Modélisation de la leucémie aiguë lymphoblastique B induite par la mutation PAX5 P80R

Manon Bayet

Université Fédérale
Toulouse Midi-Pyrénées

THÈSE

En vue de l'obtention du

DOCTORAT DE L'UNIVERSITÉ DE TOULOUSE

Délivré par Université Toulouse 3 Paul Sabatier (UT3 Paul Sabatier)

Présentée et soutenue par

Manon Bayet

Le 26 Janvier 2024

Modélisation de la leucémie aiguë lymphoblastique B induite par la mutation PAX5 P80R

École doctorale et discipline ou spécialité
BSB Biologie Santé et Biotechnologie, Cancérologie

Unité de recherche
Centre de Recherches en Cancérologie de Toulouse, Equipe IGAALD

Directrice(s) ou Directeur(s) de Thèse
Dr Bastien Gerby

Jury

Dr Susan Chan	*Directrice de recherche*	Rapporteure
Dr Laurent Delva	*Directeur de recherche*	Rapporteur
Dr Catherine Sawai	*Chargée de recherche*	Rapporteure
Pr Véronique De Mas	*PU-PH*	Examinatrice
Dr Bastien Gerby	*Chargé de recherche*	Directeur

Université Fédérale
Toulouse Midi-Pyrénées

THÈSE

En vue de l'obtention du

DOCTORAT DE L'UNIVERSITÉ DE TOULOUSE

Délivré par Université Toulouse 3 Paul Sabatier (UT3 Paul Sabatier)

Présentée et soutenue par

Manon Bayet

Le 26 Janvier 2024

Modélisation de la leucémie aiguë lymphoblastique B induite par la mutation PAX5 P80R

École doctorale et discipline ou spécialité
BSB Biologie Santé et Biotechnologie, Cancérologie

Unité de recherche
Centre de Recherches en Cancérologie de Toulouse, Equipe IGAALD

Directrice(s) ou Directeur(s) de Thèse
Dr Bastien Gerby

Jury

Dr Susan Chan	*Directrice de recherche*	Rapporteure
Dr Laurent Delva	*Directeur de recherche*	Rapporteur
Dr Catherine Sawai	*Chargée de recherche*	Rapporteure
Pr Véronique De Mas	*PU-PH*	Examinatrice
Dr Bastien Gerby	*Chargé de recherche*	Directeur

Remerciements

Il est temps maintenant de parfaire ce manuscrit avec des remerciements envers toutes les personnes qui m'ont permis de m'épanouir pendant ces quatre années de travail intense que fut ma thèse !

Il me tenait à cœur de commencer par remercier Bastien Gerby, mon directeur de thèse, qui m'a guidé d'une main de maitre pendant toutes ces années. Merci de m'avoir laissé une chance de prouver que j'étais capable de faire une thèse ! J'ai adoré grandir, évoluer, et devenir ce que je suis maintenant à tes côtés grâce à ton enthousiasme et ta passion pour la recherche. Tu es un super directeur de thèse, toujours à l'écoute, et qui arrive toujours à trouver les mots pour motiver les gens. Merci pour tout !

Un grand merci aux Dr Laurent Delva, Dr Susan Chan et Dr Catherine Sawai, qui m'ont fait l'honneur d'être rapporteurs de ma thèse. J'ai ainsi eu l'opportunité d'être évaluer par des experts aussi renommés dans leur domaine. Merci au Pr Veronique De Mas d'avoir accepté d'être la présidente de mon jury.

Merci aux Dr Philippe Brunet De La Grange et Dr Ahmed Amine Khamlichi d'avoir accepté de faire parti de mon comité de suivi de thèse. Merci pour ces échanges très enrichissants !

Je tenais également à remercier notre directeur d'équipe, Eric Delabesse, de m'avoir accepté dans l'équipe. Merci également à Cyril, Christine et Marlène pour leurs conseils dès que j'avais une question. Je pense notamment à toutes mes questions sur le clonage que j'ai pu te poser Cyril. Et à tes solutions, qui à chaque fois ont pu débloquer la situation après avoir été bloqué pendant très longtemps….

Enfin je tiens à remercier le reste de mon équipe, qui a été comme une seconde famille pour moi (ça c'est à force de passer la plupart du temps au labo, on finit par mieux connaitre ses collègues que sa propre famille). Un énorme merci (et encore, ces mots ne sont pas assez puissants pour exprimer toute ma gratitude) à Camille, que je connais depuis le master, et qui a été ingénieure dans l'équipe pendant une bonne partie de ma thèse : ta joie de vivre rendait les

journées tellement plus agréables. Tu es bien plus qu'une simple collègue et j'ai hate de continuer à vivre de belles aventures avec toi !

Merci à Sylvie, notre technicienne ou comme j'aime l'appelé ma deuxième maman, d'avoir toujours été là. Tu as été d'un grand soutien et comme j'aime souvent te le dire, la thèse n'aurait pas été pareil sans toi !

Un grand merci à ma grande copine de bureau Esmaa, pour toutes ces discussions interminables. J'ai pu découvrir une personne extraordinaire avec le cœur sur la main ! Je te passe le flambeau, c'est à toi d'être la doyenne des doctorants. Je te fais confiance, je sais que tu prendras ce rôle à cœur !

Merci à Clémence, stagiaire dans l'équipe mais surtout future doctorante. J'ai réellement adoré apprendre à te connaitre, et j'espère que ces quelques mois passés à mes côtés t'auront donné envie de continuer dans la recherche. J'aurais aimé avoir plus de temps pour te former intégralement, mais j'espère que le peu que je t'ai appris te serviront pour tes années futures !

Merci à Mathieu, l'ingénieur de l'équipe, qui a été d'une grande aide lors des grosses manips. Tu as toujours été disponible, et les projets ont ainsi pu bien avancer.

Un grand merci à Vincent, pour tous ces échanges qu'on a pu avoir qui ont été plus qu'enrichissants. Les manips avec toi ont été plus que folkoriques avec ton organisation légendaire, mais ça ne m'a pas empêché de m'éclater avec toi !

Enfin un grand merci à Laura, Laetitia, Antoine et Pauline pour leurs échanges au quotidien qui ont permis de m'enrichir au niveau scientifique.

Un énorme merci à ma maman ! Grâce à tous les sacrifices que tu as fais depuis de nombreuses années, j'ai pu réaliser mes rêves et devenir la personne que je suis maintenant. Malgré les difficultés que l'on a pu traverser, merci de m'avoir laissé m'épanouir. Je t'en serais reconnaissante toute ma vie. J'espère que tu es fière de moi. En tout cas, moi je suis fière d'avoir une maman comme toi !

Merci à mes sœurs, Camille et Elisa, d'avoir été présente et de m'avoir écouté durant ces dernières années. Merci à vous de m'avoir fait l'honneur d'être tata de cinq petits monstres, qui égayent de plus en plus mes journées !

Enfin, il me tenait à cœur de finir ces remerciements par mon copain Adrien, qui est entré dans ma vie depuis un bon petit moment ! Merci d'être la au quotidien, de me faire rire et de me rassurer. Sans toi, je n'aurais pas pu autant m'épanouir au labo. Et surtout un grand merci d'avoir tout abandonné plusieurs fois pour me suivre dans ce périple, je te serais a jamais reconnaissante !

Résumé

L'équipe s'intéresse aux altérations de facteurs de transcription impliquées dans les leucémies aiguës, dont *PAX5* qui est essentiel pour le développement des cellules B. C'est pourquoi le modèle murin transgénique PAX5-ELN a été généré, qui exprime la protéine de fusion oncogénique durant le développement des lymphocytes B, et récapitule le processus multi-étapes des LAL-B (*Jamrog L et al., PNAS, 2018*). J'ai participé à l'identification des cellules à l'origine de la LAL-B et à la caractérisation de leur propriétés fonctionnelles et moléculaires. Nos travaux indiquent qu'au stade pré-leucémique, PAX5-ELN induit l'émergence d'une population aberrante de progéniteurs B avec une propriété anormale d'auto-renouvellement. Cette population est enrichie en cellules quiescentes résistantes aux agents de chimiothérapie, activent un programme moléculaire de cellule souche, et sont le support de l'initiation leucémique à long terme. Ce travail fait l'objet d'une publication récente que je signe en deuxième auteure (*Fregona V, **Bayet M** et al., J Exp Med, in press*) (Annexe I).

En parallèle, ma thèse s'est tournée vers la modélisation de l'initiation et de la transformation leucémique induite par la mutation *PAX5*^{P80R}, une altération initiatrice fréquente chez les patients. J'ai donc utilisé des cellules de foie fœtal issus d'embryon de souris *Pax5*$^{-/-}$ pour sélectionner les progéniteurs lymphoïdes non engagés dans le lignage B. Après transduction avec des rétrovirus CTL, PAX5 Wt ou PAX5^{P80R}, j'ai montré que PAX5^{P80R} ne restaure pas efficacement l'engagement définitif des cellules vers le lignage B. Les études de transplantation ont permis de montrer que PAX5^{P80R} induit un potentiel de prise de greffe aberrant suivi du développement de la LAL-B. Cette transformation leucémique est associée à la sélection de clones porteurs de mutations additionnelles affectant la voie JAK/STAT. Nos analyses ont permis d'identifier *Hif2α* comme un candidat potentiel dans la leucémogenèse. Enfin, un criblage pharmacologique d'inhibiteurs de Hifα révèle l'Acriflavine comme un composé intéressant ciblant les cellules leucémiques. Ainsi, la modélisation de la LAL-B par la mutation PAX5^{P80R} fournit à l'équipe un nouvel outil mimant le processus multi-étapes de la LAL-B, et permet de déchiffrer les mécanismes biologiques par lesquels la mutation mène à la transformation tumorale. Ce travail fait l'objet d'un manuscrit en préparation que je signe en première auteure (***Bayet M** et al., in preparation*).

Les modèles PAX5-ELN et PAX5^{P80R} permettent non seulement d'étudier les différentes étapes de la leucémogenèse B, mais servent aussi de support pour le développement de criblage

de petites molécules sur cellules primaires. J'ai donc mis en place un protocole miniaturisé et robuste par FACS pour cribler des composés chimiques ciblant les cellules pré-leucémiques. Notre approche multiparamétrique permet d'évaluer simultanément l'effet des composés sur les cellules pré-leucémiques et les sous-populations B normales. J'ai donc criblé une banque de 1040 composés synthétiques et naturels (chimiothèque essentielle) reflétant la diversité chimique de la chimiothèque nationale française. Ce criblage, associé à des contre-criblages en dose-réponse, m'a permis d'identifier 5 molécules d'intérêt. Dans l'ensemble, mon travail montre la faisabilité d'un criblage de petites molécules sur une population enrichie en cellules initiatrice de la leucémie et prenant en compte la complexité intrinsèque des cellules primaires du lignage B.

Enfin, j'ai procédé à la rédaction et la publication d'une revue dans le journal ***Cancers*** qui expose les concepts d'hétérogénéité tumorales des cellules leucémiques des patients, l'utilité des modèles de souris transgéniques pour explorer le compartiment des cellules initiatrices de la leucémie, et les efforts actuels visant à découvrir de nouvelles thérapies ciblées (*Fregona V*, **Bayet M*** et al, Cancers (Basel), 2021*), que je signe en co-première auteure (Annexe II).

Abstract

The team is interested in alterations in transcription factors involved in acute leukemia, including *PAX5*, which is essential for B-cell development. This is why the PAX5-ELN transgenic mouse model was generated, which expresses the oncogenic fusion protein during B-cell development and recapitulates the multi-step process of B-ALL (*Jamrog L et al., PNAS, 2018*). I was involved in identifying the cells at the origin of-B-ALL and characterizing their functional and molecular properties. Our work indicates that at pre-leukemic stage, PAX5-ELN induces the emergence of an aberrant population of B-progenitors with an abnormal self-renewal property. This population is enriched in quiescent cells resistant to chemotherapeutic agents, activating a molecular stem cell program and supporting long-term leukemic initiation. This work is the subject of a recent publication signed by myself as second author (*Fregona V, **Bayet M** et al., J Exp Med, in press*).

In parallel, my thesis focused on modeling the initiation and leukemic transformation induced by the *PAX5*^{P80R} mutation, a frequent initiating alteration in patients. I used fetal liver cells derived from *Pax5*$^{-/-}$ mouse embryos to select lymphoid progenitors not committed to the B lineage. After transduction with CTL, PAX5 Wt or PAX5^{P80R} retroviruses, I showed that PAX5^{P80R} does not restore efficiently definitive commitment of cells to the B lineage. Transplantation experiments have shown that PAX5^{P80R} induces aberrant engraftment potential followed by the development of B-ALL. This leukemic transformation is associated with the selection of clones carrying additional mutations affecting the JAK/STAT signaling pathway. Our analyses identified Hif2α as a potential candidate for leukemogenesis. Finally, pharmalogical screening of Hifα inhibitors revealed Acriflavine as an interesting compound targeting leukemic cells. Thus, the modeling of B-ALL by the PAX5^{P80R} mutation provides the team with a new tool to mimic the multi-step process of B-ALL, and to decipher the biological mechanisms by which the mutation leads to tumor transformation. This work is the subject of a manuscript in preparation which I have signed as first author (***Bayet M***, *Fregona V, et al., in preparation*).

The PAX5-ELN and PAX5^{P80R} models not only make it possible to study the various stages of B leukemogeneis, but also serve as a basis for the development of small molecule screening on primary cells. I therefore set up a miniaturized and robust protocol by FACS to screen chemical compounds targeting pre-leukemic cells. Our multiparametric approach enables us to simultaneously assess the effect of compounds on pre-leukeic cells and normal B

subpopulations. I screened a bank of 1040 synthetic and natural compounds (essential chemical library) reflecting the chemical diversity of the French national chemical library. This screening, combined with dose-response counter-screening, enabled me to identify 5 molecules of interest. Overall, my work demonstrates the feasibility of small-molecule screening on a population enriched in leukemia-initiating cells, taking into account the intrinsic complexity of primary B-cells.

Finally, I edited and published a review in the journal ***Cancers*** outlining the concepts of tumor heterogeneity in patients' leukemic cells, the utility of transgenic mouse models to explore the leukemia initiating cell compartment, and current efforts to discover new targeted therapies (*Fregona V*, **Bayet M*** et al, Cancers (Basel), 2021*), wich I co-authored.

Liste des abréviations

ALP : *All-Lymphoid Progenitor*

BCR : *B-Cell Receptor*

BLP : *B-cell biased Lymphoid Progenitor*

Cas : *CRISPR-Associated genes*

CLP : Progéniteur Lymphoïde Commun

CMP : Progéniteur Myéloïde Commun

CRD : *Carbohydrate Recognition Domain*

CRISPR : *Clustered Regularly Interspaced Short Palindromic Repeats*

CSH : Cellule Souche Hématopoïétique

CSL : Cellule Souche Leucémique

CSPH : Cellule Souche et Progéniteur Hématopoïétique

EdU : 5-éthynyl-2'-désoxyuridine

EGIL : *European Group for the Immunological characterization of Leukaemias*

HD : HoméoDomaine

ID : Domaine Inhibiteur

Ig : Immunoglobuline

IgH : chaine lourde des immunoglobulines

IgL : chaine légère des immunoglobulines

IL-7 : Interleukine-7

IL-7R : récepteur à l'interleukine-7

GAL-1 : Galectine-1

Grg4 : Groucho 4

LAL : Leucémie Aiguë Lymphoblastique

LAL-B : Leucémie Aiguë Lymphoblastique B

LAL-T : Leucémie Aiguë Lymphoblastique T

LAM : Leucémie Aiguë Myéloïde

LB : Lymphocyte B

LMPP : *Lymphoid-primed MultiPotent Progenitor*

LT : Lymphocyte T

MHB : *Midbrain-Hindbrain Boundary*

MPP : Progéniteur MultiPotent

MPP4 : Progéntieur MultiPotent 4

NHEJ : *Non Homologous End Joining*

NLS : Signal de Localisation Nucléaire

NK : *Natural Killer*

OP : OctaPeptide

PAM : *Protospacer Adjacent Motif*

PAX : *PAired boX*

PBD : *Paired Box Domain*

PIP2 : Phosphoinositide phosphate 2

PIP3 : Phosphoinositide phosphate 3

Pré-BCR : *pré B-Cell Receptor*

Pré-CSL : Cellule Souche pré-Leucémique

Rb1 : *RB transcriptional corepressor 1*

ROS : *Reactive Oxygen Species*

RSS : *Recombination Signal Sequence*

SCF : *Stem Cell Factor*

SNC : Système Nerveux Central

TAD : Domaine Activateur de la Transcription

TBP : *TATA-box Binding Protein*

Table des matières

Partie I : Introduction

Chapitre 1 : La lymphopoïèse B

1.1. Généralités sur l'hématopoïèse

L'hématopoïèse est définie comme étant un processus physiologique finement régulé qui permet la production et le remplacement de tous les éléments figurés du sang **(Figure 1)**. Schématiquement, les cellules du système hématopoïétique peuvent être séparées en cellules souches (CSH), progéniteurs (MPP, LMPP et CMP), précurseurs (CLP, GMP et MEP) et cellules matures (NK, cellules T CD4 et CD8, cellules B, cellules dendritiques, monocytes, granulocytes, globules rouges et mégacaryocytes). Chaque cellule mature possède un rôle spécifique et collabore avec les autres cellules hématopoïétiques afin de maintenir l'homéostasie tissulaire. Les cellules matures possèdent diverses fonctions comme le transport de l'oxygène dans le sang, la défense immunitaire ou le contrôle de la fluidité du sang.

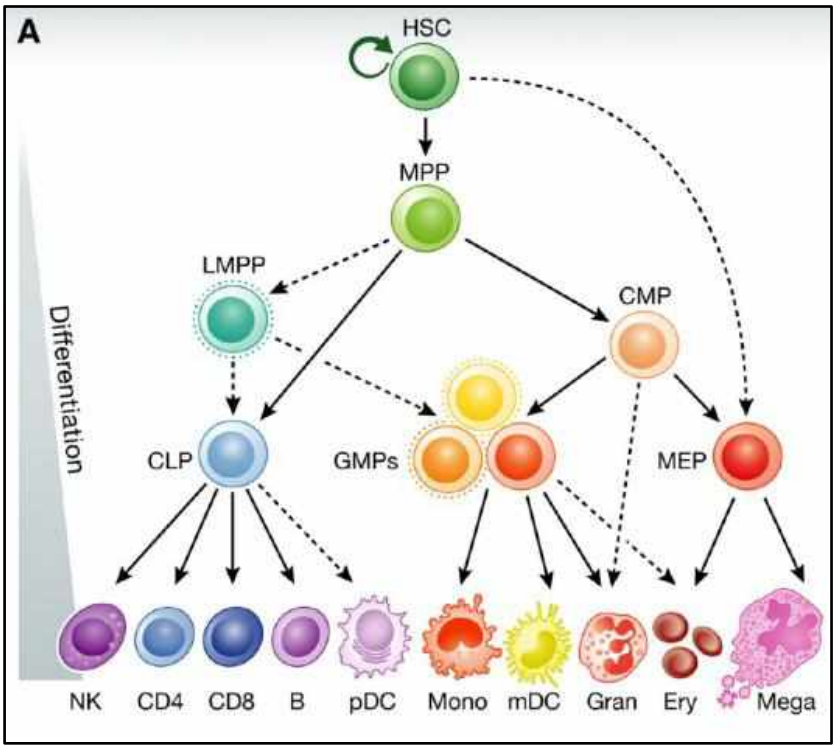

Figure 1 : Représentation schématique de l'hématopoïèse (D'après Bao et al., 2019).
Les flèches pleines correspondent au modèle d'hématopoïèse hiérarchique classique. Les flèches en pointillés présentent le processus hématopoïétique révisé plus complexe. Abréviations : **HSC** *: Hematopoietic Stem Cell ;* **MPP** *: MultiPotent Progenitor ;* **LMPP** *: Lymphoid MultiPotent Progenitor;* **CMP***: Common Myeloid Progenitor;* **CLP***: Common Lymphoid Progenitor;* **GMP***: Granulocyte Macrophage Progenitor,* **MEP***: Megakaryocyte Erythroid Progenitor;* **NK** *: Natural Killer,* **pDC** *: plasmacytoid Dendritic Cell ;* **Mono** *: Monocyte ;* **mDC** *: myeloid Dendritic Cell,* **Gran***: Granulocyte;* **Ery** *: Erythrocyte;* **Mega** *: Megakaryocyte)*

Le système hématopoïétique peut être divisé en différents lignages :

- **Le lignage lymphoïde** regroupe les lymphocytes B à l'origine de la réponse humorale, les lymphocytes T à l'origine de la réponse immunitaire adaptative, et les cellules NK (cellules lymphoïdes innées) à l'origine de la réponse cytotoxique face aux infections.
- **Le lignage myéloïde** peut être déconvolué en compartiments granuleux, monocytaire, érythroïde et mégacaryocytaire. Les granulocytes sont à l'origine de la réponse immunitaire innée en phagocytant les pathogènes ou en libérant des granules cytotoxiques. Les monocytes sont à l'origine de la présentation des antigènes aux cellules dendritiques ou dans la phagocytose par les macrophages. Les globules rouges sont à l'origine de l'oxygénation de tous les tissus. Les mégacaryocytes sont à l'origine de la production des plaquettes qui permettent de moduler la fluidité du sang.

Le renouvellement cellulaire permanent est assuré par une population de cellules, appelées cellules souches hématopoïétiques (CSH), présentes en nombre restreint dans la moelle osseuse adulte. Les CSH sont caractérisées par leur capacité d'auto-renouvellement, qui désigne leur aptitude à se diviser tout en transmettant leur potentiel initial à au moins une de ces deux cellules filles. Ces cellules sont donc capables de s'auto-renouveler, c'est-à-dire proliférer sans se différencier, permettant ainsi de maintenir un pool de CSH. Les CSH sont également caractérisées par leur multipotence, terme qui désigne leur aptitude à se différencier vers tous les lignages hématopoïétiques.

Le modèle traditionnel tel qu'on le connait présente l'hématopoïèse comme un système hiérarchique dans lequel les rares CSH restent quiescentes et se divisent de façon asymétrique, en restreignant graduellement ses alternatives de différenciation vers un lignage précis par le biais de progéniteurs intermédiaires de plus en plus différenciés. Ainsi, les CSH se différencient successivement en progéniteurs multipotents (MPP) puis en progéniteurs myéloïdes communs (CMP) ou en progéniteurs multipotents possédant un biais lymphoïde (LMPP). Les CMP sont à l'origine des cellules mono-granulocytaires, érythrocytaires et mégacaryocytaires, tandis que les LMPP se différencient en progéniteurs lymphoïdes communs (CLP) qui génèrent par la suite les cellules NK, les lymphocytes B et les lymphocytes T (Dick, 2003).

Les nouvelles technologies qui ont été développées ont permis de montrer que l'hématopoïèse est un système moins linéaire et plus complexe, et qui s'avère être plus dynamique et adaptatif (**Figure 2**). Il existe en effet une hétérogénéité phénotypique et fonctionnelle au sein du compartiment des CSH, mais également au niveau des compartiments des progéniteurs. Ce modèle révisé encourage donc à voir la différenciation hématopoïétique comme étant un processus continu et implique l'environnement comme jouant un rôle essentiel dans le choix de la différenciation des CSH et la diversification des cellules matures. En effet, la caractérisation du microenvironnement médullaire a permis de démontrer que la destinée des cellules souches et progéniteurs hématopoïétiques est influencée par leurs localisations dans la niche hématopoïétique, et par leurs interactions avec les composants du microenvironnement (Méndez-Ferrer et al., 2020).

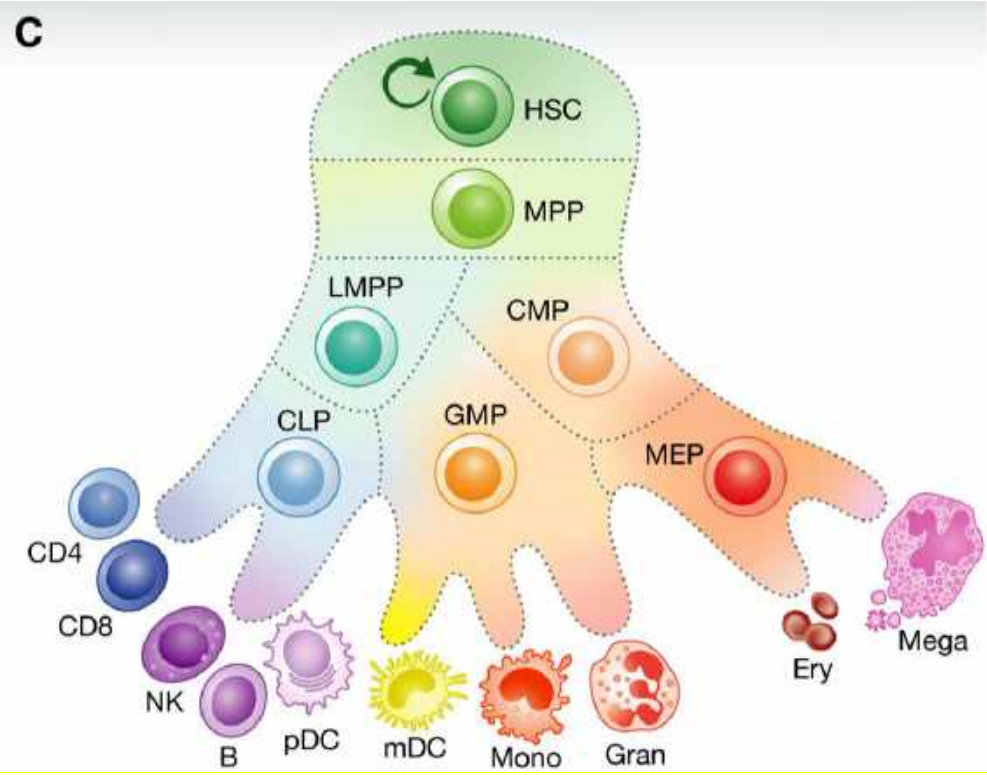

Figure 2 : Schéma de la hiérarchie du système hématopoïétique dans lequel l'engagement vers un lignage s'effectue en continuum plutôt que via des stades distincts (D'après Bao et al., 2019).

La transition entre les CSH très immatures et les cellules matures circulantes est permise par des processus progressifs d'engagement vers une voie de différenciation. Tout au long de ces différentes étapes, la cellule acquiert de façon irréversible des caractéristiques spécifiques de sa lignée et perd sa capacité de prolifération en différenciation terminale. Le maintien du pool de CSH et le choix d'engagement dans la différenciation s'effectue en réponse à des facteurs extrinsèques qui sont fournis par le stroma médullaire (cytokines, facteurs de

croissance, molécules d'adhérence), qui vont moduler l'activité et l'expression de facteurs intrinsèques (facteurs de transcription), ces derniers permettant de modifier le programme génique pour engager les cellules dans la différenciation.

1.2. La lymphopoïèse B

La lymphopoïèse B correspond au processus impliqué dans la production des lymphocytes B, qui sont à l'origine de l'immunité humorale par la production des anticorps.

1.2.A. Classification phénotypique des différents stades du développement des cellules B

Dans la moelle osseuse, la différenciation des cellules lymphoïdes B est subdivisée en différents stades cellulaires. Il existe deux nomenclatures, qui ont comme caractéristique commune d'utiliser l'expression des marqueurs de surface B220 et Cd19 **(Figure 3)** :

- La nomenclature de Bâle (Basel) qui prend en compte la taille des cellules, ainsi que l'expression du CD117 (Kit), CD25 et du CD43 à leur surface, pour différencier les différents sous-types cellulaires (Melchers, n.d.; Melchers et al., 1991, 1994).
- La classification de Hardy qui prend en compte l'expression du CD43, CD24 et du CD249 (BP-1) à la surface des cellules par cytométrie en flux pour différencier les différents sous-types cellulaires (Hardy et al., 2012; Hardy & Hayakawa, 2001).

La lymphopoïèse B se caractérise donc par une succession de stades cellulaires que sont les stades pré-pro-B (Fraction A), pro-B (Fraction B), pré-BI (Fraction C), pré-BII précoce (Fraction C'), pré-BII tardive (Fraction D), immature B (Fraction E) et mature B recirculante (Fraction F).

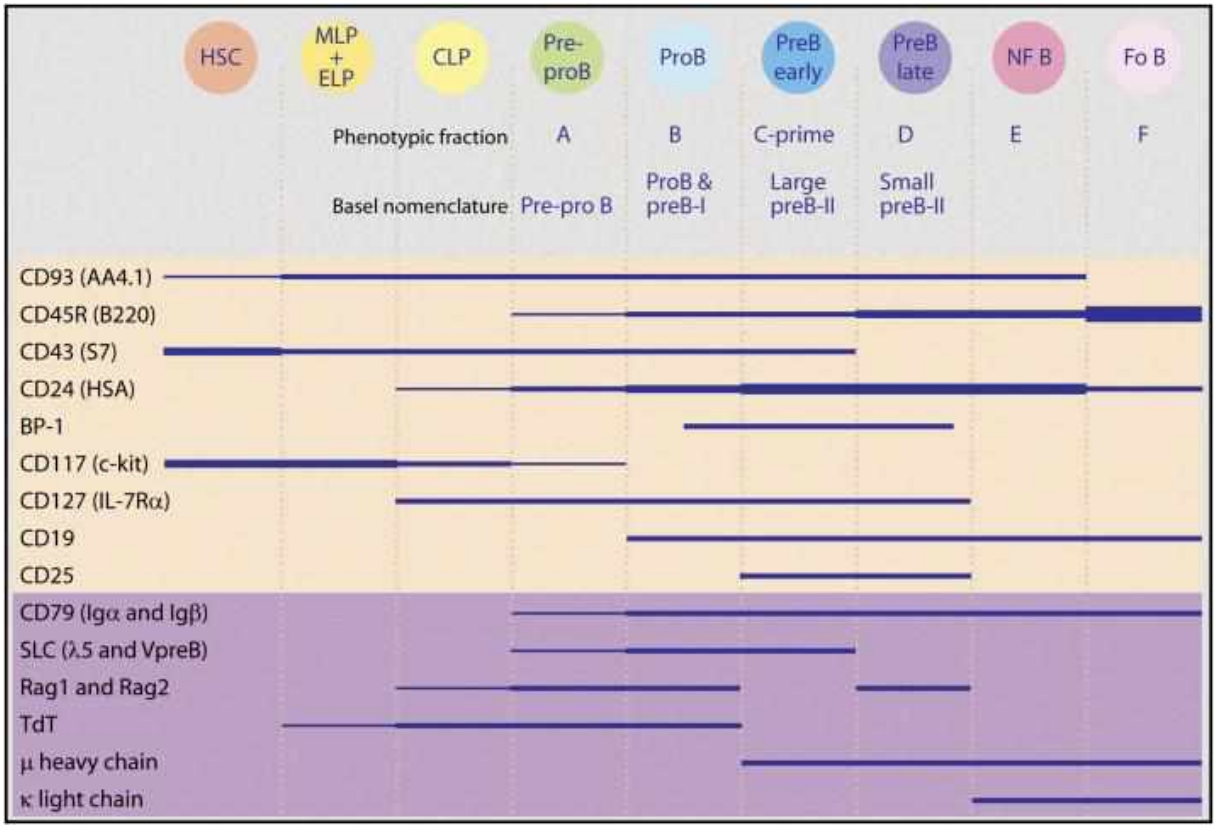

Figure 3 : ***Classification phénotypique de la différenciation des cellules lymphoïdes B permettant de discriminer les différents stades de la lymphopoïèse B dans la moelle osseuse (D'après Hardy et al., 2007).***
L'expression des marqueurs de surface (cadre beige) a été évaluée par cytométrie en flux. L'expression des gènes (cadre violet) a été évaluée par analyses d'ARNm, d'expression de gène-rapporteur ou de marquage cytoplasmiques. La largeur de chaque ligne correspond au niveau d'expression des marqueurs pour les différents stades de la lymphopoïèse B.
Abréviations: **HSC** *: Hematopoietic Stem Cells;* **MLP** *: MultiLineage Progenitor;* **ELP** *: Early Lymphoid Progenitor;* **NF B** *: Newly Formed B cell;* **Fo B** *: Follicular B cell;* **Tdt** *: Terminal deoxynucleotidyl transferase*

1.2.B. Mécanisme de la lymphopoïèse B dans la moelle osseuse

1.2.B.i. Entrée dans le lignage lymphoïde

Dans un premier temps, les CSH vont se différencier en progéniteurs multipotents qui possèdent un biais lymphoïde (mais qui gardent quand même un potentiel myéloïde) : ce sont les MPP4 (*Multipotent Progenitor subset 4*), aussi couramment appelés LMPP (*Lymphoid-primed MultiPotent Progenitor)* (Adolfsson et al., 2005; Pietras et al., 2015). Les LMPP se différencient par la suite en CLP (*Common Lymphoid Progenitor*) qui ont une capacité limitée pour générer des cellules myéloïdes (Alberti-Servera et al., 2017; Rumfelt et al., 2006).

Les CLP constituent une population hétérogène fonctionnellement, et peuvent être divisés en deux sous-populations distinctes sur la base de l'expression du Ly6d (Alberti-Servera et al., 2017; Inlay et al., 2009; Mansson et al., 2010) : les ALP (*All Lymphoid Progenitor*) qui sont Ly6d- ; et les BLP (*B cell-biaised Lymphoid Progenitor*) qui sont Ly6d+ (**Figure 4**). En plus de leur aptitude à générer des lymphocytes B, les ALP arborent également la capacité à générer des cellules de la lignée lymphoïde T et des cellules NK. Les BLP, quant à eux, ne sont capables de générer que des cellules de la lignée lymphoïde B.

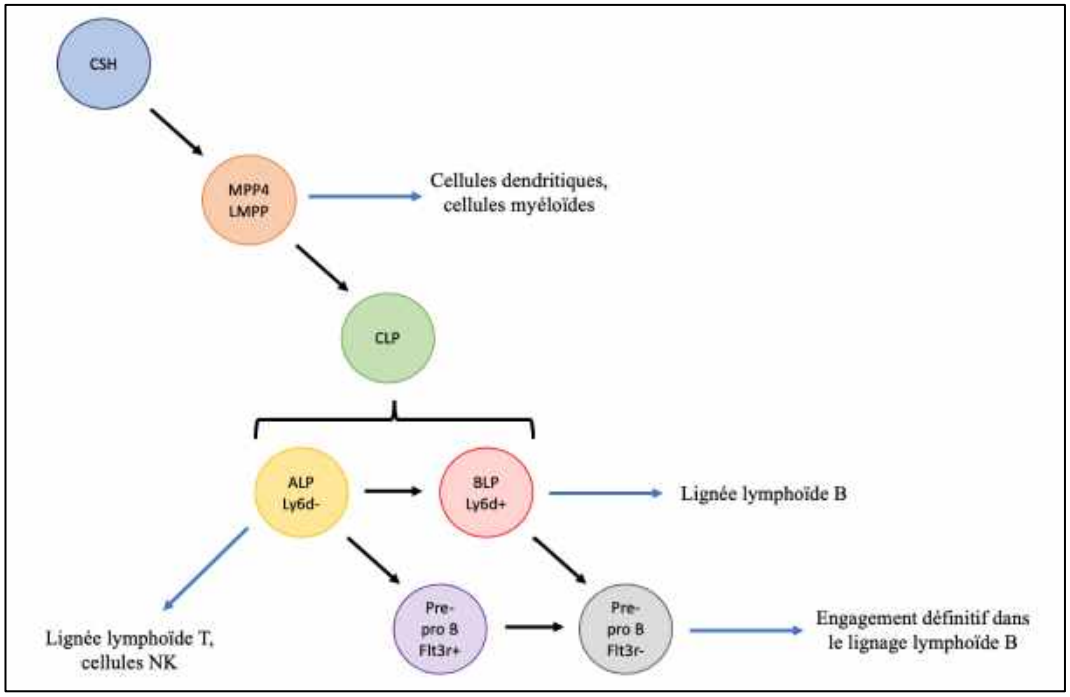

***Figure 4 :** Modèle de spécification dans la lignée lymphoïde B (Adaptée de Inlay et al., 2009).*

Les CLP vont ensuite se différencier en cellules pré-pro-B. Il existe également une hétérogénéité au sein de ce compartiment et peut également être divisé en deux sous-populations (Ogawa et al., 2000) : les cellules pré-pro-B Flt3r+ et les cellules pré-pro-B Flt3r-. Celles exprimant Flt3r sont issues des ALP alors que celles ne l'exprimant pas sont soit issues des BLP soit des cellules pré-pro-B Flt3r+. Les cellules pré-pro-B Flt3r- correspondent à la population de progéniteurs qui est destinée à s'engager uniquement dans la différenciation lymphoïde B.

Jusqu'au stade pré-pro-B Flt3r-, les cellules ne sont pas strictement engagées dans la voie de différenciation lymphoïde B ; mais elles expriment un ensemble de gènes impliqués dans la différenciation des cellules B tels que Ebf1, Pax5, et sont prêtes à s'engager dans un lignage à la suite d'une stimulation cytokinique telle que l'IL7 (Månsson et al., 2007). C'est à

partir du stade suivant, appelé stade pro-B, caractérisé par l'expression du marqueur de surface CD19 qui est transactivé directement par le facteur de transcription Pax5 (Kozmik et al., 1992a), que les cellules sont engagées de façon irréversible dans la lignée lymphoïde B **(Figure 4)**.

1.2.B.ii. Mécanismes moléculaires de la lymphopoïèse B

1.2.B.ii.a. La recombinaison V(D)J des loci des gènes des immunoglobulines

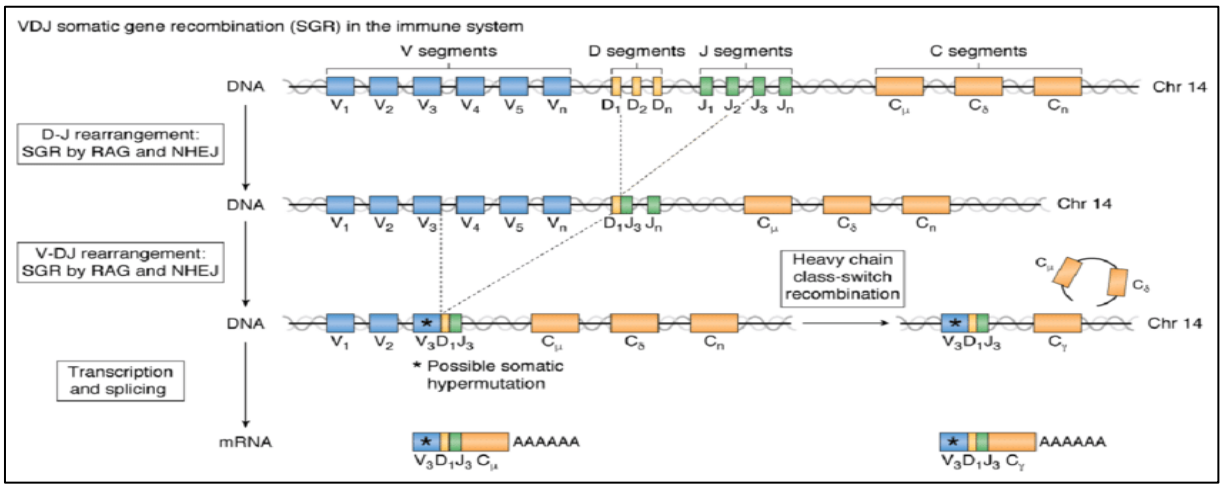

Figure 5 : Schéma récapitulant le processus de recombinaison V(D)J des gènes des immunoglobulines (D'après Kaeser & Chun, 2020).

Le développement des cellules de la lignée lymphoïde B est permis par les réarrangements aléatoires des loci du gène des chaines lourdes puis des chaines légères des immunoglobulines (Ig). Le mécanisme qui est à l'origine de ce processus s'appelle la recombinaison V(D)J (**Figure 5**), et se caractérise par différentes étapes d'assemblage des segments géniques V (Variable), D (Diversité) et J (Jonction) pour ce qui est des chaines lourdes, et l'assemblage des segments géniques V et J pour ce qui est des chaines légères ; qui permettra de constituer finalement la région variable du BCR. Ce processus de recombinaison se trouve donc être à l'origine de la diversité combinatoire, permettant de reconnaitre un large spectre d'antigènes.

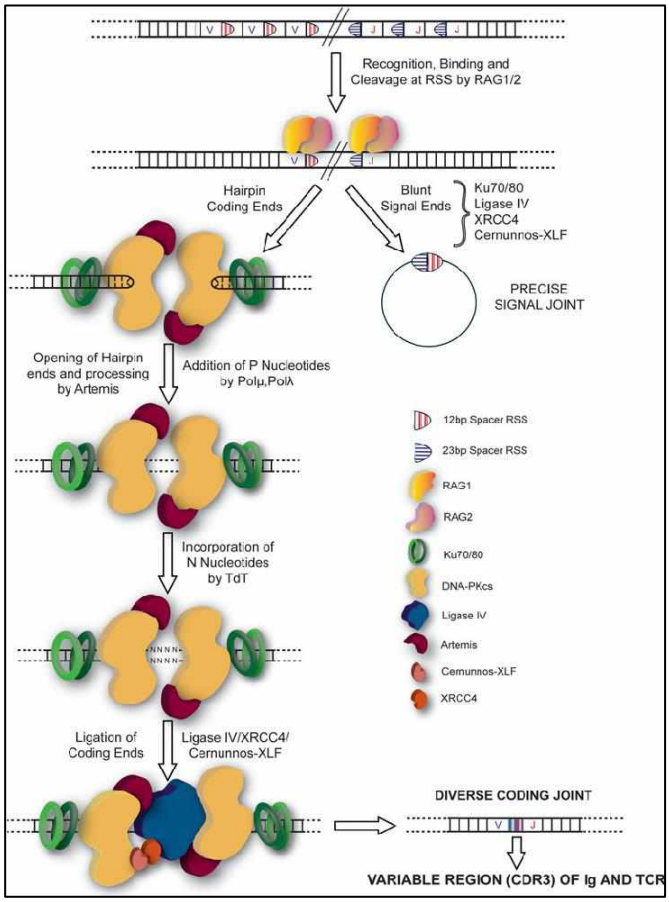

<u>Figure 6 :</u> Schéma représentant le mécanisme d'action des enzymes RAG lors du processus des réarrangements des gènes des immunoglobulines (D'après Malu et al., 2012).

La recombinaison est permise par la reconnaissance sur l'ADN de courtes séquences cibles, appelées signaux de recombinaison (RSS), de 12 nucléotides pour les régions D et de 23 nucléotides pour les régions V et J (**Figure 6**). Le complexe formé par les enzymes RAG1 et RAG2 permet d'initier la recombinaison en se fixant sur les RSS, et vont par la suite entrainer des cassures double brin (Nishana & Raghavan, 2012). Une fois le clivage de l'ADN réalisé, la machinerie de la réparation de l'ADN appelée NHEJ (*Non Homologous End Joining*), qui est dite « erreur prône », va se mettre en place afin de joindre les deux extrémités des régions clivées tout en incorporant des erreurs d'insertions/et ou de délétions de nucléotides au niveau de la jonction. Ce sont ces erreurs de réparation de l'ADN qui sont à l'origine de l'augmentation de la diversité moléculaire des immunoglobulines (Lieber et al., 2006).

1.2.B.ii.b. Formation du pré-BCR

Le réarrangement des chaines des immunoglobulines est un processus qui se produit de manière séquentielle (**Figure 7**).

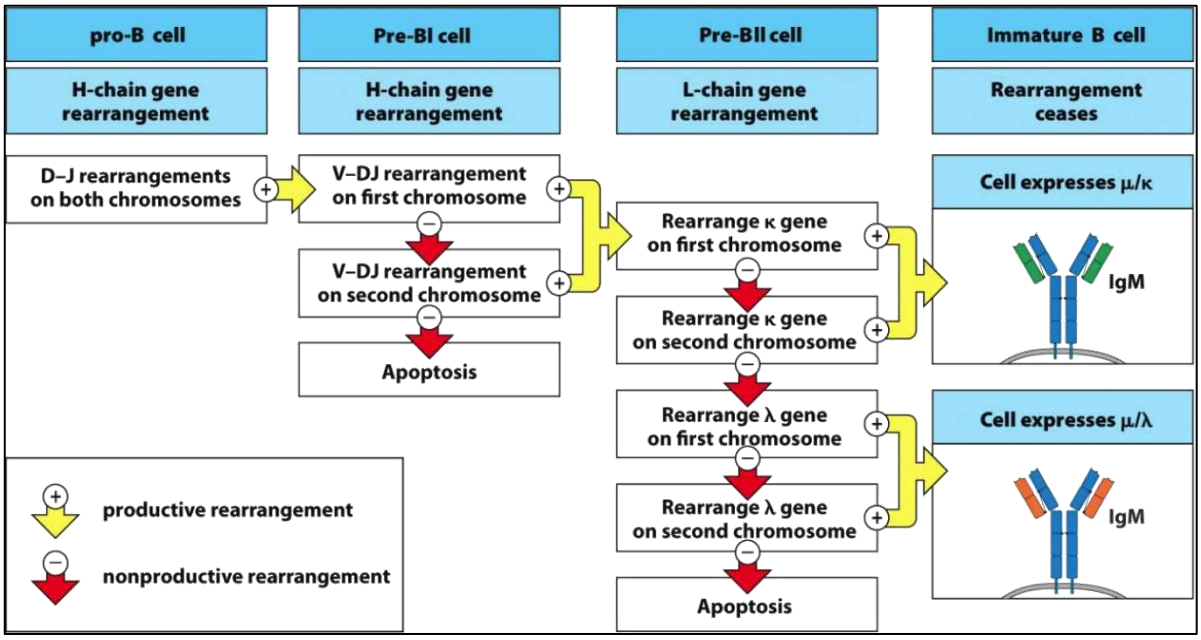

Figure 7 : Schéma représentant les réarrangements successifs des gènes des immunoglobulines permettant la progression des cellules dans la différenciation lymphoïde B.

Dans un premier temps, les réarrangements D_H-J_H s'effectuent sur les deux allèles des cellules pro-B (Fraction B) ; puis dans un second temps ce sont les réarrangement V_H-DJ_H s'effectuant sur un allèle qui s'achèvent dans les cellules pré-BI (Fraction C). A la transition entre le stade pro-B/pré-B, des pseudo-chaines légères sont exprimées pour former un complexe fonctionnel avec la chaine lourde précédemment produite : c'est ce que l'on appelle le pré-BCR (**Figure 8**). Les pseudo-chaines légères sont composées d'un hétérodimère de protéines qui sont toujours les mêmes : VpreB1 ou CD179a et lambda-5 ou CD179b (Vettermann et al., 2006).

La formation du pré-BCR à la surface ainsi que la signalisation qui en découle sert de point de contrôle pour la progression dans la différenciation des cellules lymphoïdes B. Grâce à un signal dépendant des protéines CD79A (Igα) et CD79b (Igβ) codées respectivement par les gènes *mb-1* et *B28*, le pré-BCR va pouvoir informer à la cellule qu'une chaine lourde fonctionnelle a été générée. Si la recombinaison V_H-DJ_H du premier allèle des IgH n'a pas été productive, elle va finalement se produire sur le second allèle des IgH. L'expression d'un pré-BCR fonctionnel à la surface des cellules pré-BI conduit à la répression transitoire des enzymes RAG1/2 pour éviter que la recombinaison ait lieu sur le second allèle des IgH : ce processus est

appelé mécanisme d'exclusion allélique (Grawunder et al., 1995). Les cellules pré-BII précoces (Fraction C') qui possèdent un pré-BCR fonctionnel à la surface vont subir une expansion clonale avant de progresser dans la différenciation : elles rentrent donc en cycle, d'où l'adjectif de « *large* » qu'on utilise également pour les caractériser.

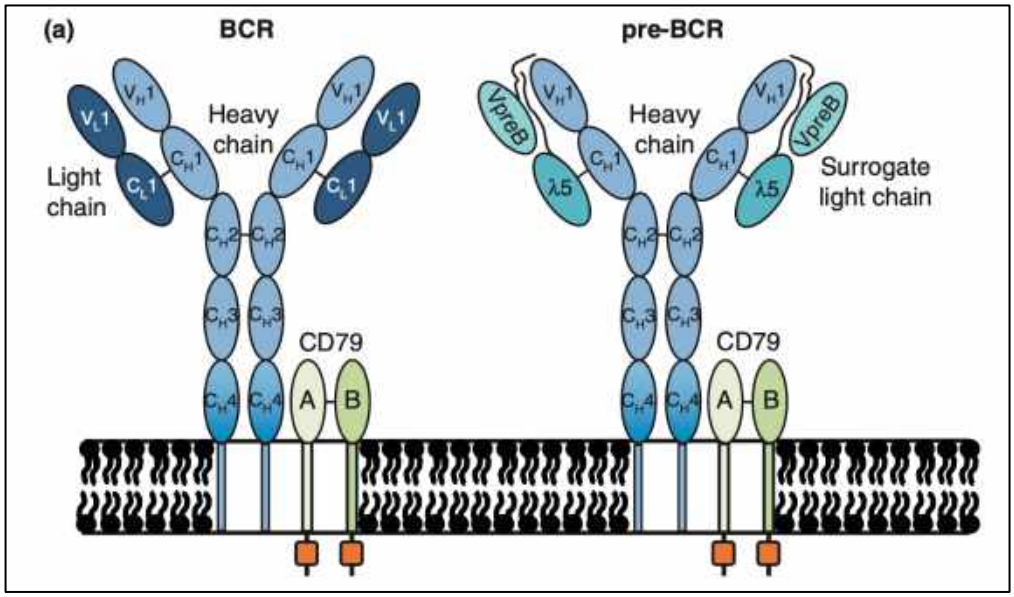

Figure 8 : Schéma du pré-BCR et du BCR respectivement localisés à la surface des cellules pré-B et des cellules immatures (D'après Berry et al., 2011).

Enfin, dans un second temps, la signalisation induite par le pré-BCR va enclencher la recombinaison du locus des chaines légères des Ig (IgL). Pour cela, les cellules doivent stopper leur progression dans le cycle cellulaire pour devenir des cellules pré-BII tardives (Fraction D) : elles sont communément qualifiées de « *small* ». La recombinaison va agir sur l'expression des facteurs de transcription impliqués dans les réarrangements des IgL, mais aussi activer la transcription des gènes des chaines légères kappa et lambda (Melchers et al., 2000). La recombinaison efficace des IgL conduit à la formation du BCR (**Figure 8**) à la surface des cellules, et permet ainsi leur progression dans la différenciation en cellules immatures (Fraction E). Ces cellules vont ensuite sortir de la moelle osseuse pour se diriger vers les organes lymphoïdes secondaires, dans le but de finir la maturation de leur BCR et de devenir des lymphocytes B matures.

1.2.B.iii. Voies de signalisation essentielles dans la différenciation B

Chez la souris, il existe deux voies de signalisation intracellulaires essentielles pour la progression dans la lymphopoïèse B : la signalisation induite par le récepteur à l'IL-7 et la signalisation induite par le pré-BCR.

1.2.B.iii.a. Signalisation induite par le récepteur à l'IL-7

Le récepteur à l'IL-7 (IL-7R) est constitué de la chaine α du récepteur à l'IL-7 (IL-7Rα) (exprimée exclusivement dans le lignage lymphoïde), et de la chaine γ du récepteur à l'IL-2 (IL-2Rγ) (exprimée de façon ubiquitaire dans les cellules hématopoïétiques). Il est exprimé précocement au cours de la lymphopoïèse B, puisqu'il se retrouve exprimé dès le stade CLP. Les souris KO pour l'IL-7R (Corcoran et al., 1998) ou pour l'IL-7 (von Freeden-Jeffry et al., 1995) ont la caractéristique de n'avoir presque plus de progéniteurs B, démontrant ainsi que la voie de signalisation induite par l'IL-7R est essentielle pour l'engagement et le développement des cellules lymphoïdes B (**Figure 9**). La production de l'IL-7, quant à elle, est permise par les cellules stromale du micro-environnement de la moelle osseuse, de la rate et du thymus.

L'induction de la voie, permise grâce à la fixation de l'IL-7 sur le récepteur, a pour conséquence d'activer deux voies de signalisation qui sont connectées mais qui possèdent des rôles différents au cours de la lymphopoïèse B : il s'agit de la voie JAK/STAT et de la voie PI3K/AKT/mTOR. Ces deux voies agissent ensemble et induisent des signaux de survie et de prolifération cellulaire, permettant ainsi aux cellules de progresser dans leur différenciation.

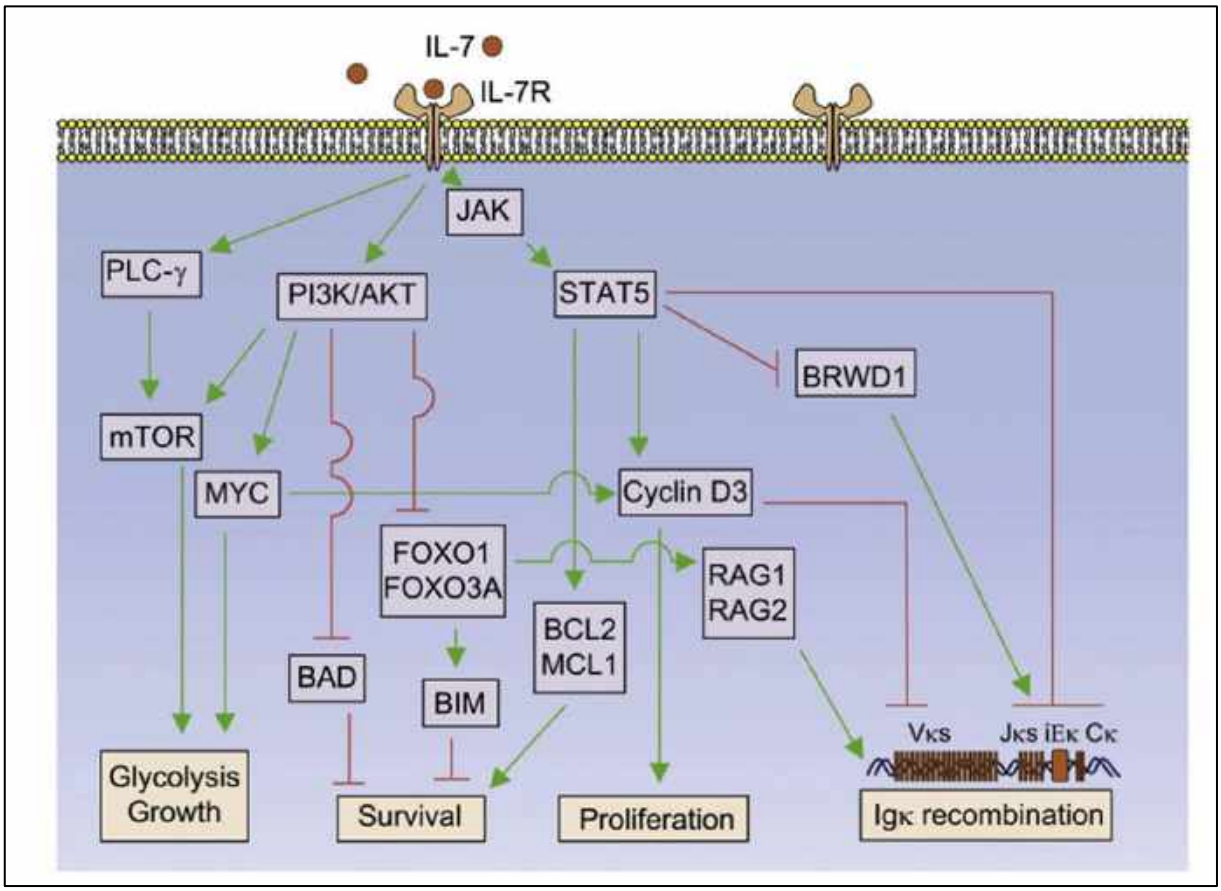

Figure 9 : ***Illustration schématique représentant la voie de signalisation IL-7R activée au cours de la différenciation des progéniteurs lymphoïdes B dans la moelle osseuse (D'après McLean & Mandal, 2020).***

Induction d'un signal de survie cellulaire

Les réarrangements des chaines lourdes des immunoglobulines qui s'effectuent au stade pro-B induisent des dommages à l'ADN. Pour que les cellules puissent y échapper, elles mettent en place une signalisation pro-survie qui est rendue possible par la voie de signalisation JAK/STAT.

En effet lorsque l'IL-7 se fixe sur son récepteur, un changement conformationnel de celui-ci phosphoryle JAK1 et/ou JAK3, qui phosphorylent à leur tour les facteurs de transcription STAT5A/B dans le cytoplasme. Une fois leur phosphorylation terminée, les facteurs STAT vont se dimériser et vont être transloqués dans le noyau pour induire l'expression de gènes pro-survie (Q. Jiang et al., 2004). Différentes études ont montré l'importance de la voie JAK/STAT dans la lymphopoïèse B puisque les souris KO pour STAT5 présentent leurs cellules bloquées au stade pro-B (Goetz et al., 2004), mais ce blocage peut être levé

partiellement par la surexpression de BCL2 (Malin et al., 2010) ou par l'expression d'une forme constitutivement active de pSTAT5 (Goetz et al., 2004).

La fixation de l'IL-7 sur son récepteur peut aussi induire l'activation de la voie PI3K/AKT. Une fois l'IL-7R activé, l'enzyme PI3K, constituée d'une sous-unité régulatrice p85 et d'une sous-unité catalytique p110, va être recrutée pour phosphoryler les Phosphoinositides phosphate 2 (PIP2) en Phosphoinositides phosphate 3 (PIP3). Cette phosphorylation va induire un signal anti-apoptotique notamment en phosphorylant le facteur de transcription Foxo1. Sa phosphorylation va bloquer sa translocation dans le noyau et empêche ainsi la transcription de cibles pro-apoptotiques (Danial & Korsmeyer, 2004).

Induction d'un signal de prolifération cellulaire

STAT5 promeut la prolifération des cellules en régulant l'expression de cyclines impliquées dans la progression du cycle cellulaire, et en activant la voie de signalisation PI3K/AKT. En effet, il a été montré que les cellules pro-B ont une prolifération diminuée en présence d'IL-7 lorsque la sous-unité catalytique p110 de PI3K est absente (Ramadani et al., 2010). De plus, l'activation de Myc induit par la signalisation PI3K/AKT est essentielle pour la prolifération des cellules du stade pré-BI (Fraction C) au stade pré-BII précoce (Fraction C'), montrant ainsi l'importance de la voie PI3K/AKT pour la prolifération et la progression dans la différenciation des cellules B (Vallespinós et al., 2011).

1.2.B.iii.b. Signalisation induite par le pré-BCR

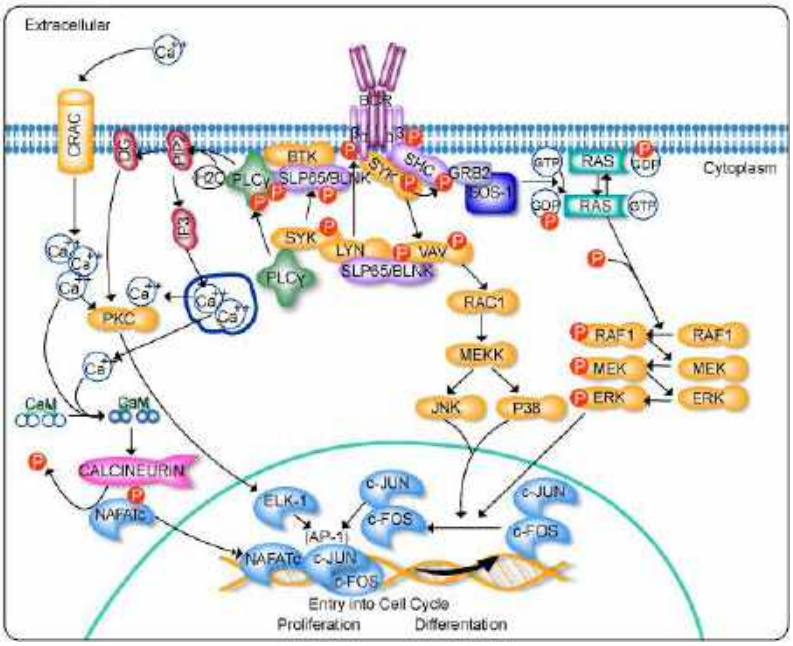

***Figure 10 :** Illustration schématique représentant la voie de signalisation induite par le pré-BCR se trouvant à la surface des cellules pré-BI.*

Induction d'un signal de prolifération cellulaire

Une fois le pré-BCR fonctionnel à la surface des cellules, les voies de signalisation PI3K/AKT et ERK/MAPK sont activées (**Figure 10**). La transduction du signal émis par le pré-BCR est permise par les kinases LYN, FYN et BLK qui vont phosphoryler les motifs ITAMs composés de quatre acides aminés (Tyrosine, deux acides aminés et une Leucine ou Isoleucine) répétés deux fois dans les queues cytoplasmiques à l'extrémité des protéines CD79a et CD79b. Ces deux protéines phosphorylées vont recruter la kinase SYK, qui va s'autophosphoryler pour augmenter son activité kinase. L'absence de SYK induit un blocage dans la différenciation des cellules B avant le stade pré-BII tardives (Fraction D). De plus, la surexpression de SYK dans les cellules pré-BII précoces (Fraction C') augmente leur prolifération en présence d'IL-7 et du pré-BCR, due à l'augmentation de la quantité de protéine MYC (Wossning et al., 2006).

Induction d'un signal de différenciation cellulaire

La transduction du signal de différenciation cellulaire émis par le pré-BCR depuis la surface des cellules est permise par SYK, BTK et BLNK (SLP65). Chez les souris délétées pour BLNK, les cellules sont bloquées au stade pré-BII précoces, montrant ainsi son rôle clé dans le contrôle de la différenciation (Flemming et al., 2003). La phosphorylation de BLNK par SYK

a pour conséquence l'activation d'une cascade de signalisation via le recrutement de PLCγ2. Cette signalisation permet l'activation de l'expression de facteur de transcription qui promeut la différenciation tels que Aiolos (Ikzf3) et IRF4.

La transduction du signal émis par l'activation du pré-BCR est également permise par la voie ERK/MAPK. Celle-ci va stopper la prolifération cellulaire, et permettre aux cellules de progresser dans la différenciation B. En effet, les cellules sont bloquées au stade pré-BII précoce dans des modèles de souris présentant une délétion pour Erk1 et Erk2 (Yasuda et al., 2008).

1.3. Les facteurs extrinsèques et intrinsèques à l'origine de la lymphopoïèse B

1.3.A. Les niches stromales impliquées dans le développement des cellules B

La moelle osseuse est constituée de deux niches hématopoïétiques : la niche périsinusoïdale et la niche endostéale/péri-artériolaire (**Figure 11**).

La niche endostéale/péri-artériolaire

Cette niche, qui se trouve à la surface de l'os, serait impliquée dans le maintien de la dormance des CSH. En effet, il a été montré que le nombre de CSH quiescentes est plus élevé dans cette région (Sugimura et al., 2012). De plus, c'est dans cette région que se trouve la plus forte concentration en calcium. Il a été montré que le nombre de CSH, qui à leur surface expriment le récepteur sensible au calcium CaSR, est diminué dans des souris *Casr*$^{-/-}$ et qu'elles ne sont pas capables de se nicher près de la région endostéale lorsqu'elles sont transplantées (G. B. Adams et al., 2006). Les CSH quiescentes, localisées à proximité des cellules artériolaires (Itkin et al., 2016; Kunisaki et al., 2013; Nombela-Arrieta et al., 2013) présentent une capacité à incorporer à long terme l'EdU (5-ethynyl-2'-désoxyuridine), un faible taux de ROS (*Reactive Oxygen Species*) et une forte expression du facteur de transcription HIF-1α. De plus, les péricytes NG2+Nestin+ localisés sur les artérioles expriment des gènes impliqués dans la niche des CSH, comme par exemple le CXCL12 (Asada et al., 2017; Kunisaki et al., 2013).

La niche périsinusoïdale

Cette niche, localisée à proximité des sinusoïdes, serait impliquée dans le maintien et la rétention des CSH.

La chimiokine CXCL12, qui a été initialement décrite pour être un facteur de croissance des cellules B précoces, joue un rôle majeur dans le maintien des CSH puisque l'absence de son récepteur CXCR4 induit d'importants défauts hématopoïétiques (Q. Ma et al., 1998; Nagasawa et al., 1994). De plus, il a été montré que le CXCL12 est un chimioattractant pour les progéniteurs hématopoïétiques murins et humains, qui leur permet d'être retenus dans la moelle osseuse (Aiuti et al., 1997; Broxmeyer et al., 2005; Q. Ma et al., 1999). Les cellules réticulaires aussi appelées cellules CAR (*CXCL12-abundant reticular cells*) correspondent aux cellules de la niche périsinusoïdale qui expriment de façon très importante CXCL12. En effet il a été montré par l'utilisation d'un modèle murin exprimant la GFP sous le promoteur du CXCL12, que la GFP était fortement exprimée par ces cellules qui se trouvent au contact des sinusoïdes (Sugiyama et al., 2006). Les CSH sont donc essentiellement localisées à proximité des sinusoïdes et en contact avec les cellules CAR (Kiel et al., 2005; Sugiyama et al., 2006). En effet, l'absence d'expression de CXCL12 par les cellules stromales périsinusoïdales (PSS) induit une augmentation de CSH circulantes.

Le SCF (*Stem Cell Factor*), correspondant au ligand du récepteur Kit, est également impliqué dans le maintien du pool de CSH (Broudy, 1997). Il est exprimé par les cellules endothéliales de la moelle osseuse, et est co-exprimé avec le CXCL12 par les cellules stromales périsinusoïdales (Ding et al., 2012; Ding & Morrison, 2013). De plus, il a été montré que la délétion de *Kitl*, qui code SCF, dans les cellules PSS diminue le maintien et la rétention des CSH (Ding et al., 2012).

L'ensemble de ces résultats démontrent que les régions périsinusoïdale et endostéale/péri-artériolaire favorisent le nichage des CSH par une forte expression du CXCL12 et du SCF. Cependant, la niche périsinusoïdale est plutôt impliquée dans le maintien et la rétention des CSH, tandis que la niche endostéale/péri-artériolaire joue un rôle critique dans le maintien et la dormance des CSH.

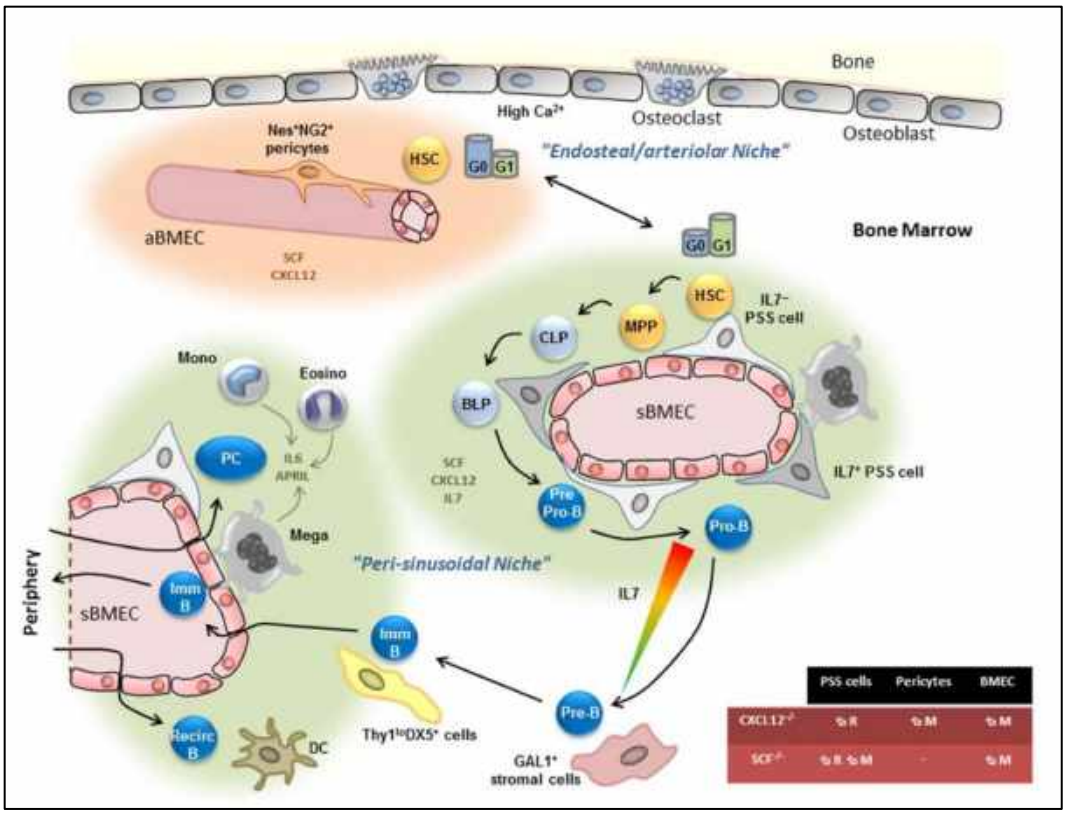

Figure 11 : Schéma représentant les différentes niches médullaires (D'après Aurrand-Lions & Mancini, 2018).

La niche périsinusoidale est également impliquée dans le développement précoce des cellules B jusqu'au stade pro-B, du fait de la présence de cellules PSS qui expriment fortement l'IL7 et le CXCL12 (**Figure 12**). En effet, la lymphophoïèse B est fortement altérée dans le foie fœtal et la moelle osseuse des souris déficientes pour *Cxcl12* et *Cxcr4* (Q. Ma et al., 1998; Nagasawa et al., 1996; Zou et al., 1998). De plus, l'IL-7 joue un rôle clé dans la prolifération des cellules pré-pro-B et pro-B (Namen et al., 1988; A. Rolink et al., 1991). L'absence de cellules PSS exprimant l'IL-7 diminue fortement de nombre de progéniteurs B à partir du stade CLP, alors que l'absence de cellules endothéliales (BMEC) induit une diminution du nombre de progéniteurs B seulement à partir du stade pro-B (Cordeiro Gomes et al., 2016), montrant ainsi que la prolifération des cellules pro-B nécessite un haut niveau d'IL-7.

Les cellules pré-pro-B et pro-B sont donc situées au contact des cellules PSS IL7+ qui expriment la chimiokine CXCL12 et le récepteur VCAM-1. Elles expriment fortement à leur surface le récepteur CXCR4 et induisent une augmentation significative de leur adhérence sur

les cellules stromales VCAM-1+, en réponse à la fixation du CXCL12 sur le récepteur CXCR4 (Glodek et al., 2003).

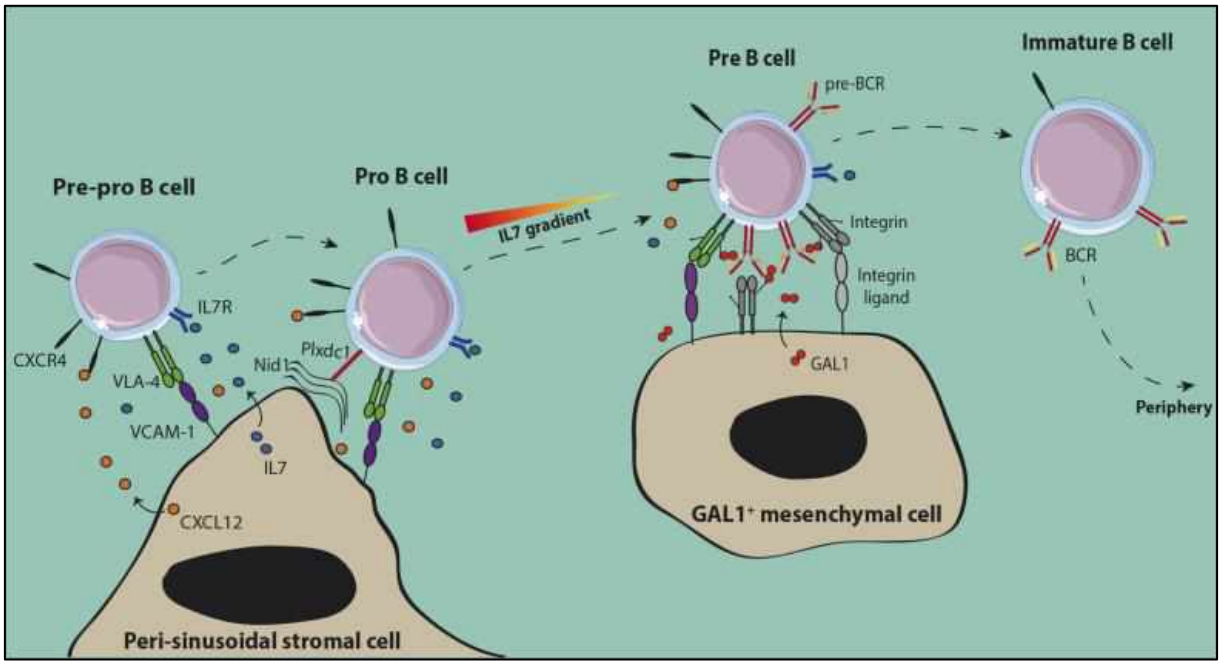

Figure 12 : Schéma représentant la différenciation des cellules B au sein de la moelle osseuse (D'après Delahaye et al., 2021).

Le niveau d'expression du récepteur CXCR4 est plus faible dans les cellules pro-B et pré-BI. Elles ne sont donc plus sensibles au chimiotactisme induit par CXCL12. Les cellules pro-B / pré-BI sont donc retrouvées au contact des cellules périsinusoïdales PSS IL7+ CXCL12- (Tokoyoda et al., 2004). Elles rentrent activement en mitose et ont besoin de l'IL-7 pour favoriser leur prolifération et leur survie (von Freeden-Jeffry et al., 1995).

L'expression en surface du pré-BCR sur les cellules pré-BII les rend moins dépendantes à l'IL7 (Marshall et al., 1998), ce qui leur permet de sortir de la niche périsinusoïdale et de migrer vers les cellules stromales exprimant la galectine 1 (GAL-1). GAL-1 fait partie de la sous-famille des galectines prototypes, c'est-à-dire qu'elle contient seulement un domaine CRD (pour *Carbohydrate Recognition Domain*) par sous-unité et qu'elle est fonctionnelle sous la forme d'un homodimère non covalent. La GAL-1 a été identifiée comme un ligand du pré-BCR via une interaction avec l'extra-boucle de λ5 (Elantak et al., 2012; Gauthier et al., 2002). GAL-1 est sécrétée par les cellules stromales (Mourcin et al., 2011), et sert de protéine d'amarrage en interagissant avec le pré-BCR et les chaines glygosylées des intégrines qui se trouvent à la surface des cellules pré-B afin de former un complexe (Espeli et al., 2009; Rossi et al., 2006),

permettant d'activer la signalisation du pré-BCR. De plus, l'inactivation de l'expression de GAL-1 par les cellules stromales *in vitro* et *in vivo* altère la différenciation et la prolifération des cellules pré-BII (Espeli et al., 2009), suggérant que l'interaction avec les cellules stromales GAL-1^+ est indispensable pour que les cellules puissent progresser dans la différenciation B.

Lorsque les cellules se différencient au stade des cellules B immatures, elles expriment le B-cell receptor (BCR) à leur surface. La sélection négative se met alors en place afin de tester le BCR se trouvant à la surface des cellules en leur présentant des auto-antigènes. Si les cellules immatures possèdent un BCR auto-réactif alors elles vont mourir par apoptose. A l'inverse, si les cellules ne possèdent pas de BCR auto-réactif, elles vont migrer vers la périphérie pour se rendre dans la rate afin de finaliser leur différenciation terminale en plasmocytes.

1.3.B. Les facteurs de transcription impliqués dans la lymphopoïèse B

L'engagement des CSH en cellules lymphoïdes B est permise par un réseau complexe de facteurs de transcription tels que PU.1, Ikaros, E2a, Ebf1 et Pax5 (**Figure 13**). La régulation de l'entrée et la spécification des cellules dans la lymphopoïèse B par ces facteurs de transcription s'effectue de manière séquentielle.

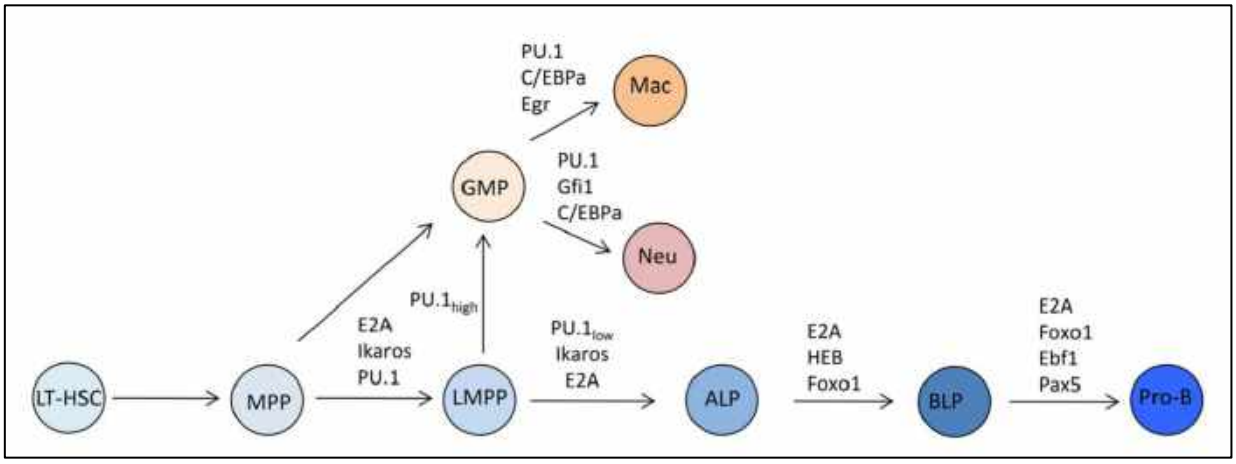

Figure 13 : Illustration schématique représentant l'expression des différents facteurs de transcription impliqués dans la régulation de l'entrée dans le lignage lymphoïde B (D'après Murre, 2018).

Chez les progéniteurs non engagés dans la différenciation lymphoïde B, on trouve une faible expression de certains facteurs de transcription associés au lignage B (Månsson et al., 2007). L'engagement dans la lignée lymphoïde est permis notamment par Ikaros ou *Ikzf1*

(Yoshida et al., 2006) et PU.1 (Scott et al., 1997). La perte d'un seul de ces facteurs bloque l'entrée dans la lignée lymphoïde.

Les souris délétées pour *Ikzf1* (codant le facteur de transcription Ikaros) présentent une hématopoïèse altérée car elles ne possèdent plus de cellules B, T et NK (Georgopoulos et al., 1994; Sellars, 2011). Ikaros joue un rôle crucial dans la maturation des LMPP en CLP. En effet, les LMPP *Ikaros*$^{-/-}$ n'expriment pas les protéines essentielles à la différenciation lymphoïde telles que le Flt3, le récepteur à l'IL7 et les protéines Rag1 et Rag2 (Yoshida et al., 2006). Au niveau mécanistique, Ikaros active l'expression de Flt3 et, à l'inverse, inhibe l'expression des gènes spécifiques pour l'engagement des cellules vers la voie myéloïde (Nichogiannopoulou et al., 1999). Ikaros joue également un rôle clé dans le développement des cellules B après leur engagement définitif dans le lignage lymphoïde B. En effet, les souris avec un allèle hypomorphique d'Ikaros présentent un blocage dans le développement des cellules B entre le stade pro-B et le stade pré-B (Kirstetter et al., 2002; Sellars, 2011).

Les souris déficientes pour PU.1 ne sont pas viables, mais les embryons *PU.1*$^{-/-}$ présentent un défaut dans la production des progéniteurs des lymphocytes B, lymphocytes T, granulocytes, monocytes et ostéoclastes. Les effets de PU.1 s'effectuent de manière dose-dépendante : PU.1 favorise la différenciation des LMPP vers le lignage lymphoïde lorsqu'il est exprimé à un faible niveau, alors qu'il favorise la différenciation myéloïde lorsqu'il est exprimé à fortes doses (DeKoter & Singh, 2000).

Lorsque les cellules sont engagées dans la lignée lymphoïde B, les facteurs de transcription E2a, Ebf1 et Pax5 vont permettre de spécifier cet engagement de manière irréversible.

Les facteurs de transcription E2a et Ebf1 interviennent en amont du gène Pax5 (Bain et al., 1994; H. Lin & Grosschedl, 1995). En effet, il a été montré que les progéniteurs de souris *Pax5*$^{-/-}$ expriment E2a et Ebf1, alors que Pax5 n'est pas exprimé dans les progéniteurs de souris *E2a*$^{-/-}$ ou *Ebf1*$^{-/-}$. En absence de E2A et Ebf1, les progéniteurs gardent leur capacité à se différencier *in vitro* en cellules myéloïdes et lymphoïdes (autre que B), montrant ainsi qu'ils ne sont pas totalement engagés dans le lignage B (Ikawa et al., 2004; Pongubala et al., 2008). Dans le développement précoce des cellules B, E2A agit en amont de Ebf1 : E2A se fixe directement

sur Ebf1, et l'active pendant la progression des progéniteurs lymphoïdes en cellules pro-B (Y. C. Lin et al., 2010; Seet et al., 2004).

L'activation complète de Ebf1 est permise uniquement lorsque Pax5 est exprimé : l'expression de Ebf1 est 5 fois plus faible dans des cellules pro-B qui n'expriment pas Pax5 comparativement à des cellules pro-B qui l'expriment (Fuxa et al., 2004; Roessler et al., 2007). De plus, en absence de Ebf1, les progéniteurs sont incapables de se différencier en cellules pro-B sans expression de Pax5 (Medina et al., 2004). Il a également été montré qu'une coopération existe entre Ebf1 et Pax5 afin de contrôler l'engagement des cellules vers le lignage B (Treiber et al., 2010) : la plupart des gènes cibles régulés par Ebf1 le sont également par Pax5.

Pax5 à la capacité de se fixer directement sur des séquences situées dans le promoteur de *Ebf1*, l'identifiant comme un gène cible activé par Pax5 (Roessler et al., 2007). Ebf1 est aussi capable d'interagir directement sur le promoteur de *Pax5*, l'identifiant comme un gène cible direct (Decker et al., 2009). Ceci montre donc l'existence d'une boucle de régulation de rétrocontrôle entre Ebf1 et Pax5, permettant de stabiliser le programme d'expression B-spécifique au cours du développement des cellules pro-B. Ce n'est donc qu'une fois Pax5 exprimé que les cellules sont irréversiblement engagées dans le lignage B.

Les organisations génomique et structurelle de Pax5, ainsi que sa fonction dans la lymphopoïèse B font l'objet du prochain chapitre.

Chapitre 2 : Le facteur de transcription Pax5

Les gènes de la famille PAX (*Paired Box*) sont très conservés au cours de l'évolution et sont impliqués dans le développement de divers organes et la spécialisation des différents sous-types cellulaires (Stoykova & Gruss, 1994). À ce jour, on dénombre neuf homologues (Pax1 à Pax9) chez les Vertébrés supérieurs (Paixão-Côrtes et al., 2015; Stapleton et al., 1993; Walther et al., 1991). Ils se trouvent sur différents chromosomes que ce soit chez la souris (Wallin et al., 1993; Walther et al., 1991) ou chez l'Homme (Stapleton et al., 1993; Ton et al., 1991; Tsukamoto et al., 1994; Wilcox et al., 1992). Tous sont exprimés au cours du développement embryonnaire à la seule différence que Pax5 et Pax8 sont encore exprimés au stade adulte.

2.1. Classification des homologues de la famille PAX

Les membres de la famille *PAX* codent pour des facteurs de transcription qui possèdent tous la même structure de base : un domaine de liaison à l'ADN appelé *Paired Box Domain* (PBD) situé en N-terminal, un signal de localisation nucléaire (NLS) en partie centrale (leur permettant d'être transloqué dans le noyau afin d'exercer leur fonction de facteur de transcription), une région régulatrice de la transcription des gènes cibles (composée d'un domaine activateur et d'un domaine inhibiteur) située en C-terminal ; à laquelle peut s'ajouter un octamère et/ou un homéodomaine partiel ou complet.

PAX family Group	Protein structure/domains Paired octapeptide homeodomain	Protein family member	Embryonic Expression Domain	Expression/Mutation in human disease
I		PAX1	Skeleton, thymus 3rd/4th pharyngeal pouch	Klippel-Feil Syndrome, Jarcho-Levin Syndrome
		PAX9	Skeleton, Teeth, Thymus	Jarcho-Levin Syndrome, Oligodontia
II	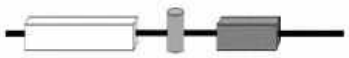	PAX2	Kidney, CNS	Hyperproliferative dysplastic kidney, Renal hyperplasia, Bladder and renal cancer,Coloboma Syndrome
		PAX5	B-Cells, CNS	Lymphomas
		PAX8	Kidney, Thyroid, CNS	Congenital hypothyroidism, Thyroid carcinomas/adenomas
III	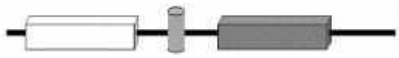	PAX3	Neural Crest, CNS somites/muscle	Waardenburg Syndrome Types I/III, Melanoma, Rhabdomyosarcoma
		PAX7	Neural Crest, CNS somites/muscle	Rhabdomyosarcoma
IV		PAX4	Pancreas, gut	Diabetes
		PAX6	Pancreas, gut, CNS and eye	Aniridia,GI tumors Cataracts/Peter's Anomaly

Figure 14 : Les différentes classes des homologues PAX en fonction de leur structure protéique (D'après Lang et al., 2007).

La classification des différents membres de la famille PAX varie du fait de la présence ou l'absence de l'octapeptide (cylindre gris) et/ou de l'homéodomaine (pavé gris). Le domaine PBD *(pour Paired Box Domain) est représenté par un pavé blanc. Les territoires d'expression embryonnaire sont listés ainsi que les pathologies humaines associées. (*CNS *: Central Nervous System)*

Bien que la structure des différents membres de cette famille soit très similaire, les gènes *Pax* sont actuellement répartis en quatre classes selon différents critères : le degré d'homologie des séquences primaires, leur similarité en termes d'organisation génomique, les différents domaines structuraux que possèdent la protéine, et le profil d'expression durant le développement embryonnaire (Balczarek et al., 1997; D. Lang et al., 2007; Mayran et al., 2015; Noll, 1993) **(Figure 14)** :

- Classe I : La protéine contient l'octapeptide mais ne possède pas d'homéodomaine (Pax1 et Pax9).
- Classe II : La protéine possède l'octapeptide et un homéodomaine mais qui est partiel (Pax2, Pax5 et Pax8).
- Classe III : La protéine possède l'octapeptide et l'homéodomaine complet (Pax3 et Pax7).
- Classe IV : La protéine possède l'homéodomaine complet mais l'octapeptide est absent (Pax4 et Pax6).

2.2. Les différentes classes de la famille PAX

Les gènes *Pax* possèdent de nombreux rôles essentiels lors de la formation de divers organes pendant le développement embryonnaire tels que la prolifération et le renouvellement cellulaire, la résistance à l'apoptose, la migration des cellules précurseurs embryonnaires et la coordination de différents programmes de différenciation spécifiques. Leur spécialisation dépend cependant du type cellulaire au sein duquel chaque gène est exprimé.

2.2.A. Groupe I (Pax1 et Pax9)

Ces deux membres de la famille ne sont pas exprimés dans le système nerveux central (SNC). Ils ont la particularité d'être exprimés dans les mêmes territoires et peuvent donc accomplir des fonctions compensatoires. Malgré cela, ils ne peuvent pas remplacer la fonction de l'autre dans les tissus où ils ne sont pas tous les deux exprimés. Ils sont impliqués dans le développement de la colonne vertébrale, le sternum et la ceinture osseuse pectorale/scapulaire (permettant de rattacher les membres antérieurs à la colonne vertébrale). Ils sont également

fortement impliqués dans le développement de la glande parathyroïde, dans le développement des dents et dans la formation de la mâchoire (Peters et al., 1998; Sivakamasundari et al., 2018).

2.2.B. Groupe II (Pax2, Pax5 et Pax8)

Pax2 est essentiel pour la bonne formation du mésencéphale, puisque l'absence de celui-ci impacte son développement (Stoykova & Gruss, 1994). Il est également associé aux fonctions de maturation du sperme étant donné son rôle dans le fonctionnement de l'épithélium de l'épididyme (Oefelein et al., 1996). Il est impliqué dans le développement des reins et régule aussi la sécrétion du glucagon par les ilots pancréatiques (Goode & Elgar, 2009; Ritz-Laser et al., 2000). Pour finir, il joue également un rôle dans la protection des cellules contre l'apoptose à la suite d'un stress osmotique dû à une accumulation de NaCl dans le canal collecteur du rein (Cai et al., 2005).

Pax8 est essentiel dans le maintien de la différenciation fonctionnelle des cellules thyroïdiennes car il permet l'activation de tous les gènes spécifiques de la thyroïde tels que la thyroglobuline ou la thyroperoxidase (Pasca di Magliano et al., 2000). Il se trouve être également exprimé dans le système nerveux central (SNC) et le rein.

Pax5 quant à lui, est impliqué dans la formation du mésencéphale, et joue un rôle dans la spermatogenèse ainsi que l'hématopoïèse (B. Adams et al., 1992; Stoykova & Gruss, 1994). Il a la particularité d'être le seul membre de la famille *Pax* à être exprimé dans le système hématopoïétique. Le rôle de Pax5 dans le développement B normal et pathologique est détaillé plus loin dans ce manuscrit.

2.2.C. Groupe III (Pax3 et Pax7)

Pax3 et Pax7 jouent un rôle important dans la formation du muscle strié squelettique dès les stades les plus précoces en permettant l'engagement des cellules dans la différenciation (Seale et al., 2001). Ils sont également très fortement impliqués dans la formation du SNC (Shin et al., 2003; J. Thompson et al., 2004; J. A. Thompson et al., 2007, 2008).

2.2.D. Groupe IV (Pax4 et Pax6)

En plus de la fonction cruciale de Pax6 durant le développement embryonnaire des yeux, Pax4 et Pax6 jouent un rôle essentiel dans la rétine puisque Pax4 est exprimé dans les cellules photoréceptrices et Pax6 dans l'épiphyse (Rath et al., 2009).

Pax4 et Pax6 participent également au développement des cellules pancréatiques. Pax4 joue un rôle déterminant dans le contrôle de l'homéostasie des cellules β pancréatiques qui produisent l'insuline (Brun et al., 2004), tandis que Pax6 est impliqué dans la différenciation des cellules α pancréatiques qui produisent le glucagon, mais participe également aux modulations du fonctionnement et de l'architecture des ilots pancréatiques (Hamasaki et al., 2007; Paixão-Côrtes et al., 2015). Ils sont également nécessaires pour le destin du système endocrinien dans le pancréas (St-Onge et al., 1997).

2.3. Le facteur de transcription Pax5

2.3.A. Organisation du gène

Le gène humain *PAX5* se trouve sur le bras court du chromosome 9 dans la région p13.2 (Stapleton et al., 1993). Son orthologue murin *Pax5* quant à lui, est situé sur le chromosome 4 (Walther et al., 1991). Il est extrêmement conservé entre les espèces, surtout entre l'Homme et la souris puisque les protéines possèdent 99% d'identité.

Le gène *Pax5* est composé de 11 exons **(Figure 15)**. La séquence génique qui va produire un transcrit inclut 10 exons dont les deux premiers exons qui se trouvent en 5' (exon 1A et exon 1B) ; qui sont mutuellement exclusifs lors de la transcription (Busslinger et al., 1996).

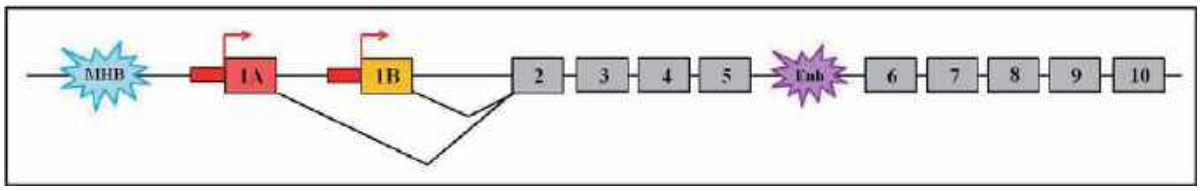

Figure 15 : Organisation génomique de Pax5.
Les deux promoteurs alternatifs de Pax5 sont représentés en rouge. L'exon 1A est en rouge clair et l'exon 1B en orange ; les exons 2 à 10 sont représentés en gris. Les enhancers de Pax5 sont représentés par des étoiles, en bleu l'enhancer MHB (Midbrain-Hindbrain Boundary) et en violet l'enhancer B-spécifique.

2.3.B. *Éléments de régulation transcriptionnelle*

La transcription du gène *Pax5* est régulée par deux promoteurs distincts : un promoteur distal contenant la TATA-box et est associé à l'exon 1A, et un promoteur proximal ne contenant pas de TATA-box et est associé à l'exon 1B (Busslinger et al., 1996). Ces deux promoteurs vont permettre d'initier la transcription de *Pax5* à partir de l'exon 1A ou de l'exon 1B suivi des neuf exons communs (exons 2 à 10). Ce démarrage alternatif de la transcription peut donc donner naissance à deux transcrits *Pax5A* et *Pax5B* (Liu et al., 2002), qui diffèrent uniquement par leur premier exon (exon 1A ou exon 1B). Les deux isoformes protéiques Pax5A et Pax5B contiennent uniquement une différence de séquence au niveau de l'extrémité N-terminale : l'exon 1A est constitué de 15 acides aminés qui sont complètement différents des 14 acides aminés qui constituent l'exon 1B (Busslinger et al., 1996).

Ces deux promoteurs sont eux aussi régulés différemment. Le promoteur distal est exclusivement actif dans le lignage lymphoïde B. Le promoteur proximal quant à lui, est actif dans tous les tissus où *Pax5* est exprimé : dans le SNC pendant le développement embryonnaire, le lignage lymphoïde B, et enfin les testicules (B. Adams et al., 1992; Busslinger et al., 1996). Malgré le fait que ces deux promoteurs soient actifs dans le lignage lymphoïde B, il y a quand même une différence d'expression entre les deux isoformes au cours de la différenciation des cellules B : Pax5a est plus exprimé que Pax5b dans la moelle osseuse de souris (Cresson, Péron, et al., 2018), ainsi que dans la rate (Busslinger et al., 1996)

Pax5 contient également deux enhancers, qui permettent eux aussi de moduler son expression **(Figure 15)** :

- Le Midbrain-Hindbrain Boundary (MHB) se situe en amont du promoteur de l'exon 1A, et régule l'expression de Pax5 lors du développement embryonnaire dans le système nerveux central (Pfeffer et al., 2000).
- Le second enhancer se trouve dans l'intron entre l'exon 5 et l'exon 6, et contrôle l'expression de Pax5 uniquement pendant la différenciation B (Decker et al., 2009). Sa régulation est complexe et se fait donc par étape. Dans un premier temps, à l'état basal dans les cellules souches embryonnaires, l'enhancer inactif est méthylé. Puis il est ensuite activé par déméthylation dans les progéniteurs hématopoïétiques multipotents. Il possède les sites de liaison pour les facteurs de transcription PU-1, IRF4, IRF8 et NF-kB, qui vont servir de régulateurs pour son activation pendant la lymphopoïèse B précoce (Decker et al., 2009). La

région promotrice est activée pendant le stade pro-B par Ebf1, nécessaire pour le remodelage de la chromatine. L'ouverture de la chromatine participe à l'activation de *Pax5* en permettant une interaction entre le promoteur et l'enhancer, activé avant l'expression d'Ebf1.

2.3.C. Structure et fonction des domaines de la protéine

Le gène *Pax5* code une protéine de 391 acides aminés **(Figure 16)** chez la souris tout comme chez l'Homme. Celle-ci est composée de différents domaines qui ont chacun leurs propres fonctions.

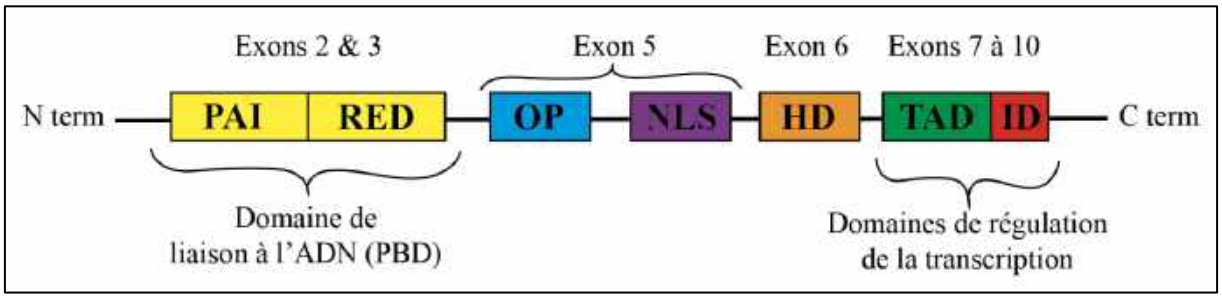

Figure 16 : Schéma de l'organisation protéique de Pax5 avec ses différents domaines structuraux.
PBD *: Paired Box Domain ;* OP *: Octapeptide ;* NLS *: Nuclear Localization Sequence;* HD *: HomeoDomain;* TAD *: TransActivation Domain;* ID *: Inhibitory Domain*

2.3.C.i. Le domaine Paired (PBD)

Il permet la liaison à l'ADN et est très conservé chez les différents membres de la famille Pax (Czerny et al., 1993; Treisman et al., 1991). Ce domaine possède une structure bipartite divisé lui-même en deux sous-domaines : un sous-domaine N-terminal (PAI) et un sous-domaine C-terminal (RED) (Czerny et al., 1993; W. Xu et al., 1995). La seule différence entre ces deux sous-domaines est la présence de deux feuillets β dans le sous-domaine PAI (en plus des trois hélices a que l'on retrouve dans les deux sous-domaines). Ces deux sous-domaines sont reliés entre eux par une région flexible appelée linker, permettant ainsi des contacts étendus avec l'ADN (H. E. Xu et al., 1999).

Ils reconnaissent tous les deux une séquence consensus TCACGC/G, qui se trouve être commune avec toutes les autres protéines Pax (avec quelques changements mineurs entre les différents homologues) (Czerny et al., 1993; Czerny & Busslinger, 1995). Un seul des deux sous-domaines suffit pour se fixer sur les cibles de Pax5. En effet, il, a été montré qu'une forme tronquée du domaine PAIRED de Pax5 garde sa capacité à se lier à certaines séquences cibles,

mais avec une affinité plus faible (Czerny et al., 1993). Il existe une spécificité des séquences de liaison pour chaque sous-domaine : les sous-domaines PAI et RED se lient à des séquences d'ADN spécifiques et différentes, et donc peuvent réguler des ensembles de gènes bien distincts. Bien que la séquence consensus minimale qu'ils reconnaissent est proche, le reste de la séquence reconnu peut être très varié, aboutissant à un motif d'interaction dégénéré avec l'ADN : le site de liaison à l'ADN de Pax5 peut donc être très différent de la séquence consensus.

Le domaine PAIRED intervient également dans des interactions protéiques qui permettent d'agir sur l'activité transcriptionnelle de Pax5. Il recrute directement l'enzyme AID et interagit avec le facteur de transcription E2A pendant les réarrangements des chaines des immunoglobulines (Hauser et al., 2016).

2.3.C.ii. L'octapeptide (OP)

Ce domaine est impliqué dans des interactions protéiques de type répressive. En effet, il permet un contact direct avec une protéine co-répressive de la transcription Groucho4 (Grg4) (Eberhard et al., 2000; Koop et al., 1996). Sa fixation sur l'octapeptide fait diminuer l'activité transcriptionnelle de Pax5 (Eberhard et al., 2000; Fisher & Caudy, 1998). La fixation de Grg4 peut empêcher le recrutement des médiateurs par l'homéodomaine, masquer ou encore réprimer l'activité du domaine TAD (Barlev et al., 2003; Emelyanov et al., 2002).

2.3.C.iii. Un signal de localisation nucléaire (NLS)

Il permet le transport de la protéine Pax5 dans le noyau, où elle va pouvoir aller se fixer sur ses gènes cibles, à la suite de la fixation de l'importine α1 sur la séquence NLS (Kovac et al., 2000).

2.3.C.iv. Un homéodomaine partiel (HD)

Le domaine HD permet également à Pax5 d'interagir avec l'ADN, et est très conservé au cours de l'évolution (Chi & Epstein, 2002). Il se lie aux protéines de la TATA-box pour réguler la machinerie transcriptionnelle.

Le domaine HD peut également servir d'interface pour des interactions avec d'autres protéines. Suite à sa fixation sur l'homéodomaine de Pax5, la protéine Daxx peut soit réprimer

soit activer la transcription (Emelyanov et al., 2002). Le domaine HD interagit également avec Rb1 (RB transcriptional corepressor 1) et TBP (TATA-box binding protein). TBP correspond à la sous-unité de liaison à l'ADN du complexe général de la transcription TFIID, permettant de faciliter le recrutement du complexe TFIID au niveau des séquences promotrices ciblées par Pax5 (Cvekl et al., 1999; Eberhard & Busslinger, 1999).

2.3.C.v. Un domaine activateur (TAD) et un domaine inhibiteur (ID)

Les domaines activateur et inhibiteur possèdent en C-terminal des régions riches en proline, sérine et thréonine (sites PST), et permettent de réguler la transcription des gènes cibles de Pax5 (Dörfler & Busslinger, 1996). Pax5 a besoin de réaliser des interactions protéiques pour exercer sa fonction. Pax5 recrute via son domaine régulateur TAD des acétyltransférases d'histones (HAT) et des protéines adaptatrices pour assurer la régulation épigénétique (Barlev et al., 2003; Emelyanov et al., 2002; He et al., 2011). Ce domaine participe également au recrutement de co-répresseurs de la transcription, tout comme l'octapeptide (Eberhard et al., 2000). L'équipe de Busslinger a d'ailleurs très récemment démontré le rôle clé de ces deux domaines dans le contrôle du développement des cellules B, puisque leur absence résulte en un blocage de différenciation avant l'engagement définitif dans le lignage lymphoïde B (Gruenbacher et al., 2023).

2.3.D. Variants des transcrits issus de l'épissage alternatif

On dénombre à ce jour jusqu'à 16 variants qui résultent de l'épissage alternatif de *PAX5* chez l'Homme et chez la souris, mais ces variants ne sont pas tous traduits en protéine (Oppezzo et al., 2005; Robichaud et al., 2004). L'épissage alternatif peut conduire à la formation de transcrits possédant un domaine PAIRED tronqué ou à la formation de transcrits avec un ou plusieurs exons 6 à 10 manquants. Ces différences peuvent conduire à des modifications de propriétés de fixation à l'ADN et de transactivation (Lowen et al., 2001; Robichaud et al., 2004). Les variants tronqués pourraient être impliqués dans la régulation de l'activité de Pax5a. Ils ont notamment été décrits comme modulant la fonction de Pax5a dans l'activation de la différenciation des cellules B (Lowen et al., 2001; Oppezzo et al., 2005).

L'isoforme Pax5d, qui possède l'entièreté du domaine de liaison à l'ADN, est capable d'interagir avec les sites de reconnaissance de Pax5 ; et donc de rentrer en compétition avec

Pax5a en exerçant une fonction répressive (Lowen et al., 2001). A l'inverse, l'isoforme Pax5e peut servir d'amplificateur de l'activité de transactivation de Pax5a.

2.3.E. *Fonctions de Pax5 dans la lymphopoïèse B*

Une fois que les cellules sont engagées dans le lignage B, le facteur de transcription Pax5 devient critique pour le maintien des cellules pro-B dans leur voie de différenciation (Cobaleda, Schebesta, et al., 2007). Celui-ci est exprimé à partir du stade pro-B jusqu'au stade B mature, puis son expression s'éteint pour permettre la différenciation B terminale en plasmocytes.

La grande majorité des souris déficientes pour *Pax5* meurent en période périnatale due à un défaut majeur du mésencéphale. Chez les rares souris survivant assez longtemps pour être analysées ou dans les foies fœtaux des embryons déficients, la lymphopoïèse B est défectueuse et bloquée dès les premiers stades de la différenciation B (Nutt, Thévenin, et al., 1997; Urbánek et al., 1994).

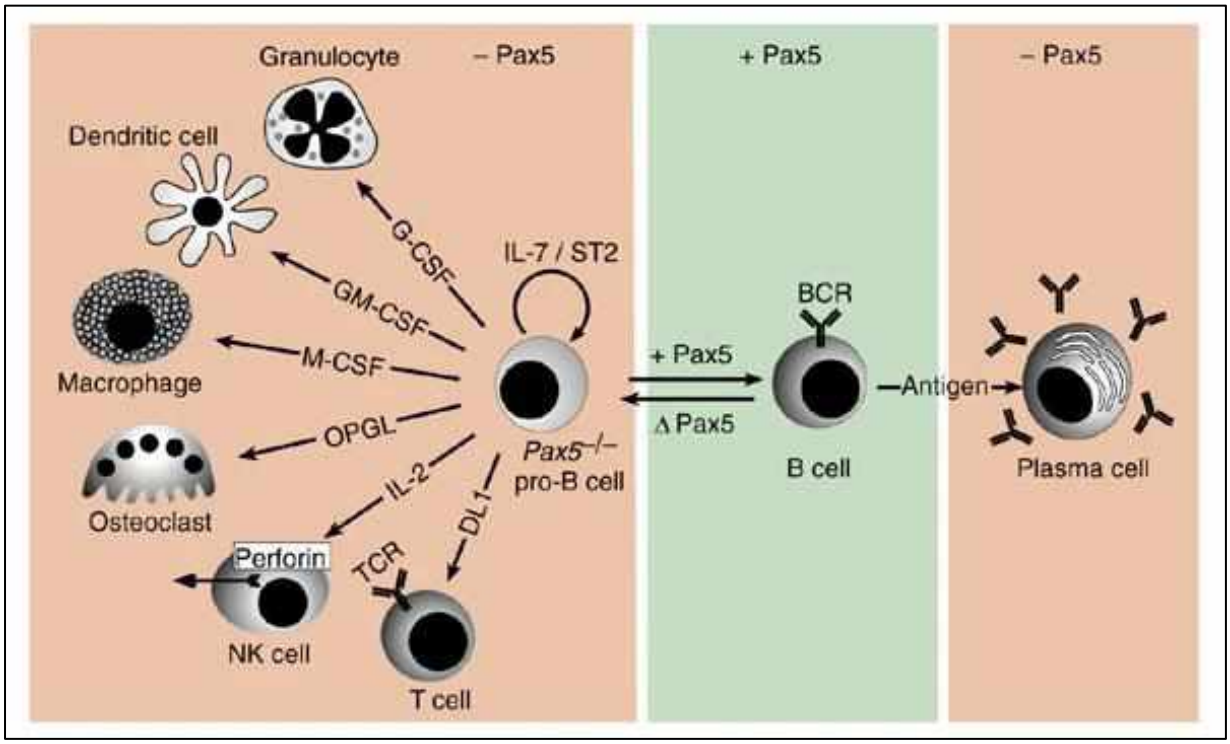

Figure 17 : Schéma représentatif de l'importance de PAX5 dans la restriction des cellules au lignage B (D'après *Cobaleda, Schebesta, et al., 2007*).

La perte de l'expression de Pax5 induit une plasticité des cellules lymphoïdes B en conférant aux cellules un potentiel de dédifférenciation. L'équipe de Busslinger a pu démontrer que les progéniteurs B *Pax5*$^{-/-}$ sont capables de générer une diversité de lignages hématopoïétiques *in vitro* **(Figure 17)** (macrophages, ostéoclastes, cellules dendritiques granulocytes et cellules NK) sous l'action de cytokines appropriées (Nutt et al., 1999a). Cette plasticité cellulaire des lymphocytes B a été démontrée directement *in vivo* en transplantant des progéniteurs B *Pax5*$^{-/-}$, qui, après prise de greffe, sont capables de générer des lymphocytes T, des macrophages, des granulocytes et des globules rouges (A. G. Rolink et al., 1999a; Schaniel et al., 2002a). La plasticité cellulaire induite en absence de Pax5 est possible quel que soit le niveau de différenciation des cellules lymphoïdes B : la délétion conditionnelle de *Pax5* dans des lymphocytes B matures leur redonne une capacité à se différencier en lymphocyte T par dédifférenciation (Cobaleda, Jochum, et al., 2007a). L'ensemble de ces résultats démontrent l'importance de l'activité de Pax5 et de sa dose pour réprimer la plasticité cellulaire des lymphocytes B.

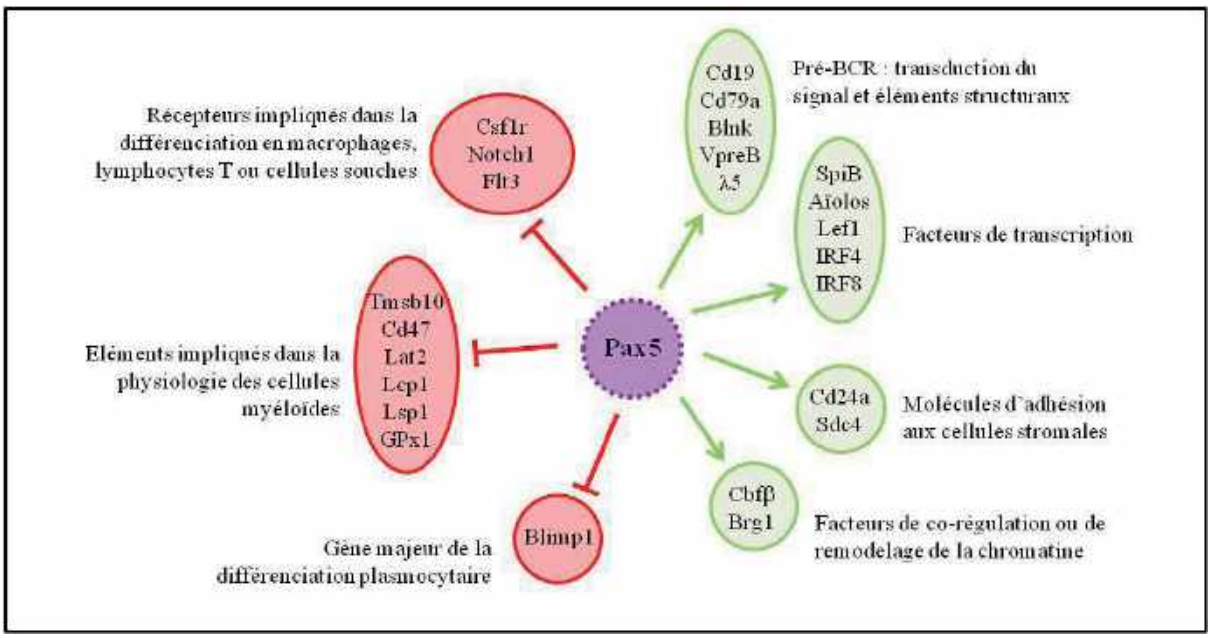

***Figure 18 :* Exemple de gènes régulés par Pax5.**
En vert sont représentés les gènes dont l'expression est activée par Pax5 et en rouge ceux réprimée. Les grandes fonctions dans lesquelles sont impliqués les gènes cibles sont notées à côté de chaque groupe.

Avant leur engagement exclusif vers un lignage cellulaire conduisant à leur différenciation, les CSH doivent activer un certain nombre de programmes d'expression génique différents. En ce qui concerne la différenciation lymphoïde B, une cellule doit exprimer

Pax5 qui va par la suite modifier son programme d'expression génique en activant des gènes spécifiques du lignage B (Cobaleda, Schebesta, et al., 2007) tout en réprimant des gènes activant les autres lignages (Delogu et al., 2006) **(Figure 18)**.

La comparaison du profil d'expression de cellules n'exprimant pas Pax5 avec des cellules sauvages a permis d'identifier 170 gènes activés par Pax5 (A. Schebesta et al., 2007). Les gènes identifiés codent pour des protéines régulatrices et structurales pouvant être classifiés dans différents processus cellulaires des lymphocytes B tels que la signalisation, l'adhérence, la migration, la présentation antigénique et la différenciation jusqu'au stade B mature.

L'identification des gènes activés par Pax5 a permis de confirmer son rôle essentiel dans le contrôle de la transduction du signal du pré-BCR et du BCR, qui constituent des points de contrôle clés dans le développement B (Busslinger, 2004a). En effet, il active l'expression de gènes cibles des composants essentiels des voies de signalisation des pré-BCR comme le Cd79a, les récepteurs stimulateurs CD19 et CD21, et l'adaptateur central Blnk (Fitzsimmons et al., 1996; Horcher et al., 2001; Kozmik et al., 1992; Nutt et al., 1997; M. Schebesta et al., 2002).

Le deuxième rôle majeur de Pax5 consiste à réprimer les gènes inappropriés pour le développement des lymphocytes B. Cela englobe à la fois des gènes de la différenciation terminale en plasmocytes et des gènes spécifiques à d'autres lignages hématopoïétiques. Une analyse transcriptomique a permis d'identifier plus de 100 gènes réprimés, et démontre que Pax5 réprime diverses activités biologiques telles que la signalisation des récepteurs, l'adhérence cellulaire, la migration, le contrôle de la transcription et le métabolisme cellulaire (Delogu et al., 2006).

Pax5 réprime l'expression de plusieurs gènes des progéniteurs hématopoïétiques, des cellules myéloïdes et des lymphocytes T dans le but de restreindre le développement des progéniteurs et de favoriser leur engagement dans la voie de différenciation de la lignée B (Cobaleda, Schebesta, et al., 2007; Delogu et al., 2006). Pax5 réprime notamment *Flt3* ou CD135, responsable du caractère pluripotent des cellules progénitrices lymphoïdes précoces. Il s'agit d'ailleurs d'une répression cruciale pour l'engagement des progéniteurs dans la voie des lymphocytes B (Holmes et al., 2006). En effet, les cellules pro-B sauvages ne sont pas stimulées par le Flt3-L car Pax5 réprime l'expression de *Flt3* (Delogu et al., 2006; Holmes et al., 2006).

Pax5 est également capable de réprimer la transcription de *Csfr1*, récepteur du CSF-1, indispensable pour la différenciation des cellules en macrophage. Dans les cellules lymphoïdes n'exprimant pas Pax5, la stimulation par le M-CSF favorise la différenciation macrophagique alors que les pro-B exprimant Pax5 sont complètement insensibles à cette cytokine (Nutt et al., 1999).

La répression de la transcription de *Notch1* (récepteur de DL1 : facteur de différenciation T) par Pax5 insensibilise les cellules au ligand de Notch et empêche donc l'engagement vers les cellules T. À l'inverse, la surexpression de Pax5 dans les cellules hématopoïétiques provoque une diminution de l'expression de *Notch1* dans les progéniteurs thymiques, altérant leur développement en lymphocytes T (Souabni et al., 2002).

Chapitre 3 : Les leucémies aiguës lymphoblastiques B

3.1. Généralités

3.1.A. Incidences

Les leucémies aiguës lymphoblastiques (LAL) correspondent aux cancers pédiatriques les plus fréquemment retrouvés (environ 25% de l'ensemble des cancers de l'enfant de moins de 15 ans). Celles qui affectent le lignage B (LAL-B) correspondent à 85% des LAL, les 15% restant affectant le lignage T (LAL-T). Bien que les LAL touchent très fréquemment les enfants, on les retrouve également chez les adultes.

L'incidence des LAL varie en fonction de l'âge : on retrouve un premier pic d'incidence entre 2 et 5 ans, et un second pic après 50 ans avec 75% des diagnostics de LAL établit avant l'âge de 6 ans. On dénombre environ 800 à 900 nouveaux cas par an en France.

3.1.B. Caractéristiques biologique et clinique

Les LAL-B apparaissent dans la moelle osseuse et sont caractérisées par un blocage de la différenciation des lymphocytes B au stade progéniteur B ou précurseur B. Ce blocage de différenciation est associé à une prolifération excessive de cellules anormales, envahissant rapidement la moelle osseuse et les organes lymphoïdes secondaires tels que la rate et les ganglions lymphatiques.

Les signes cliniques amenant au diagnostic d'une LAL-B sont des anomalies de numération de la formule sanguine (anémie, thrombopénie et neutropénie) qui induisent généralement fatigue et pâleur, des infections et des saignements. Les infiltrations de cellules leucémiques dans les organes lymphoïdes secondaires et le foie sont fréquentes, provoquant ainsi une splénomégalie, une hypertrophie ganglionnaire et une hépatomégalie.

3.1.C. Traitement et taux de survie

Les LAL-B sont actuellement traitées avec une combinaison de chimiothérapies, qui éliminent efficacement les cellules qui prolifèrent. Le traitement se caractérise par une phase d'induction de 4 à 6 semaines avec l'utilisation d'agents de chimiothérapie (Vincristine,

Methotrexate, Doxorubicine, L-asparaginase) associés à des glucocorticoïdes (Dexaméthasone) : celle-ci a pour objectif d'induire une rémission chez le patient s'il est répondeur au traitement. Cette phase peut être combinée avec une allogreffe de CSH pour stimuler l'apparition d'une nouvelle hématopoïèse saine. La deuxième partie de la thérapie correspond à une phase de consolidation ou d'intensification de 6 à 8 mois pour préserver la rémission induite lors de la phase d'induction. Enfin dans un dernier temps, un traitement d'entretien de moindre intensité est mis en place jusqu'à 2 ans après le début du traitement.

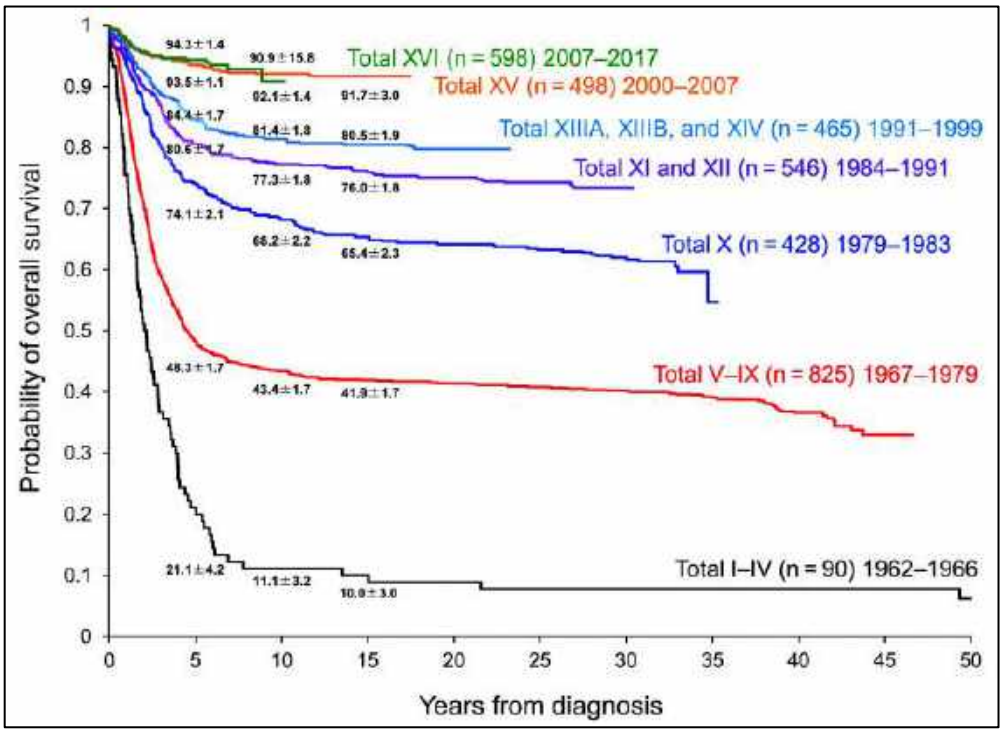

Figure 19 : Évolution de la survie globale des enfants de moins de 15 ans atteints de LAL-B inclus dans des essais cliniques de 1962 à 2017 (D'après Inaba & Mullighan, 2020).

Les doses de chimiothérapie prescrites sont adaptées à l'âge du patient. En effet, les adultes présentent une tolérance plus faible que les enfants face à la chimiothérapie. L'utilisation de plus fortes doses de chimiothérapies chez les enfants a permis d'augmenter considérablement la survie globale depuis le début des années 1960 (**Figure 19**). La survie globale est passée de 10% dans les années 1960 à plus de 90% en 2017. Environ 98% des enfants souffrant de LAL atteignent la rémission, et 80 à 90% d'entre eux sont considérés comme guéris.

Cependant, la chimiothérapie est associée à une toxicité qui peut persister toute la vie du patient avec des effets secondaires indésirables comme des anomalies endocriniennes, une cardiotoxicité, le développement de tumeurs malignes induites par la chimiothérapie et des

problèmes de fertilité. Chez les patients âgés, le pronostic de survie globale est beaucoup plus péjoratif puisque seulement 50% des patients survivent après 5 ans (Roberts, 2018) : ce mauvais pronostic est lié à leurs rechutes plus fréquentes ayant lieu dans 40 à 75% des adultes.

3.2. Caractérisation des LAL-B

3.2.A. Caractérisation immunophénotypique

Afin de connaitre à quel stade les cellules leucémiques sont bloquées, l'expression de différents marqueurs caractéristiques de la différenciation B (CD10, CD19, CD20, CD22 et CD34 pour les marqueurs membranaires, CD79a, IgH et IgL pour les marqueurs intracellulaires) est analysée par cytométrie en flux. L'expression de ces marqueurs permet en clinique de discriminer les LAL de type B, T et les leucémies aiguës myéloïdes (LAM), permettant ainsi d'adapter le traitement. Le marqueur CD19 est notamment utilisé comme marqueur de diagnostic et de suivi des LAL-B.

Le consortium EGIL (*European Group for the Immunological characterization of Leukaemias*) utilise les différents marqueurs de la différenciation B pour classer les LAL-B en quatre groupes distincts :

- Les LAL pro-B (sous-type B-I) qui se caractérisent par l'expression d'au moins deux des marqueurs de la différenciation B précoce (CD19, CD22, CD79A).
- Les LAL communes (sous-type B-II) qui se caractérisent par la co-expression du CD19 et du CD10. Elles représentent d'ailleurs le sous-type de LAL-B le plus fréquent, que ce soit chez l'adulte ou chez l'enfant.
- Les LAL pré-B (sous-type B-III) qui se caractérisent par l'expression intracellulaire de la chaine lourde μ des immunoglobulines.
- Les LAL mature B (sous-type B-IV) qui se caractérisent par l'expression membranaire des immunoglobulines (IgM de surface).

3.2.B. Caractérisation moléculaire

La classification moléculaire des LAL-B se réalise par l'identification des réarrangements moléculaires ou modifications chromosomiques dans les cellules leucémiques. 75% des LAL-B pédiatriques sont concernées par ce type d'altérations, qui sont détectées par caryotypage ou par FISH (technique d'hybridation de sondes fluorescentes *in situ*). Grâce aux nouvelles technologies, il a été possible de préciser ces sous-types et de caractériser

l'hétérogénéité des altérations oncogéniques des LAL-B (Brady et al., 2022; Gu et al., 2019a). À ce jour, on identifie 23 sous-types oncogéniques (**Figure 20**) classés en fonction de l'identité de la première altération acquise.

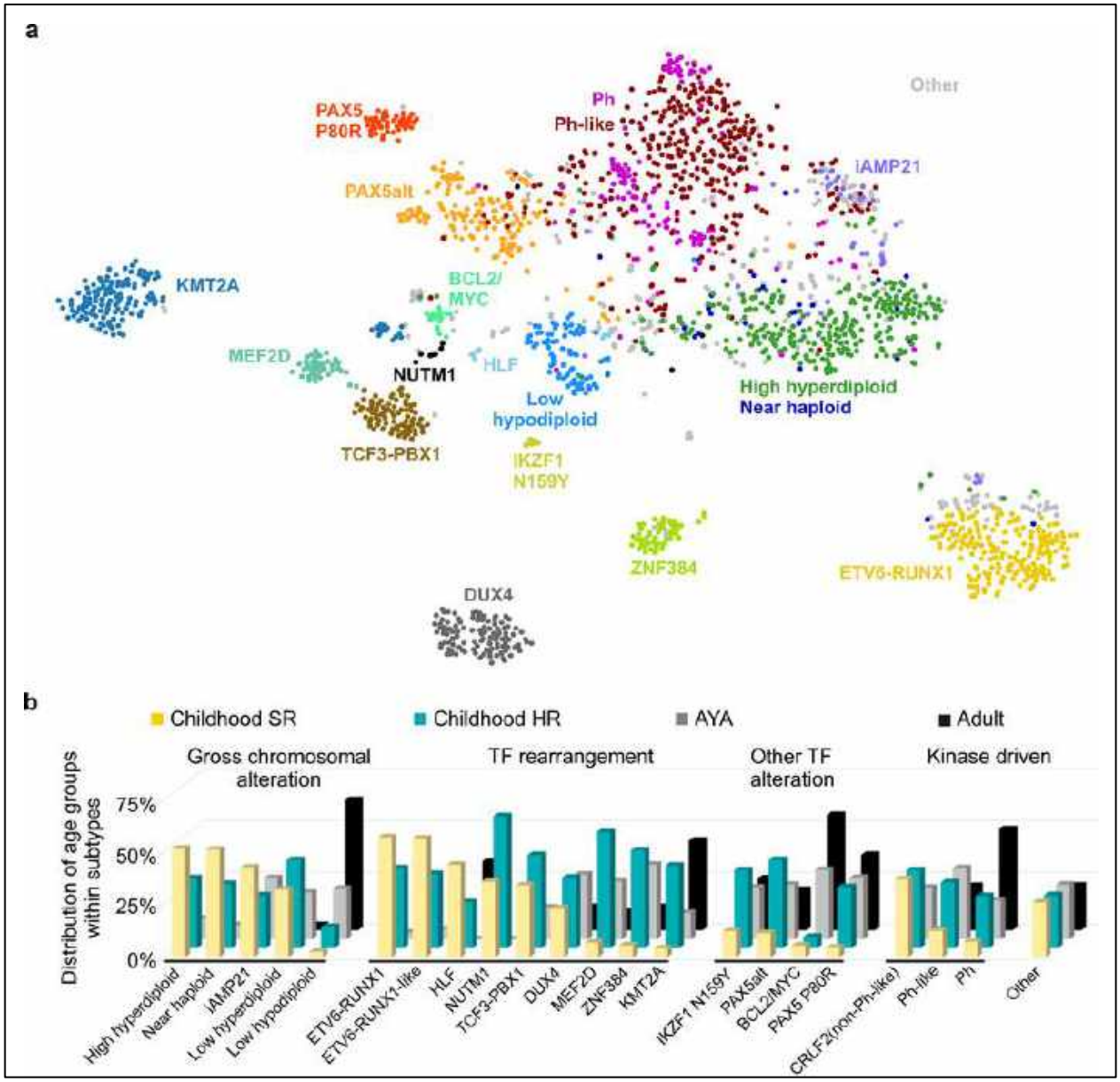

Figure 20 : Classification des différents sous-types oncogéniques des LAL-B (D'après Mullighan, 2019).

A. Principaux sous-types génétiques de LAL-B basés sur le profil d'expression génique de 1988 cas classés en 3 catégories d'âge : enfants entre 0,2 et 15 ans, adolescents et jeunes adultes (AYAs) de 15 à 39 ans, et adultes de 40 ans et plus. B. Distribution des sous-types génétiques de LAL-B au sein de chaque catégorie d'âge. Les sous-types sont regroupés entre anomalies chromosomiques de nombre (Aneuploid/copy number gain) et anomalies de structure comprenant les réarrangements chromosomiques impliquant des facteurs de transcription (TF rearrangement), les autres altérations de FTs (TF-driven) ou de kinases (kinase-driven), ou toute autre aberration qui n'entre pas dans ces sous-groupes ('other').

LAL-B hyperdiploïdes

Les LAL-B hyperdiploïdes sont détectées dans plus de 30% des cas, et constituent ainsi le sous-groupe oncogénique le plus courant, notamment chez les enfants (Moorman et al., 2010). Il s'agit d'une accumulation anormale de chromosomes due à une mauvaise séparation du matériel génétique lors de la division cellulaire de la cellule mère en deux cellules filles. Dans les LAL-B, ce sont les chromosomes X, 4, 6, 10, 14, 17 et 21 qui sont concernés.

LAL-B BCR-ABL

La protéine de fusion BCR-ABL est issue de la translocation chromosomique t(9 ;22)(q34 ;q11), et est retrouvée aussi bien dans les LAM que dans les LAL-B. Elles sont communément appelées Ph^+ (chromosome de Philadelphie), et ne sont retrouvées que chez les adultes âgés de plus de 40 ans. Les altérations oncogéniques secondaires fréquemment retrouvées correspondent à des délétions d'IKZF1, potentiellement associées à des délétions de PAX5. La présence de la protéine de fusion BCR-ABL provoque une activité tyrosine kinase constitutive et incontrôlée. Elles sont considérées comme étant de mauvais pronostic car elles sont très fortement associées à un haut niveau de rechute et à une réponse faible aux chimiothérapies. L'utilisation d'inhibiteurs de tyrosine kinase (comme l'Imatinib par exemple), en plus d'une chimiothérapie conventionnelle, a ainsi permis d'améliorer la survie des patients atteints de LAL-B Ph+ (Schultz et al., 2014).

LAL-B ETV6-RUNX1

La protéine de fusion ETV6-RUNX1 issue de la translocation chromosomique t(12 ;21)(p13 ;q22) correspond à l'altération génétique la plus commune dans les LAL-B pédiatriques (25% des cas de LAL-B chez les patients de moins de 18 ans). Les LAL-B ETV6-RUNX1 sont considérées comme étant de bon pronostic avec plus de 80% de rémission à long terme (Forestier et al., 2008; Moorman et al., 2010). Les altérations oncogéniques secondaires communément associées correspondent à des délétions du second allèle de ETV6, d'un allèle de CDKN2A ou de PAX5. Les deux facteurs de transcription impliqués dans la translocation sont des régulateurs clés de l'hématopoïèse. Notamment, la protéine de fusion perturbe le programme de transcription génique en réprimant l'expression des gènes qui est normalement activée par RUNX1 (Hiebert et al., 1996).

LAL-B TCF3-PBX1

La protéine de fusion issue de la translocation chromosomique t(4 ;11)(q21 ;q23) constitue un sous-groupe oncogénique correspondant à 5% des LAL-B pédiatriques. Les altérations oncogéniques secondaires associées correspondent à des délétions de CDKN2A et de PAX5. Elles ont été initialement considérées comme étant de pronostic intermédiaire, mais les derniers protocoles de polychimiothérapies associés à l'allotransplantation de CSH permettent une rémission complète dans plus de 95% des cas (Zhou et al., 2021).

LAL-B KMT2A

Les translocations de KMT2A ou MLL correspondent au sous-type oncogénique des LAL-B le plus fréquemment retrouvé chez les enfants âgés de moins d'un an (environ 80%). Elles sont considérées comme étant de très mauvais pronostic. Les translocations MLL sont très peu associées à d'autres altérations oncogéniques, malgré la présence de quelques mutations de la voie RAS/MAPK et de PAX5 (Driessen et al., 2013), suggérant ainsi que la translocation seule pourrait suffire à induire la leucémie.

3.3. Altérations génétiques de PAX5 dans les LAL-B

Parmi les différents sous-types oncogéniques, on en trouve deux contenant des altérations de PAX5 et qui sont définis par des profils d'expression génique distincts (Bastian, Schroeder, Eckert, Schlee, Tanchez, Kämpf, et al., 2019; Brady et al., 2022; Gu et al., 2019a; Passet, Boissel, Sigaux, Saillard, Bargetzi, Ba, Thomas, Graux, Chalandon, Leguay, Lengliné, et al., 2019) : un premier sous-type contenant exclusivement des altérations de PAX5 (PAX5alt comprenant délétion, translocation et mutations autres que P80R) et un autre sous-type exclusivement porteur de la mutation PAX5 P80R.

PAX5 correspond à la cible d'altérations génétiques la plus fréquente dans les LAL-B, puisqu'il est retrouvé altéré dans un tiers des cas que ce soit chez les enfants ou chez les adultes (Familiades et al., 2009; Mullighan et al., 2007).

3.3.A. Délétions de PAX5

PAX5 est inactivé dans environ un tiers des cas de LAL-B pédiatriques et adultes (Familiades et al., 2009; Mullighan et al., 2007), le qualifiant ainsi de gène suppresseur de tumeur dans les LAL-B.

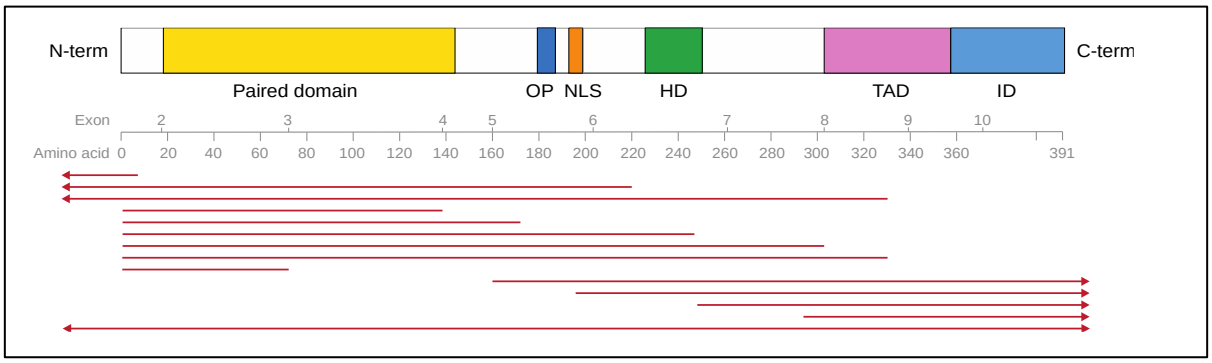

Figure 21 : Schéma représentant les délétions partielles ou totales de PAX5 dans les LAL-B.

Les inactivations de PAX5 correspondent généralement à des délétions mono-alléliques ayant pour conséquence des délétions partielles ou totales de la protéine. (**Figure 21**) Ces altérations induisent une haploinsuffisance de PAX5, dont la conséquence est difficile à déterminer car les souris hétérozygotes *Pax5*$^{+/-}$ présentent un phénotype normal (Urbánek et al., 1994). Cependant, les délétions de PAX5 sont maintenant considérées comme des événements coopérateurs en association avec d'autres évènements oncogéniques. Par exemple, la délétion de PAX5 est très souvent associée aux délétions de CDKN2A et de CDKN2B. Ces deux gènes sont localisés dans la même région chromosomique que *PAX5* (9p). Cette association de délétions pourrait participer à l'aggravation de la pathologie car CDKN2A et CDKN2B sont connus pour être des gènes suppresseurs de tumeurs (Kamb, Gruis, et al., 1994; Kamb, Shattuck-Eidens, et al., 1994; Nobori et al., 1994).

3.3.B. Diversité des réarrangements chromosomiques de PAX5

Les réarrangements structuraux du gène *PAX5* se caractérisent par la juxtaposition de la partie 5' de *PAX5* avec une diversité de partenaires de fusion. Toutes les protéines de fusion impliquant PAX5, résultant d'une translocation chromosomique, conservent systématiquement le domaine de liaison à l'ADN situé en N-terminal de la protéine. En revanche, elles perdent en partie ou en totalité le complexe de régulation de la transcription situé en C-terminal de la

protéine. Les réarrangements de *PAX5* mènent à l'expression de transcrits de fusion dans approximativement 2,5% des LAL-B (la protéine de fusion la plus fréquente étant PAX5-ETV6) (Coyaud et al., 2010b; Nebral, Denk, Attarbaschi, König, et al., 2009).

PAX5 se retrouve fusionné avec de nombreux partenaires (**Figure 22**). Actuellement, plus d'une cinquantaine de réarrangements chromosomiques impliquant *PAX5* ont été identifiés. Les partenaires de fusion correspondent à des gènes qui codent des facteurs de transcription (tels que ETV6, FOXP1), des récepteurs nucléaires, des protéines transmembranaires, des protéines structurales nucléaires ou extracellulaires (telles que l'élastine ou ELN), des kinases impliquées dans des voies de signalisation (telles que JAK2), des protéines impliquées dans l'épissage alternatif ou même encore des protéines aux fonctions inconnues (telles que AUTS2) (Coyaud et al., 2010; Mullighan et al., 2007; Nebral et al., 2009).

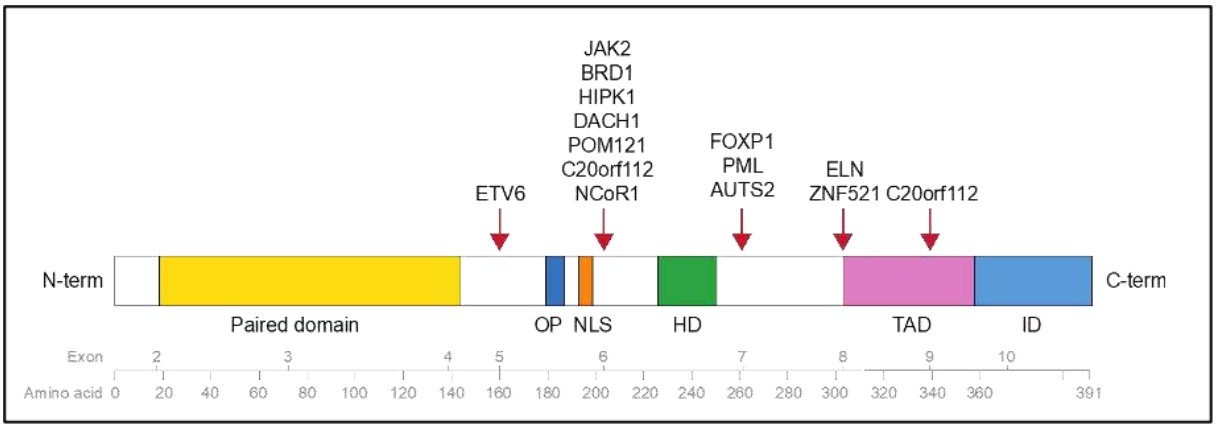

Figure 22 : Représentation schématique des points de fusion de certains partenaires de fusion de PAX5 impliqués dans les translocations retrouvées dans les LAL-B.

3.3.C. Diversité des mutations de séquence de PAX5

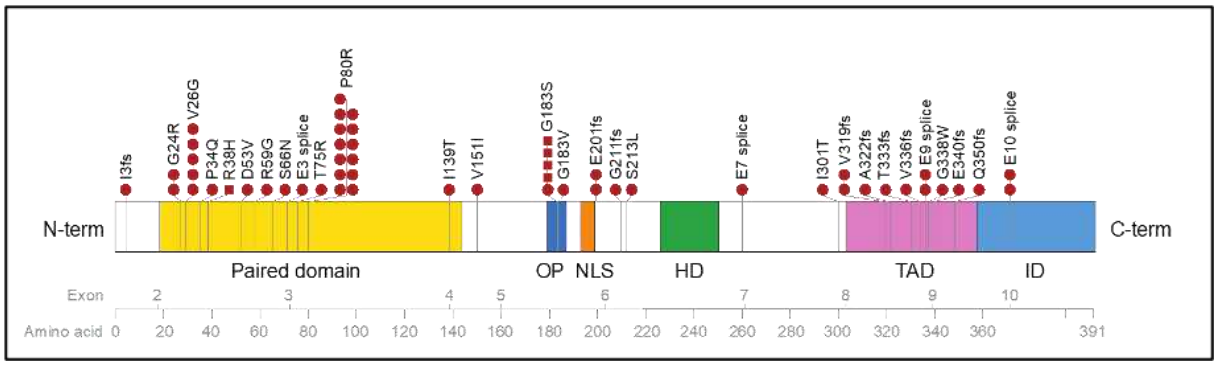

Figure 23 : Schéma des domaines protéines de PAX5 recensant les différentes mutations ponctuelles impliquées dans le développement des LAL-B.

Les mutations ponctuelles de la phase codante de PAX5 sont identifiées dans 6 à 7% des cas de LAL-B (Familiades et al., 2009; Mullighan et al., 2007). Il existe de très nombreuses mutations ponctuelles (**Figure 23**) qui se répartissent sur tout le gène *PAX5*, mais elles se concentrent principalement sur les domaines fonctionnels de la protéine.

Les mutations ponctuelles affectant la moitié N-terminale de PAX5 sont considérées comme apportant un gain de fonction. À l'inverse, les mutations affectant la moitié C-terminale de PAX5 sont considérées comme entrainant une perte de fonction (notamment due à la perte des domaines de régulation de la transcription).

3.3.D. Le hotspot mutationnel PAX5 P80R

La mutation ponctuelle de PAX5 la plus fréquente dans les cas de LAL-B correspond à la mutation PAX5 P80R, qui est retrouvée dans 5% des cas de LAL-B (Bastian, Schroeder, Eckert, Schlee, Tanchez, Kämpf, et al., 2019; Gu et al., 2019a; Passet, Boissel, Sigaux, Saillard, Bargetzi, Ba, Thomas, Graux, Chalandon, Leguay, Lengliné, et al., 2019). La mutation PAX5 P80R est plutôt considérée comme une mutation gain de fonction du fait de sa récurrence et de sa capacité à induire une signature d'expression génique distincte : elle définit donc un sous-type oncogénique des LAL-B. Elles sont considérées comme étant de pronostic intermédiaire. Les altérations oncogéniques retrouvées fréquemment associées à cette mutation correspondent à l'inactivation du second allèle de *PAX5* (par délétion ou par mutation), de la délétion bi-allélique de CDKN2A et des mutations affectant les voies de signalisation RAS/MAPK et JAK/STAT.

Cette mutation se caractérise par la substitution d'une proline en arginine, en position 80 au niveau du domaine de liaison à l'ADN de *PAX5*. L'analyse de prédiction *in silico* de l'effet de cette mutation au niveau de la conformation de la protéine a révélé un changement conformationnel, qui suggère une diminution de la capacité de fixation sur l'ADN (Passet, Boissel, Sigaux, Saillard, Bargetzi, Ba, Thomas, Graux, Chalandon, Leguay, Lengliné, et al., 2019). Au niveau transcriptionnel, un enrichissement négatif des cibles de PAX5 est observé chez les patients PAX5 P80R. La moitié des gènes régulés négativement par PAX5 P80R le sont aussi par PAX5alt, démontrant ainsi que ces deux sous-groupes se caractérisent par une perte de l'activité transcriptionnelle de PAX5. De plus, la comparaison du profil d'expression génique entre les sous-types oncogéniques P80R et PAX5alt montre un enrichissement négatif pour les gènes spécifiques du lignage lymphoïde B, suggérant que la mutation PAX5 P80R a

un effet plus délétère sur le développement des cellules B comparé aux altérations constituant le sous-groupe PAX5alt. L'ensemble de ces résultats suggère une perte de fonction partielle de PAX5.

Chapitre 4 : Hétérogénéité et processus multi-étapes de la leucémogenèse

4.1. Hétérogénéités moléculaire et cellulaire des leucémies aiguës

4.1.A. Origine du concept des cellules souches leucémiques

En accord avec différentes études pionnières, l'hématopoïèse normale est un processus finement régulé basé sur une organisation hiérarchique dans laquelle un petit nombre de cellules souches multipotentes maintient l'ensemble du lignage hématopoïétique (Berenson et al., 1988; M. Bhatia et al., 1997; Morrison & Weissman, 1994; Osawa et al., 1996; Spangrude et al., 1988; TILL & McCULLOCH, 1961).

Tout comme pour le système hématopoïétique normal, le concept des cellules souches leucémiques (CSL) supporte l'idée que les cellules leucémiques sont hétérogènes fonctionnellement, et suivent un modèle hiérarchique au sein duquel une population mineure de CSL est capable d'initier et de maintenir indéfiniment la maladie.

Ce concept provient d'études pionnières du laboratoire de John Dick, qui ont permis d'identifier une sous-population distincte de cellules tumorales issues de patients atteints de LAM, capables d'initier et de propager la maladie après xénogreffes dans des souris immunodéficientes (Bonnet & Dick, 1997; Lapidot et al., 1994). Depuis, la transplantation de cellules leucémiques humaines est devenue le test standard de référence pour étudier l'activité des cellules souches leucémiques (Kreso & Dick, 2014). Basée sur une caractérisation phénotypique, plusieurs études décrivent une population rare et spécialisée enrichie en CSL dans la fraction CD34+CD38-Lin- de patients LAM (Eppert et al., 2011; Goardon et al., 2011; Hope et al., 2004; Ishikawa et al., 2007). Cependant, les CSL transplantables ont aussi être trouvées dans les sous-populations CD34+CD38+ et CD34-, mais avec des fréquences plus faible (Eppert et al., 2011; Goardon et al., 2011; Kreso & Dick, 2014; Sarry et al., 2011), et peuvent être ainsi phénotypiquement plus diverses que pensé initialement. Malgré ce débat, contrairement aux cellules leucémiques propagatrices, les CSL restent considérées comme au sommet de la hiérarchie leucémique, étant capables de maintenir le développement tumoral à long terme et constituant un driver important de rechute grâce à leur faible taux de division qui

les rendent résistantes aux chimiothérapies conventionnelles (Greaves, 2016; Kreso & Dick, 2014).

4.1.B. Plasticités phénotypique et fonctionnelle des LAL

La notion d'hétérogénéité cellulaire et fonctionnelle dans les cellules leucémiques est d'un intérêt fondamental afin de comprendre l'initiation et le développement leucémique chez les patients. Le modèle hiérarchique du concept de CSL a donc été appliqué aux LAL-B et aux LAL-T.

Dans les LAL-B, les marqueurs CD34, CD38 et CD19 ont été utilisés pour explorer l'hétérogénéité des blastes leucémiques de patients pédiatriques et adultes, ce qui a mené à de nombreuses controverses (F. Lang et al., 2015). Initialement, il a été proposé que les cellules leucémiques au phénotype proche d'une CSH, c'est-à-dire CD34+CD19-, étaient porteuses du compartiment CSL (Cobaleda et al., 2000; Cox et al., 2004). Cependant, il a été démontré par la suite que l'activité d'auto-renouvellement pouvait être également enrichie dans les sous-populations leucémiques exprimant le marqueur CD19 (Castor et al., 2005; Hotfilder et al., 2002; Kong et al., 2008; le Viseur et al., 2008), correspondant phénotypiquement à des précurseurs B normaux. Ainsi, l'enrichissement potentiel de CSL dans les LAL-B en utilisant les marqueurs de surface CD34 et CD38, associé ou non au CD19, a conduit à des résultats variables (Aoki et al., 2015; Kong et al., 2008; F. Lang et al., 2015; le Viseur et al., 2008).

En effet, le concept hiérarchique a été challengé par l'utilisation de tests de dilution limite (LDA), montrant que les cellules de LAL-B capables de greffer dans des souris immunodéficientes sont très fréquentes et ne sont pas restreintes à une seule population avec un phénotype spécifique (Aoki et al., 2015; le Viseur et al., 2008; Rehe et al., 2013). Il a également été démontré au niveau unicellulaire que l'expression du CD34 et du CD38 est un processus plastique et dynamique à la surface des cellules blastiques (F. Lang et al., 2017), qui peut aussi expliquer les différentes controverses quant à l'utilisation de ces deux marqueurs pour l'enrichissement des CSL. De la même manière, la perte de l'expression de l'antigène CD19 à la surface des cellules leucémiques permettant à la tumeur d'échapper à l'immunothérapie par CAR-T cells (*Chimeric Antigen Receptor*) (Orlando et al., 2018; Rabilloud et al., 2021), correspond à un exemple représentatif de plasticité antigénique et d'adaptation des cellules leucémiques durant le traitement. L'identification de différents marqueurs de surface stables exprimés de façon aberrante sur les cellules leucémiques semble

donc indispensable pour suivre l'évolution de la maladie et pour traquer les cellules résistantes (Sędek et al., 2019; Tsitsikov et al., 2018).

L'utilisation de modèles de xénogreffes de LAL combinée à un test de division cellulaire *in vivo* a permis de démontrer que les propriétés des cellules souches, telles que la dormance, la résistance aux traitements et l'activité initiatrice de la leucémie, sont réversibles (Ebinger et al., 2016). De plus, les auteurs ont également montré que la plasticité fonctionnelle des clones quiescents est dépendante de l'environnement *in vivo* et suggère que ces mécanismes réversibles pourraient être impliqués dans l'échec aux traitements et la rechute de la maladie. Ainsi, la plasticité phénotypique et fonctionnelle doit être prise en compte dans les approches expérimentales pour identifier les populations enrichies en cellules souches leucémiques, mais également au niveau clinique, pour expliquer les mécanismes d'échappement thérapeutique et la rechute des LAL-B.

4.2. Diversité moléculaire et évolution clonale

Le développement des leucémies aiguës est caractérisé par un processus multi-étapes par l'acquisition de diverses mutations. En lien avec l'observation que les leucémies aiguës présentent un nombre limité d'altérations génétiques (Alexandrov et al., 2013), chaque mutation acquise peut perturber des fonctions cellulaires critiques et leur combinaison peut être suffisante pour induire la transformation tumorale.

Grâce à une approche de cytogénétique par hybridation *in situ* de sondes fluorescentes multiplex (M-FISH), des travaux pionniers ont permis à l'équipe de Mel Greaves d'établir l'architecture génétique intraclonale des cellules leucémiques de patients atteints de LAL-B. Cette approche, permettant de détecter jusqu'à huit altérations génétiques par cellule, a permis de mettre en évidence la diversité clonale des cellules leucémiques, de hiérarchiser l'acquisition des différentes altérations et d'établir des arbres phylogénétiques de l'évolution clonale pour chaque patient (Anderson et al., 2011). Ces travaux ont également permis de déterminer la présence au sein de la masse tumorale de clones ancestraux ne présentant qu'une seule altération génétique.

La composition et la dynamique de sous-clones leucémiques ont également été étudiées en comparant les altérations génétiques entre des échantillons de LAL au diagnostic et à la rechute (Kuster et al., 2011; Mullighan et al., 2008; Theunissen et al., 2019; Waanders et al.,

2020; Yang et al., 2008). Les analyses par techniques de séquençage nouvelle génération (NGS), de polymorphisme d'un seul nucléotide (SNP), d'hybridation génomique comparative (CGH) d'échantillons de LAL au diagnostic et à la rechute ont permis de caractériser le profil génétique des patients au cours de l'évolution de la maladie. Toutes ces techniques ont établi une architecture complexe de chaque leucémie et révélé que la rechute pouvait être générée à partir d'un clone mineur, majeur ou ancestral du diagnostic. L'équipe de Mullighan a notamment montré que plus de la moitié des échantillons de LAL à la rechute n'avaient pas toutes les altérations génétiques présentes au diagnostic, et présentaient également de nouvelles lésions génétiques qui étaient absentes au diagnostic (Mullighan, 2012; Mullighan et al., 2008; Waanders et al., 2020). Ils ont pu démontrer que dans la majorité des rechutes de LAL, les cellules leucémiques proviennent d'un clone avec un nombre limité d'altérations génétiques. En effet, alors qu'une rechute peut être induite par un clone prédominant au diagnostic, la majorité d'entre-elles apparaissent à partir d'un sous-clone mineur préexistant fortement dilué ou à partir d'une évolution clonale d'un clone ancestral (X. Ma et al., 2015; Mullighan et al., 2008; Oshima et al., 2016; Waanders et al., 2020).

Ces différentes études démontrent donc une diversité sous-clonale dans les cellules leucémiques de LAL, résultant d'une évolution complexe, non linéaire et ramifiée. Ces travaux prédisent également l'existence d'un clone ancestral présent avant le diagnostic arborant un nombre restreint d'altérations génétiques (altérations primaires), qui n'est pas encore transformé mais qui se trouve au sommet de la hiérarchie et de l'hétérogénéité tumorale.

4.3. Processus multi-étapes de la leucémogenèse

La notion de processus multi-étapes et d'origine prénatale du développement de la LAL a beaucoup été étudié par l'équipe de Mel Greaves avec notamment l'étude de l'initiation et de la progression leucémiques chez des jumelles monochorioniques (Greaves, 2018). Ces études ont permis de montrer que les translocations chromosomiques, en particulier ETV6-RUNX1, pouvaient être détectées dans les cellules sanguines plusieurs années avant l'apparition de la maladie, établissant ainsi un état pré-leucémique. Ces cellules pré-leucémiques portent donc l'altération génétique fondatrice mais n'ont pas la capacité d'induire la maladie par elles-mêmes. L'acquisition, plus tard dans la vie de l'individu, de mutations complémentaires transforment ces cellules en cellules leucémiques malignes, sujettes à des processus d'évolution et de sélection clonale, et mènent à l'hétérogénéité génétique de la masse tumorale au moment du diagnostic (Greaves, 2018). La translocation ETV6-RUNX1 survient donc durant

l'hématopoïèse fœtale et agit comme premier évènement oncogénique dans les cellules B conduisant à l'émergence d'un clone pré-leucémique ayant des propriétés aberrantes d'auto-renouvellement et de survie (Hong et al., 2008).

4.4. *Mécanisme causal des LAL-B et prédisposition génétique*

Le mécanisme causal de développement des LAL-B pédiatriques est présenté comme multifactoriel, mettant en cause notamment des expositions à des infections, la prédisposition génétique ou encore un microbiote intestinal immature (Greaves, 2018; Peppas et al., 2023).

Selon les travaux de Mel Greaves, les LAL pédiatriques s'établissent en deux étapes distinctes à l'échelle de l'individu appelé le « two hits model » initialement (**Figure 24**) :

- ***Première étape : Émergence d'un clone pré-leucémique par acquisition d'une lésion in utero :***

Le premier évènement oncogénique se produit in utéro par l'acquisition d'une altération génétique telle que la translocation ETV6-RUNX1 (Wiemels et al., 1999) ou une hyperdiploïdie (Maia et al., 2003; Taub et al., 2002), conduisant au développement d'un clone pré-leucémique. La fusion ETV6-RUNX1 est présente dans 1 à 5% des nouveaux nés sains mais la majorité ne développe jamais de leucémie, montrant ainsi la faible pénétrance de la maladie et la nécessité d'acquisition de mutations additionnelles post-natales (Mori et al., 2002; Schäfer et al., 2018).

- ***Deuxième étape : Conversion en un clone leucémique post-natale :***

Chez une faible proportion des enfants (environ 1%), un second évènement subvient après la naissance et convertit le clone pré-leucémique en leucémie. L'hypothèse de « l'infection retardée » suggère que le développement de la leucémie apparaitrait à la suite d'une réaction immunitaire aberrante en réponse à une ou plusieurs infections dont l'exposition aurait anormalement lieu tardivement (Greaves, 2018). Cette exposition dite retardée pourrait expliquer notamment le pic d'incidence des LAL-B pédiatriques entre 2 et 5 ans. Cette réponse immunitaire anormale permettrait de déclencher indirectement l'acquisition de mutations secondaires requises pour l'évolution clonale et la transformation maligne (Isidro-Hernández et al., 2020, 2023).

Il a été montré plus récemment que les expositions très précoces à des pathogènes dans la vie de l'enfant avaient un impact profond sur la maturation correcte du microbiote intestinal

(Amir et al., 2022; Reyman et al., 2019; Shao et al., 2019; Stewart et al., 2018), qui est reconnu comme indispensable pour la bonne maturation du système immunitaire chez l'enfant (Olin et al., 2018). Ceci amène à la suggestion que la sous-exposition microbienne induirait l'apparition d'un microbiote intestinal déficient chez les patients qui développent une LAL-B pédiatriques (Peppas et al., 2023).

L'implication de l'exposition à des agents pathogènes (Isidro-Hernández et al., 2023; Martín-Lorenzo et al., 2015; Rodríguez-Hernández et al., 2019) ou d'un microbiote intestinal altéré (Vicente-Dueñas et al., 2020) dans le développement leucémique, a été démontré expérimentalement par l'utilisation de modèles murins Pax5 hétérozygote ou exprimant la protéine de fusion ETV6-RUNX1. En effet, le taux de développement de LAL-B augmente lorsque ces souris sont exposées à des infections après les avoir placées dans des animaleries conventionnelles. De plus, la production de cytokines inflammatoires causée par les infections peut provoquer le développement de la leucémie (Isidro-Hernández et al., 2020).

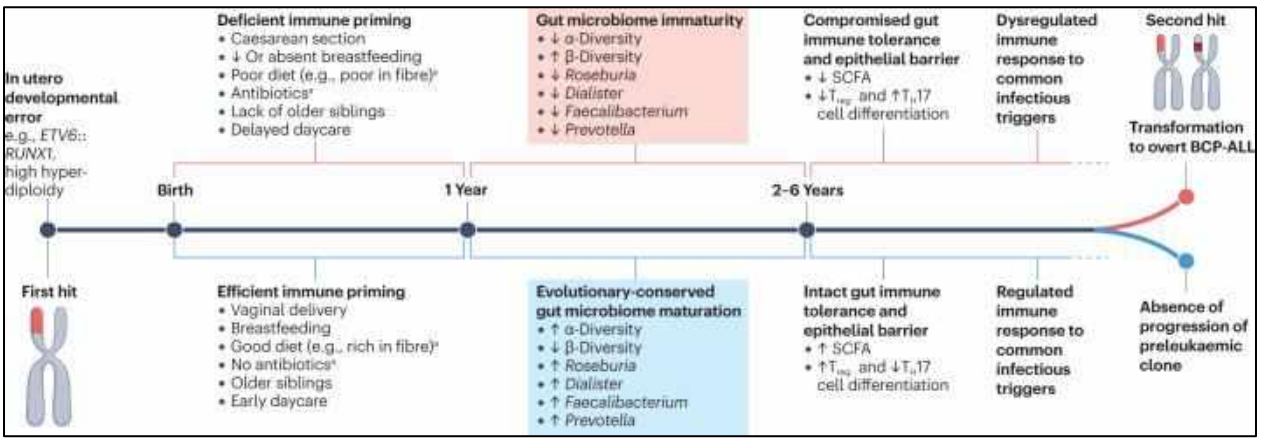

<u>Figure 24 :</u> Modèle de développement de la LAL-B suivant l'hypothèse de « l'infection retardée » (aussi appelée « two-hit model ») (D'après Peppas et al., 2023).

4.5. <u>Reprogrammation oncogénique et émergence des cellules souches pré-leucémiques</u>

Donc, excepté dans de rare cas de jumelles monochorioniques leucémique et pré-leucémique (Greaves, 2018), explorer le développement multi-étapes ainsi que les propriétés biologiques des cellules pré-leucémiques constituent un grand challenge. Pour pallier ce problème, le développement de modèles murins transgéniques dans lesquels sont activés des oncogènes particuliers au sein de lignages spécifiques est d'un intérêt majeur. En effet, ces

modèles murins servent d'outils pour comprendre les mécanismes biologiques par lesquels un premier évènement oncogénique induit l'apparition de la maladie, et leur utilisation ouvre de nouvelles perspectives (**Figure 25**). En effet, ils permettent de déchiffrer les mécanismes biologiques par lequel une voie oncogénique perturbe le développement de l'hématopoïèse normale et reprogramme un progéniteur commis en cellule souche pré-leucémique (pré-CSL) durant l'initiation de la maladie. Les modèles de souris permettent également de comprendre le processus multi-étapes de la maladie à partir du stade pré-leucémique jusqu'au stade leucémique en identifiant les évènements collaborateurs qui conduisent à la transformation maligne. Pour finir, ils permettent d'explorer aux niveaux moléculaire et fonctionnel le lien entre les cellules pré-leucémiques et leucémiques avec leur microenvironnement ; et permettent de développer des thérapies qui ciblent spécifiquement des marqueurs et/ou des mécanismes biologiques impliqués dans le développement leucémique et la résistance.

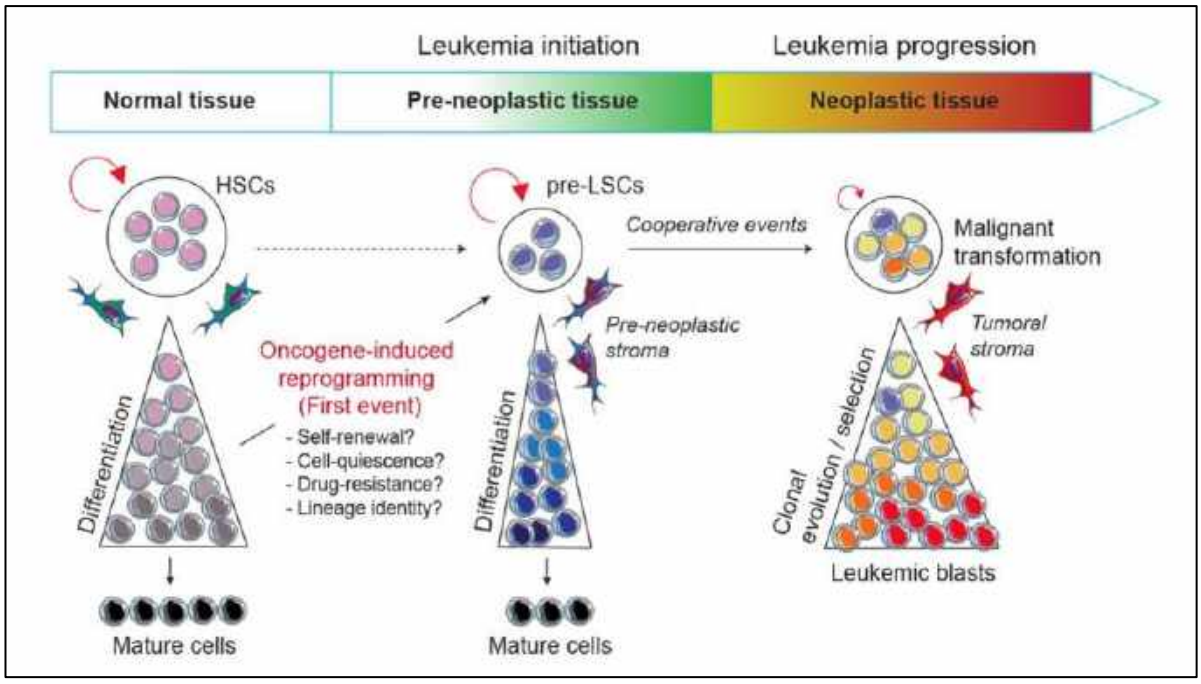

***Figure 25 :** Modèle d'évolution leucémique (D'après Fregona et al., 2021).*

L'utilisation de modèles murins de LAM corrobore l'idée que les altérations ciblant les facteurs de transcription correspondent à des évènements précoces de la maladie, et peuvent interférer avec des fonctions cellulaires essentielles des cellules. Par exemple, des oncogènes comme MLL-AF9, MLL-ENL ou PML-RAR ont été montré comme capables d'induire le développement d'une LAM quand ils sont introduits dans des cellules engagées dans la différenciation myéloïde (Cozzio et al., 2003; Guibal et al., 2009; Krivtsov et al., 2006; Wojiski et al., 2009). De plus, la caractérisation moléculaire de la cellule d'origine indique que ces

facteurs de transcription oncogéniques peuvent reprogrammer au sein de progéniteurs myéloïdes des signatures d'expression géniques proches de celles de CSH. Ces observations supportent l'idée qu'un événement oncogénique primaire peut causer au sein d'un progéniteur engagé une reprogrammation suffisante pour lui conférer une aptitude d'auto-revouvellement aberrante et le convertir en pré-CSL.

4.5.A. Auto-renouvellement des thymocytes pré-leucémiques

Dans les LAL, l'observation qu'un facteur de transcription oncogénique peut reprogrammer un progéniteur engagé en pré-CSL a été faite pour la première fois dans les thymocytes. Comme les thymocytes normaux ne présentent pas d'activité d'auto-renouvellement, le thymus représente une plateforme cellulaire d'intérêt pour étudier la reprogrammation induite par un oncogène. En réalisant des transplantations en série de thymocytes pré-leucémiques, il a été montré que la surexpression de l'oncogène Lmo2 dans le thymus provoque l'émergence d'une population de cellules souches pré-leucémiques (McCormack et al., 2010). Il a été effectivement démontré, par l'utilisation du modèle murin transgénique *Cd2-Lmo2* qui récapitule la LAL-T humaine, que l'expression forcée de Lmo2 convertie des thymocytes DN3 normaux en une population pré-leucémique qui s'autorenouvelle, associé à la réactivation partielle d'un programme de cellules souches.

Au niveau physiologique, les protéines LMO ont besoin d'une interaction protéique avec des facteurs de transcription de type bHLH (*basic Helix-Loop-Helix*) comme SCL/TAL1 ou LYL1 afin de former un complexe sur l'ADN et d'activer la transcription génique qui contrôle les fonctions des cellules souches et progéniteurs hématopoïétiques (CSPH) (Wilson et al., 2010). Il a été effectivement montré par la suite que l'expression ectopique, l'interaction et la collaboration de SCL et de l'oncoprotéine LMO1 sont indispensables pour altérer la différenciation des thymocytes (Herblot et al., 2000), mais également pour induire un réseau moléculaire d'auto-renouvellement nécessaire à l'émergence de pré-CSL dans le thymus (Gerby et al., 2014; Goossens & Van Vlierberghe, 2014).

Les modèles murins transgéniques permettent donc d'avoir un accès non restreint et reproductible aux pré-CSL, et ainsi d'étudier leurs mécanismes moléculaire et cellulaire, en particulier ceux impliqués dans la résistance aux chimiothérapies. En effet, des travaux ont

permis de démontrer la résistance des pré-CSL à la chimiothérapie dû à leur faible taux de division (Gerby, Veiga, Krosl, Nourreddine, Ouellette, Haman, Lavoie, Fares, Tremblay, Litalien, Ottoni, Kosic, Geoffrion, Ryan, Maddox, Chagraoui, Marinier, Hébert, et al., 2016; Tremblay et al., 2018). Il a été démontré par l'utilisation de la souris H2B-GFP^{tg} inductible à la doxycycline (modèle *in vivo* de référence pour étudier la quiescence des CSH) que l'auto-renouvellement, la résistance aux chimiothérapies et l'évolution clonale étaient restreintes à une population rare et peu cyclante de pré-CSL dans le modèle murin de LAL-T induite par l'oncogène LMO2 (Tremblay et al., 2018). Cette étude a permis de montrer pour la première fois l'importance de la restriction du cycle cellulaire dans l'activité des pré-CSL, mais aussi montre que le système H2B-GFP s'avère être un modèle puissant pour isoler les pré-CSL peu cyclantes et permettre de développer des stratégies ciblant leur mécanisme de résistance.

4.5.B. Reprogrammation cellulaire par les mutants de PAX5

PAX5 a d'abord été initialement caractérisé comme étant un gène suppresseur de tumeur dans les LAL, puisque les délétions de PAX5 sont retrouvées dans 1/3 des cas de LAL-B. Cependant, les souris hétérozygotes pour *Pax5* présentent un développement des cellules B normal et n'est pas suffisant pour induire le développement de la LAL-B en absence d'autres lésions oncogéniques (Cobaleda, Schebesta, et al., 2007). Le rôle suppresseur de Pax5 a été révélé en utilisant les souris *Pax5* hétérozygotes avec une approche de mutagenèse induite chimiquement (Dang et al., 2015a). Puis il a été confirmé en modulant d'autres facteurs de transcription impliqués dans le développement des cellules B, comme Ebf1 (M. A. J. Prasad et al., 2015; Ramamoorthy, Kometani, Herman, Bayer, Boller, Edwards-Hicks, Ramachandran, Li, Klein-Geltink, Pearce, Grün, et al., 2020), Ikzf1 (Chan, Chen, Braas, Lee, Xiao, Geng, Cosgun, Hurtz, Shojaee, Cazzaniga, Schjerven, Ernst, Hochhaus, Kornblau, Konopleva, Pufall, Cazzaniga, Liu, Milne, Koeffler, Ross, Sánchez-García, et al., 2017) et Stat5 (Heltemes-Harris et al., 2011a). En effet, les altérations génétiques de PAX5, EBF1 et IKZF1 sont communément retrouvées dans les LAL-B humaines, suggérant ainsi que le dosage de ces trois gènes est extrêmement important pour protéger de la leucémie (Roberts & Mullighan, 2020; Somasundaram et al., 2015). De façon intéressante, il a été montré que la délétion hétérozygote de Pax5 et Ebf1 bloque de manière partielle la différenciation des cellules pro-B, et augmente leur plasticité avant l'apparition de la leucémie (M. A. J. Prasad et al., 2015; Ramamoorthy, Kometani, Herman, Bayer, Boller, Edwards-Hicks, Ramachandran, Li, Klein-Geltink, Pearce,

Grün, et al., 2020; Ungerbäck et al., 2015). Les cellules pro-B hétérozygotes pour Pax5 et Ebf1 diminuent l'expression de gènes indispensables pour le maintien de l'identité des cellules B, permettant de révéler leur réponse à la signalisation NOTCH provoquant un potentiel T *in vitro* et *in vivo*. La diminution combinée de l'expression de Pax5 et Ebf1 induit au niveau moléculaire et fonctionnel un processus de conversion de lignage en cellules pro-B pré-leucémiques (Ungerbäck et al., 2015). Ces différents travaux suggèrent donc que la reprogrammation moléculaire, la perte partielle de l'identité des cellules B et l'acquisition d'une fonction d'auto-renouvellement sont des mécanismes clés impliqués dans l'initiation leucémique.

La question d'auto-renouvellement des pré-CSL a beaucoup été étudiée dans des modèles murins de LAL-T, mais est cependant très peu décrite dans les LAL-B. En effet de très nombreux modèles murins ont été générés pour essayer de mimer la pathologie humaine, mais très peu parviennent à développer spontanément la LAL-B. Notre équipe a récemment généré un modèle murin de LAL-B induite par l'oncogène PAX5-ELN, correspondant à une protéine de fusion initialement identifiée chez des patients toulousains atteints de LAL-B (Bousquet et al., 2007a). L'oncogène a la particularité d'être contrôlé par le locus des IgH, qui lui permet d'être exprimé uniquement dans les cellules B (Jamrog, Chemin, Fregona, Coster, Pasquet, Oudinet, Rouquié, et al., 2018). PAX5-ELN induit de façon efficace le développement de la LAL-B, et est associé à l'acquisition de mutations secondaires affectant les voies de signalisation JAK/STAT et RAS/MAPK. Ces mutations sont communément retrouvées chez les patients atteints de LAL-B (Mullighan et al., 2007), mais également dans d'autres modèles murins de LAL-B (Duque-Afonso et al., 2015b; van der Weyden et al., 2015b). Notre modèle mime donc le processus multi-étapes de la LAL-B humaine. De façon importante, le développement leucémique est précédé d'une phase pré-leucémique de trois mois, qui est associée à un blocage partiel de la différenciation. Ce modèle murin nous donne donc l'opportunité d'étudier les mécanismes biologiques par lesquels une protéine de fusion de PAX5 reprogramme des progéniteurs B normaux, perturbe l'identité des cellules B et mène à l'émergence d'une population de pré-CSL.

Chapitre 5 : Le système CRISPR-Cas9

5.1. Découverte chez les bactéries

La découverte du système CRISPR dans les bactéries s'est effectuée de manière séquentielle en différentes étapes (**Figure 26**).

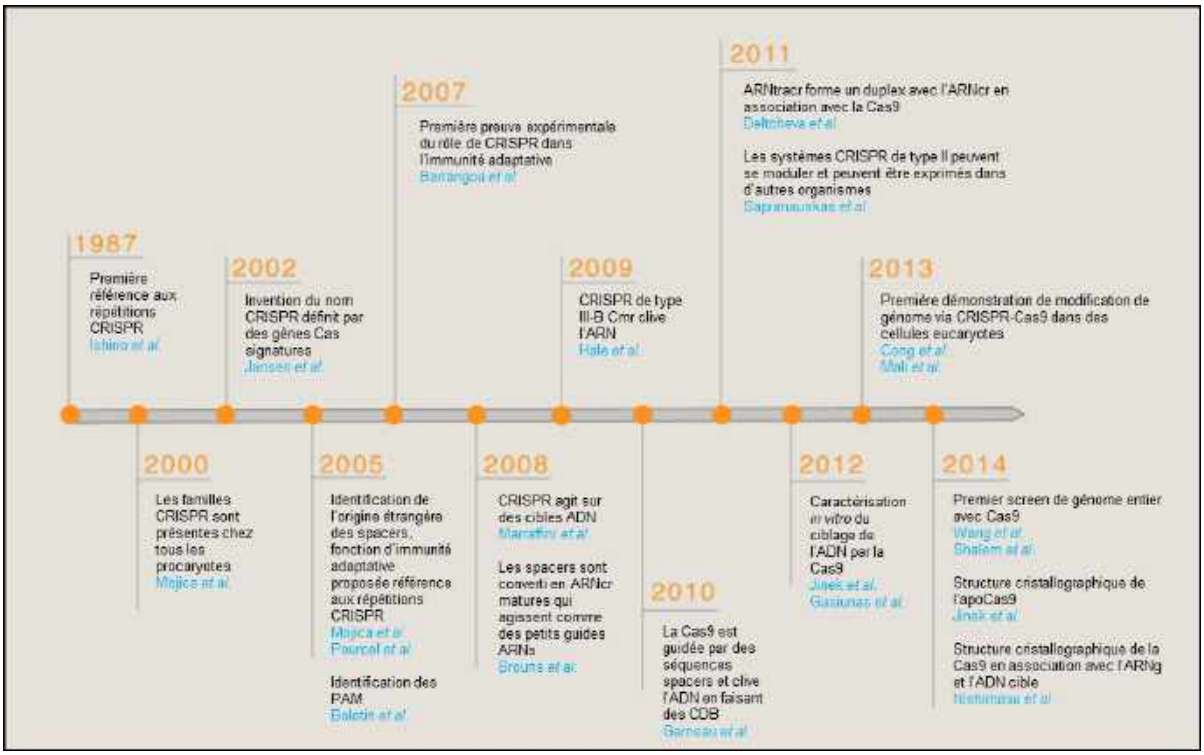

Figure 26 : Frise chronologique représentant les études clés portant sur le système CRISPR-Cas. (D'après Hsu et al., 2014).

Il a été observé pour la première fois par des chercheurs japonais en 1987 dans la bactérie E. coli des petites séquences répétées palindromiques (appelées spacers) séparées par des séquences géniques (Ishino et al., 1987). Ces loci particuliers ont été définis en 2002 sous le nom de « CRISPR » (*Clustered Regularly Interspaced Short Palindromic Repeats*), ce qui signifie « courtes régions palindromiques régulièrement espacées » (Jansen et al., 2002).

En 2005, Francisco Mojica et Christine Pourcel découvrent, de façon indépendante, que les régions localisées entre les spacers sont homologues à celles de séquences d'ADN que l'on retrouve dans des bactériophages, prophages et plasmides (Mojica et al., 2005; Pourcel et al., 2005). En se basant sur la littérature, ils remarquent que les phages et les plasmides ne peuvent pas infecter les hôtes qui possèdent ces séquences homologues dans leur locus CRISPR. Ils en

concluent alors que les séquences CRISPR apportent un système de défense similaire au processus de l'ARN interférence, en protégeant les cellules contre l'entrée d'éléments génétiques étrangers. Ils découvrent également que CRISPR permet de capturer des morceaux de l'ADN étranger pour constituer une mémoire génétique des précédentes infections (Bolotin et al., 2005).

La comparaison des régions CRISPR dans différents organismes a permis la découverte de quatre gènes conservés très souvent situés à proximité des régions CRISPR : les gènes *Cas* (*CRISPR-Associated genes*) numérotés de 1 à 4 (Jansen et al., 2002). Ils suggèrent alors que les protéines codées par ces gènes pourraient jouer un rôle dans la fonction de défense immunitaire des procaryotes. Pour valider cette hypothèse, l'équipe de Makarova a analysé les séquences des protéines Cas afin de prédire leurs fonctions (Makarova et al., 2006), et remarque que le système CRISPR-Cas possède des similarités avec le système immunitaire des Vertébrés, mais à la grande différence que celui-ci n'est pas transmissible à la descendance.

En 2007, la fonction du système CRISPR-Cas9 a été étudiée expérimentalement par l'équipe de Barrangou, en utilisant la bactérie S. thermophilus (Barrangou et al., 2007). En effet dans cette étude, il a été montré que l'insertion de séquences de phage dans les régions spacers de la bactérie a pour conséquence de rendre la bactérie résistante à ce même phage. A l'inverse, cette résistance n'existe plus lorsque la séquence correspondante dans le génome du phage est supprimée. Cette étude a donc permis de confirmer le rôle du système CRISPR dans le système immunitaire adaptatif des bactéries contre les bactériophages, prophages et plasmides.

En 2010, une étude a démontré que la protéine Cas9 que l'on retrouve chez S. pyogenes est la seule enzyme de la famille à pouvoir cliver l'ADN par des cassures double brin : c'est d'ailleurs cette protéine qui sera la première à être utilisée pour éditer le génome (Garneau et al., 2010).

En 2011, l'équipe de Charpentier fait la découverte du crRNA (CRISPR-ARN), qui s'hybride avec le tracrARN (*trans-activating crARN*), formant ainsi à eux deux ce que l'on appelle communément l'ARN guide, qui permet de guider l'endonucléase Cas9 jusqu'à son site de clivage (Deltcheva et al., 2011). En 2020, le prix Nobel de Chimie est décerné à Emmanuelle Charpentier et à Jennifer Anne Doudna pour leurs travaux révolutionnaires sur le système CRISPR-Cas9.

5.2. *Fonctionnement général du mécanisme CRISPR-Cas9*

Le système CRISPR se déconvolue en trois grandes étapes, permettant finalement l'immunisation de l'hôte contre une prochaine infection de cet ADN étranger (**Figure 27**) :

- La première étape consiste en l'étape d'adaptation : des fragments de l'ADN du pathogène, communément appelés « protospacers », sont intégrés dans le génome de la bactérie au niveau du locus CRISPR entre des séquences répétées.
- La deuxième étape consiste en l'étape d'interférence. La région CRISPR avec les séquences nouvellement intégrées est transcrite en un précurseur ARN, que l'on appelle également pré-crARN. Ce précurseur va alors subir un clivage enzymatique, pour aboutir à un crARN mature. Il servira alors de guide ARN pour cibler l'ADN exogène lors de la seconde infection par ce même pathogène. Il est constitué en 5' du spacer, correspondant à un court fragment d'ARN, et est complémentaire de la séquence protospacer de l'ADN étranger ciblé. La partie 3' quant à elle, est composée d'un morceau de la séquence CRISPR répétée.
- La troisième étape, qui a lieu uniquement lorsqu'une nouvelle infection avec ce même pathogène se produit, consiste en la reconnaissance de la séquence d'ADN du pathogène par le spacer du crARN, et qui induit le clivage de la séquence d'ADN par les protéines endonucléases Cas.

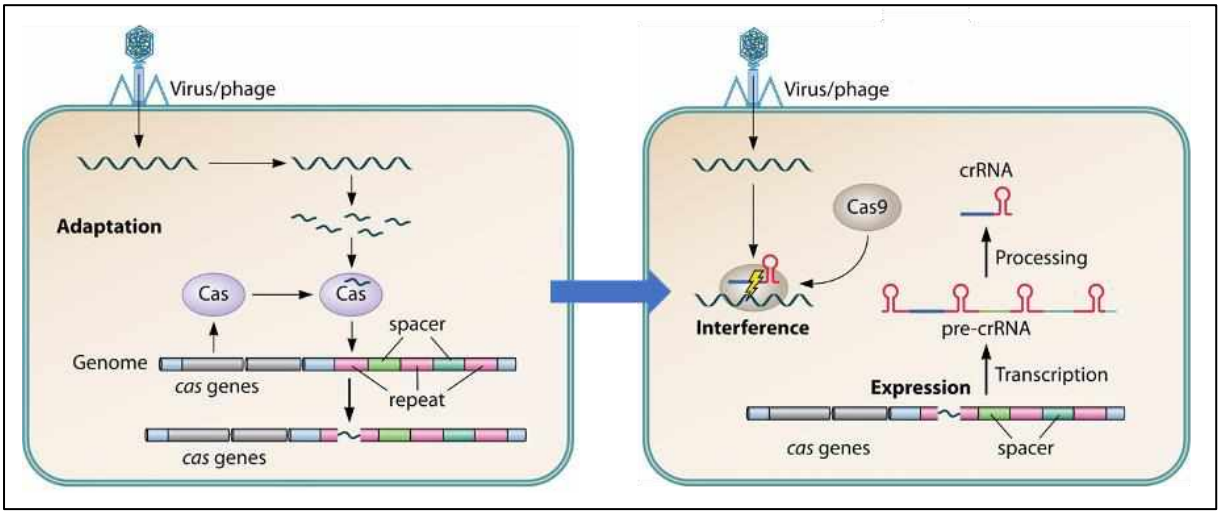

Figure 27 : Mécanisme d'acquisition de l'immunité chez les Bactéries grâce au système CRISPR-Cas9 (D'après Ishino et al., 2018).

La plupart des systèmes CRISPR sont dépendants de la présence d'une séquence spécifique adjacente à la séquence ciblée par le crARN dans le génome du pathogène : il s'agit

de la séquence PAM (*Protospacer Adjacent Motif*). Cette séquence est essentielle pour la sélection et la dégradation de l'ADN cible.

5.3. *Une multitude de systèmes CRISPR*

Il existe une multitude de systèmes CRISPR qui diffèrent selon leurs caractéristiques et la fonction des protéines Cas. En effet, la longueur des séquences répétées, le nombre de spacers, leur taille, la séquence PAM associée ou bien encore le nombre de locus CRISPR diffèrent en fonction des systèmes.

La classification actuelle se base sur deux grandes classes et six types (**Figure 28**). L'appartenance à la classe 1 ou à la classe 2 est dépendante uniquement de l'activité endonucléasique : une coopération de plusieurs protéines (entre 4 et 7) est nécessaire pour la classe 1 alors qu'une seule protéine est nécessaire pour la classe 2 (Ishino et al., 2018). La classe 2 est retrouvée uniquement chez les Bactéries et ne représente seulement que 10% de la totalité des systèmes CRISPR. Cependant, c'est cette classe de CRISPR qui est actuellement utilisée dans les systèmes d'édition génique.

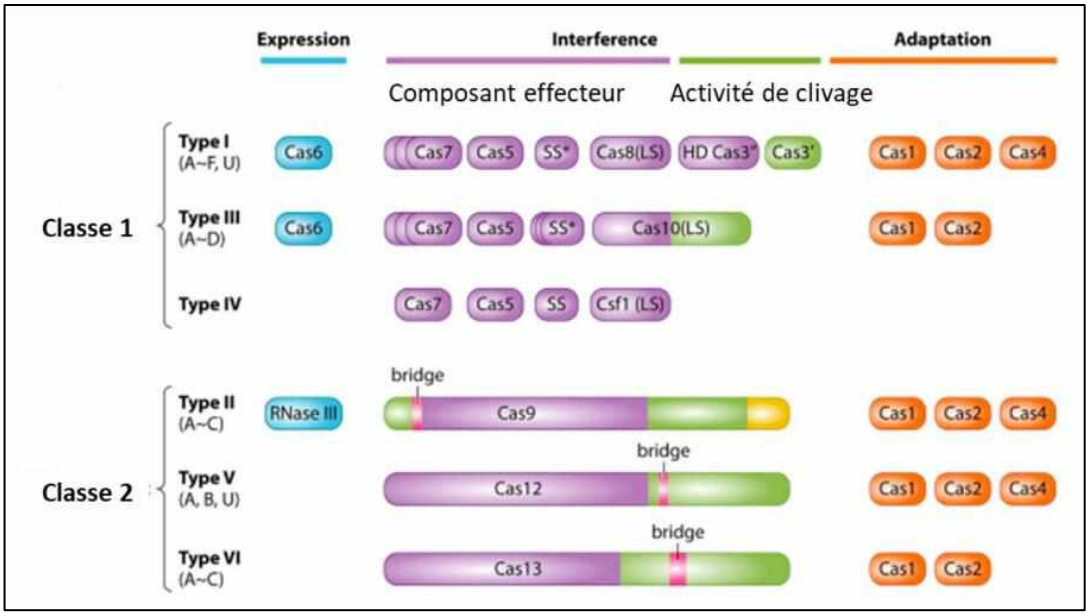

***Figure 28 :** Classification de l'ensemble des systèmes CRISPR-Cas (D'après Ishino et al., 2018).*

Chaque classe se déconvolue en trois types : I, III, IV pour la classe 1 et II, V, VI pour la classe 2. Cette classification se base sur les gènes *Cas* : en effet, chaque sous-type possède un gène ou un set de gènes *Cas* unique(s). Le premier système CRISPR utilisé pour réaliser dans des cellules eucaryotes de l'édition génomique par Jennifer Doudna et Emmanuelle

Charpentier en 2013 est le système CRISPR-Cas9 (Hsu et al., 2013; Jinek et al., 2012a). Même si de nouveaux systèmes sont utilisés pour réaliser des modifications du génome de cellules eucaryotes, le système CRISPR-Cas9 reste à ce jour le système le plus commun et le plus étudié.

5.4. *Le système CRISPR-Cas9*

Le système CRISPR-Cas9 le plus courant provient de la bactérie Streptococcus pyrogenes (SpyCas9 ou SpCas9). La protéine Cas9 est une grande endonucléase multifonctionnelle (1368 acides aminés) et est composée de deux lobes majeurs : un lobe de reconnaissance (lobe REC) et un lobe nucléase (lobe NUC). Elle est considérée comme la protéine signature des systèmes CRISPR de type 2.

5.4.A. *Fonctionnement général*

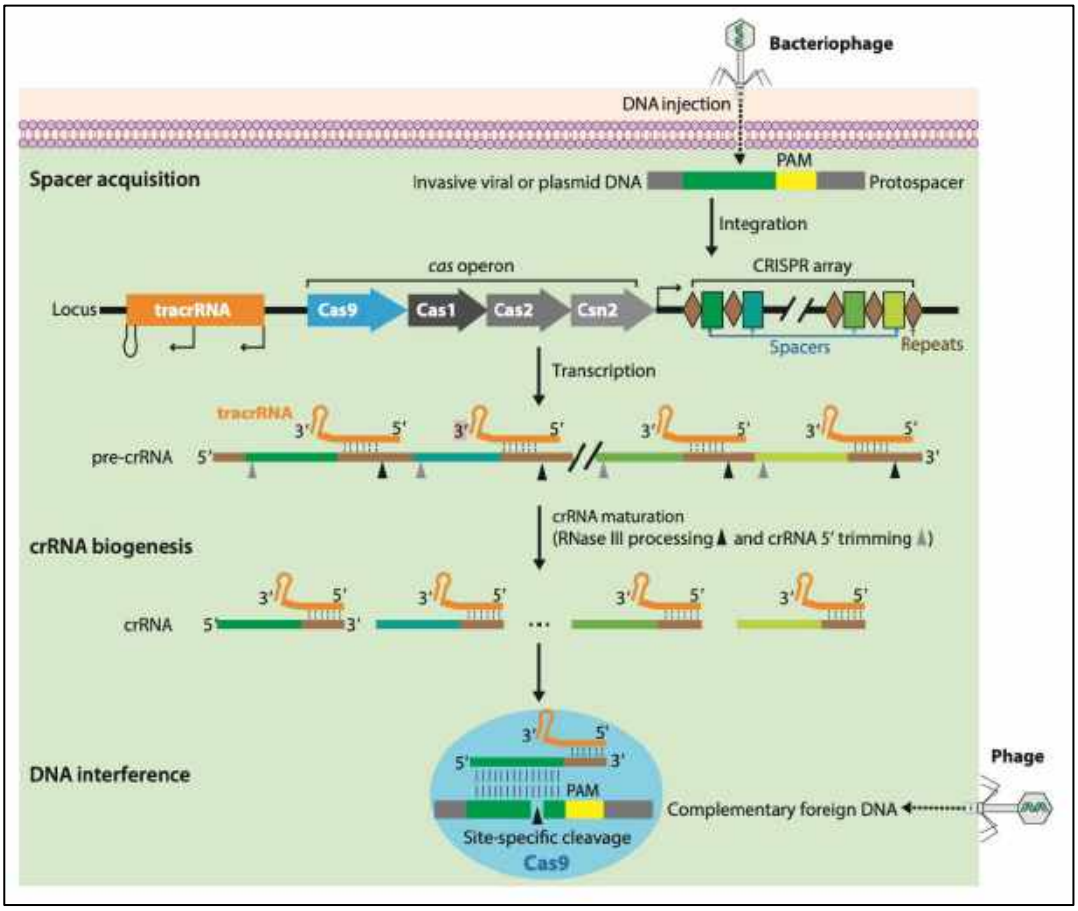

***Figure 29 :** Interférence de l'ADN dépendante de CRISPR-Cas9, impliquée dans l'immunité adaptative bactérienne (D'après F. Jiang & Doudna, 2017).*

Le mécanisme du système CRISPR-Cas9 a été découvert en 2012 simultanément par les équipes d'Emmanuelle Charpentier et de Jennifer Doudna. Le locus CRISPR est très semblable

à celui des autres types. En effet, on retrouve une alternance de séquences répétées, entre lesquelles sont insérées des séquences protospacers, issues d'une précédente infection. La caractéristique majeure de ce système se situe au niveau de la maturation du pré-crARN (**Figure 29**). En effet, les transcrits sont composés de 75 nucléotides dont les 25 premiers situés en 5' sont complémentaires des séquences répétées du pré-crARN : ces transcrits sont appelés tracrARN. L'hybridation du tracrARN avec les séquences répétées du pré-crARN aboutit à la formation d'un ARN double brin. La structure conformationnelle que prend le tracrARN est crucial pour recruter la Cas9. Cet ARN double brin nouvellement formé va permettre de recruter la Cas9 pour ensuite maturer le pré-crARN grâce à l'action de la RNaseIII (Deltcheva et al., 2011). Une fois la maturation achevée, le pré-crARN devient un ARN partiellement double brin constitué du crARN et du tracrARN. La Cas9 intervient pendant le mécanisme de la maturation du pré-crARN, mais aussi pendant le mécanisme d'interférence de la séquence d'ADN étranger via son activité endonucléasique (Hsu et al., 2013).

5.4.B. Le complexe crARN-tracrARN

Le crARN et le tracrARN (**Figure 30**) qui s'hybride et forme un complexe de double ARN, constitue un ARN guide qui permet d'amener directement l'endonucléase Cas9 sur son site de clivage (F. Jiang & Doudna, 2017) :

- Le crARN est constitué du spacer (20 nucléotides) en 5' et de la séquence répétée en 3' (21 nucléotides). La séquence du spacer permet de cibler la séquence cible de l'ADN exogène. Le crARN est donc responsable de la spécificité du système.
- Le tracrARN se caractérise quant à lui par une séquence complémentaire de la séquence répétée du crARN, permettant ainsi leur hybridation. Étant donné sa structure conformationnelle, la suite de la séquence de celui-ci permet le recrutement de la Cas9.

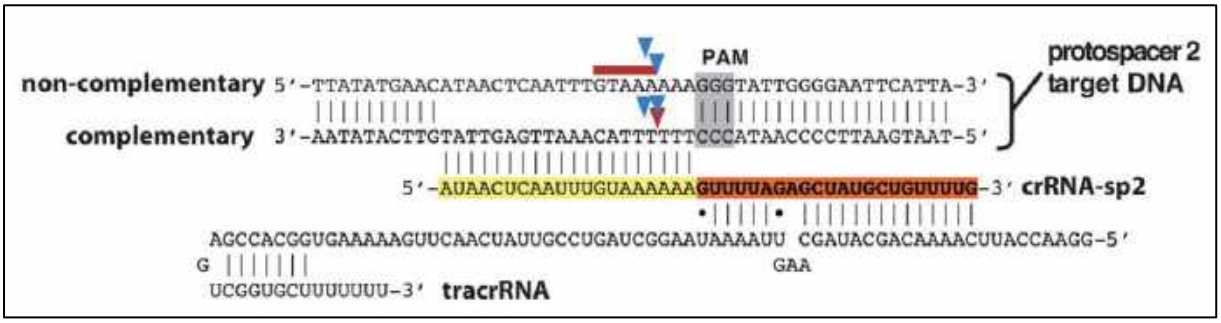

Figure 30 : Représentation schématique de l'ARN guide composé du crARN et du tracrARN (Daprès Jinek et al., 2012).
Les régions du crARN complémentaires au tracrARN sont représentées en orange, et à l'ADN protospacers en jaune. La séquence PAM est représentée en gris.

5.4.C. *Mécanisme d'action du complexe ARNg-Cas9*

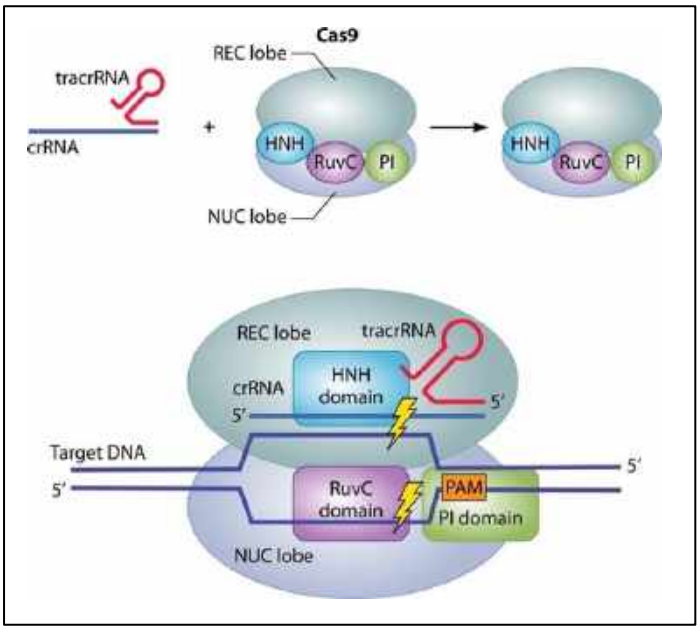

Figure 31 : Mécanisme de clivage de l'ADN par le complexe Cas9-ARN guide (D'après Ishino et al., 2018).

Le complexe formé par l'ARN guide et la Cas9 est appelé ribonucléoprotéine (RNP) (**Figure 31**). La fixation de la Cas9 sur l'ARN guide va induire un changement de conformation de la Cas9, qui va passer d'une forme inactive à une forme active, lui permettant ainsi de reconnaitre la séquence cible, de se lier et de couper l'ADN. Ce complexe RNP actif va scanner l'ADN pour rechercher la séquence cible. En effet, la fixation du complexe sur l'ADN nécessite une complémentarité de bases entre la séquence du spacer de l'ARN guide et du protospacer sur la séquence cible, et d'une séquence PAM adjacente à la séquence ciblée. La séquence PAM est absolument nécessaire pour l'activité de clivage de la Cas9 : une seule mutation présente dans cette séquence inhibe complètement l'activité endonucléasique de la Cas9 (Hsu et al., 2013). La séquence PAM correspond à la séquence 5'-NGG-3' (avec N qui peut correspondre à une des quatre bases azotées) qui est reconnue par le domaine d'interaction du PAM (PAM interacting domain ou PI). Différentes expériences ont permis de montrer que la Cas9 commence dans un premier temps par rechercher la séquence PAM, puis dans un second temps examine ensuite la séquence d'ADN adjacente pour une complémentarité potentielle avec l'ARN guide (Sternberg et al., 2014). Une fois que la Cas9 a trouvé la région ciblée avec une séquence PAM associée à une complémentarité parfaite, celle-ci va pouvoir activer sa fonction endonucléasique par changement de sa conformation. La protéine Cas9 possède deux domaines dans le lobe NUC ayant une activité nucléase (domaines HNH et RuvC). Chaque domaine va couper un brin de l'ADN : le domaine HNH coupe le brin ciblé complémentaire à l'ARN guide,

et le domaine RuvC coupe le brin opposé non ciblé. Ces deux coupures s'effectuent environ 3 bases en 5' de la séquence PAM, et induisent majoritairement des cassures double brin franches (Wang et al., 2016).

5.5. *Le système CRISPR-Cas9 comme outil pour éditer le génome*

5.5.A. *Adaptation du système pour l'édition génomique chez les Eucaryotes*

Les équipes de Jennifer Doudna et Emmanuelle Charpentier ont simplifié le système CRISPR-Cas9 en démontrant que le complexe formé par l'hybridation entre le crARN et le tracrARN pouvait être fusionné pour former un ARN guide plus court et simple brin (**Figure 32**). Ce guide permet l'utilisation du système pour l'édition génique avec une synthèse et une vectorisation simplifiée (Hsu et al., 2013). En effet, l'ARN guide chimérique conserve la même structure et la même fonctionnalité que le complexe crARN-tracrARN : il est constitué de 20 bases en 5' permettant la spécificité du guide, ainsi que d'une structure en épingle en 3' qui mime la conformation du tracrARN permettant le recrutement et l'activation de la Cas9.

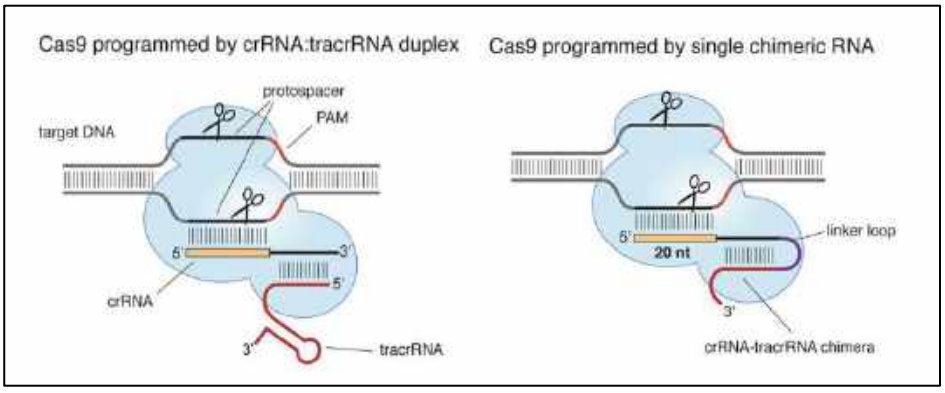

Figure 32 : L'endonucléase Cas9 peut être guidée par un duplex d'ARN (gauche) ou par un guide chimérique (droite) (D'après Jinek et al., 2012).

De manière physiologique, le protospacer est originaire de l'ADN du bactériophage qui infecte la bactérie. Dans le laboratoire, il est possible de choisir spécifiquement la séquence du protospacer pour guider de façon efficace un complexe CRISPR-Cas9 partout où l'on souhaite dans le génome.

5.5.B. *Application du système CRISPR-Cas9 pour l'édition génomique*

5.5.B.i. *Généralités*

Les nucléases programmables ont émergé ces dernières années en tant qu'outils performants pour effectuer de l'ingénierie du génome de manière précise et spécifique au sein d'une cellule vivante (Jinek et al., 2012; Urnov et al., 2010). L'utilisation des endonucléases Cas9 guidées par une molécule d'ARN est devenue la technique de référence pour cibler facilement et effectuer un clivage double brin à une séquence d'ADN spécifique (Cong et al., 2013; Mali et al., 2013).

De manière physiologique dans les cellules, les cassures double brin de l'ADN surgissent naturellement à cause de facteurs externes, tels que des rayonnements ultraviolets ou des carcinogènes par exemple (Marnett, 2000; Rastogi et al., 2010) ; ou par des facteurs internes comme lors du crossing-over au cours de la méiose (Murakami & Keeney, 2008). C'est pour cette raison que les cellules ont mis en place des mécanismes de réparation de cassures d'ADN (Chapman et al., 2012). Il existe deux types de réparation de cassures double brin de l'ADN : la recombinaison homologue et la jonction des extrémités non-homologues (« *Non Homologous End-Joining* » ou NHEJ).

La recombinaison homologue correspond à un mécanisme de réparation de cassures d'ADN double brin extrêmement fidèle mais assez minoritaire, puisque ce type de réparation se produit uniquement lorsque les cellules sont en phase S et G2 du cycle cellulaire (Johnson & Jasin, 2001). La réparation de l'ADN s'appuie sur la présence d'une molécule d'ADN homologue pour répliquer la version non-endommagée au sein du site altéré. Pour ce faire, la chromatide sœur est recrutée au niveau du site de coupure pour service de matrice pendant la réparation (**Figure 33**).

La rectification des cassures double brin de l'ADN par recombinaison homologue après clivage par CRISPR-Cas9 a été adaptée par des équipes de recherche afin de générer des mutations ponctuelles dans le génome (Aird et al., 2018; Richardson et al., 2016). Une séquence d'ADN exogène possédant la mutation d'intérêt et deux bras d'homologie doit se trouver à proximité du site de coupure pour engendrer la recombinaison homologue. Cependant, les taux

de réparation par ce système restent relativement faibles, et il n'est pas optimal dans les cellules de mammifères pour générer des mutations ponctuelles (Komor et al., 2017).

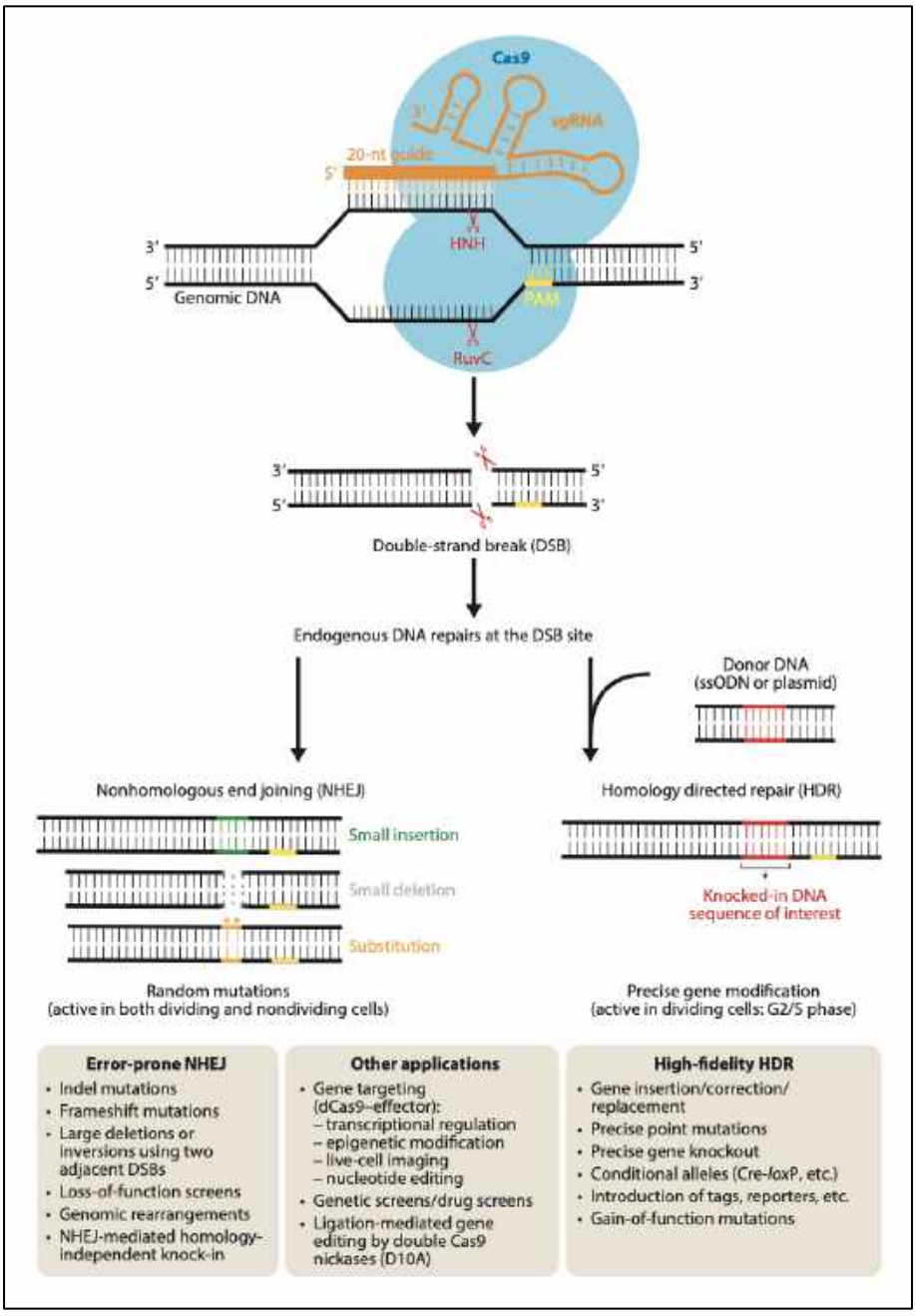

Figure 33 : Les mécanismes de réparation mis en place à la suite de cassures double brin dans l'ADN (D'après F. Jiang & Doudna, 2017).

Le second mécanisme de réparation de coupures double brin, NHEJ (**Figure 32**), est celui qui est le plus fréquemment retrouvé dans les cellules de mammifères lorsqu'elles sont en phase G0/G1 (Komor et al., 2017). À la différence de la recombinaison homologue, le système NHEJ n'a pas besoin de matrice d'ADN complémentaire pour corriger la cassure, mais raboute

directement les deux extrémités cassées (Moore & Haber, 1996). Ce mécanisme n'est pas systématiquement fidèle, et peut engendrer de courtes délétions et insertions, que l'on surnomme indels. Lorsque la cassure a lieu, un couple de protéines Ku70/80 est rapidement recruté au niveau des extrémités clivées, formant ainsi un anneau qui va protéger l'ADN d'une dégradation par exonucléase (Davis & Chen, 2013). L'hétérodimère formé par les protéines Ku70/80 recrute des protéines du complexe NHEJ, ainsi que la kinase DNA-PKcs qui va activer la ligature des deux extrémités par phosphorylation et l'activation de la ligase IV (Chapman et al., 2012; Davis & Chen, 2013). Cette réparation rapide peut soit se réaliser correctement, ou soit induire par erreur l'ajout de 1 à 4 nucléotides (McVey & Lee, 2008). À l'inverse, si le recrutement des protéines Ku70/80 est trop long, les extrémités d'ADN peuvent subir des dégradations par exonucléase et perdent plusieurs nucléotides, créant ainsi des délétions lorsque la réparation NHEJ est terminée (Heidenreich, 2003).

La technologie CRISPR-Cas9 peut être utilisée pour générer des cellules dont l'expression d'un gène est absente. Effectivement, si l'ARN guide cible un exon codant un gène, les indels produits par le mécanisme NHEJ décaleront le cadre ouvert de lecture du gène, aboutissant à l'apparition prématurée d'un codon STOP et empêchant l'expression du gène ciblé (Cong et al., 2013; Mali et al., 2013).

5.5.B.ii. ***Applications***

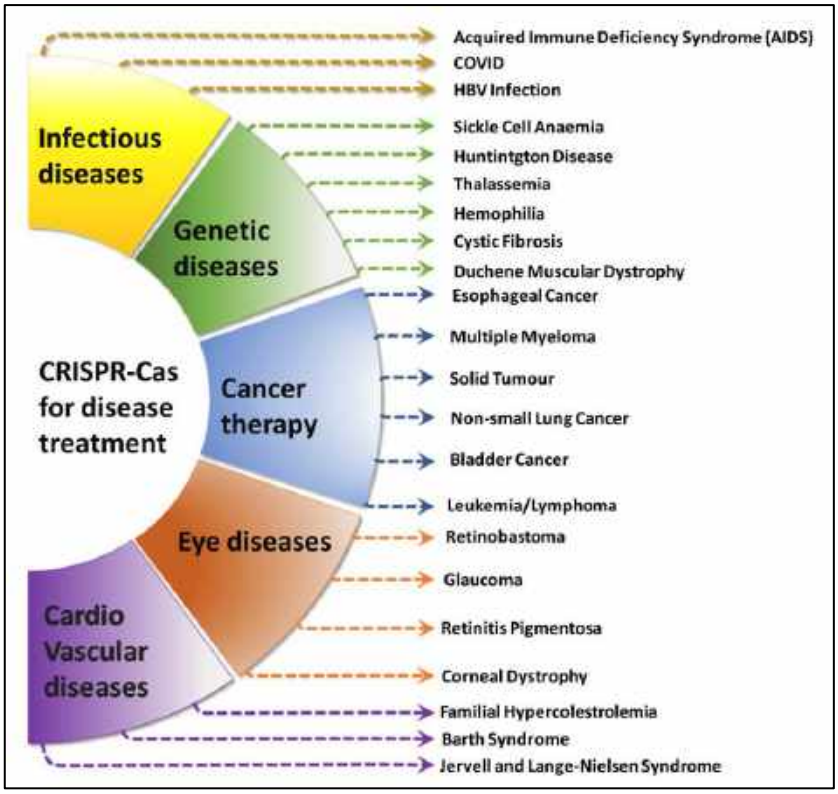

Figure 34 : Les différentes application du système CRISPR-Cas dans le traitement des maladies (D'après Bhatia et al., 2023).

Le faible coût et la facilité de mise en œuvre du système CRISPR-Cas9 en a fait un outil de premier choix pour l'édition génique. Il y a eu un véritable essor de l'utilisation de cette technologie dans de nombreux champs de la société, que ce soit dans l'agriculture, pour les plantes, les animaux, ou encore dans la recherche biomédicale, avec plus récemment des applications médicales via des essais pré-cliniques et cliniques (**Figure 34**). Le système CRISPR-Cas9 a facilité la modélisation de maladies génétiques comme certains cancers, ce qui a permis de mieux comprendre les mécanismes moléculaires à l'origine des processus pathologiques. Des essais cliniques pour des immunothérapies personnalisées sont également en cours.

Partie II : Objectifs et Résultats

La LAL-B correspond au cancer pédiatrique le plus fréquent. Le facteur de transcription PAX5 est décrit comme étant le gardien de l'identité des cellules B, mais est aussi la cible principale des altérations somatiques dans les LAL-B. Les délétions hétérozygotes de *PAX5* sont retrouvées chez un tiers des patients, et sont considérées comme des évènements oncogéniques secondaires dans le développement leucémique. De plus, les mutations ponctuelles somatiques de *PAX5* sont trouvées dans 7% des LAL-B, et sont prédites pour altérer les fonctions de fixation à l'ADN ou de régulation transcriptionnelle. Parmi elles, la mutation somatique *P80R* de *PAX5*, localisée dans le domaine de liaison à l'ADN, correspond à la mutation de PAX5 la plus fréquente des LAL-B. Contrairement aux autres mutations somatiques de *PAX5*, $PAX5^{P80R}$ induit un programme transcriptionnel unique chez les patients, et est définit comme un sous-type oncogénique indépendant, supportant ainsi la notion que la mutation $PAX5^{P80R}$ agit comme une lésion initiatrice dans le développement leucémique. $PAX5^{P80R}$ représente donc une altération génétique d'intérêt pour modéliser les étapes précoces du développement leucémique, et pour identifier ses collaborateurs oncogéniques impliqués dans la progression de la maladie. C'est dans ce contexte que s'est inscrit mon projet de thèse qui a été de modéliser la mutation $PAX5^{P80R}$ afin d'étudier son impact sur le développement normal et pathologique des cellules B. Afin de modéliser la mutation $PAX5^{P80R}$, nous avons transduit des cellules lymphoïdes de foie fœtal provenant de souris Pax5-déficientes avec des vecteurs rétroviraux CTL, PAX5 Wt ou PAX5 P80R. Les expériences *in vitro* démontrent que PAX5 P80R ne permet pas de restaurer de façon efficace la prolifération et l'engagement définitif des cellules $Pax5^{-/-}$ dans le lignage B. Nos études de transplantation nous ont permis de montrer que les cellules exprimant PAX5 P80R arborent un potentiel de prise de greffe aberrant et induisent efficacement le développement de la LAL-B *in vivo*. Sur le plan moléculaire, nos analyses révèlent que la transformation en LAL-B est associée à une sélection de clones leucémiques qui ont acquis des mutations additionnelles affectant la voie de signalisation JAK/STAT. De plus, nos analyses transcriptomiques nous ont orienté vers le facteur de transcription Hif2α, représentant un candidat potentiel impliqué dans le développement de la LAL-B. Enfin, un criblage pharmacologique d'inhibiteurs de Hifα, a révélé l'Acriflavine comme composé relevant, présentant une activité synergique avec le Tofacitinib (inhibiteur de JAK) pour cibler les cellules leucémiques $PAX5^{P80R}$. Ainsi, notre

modèle fournit une nouvelle stratégie pour mimer le processus multi-étapes de la LAL-B, et nous permet de déchiffrer les mécanismes biologiques par lesquels la mutation *PAX5*^{P80R} mène à la transformation leucémique. Ce travail fait actuellement l'objet d'un article que je signe en première auteure, et que je vous présente ci-après.

Modeling B-cell acute lymphoblastic leukemia induced by the PAX5^{P80R} mutation

Manon Bayet[1,2], Vincent Fregona[1,2], Mathieu Bouttier[1,2], Laura Jamrog[1,2], Marie Passet[5], Naïs Prade[1,2,3,4], Stéphanie Lagarde[1,2,3,4], Sylvie Hebrard[1,2], Christine Didier[1,2], Emmanuelle Clappier[5], Éric Delabesse[1,2,3,4], Cyril Broccardo[1,2] and Bastien Gerby[1,2@].

[1]CRCT, Université de Toulouse, Inserm, CNRS, Université Toulouse III-Paul Sabatier, Centre de Recherches en Cancérologie de Toulouse, Toulouse, France.

[2]Equipe Labellisée Ligue Contre le Cancer 2023, Toulouse, France ; Équipe Labellisée Institut Carnot Opale, Toulouse, France.

[3]IUCT-Oncopole, Toulouse, France.

[4]CHU de Toulouse, Toulouse, France.

[5]Hematology Laboratory, Saint-Louis Hospital, Assistance Publique-Hôpitaux de Paris, Paris, France.

Footnotes

@, Address correspondence to Bastien Gerby, CRCT INSERM UMR1037, 2 avenue Hubert Curien, Oncopole, CS 53717, F-31037 TOULOUSE CEDEX 1 (FRANCE)

ORCID: 0000-0002-2657-4200

E-mail address: bastien.gerby@inserm.fr

Phone number: 0033 5 82 74 17 61

Abstract

The transcription factor PAX5 is a main target of genetic alterations in human B-cell precursor acute lymphoblastic leukemia (B-ALL). Among them, the mutation *P80R*, affecting its DNA-binding domain, represents the most frequent *PAX5* point mutation in B-ALL. In contrast to other somatic *PAX5* mutations, *PAX5*^{P80R} induces a unique transcriptional program in patients, and is defined as an initiating lesion in leukemia development. However, the mechanisms by which *PAX5*^{P80R} perturbs the normal B-cell differentiation and the identification of oncogenic relays involved in the malignant progression are ill-known. Using a retroviral complementation approach of *Pax5*-deficient FL cells, we demonstrate at the functional and molecular levels that *PAX5*^{P80R} mutation fails to induce the definitive B-cell commitment *in vitro*, but maintains the normal function of PAX5 in suppressing T-cell development. Moreover, *PAX5*^{P80R} eventually leads to clonal B-ALL transformation after transplantation through the acquisition of secondary mutations in genes of the JAK/STAT and RAS/MAPK pathways. Finally, our analysis of transcriptomic data, combined to pharmacological approaches, reveal the transcription factor Hif2α as a strong candidate in driving B-ALL. Hence, our study provides a new strategy to model the multi-step process of B-ALL and sheds lights on the biological mechanisms by which *PAX5*^{P80R} mutation leads to leukemia.

Keywords

B-cell acute lymphoblastic leukemia; PAX5 alterations; primary oncogenic event; leukemia initiation; oncogenic transformation.

Introduction

Normal B-cell development is permitted by the entry of hematopoietic progenitors into the B-cell lineage transcription program associated with sequential rearrangements of the immunoglobulin genes through V(D)J recombination. Leading to the generation of immune-competent plasma cells, this process can be divided into CLP, pre-pro-B, pro-B, pre-BI, pre-BII, immature B and circulating mature-B cell populations, that correspond to different stages of differentiation (Hardy et al., 2000). At the genomic level, B-lineage commitment is characterized by the rearrangement of the immunoglobin heavy-chain (*IgH*) locus that starts during the transition from the pre-pro-B to the pro-B cell stages through the recombination of the D_H-J_H locus. Then, productive V_H-D_H-J_H recombination leads to the production of the Igμ, a main protein of the pre-B cell receptor (pre-BCR), which promotes the transition from the pro-B to the pre-B cell stage (Melchers, 2005). Finally, successful immunoglobulin light-chain (*IgL*) gene rearrangement results in the emergence of immature IgM^+ B-cells that migrate and finish their maturation in peripheral lymphoid organs (Meffre et al., 2000).

At the molecular level, the developmental progression from early B-cell progenitors to plasma cells is regulated by several transcription factors (Busslinger, 2004b). In particular, the transcription factor PAX5 is an essential regulator for the commitment of lymphoid progenitors to the B-cell lineage by activating the transcription of B-cell specific genes and simultaneously, by suppressing alternative lineage programs (Nera et al., 2006; Nutt et al., 1999b; Souabni et al., 2002b). Pax5 is exclusively expressed in the B-cell lineage of the hematopoietic system and pioneer work demonstrated that embryonic B-cell differentiation is arrested at early stages in *Pax5*$^{-/-}$ mice, unraveling its critical role in B-cell commitment (Urbanek et al., 1994). In addition, functional experiments demonstrated that *Pax5*$^{-/-}$ B-cells from fetal liver (FL) have the capacity to differentiate towards several hematopoietic lineages, either *in vitro* when cultured with appropriate growth factors, or *in vivo* after transplantation (A. G. Rolink et al., 1999b). Remarkably, Pax5 inactivation in mature B-cells allowed for their reprogramming into functional T-cells through a dedifferentiation process into uncommitted progenitors (Cobaleda, Jochum, et al., 2007b). These studies not only revealed the plasticity of committed B-cells but also elected Pax5 as a guardian of B-cell identity (Cobaleda, Schebesta, et al., 2007c).

PAX5 is described as the main target of genetic alterations in B-cell acute lymphoblastic leukemia (B-ALL), which have not the same impact on the leukemic process. *PAX5* was initially identified as a haploinsufficient tumor suppressor gene in patients. Indeed, heterozygous deletions of *PAX5* are found in one-third of cases and are considered as secondary oncogenic events in the leukemogenesis process (Familiades, Bousquet, Lafage-Pochitaloff, Bene, et al., 2009; Mullighan et al., 2007a; Nebral, Denk, Attarbaschi, Konig, et al., 2009). Moreover, *PAX5* is also rearranged at a frequency of 2-3% in human B-ALL, being fused to several fusion partners such as the transcription factors ETV6 and FOXP1, the chromatin regulators NCoR1 and BRD1, the protein kinase JAK2, the estrogen-related receptor

ESRRB and the extracellular matrix protein PAX5::ELN (Bousquet et al., 2007b; Coyaud et al., 2010a; Medvedovic et al., 2011b; Nebral, Denk, Attarbaschi, Konig, et al., 2009). In contrast to *PAX5* deletions, *PAX5* fusions are considered as primary oncogenic events in B-ALL patients, the first and the most frequently described being *PAX5::ETV6* (Cazzaniga et al., 2001). Finally, *PAX5* point mutations are found in about 7% in B-ALL patients (Familiades, Bousquet, Lafage-Pochitaloff, Bene, et al., 2009; Mullighan et al., 2007a) and are predicted to result in lost or altered DNA-binding or transcriptional regulatory functions (An et al., 2008; Mullighan et al., 2007a). While our group and others have reported inherited *PAX5* mutations (Duployez et al., 2021; Shah et al., 2013), somatic *PAX5* mutations are mostly found and represent a hallmark of B-ALL. In particular, the somatic mutation *P80R* of *PAX5* (*PAX5*^{P80R}) was identified within its DNA-binding domain, and is the most frequent *PAX5* point mutation (Familiades, Bousquet, Lafage-Pochitaloff, Bene, et al., 2009; Mullighan et al., 2007a). In contrast to other somatic *PAX5* mutations, *PAX5*^{P80R} induces a unique transcriptional program in patients and defines an independent B-ALL subtype (Bastian, Schroeder, Eckert, Schlee, Tanchez, Kampf, et al., 2019; Gu et al., 2019b; Passet, Boissel, Sigaux, Saillard, Bargetzi, Ba, Thomas, Graux, Chalandon, Leguay, Lengline, et al., 2019). This finding supports the notion that *PAX5*^{P80R} mutation acts as an initiating lesion in B-ALL. Therefore, *PAX5*^{P80R} mutation represents a genetic alteration of interest to model the early steps of the B-ALL development and to identify its oncogenic collaborators involved in malignant progression (Gu et al., 2019b).

Here, using a retroviral complementation approach of *Pax5*-deficient FL cells, we demonstrate that *PAX5*^{P80R} mutation fails to induce the definitive B-cell commitment *in vitro* and eventually leads to clonal B-ALL transformation *in vivo*. Thus, ectopic expression of PAX5-P80R mutant recapitulates the multi-step process of B-ALL after transplantation, including acquired secondary mutations in the JAK/STAT and RAS/MAPK pathways. At the molecular level, we demonstrate that *PAX5*^{P80R} mutation generally antagonize the normal functions of PAX5 in pre-leukemic B-cells, but is still able to repress normal T-cell development. Finally, we identify the hypoxia-inducible factor Hif2α as a strong candidate in driving leukemogenesis in our model.

Results

PAX5^{P80R} mutation partially perturbs the normal PAX5 functions *in vitro*.

Combinations of cell surface markers were established for the phenotypic characterization of the different B-cell subsets in mice (Hardy & Hayakawa, 2001b; A. Rolink & Melchers, 1996). We therefore established a multiparametric staining by FACS integrating nine markers to cover the steps of the B-cell differentiation from CLP to mature B-cell subsets (**Figures S1A-C** and **Table S1**). To precisely identify the stage of differentiation blockade induced by *Pax5* deletion, we took advantage of this multiparametric FACS staining combined to an unsupervised clustering approach by UMAP (*Uniform Manifold Approximation and Projection*) that allow to visualize the natural phenotypic progression of lymphoid cells throughout the B-cell differentiation (**Figure 1A** and **Figure S1D**). Thus, Fetal liver (FL) cells from 17.5-day-old *Pax5*$^{-/-}$, *Pax5*$^{+/-}$ and *Pax5*$^{+/+}$ mouse embryos were co-cultured on OP9 stromal cells (Cresson, Peron, et al., 2018; Duployez et al., 2021) and *in vitro* cell expansion of each B-cell subset was monitored. Since B lymphopoiesis is arrested prior to the appearance of CD19^{+} progenitors in the fetal liver of *Pax5*-deficient embryos (Nutt, Urbanek, et al., 1997), we observed that expanded cells from *Pax5*$^{-/-}$ FL were blocked at the CLP/pre-pro-B stages (**Figures 1A, B**), as expected. In contrast, expanded cells from *Pax5*$^{+/-}$ and *Pax5*$^{+/+}$ FLs were both committed in the pro-B/pre-BI stages, while B-cell differentiation efficiency toward the pre-BI stage seems dependant of the Pax5 dosage (**Figures 1A, B**). Together, our approach confirms numerous previous findings highlighting the critical functions of Pax5 in the definitive commitment toward the B-cell lineage (Cobaleda, Schebesta, et al., 2007c; Nutt et al., 1999b; Urbanek et al., 1994). In addition, our results render *Pax5*-deficient fetal liver cells as a relevant model to evaluate B-cell commitment.

Thus, to address the impact of *PAX5*^{P80R} mutation on the B-cell commitment and differentiation, we used a complementation approach by transducing *Pax5*$^{-/-}$ FL cells with retroviral vectors expressing either empty MIG-GFP (CTL) or MIG-PAX5 Wt (PAX5 Wt) or MIG-PAX5 P80R (PAX5 P80R) (**Figure 2A** and **Figure S2A**). Our first following functional experiments aimed to compare the ability of PAX5 and PAX5 P80R to rescue the blockade of B-cell commitment in *Pax5*-deficient FL cells when co-cultured on OP9 stromal cells (**Figure 2A**). We observed that PAX5 Wt expression significantly increased the cell growth of *Pax5*$^{-/-}$ cells whereas PAX5 P80R expression did not (**Figure 2B**). Moreover, the phenotypic characterization of co-cultured cells indicated that PAX5 Wt efficiently rescued their differentiation from the CLP/pre-pro-B stages toward the pro-B and then the pre-BI/pre-BII stages (**Figures 2C, D**). This phenotypic evolution was associated with the increase of CD93 expression (**Figure S2B**) and with the progressive acquisition of the CD19 and Bp1 surface markers (**Figure 2C**). In contrast, *Pax5*$^{-/-}$ cells expressing PAX5 P80R mutant did not progress through the differentiation and remained blocked at the CLP/pre-pro-B stages (**Figures 2C, D**). However, we observed a significant progression of PAX5 P80R-expressing cells toward the pre-pro-B stage (**Figures 2C, D**) characterized by B220 and CD93

upregulation (**Figure 2C** and **Figure S2B**), as compared with *Pax5*$^{-/-}$ cells expressing the empty CTL vector. As CLP/pre-pro-B fractions are described to sustain T lineage potential *in vitro* (Rumfelt et al., 2006), we next asked the question whether PAX5 P80R-expressing cells still have the capacity to generate T-cells. Thus, we co-cultured *Pax5*$^{-/-}$ FL cells transduced with CTL, PAX5 Wt or PAX5 P80R vectors on stromal cells expressing the most physiological NOTCH1 ligand, delta-like 4 (DL4) (Gerby, Veiga, Krosl, Nourreddine, Ouellette, Haman, Lavoie, Fares, Tremblay, Litalien, Ottoni, Kosic, Geoffrion, Ryan, Maddox, Chagraoui, Marinier, Hebert, et al., 2016; Koch et al., 2008; Mohtashami et al., 2010) (**Figure S2C**). As expected, unmodified *Pax5*$^{-/-}$ FL cells transduced with CTL vector efficiently produced Thy.1^{+} cells during the co-culture on MS5-DL4 (**Figures 2E, F**) and not on MS5-CTL stromal cells (**Figures 2F** and **Figure S2D**). However, we observed that PAX5 Wt as well as PAX5 P80R mutant abrogate T-cell development on MS5-DL4 (**Figures 2E, F**).

Collectively, our *in vitro* approaches demonstrate that while PAX5 P80R mutant fails to rescue the definitive B-cell commitment of *Pax5*-deficient FL cells, it maintains the normal function of PAX5 in suppressing T-cell development.

PAX5^{P80R} mutation induces B-ALL development *in vivo*.

To address the question whether the differentiation blockade induced by *PAX5*^{P80R} mutation is associated with a pre-leukemic stage, co-cultured *Pax5*$^{-/-}$ FL cells transduced with CTL, PAX5 Wt or PAX5 P80R vectors were serially transplanted in recipient mice (**Figure 2A**). First, we observed that unmodified *Pax5*$^{-/-}$ FL cells transduced with CTL vector were able to engraft in the bone marrow (BM), the spleen and the thymus of primary recipients (**Figure 3A**). Interestingly, CTL donor-derived cells maintained their CLP/pre-pro-B phenotype (B220$^{low/-}$CD19^{-}) in the BM (**Figure 3B**) and efficiently differentiated toward the T-lineage into the thymus (**Figure 3B**). This observation reinforces the established notion that *Pax5*-deleted cells are able to self-renew and differentiate into several hematopoietic cell types, including T cells (Hoflinger et al., 2004; Nutt et al., 1999b; A. G. Rolink et al., 1999b; Schaniel et al., 2002b). In addition, PAX5 Wt overexpression abrogated the self-renewal activity of *Pax5*$^{-/-}$ FL cells and prevented their ability to engraft and to produce T-cell into the thymus (**Figure 3A**). However, the engraftment potential was drastically enhanced by the PAX5 P80R mutant that eventually led to B-ALL development in primary mice, characterized by the presence of leukemic blasts in the BM that had the capacity to spread into the thymus (**Figures 3A, B**). Of note, PAX5 P80R donor-derived cells did not produce T-cells within the thymus of recipient mice (**Figure 3B**), corroborating our results *in vitro* (**Figures 2E, F**). The leukemia development was also associated with a splenomegaly characterized by an important infiltration of donor-derived cells in the spleen (**Figures 3A, C** and **Figure S3A**). Interestingly, B-ALL PAX5 P80R cells exhibited a pre-pro-B-like immunophenotype (B220^{+}CD19^{-} IgM^{-}) in the majority of mice (n=6/9, **Figure 3B** and **Figure S3B**, *left panel*) but in some cases, leukemic cells acquired a significant proportion of CD19 and of IgM surface markers *in vivo*

(n=3/9, **Figure S3B**, *right panel*). These observations suggested that leukemic cells were frequently transformed before the definitive commitment toward the B-cell lineage, but also revealed that clonal transformation induced by PAX5 P80R can be associated in few cases with a more mature immunophenotype. Our secondary transplantations revealed that CTL donor-derived cells maintained their self-renewal capacity in the BM and their ability to produce T-cells in the thymus (**Figure 3D** and **Figure S3C**). Furthermore, our results showed that leukemic PAX5 P80R cells quickly propagate in the BM and the thymus of the secondary recipients (**Figure 3D**, *upper panel* and **Figure S3C**), with a massive infiltration in the spleen (**Figure 3D**, *lower panel*). Finally, using the intracellular staining of PAX5 with an antibody recognizing both the human and the murine forms of the protein, we controlled *in vivo* that the expression of PAX5 P80R driven by the transgene in B-ALL cells was similar to that of murine Pax5 in normal B-cells (**Figure 3E**). Together, our results indicate that $PAX5^{P80R}$ mutation perturbs the normal functions of PAX5 and triggers B-ALL *in vivo*.

Clonal transformation and collaborating events of $PAX5^{P80R}$ mutation.

We next addressed the differentiation blockade caused by $PAX5^{P80R}$ mutation at the molecular level. Combining quantitative RT-PCR and targeted next generation sequencing (NGS), we first controlled that *PAX5 Wt* and *PAX5 P80R* transgenes were expressed at similar levels in modified $Pax5^{-/-}$ FL cells after co-culture and that *PAX5 P80R* transgene expression was maintained in B-ALL cells after transplantation in primary and secondary recipients (**Figure 4A**). Moreover, we observed that PAX5 P80R mutant failed to activate the two common Pax5 target genes *CD19* and *CD79a* both *in vitro* and *in vivo* (**Figure 4B**), corroborating at the transcriptional level our observation on the B-cell differentiation (**Figure 2C**). Then, to determine the rearrangements status of the *IgH* locus of modified $Pax5^{-/-}$ FL cells *in vitro* and *in vivo*, we performed a multiplex PCR combined to NGS on genomic DNA to quantify simultaneously D_H-J_H and V_H-D_HJ_H rearrangements (**Table S2**). Interestingly, this approach revealed that both PAX5 Wt and PAX5 P80R overexpression significantly increased the diversity of D_H-J_H rearrangements of $Pax5^{-/-}$ FL cells *in vitro*, as compared to unmodified CTL cells (**Figure 4C** and **Figure S4A**). This result corroborates the phenotypic progression of PAX5 P80R-expressing cells from the CLP toward the pre-pro-B stage (**Figure 2C, D** and **Figure S2B**), in which the recombination of the D_H-J_H locus starts (**Figure S1A**). Thus, while PAX5 P80R mutant failed to drive the definitive B-cell commitment of *Pax5*-deficient FL cells *in vitro*, it was still able to trigger the early steps of differentiation. Furthermore, the data revealed prominent D_H-J_H rearrangements after transformation *in vivo* in B-ALL cells exhibiting a pre-pro-B-like immunophenotype (**Figure 4C** and **Figures S4A and S3B**). Interestingly, while V_H-D_HJ_H rearrangements have been observed neither with PAX5 Wt nor with PAX5 P80R overexpression *in vitro*, we noticed in few cases that PAX5 P80R induced the clonal transformation of a B-cell progenitor that has rearranged both D_H-J_H and V_H-D_HJ_H segments of the *IgH* locus *in vivo* (**Figure S4B**). As expected, this corresponded to leukemic cells that exhibited CD19 and of IgM surface markers (**Figure S3B**).

Our data revealed that *in vitro*-derived PAX5 P80R cells exhibited a polyclonal profile for D_H-J_H rearrangements, similar to that of PAX5 wt cells (**Figure 4C**), confirming their pre-leukemic state before transplantation. Furthermore, a minimum delay of 21 weeks is required to induce an efficient clonal selection (**Figure 4C**) and B-ALL development (**Figure 3A-C**) after transplantation in primary recipients. Thus, these observations suggest that the clonal transformation that occurs *in vivo* is associated with the acquisition of secondary mutations. To further identify the additional genetic alterations that cooperate with $PAX5^{P80R}$ in the leukemogenesis process, we performed the targeted sequencing of several exons of *Ptpn11*, *Kras*, *Jak3* and *Pax5* (**Table S2**), four genes recurrently mutated in B-ALL patients (Jamrog, Chemin, Fregona, Coster, Pasquet, Oudinet, Rouquie, et al., 2018; Mullighan et al., 2007a) and in other oncogene-induced B-ALL models (Duque-Afonso et al., 2015a; Fregona et al., 2021a; Gu et al., 2019b; Jamrog, Chemin, Fregona, Coster, Pasquet, Oudinet, Rouquie, et al., 2018; van der Weyden et al., 2015a). While no alterations were detected in *Kras* and *Pax5* genes, we identified frequent *Ptpn11* and *Jak3* mutations in leukemic PAX5 P80R cells from primary and secondary recipients (**Figure 4D**). Moreover, the absence of those mutations in pre-leukemic *in vitro*-derived PAX5 P80R cells (**Figure 4D**) confirmed that clonal transformation occurred *in vivo* after transplantation. The above results suggest that the ectopic activation of IL7r/JAK-STAT pathway favors the survival of PAX5 P80R B-ALL cells. Thus, we analysed this pathway by using a phosphoflow cytometry approach after *ex vivo* ligand stimulation. Interestingly, ligand stimulation of IL7r efficiently induced the phosphorylation of Stat5 in both *Jak3*-mutated (#1301) and *Jak3*-Wt (#1300) PAX5 P80R B-ALLs in a similar way to unmodified CTL cells, and which is abrogated in the presence of tofacitinib (TOFA), a well-known JAK-STAT inhibitor (**Figure 4E**). Accordingly, our *in vitro* dose-responses of TOFA showed that all of them were sensitive to JAK-STAT inhibition (**Figure 4F**).

Collectively, our findings indicate that $PAX5^{P80R}$ mutation induces a partial loss-of-function of *PAX5*, prevents the definitive B-cell commitment and eventually leads to clonal B-ALL transformation (**Figure 4G**). Furthermore, our work provides a robust *in vivo* approach for B-ALL induced by the primary $PAX5^{P80R}$ mutation that recapitulates the multi-step process of the human disease, including acquired secondary mutations in genes of the JAK/STAT pathway. Finally, although JAK/STAT signaling represents a logical target for therapeutic intervention in B-ALL (Downes et al., 2021; Mullighan et al., 2009), our results suggest that its physiological activation and functions in the early steps (from CLP to pre-BII stages) of B-cell development (Clark et al., 2014) does not make it a specific target.

Hif2α as a gene candidate in driving B-ALL.

Engineered mouse models in which are activated PAX5 mutants represent valuable tools to understand the biological mechanisms by which a primary oncogenic event perturbs the B-cell development and drives B-ALL transformation (Fregona et al., 2021a). As representative example, we

previously reported a transgenic line expressing the fusion protein PAX5::ELN that represents an accurate B-ALL modelization revealing a pre-leukemic phase and mimicking the key features of the human disease (Jamrog, Chemin, Fregona, Coster, Pasquet, Oudinet, Rouquie, et al., 2018). To evaluate the oncogenic potential of *PAX5*^{P80R} mutation, Mullighan and colleagues generated a transgenic model expressing *PAX5*^{P80R} from the *Pax5* locus (Gu et al., 2019b). The mice efficiently developed B-progenitor leukemia with a pre-pro-B-like immunophenotype (B220^{+}CD19^{-}), similar to that observed in our B-ALL PAX5 P80R cells (**Figure 3B** and **Figure S3B**, *left panel*), further validating our retroviral complementation approach. This observation is in stark contrast with the blockade at the pro-B/pre-B stages that occurs in our PAX5::ELN-induced B-ALL model (Jamrog, Chemin, Fregona, Coster, Pasquet, Oudinet, Rouquie, et al., 2018), as well as in transgenic mice expressing PAX5::ETV6 (Smeenk et al., 2017b). To identify shared gene candidates involved in the B-ALL development induced by those PAX5 mutants, we determined the overlap the list of genes that were activated by *PAX5*^{P80R} (Gu et al., 2019b), *PAX5::ELN* (Jamrog, Chemin, Fregona, Coster, Pasquet, Oudinet, Rouquie, et al., 2018)and *PAX5::ETV6* (Smeenk et al., 2017b) in the three transgenic lines and we found ten common genes (**Figure 5A,** *left panel*). Among them, only the hypoxia-inducible factor *Hif2α* and the endosialin *CD248* were not expressed in the normal B-cell differentiation in mice (*i.e.* multi-lymphoid progenitors (MLPs) and committed B-cells ; **Figure 5A,** *right panel*) and were ectopically expressed in B-ALL patients (**Figure S5A**), based on available RNA-sequencing data from the Immunological Genome Project (ImmGenn) consortium (https://www.immgen.org/) and from (Gu et al., 2019b), respectively. Interestingly, the analysis of the event-free survival (EFS) curves (Gu et al., 2019b) showed that the clinical outcome was significantly affected for B-ALL patients with high level of *HIF2α* or with high level of *CD248* (**Figure S5B**), making these two genes as good candidates in driving B-ALL. Finally, we observed that *HIF2α* and *CD248* expression in leukemic cells from patients harboring the *PAX5*^{P80R} mutation and other PAX5 alterations (*i.e.* PAX5alt subgroup), including the frequent *PAX5-ETV6* chromosomal rearrangements, were significantly higher than that of normal B-cells (**Figure S5C**). We noticed that *HIF2α* and *CD248* expression were particularly increased in the only *PAX5::ELN* patient of the cohort and were also significantly high in patients exhibiting the *TCF3::PBX1* and *BCR::ABL1* rearrangements. However, the two most frequent B-ALL genetic subgroups (*i.e. ETV6::RUNX1* and hyperdiploid patients) expressed higher levels of *HIF2α* but not of *CD248,* as compared with normal B-cells (**Figure S5C**). Collectively, our observations suggest that *Hif2α* ectopic activation is a common and an oncogene-independent feature of B-ALL cells.

Thus, we confirmed that PAX5 P80R-expressing cells *in vivo* from our retroviral approach and PAX5-ELN-expressing cells from our mouse model both ectopically express *Hif2α*, as compared to their respective controls (**Figures 5B, C**). We took advantage of our *PAX5::ELN* transgenic model (*PE*^{tg}), in

which *Hif2α* is drastically upregulated (**Figure 5C**), to study the effect of *Hif2α* loss-of-function by CRISPR strategy (**Figure 5D**). We generated *PE*^{tg}*Cas9*^{tg} mice by breeding *PE*^{tg} mice with *Rosa26-Cas9*^{tg} mice that express constitutively the Cas9 endonuclease (Tzelepis et al., 2016), and we designed two sgRNAs (sgHif2α T8 and sg Hif2α T12) targeting the genomic region encoding the exon 2 of *Hif2α* (**Table S2**). Then, B-cell progenitors from *PE*^{tg}*Cas9*^{tg} mice were purified (**Figure S6A**) and transduced with lentiviral vectors encoding sgHif2α T8 and sgHif2α T12 or a non-targeted control sgRNA (sgCTL). Transduced *PE*^{tg}*Cas9*^{tg} GFP^{+} cells were purified (**Figure S6B**) and we performed functional *in vitro* experiment (**Figure 5D**). Our results indicated that the expansion and the viability of *PE*^{tg}*Cas9*^{tg} GFP^{+} cells transduced with sgHif2α T8 and T12 were significantly reduced compared to sgCTL, as assessed in co-cultured assay (**Figure 5E** and **Figure S6C**) and this was associated with a counter selection of GFP$^{low/neg}$ residual viable cells during the co-culture (**Figure S6D**). In parallel, we verified that *Hif2α* expression was decreased by the two sgRNA (**Figure 5F**), caused by the induction of several genomic insertions/deletions (InDels) in the targeted *Hif2α* locus (**Figure S6E**). Finally, our transplantation experiments (**Figure 5D**) showed that *Hif2a* inhibition diminishes the engraftment capacity of PAX5-ELN-expressing B-cells (**Figure 5G**), which is associated with a counter selection of GFP^{low} residual cells *in vivo* (**Figure 5H**). Together, our results indicate that *Hif2a* is required to sustain the viability and the proliferation *in vitro* and *in vivo* of *PAX5::ELN*-expressing B-cells.

Genomic editing of *Hif2α* does not impact normal hematopoietic reconstitution of LSK cells.

The role of *Hif2α* in the maintenance of HSC properties is debated in the literature, possibly due to the different experimental approaches both in human cells and mouse models (Guitart et al., 2013a; Huang et al., 2018; Rouault-Pierre et al., 2013; Vyas, 2014). Since we observed that *Hif2α* is expressed in the LT-HSC compartment of hematopoietic stem/progenitor cells (HSPCs) (**Figure 5A,** *right panel*), we investigated whether *Hif2α* is essential for murine HSC maintenance by applying our CRISPR-Cas9 strategy. We explored the effect *in vitro* and *in vivo* of *Hif2α* loss-of-function on Lineage^{-}Sca1^{+}Kit^{+} (LSK) cells (**Figure 6A**), a population enriched in HSPCs (Miller et al., 2008). Cas9-expressing LSK cells were purified (**Figure 6B**) and transduced with sgCTL, sgHif2α T8 and T12 lentiviral vectors. The sgHif2α T8 and T12 allowed for an efficient transduction and genomic editing of LSK cells as revealed by the percentage of GFP^{+} cells and the rate of InDels in the *Hif2α* locus 11 days after *ex vivo* expansion in methylcellulose, respectively (**Figures 6C, D**). This was associated with the inhibition of *Hif2α*, at the mRNA and the protein levels (**Figures 6E, F**). Despite Hif2α inhibition in LSK-derived cells, the numbers of total, CFU-GEMM, CFU-GM, CFU-G, CFU-M and BFU-E colonies in methylcellulose were similar between sgCTL, sgHif2α T8 and T12 conditions (**Figure 6G**). This result indicates that *Hif2α* deletion does not affect the clonogenic activity of hematopoietic progenitors.

In parallel, Cas9-expressing LSK cells (CD45.2$^+$) transduced with sgCTL, sgHif2α T8 and T12 vectors were transplanted into syngenic recipient mice (CD45.1$^+$) (**Figure 6A**). The analysis of engrafted donor-derived cells (CD45.2$^+$GFP$^+$) in recipient BM 5 and 16 weeks after transplantation revealed that *Hif2a* deletion neither affected the short-term and the long-term engraftment potential (10 to 13%) of normal LSK cells (**Figure 6H**), nor their multipotent hematopoietic reconstitution (**Figure 6I**). Finally, the presence of about 13% InDels in sgHif2α T8 and T12 engrafted BM confirmed that donor-derived hematopoietic cells were still edited for *Hif2α* 16 weeks after transplantation (**Figure 6J**). As described previously using *Hif2α*-deficient HSCs (Guitart et al., 2013a), our results using CRISPR-Cas9 strategy reinforce the notion that Hif2α is dispensable for HSC functions and for the normal hematopoietic development in mouse.

Chemical screening of *Hifα* inhibitors identifies acriflavine as potent B-ALL drug.

Although the role of Hif2α was not described in B-ALL, our above results place Hif2α as an interesting target to impact the leukemia development without affecting normal B-cell and HSPC functions. Therefore, we designed a miniaturized co-cultured system that favored the viability and the proliferation of primary leukemic cells in 96-well format, and that allowed for a robust and reproducible small-molecule screening (**Figures 7A, B**). Using this protocol, we screened in duplicate a library of 19 compounds defined as potential *Hifα* inhibitors, on three PAX5 P80R and four *PAX5::ELN* B-ALL (**Figures 7A, B**). Compounds inducing reproductively more than 30% inhibition of PAX5 P80R and/or *PAX5::ELN* leukemic cell viability were defined as hits (**Figure 7B**) and we identified 5 potent drugs (**Figure 7C**). Then, we took advantage of the two REH (*ETV6::RUNX1*) and 697 (*TCF3::PBX1*) human B-ALL cell lines in which Hif2α expression is high to select the most efficient compound targeting Hif2α (**Figures S7A**). Strikingly, acriflavine (ACF) was the only compound for which we observed an efficient (~80%) inhibition of Hif2α protein levels in both cell lines (**Figures S7A, B**). In addition, dose-response experiments of ACF on primary PAX5 P80R B-ALLs revealed an IC50 of ~400 nM (**Figure 7D**) associated with an efficient inhibition of Hif2α expression (**Figures 7E, F**). Interestingly, we observed that the treatment with TOFA, that inhibit efficiently Stat5 phosphorylation (**Figure 4E**), did not modify Hif2α protein levels in the same experimental conditions (**Figures S7C, D**).

Finally, we explored the effect of ACF on the human B-ALL cell lines REH and 697, as well as on patient-derived xenograft models (PDX #112 and PDX #214) that we generated by transplantation of leukemic blasts from two "*de novo*" P80R B-ALL patients into immunodeficient NOD.*Cg-Prkdc^{scid}Il2rg^{tmWjl}* (NSG) mice. We observed that B-ALL cell lines and the P80R B-ALL PDXs were all sensitive to ACF (**Figure 7G**). At the molecular level, we confirmed that ACF, but not TOFA, inhibits Hif2α expression of leukemic cells from patients in a dose-dependent manner (**Figures 7H, I** and **Figure S7E**). Conversely, we observed that in contrast to TOFA, ACF does not have the capacity to abrogated Stat5

phosphorylation induced by ligand stimulation of IL7r (**Figure S7F**). Together, our pharmacological approach identifies ACF as a potent B-ALL drug and demonstrates that Hif2α and JAK-STAT are two independent signaling pathways in B-ALL.

Discussion

Although the critical functions of Pax5 in normal B-cell development are well established, the question of whether genetic alterations involving *PAX5* perturb the differentiation of B-cell progenitors and lead to B-ALL remains to be fully explored (Fregona et al., 2021a). In mice, the tumor suppressor role of *Pax5* has been revealed by mutagenesis approach (Dang et al., 2015b), through the modulation of other key transcription factors such as Ebf1 (M. A. Prasad et al., 2015; Ramamoorthy, Kometani, Herman, Bayer, Boller, Edwards-Hicks, Ramachandran, Li, Klein-Geltink, Pearce, Grun, et al., 2020), Ikzf1 (Chan, Chen, Braas, Lee, Xiao, Geng, Cosgun, Hurtz, Shojaee, Cazzaniga, Schjerven, Ernst, Hochhaus, Kornblau, Konopleva, Pufall, Cazzaniga, Liu, Milne, Koeffler, Ross, Sanchez-Garcia, et al., 2017) or Stat5 (Heltemes-Harris et al., 2011b), by infection exposure (Isidro-Hernandez et al., 2020; Martin-Lorenzo et al., 2015; Rodriguez-Hernandez et al., 2019) or by altering the gut microbiome (Vicente-Duenas et al., 2020). Although still limited, the development of animal models and/or *in vivo* approaches to study the impact of primary oncogenic *PAX5* fusions or mutations on B-ALL has significantly increased over the past years (Duployez et al., 2021; Fregona et al., 2021a; Gu et al., 2019b; Jamrog, Chemin, Fregona, Coster, Pasquet, Oudinet, Rouquie, et al., 2018; Jurado et al., 2022; Smeenk et al., 2017b). In particular, while transgenic lines expressing *PAX5-ETV6* and *PAX5-FOXP1* from the *Pax5* locus failed to drive B-ALL on their own, it has been shown that both fusions perturbed the early stages of B-cell differentiation (Smeenk et al., 2017b). Furthermore, the oncogenic function of *PAX5-ETV6* was revealed in combination with the loss of *Cdkn2a/b* tumor suppressor genes (Smeenk et al., 2017b). Recently, mice expressing PAX5-JAK2 fusion protein from the *Pax5* locus have been also generated. In contrast to *PAX5-ETV6* mice, *PAX5-JAK2* mice rapidly developed an aggressive B-ALL without introducing complementary oncogenic event (Jurado et al., 2022).

Element de discussion : Hif2a semble etre un gene candidat activé par les oncogenes PAX5 mais independant du blocage de differentiation qu'ils induise (stress oncogenique)

The role of *Hif2α* in the maintenance of HSC properties is debated in the literature, possibly due to the different experimental approaches both in human cells and mouse models (Guitart et al., 2013a; Huang et al., 2018; Rouault-Pierre et al., 2013; Vyas, 2014).

Experimental procedures

Mice

Pax5$^{-/-}$ mice were obtained by breeding *Pax5*$^{+/-}$ mice (Urbanek et al., 1994) which were kindly provided by Meinrad Busslinger (Research Institute of Molecular Pathology, Vienna, Austria) and backcrossed on a C57BL/6J background. *PAX5-ELN* (*PE*^{tg}) transgenic mouse model was developed by our team as previously described (Jamrog et al., 2018). *Rosa26-Cas9* (*Cas9*^{tg}) mice (Tzelepis et al., 2016) were generously provided by the Trust Sanger Institute de Cambridge (UK). Homozygous *PE*^{tg} and *Cas9*^{tg} mice were maintained by cross-breeding, their genotypes were verified by PCR and all the experiments were performed in heterozygous mice. C57BL6 (Ly6.2, CD45.2) mice were purchased from Charles River Laboratories (France) and Pep3b (Ly6.1, CD45.1) B6.SJL congenic mice were initially obtained from The Jackson Laboratory (Bar Harbor, ME). All animals were housed in pathogen-free conditions (Anexplo US006 CREFRE, Toulouse, France) in accordance with the European Directive 2010/63/EU and the French Institutional Guidelines for animal handling. Mice were handled according to protocols approved by the Regional Ethical Committee (Agreement #A31555010). Mice were backcrossed into the C57BL6 background for more than 10 generations.

FACS analysis, antibodies and cell sorting

Single cell suspensions from FL *Pax5*$^{-/-}$, *Pax5*$^{+/-}$ and *Pax5*$^{+/+}$ mice (E17.5) were prepared in Iscove's Modified Dulbecco's Medium (IMDM; Gibco) supplemented with 2% Fetal Bovine Serum (FBS) (Stemcell technologies). Immunostainings were performed using antibodies for flow cytometry obtained from Pharmingen (BD Biosciences), Invitrogen and Miltenyi are listed in **Table S1**. For surface staining, cells were incubated with the antibodies for 20 minutes in IMDM 2% FBS at 4°C and washed twice with PBS1X before analysis. FACS analysis was performed on a Fortessa cytometer (BD Biosciences) using FlowJo (BD Biosciences) softwares and cell sorting was performed on a MoFlo Astrios sorter (Beckman Coulter).

Co-culture of primary fetal liver cells

Fetal liver (FL) cells were co-cultured on irradiated OP9 stromal cells in Iscove's Modified Dulbecco's Medium (IMDM; Gibco), supplemented with 5% Fetal Bovine Serum (FBS) (Stemcell technologies), 0.05 mM β-mercaptoethanol (Sigma-Aldrich), 2mM L-glutamine (Invitrogen), penicillin (100 units/ml) and streptomycin (100 units/ml). *In vitro* experiments were performed in the presence of 2ng/ml IL7. Every 3 days, FL cells were harvested and propagated on fresh OP9 stromal cells.

UMAP analysis

UMAP analysis was performed using FlowJo software. At least 4 samples per condition were pre-gated on single cells of the population of interest. Then, informatic cleaning and normalization were performed using FlowAI package (V2.1) (Monaco et al., 2016) and CytoNorm package (V1.0) (Van Gassen et al., 2020) for each sample and the same number of cells were then concatenated. Arc sin transformation was performed manually for each marker to discriminate the different B-cell populations. The dimension reduction algorithm UMAP (umap-learn Python package v2.4.0) (Becht et al., 2018) was run using Euclidian distance with 15 nearest neighbors and 0.5 distance parameters.

Retroviral production and transduction of FL *Pax5*$^{-/-}$ cells

Full-length human *PAX5* and *PAX5-P80R* cDNA were amplified, sequenced and inserted into the retroviral vector pMSCV-IRES-GFP II (pMIG II). Retroviral supernatants were produced using the Phoenix retrovirus producer line (Orbigen) and Lipofectamine 2000 (Invitrogen) reagent for transfection and proceeding according to the manufacturer's instructions. After overnight incubation of the transfection mix, cells were treated with 10 mM sodium butyrate (Millipore) and washed with PBS before pro-B-cell medium was added. Viral supernatants were harvested after 24 h of incubation at 32°C, passed on a 0.45 µm filter, aliquoted and frozen at -80°C. Lymphoid cells from *Pax5*$^{-/-}$ embryonic liver at E17.5 were amplified on irradiated OP9 stromal cells in the presence of 2 ng/mL IL7, purified by cell sorting and transduced with retroviral vectors expressing either empty MIG-GFP (CTL) or MIG-PAX5 Wt or MIG-PAX5 P80R vectors. Retroviral supernatant was diluted at 1:3, supplemented with 4µg/ml polybrene (Sigma) and 2 ng/mL of IL7. Spinoculation was performed at 1,000 g at 32°C for 90 min. After centrifugation, 1mL of fresh medium supplemented with IL7 is added and the cells are incubated overnight at 37°C. After transduction, cells were washed and plated in IMDM, 5% FCS, 0.05 mM β-mercaptoethanol and 2 mM L-glutamine on irradiated OP9-derived stromal cells with 2 ng/mL IL7.

Transplantation assay of transduced FL *Pax5*$^{-/-}$ cells.

Transduced, purified and co-cultured GFP$^+$ cells from FL *Pax5*$^{-/-}$ mice (CD45.2$^+$GFP$^+$) were intravenously transplanted (2x10^5 cells per mouse) into 6-8 weeks old primary and secondary recipient mice (CD45.1$^+$) pre-treated, 24h before transplantation, with 30 mg/kg of Busulfan (Busilvex, Pierre Fabre). Chimerism was analyzed by flow cytometry (FACS) and was illustrated by the percentage of donor-derived cells (% CD45.2$^+$GFP$^+$) found in the recipient BM, spleen and thymus.

IL7r-ligand stimulation and phosphoflow cytometry.

B-ALL#1300 and #1301 PAX5 P80R GFP$^+$ cells of B-ALL cell lines (REH, 697) were treated or not (Vehicle) with 1µM Tofacitinib (Tofa) during 10 minutes. IL7r-ligand stimulation was assessed by phosphoflow

cytometry after the *ex vivo* activation with 30 ng/mL IL-7 (Peprotech) during 15 minutes (+IL-7) at 37°C in RPMI 2% FBS. Unstimulated (-IL-7) cells were used as control. For the staining of pStat5, cells were then fixed with pre-warmed Lyse/Fix buffer 1X for 12 minutes at 37°C, washed twice (centrifugation 7 minutes; 500 rpm) in RPMI 2% FBS and permeabilized with cold Perm Buffer III for 30 minutes at 4°C, according the manufacturer's instructions (BD Phosphoflow™). Cells were washed twice in PermWash buffer and the intracellular immunostaining with the anti-pStat5 antibody (Invitrogen) was performed for 30 minutes at RT, followed by two washes before FACS analysis.

Lentiviral production of sgRNA *Hif2α*.

Single-guide RNAs (sgRNAs) targeting the exon 2 of *Hif2α* (**Table S2**) were designed using CCTop - CRISPR/Cas9 target online predictor software (Center for Organismal Studies Heidelberg) and subcloned in pLKO5-sgRNA-EFS-GFP, in which the sgRNA and GFP coding sequences are controlled by the U6 and the EF1α promoters, respectively (Heckl et al., 2014). Concentrated VSV/G pseudotyped lentiviral vectors pLKO5-sgRNA-EFS-GFP encoding sgRNA *Hif2α* (sg*Hif2α* T8 and T12) or sgRNA CTL (sgCTL) were produced by triple transfection method. Briefly, 12.10^6 293FT cells are seeded on each T175 flask the day before the calcium phosphate-mediated transfection. Each T175 Flask of 80% confluence 293 cells were co-transfected with 20µg of the transfer vector plasmid, 12µg of pRSV-Rev, 20µg of the pMDLgag/pol packaging plasmid and 10 µg of the pVSVg envelope plasmid. Six hours after transfection, the medium was replaced by 24 ml of OptiMEM medium (Life Technologies, ThermoFisher Scientific). Twenty-six hours after transfection, the conditioned medium was collected, cleared by centrifugation and filtered through 0.45 µm-pore-size PVDF filters. The lentiviral particles were concentrated by ultracentrifugation 2 hours at 24.000 rpm and resuspended in 40µl of PBS with Calcium and Magnesium. Titrations of produced lentiviral vectors were performed on HT1080 cell line.

Purification, gene transfer and functional assays of *PE*^{tg}*Cas9*^{tg} B-cells or *Cas9*^{tg} LSK cells.

Homozygous *PE*^{tg} mice were bred with homozygous *Cas9*^{tg} mice to obtain heterozygous *PE*^{tg}*Cas9*^{tg} mice. B-cell progenitors (CD19$^+$CD23$^-$ Kit$^+$) from the BM of *PE*^{tg}*Cas9*^{tg} mice were purified by cell sorting, plated in suspension culture in B-cell medium supplemented with Il7 (5ng/mL), Flt3L (10ng/mL) and SCF (10ng/mL) and transduced with lentiviral vectors at a multiplicity of infection (MOI) of 10 in the presence of 2 µg/mL of polybrene (Sigma Aldrich) for 24h. Transduced cells were then washed in PBS1X and co-cultured on MS5 stromal cells in fresh supplemented B-cell medium for 3 days. Transduced GFP$^+$ cells were then purified by cell sorting to perform *in vitro* functional assays. Purified transduced GFP$^+$ cells (Cd45.2$^+$) were also transplanted intravenously ($2.5x10^4$ cells/mouse, n=6 to 8 for each condition) into 6-8 weeks old recipient mice (CD45.1$^+$) pre-treated, 24h before transplantation, with 30 mg/kg of

Busulfan. Chimerism of engrafted and transduced cells was analyzed by flow cytometry (FACS) and was illustrated by the percentage of donor-derived cells (%Cd45.2$^+$GFP$^+$) found in the recipient BM.

BM cells from heterozygous Cas9-expressing mice were flushed and Lineage$^-$ (Lin$^-$) cells were enriched by magnetics microbead separation using Lineage Cell Depletion Kit (Miltenyi Biotech). Immunostaining was performed using antibodies used for flow cytometry obtained from Pharmingen (BD Biosciences): Lin$^-$ cell fraction was subsequently incubated with PE-labelled anti-Sca1 (E13-161.7), PeCy5-labelled anti-c-Kit (2B8) and biotin-labelled anti-CD3e (145.2), anti-B220 (RA3-6B2), anti-Ter119 (TER-119), anti-Gr1 (RB6-8C5), anti CD11b+c (M1/70) antibodies. Cells were then incubated with AF488-labelled streptavidin (BD Biosciences). Cell sorting of LSK cell population was performed on a MoFlo Astrios sorter (Beckman Coulter). Purified *Cas9*^{tg} LSK cells were plated in suspension culture in StemSpan medium (StemCell Technologies) with 50 ng/mL murine thrombopoietin (TPO) and 50 ng/mL murine stem cell factor (SCF). After 24h of pre-stimulation, LSK cells were transduced with lentiviral vectors at a multiplicity of infection of 10 (MOI10) in the presence of 2 µg/mL of polybrene (Sigma Aldrich) for 24h before performing functional assays. Transduced *Cas9*^{tg} LSK cells were plated in triplicate in multipotential methylcellulose (MethoCult 3434, Stem Cell Technologies, Vancouver, Canada) at 300 cells per dish, and GFP$^+$ colonies were numbered and characterized 11 days later. In parallel, transduced *Cas9*^{tg} LSK (Cd45.2$^+$) were transplanted intravenously (10^4 LSK cells/mouse, n=6 to 7 for each condition) into 6-8 weeks old recipient mice (Cd45.1$^+$) pre-treated, 24h before transplantation, with 30 mg/kg of Busulfan. Chimerism of engrafted and transduced cells was analyzed by flow cytometry (FACS) and was illustrated by the percentage of donor-derived cells (%CD45.2$^+$GFP$^+$) found in the recipient BM.

RT-qPCR

RNA was isolated using Trizol method and cDNA was synthesized using SuperScript® VILO™ cDNA Synthesis Kit (Invitrogen™) according to the manufacturer's instructions. Quantitative SYBR Green PCR was performed on a LightCycler®480 II System (Roche) to quantify human *PAX5* and murine *CD19* and *CD79a* cDNAs expression in GFP$^+$ CTL, PAX5 Wt and PAX5 P80R cells 14 days after co-culture and from GFP$^+$ PAX5 P80R cells in the BM of engrafted primary and secondary recipients using LightCycler®480 SYBR Green I Master (Roche Diagnostics GmbH) according to the manufacturer's instructions. All PCR were carried out as follows in a 20 µl volume: 5 min at 95°C, followed by 45 cycles of 10 s at 95°C, 10 s at annealing temperature of 60°C and 10 s at 72°C. Quantification was performed using the Δ*Ct* method with normalization to the *Abl1* gene expression levels. Data were analyzed using the LC480 software (Roche Diagnostics). The same approach was performed to quantify *Hif2*α expression. Targets and primers are listed in **Table S2**.

Next generation sequencing (NGS) of targeted gene regions

mRNA and genomic DNA extraction was performed using a AllPrep® DNA/RNA micro-Kit (#80284) according to manufacturer's instruction (QIAGEN). For the sequencing of genomic mutations, a library was generated using PCR from 7 specific mouse regions of *Ptpn11*, *Kras*, *Pax5*, and *Jak3* genes previously identified by whole exome sequencing (Jamrog, Chemin, Fregona, Coster, Pasquet, Oudinet, Rouquie, et al., 2018). The library was sequenced with a MiSeq sequencer (Illumina, San Diego, USA) using a Miseq Reagent Kit V2 (paired-end sequencing 2 x 150 cycles). Alignment was performed using BWA aligner and variant calling was performed using FreeBayes and Mutect2 variant callers. To evaluate the proportion of *PAX5-P80R* transcript, cDNA was amplified with primers that detect both human *PAX5* and *PAX5-P80R* transgene and sequenced by NGS. Sequences were then aligned on human PAX5 gene as reference. Genome editing efficiency of targeted *Hif2α* region (Exon 2) was analysed using the online CRISPResso software (https://crispresso.pinellolab.partners.org/submission ; (Canver et al., 2018)). Targets and primers are listed in **Table S2**.

Chemical screen of potential Hifα inhibitors

MS5 stromal cells (10^4 per 90 µl per well) were seeded in 96-well plates in B-cell medium supplemented with Il7 (5ng/mL), Flt3L (10ng/mL) and SCF (10ng/mL). Twenty-four hours later, PAX5 P80R and PAX5-ELN leukemic cells were seeded on MS5 stromal cells and exposed to 19 individual potential *Hifα* inhibitors (MCE, MedChemExpress) at the dose of 500nM in duplicate. Absolute numbers of B-ALL $CD19^+$ cells were determined after 48 hours of culture using flow cytometry. 18 wells containing B-ALL cells were treated with DMSO (vehicle) as negative controls, respectively. The inhibition (percentage) of cell viability by individual compounds was calculated based on the absolute numbers of cells recovered from the co-culture according to the formula 100 – ((test compound/median vehicle) × 100).

Human B-ALL cell lines and Patient-Derived Xenografted Model.

The human B-ALL cell lines REH and 697 were obtained from DSMZ Leibniz-Institut and the human B-ALL samples were obtained from the Hematology Laboratory of Saint-Louis Hospital (Paris, France) after signed written informed consent for research use in accordance with the Declaration of Helsinki and stored at the HIMIP collection (BB-0033-00060). Patient-derived xenograft models (PDX #112 and PDX #214) have been generated by transplantation of leukemic blasts from two "*de novo*" P80R B-ALL patients and amplification into immunodeficient NOD.*Cg-Prkdc*^{scid}*Il2rg*^{tmWjl} (NSG) mice. NSG mice were produced at the Génotoul-Anexplo platform at Toulouse, France, using breeders obtained from Charles River Laboratories. Mice were housed in sterile conditions using high-efficiency particulate arrestance filtered microisolators and fed with irradiated food and sterile water. Mice (6–9 weeks old) were sub-lethally treated with busulfan 30 mg/kg 24 h before injection of leukemic cells. Leukemia engraftment

was monitored by FACS with hCD45 (BD Bioscience, 557748) and hCD19 (BD Bioscience, 562294) staining and leukemic cells from the BM were used for experiments.

Western blot

Protein extraction was performed using RIPA buffer (20 mM Tris pH 8.0, 150 mM NaCl, 1% NP-40, 0.1% SDS, 0.5% Sodium Desoxycholate). The concentrations of protein extracts were determined using Bicinchroninic Acid Kit (Sigma). Proteins were then separated on sodium dodecyl sulfate–PAGE (SDS-PAGE) and transferred on poly-vinylidene difluoride (PVDF) membranes (Millipore Corporation). Immunodetection was revealed using ECL Plus (Amersham Biosciences). The membranes were blocked and the antibodies were diluted in 5% dried milk in TBST (10 mM Tris-HCl pH 8.0, 150 mM NaCl, 0.05% Tween-20). The rabbit polyclonal anti-Hif2α (Novus Biological, NB100-122) and the rabbit monoclonal anti-α-Actin (Cell Signaling Technology, D18C11, 8456S) antibodies were diluted 1/1000. The secondary antibodies against rabbit IgG(H+L)-HRP conjugate were obtained from Cell Signaling Technology (Danvers, MA, USA) and diluted at 1/2000.

Statistical analysis

Student's *t* test was used for comparison of quantitative variable (***p<0.0005, **p<0.005, *p< 0.05), assuming normality and equal distribution of variance between the different groups analyzed. Survival in mouse experiments was represented with Kaplan-Meier curves (Prism GraphPad).

Author contributions

MBa designed the study, performed and analysed the experiments and wrote the manuscript. VF, MBo, LJ, NP, SL and SH performed experiments. MP and EC provided human P80R B-ALL cells from PDXs. CD, ED and CB reviewed the data and the manuscript. BG performed and analysed experiments, conceived and supervised the project and wrote the manuscript. All authors contributed to the final draft.

Acknowledgments

We acknowledge Manon Farcé from the cytometry and cell sorting facility of the Cancer Research Center of Toulouse (INSERM U1037) and the Anexplo/Genotoul platforms (UMS006) for technical assistances. This study was supported by institutional grants from the Institut National de la Santé et de la Recherche Médicale (INSERM, France), France, from the Centre National de la Recherche Scientifique (CNRS, France), the Institut National du Cancer, France (INCa-2020-096, France), the Agence Nationale de la Recherche (ANR-18-CE13-0002-01, France) and the Fondation ARC pour la Recherche sur le Cancer (PJA-20181207977, France). The team is supported by the Ligue Contre le

Cancer and the associations “Laurette Fugain”, “111 des arts”, “Cassandra” and “Constance la petite guerrière astronaute”.

Declaration of interests

The authors declare no competing interests.

Cliquez ou appuyez ici pour entrer du texte.

Figure 1

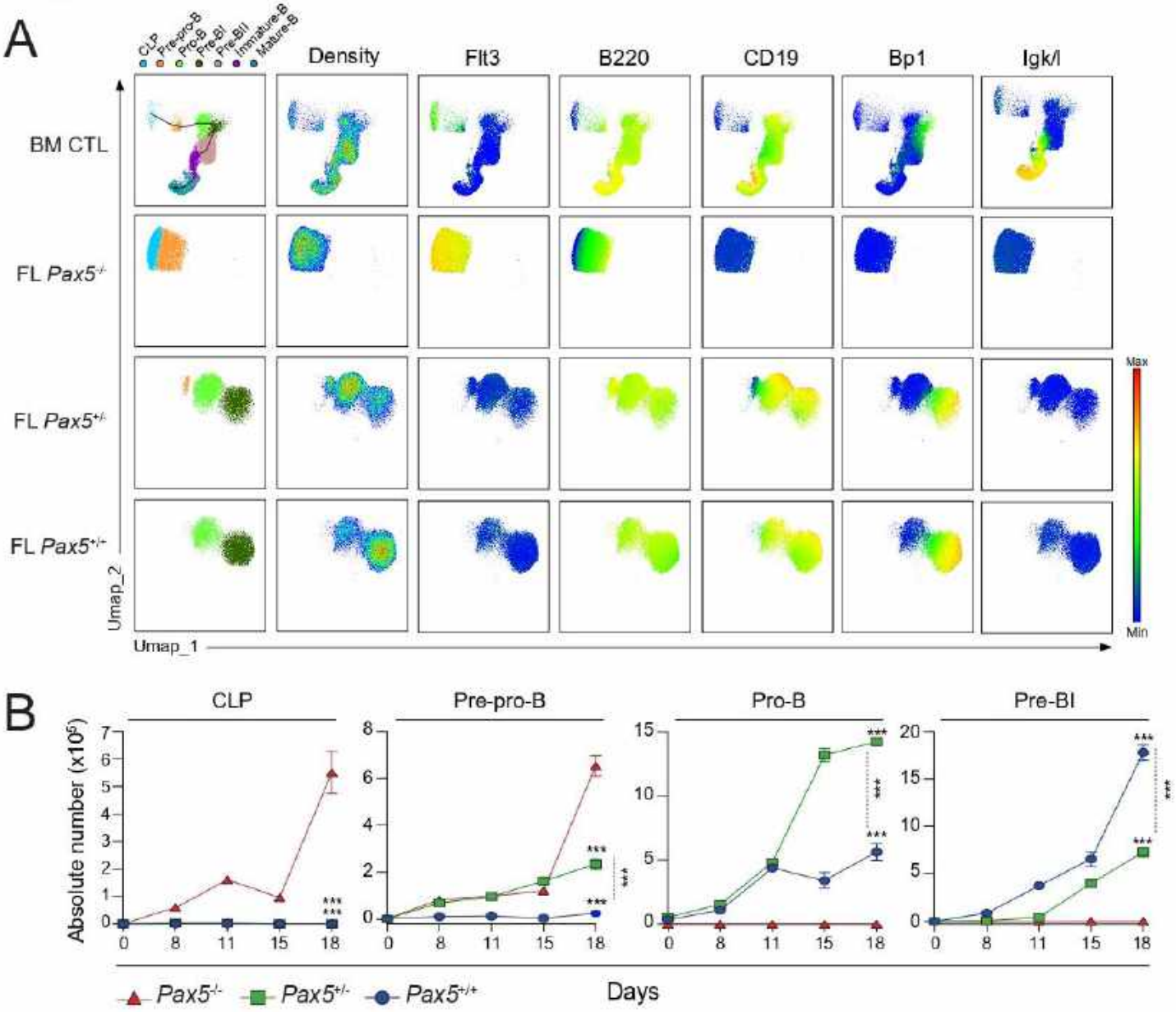
A
CLP
Pre-pro-B
Pro-B
Pre-BI
Pre-BII
Immature-B
Mature-B
Density
Flt3
B220
CD19
Bp1
Igk/l
BM CTL
FL Pax5-/-
FL Pax5+/-
FL Pax5+/+
Max
Min
Umap_2
Umap_1
B
CLP
Pre-pro-B
Pro-B
Pre-BI
Absolute number (x10^5)
Days
Pax5-/-
Pax5+/-
Pax5+/+

Figure 2

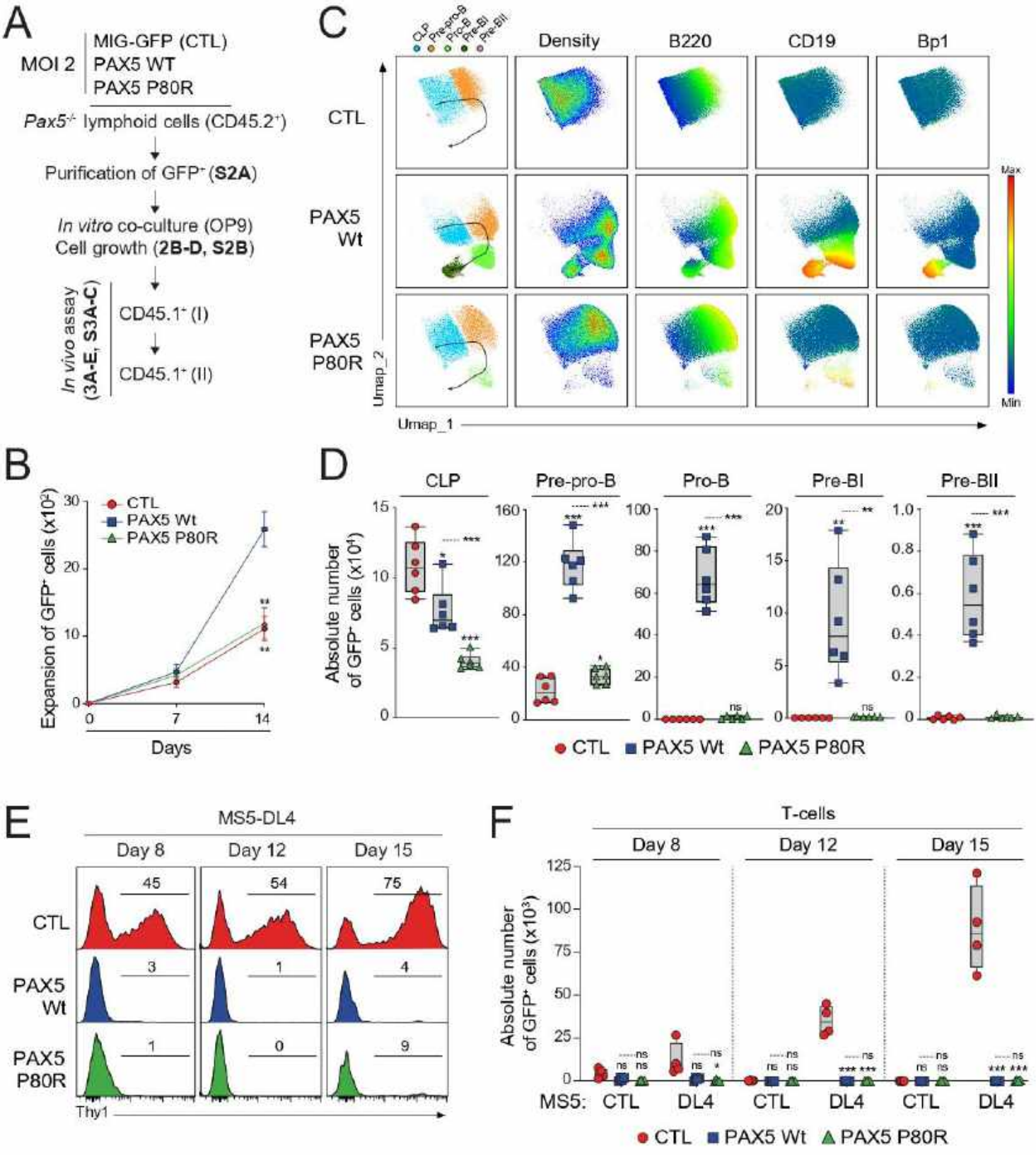
A
MOI 2
MIG-GFP (CTL)
PAX5 WT
PAX5 P80R
Pax5-/- lymphoid cells (CD45.2+)
Purification of GFP+ (S2A)
In vitro co-culture (OP9)
Cell growth (2B-D, S2B)
In vivo assay (3A-E, S3A-C)
CD45.1+ (I)
CD45.1+ (II)
C
CLP
Pre-pro-B
Pro-B
Pre-BI
Pre-BII
Density
B220
CD19
Bp1
CTL
PAX5 Wt
PAX5 P80R
Max
Min
Umap_2
Umap_1
B
Expansion of GFP+ cells (x10³)
CTL
PAX5 Wt
PAX5 P80R
Days
D
CLP
Pre-pro-B
Pro-B
Pre-BI
Pre-BII
Absolute number of GFP+ cells (x10³)
CTL
PAX5 Wt
PAX5 P80R
E
MS5-DL4
Day 8
Day 12
Day 15
CTL
PAX5 Wt
PAX5 P80R
45
54
75
3
1
4
1
0
9
Thy1
F
T-cells
Day 8
Day 12
Day 15
Absolute number of GFP+ cells (x10³)
MS5: CTL DL4 CTL DL4 CTL DL4
CTL
PAX5 Wt
PAX5 P80R

Figure 3

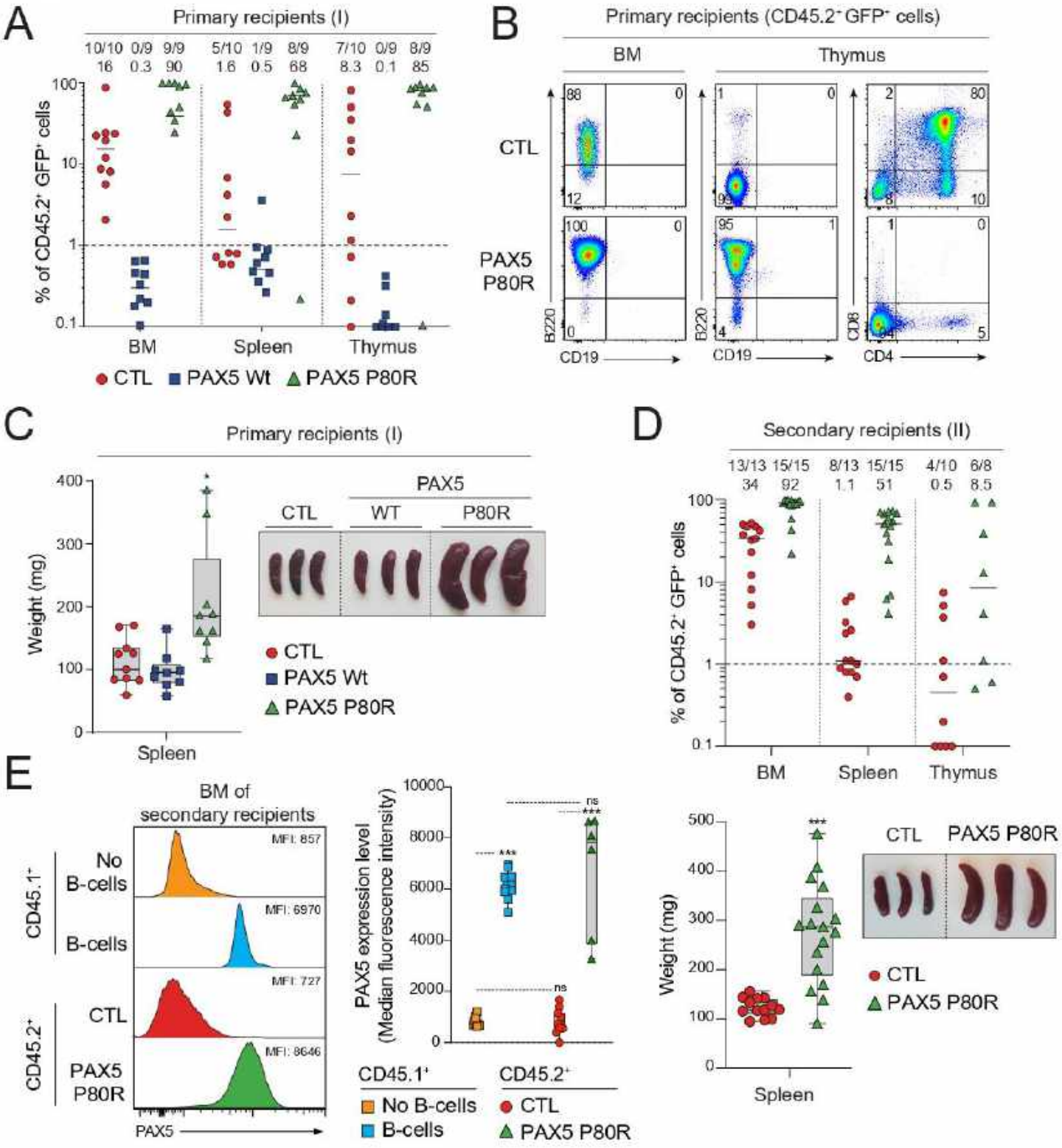
A
Primary recipients (I)
10/10 0/9 9/9
16 0.3 90
5/10 1/9 8/9
1.6 0.5 68
7/10 0/9 8/9
8.3 0.1 85
% of CD45.2+ GFP+ cells
BM
Spleen
Thymus
CTL
PAX5 Wt
PAX5 P80R
B
Primary recipients (CD45.2- GFP+ cells)
BM
Thymus
CTL
PAX5 P80R
B220
CD19
CD8
CD4
C
Primary recipients (I)
Weight (mg)
PAX5
CTL
WT
P80R
Spleen
CTL
PAX5 Wt
PAX5 P80R
D
Secondary recipients (II)
13/13 15/15 8/13 15/15 4/10 6/8
34 92 1.1 51 0.5 8.5
% of CD45.2+ GFP+ cells
BM
Spleen
Thymus
Weight (mg)
CTL
PAX5 P80R
Spleen
E
BM of
secondary recipients
CD45.1+
No B-cells
B-cells
CD45.2+
CTL
PAX5 P80R
MFI: 857
MFI: 6970
MFI: 727
MFI: 8646
PAX5
PAX5 expression level
(Median fluorescence intensity)
ns
CD45.1+
No B-cells
B-cells
CD45.2+
CTL
PAX5 P80R

Figure 4

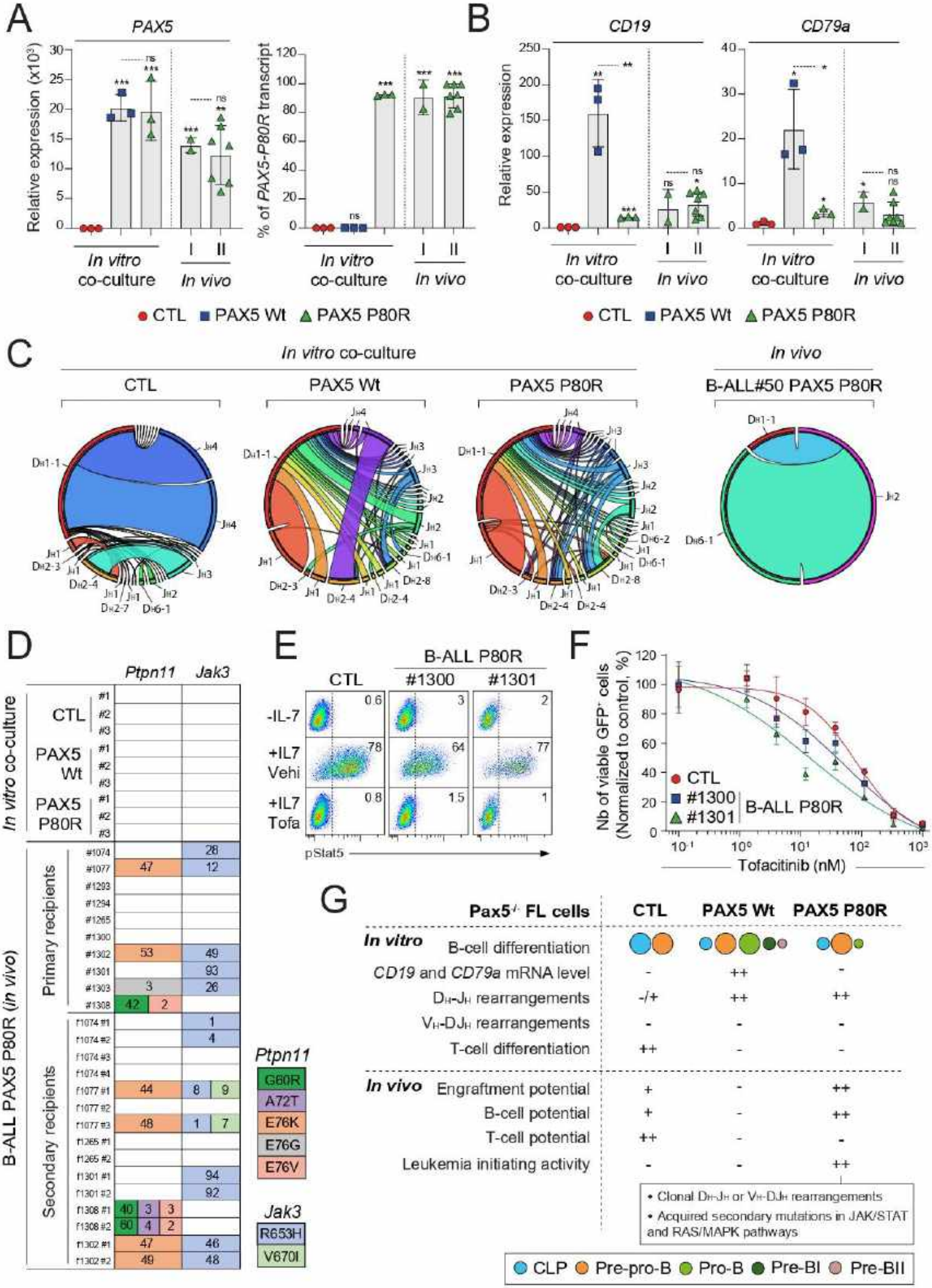
A
PAX5
Relative expression (x10³)
% of PAX5-P80R transcript
In vitro co-culture
In vivo
I
II
CTL
PAX5 Wt
PAX5 P80R
B
CD19
CD79a
Relative expression
C
In vitro co-culture
In vivo
CTL
PAX5 Wt
PAX5 P80R
B-ALL#50 PAX5 P80R
D
Ptpn11
Jak3
In vitro co-culture
B-ALL PAX5 P80R (in vivo)
Primary recipients
Secondary recipients
G60R
A72T
E76K
E76G
E76V
R653H
V670I
E
B-ALL P80R
#1300
#1301
-IL-7
+IL7 Vehi
+IL7 Tofa
pStat5
F
Nb of viable GFP⁺ cells (Normalized to control, %)
Tofacitinib (nM)
B-ALL P80R
G
Pax5⁻/⁻ FL cells
In vitro
B-cell differentiation
CD19 and CD79a mRNA level
DH-JH rearrangements
VH-DJH rearrangements
T-cell differentiation
In vivo
Engraftment potential
B-cell potential
T-cell potential
Leukemia initiating activity
• Clonal DH-JH or VH-DJH rearrangements
• Acquired secondary mutations in JAK/STAT and RAS/MAPK pathways
CLP
Pre-pro-B
Pro-B
Pre-BI
Pre-BII

Figure 5

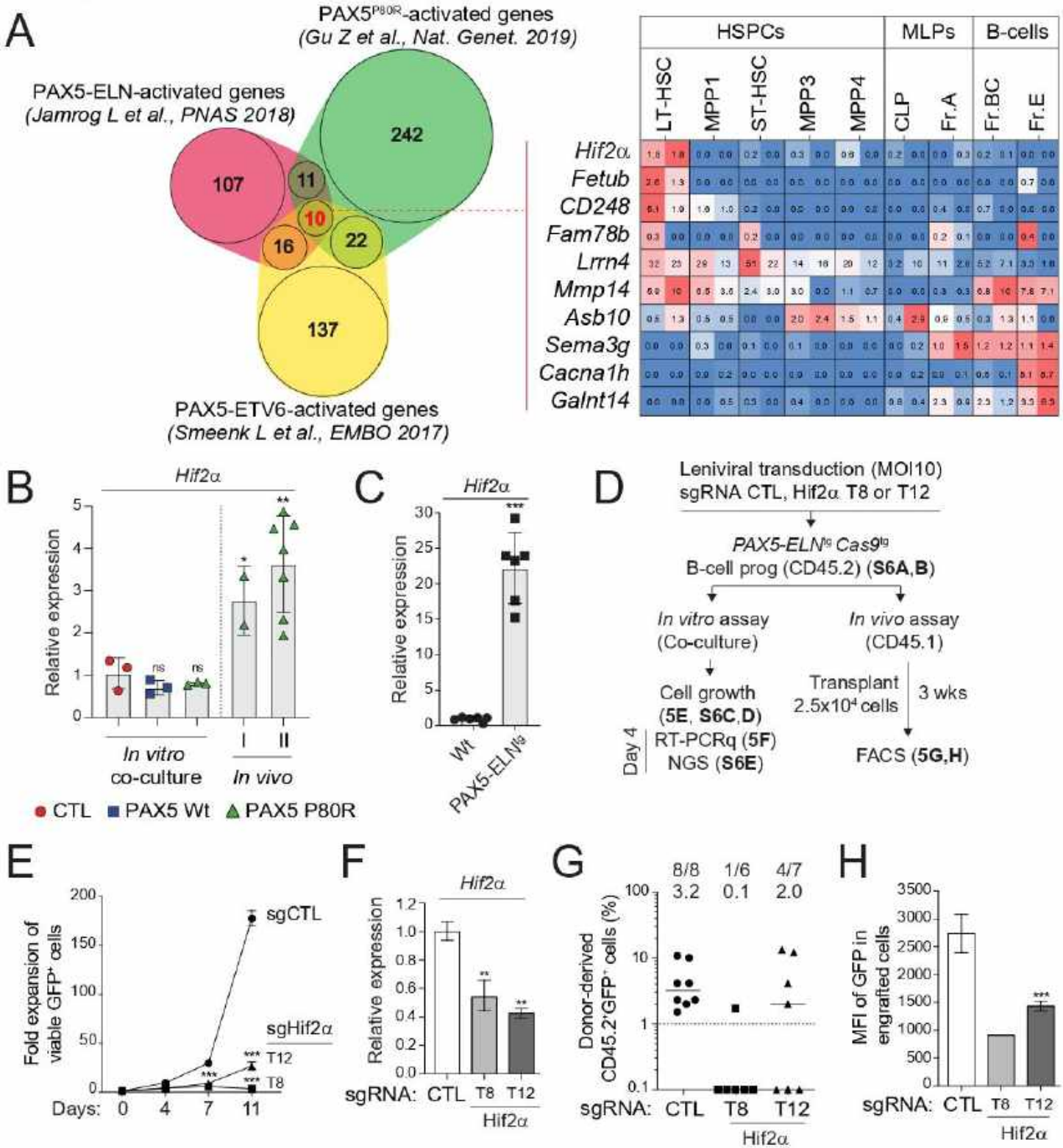
A
PAX5P80R-activated genes
(Gu Z et al., Nat. Genet. 2019)
PAX5-ELN-activated genes
(Jamrog L et al., PNAS 2018)
PAX5-ETV6-activated genes
(Smeenk L et al., EMBO 2017)
242
107
11
10
16
22
137
HSPCs
MLPs
B-cells
LT-HSC
MPP1
ST-HSC
MPP3
MPP4
CLP
Fr.A
Fr.BC
Fr.E
Hif2α
Fetub
CD248
Fam78b
Lrrn4
Mmp14
Asb10
Sema3g
Cacna1h
Galnt14
B
Hif2α
Relative expression
ns
In vitro co-culture
In vivo
CTL
PAX5 Wt
PAX5 P80R
C
Hif2α
Relative expression
Wt
PAX5-ELNtg
D
Leniviral transduction (MOI10)
sgRNA CTL, Hif2α T8 or T12
PAX5-ELNtg Cas9tg
B-cell prog (CD45.2) (S6A,B)
In vitro assay
(Co-culture)
In vivo assay
(CD45.1)
Cell growth
(5E, S6C,D)
Day 4
RT-PCRq (5F)
NGS (S6E)
Transplant
2.5x10⁴ cells
3 wks
FACS (5G,H)
E
Fold expansion of viable GFP+ cells
sgCTL
sgHif2α
T12
T8
Days: 0 4 7 11
F
Hif2α
Relative expression
sgRNA: CTL T8 T12
Hif2α
G
8/8 1/6 4/7
3.2 0.1 2.0
Donor-derived CD45.2+GFP+ cells (%)
sgRNA: CTL T8 T12
Hif2α
H
MFI of GFP in engrafted cells
sgRNA: CTL T8 T12
Hif2α

Figure 6

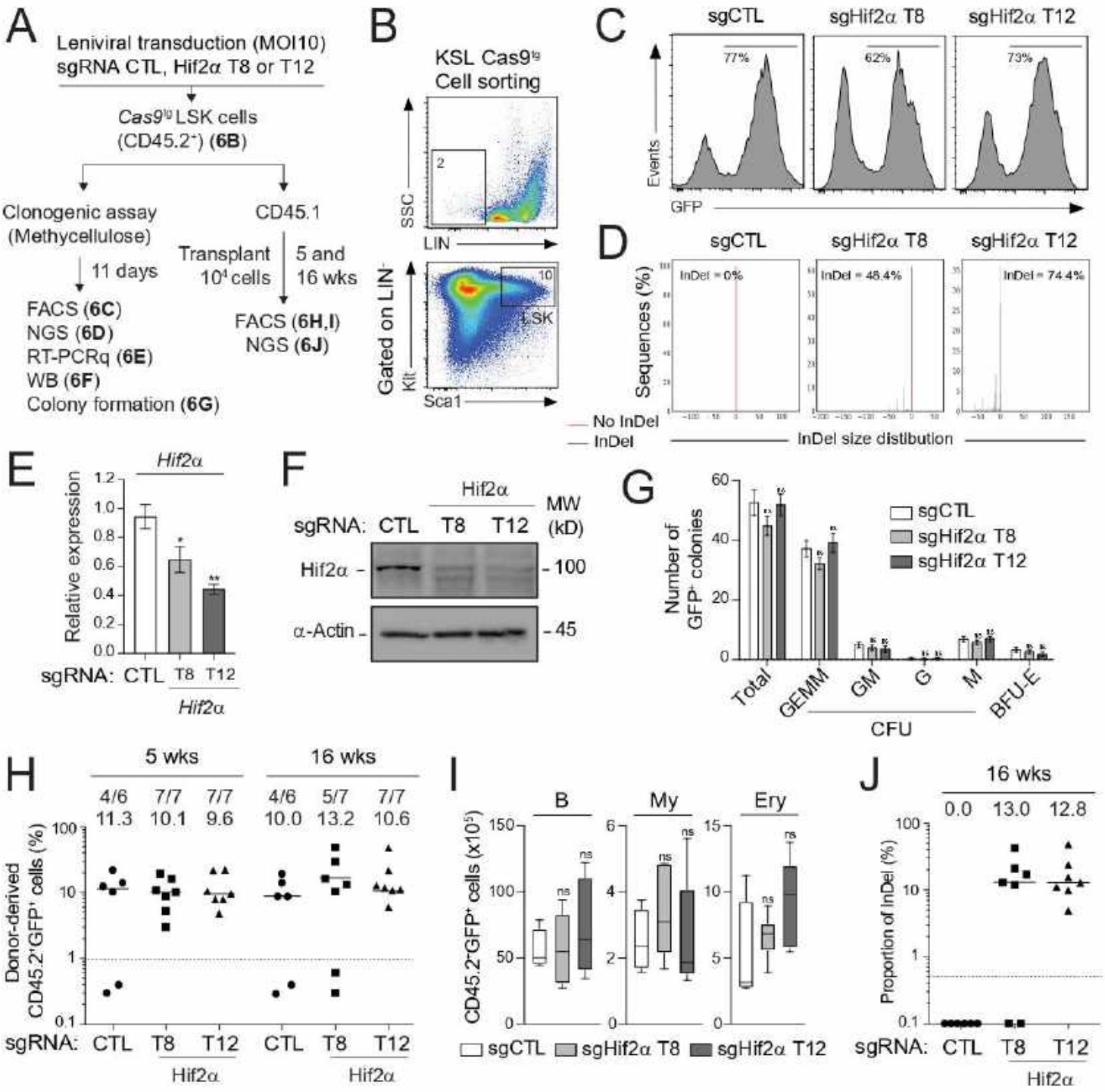
A
Leniviral transduction (MOI10)
sgRNA CTL, Hif2α T8 or T12
Cas9tg LSK cells
(CD45.2+) (6B)
Clonogenic assay
(Methycellulose)
11 days
FACS (6C)
NGS (6D)
RT-PCRq (6E)
WB (6F)
Colony formation (6G)
CD45.1
Transplant
10⁴ cells
5 and
16 wks
FACS (6H,I)
NGS (6J)
B
KSL Cas9tg
Cell sorting
SSC
LIN
Gated on LIN-
Kit
Sca1
LSK
C
sgCTL
sgHif2α T8
sgHif2α T12
77%
62%
73%
Events
GFP
D
sgCTL
sgHif2α T8
sgHif2α T12
Sequences (%)
InDel = 0%
InDel = 46.4%
InDel = 74.4%
No InDel
InDel
InDel size distibution
E
Hif2α
Relative expression
sgRNA: CTL T8 T12
Hif2α
F
Hif2α
sgRNA: CTL T8 T12
MW (kD)
Hif2α
α-Actin
100
45
G
Number of GFP+ colonies
sgCTL
sgHif2α T8
sgHif2α T12
Total
GEMM
GM
G
M
BFU-E
CFU
H
5 wks
16 wks
4/6 7/7 7/7
11.3 10.1 9.6
4/6 5/7 7/7
10.0 13.2 10.6
Donor-derived CD45.2+GFP+ cells (%)
sgRNA: CTL T8 T12 CTL T8 T12
Hif2α
Hif2α
I
B
My
Ery
CD45.2+GFP+ cells (x10⁵)
ns
sgCTL
sgHif2α T8
sgHif2α T12
J
16 wks
0.0 13.0 12.8
Proportion of InDel (%)
sgRNA: CTL T8 T12
Hif2α

Figure 7

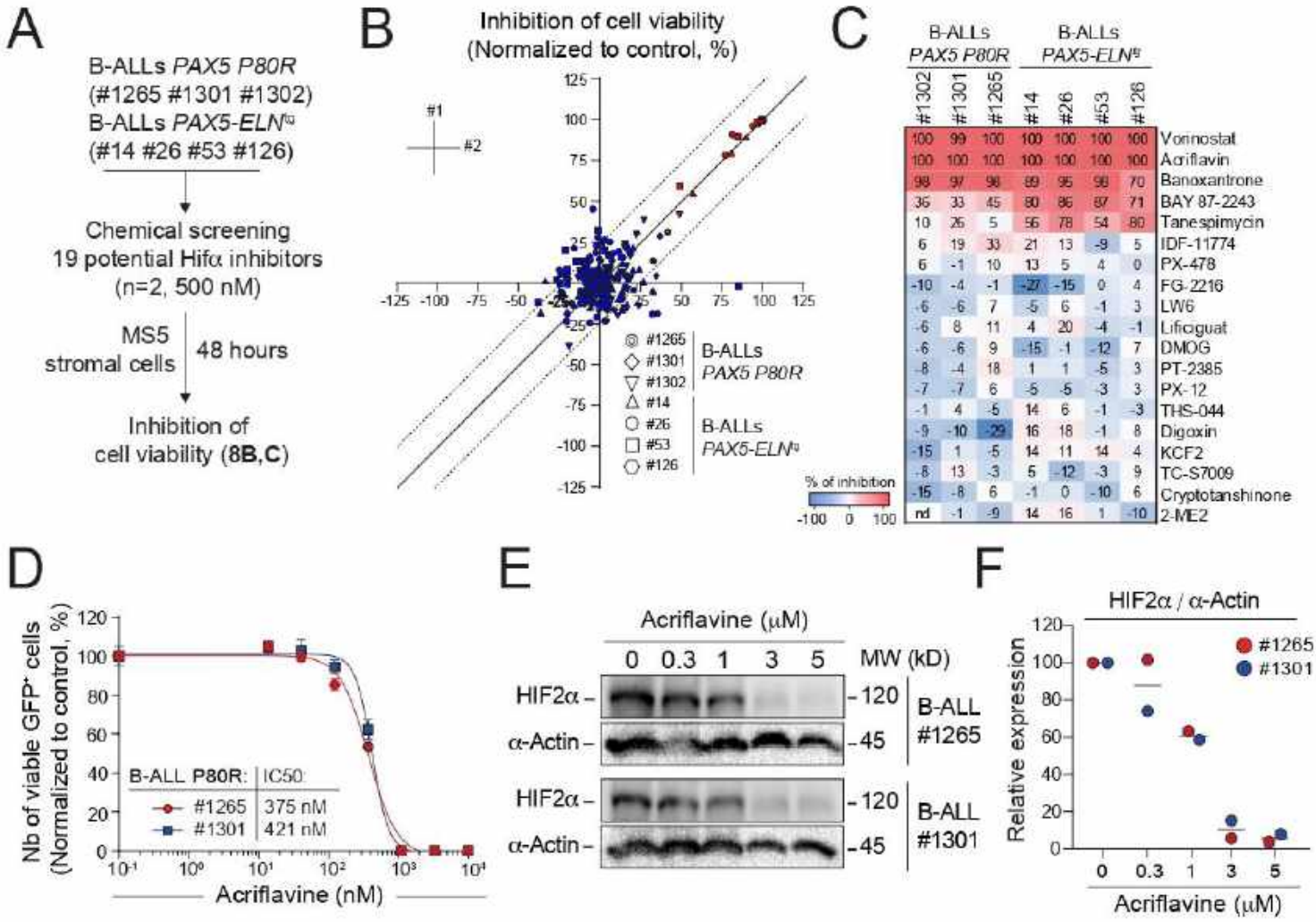
A
B-ALLs PAX5 P80R
(#1265 #1301 #1302)
B-ALLs PAX5-ELNfu
(#14 #26 #53 #126)
Chemical screening
19 potential Hifα inhibitors
(n=2, 500 nM)
MS5 stromal cells
48 hours
Inhibition of cell viability (8B,C)
B
Inhibition of cell viability
(Normalized to control, %)
#1
#2
#1265
#1301
#1302
#14
#26
#53
#126
B-ALLs PAX5 P80R
B-ALLs PAX5-ELNfu
% of inhibition
-100 0 100
C
B-ALLs PAX5 P80R
B-ALLs PAX5-ELNfu
#1302 #1301 #1265 #14 #26 #53 #126
100 99 100 100 100 100 100 Vorinostat
100 100 100 100 100 100 100 Acriflavin
98 97 98 89 95 98 70 Banoxantrone
36 33 45 80 86 87 71 BAY 87-2243
10 26 5 56 78 54 80 Tanespimycin
6 19 33 21 13 -9 5 IDF-11774
6 -1 10 13 5 4 0 PX-478
-10 -4 -1 -27 -15 0 4 FG-2216
-6 -6 7 -5 6 -1 3 LW6
-6 8 11 4 20 -4 -1 Lificiguat
-6 -6 9 -15 -1 -12 7 DMOG
-8 -4 18 1 1 -5 3 PT-2385
-7 -7 6 -5 -5 -3 3 PX-12
-1 4 -5 14 6 -1 -3 THS-044
-9 -10 -29 16 18 -1 8 Digoxin
-15 1 -5 14 11 14 4 KCF2
-8 13 -3 5 -12 -3 9 TC-S7009
-15 -8 6 -1 0 -10 6 Cryptotanshinone
nd -1 -9 14 16 1 -10 2-ME2
D
Nb of viable GFP+ cells
(Normalized to control, %)
B-ALL P80R: IC50:
#1265 375 nM
#1301 421 nM
Acriflavine (nM)
E
Acriflavine (μM)
0 0.3 1 3 5
MW (kD)
HIF2α
α-Actin
120
45
B-ALL #1265
B-ALL #1301
F
HIF2α / α-Actin
Relative expression
#1265
#1301
Acriflavine (μM)

Figure legends.

Figure 1. (**A**) Phenotypic characterization of lymphoid cells from the fetal liver (FL) of *Pax5*$^{-/-}$, *Pax5*$^{+/-}$ and *Pax5*$^{+/+}$ mice (E17.5) after co-culture and expansion on OP9 stromal cells during 18 days. Multiparametric staining by FACS integrating the nine markers shown in **Figures S1A-C** covering all the steps of the B-cell differentiation was used. UMAP (Uniform Manifold Approximation and Projection) representation of the clustering analysis of the different B-cell subpopulations based on the gating strategy shown in **Figures S1B, C**. Total bone marrow (BM) cells from wt adult mice were used as reference (BM CTL) to identify all B-cell subsets. Each subset (CLP, pre-pro-B, pro-B, pre-BI, pre-BII, immature-B and mature-B) is represented by one color and black arrow indicates the physiological phenotypic progression of B-cells in the differentiation (*left panels*). Visualization of the cell density and the expression level of Flt3, B220, CD19, Bp1 and Igκ/λ were shown for all the conditions (*right panels*). (**B**) Absolute numbers of CLP, pre-pro-B, pro-B and pre-BI cells during the co-culture of *Pax5*$^{-/-}$, *Pax5*$^{+/-}$ and *Pax5*$^{+/+}$ FL were calculated for each time points (n=3, ***p<0.001). Representative of two independent experiments.

Figure 2. (**A**) Experimental procedure to study the functional impact of *PAX5*^{P80R} mutation on normal B-cell development and leukemia transformation. Lymphoid cells (CLP/Pre-pro-B) from FL *Pax5*$^{-/-}$ mice (CD45.2) were expanded on OP9 stromal cells during 10 days, purified by cell sorting and transduced with retroviral vectors expressing either empty MIG-GFP (CTL) or MIG-PAX5 Wt (PAX5 Wt) or MIG-PAX5 P80R (PAX5 P80R) vectors. Transduced GFP$^+$ cells were purified (**Figure S2A**) and co-cultured on OP9 stromal cells during 14 days. At the end of the co-culture, transduced cells (CD45.2$^+$GFP$^+$) were intravenously transplanted in equal number in primary and secondary CD45.1 recipient mice. (**B**-**D**) *In vitro* cell growth of transduced GFP$^+$ MIG-GFP (CTL), PAX5 Wt and PAX5 P80R cells. Results represent the cumulative fold expansion of GFP$^+$ cells during 14 days of co-culture on OP9 stromal cells (B, n=6, **p<0.01). UMAP representation of GFP$^+$ B-cell subsets generated 14 days after co-culture. Each subset is represented by one color and black arrow indicates the phenotypic progression of cells in the differentiation (C, *left panels*). Visualization of the cell density and the expression level of B220, CD19 and Bp1 were shown for all the conditions (C, *right panels*). Absolute numbers of each subset 14 days after co-culture were calculated for each condition (D, n=6, ns=non-significant, *p<0.05, **p<0.01, ***p<0.001). Representative of two independent experiments.

Figure 3. (**A**) Transduced GFP$^+$ MIG-GFP (CTL), PAX5 Wt and PAX5 P80R cells were serially transplanted according to **Figure 2A**. Engraftment efficiency (% CD45.2$^+$GFP$^+$) in the BM, the spleen and the thymus from primary recipients was analyzed 21 weeks after transplantation. The number of positive mice and the median of engraftment are indicated. (**B**) Representative immunophenotype of donor-derived

$CD45.2^+GFP^+$ cells from the BM and the thymus of primary recipients engrafted with CTL and PAX5 P80R cells. FACS analysis of B220, CD19, CD4 and CD8 expression was shown. (**C**) Weight of spleens from primary recipients transplanted with CTL, PAX5 Wt and PAX5 P80R cells (*left panel*, ns=non-significant, *p<0.05) and representative pictures of spleens are shown (*right panel*). (**D**) Engraftment efficiency ($CD45.2^+GFP^+$) in the BM, the spleen and the thymus from secondary recipients was analyzed 2-3 weeks after the transplantation of CTL and PAX5 P80R cells. The number of positive mice and the median of engraftment are indicated (*upper panel*). Weight and representative pictures of spleens from secondary recipients are shown (*lower panel*, ***p<0.001). (**E**) Representative FACS analysis (*left panel*) and quantification (*right panel*, ns=non-significant, ***p<0.001) of PAX5 expression level in donor-derived $CD45.2^+$ cells from the BM of secondary recipients engrafted with CTL and PAX5 P80R cells. PAX5 expression level in host-derived $CD45.1^+$ B-cells ($B220^+$) and non-B-cells ($B220^-$) was measured as controls.

Figure 4. (**A**-**B**) Total mRNA was extracted from transduced GFP^+ CTL, PAX5 Wt and PAX5 P80R cells 14 days after co-culture (**Figures 2B-D**) and from B-ALL GFP^+ PAX5 P80R cells in the BM of engrafted primary (I) and secondary (II) recipients (**Figures 3A, E**). mRNA levels of the human *PAX5* transgene (A, *left panel*) and of its murine target genes *CD19* and *CD79a* (B) were determined by quantitative RT-PCR and normalized to *Abl1* gene (mean ± SD, n=3 to 6, *p<0.05, **p<0.01, ***p<0.001). Representative of two independent experiments. The proportion of *PAX5-P80R* transcript was measured by targeted next-generation sequencing (NGS, ***p<0.001). Representative of two independent experiments (A, *right panel*). (**C**) *IgH* gene rearrangements of transduced GFP^+ CTL, PAX5 Wt and PAX5 P80R cells 14 days after co-culture on OP9 stromal cells were performed (*left panels*). *IgH* locus was analyzed by multiplex PCR to quantify D_H-J_H and V_H-D_HJ_H rearrangements using primers listed in **Table S2**. Results were analyzed using the Vidjil software (**Figures S4A, C**). The proportions of the different D_H-J_H rearrangements for each condition were represented by Circos diagrams. V_H-D_HJ_H rearrangements were not observed. Representative of two independent experiments. D_H-J_H rearrangements of B-ALL#50 PAX5 P80R cells was shown (*right panel*). (**D**) Recurrent mutations in leukemic cells induced by $PAX5^{P80R}$ mutation. Mutations on *Ptpn11*, *Kras*, *Jak3* and *Pax5* genes were screened for recurrence by targeted next-generation sequencing (NGS) on GFP^+ CTL, PAX5 Wt and PAX5 P80R cells after co-culture and on B-ALL GFP^+ PAX5 P80R cells from the BM of engrafted primary (I) and secondary (II) recipients. Each row represents a sample, and each column represents a genetic alteration. Colors indicate the position of the mutation, and numbers represent the variant allele frequency of each mutation. (**E**) Representative FACS analysis of pStat5 expression after IL-7 stimulation (+IL-7) in presence or not (vehicle) of Tofacitinib (Tofa) in transduced GFP^+ CTL cells and in B-ALL#1300 and B-ALL#1301 PAX5 P80R GFP^+ cells. Unstimulated (-IL-7) B-ALL cells were used as controls. (**F**) B-ALL#1300 and B-ALL#1301

PAX5 P80R GFP$^+$ cells were treated *in vitro* with a dose-response of Tofacitinib for 48 hours. Transduced GFP$^+$ CTL cells has been used as control. Absolute numbers of GFP$^+$ cells were then analyzed by FACS and normalized to the number of untreated cells. (**G**) Schematic table and diagrams summarizing our finding about the impact of *PAX5*^{P80R} mutation on the B-cell differentiation and the B-ALL development.

Figure 5. (**A**) Venn diagram indicating the overlap of up-regulated genes in B-cells from the PAX5^{P80R} (Gu et al., 2019b) PAX5-ELN (Jamrog, Chemin, Fregona, Coster, Pasquet, Oudinet, Rouquie, et al., 2018) and PAX5-ETV6 (Smeenk et al., 2017b) transgenic mouse models. Genes are selected for an expression difference of >2-, 1.5-, and 5-fold, respectively (*left panel*). The list of overlapping genes is indicated and their expression profiles in murine hematopoietic stem and progenitor cells (HSPCs) (LT-HSCs, MPP1, ST-HSCs, MPP3, MPP4), multi-lymphoid progenitors (MLPs, *i.e.* common lymphoid progenitor (CLP) and Fr.A/Pre-pro-B) and committed B-cells (Fr.B/Pro-B to Fr.E/immature-B) were extracted from RNA-seq data from the Immunological Genome Project (ImmGenn) consortium (https://www.immgen.org/). Values represent transcripts per million (TPM) and color normalization was done for each gene (*right panel*). (**B**-**C**) mRNA levels of *Hif2*α were determined by quantitative RT-PCR and normalized to *Abl1* gene (mean $\pm$ SD, n=3 to 6, *p<0.05, **p<0.01) from GFP$^+$ *in vitro*-derived CTL, PAX5 Wt and PAX5 P80R cells and from *in vivo*-derived B-ALL GFP$^+$ PAX5 P80R cells. Representative of two independent experiments (B). *Hif2*α relative expression was also determined in B-cell progenitors (CD19$^+$CD23$^-$Kit$^+$) from the BM of Wt and *PAX5-ELN*^{tg} mice (mean $\pm$ SD, n=6, ***p<0.001). Representative of two independent experiments (C). (**D**) Experimental procedure to study the effect of Hif2α genomic editing on PAX5-ELN B-cell progenitors. B-cell progenitors (CD19$^+$CD23$^-$Kit$^+$) from the BM of *PAX5-ELN*^{tg}*Cas9*^{tg} mice were purified and transduced with lentiviral vectors expressing sgRNA CTL (sgCTL) or sgRNA Hif2α T8 and T12 targeting the exon 2 of *Hif2*α (sgHif2α T8 and sgHif2α T12). Transduced *PAX5-ELN*^{tg}*Cas9*^{tg} GFP$^+$ B-cells were purified and co-cultured in 24-well plates (10^5 cells / well) on MS5 stromal cells. In parallel, purified transduced sgCTL, sgHif2α T8 and T12 cells (CD45.2$^+$GFP$^+$) were intravenously transplanted in equal number ($2.5x10^4$ per mouse) in recipient CD45.1 mice. (**E-F**) *In vitro* cell growth of transduced GFP$^+$ sgCTL, sgHif2α T8 and T12 cells. Results represent the cumulative fold expansion of *PAX5-ELN*^{tg}*Cas9*^{tg} GFP$^+$ B-cells during 11 days of co-culture (E, n=3, ***p<0.001). Total mRNA was extracted from transduced GFP$^+$ cells 4 days after co-culture and mRNA levels of *Hif2*α were determined by qRT-PCR and normalized to *Abl1* gene (F, mean $\pm$ SD, n=3, **p<0.01). (**G**-**H**) Engraftment efficiency in the BM of recipient CD45.1$^+$ mice transplanted with transduced sgCTL, sgHif2α T8 and T12 cells was analyzed by FACS 3 weeks after transplantation. The number of positive mice and the median of engraftment are indicated (G). The mean fluorescence

intensity (MFI) of the GFP in the BM engrafted cells of positive recipient mice was measured (H, *right panel*).

Figure 6. (**A**) Experimental procedure to study the effect of Hif2α genomic editing on murine hematopoietic development. LSK cells from Cas9-expressing mice were purified by cell sorting and transduced with either sgCTL or sgHif2α T8 and T12 lentiviral vectors. Transduced Cas9-expressing LSK cells (CD45.2$^+$) were either plated in clonogenic assay during 11 days or transplanted into syngenic recipient mice (CD45.1$^+$, n=6 to 7 mice for each condition). (**B**) Gating strategy used for the purification of LSK from *Cas9*^{tg} mice by cell sorting. (**C**) Transduction efficiency was assessed on cells from sgCTL or sgHif2a T8 and T12 *Cas9*^{tg} LSK-derived colonies. The percentage of GFP was analysed by FACS for each condition. (**D**-**F**) Genomic DNA (D), total mRNA (E) and protein (F) were extracted from transduced sgCTL or sgHif2a T8 and T12 *Cas9*^{tg} LSK-derived colonies. The targeted region (exon 2) of *Hif2α* was performed by NGS and the genomic editing efficiency was analyzed by the proportion (%) of insertions and deletions (InDel) induced by the sgHif2α T8 and T12 using the online CRISPResso software (D). mRNA levels of *Hif2α* were determined by qRT-PCR and normalized to *Abl1* gene (E, mean ± SD, n=3, *p<0.05, **p<0.01). Protein extract was subjected to immunoblotting with anti-Hif2α antibody. α-Actin was used as a loading control (F). (**G**) Number of GFP$^+$ total, CFU-GEMM, CFU-GM and BFU-E colonies was calculated for each condition (n=3). (**H**-**I**) Engraftment efficiency in the BM of recipient CD45.1$^+$ mice transplanted with *Cas9*^{tg} LSK cells transduced by sgCTL, sgHif2α T8 and T12 lentiviral vectors was analyzed by FACS 5 and 16 weeks after transplantation. Representative FACS profile illustrating the percentage of transduced donor cells (%CD45.2$^+$GFP$^+$) found in the recipient BM (H, *left panel*). The number of positive mice and the median of engraftment are indicated (H, *right panel*). Immunophenotype of engrafted donor-derived cells (CD45.2$^+$GFP$^+$) was analyzed using CD19 (B cells), Gr1 (Myeloid cells) and Ter119 (Erythroid cells) markers. The absolute number of B, myeloid (My) and erythroid (Ery) cells in donor-derived cells (%CD45.2$^+$GFP$^+$) was then calculated 16 weeks after transplantation (I). (**J**) The percentage of Insertion/Deletion (InDel) in total BM cells from the recipient mice 16 weeks after transplantation was analysed using the online CRISPResso software.

Figure 7. (**A**) Experimental procedure for the chemical screening of 19 potential *Hifα* inhibitors. Three PAX5 P80R B-ALL (#1302, #1301, #1265) and four PAX5-ELN B-ALL (#14, #26, #53, #126) were co-cultured in 96-well plates (10^4 cells / well) on MS5 stromal cells in presence or not with 19 potential *Hifα* inhibitors in duplicate at 500nM during 48 hours. (**B**) The absolute number of treated cells by each compound was measured by FACS and normalized by the absolute number of untreated cells (vehicle, n=18). Data represents the percentage of inhibition induced by each compound (n=2, #1 and #2). Each

dot represents an individual well. Solid lines and dashed lines represent the mean and 3-fold the SD, respectively. Compounds inducing more than 30% inhibition, and in a reproducible manner, were selected as hits (red dots). (**C**) List of the 19 compounds ranked according to their efficiency to inhibit the cell viability of PAX5 P80R and PAX5-ELN B-ALL cells. The values indicate the percentage of inhibition induced by each compound (mean of the duplicate). (**D**) B-ALL#1265 and B-ALL#1301 PAX5 P80R GFP^+ cells were treated *in vitro* with a dose-response of Acriflavine for 48 hours. Absolute numbers of GFP^+ cells were then analyzed by FACS and normalized to the number of untreated cells and IC50 have been calculated. (**E**-**F**) B-ALL#1265 and B-ALL#1301 PAX5 P80R GFP^+ cells were treated for 16 hours at the indicated doses of Acriflavine. Total protein extracts were subjected to immunoblotting with HIF2α antibodies. α-Actin was used as a loading control (E) and to normalized HIF2α expression for each dose (F). (**G**) *In vitro* dose-response of Acriflavine on human B-ALL cell lines (REH and 697) and on leukemic blasts from P80R B-ALL PDXs (PDX #112 and PDX #214). Absolute numbers of cells were then analyzed 48h after treatment by FACS and normalized to the number of untreated cells and IC50 have been calculated. (**H**-**I**) HIF2α expression assessed by WB in REH, 697, PDX #112 and PDX #214 16 hours after 16 hours of treatment with the indicated doses of Acriflavine. α-Actin was used as a loading control (H) and to normalized HIF2α expression for each dose (I).

Figure S1

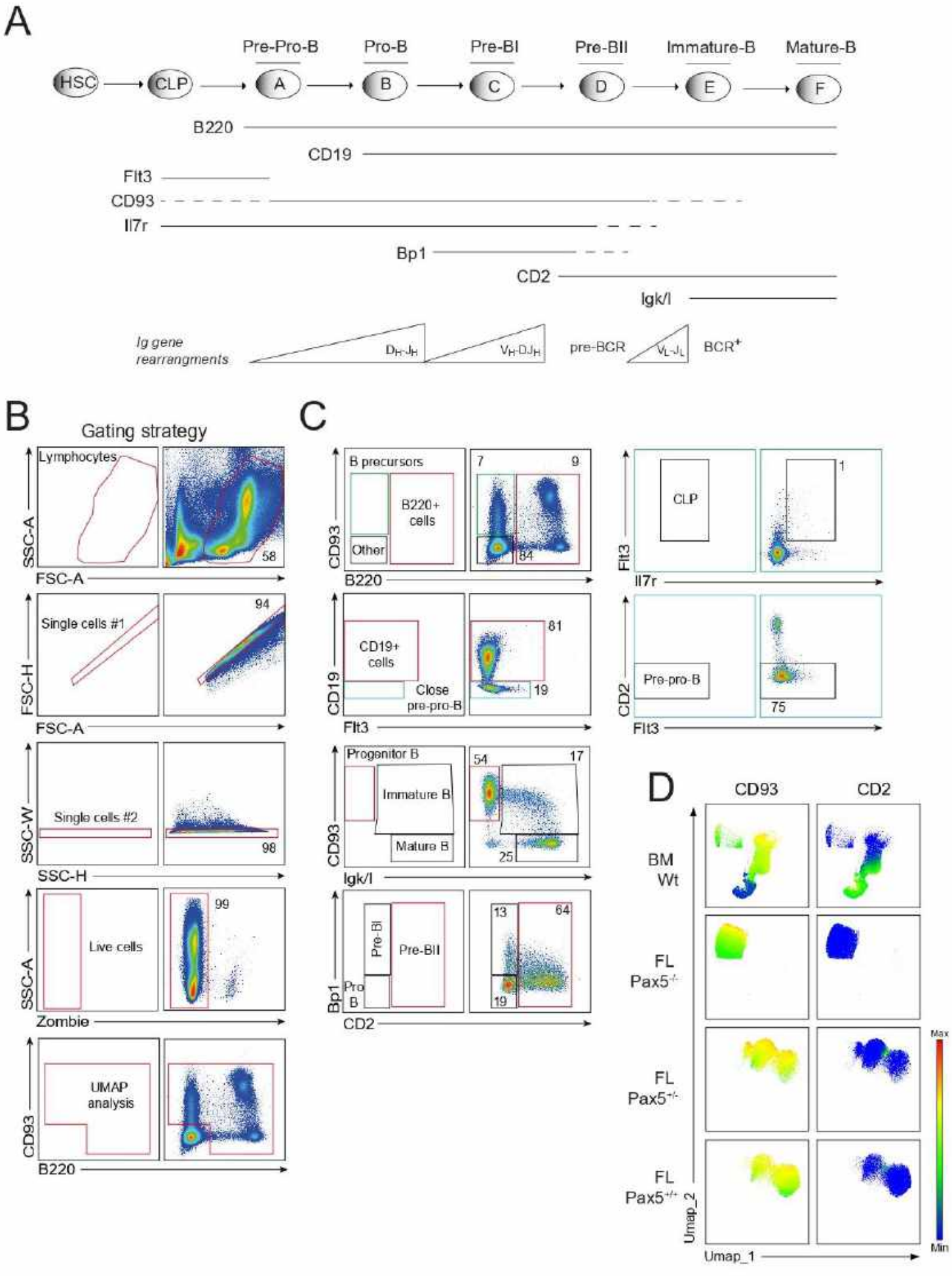
A
Pre-Pro-B
Pro-B
Pre-BI
Pre-BII
Immature-B
Mature-B
HSC
CLP
A
B
C
D
E
F
B220
CD19
Flt3
CD93
Il7r
Bp1
CD2
Igk/l
Ig gene rearrangments
DH-JH
VH-DJH
pre-BCR
VL-JL
BCR+
B
Gating strategy
Lymphocytes
SSC-A
FSC-A
58
Single cells #1
FSC-H
94
Single cells #2
SSC-W
SSC-H
98
Live cells
99
Zombie
UMAP analysis
CD93
B220
C
B precursors
B220+ cells
Other
7
9
84
CD19+ cells
Close pre-pro-B
81
19
Progenitor B
Immature B
Mature B
54
17
25
Pre-BI
Pre-BII
Pro B
13
64
19
Bp1
CD2
CLP
1
Pre-pro-B
75
D
CD93
CD2
BM Wt
FL Pax5-/-
FL Pax5-/-
FL Pax5+/+
Max
Min
Umap_2
Umap_1

Figure S2

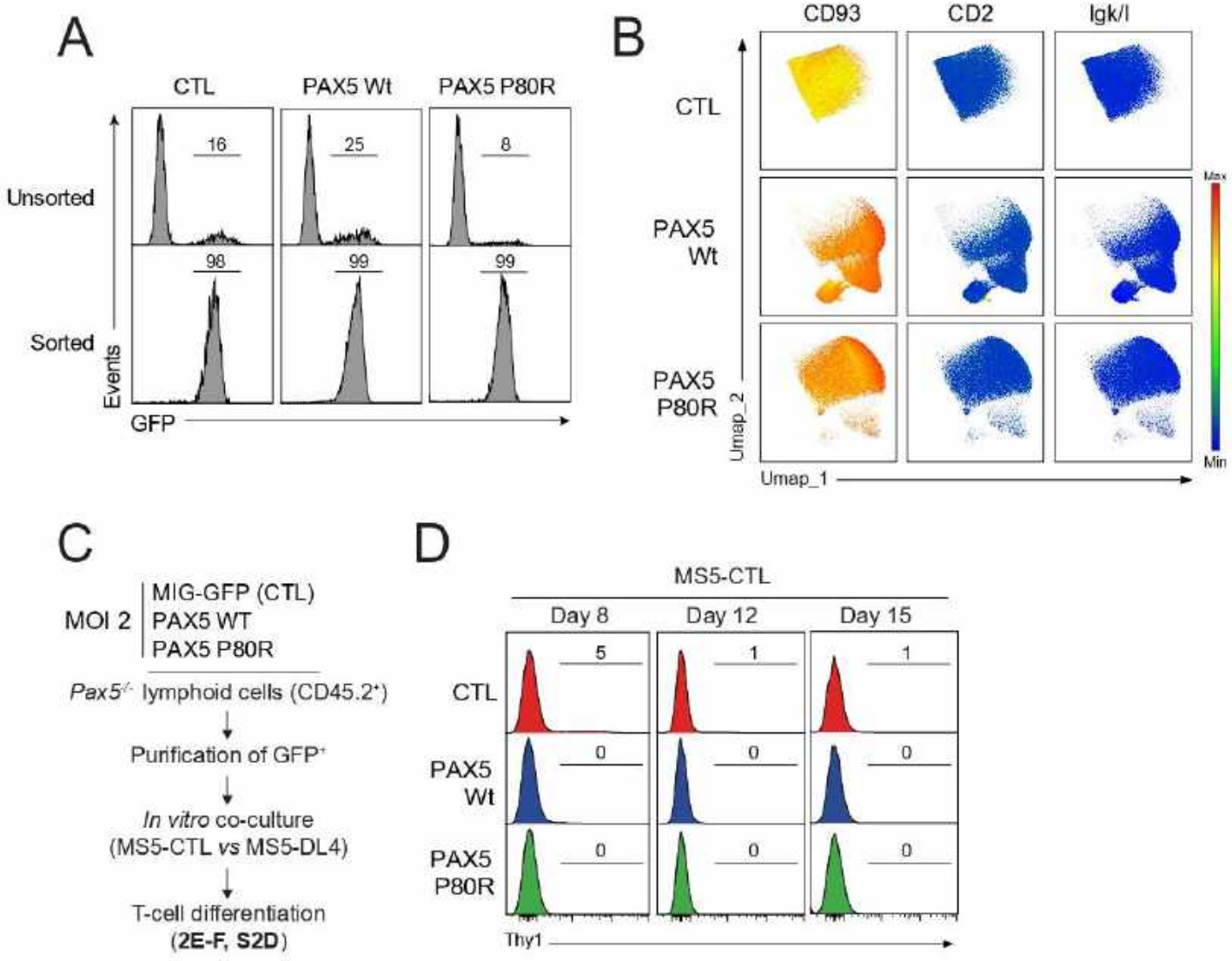
A
CTL
PAX5 Wt
PAX5 P80R
Unsorted
Sorted
16
25
8
98
99
99
Events
GFP
B
CD93
CD2
Igk/l
CTL
PAX5 Wt
PAX5 P80R
Umap_2
Umap_1
Max
Min
C
MOI 2
MIG-GFP (CTL)
PAX5 WT
PAX5 P80R
Pax5-/- lymphoid cells (CD45.2+)
Purification of GFP+
In vitro co-culture
(MS5-CTL vs MS5-DL4)
T-cell differentiation
(2E-F, S2D)
D
MS5-CTL
Day 8
Day 12
Day 15
CTL
PAX5 Wt
PAX5 P80R
5
1
1
0
0
0
0
0
0
Thy1

Figure S3

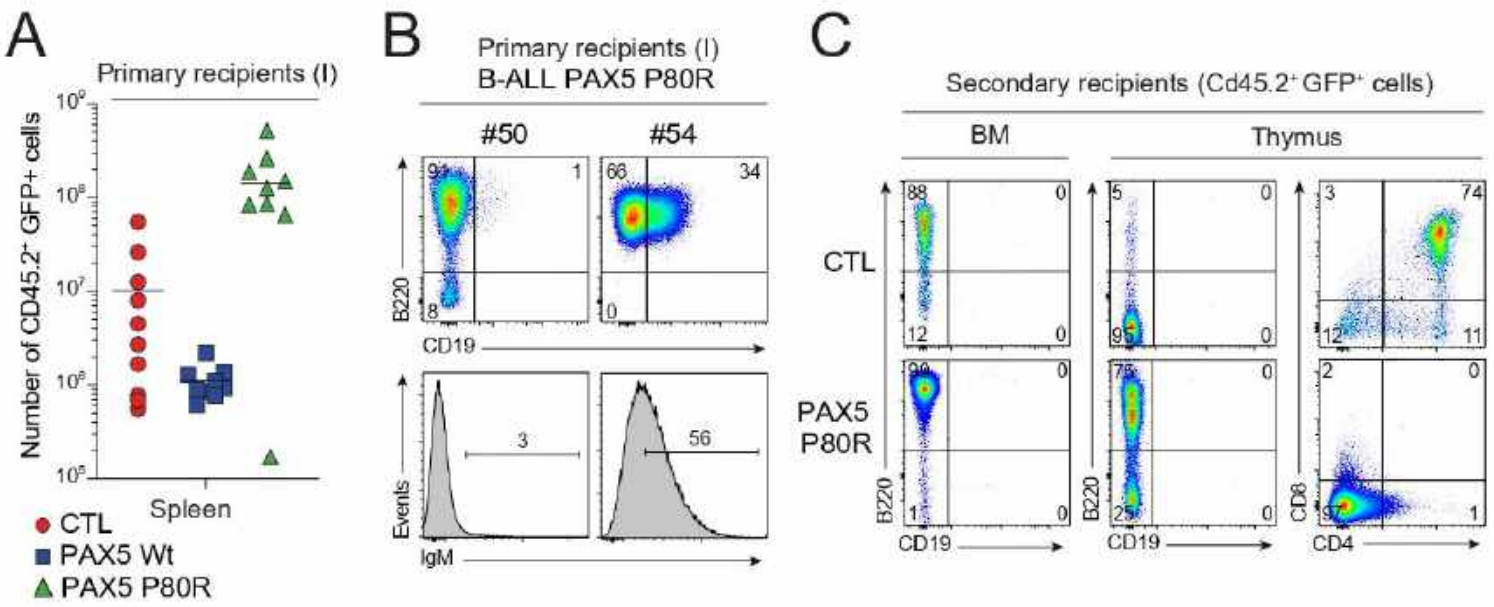
A
Primary recipients (I)
Number of CD45.2+ GFP+ cells
Spleen
CTL
PAX5 Wt
PAX5 P80R
B
Primary recipients (I)
B-ALL PAX5 P80R
#50
#54
B220
CD19
Events
IgM
C
Secondary recipients (Cd45.2+ GFP+ cells)
BM
Thymus
CTL
PAX5 P80R
CD19
CD4
CD8

Figure S4

A

CTL

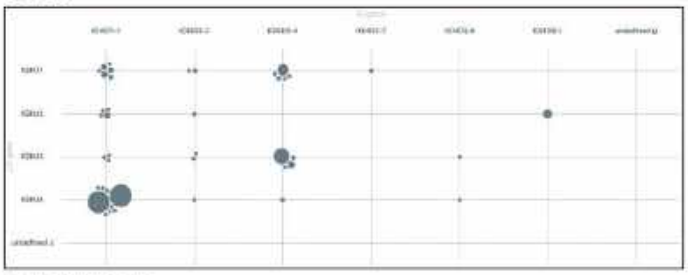

PAX5 Wt

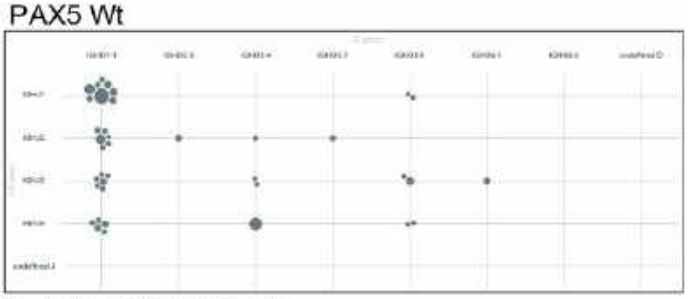

PAX5 P80R

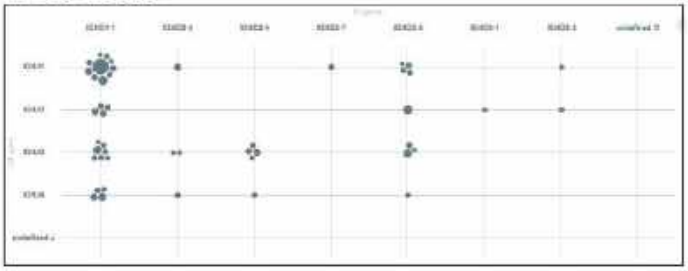

B-ALL#50 PAX5 P80R

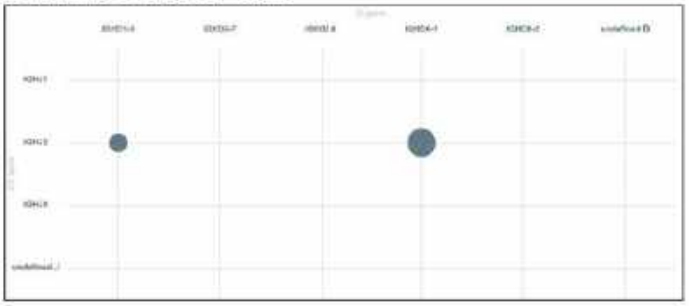

B

B-ALL#54 PAX5 P80R

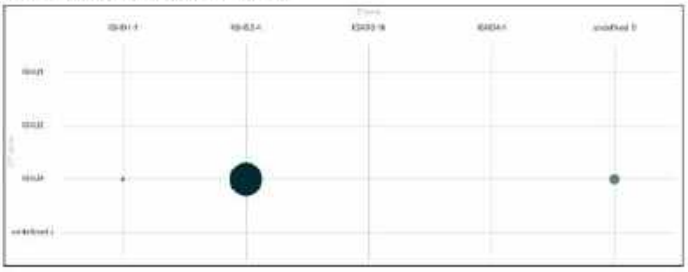

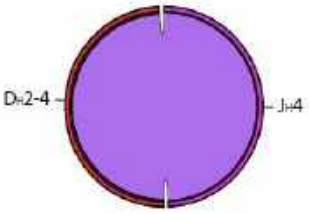

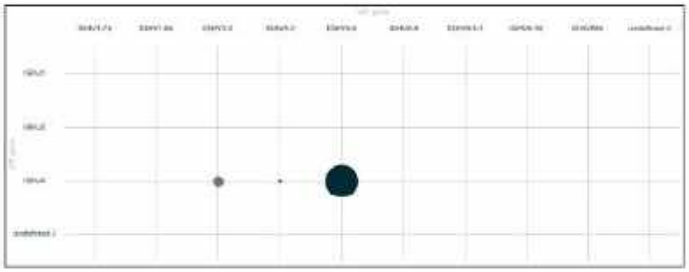

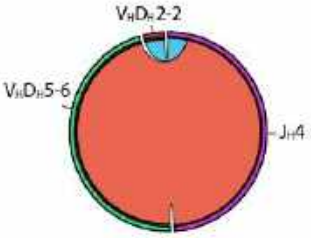

Figure S5

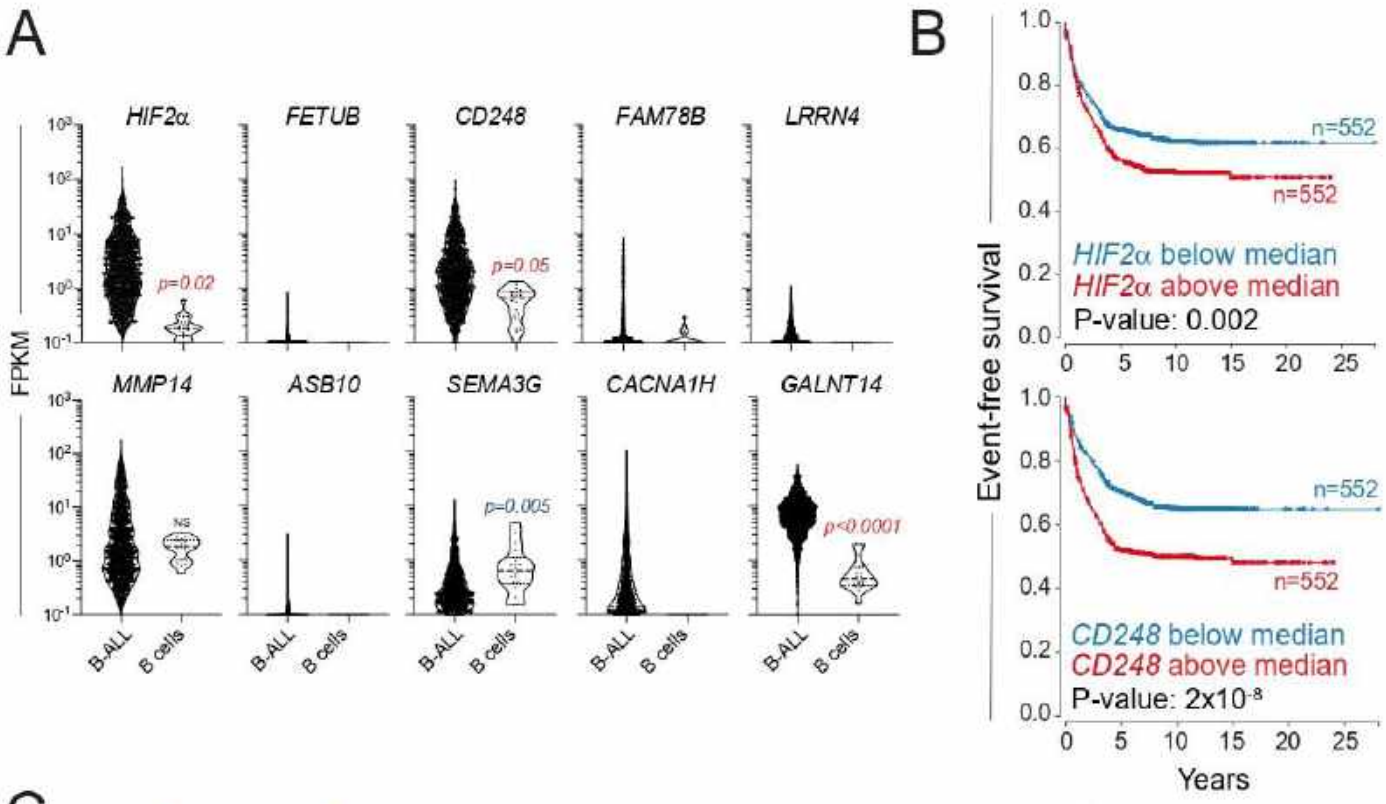
A
HIF2α
FETUB
CD248
FAM78B
LRRN4
MMP14
ASB10
SEMA3G
CACNA1H
GALNT14
FPKM
p=0.02
p=0.05
NS
p=0.005
p<0.0001
B-ALL
B cells
B
Event-free survival
n=552
n=552
HIF2α below median
HIF2α above median
P-value: 0.002
CD248 below median
CD248 above median
P-value: 2x10-8
Years

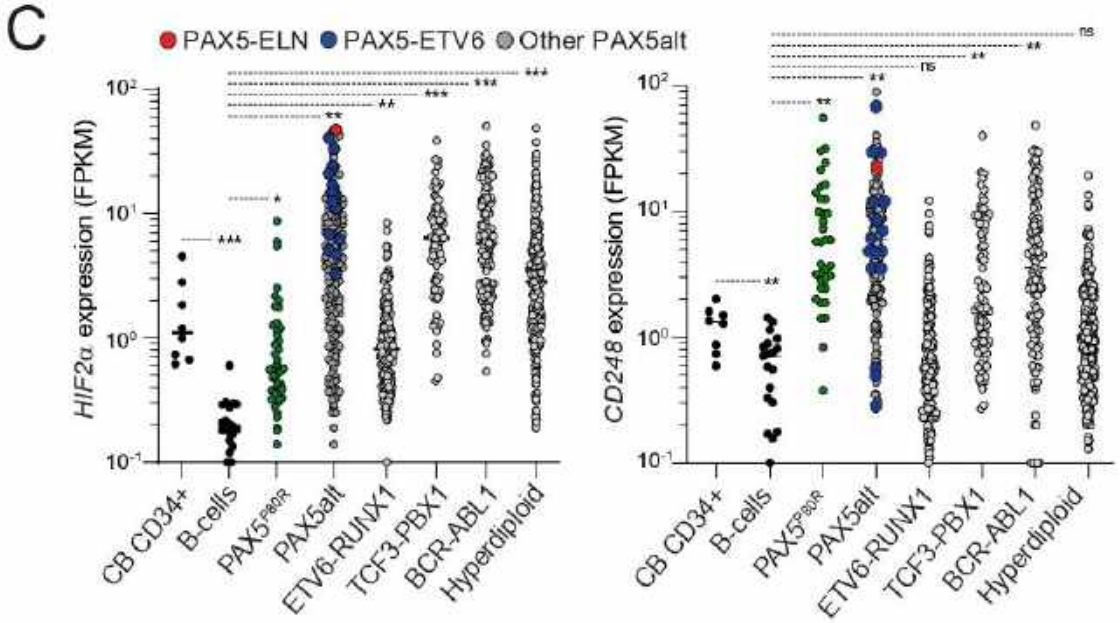
C
PAX5-ELN
PAX5-ETV6
Other PAX5alt
HIF2α expression (FPKM)
CD248 expression (FPKM)
CB CD34+
B-cells
PAX5P80R
PAX5alt
ETV6-RUNX1
TCF3-PBX1
BCR-ABL1
Hyperdiploid

Figure S6

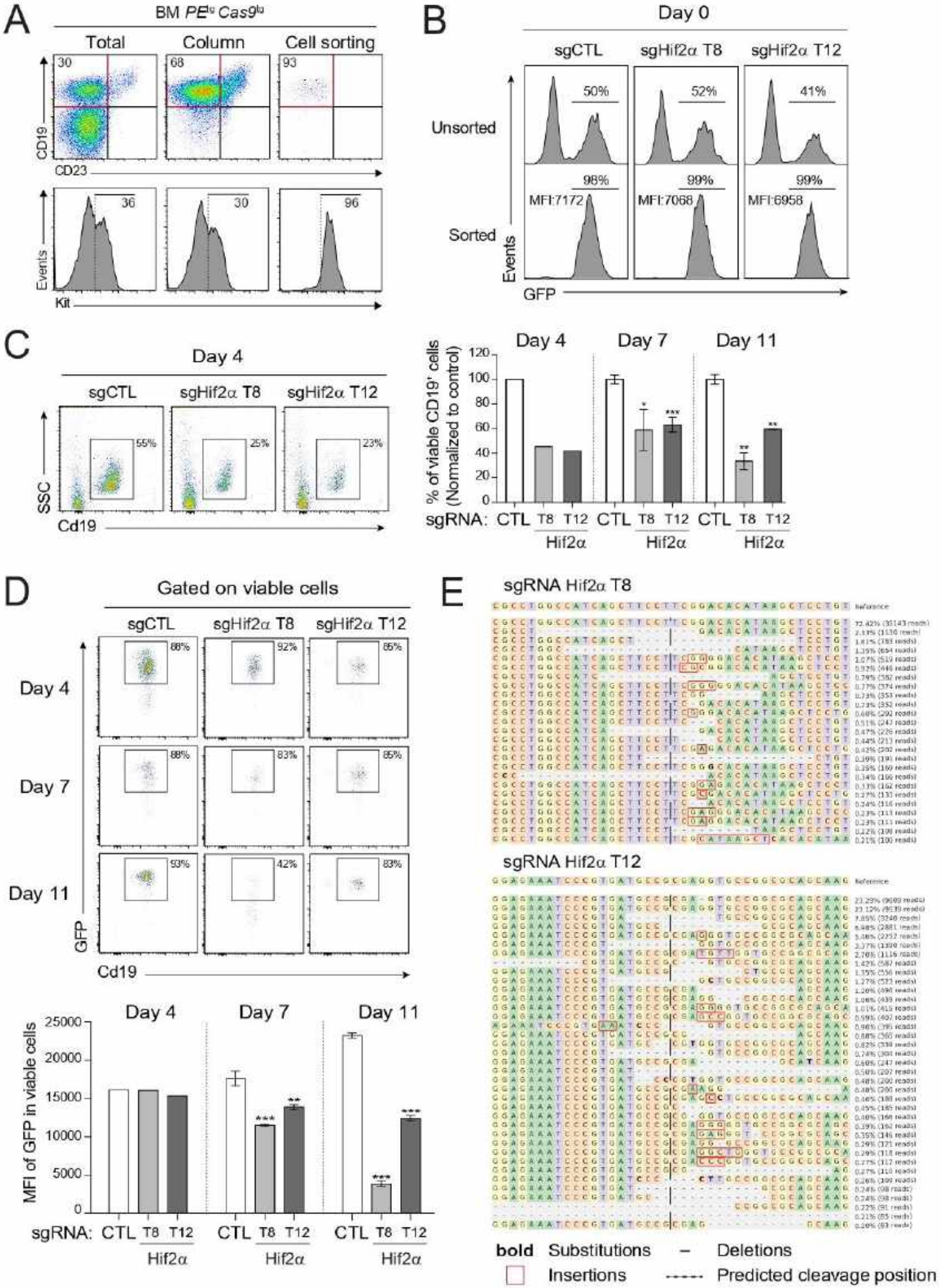
A
BM PE^tg Cas9^tg
Total
Column
Cell sorting
30
68
93
CD19
CD23
36
30
96
Events
Kit
B
Day 0
sgCTL
sgHif2α T8
sgHif2α T12
Unsorted
Sorted
50%
52%
41%
98%
99%
99%
MFI:7172
MFI:7068
MFI:6958
Events
GFP
C
Day 4
sgCTL
sgHif2α T8
sgHif2α T12
55%
25%
23%
SSC
Cd19
Day 4
Day 7
Day 11
% of viable CD19+ cells (Normalized to control)
120
100
80
60
40
20
0
sgRNA: CTL T8 T12 CTL T8 T12 CTL T8 T12
Hif2α
Hif2α
Hif2α
D
Gated on viable cells
sgCTL
sgHif2α T8
sgHif2α T12
Day 4
Day 7
Day 11
88%
92%
85%
88%
83%
85%
93%
42%
83%
GFP
Cd19
Day 4
Day 7
Day 11
MFI of GFP in viable cells
25000
20000
15000
10000
5000
0
sgRNA: CTL T8 T12 CTL T8 T12 CTL T8 T12
Hif2α
Hif2α
Hif2α
E
sgRNA Hif2α T8
sgRNA Hif2α T12
bold Substitutions
Insertions
– Deletions
Predicted cleavage position

Figure S7

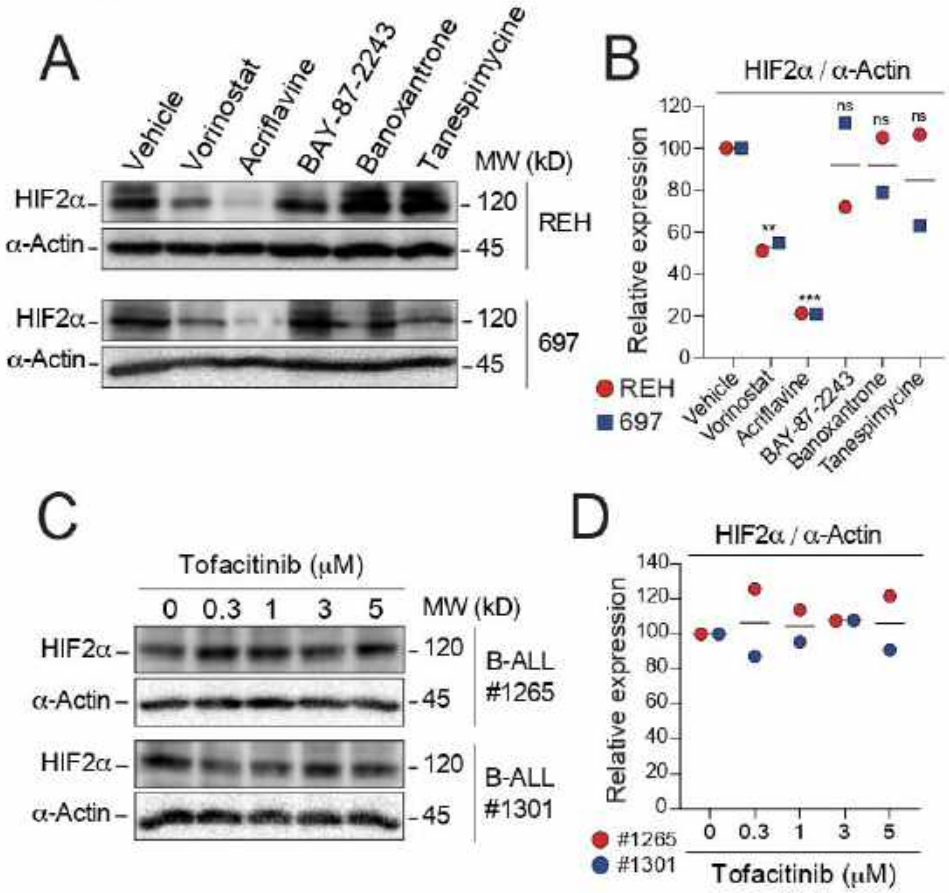
A
Vehicle
Vorinostat
Acriflavine
BAY-87-2243
Banoxantrone
Tanespimycine
MW (kD)
HIF2α
α-Actin
120
45
REH
697
B
HIF2α / α-Actin
Relative expression
ns
**
***
REH
697
C
Tofacitinib (μM)
0 0.3 1 3 5
B-ALL #1265
B-ALL #1301
D
HIF2α / α-Actin
Relative expression
#1265
#1301
Tofacitinib (μM)

Supplementary figure legends.

Figure S1. (**A**) Schematic representation of the murine B-cell development. Representation of the different B-cell differentiation stages (HSC, CLP, pre-pro-B, pro-B, pre-BI, pre-BII, immature-B and mature-B) and pattern of expression of the main markers used to characterize each subset. The thickness of the line is representative of the expression level. The dotted lines indicate subsets where expression is progressively acquired or lost. $V_HD_HJ_H$ and V_LJ_L rearrangements are indicated. (**B**-**C**) Gating strategy of the lymphoid compartment (B) and of the different B-cell subpopulations (C) to perform the clustering analysis by UMAP shown in **Figure 1A**. Gates from total BM cells of wt adult mice were shown as reference. Each red gate represents the parent population of the following below set of FACS plots. Green and blue gates represent the parent populations allowing the identification of CLP and pre-pro-B subpopulations, respectively. (**D**) Visualization of the expression level of CD93 and CD2 in the BM cells from wt mice and in the fetal liver (FL) from *Pax5*$^{-/-}$, *Pax5*$^{+/-}$ and *Pax5*$^{+/+}$ mice was shown according to the UMAP approach from **Figure 1A**.

Figure S2. (**A**) Transduction efficiency of FL cells from *Pax5*$^{-/-}$ mice expressing MIG-GFP (CTL) or MIG-PAX5 Wt (PAX5 Wt) or MIG-PAX5 P80R (PAX5 P80R) vectors was assessed by FACS by monitoring the percentage of GFP for each condition (*upper panels*). Transduced GFP$^+$ cells were then purified by cell sorting and cell purity was then verified (*lower panels*). (**B**) Visualization of the expression level of CD93, CD2 and Igκ/λ were shown in GFP$^+$ B-cell subsets according to the UMAP approach from **Figure 2C**.

Figure S3. (**A**) Absolute number of donor-derived (CD45.2$^+$GFP$^+$) cells from the spleen of primary recipients transplanted with CTL, PAX5 Wt and PAX5 P80R cells. (**B**) Immunophenotype of B-ALL PAX5 P80R cells from two representative mice (#50 and #54). FACS analysis of B220, CD19 and IgM expression was shown. (**C**) Representative immunophenotype of donor-derived CD45.2$^+$GFP$^+$ cells from the BM and the thymus of secondary recipients engrafted with CTL and PAX5 P80R cells. FACS analysis of B220, CD19, CD4 and CD8 expression was shown.

Figure S4. (**A**) *IgH* gene rearrangements of transduced GFP$^+$ CTL, PAX5 Wt and PAX5 P80R cells cultured *in vitro* and of B-ALL#50 PAX5 P80R cells were performed according to **Figure 4C** and were visualized with the Vidjil software. D_H-J_H rearrangements are displayed as circles whose size is proportional to the number of reads which is assumed to reflect the proportion of each rearrangement in the sample. The coordinates of the positions of the circles correspond to the *IgH* gene segments involved in each rearrangement (D_H segments on the x-axis and J_H segments on the y-axis). V_H-D_HJ_H rearrangements were not observed. (**B**) D_H-J_H (*upper panel*) and V_H-D_HJ_H (*lower panel*) clonal rearrangements of B-ALL cells

from mouse #54 were visualized with the Vidjil software. The proportions of the rearrangements were represented by Circos diagrams (*right panels*).

Figure S5. (**A**) Expression of *HIF2α, FETUB, CD248, FAM78B, LRRN4, MMP14, ASB10, SEMA3G, CACNA1H* and *GALNT14* in total B-ALL patients and in normal B-cells ($CD19^+$) from cord blood subgroups extracted from (Gu et al., 2019b). (**B**) *HIF2α* and *CD248* expressions and their associated clinical outcome in B-ALL patient extracted from (Gu et al., 2019b). Event-free survival (EFS) curves of total B-ALL patients with *HIF2α* or *CD248* expression below (blue) and above (red) to the median. Data were visualized using the St. Jude Cloud visualization community tool (https://viz.stjude.cloud/st-jude-childrens-research-hospital/visualization). (**C**) *HIF2α* and *CD248* expression in B-ALL patients belonging to the $PAX5^{P80R}$ (green), PAX5alt (including PAX5-ELN and PAX5-ETV6 patients in red and blue, respectively), ETV6-RUNX1, TCF3-PBX1, BCR-ABL1 and Hyperdyploid oncogenic subgroups extracted from (Gu et al., 2019b). Normal HSPCs ($CD34^+$) and normal B-cells ($CD19^+$) from cord blood are used as control.

Figure S6. (**A**) Purification of B-cell progenitors ($CD19^+CD23^-Kit^+$) from the BM of *PAX5-ELN*^{tg}*Cas9*^{tg} mice. (**B**) Transduction efficiency of *PAX5-ELN*^{tg}*Cas9*^{tg} B-cells expressing sgCTL, sgHif2α T8 and sgHif2α T12 was assessed by FACS by monitoring the percentage of GFP for each condition (*upper panels*). Transduced cells were then purified by cell sorting and cell purity was verified (*lower panels*). (**C**) The percentage of viable $CD19^+$ cells was monitored by FACS at day 4, 7 and 11 of co-culture for each condition. Representative FACS profile at day 4 (*left panel*) and quantification for each time point (*right panel*) were shown. (**D**) Representative FACS profile illustrating the proportion of GFP^+ cells at day 4, 7 and 11 of co-culture for each condition (*upper panel*) and the MFI of the GFP was measured (*lower panel*). (**E**) Genomic DNA were extracted from transduced GFP^+ cells 4 days after co-culture. The targeted region (exon 2) of *Hif2α* was performed by NGS and the genomic editing efficiency was analyzed by the proportion (%) of insertions and deletions (InDel) induced by the sgHif2α T8 and T12 using the online CRISPResso software. Sequence alignments illustrating the genomic editing efficiency of the *Hif2α* locus was shown.

Figure S7. (**A**-**B**) Human REH and 697 B-ALL cell lines were treated for 16 hours at 5µM with the indicated compounds. Total protein extracts were subjected to immunoblotting with HIF2α antibodies. α-Actin was used as a loading control (A) and to normalized HIF2α expression for each compound (B). (**C**-**D**) B-ALL#1265 and B-ALL#1301 PAX5 P80R GFP^+ cells were treated for 16 hours at the indicated doses of Tofacitinib. Total protein extracts were subjected to immunoblotting with HIF2α antibodies.

α-Actin was used as a loading control (C) and to normalized HIF2α expression for each dose (D). (**E**) HIF2α expression assessed by WB in leukemic blasts from P80R B-ALL PDXs (PDX #112 and PDX #214) after 16 hours of treatment with the indicated doses of Tofacitinib. α-Actin was used as a loading control. (**F**) Representative FACS analysis of pStat5 expression after IL-7 stimulation (+IL-7) in presence or not (vehicle) of 1 μM Tofacitinib (Tofa) and of a dose-response of Acriflavine in REH and 697 B-ALL cell lines and in P80R B-ALL PDX #112 and PDX #214. Unstimulated (-IL-7) cells and were used as controls.

Table S1. List of FACS antibodies used for the phenotypic characterization of the B-cell lineage. The combination of markers for the multiparametric immunostaining used in each figure were indicated.

Table S2. Sequences of oligonucleotide primers used for the targeted NGS, for the subcloning of sgRNAs in pLKO5-sgRNA-EFS-GFP to generate lentiviral vectors, for RT-qPCR and for IgH gene rearrangements.

References.

Adams, B., Dörfler, P., Aguzzi, A., Kozmik, Z., Urbánek, P., Maurer-Fogy, I., & Busslinger, M. (1992). Pax-5 encodes the transcription factor BSAP and is expressed in B lymphocytes, the developing CNS, and adult testis. *Genes & Development*, *6*(9), 1589–1607. https://doi.org/10.1101/gad.6.9.1589

Adams, G. B., Chabner, K. T., Alley, I. R., Olson, D. P., Szczepiorkowski, Z. M., Poznansky, M. C., Kos, C. H., Pollak, M. R., Brown, E. M., & Scadden, D. T. (2006). Stem cell engraftment at the endosteal niche is specified by the calcium-sensing receptor. *Nature*, *439*(7076), 599–603. https://doi.org/10.1038/nature04247

Adolfsson, J., Månsson, R., Buza-Vidas, N., Hultquist, A., Liuba, K., Jensen, C. T., Bryder, D., Yang, L., Borge, O.-J., Thoren, L. A. M., Anderson, K., Sitnicka, E., Sasaki, Y., Sigvardsson, M., & Jacobsen, S. E. W. (2005). Identification of Flt3+ Lympho-Myeloid Stem Cells Lacking Erythro-Megakaryocytic Potential. *Cell*, *121*(2), 295–306. https://doi.org/10.1016/j.cell.2005.02.013

Aird, E. J., Lovendahl, K. N., St. Martin, A., Harris, R. S., & Gordon, W. R. (2018). Increasing Cas9-mediated homology-directed repair efficiency through covalent tethering of DNA repair template. *Communications Biology*, *1*(1), 54. https://doi.org/10.1038/s42003-018-0054-2

Aiuti, A., Webb, I. J., Bleul, C., Springer, T., & Gutierrez-Ramos, J. C. (1997). The Chemokine SDF-1 Is a Chemoattractant for Human CD34+ Hematopoietic Progenitor Cells and Provides a New Mechanism to Explain the Mobilization of CD34+ Progenitors to Peripheral Blood. *The Journal of Experimental Medicine*, *185*(1), 111–120. https://doi.org/10.1084/jem.185.1.111

Alberti-Servera, L., von Muenchow, L., Tsapogas, P., Capoferri, G., Eschbach, K., Beisel, C., Ceredig, R., Ivanek, R., & Rolink, A. (2017). Single-cell RNA sequencing reveals developmental heterogeneity among early lymphoid progenitors. *The EMBO Journal*, *36*(24), 3619–3633. https://doi.org/10.15252/embj.201797105

Alexandrov, L. B., Nik-Zainal, S., Wedge, D. C., Aparicio, S. A. J. R., Behjati, S., Biankin, A. V., Bignell, G. R., Bolli, N., Borg, A., Børresen-Dale, A.-L., Boyault, S., Burkhardt, B., Butler, A. P., Caldas, C., Davies, H. R., Desmedt, C., Eils, R., Eyfjörd, J. E., Foekens, J. A., … Stratton, M. R. (2013). Signatures of mutational processes in human cancer. *Nature*, *500*(7463), 415–421. https://doi.org/10.1038/nature12477

Amir, A., Erez-Granat, O., Braun, T., Sosnovski, K., Hadar, R., BenShoshan, M., Heiman, S., Abbas-Egbariya, H., Glick Saar, E., Efroni, G., & Haberman, Y. (2022). Gut microbiome development in early childhood is affected by day care attendance. *Npj Biofilms and Microbiomes*, *8*(1), 2. https://doi.org/10.1038/s41522-021-00265-w

An, Q., Wright, S. L., Konn, Z. J., Matheson, E., Minto, L., Moorman, A. V, Parker, H., Griffiths, M., Ross, F. M., Davies, T., Hall, A. G., Harrison, C. J., Irving, J. A., & Strefford, J. C. (2008). Variable breakpoints target PAX5 in patients with dicentric chromosomes: a model for the basis of unbalanced translocations in cancer. *Proc Natl Acad Sci U S A*, *105*(44), 17050–17054. https://doi.org/10.1073/pnas.0803494105

Anderson, K., Lutz, C., van Delft, F. W., Bateman, C. M., Guo, Y., Colman, S. M., Kempski, H., Moorman, A. V., Titley, I., Swansbury, J., Kearney, L., Enver, T., & Greaves, M. (2011). Genetic variegation of clonal architecture and propagating cells in leukaemia. *Nature*, *469*(7330), 356–361. https://doi.org/10.1038/nature09650

Aoki, Y., Watanabe, T., Saito, Y., Kuroki, Y., Hijikata, A., Takagi, M., Tomizawa, D., Eguchi, M., Eguchi-Ishimae, M., Kaneko, A., Ono, R., Sato, K., Suzuki, N., Fujiki, S., Koh, K., Ishii, E.,

Shultz, L. D., Ohara, O., Mizutani, S., & Ishikawa, F. (2015). Identification of CD34+ and CD34− leukemia-initiating cells in MLL-rearranged human acute lymphoblastic leukemia. *Blood*, *125*(6), 967–980. https://doi.org/10.1182/blood-2014-03-563304

Asada, N., Kunisaki, Y., Pierce, H., Wang, Z., Fernandez, N. F., Birbrair, A., Ma'ayan, A., & Frenette, P. S. (2017). Differential cytokine contributions of perivascular haematopoietic stem cell niches. *Nature Cell Biology*, *19*(3), 214–223. https://doi.org/10.1038/ncb3475

Aurrand-Lions, M., & Mancini, S. (2018). Murine Bone Marrow Niches from Hematopoietic Stem Cells to B Cells. *International Journal of Molecular Sciences*, *19*(8), 2353. https://doi.org/10.3390/ijms19082353

Bain, G., Maandag, E. C., Izon, D. J., Amsen, D., Kruisbeek, A. M., Weintraub, B. C., Krop, I., Schlissel, M. S., Feeney, A. J., & van Roon, M. (1994). E2A proteins are required for proper B cell development and initiation of immunoglobulin gene rearrangements. *Cell*, *79*(5), 885–892. https://doi.org/10.1016/0092-8674(94)90077-9

Balczarek, K. A., Lai, Z. C., & Kumar, S. (1997). Evolution of functional diversification of the paired box (Pax) DNA- binding domains. *Molecular Biology and Evolution*, *14*(8), 829–842. https://doi.org/10.1093/oxfordjournals.molbev.a025824

Bao, E. L., Cheng, A. N., & Sankaran, V. G. (2019). The genetics of human hematopoiesis and its disruption in disease. *EMBO Molecular Medicine*, *11*(8). https://doi.org/10.15252/emmm.201910316

Barlev, N. A., Emelyanov, A. V., Castagnino, P., Zegerman, P., Bannister, A. J., Sepulveda, M. A., Robert, F., Tora, L., Kouzarides, T., Birshtein, B. K., & Berger, S. L. (2003). A Novel Human Ada2 Homologue Functions with Gcn5 or Brg1 To Coactivate Transcription. *Molecular and Cellular Biology*, *23*(19), 6944–6957. https://doi.org/10.1128/MCB.23.19.6944-6957.2003

Barrangou, R., Fremaux, C., Deveau, H., Richards, M., Boyaval, P., Moineau, S., Romero, D. A., & Horvath, P. (2007). CRISPR Provides Acquired Resistance Against Viruses in Prokaryotes. *Science*, *315*(5819), 1709–1712. https://doi.org/10.1126/science.1138140

Bastian, L., Schroeder, M. P., Eckert, C., Schlee, C., Tanchez, J. O., Kämpf, S., Wagner, D. L., Schulze, V., Isaakidis, K., Lázaro-Navarro, J., Hänzelmann, S., James, A. R., Ekici, A., Burmeister, T., Schwartz, S., Schrappe, M., Horstmann, M., Vosberg, S., Krebs, S., … Baldus, C. D. (2019). PAX5 biallelic genomic alterations define a novel subgroup of B-cell precursor acute lymphoblastic leukemia. *Leukemia*, *33*(8), 1895–1909. https://doi.org/10.1038/s41375-019-0430-z

Bastian, L., Schroeder, M. P., Eckert, C., Schlee, C., Tanchez, J. O., Kampf, S., Wagner, D. L., Schulze, V., Isaakidis, K., Lazaro-Navarro, J., Hanzelmann, S., James, A. R., Ekici, A., Burmeister, T., Schwartz, S., Schrappe, M., Horstmann, M., Vosberg, S., Krebs, S., … Baldus, C. D. (2019). PAX5 biallelic genomic alterations define a novel subgroup of B-cell precursor acute lymphoblastic leukemia. *Leukemia*, *33*(8), 1895–1909. https://doi.org/10.1038/s41375-019-0430-z

Becht, E., McInnes, L., Healy, J., Dutertre, C. A., Kwok, I. W. H., Ng, L. G., Ginhoux, F., & Newell, E. W. (2018). Dimensionality reduction for visualizing single-cell data using UMAP. *Nat Biotechnol*. https://doi.org/10.1038/nbt.4314

Berenson, R. J., Andrews, R. G., Bensinger, W. I., Kalamasz, D., Knitter, G., Buckner, C. D., & Bernstein, I. D. (1988). Antigen CD34+ marrow cells engraft lethally irradiated baboons. *Journal of Clinical Investigation*, *81*(3), 951–955. https://doi.org/10.1172/JCI113409

Berry, R., Chen, Z., McCluskey, J., & Rossjohn, J. (2011). Insight into the basis of autonomous immunoreceptor activation. *Trends in Immunology*, *32*(4), 165–170. https://doi.org/10.1016/j.it.2011.01.007

Bhatia, M., Wang, J. C. Y., Kapp, U., Bonnet, D., & Dick, J. E. (1997). Purification of primitive human hematopoietic cells capable of repopulating immune-deficient mice. *Proceedings of the National Academy of Sciences*, *94*(10), 5320–5325. https://doi.org/10.1073/pnas.94.10.5320

Bhatia, S., Pooja, & Yadav, S. K. (2023). CRISPR-Cas for genome editing: Classification, mechanism, designing and applications. *International Journal of Biological Macromolecules*, *238*, 124054. https://doi.org/10.1016/j.ijbiomac.2023.124054

Bolotin, A., Quinquis, B., Sorokin, A., & Ehrlich, S. D. (2005). Clustered regularly interspaced short palindrome repeats (CRISPRs) have spacers of extrachromosomal origin. *Microbiology*, *151*(8), 2551–2561. https://doi.org/10.1099/mic.0.28048-0

Bonnet, D., & Dick, J. E. (1997). Human acute myeloid leukemia is organized as a hierarchy that originates from a primitive hematopoietic cell. *Nature Medicine*, *3*(7), 730–737. https://doi.org/10.1038/nm0797-730

Bousquet, M., Broccardo, C., Quelen, C., Meggetto, F., Kuhlein, E., Delsol, G., Dastugue, N., & Brousset, P. (2007a). A novel PAX5-ELN fusion protein identified in B-cell acute lymphoblastic leukemia acts as a dominant negative on wild-type PAX5. *Blood*, *109*(8), 3417–3423. https://doi.org/10.1182/blood-2006-05-025221

Bousquet, M., Broccardo, C., Quelen, C., Meggetto, F., Kuhlein, E., Delsol, G., Dastugue, N., & Brousset, P. (2007b). A novel PAX5-ELN fusion protein identified in B-cell acute lymphoblastic leukemia acts as a dominant negative on wild-type PAX5. *Blood*, *109*(8), 3417–3423. https://doi.org/10.1182/blood-2006-05-025221

Brady, S. W., Roberts, K. G., Gu, Z., Shi, L., Pounds, S., Pei, D., Cheng, C., Dai, Y., Devidas, M., Qu, C., Hill, A. N., Payne-Turner, D., Ma, X., Iacobucci, I., Baviskar, P., Wei, L., Arunachalam, S., Hagiwara, K., Liu, Y., … Mullighan, C. G. (2022). The genomic landscape of pediatric acute lymphoblastic leukemia. *Nature Genetics*, *54*(9), 1376–1389. https://doi.org/10.1038/s41588-022-01159-z

Broudy, V. C. (1997). Stem cell factor and hematopoiesis. *Blood*, *90*(4), 1345–1364.

Broxmeyer, H. E., Orschell, C. M., Clapp, D. W., Hangoc, G., Cooper, S., Plett, P. A., Liles, W. C., Li, X., Graham-Evans, B., Campbell, T. B., Calandra, G., Bridger, G., Dale, D. C., & Srour, E. F. (2005). Rapid mobilization of murine and human hematopoietic stem and progenitor cells with AMD3100, a CXCR4 antagonist. *The Journal of Experimental Medicine*, *201*(8), 1307–1318. https://doi.org/10.1084/jem.20041385

Brun, T., Franklin, I., St-Onge, L., Biason-Lauber, A., Schoenle, E. J., Wollheim, C. B., & Gauthier, B. R. (2004). The diabetes-linked transcription factor PAX4 promotes β-cell proliferation and survival in rat and human islets. *Journal of Cell Biology*, *167*(6), 1123–1135. https://doi.org/10.1083/jcb.200405148

Busslinger, M. (2004a). Transcriptional Control of Early B Cell Development. *Annual Review of Immunology*, *22*(1), 55–79. https://doi.org/10.1146/annurev.immunol.22.012703.104807

Busslinger, M. (2004b). Transcriptional control of early B cell development. *Annu Rev Immunol*, *22*, 55–79. https://doi.org/10.1146/annurev.immunol.22.012703.104807

Busslinger, M., Klix, N., Pfeffer, P., Graninger, P. G., & Kozmik, Z. (1996). Deregulation of PAX-5 by translocation of the Emu enhancer of the IgH locus adjacent to two alternative PAX-5

promoters in a diffuse large-cell lymphoma. *Proceedings of the National Academy of Sciences*, *93*(12), 6129–6134. https://doi.org/10.1073/pnas.93.12.6129

Cai, Q., Dmitrieva, N. I., Ferraris, J. D., Brooks, H. L., van Balkom, B. W. M., & Burg, M. (2005). Pax2 expression occurs in renal medullary epithelial cells *in vivo* and in cell culture, is osmoregulated, and promotes osmotic tolerance. *Proceedings of the National Academy of Sciences*, *102*(2), 503–508. https://doi.org/10.1073/pnas.0408840102

Canver, M. C., Haeussler, M., Bauer, D. E., Orkin, S. H., Sanjana, N. E., Shalem, O., Yuan, G. C., Zhang, F., Concordet, J. P., & Pinello, L. (2018). Integrated design, execution, and analysis of arrayed and pooled CRISPR genome-editing experiments. *Nat Protoc*, *13*(5), 946–986. https://doi.org/10.1038/nprot.2018.005

Castor, A., Nilsson, L., Åstrand-Grundström, I., Buitenhuis, M., Ramirez, C., Anderson, K., Strömbeck, B., Garwicz, S., Békássy, A. N., Schmiegelow, K., Lausen, B., Hokland, P., Lehmann, S., Juliusson, G., Johansson, B., & Jacobsen, S. E. W. (2005). Distinct patterns of hematopoietic stem cell involvement in acute lymphoblastic leukemia. *Nature Medicine*, *11*(6), 630–637. https://doi.org/10.1038/nm1253

Cazzaniga, G., Daniotti, M., Tosi, S., Giudici, G., Aloisi, A., Pogliani, E., Kearney, L., & Biondi, A. (2001). The paired box domain gene PAX5 is fused to ETV6/TEL in an acute lymphoblastic leukemia case. *Cancer Res*, *61*(12), 4666–4670. https://www.ncbi.nlm.nih.gov/pubmed/11406533

Chan, L. N., Chen, Z., Braas, D., Lee, J. W., Xiao, G., Geng, H., Cosgun, K. N., Hurtz, C., Shojaee, S., Cazzaniga, V., Schjerven, H., Ernst, T., Hochhaus, A., Kornblau, S. M., Konopleva, M., Pufall, M. A., Cazzaniga, G., Liu, G. J., Milne, T. A., … Muschen, M. (2017). Metabolic gatekeeper function of B-lymphoid transcription factors. *Nature*, *542*(7642), 479–483. https://doi.org/10.1038/nature21076

Chan, L. N., Chen, Z., Braas, D., Lee, J.-W., Xiao, G., Geng, H., Cosgun, K. N., Hurtz, C., Shojaee, S., Cazzaniga, V., Schjerven, H., Ernst, T., Hochhaus, A., Kornblau, S. M., Konopleva, M., Pufall, M. A., Cazzaniga, G., Liu, G. J., Milne, T. A., … Müschen, M. (2017). Metabolic gatekeeper function of B-lymphoid transcription factors. *Nature*, *542*(7642), 479–483. https://doi.org/10.1038/nature21076

Chapman, J. R., Taylor, M. R. G., & Boulton, S. J. (2012). Playing the End Game: DNA Double-Strand Break Repair Pathway Choice. *Molecular Cell*, *47*(4), 497–510. https://doi.org/10.1016/j.molcel.2012.07.029

Chi, N., & Epstein, J. A. (2002). Getting your Pax straight: Pax proteins in development and disease. *Trends in Genetics*, *18*(1), 41–47. https://doi.org/10.1016/S0168-9525(01)02594-X

Clark, M. R., Mandal, M., Ochiai, K., & Singh, H. (2014). Orchestrating B cell lymphopoiesis through interplay of IL-7 receptor and pre-B cell receptor signalling. *Nat Rev Immunol*, *14*(2), 69–80. https://doi.org/10.1038/nri3570

Cobaleda, C., Gutiérrez-Cianca, N., Pérez-Losada, J., Flores, T., García-Sanz, R., González, M., & Sánchez-García, I. (2000). A primitive hematopoietic cell is the target for the leukemic transformation in human philadelphia-positive acute lymphoblastic leukemia. *Blood*, *95*(3), 1007–1013.

Cobaleda, C., Jochum, W., & Busslinger, M. (2007a). Conversion of mature B cells into T cells by dedifferentiation to uncommitted progenitors. *Nature*, *449*(7161), 473–477. https://doi.org/10.1038/nature06159

Cobaleda, C., Jochum, W., & Busslinger, M. (2007b). Conversion of mature B cells into T cells by dedifferentiation to uncommitted progenitors. *Nature*, *449*(7161), 473–477. https://doi.org/10.1038/nature06159

Cobaleda, C., Schebesta, A., Delogu, A., & Busslinger, M. (2007a). Pax5: the guardian of B cell identity and function. *Nature Immunology*, *8*(5), 463–470. https://doi.org/10.1038/ni1454

Cobaleda, C., Schebesta, A., Delogu, A., & Busslinger, M. (2007b). Pax5: the guardian of B cell identity and function. *Nature Immunology*, *8*(5), 463–470. https://doi.org/10.1038/ni1454

Cobaleda, C., Schebesta, A., Delogu, A., & Busslinger, M. (2007c). Pax5: the guardian of B cell identity and function. *Nat Immunol*, *8*(5), 463–470. https://doi.org/10.1038/ni1454

Cong, L., Ran, F. A., Cox, D., Lin, S., Barretto, R., Habib, N., Hsu, P. D., Wu, X., Jiang, W., Marraffini, L. A., & Zhang, F. (2013). Multiplex Genome Engineering Using CRISPR/Cas Systems. *Science*, *339*(6121), 819–823. https://doi.org/10.1126/science.1231143

Corcoran, A. E., Riddell, A., Krooshoop, D., & Venkitaraman, A. R. (1998). Impaired immunoglobulin gene rearrangement in mice lacking the IL-7 receptor. *Nature*, *391*(6670), 904–907. https://doi.org/10.1038/36122

Cordeiro Gomes, A., Hara, T., Lim, V. Y., Herndler-Brandstetter, D., Nevius, E., Sugiyama, T., Tani-ichi, S., Schlenner, S., Richie, E., Rodewald, H.-R., Flavell, R. A., Nagasawa, T., Ikuta, K., & Pereira, J. P. (2016). Hematopoietic Stem Cell Niches Produce Lineage-Instructive Signals to Control Multipotent Progenitor Differentiation. *Immunity*, *45*(6), 1219–1231. https://doi.org/10.1016/j.immuni.2016.11.004

Cox, C. V., Evely, R. S., Oakhill, A., Pamphilon, D. H., Goulden, N. J., & Blair, A. (2004). Characterization of acute lymphoblastic leukemia progenitor cells. *Blood*, *104*(9), 2919–2925. https://doi.org/10.1182/blood-2004-03-0901

Coyaud, E., Struski, S., Prade, N., Familiades, J., Eichner, R., Quelen, C., Bousquet, M., Mugneret, F., Talmant, P., Pages, M. P., Lefebvre, C., Penther, D., Lippert, E., Nadal, N., Taviaux, S., Poppe, B., Luquet, I., Baranger, L., Eclache, V., … Broccardo, C. (2010a). Wide diversity of PAX5 alterations in B-ALL: a Groupe Francophone de Cytogenetique Hematologique study. *Blood*, *115*(15), 3089–3097. https://doi.org/10.1182/blood-2009-07-234229

Coyaud, E., Struski, S., Prade, N., Familiades, J., Eichner, R., Quelen, C., Bousquet, M., Mugneret, F., Talmant, P., Pages, M.-P., Lefebvre, C., Penther, D., Lippert, E., Nadal, N., Taviaux, S., Poppe, B., Luquet, I., Baranger, L., Eclache, V., … Broccardo, C. (2010b). Wide diversity of PAX5 alterations in B-ALL: a Groupe Francophone de Cytogénétique Hématologique study. *Blood*, *115*(15), 3089–3097. https://doi.org/10.1182/blood-2009-07-234229

Cozzio, A., Passegué, E., Ayton, P. M., Karsunky, H., Cleary, M. L., & Weissman, I. L. (2003). Similar MLL-associated leukemias arising from self-renewing stem cells and short-lived myeloid progenitors. *Genes & Development*, *17*(24), 3029–3035. https://doi.org/10.1101/gad.1143403

Cresson, C., Péron, S., Jamrog, L., Rouquié, N., Prade, N., Dubois, M., Hébrard, S., Lagarde, S., Gerby, B., Mancini, S. J. C., Cogné, M., Delabesse, E., Delpy, L., & Broccardo, C. (2018). *PAX5A* and *PAX5B* isoforms are both efficient to drive B cell differentiation. *Oncotarget*, *9*(67), 32841–32854. https://doi.org/10.18632/oncotarget.26003

Cresson, C., Peron, S., Jamrog, L., Rouquie, N., Prade, N., Dubois, M., Hebrard, S., Lagarde, S., Gerby, B., Mancini, S. J. C., Cogne, M., Delabesse, E., Delpy, L., & Broccardo, C. (2018).

PAX5A and PAX5B isoforms are both efficient to drive B cell differentiation. *Oncotarget*, *9*(67), 32841–32854. https://doi.org/10.18632/oncotarget.26003

Cvekl, A., Kashanchi, F., Brady, J. N., & Piatigorsky, J. (1999). Pax-6 interactions with TATA-box-binding protein and retinoblastoma protein. *Investigative Ophthalmology & Visual Science*, *40*(7), 1343–1350.

Czerny, T., & Busslinger, M. (1995). DNA-Binding and Transactivation Properties of Pax-6: Three Amino Acids in the Paired Domain Are Responsible for the Different Sequence Recognition of Pax-6 and BSAP (Pax-5). *Molecular and Cellular Biology*, *15*(5), 2858–2871. https://doi.org/10.1128/MCB.15.5.2858

Czerny, T., Schaffner, G., & Busslinger, M. (1993). DNA sequence recognition by Pax proteins: bipartite structure of the paired domain and its binding site. *Genes & Development*, *7*(10), 2048–2061. https://doi.org/10.1101/gad.7.10.2048

Dang, J., Wei, L., de Ridder, J., Su, X., Rust, A. G., Roberts, K. G., Payne-Turner, D., Cheng, J., Ma, J., Qu, C., Wu, G., Song, G., Huether, R. G., Schulman, B., Janke, L., Zhang, J., Downing, J. R., van der Weyden, L., Adams, D. J., & Mullighan, C. G. (2015a). PAX5 is a tumor suppressor in mouse mutagenesis models of acute lymphoblastic leukemia. *Blood*, *125*(23), 3609–3617. https://doi.org/10.1182/blood-2015-02-626127

Dang, J., Wei, L., de Ridder, J., Su, X., Rust, A. G., Roberts, K. G., Payne-Turner, D., Cheng, J., Ma, J., Qu, C., Wu, G., Song, G., Huether, R. G., Schulman, B., Janke, L., Zhang, J., Downing, J. R., van der Weyden, L., Adams, D. J., & Mullighan, C. G. (2015b). PAX5 is a tumor suppressor in mouse mutagenesis models of acute lymphoblastic leukemia. *Blood*, *125*(23), 3609–3617. https://doi.org/10.1182/blood-2015-02-626127

Danial, N. N., & Korsmeyer, S. J. (2004). Cell Death. *Cell*, *116*(2), 205–219. https://doi.org/10.1016/S0092-8674(04)00046-7

Davis, A. J., & Chen, D. J. (2013). DNA double strand break repair via non-homologous end-joining. *Translational Cancer Research*, *2*(3), 130–143. https://doi.org/10.3978/j.issn.2218-676X.2013.04.02

Decker, T., Pasca di Magliano, M., McManus, S., Sun, Q., Bonifer, C., Tagoh, H., & Busslinger, M. (2009). Stepwise Activation of Enhancer and Promoter Regions of the B Cell Commitment Gene Pax5 in Early Lymphopoiesis. *Immunity*, *30*(4), 508–520. https://doi.org/10.1016/j.immuni.2009.01.012

DeKoter, R. P., & Singh, H. (2000). Regulation of B Lymphocyte and Macrophage Development by Graded Expression of PU.1. *Science*, *288*(5470), 1439–1441. https://doi.org/10.1126/science.288.5470.1439

Delahaye, M. C., Salem, K.-I., Pelletier, J., Aurrand-Lions, M., & Mancini, S. J. C. (2021). Toward Therapeutic Targeting of Bone Marrow Leukemic Niche Protective Signals in B-Cell Acute Lymphoblastic Leukemia. *Frontiers in Oncology*, *10*. https://doi.org/10.3389/fonc.2020.606540

Delogu, A., Schebesta, A., Sun, Q., Aschenbrenner, K., Perlot, T., & Busslinger, M. (2006). Gene Repression by Pax5 in B Cells Is Essential for Blood Cell Homeostasis and Is Reversed in Plasma Cells. *Immunity*, *24*(3), 269–281. https://doi.org/10.1016/j.immuni.2006.01.012

Deltcheva, E., Chylinski, K., Sharma, C. M., Gonzales, K., Chao, Y., Pirzada, Z. A., Eckert, M. R., Vogel, J., & Charpentier, E. (2011). CRISPR RNA maturation by trans-encoded small RNA and host factor RNase III. *Nature*, *471*(7340), 602–607. https://doi.org/10.1038/nature09886

Dick, J. E. (2003). Self-renewal writ in blood. *Nature*, *423*(6937), 231–232. https://doi.org/10.1038/423231a

Ding, L., & Morrison, S. J. (2013). Haematopoietic stem cells and early lymphoid progenitors occupy distinct bone marrow niches. *Nature*, *495*(7440), 231–235. https://doi.org/10.1038/nature11885

Ding, L., Saunders, T. L., Enikolopov, G., & Morrison, S. J. (2012). Endothelial and perivascular cells maintain haematopoietic stem cells. *Nature*, *481*(7382), 457–462. https://doi.org/10.1038/nature10783

Dörfler, P., & Busslinger, M. (1996). C-terminal activating and inhibitory domains determine the transactivation potential of BSAP (Pax-5), Pax-2 and Pax-8. *The EMBO Journal*, *15*(8), 1971–1982.

Downes, C. E. J., McClure, B. J., Bruning, J. B., Page, E., Breen, J., Rehn, J., Yeung, D. T., & White, D. L. (2021). Acquired JAK2 mutations confer resistance to JAK inhibitors in cell models of acute lymphoblastic leukemia. *NPJ Precision Oncology*, *5*(1), 75. https://doi.org/10.1038/s41698-021-00215-x

Driessen, E. M. C., van Roon, E. H. J., Spijkers-Hagelstein, J. A. P., Schneider, P., de Lorenzo, P., Valsecchi, M. G., Pieters, R., & Stam, R. W. (2013). Frequencies and prognostic impact of RAS mutations in MLL-rearranged acute lymphoblastic leukemia in infants. *Haematologica*, *98*(6), 937–944. https://doi.org/10.3324/haematol.2012.067983

Duployez, N., Jamrog, L. A., Fregona, V., Hamelle, C., Fenwarth, L., Lejeune, S., Helevaut, N., Geffroy, S., Caillault, A., Marceau-Renaut, A., Poulain, S., Roche-Lestienne, C., Largeaud, L., Prade, N., Dufrechou, S., Hebrard, S., Berthon, C., Nelken, B., Fernandes, J., … Broccardo, C. (2021). Germline PAX5 mutation predisposes to familial B-cell precursor acute lymphoblastic leukemia. *Blood*, *137*(10), 1424–1428. https://doi.org/10.1182/blood.2020005756

Duque-Afonso, J., Feng, J., Scherer, F., Lin, C. H., Wong, S. H., Wang, Z., Iwasaki, M., & Cleary, M. L. (2015a). Comparative genomics reveals multistep pathogenesis of E2A-PBX1 acute lymphoblastic leukemia. *J Clin Invest*, *125*(9), 3667–3680. https://doi.org/10.1172/JCI81158

Duque-Afonso, J., Feng, J., Scherer, F., Lin, C.-H., Wong, S. H. K., Wang, Z., Iwasaki, M., & Cleary, M. L. (2015b). Comparative genomics reveals multistep pathogenesis of E2A-PBX1 acute lymphoblastic leukemia. *Journal of Clinical Investigation*, *125*(9), 3667–3680. https://doi.org/10.1172/JCI81158

Eberhard, D., & Busslinger, M. (1999). The partial homeodomain of the transcription factor Pax-5 (BSAP) is an interaction motif for the retinoblastoma and TATA-binding proteins. *Cancer Research*, *59*(7 Suppl), 1716s–1724s; discussion 1724s-1725s.

Eberhard, D., Jiménez, G., Heavey, B., & Busslinger, M. (2000). Transcriptional repression by Pax5 (BSAP) through interaction with corepressors of the Groucho family. *The EMBO Journal*, *19*(10), 2292–2303. https://doi.org/10.1093/emboj/19.10.2292

Ebinger, S., Özdemir, E. Z., Ziegenhain, C., Tiedt, S., Castro Alves, C., Grunert, M., Dworzak, M., Lutz, C., Turati, V. A., Enver, T., Horny, H.-P., Sotlar, K., Parekh, S., Spiekermann, K., Hiddemann, W., Schepers, A., Polzer, B., Kirsch, S., Hoffmann, M., … Jeremias, I. (2016). Characterization of Rare, Dormant, and Therapy-Resistant Cells in Acute Lymphoblastic Leukemia. *Cancer Cell*, *30*(6), 849–862. https://doi.org/10.1016/j.ccell.2016.11.002

Elantak, L., Espeli, M., Boned, A., Bornet, O., Bonzi, J., Gauthier, L., Feracci, M., Roche, P., Guerlesquin, F., & Schiff, C. (2012). Structural Basis for Galectin-1-dependent Pre-B Cell

Receptor (Pre-BCR) Activation. *Journal of Biological Chemistry*, *287*(53), 44703–44713. https://doi.org/10.1074/jbc.M112.395152

Emelyanov, A. V., Kovac, C. R., Sepulveda, M. A., & Birshtein, B. K. (2002). The Interaction of Pax5 (BSAP) with Daxx Can Result in Transcriptional Activation in B Cells. *Journal of Biological Chemistry*, *277*(13), 11156–11164. https://doi.org/10.1074/jbc.M111763200

Eppert, K., Takenaka, K., Lechman, E. R., Waldron, L., Nilsson, B., van Galen, P., Metzeler, K. H., Poeppl, A., Ling, V., Beyene, J., Canty, A. J., Danska, J. S., Bohlander, S. K., Buske, C., Minden, M. D., Golub, T. R., Jurisica, I., Ebert, B. L., & Dick, J. E. (2011). Stem cell gene expression programs influence clinical outcome in human leukemia. *Nature Medicine*, *17*(9), 1086–1093. https://doi.org/10.1038/nm.2415

Espeli, M., Mancini, S. J. C., Breton, C., Poirier, F., & Schiff, C. (2009). Impaired B-cell development at the pre-BII-cell stage in galectin-1–deficient mice due to inefficient pre-BII/stromal cell interactions. *Blood*, *113*(23), 5878–5886. https://doi.org/10.1182/blood-2009-01-198465

Familiades, J., Bousquet, M., Lafage-Pochitaloff, M., Bene, M. C., Beldjord, K., De Vos, J., Dastugue, N., Coyaud, E., Struski, S., Quelen, C., Prade-Houdellier, N., Dobbelstein, S., Cayuela, J. M., Soulier, J., Grardel, N., Preudhomme, C., Cave, H., Blanchet, O., Lheritier, V., … Delabesse, E. (2009). PAX5 mutations occur frequently in adult B-cell progenitor acute lymphoblastic leukemia and PAX5 haploinsufficiency is associated with BCR-ABL1 and TCF3-PBX1 fusion genes: a GRAALL study. *Leukemia*, *23*(11), 1989–1998. https://doi.org/10.1038/leu.2009.135

Familiades, J., Bousquet, M., Lafage-Pochitaloff, M., Béné, M.-C., Beldjord, K., De Vos, J., Dastugue, N., Coyaud, E., Struski, S., Quelen, C., Prade-Houdellier, N., Dobbelstein, S., Cayuela, J.-M., Soulier, J., Grardel, N., Preudhomme, C., Cavé, H., Blanchet, O., Lhéritier, V., … Delabesse, É. (2009a). PAX5 mutations occur frequently in adult B-cell progenitor acute lymphoblastic leukemia and PAX5 haploinsufficiency is associated with BCR-ABL1 and TCF3-PBX1 fusion genes: a GRAALL study. *Leukemia*, *23*(11), 1989–1998. https://doi.org/10.1038/leu.2009.135

Familiades, J., Bousquet, M., Lafage-Pochitaloff, M., Béné, M.-C., Beldjord, K., De Vos, J., Dastugue, N., Coyaud, E., Struski, S., Quelen, C., Prade-Houdellier, N., Dobbelstein, S., Cayuela, J.-M., Soulier, J., Grardel, N., Preudhomme, C., Cavé, H., Blanchet, O., Lhéritier, V., … Delabesse, É. (2009b). PAX5 mutations occur frequently in adult B-cell progenitor acute lymphoblastic leukemia and PAX5 haploinsufficiency is associated with BCR-ABL1 and TCF3-PBX1 fusion genes: a GRAALL study. *Leukemia*, *23*(11), 1989–1998. https://doi.org/10.1038/leu.2009.135

Fisher, A. L., & Caudy, M. (1998). Groucho proteins: transcriptional corepressors for specific subsets of DNA-binding transcription factors in vertebrates and invertebrates. *Genes & Development*, *12*(13), 1931–1940. https://doi.org/10.1101/gad.12.13.1931

Fitzsimmons, D., Hodsdon, W., Wheat, W., Maira, S. M., Wasylyk, B., & Hagman, J. (1996). Pax-5 (BSAP) recruits Ets proto-oncogene family proteins to form functional ternary complexes on a B-cell-specific promoter. *Genes & Development*, *10*(17), 2198–2211. https://doi.org/10.1101/gad.10.17.2198

Flemming, A., Brummer, T., Reth, M., & Jumaa, H. (2003). The adaptor protein SLP-65 acts as a tumor suppressor that limits pre-B cell expansion. *Nature Immunology*, *4*(1), 38–43. https://doi.org/10.1038/ni862

Forestier, E., Heyman, M., Andersen, M. K., Autio, K., Blennow, E., Borgström, G., Golovleva, I., Heim, S., Heinonen, K., Hovland, R., Johannsson, J. H., Kerndrup, G., Nordgren, A.,

Rosenquist, R., Swolin, B., & Johansson, B. (2008). Outcome of ETV6/RUNX1-positive childhood acute lymphoblastic leukaemia in the NOPHO-ALL-1992 protocol: frequent late relapses but good overall survival. *British Journal of Haematology*, *140*(6), 665–672. https://doi.org/10.1111/j.1365-2141.2008.06980.x

Fregona, V., Bayet, M., & Gerby, B. (2021a). Oncogene-Induced Reprogramming in Acute Lymphoblastic Leukemia: Towards Targeted Therapy of Leukemia-Initiating Cells. *Cancers (Basel)*, *13*(21). https://doi.org/10.3390/cancers13215511

Fregona, V., Bayet, M., & Gerby, B. (2021b). Oncogene-Induced Reprogramming in Acute Lymphoblastic Leukemia: Towards Targeted Therapy of Leukemia-Initiating Cells. *Cancers*, *13*(21), 5511. https://doi.org/10.3390/cancers13215511

Fuxa, M., Skok, J., Souabni, A., Salvagiotto, G., Roldan, E., & Busslinger, M. (2004). Pax5 induces *V* -to- *DJ* rearrangements and locus contraction of the *immunoglobulin heavy-chain* gene. *Genes & Development*, *18*(4), 411–422. https://doi.org/10.1101/gad.291504

Garneau, J. E., Dupuis, M.-È., Villion, M., Romero, D. A., Barrangou, R., Boyaval, P., Fremaux, C., Horvath, P., Magadán, A. H., & Moineau, S. (2010). The CRISPR/Cas bacterial immune system cleaves bacteriophage and plasmid DNA. *Nature*, *468*(7320), 67–71. https://doi.org/10.1038/nature09523

Gauthier, L., Rossi, B., Roux, F., Termine, E., & Schiff, C. (2002). Galectin-1 is a stromal cell ligand of the pre-B cell receptor (BCR) implicated in synapse formation between pre-B and stromal cells and in pre-BCR triggering. *Proceedings of the National Academy of Sciences*, *99*(20), 13014–13019. https://doi.org/10.1073/pnas.202323999

Georgopoulos, K., Bigby, M., Wang, J.-H., Molnar, A., Wu, P., Winandy, S., & Sharpe, A. (1994). The ikaros gene is required for the development of all lymphoid lineages. *Cell*, *79*(1), 143–156. https://doi.org/10.1016/0092-8674(94)90407-3

Gerby, B., Tremblay, C. S., Tremblay, M., Rojas-Sutterlin, S., Herblot, S., Hébert, J., Sauvageau, G., Lemieux, S., Lécuyer, E., Veiga, D. F. T., & Hoang, T. (2014). SCL, LMO1 and Notch1 Reprogram Thymocytes into Self-Renewing Cells. *PLoS Genetics*, *10*(12), e1004768. https://doi.org/10.1371/journal.pgen.1004768

Gerby, B., Veiga, D. F., Krosl, J., Nourreddine, S., Ouellette, J., Haman, A., Lavoie, G., Fares, I., Tremblay, M., Litalien, V., Ottoni, E., Kosic, M., Geoffrion, D., Ryan, J., Maddox, P. S., Chagraoui, J., Marinier, A., Hebert, J., Sauvageau, G., … Hoang, T. (2016). High-throughput screening in niche-based assay identifies compounds to target preleukemic stem cells. *J Clin Invest*. https://doi.org/10.1172/JCI86489

Gerby, B., Veiga, D. F. T., Krosl, J., Nourreddine, S., Ouellette, J., Haman, A., Lavoie, G., Fares, I., Tremblay, M., Litalien, V., Ottoni, E., Kosic, M., Geoffrion, D., Ryan, J., Maddox, P. S., Chagraoui, J., Marinier, A., Hébert, J., Sauvageau, G., … Hoang, T. (2016). High-throughput screening in niche-based assay identifies compounds to target preleukemic stem cells. *Journal of Clinical Investigation*, *126*(12), 4569–4584. https://doi.org/10.1172/JCI86489

Glodek, A. M., Honczarenko, M., Le, Y., Campbell, J. J., & Silberstein, L. E. (2003). Sustained Activation of Cell Adhesion Is a Differentially Regulated Process in B Lymphopoiesis. *The Journal of Experimental Medicine*, *197*(4), 461–473. https://doi.org/10.1084/jem.20021477

Goardon, N., Marchi, E., Atzberger, A., Quek, L., Schuh, A., Soneji, S., Woll, P., Mead, A., Alford, K. A., Rout, R., Chaudhury, S., Gilkes, A., Knapper, S., Beldjord, K., Begum, S., Rose, S., Geddes, N., Griffiths, M., Standen, G., … Vyas, P. (2011). Coexistence of LMPP-

like and GMP-like Leukemia Stem Cells in Acute Myeloid Leukemia. *Cancer Cell*, *19*(1), 138–152. https://doi.org/10.1016/j.ccr.2010.12.012

Goetz, C. A., Harmon, I. R., O'Neil, J. J., Burchill, M. A., & Farrar, M. A. (2004). STAT5 Activation Underlies IL7 Receptor-Dependent B Cell Development. *The Journal of Immunology*, *172*(8), 4770–4778. https://doi.org/10.4049/jimmunol.172.8.4770

Goode, D. K., & Elgar, G. (2009). The *PAX258* gene subfamily: A comparative perspective. *Developmental Dynamics*, *238*(12), 2951–2974. https://doi.org/10.1002/dvdy.22146

Goossens, S., & Van Vlierberghe, P. (2014). Controlling Pre-leukemic Thymocyte Self-Renewal. *PLoS Genetics*, *10*(12), e1004881. https://doi.org/10.1371/journal.pgen.1004881

Grawunder, U., Leu, T. M. J., Schatz, D. G., Werner, A., Rolink, A. G., Melchers, F., & Winkler, T. H. (1995). Down-regulation of RAG1 and RAG2 gene expression in PreB cells after functional immunoglobulin heavy chain rearrangement. *Immunity*, *3*(5), 601–608. https://doi.org/10.1016/1074-7613(95)90131-0

Greaves, M. (2016). Leukaemia "firsts" in cancer research and treatment. *Nature Reviews Cancer*, *16*(3), 163–172. https://doi.org/10.1038/nrc.2016.3

Greaves, M. (2018a). A causal mechanism for childhood acute lymphoblastic leukaemia. *Nature Reviews Cancer*, *18*(8), 471–484. https://doi.org/10.1038/s41568-018-0015-6

Greaves, M. (2018b). A causal mechanism for childhood acute lymphoblastic leukaemia. *Nature Reviews Cancer*, *18*(8), 471–484. https://doi.org/10.1038/s41568-018-0015-6

Gruenbacher, S., Jaritz, M., Hill, L., Schäfer, M., & Busslinger, M. (2023). Essential role of the Pax5 C-terminal domain in controlling B cell commitment and development. *Journal of Experimental Medicine*, *220*(12). https://doi.org/10.1084/jem.20230260

Gu, Z., Churchman, M. L., Roberts, K. G., Moore, I., Zhou, X., Nakitandwe, J., Hagiwara, K., Pelletier, S., Gingras, S., Berns, H., Payne-Turner, D., Hill, A., Iacobucci, I., Shi, L., Pounds, S., Cheng, C., Pei, D., Qu, C., Newman, S., … Mullighan, C. G. (2019a). PAX5-driven subtypes of B-progenitor acute lymphoblastic leukemia. *Nature Genetics*, *51*(2), 296–307. https://doi.org/10.1038/s41588-018-0315-5

Gu, Z., Churchman, M. L., Roberts, K. G., Moore, I., Zhou, X., Nakitandwe, J., Hagiwara, K., Pelletier, S., Gingras, S., Berns, H., Payne-Turner, D., Hill, A., Iacobucci, I., Shi, L., Pounds, S., Cheng, C., Pei, D., Qu, C., Newman, S., … Mullighan, C. G. (2019b). PAX5-driven subtypes of B-progenitor acute lymphoblastic leukemia. *Nat Genet*, *51*(2), 296–307. https://doi.org/10.1038/s41588-018-0315-5

Guibal, F. C., Alberich-Jorda, M., Hirai, H., Ebralidze, A., Levantini, E., Di Ruscio, A., Zhang, P., Santana-Lemos, B. A., Neuberg, D., Wagers, A. J., Rego, E. M., & Tenen, D. G. (2009). Identification of a myeloid committed progenitor as the cancer-initiating cell in acute promyelocytic leukemia. *Blood*, *114*(27), 5415–5425. https://doi.org/10.1182/blood-2008-10-182071

Guitart, A. V, Subramani, C., Armesilla-Diaz, A., Smith, G., Sepulveda, C., Gezer, D., Vukovic, M., Dunn, K., Pollard, P., Holyoake, T. L., Enver, T., Ratcliffe, P. J., & Kranc, K. R. (2013a). Hif-2alpha is not essential for cell-autonomous hematopoietic stem cell maintenance. *Blood*, *122*(10), 1741–1745. https://doi.org/10.1182/blood-2013-02-484923

Guitart, A. V, Subramani, C., Armesilla-Diaz, A., Smith, G., Sepulveda, C., Gezer, D., Vukovic, M., Dunn, K., Pollard, P., Holyoake, T. L., Enver, T., Ratcliffe, P. J., & Kranc, K. R. (2013b). Hif-2α is not essential for cell-autonomous hematopoietic stem cell maintenance. *Blood*, *122*(10), 1741–1745. https://doi.org/10.1182/blood-2013-02-484923

Hallal, R., Nehme, R., Brachet-Botineau, M., Nehme, A., Dakik, H., Deynoux, M., Dello Sbarba, P., Levern, Y., Zibara, K., Gouilleux, F., & Mazurier, F. (2020). Acriflavine targets oncogenic

STAT5 signaling in myeloid leukemia cells. *Journal of Cellular and Molecular Medicine*, *24*(17), 10052–10062. https://doi.org/10.1111/jcmm.15612

Hamasaki, A., Yamada, Y., Kurose, T., Ban, N., Nagashima, K., Takahashi, A., Fujimoto, S., Shimono, D., Fujiwara, M., Toyokuni, S., Seino, Y., & Inagaki, N. (2007). Adult pancreatic islets require differential pax6 gene dosage. *Biochemical and Biophysical Research Communications*, *353*(1), 40–46. https://doi.org/10.1016/j.bbrc.2006.11.105

Hardy, R. R., Carmack, C. E., Shinton, S. A., Kemp, J. D., & Hayakawa, K. (2012). Resolution and characterization of pro-B and pre-pro-B cell stages in normal mouse bone marrow. 1991. *Journal of Immunology (Baltimore, Md. : 1950)*, *189*(7), 3271–3283.

Hardy, R. R., & Hayakawa, K. (2001a). B Cell Development Pathways. *Annual Review of Immunology*, *19*(1), 595–621. https://doi.org/10.1146/annurev.immunol.19.1.595

Hardy, R. R., & Hayakawa, K. (2001b). B cell development pathways. *Annu Rev Immunol*, *19*, 595–621. https://doi.org/10.1146/annurev.immunol.19.1.595

Hardy, R. R., Kincade, P. W., & Dorshkind, K. (2007). The Protean Nature of Cells in the B Lymphocyte Lineage. *Immunity*, *26*(6), 703–714. https://doi.org/10.1016/j.immuni.2007.05.013

Hardy, R. R., Li, Y. S., Allman, D., Asano, M., Gui, M., & Hayakawa, K. (2000). B-cell commitment, development and selection. *Immunol Rev*, *175*, 23–32. https://www.ncbi.nlm.nih.gov/pubmed/10933588

Hauser, J., Grundström, C., Kumar, R., & Grundström, T. (2016). Regulated localization of an AID complex with E2A, PAX5 and IRF4 at the Igh locus. *Molecular Immunology*, *80*, 78–90. https://doi.org/10.1016/j.molimm.2016.10.014

He, T., Hong, S. Y., Huang, L., Xue, W., Yu, Z., Kwon, H., Kirk, M., Ding, S., Su, K., & Zhang, Z. (2011). Histone Acetyltransferase p300 Acetylates Pax5 and Strongly Enhances Pax5-mediated Transcriptional Activity. *Journal of Biological Chemistry*, *286*(16), 14137–14145. https://doi.org/10.1074/jbc.M110.176289

Heckl, D., Kowalczyk, M. S., Yudovich, D., Belizaire, R., Puram, R. V, McConkey, M. E., Thielke, A., Aster, J. C., Regev, A., & Ebert, B. L. (2014). Generation of mouse models of myeloid malignancy with combinatorial genetic lesions using CRISPR-Cas9 genome editing. *Nat Biotechnol*, *32*(9), 941–946. https://doi.org/10.1038/nbt.2951

Heidenreich, E. (2003). Non-homologous end joining as an important mutagenic process in cell cycle-arrested cells. *The EMBO Journal*, *22*(9), 2274–2283. https://doi.org/10.1093/emboj/cdg203

Heltemes-Harris, L. M., Willette, M. J. L., Ramsey, L. B., Qiu, Y. H., Neeley, E. S., Zhang, N., Thomas, D. A., Koeuth, T., Baechler, E. C., Kornblau, S. M., & Farrar, M. A. (2011a). *Ebf1* or *Pax5* haploinsufficiency synergizes with STAT5 activation to initiate acute lymphoblastic leukemia. *Journal of Experimental Medicine*, *208*(6), 1135–1149. https://doi.org/10.1084/jem.20101947

Heltemes-Harris, L. M., Willette, M. J., Ramsey, L. B., Qiu, Y. H., Neeley, E. S., Zhang, N., Thomas, D. A., Koeuth, T., Baechler, E. C., Kornblau, S. M., & Farrar, M. A. (2011b). Ebf1 or Pax5 haploinsufficiency synergizes with STAT5 activation to initiate acute lymphoblastic leukemia. *J Exp Med*, *208*(6), 1135–1149. https://doi.org/10.1084/jem.20101947

Herblot, S., Steff, A.-M., Hugo, P., Aplan, P. D., & Hoang, T. (2000). SCL and LMO1 alter thymocyte differentiation: inhibition of E2A-HEB function and pre-Tα chain expression. *Nature Immunology*, *1*(2), 138–144. https://doi.org/10.1038/77819

Hiebert, S. W., Sun, W., Nathan Davis, J., Golub, T., Shurtleff, S., Buijs, A., Downing, J. R., Grosveld, G., Roussel, M. F., Gary Gilliland, D., Lenny, N., & Meyers, S. (1996). The t(12;21) Translocation Converts AML-1B from an Activator to a Repressor of Transcription. *Molecular and Cellular Biology*, *16*(4), 1349–1355. https://doi.org/10.1128/MCB.16.4.1349

Hoflinger, S., Kesavan, K., Fuxa, M., Hutter, C., Heavey, B., Radtke, F., & Busslinger, M. (2004). Analysis of Notch1 function by in vitro T cell differentiation of Pax5 mutant lymphoid progenitors. *J Immunol*, *173*(6), 3935–3944. https://doi.org/10.4049/jimmunol.173.6.3935

Holmes, M. L., Carotta, S., Corcoran, L. M., & Nutt, S. L. (2006). Repression of *Flt3* by Pax5 is crucial for B-cell lineage commitment. *Genes & Development*, *20*(8), 933–938. https://doi.org/10.1101/gad.1396206

Hong, D., Gupta, R., Ancliff, P., Atzberger, A., Brown, J., Soneji, S., Green, J., Colman, S., Piacibello, W., Buckle, V., Tsuzuki, S., Greaves, M., & Enver, T. (2008). Initiating and Cancer-Propagating Cells in *TEL-AML1* -Associated Childhood Leukemia. *Science*, *319*(5861), 336–339. https://doi.org/10.1126/science.1150648

Hope, K. J., Jin, L., & Dick, J. E. (2004). Acute myeloid leukemia originates from a hierarchy of leukemic stem cell classes that differ in self-renewal capacity. *Nature Immunology*, *5*(7), 738–743. https://doi.org/10.1038/ni1080

Horcher, M., Souabni, A., & Busslinger, M. (2001). Pax5/BSAP Maintains the Identity of B Cells in Late B Lymphopoiesis. *Immunity*, *14*(6), 779–790. https://doi.org/10.1016/S1074-7613(01)00153-4

Hotfilder, M., Röttgers, S., Rosemann, A., Jürgens, H., Harbott, J., & Vormoor, J. (2002). Immature CD34+CD19− progenitor/stem cells in TEL/AML1-positive acute lymphoblastic leukemia are genetically and functionally normal. *Blood*, *100*(2), 640–646. https://doi.org/10.1182/blood.V100.2.640

Hsu, P. D., Lander, E. S., & Zhang, F. (2014). Development and Applications of CRISPR-Cas9 for Genome Engineering. *Cell*, *157*(6), 1262–1278. https://doi.org/10.1016/j.cell.2014.05.010

Hsu, P. D., Scott, D. A., Weinstein, J. A., Ran, F. A., Konermann, S., Agarwala, V., Li, Y., Fine, E. J., Wu, X., Shalem, O., Cradick, T. J., Marraffini, L. A., Bao, G., & Zhang, F. (2013). DNA targeting specificity of RNA-guided Cas9 nucleases. *Nature Biotechnology*, *31*(9), 827–832. https://doi.org/10.1038/nbt.2647

Huang, X., Trinh, T., Aljoufi, A., & Broxmeyer, H. E. (2018). Hypoxia Signaling Pathway in Stem Cell Regulation: Good and Evil. *Current Stem Cell Reports*, *4*(2), 149–157. https://doi.org/10.1007/s40778-018-0127-7

Ikawa, T., Kawamoto, H., Wright, L. Y. T., & Murre, C. (2004). Long-Term Cultured E2A-Deficient Hematopoietic Progenitor Cells Are Pluripotent. *Immunity*, *20*(3), 349–360. https://doi.org/10.1016/S1074-7613(04)00049-4

Inaba, H., & Mullighan, C. G. (2020). Pediatric acute lymphoblastic leukemia. *Haematologica*, *105*(11), 2524–2539. https://doi.org/10.3324/haematol.2020.247031

Inlay, M. A., Bhattacharya, D., Sahoo, D., Serwold, T., Seita, J., Karsunky, H., Plevritis, S. K., Dill, D. L., & Weissman, I. L. (2009). Ly6d marks the earliest stage of B-cell specification and identifies the branchpoint between B-cell and T-cell development. *Genes & Development*, *23*(20), 2376–2381. https://doi.org/10.1101/gad.1836009

Ishikawa, F., Yoshida, S., Saito, Y., Hijikata, A., Kitamura, H., Tanaka, S., Nakamura, R., Tanaka, T., Tomiyama, H., Saito, N., Fukata, M., Miyamoto, T., Lyons, B., Ohshima, K., Uchida, N.,

Taniguchi, S., Ohara, O., Akashi, K., Harada, M., & Shultz, L. D. (2007). Chemotherapy-resistant human AML stem cells home to and engraft within the bone-marrow endosteal region. *Nature Biotechnology*, *25*(11), 1315–1321. https://doi.org/10.1038/nbt1350

Ishino, Y., Krupovic, M., & Forterre, P. (2018). History of CRISPR-Cas from Encounter with a Mysterious Repeated Sequence to Genome Editing Technology. *Journal of Bacteriology*, *200*(7). https://doi.org/10.1128/JB.00580-17

Ishino, Y., Shinagawa, H., Makino, K., Amemura, M., & Nakata, A. (1987). Nucleotide sequence of the iap gene, responsible for alkaline phosphatase isozyme conversion in Escherichia coli, and identification of the gene product. *Journal of Bacteriology*, *169*(12), 5429–5433. https://doi.org/10.1128/jb.169.12.5429-5433.1987

Isidro-Hernández, M., Casado-García, A., Oak, N., Alemán-Arteaga, S., Ruiz-Corzo, B., Martínez-Cano, J., Mayado, A., Sánchez, E. G., Blanco, O., Gaspar, M. L., Orfao, A., Alonso-López, D., De Las Rivas, J., Riesco, S., Prieto-Matos, P., González-Murillo, Á., Criado, F. J. G., Cenador, M. B. G., Ramírez-Orellana, M., … Sánchez-García, I. (2023a). Immune stress suppresses innate immune signaling in preleukemic precursor B-cells to provoke leukemia in predisposed mice. *Nature Communications*, *14*(1), 5159. https://doi.org/10.1038/s41467-023-40961-z

Isidro-Hernández, M., Casado-García, A., Oak, N., Alemán-Arteaga, S., Ruiz-Corzo, B., Martínez-Cano, J., Mayado, A., Sánchez, E. G., Blanco, O., Gaspar, M. L., Orfao, A., Alonso-López, D., De Las Rivas, J., Riesco, S., Prieto-Matos, P., González-Murillo, Á., Criado, F. J. G., Cenador, M. B. G., Ramírez-Orellana, M., … Sánchez-García, I. (2023b). Immune stress suppresses innate immune signaling in preleukemic precursor B-cells to provoke leukemia in predisposed mice. *Nature Communications*, *14*(1), 5159. https://doi.org/10.1038/s41467-023-40961-z

Isidro-Hernández, M., Mayado, A., Casado-García, A., Martínez-Cano, J., Palmi, C., Fazio, G., Orfao, A., Ribera, J., Ribera, J. M., Zamora, L., Raboso-Gallego, J., Blanco, O., Alonso-López, D., De Las Rivas, J., Jiménez, R., García Criado, F. J., García Cenador, M. B., Ramírez-Orellana, M., Cazzaniga, G., … Sánchez-García, I. (2020a). Inhibition of inflammatory signaling in Pax5 mutant cells mitigates B-cell leukemogenesis. *Scientific Reports*, *10*(1), 19189. https://doi.org/10.1038/s41598-020-76206-y

Isidro-Hernández, M., Mayado, A., Casado-García, A., Martínez-Cano, J., Palmi, C., Fazio, G., Orfao, A., Ribera, J., Ribera, J. M., Zamora, L., Raboso-Gallego, J., Blanco, O., Alonso-López, D., De Las Rivas, J., Jiménez, R., García Criado, F. J., García Cenador, M. B., Ramírez-Orellana, M., Cazzaniga, G., … Sánchez-García, I. (2020b). Inhibition of inflammatory signaling in Pax5 mutant cells mitigates B-cell leukemogenesis. *Scientific Reports*, *10*(1), 19189. https://doi.org/10.1038/s41598-020-76206-y

Isidro-Hernandez, M., Mayado, A., Casado-Garcia, A., Martinez-Cano, J., Palmi, C., Fazio, G., Orfao, A., Ribera, J., Ribera, J. M., Zamora, L., Raboso-Gallego, J., Blanco, O., Alonso-Lopez, D., De Las Rivas, J., Jimenez, R., Garcia Criado, F. J., Garcia Cenador, M. B., Ramirez-Orellana, M., Cazzaniga, G., … Sanchez-Garcia, I. (2020). Inhibition of inflammatory signaling in Pax5 mutant cells mitigates B-cell leukemogenesis. *Sci Rep*, *10*(1), 19189. https://doi.org/10.1038/s41598-020-76206-y

Itkin, T., Gur-Cohen, S., Spencer, J. A., Schajnovitz, A., Ramasamy, S. K., Kusumbe, A. P., Ledergor, G., Jung, Y., Milo, I., Poulos, M. G., Kalinkovich, A., Ludin, A., Golan, K., Khatib, E., Kumari, A., Kollet, O., Shakhar, G., Butler, J. M., Rafii, S., … Lapidot, T. (2016). Distinct

bone marrow blood vessels differentially regulate haematopoiesis. *Nature*, *532*(7599), 323–328. https://doi.org/10.1038/nature17624

Jamrog, L., Chemin, G., Fregona, V., Coster, L., Pasquet, M., Oudinet, C., Rouquié, N., Prade, N., Lagarde, S., Cresson, C., Hébrard, S., Nguyen Huu, N. S., Bousquet, M., Quelen, C., Brousset, P., Mancini, S. J. C., Delabesse, E., Khamlichi, A. A., Gerby, B., & Broccardo, C. (2018). PAX5-ELN oncoprotein promotes multistep B-cell acute lymphoblastic leukemia in mice. *Proceedings of the National Academy of Sciences*, *115*(41), 10357–10362. https://doi.org/10.1073/pnas.1721678115

Jamrog, L., Chemin, G., Fregona, V., Coster, L., Pasquet, M., Oudinet, C., Rouquie, N., Prade, N., Lagarde, S., Cresson, C., Hebrard, S., Nguyen Huu, N. S., Bousquet, M., Quelen, C., Brousset, P., Mancini, S. J. C., Delabesse, E., Khamlichi, A. A., Gerby, B., & Broccardo, C. (2018). PAX5-ELN oncoprotein promotes multistep B-cell acute lymphoblastic leukemia in mice. *Proc Natl Acad Sci U S A*, *115*(41), 10357–10362. https://doi.org/10.1073/pnas.1721678115

Jansen, Ruud., Embden, Jan. D. A. van, Gaastra, Wim., & Schouls, Leo. M. (2002). Identification of genes that are associated with DNA repeats in prokaryotes. *Molecular Microbiology*, *43*(6), 1565–1575. https://doi.org/10.1046/j.1365-2958.2002.02839.x

Jiang, F., & Doudna, J. A. (2017). CRISPR–Cas9 Structures and Mechanisms. *Annual Review of Biophysics*, *46*(1), 505–529. https://doi.org/10.1146/annurev-biophys-062215-010822

Jiang, Q., Li, W. Q., Hofmeister, R. R., Young, H. A., Hodge, D. R., Keller, J. R., Khaled, A. R., & Durum, S. K. (2004). Distinct Regions of the Interleukin-7 Receptor Regulate Different Bcl2 Family Members. *Molecular and Cellular Biology*, *24*(14), 6501–6513. https://doi.org/10.1128/MCB.24.14.6501-6513.2004

Jinek, M., Chylinski, K., Fonfara, I., Hauer, M., Doudna, J. A., & Charpentier, E. (2012a). A Programmable Dual-RNA–Guided DNA Endonuclease in Adaptive Bacterial Immunity. *Science*, *337*(6096), 816–821. https://doi.org/10.1126/science.1225829

Jinek, M., Chylinski, K., Fonfara, I., Hauer, M., Doudna, J. A., & Charpentier, E. (2012b). A Programmable Dual-RNA–Guided DNA Endonuclease in Adaptive Bacterial Immunity. *Science*, *337*(6096), 816–821. https://doi.org/10.1126/science.1225829

Johnson, R. D., & Jasin, M. (2001). Double-strand-break-induced homologous recombination in mammalian cells. *Biochemical Society Transactions*, *29*(2), 196. https://doi.org/10.1042/0300-5127:0290196

Jurado, S., Fedl, A. S., Jaritz, M., Kostanova-Poliakova, D., Malin, S. G., Mullighan, C. G., Strehl, S., Fischer, M., & Busslinger, M. (2022). The PAX5-JAK2 translocation acts as dual-hit mutation that promotes aggressive B-cell leukemia via nuclear STAT5 activation. *EMBO J*, *41*(7), e108397. https://doi.org/10.15252/embj.2021108397

Kaeser, G., & Chun, J. (2020). Brain cell somatic gene recombination and its phylogenetic foundations. *Journal of Biological Chemistry*, *295*(36), 12786–12795. https://doi.org/10.1074/jbc.REV120.009192

Kamb, A., Gruis, N. A., Weaver-Feldhaus, J., Liu, Q., Harshman, K., Tavtigian, S. V., Stockert, E., Day, R. S., Johnson, B. E., & Skolnick, M. H. (1994). A Cell Cycle Regulator Potentially Involved in Genesis of Many Tumor Types. *Science*, *264*(5157), 436–440. https://doi.org/10.1126/science.8153634

Kamb, A., Shattuck-Eidens, D., Eeles, R., Liu, Q., Gruis, N. A., Ding, W., Hussey, C., Tran, T., Miki, Y., Weaver-Feldhaus, J., McClure, M., Aitken, J. F., Anderson, D. E., Bergman, W., Frants, R., Goldgar, D. E., Green, A., MacLennan, R., Martin, N. G., … Cannon-Albright, L. A. (1994). Analysis of the p16 gene (CDKN2) as a candidate for the chromosome 9p

melanoma susceptibility locus. *Nature Genetics*, *8*(1), 22–26. https://doi.org/10.1038/ng0994-22

Kiel, M. J., Yilmaz, Ö. H., Iwashita, T., Yilmaz, O. H., Terhorst, C., & Morrison, S. J. (2005). SLAM Family Receptors Distinguish Hematopoietic Stem and Progenitor Cells and Reveal Endothelial Niches for Stem Cells. *Cell*, *121*(7), 1109–1121. https://doi.org/10.1016/j.cell.2005.05.026

Kirstetter, P., Thomas, M., Dierich, A., Kastner, P., & Chan, S. (2002). Ikaros is critical for B cell differentiation and function. *European Journal of Immunology*, *32*(3), 720. https://doi.org/10.1002/1521-4141(200203)32:3<720::AID-IMMU720>3.0.CO;2-P

Koch, U., Fiorini, E., Benedito, R., Besseyrias, V., Schuster-Gossler, K., Pierres, M., Manley, N. R., Duarte, A., Macdonald, H. R., & Radtke, F. (2008). Delta-like 4 is the essential, nonredundant ligand for Notch1 during thymic T cell lineage commitment. *J Exp Med*, *205*(11), 2515–2523. https://doi.org/10.1084/jem.20080829

Komor, A. C., Badran, A. H., & Liu, D. R. (2017). CRISPR-Based Technologies for the Manipulation of Eukaryotic Genomes. *Cell*, *169*(3), 559. https://doi.org/10.1016/j.cell.2017.04.005

Kong, Y., Yoshida, S., Saito, Y., Doi, T., Nagatoshi, Y., Fukata, M., Saito, N., Yang, S. M., Iwamoto, C., Okamura, J., Liu, K. Y., Huang, X. J., Lu, D. P., Shultz, L. D., Harada, M., & Ishikawa, F. (2008). CD34+CD38+CD19+ as well as CD34+CD38−CD19+ cells are leukemia-initiating cells with self-renewal capacity in human B-precursor ALL. *Leukemia*, *22*(6), 1207–1213. https://doi.org/10.1038/leu.2008.83

Koop, K. E., MacDonald, L. M., & Lobe, C. G. (1996). Transcripts of Grg4, a murine groucho-related gene, are detected in adjacent tissues to other murine neurogenic gene homologues during embryonic development. *Mechanisms of Development*, *59*(1), 73–87. https://doi.org/10.1016/0925-4773(96)00582-5

Kovac, C. R., Emelyanov, A., Singh, M., Ashouian, N., & Birshtein, B. K. (2000). BSAP (Pax5)-Importin α1 (Rch1) Interaction Identifies a Nuclear Localization Sequence. *Journal of Biological Chemistry*, *275*(22), 16752–16757. https://doi.org/10.1074/jbc.M001551200

Kozmik, Z., Wang, S., Dörfler, P., Adams, B., & Busslinger, M. (1992a). The Promoter of the CD19 Gene Is a Target for the B-Cell-Specific Transcription Factor BSAP. *Molecular and Cellular Biology*, *12*(6), 2662–2672. https://doi.org/10.1128/mcb.12.6.2662-2672.1992

Kozmik, Z., Wang, S., Dörfler, P., Adams, B., & Busslinger, M. (1992b). The Promoter of the CD19 Gene Is a Target for the B-Cell-Specific Transcription Factor BSAP. *Molecular and Cellular Biology*, *12*(6), 2662–2672. https://doi.org/10.1128/mcb.12.6.2662-2672.1992

Kreso, A., & Dick, J. E. (2014). Evolution of the Cancer Stem Cell Model. *Cell Stem Cell*, *14*(3), 275–291. https://doi.org/10.1016/j.stem.2014.02.006

Krivtsov, A. V., Twomey, D., Feng, Z., Stubbs, M. C., Wang, Y., Faber, J., Levine, J. E., Wang, J., Hahn, W. C., Gilliland, D. G., Golub, T. R., & Armstrong, S. A. (2006). Transformation from committed progenitor to leukaemia stem cell initiated by MLL–AF9. *Nature*, *442*(7104), 818–822. https://doi.org/10.1038/nature04980

Kunisaki, Y., Bruns, I., Scheiermann, C., Ahmed, J., Pinho, S., Zhang, D., Mizoguchi, T., Wei, Q., Lucas, D., Ito, K., Mar, J. C., Bergman, A., & Frenette, P. S. (2013). Arteriolar niches maintain haematopoietic stem cell quiescence. *Nature*, *502*(7473), 637–643. https://doi.org/10.1038/nature12612

Kuster, L., Grausenburger, R., Fuka, G., Kaindl, U., Krapf, G., Inthal, A., Mann, G., Kauer, M., Rainer, J., Kofler, R., Hall, A., Metzler, M., Meyer, L. H., Meyer, C., Harbott, J., Marschalek, R., Strehl, S., Haas, O. A., & Panzer-Grümayer, R. (2011). ETV6/RUNX1-positive relapses

evolve from an ancestral clone and frequently acquire deletions of genes implicated in glucocorticoid signaling. *Blood*, *117*(9), 2658–2667. https://doi.org/10.1182/blood-2010-03-275347

Lang, D., Powell, S. K., Plummer, R. S., Young, K. P., & Ruggeri, B. A. (2007). PAX genes: Roles in development, pathophysiology, and cancer. *Biochemical Pharmacology*, *73*(1), 1–14. https://doi.org/10.1016/j.bcp.2006.06.024

Lang, F., Wojcik, B., Bothur, S., Knecht, C., Falkenburg, J. H. F., Schroeder, T., Serve, H., Ottmann, O. G., & Rieger, M. A. (2017). Plastic CD34 and CD38 expression in adult B–cell precursor acute lymphoblastic leukemia explains ambiguity of leukemia-initiating stem cell populations. *Leukemia*, *31*(3), 731–734. https://doi.org/10.1038/leu.2016.315

Lang, F., Wojcik, B., & Rieger, M. A. (2015). Stem Cell Hierarchy and Clonal Evolution in Acute Lymphoblastic Leukemia. *Stem Cells International*, *2015*, 1–13. https://doi.org/10.1155/2015/137164

Lapidot, T., Sirard, C., Vormoor, J., Murdoch, B., Hoang, T., Caceres-Cortes, J., Minden, M., Paterson, B., Caligiuri, M. A., & Dick, J. E. (1994). A cell initiating human acute myeloid leukaemia after transplantation into SCID mice. *Nature*, *367*(6464), 645–648. https://doi.org/10.1038/367645a0

le Viseur, C., Hotfilder, M., Bomken, S., Wilson, K., Röttgers, S., Schrauder, A., Rosemann, A., Irving, J., Stam, R. W., Shultz, L. D., Harbott, J., Jürgens, H., Schrappe, M., Pieters, R., & Vormoor, J. (2008). In Childhood Acute Lymphoblastic Leukemia, Blasts at Different Stages of Immunophenotypic Maturation Have Stem Cell Properties. *Cancer Cell*, *14*(1), 47–58. https://doi.org/10.1016/j.ccr.2008.05.015

Lieber, M. R., Yu, K., & Raghavan, S. C. (2006). Roles of nonhomologous DNA end joining, V(D)J recombination, and class switch recombination in chromosomal translocations. *DNA Repair*, *5*(9–10), 1234–1245. https://doi.org/10.1016/j.dnarep.2006.05.013

Lin, H., & Grosschedl, R. (1995). Failure of B-cell differentiation in mice lacking the transcription factor EBF. *Nature*, *376*(6537), 263–267. https://doi.org/10.1038/376263a0

Lin, Y. C., Jhunjhunwala, S., Benner, C., Heinz, S., Welinder, E., Mansson, R., Sigvardsson, M., Hagman, J., Espinoza, C. A., Dutkowski, J., Ideker, T., Glass, C. K., & Murre, C. (2010). A global network of transcription factors, involving E2A, EBF1 and Foxo1, that orchestrates B cell fate. *Nature Immunology*, *11*(7), 635–643. https://doi.org/10.1038/ni.1891

Liu, M.-L., Rahman, M., Hirabayashi, Y., & Sasaki, T. (2002). Sequence analysis of 5'-flanking region of human pax-5 gene exon 1B. *Zhongguo Shi Yan Xue Ye Xue Za Zhi*, *10*(2), 100–103.

Lowen, M., Scott, G., & Zwollo, P. (2001). Functional Analyses of Two Alternative Isoforms of the Transcription Factor Pax-5. *Journal of Biological Chemistry*, *276*(45), 42565–42574. https://doi.org/10.1074/jbc.M106536200

Ma, Q., Jones, D., Borghesani, P. R., Segal, R. A., Nagasawa, T., Kishimoto, T., Bronson, R. T., & Springer, T. A. (1998). Impaired B-lymphopoiesis, myelopoiesis, and derailed cerebellar neuron migration in CXCR4- and SDF-1-deficient mice. *Proceedings of the National Academy of Sciences*, *95*(16), 9448–9453. https://doi.org/10.1073/pnas.95.16.9448

Ma, Q., Jones, D., & Springer, T. A. (1999). The Chemokine Receptor CXCR4 Is Required for the Retention of B Lineage and Granulocytic Precursors within the Bone Marrow Microenvironment. *Immunity*, *10*(4), 463–471. https://doi.org/10.1016/S1074-7613(00)80046-1

Ma, X., Edmonson, M., Yergeau, D., Muzny, D. M., Hampton, O. A., Rusch, M., Song, G., Easton, J., Harvey, R. C., Wheeler, D. A., Ma, J., Doddapaneni, H., Vadodaria, B., Wu, G., Nagahawatte, P., Carroll, W. L., Chen, I.-M., Gastier-Foster, J. M., Relling, M. V., … Zhang, J. (2015). Rise and fall of subclones from diagnosis to relapse in pediatric B-acute lymphoblastic leukaemia. *Nature Communications*, *6*(1), 6604. https://doi.org/10.1038/ncomms7604

Mahuteau-Betzer, F. (2015). Chimiothèque Nationale. *Médecine/Sciences*, *31*(4), 417–422. https://doi.org/10.1051/medsci/20153104016

Maia, A. T., van der Velden, V. H. J., Harrison, C. J., Szczepanski, T., Williams, M. D., Griffiths, M. J., van Dongen, J. J. M., & Greaves, M. F. (2003). Prenatal origin of hyperdiploid acute lymphoblastic leukemia in identical twins. *Leukemia*, *17*(11), 2202–2206. https://doi.org/10.1038/sj.leu.2403101

Makarova, K. S., Grishin, N. V, Shabalina, S. A., Wolf, Y. I., & Koonin, E. V. (2006). A putative RNA-interference-based immune system in prokaryotes: computational analysis of the predicted enzymatic machinery, functional analogies with eukaryotic RNAi, and hypothetical mechanisms of action. *Biology Direct*, *1*(1), 7. https://doi.org/10.1186/1745-6150-1-7

Mali, P., Yang, L., Esvelt, K. M., Aach, J., Guell, M., DiCarlo, J. E., Norville, J. E., & Church, G. M. (2013). RNA-Guided Human Genome Engineering via Cas9. *Science*, *339*(6121), 823–826. https://doi.org/10.1126/science.1232033

Malin, S., McManus, S., Cobaleda, C., Novatchkova, M., Delogu, A., Bouillet, P., Strasser, A., & Busslinger, M. (2010). Role of STAT5 in controlling cell survival and immunoglobulin gene recombination during pro-B cell development. *Nature Immunology*, *11*(2), 171–179. https://doi.org/10.1038/ni.1827

Malu, S., Malshetty, V., Francis, D., & Cortes, P. (2012). Role of non-homologous end joining in V(D)J recombination. *Immunologic Research*, *54*(1–3), 233–246. https://doi.org/10.1007/s12026-012-8329-z

Månsson, R., Hultquist, A., Luc, S., Yang, L., Anderson, K., Kharazi, S., Al-Hashmi, S., Liuba, K., Thorén, L., Adolfsson, J., Buza-Vidas, N., Qian, H., Soneji, S., Enver, T., Sigvardsson, M., & Jacobsen, S. E. W. (2007). Molecular Evidence for Hierarchical Transcriptional Lineage Priming in Fetal and Adult Stem Cells and Multipotent Progenitors. *Immunity*, *26*(4), 407–419. https://doi.org/10.1016/j.immuni.2007.02.013

Mansson, R., Zandi, S., Welinder, E., Tsapogas, P., Sakaguchi, N., Bryder, D., & Sigvardsson, M. (2010). Single-cell analysis of the common lymphoid progenitor compartment reveals functional and molecular heterogeneity. *Blood*, *115*(13), 2601–2609. https://doi.org/10.1182/blood-2009-08-236398

Marnett, L. J. (2000). Oxyradicals and DNA damage. *Carcinogenesis*, *21*(3), 361–370. https://doi.org/10.1093/carcin/21.3.361

Marshall, A. J., Fleming, H. E., Wu, G. E., & Paige, C. J. (1998). Modulation of the IL-7 dose-response threshold during pro-B cell differentiation is dependent on pre-B cell receptor expression. *Journal of Immunology (Baltimore, Md. : 1950)*, *161*(11), 6038–6045.

Martín-Lorenzo, A., Auer, F., Chan, L. N., García-Ramírez, I., González-Herrero, I., Rodríguez-Hernández, G., Bartenhagen, C., Dugas, M., Gombert, M., Ginzel, S., Blanco, O., Orfao, A., Alonso-López, D., Rivas, J. D. Las, García-Cenador, M. B., García-Criado, F. J., Müschen, M., Sánchez-García, I., Borkhardt, A., … Hauer, J. (2018). Loss of Pax5 Exploits Sca1-BCR-ABLp190 Susceptibility to Confer the Metabolic Shift Essential for pB-ALL. *Cancer Research*, *78*(10), 2669–2679. https://doi.org/10.1158/0008-5472.CAN-17-3262

Martin-Lorenzo, A., Hauer, J., Vicente-Duenas, C., Auer, F., Gonzalez-Herrero, I., Garcia-Ramirez, I., Ginzel, S., Thiele, R., Constantinescu, S. N., Bartenhagen, C., Dugas, M., Gombert, M., Schafer, D., Blanco, O., Mayado, A., Orfao, A., Alonso-Lopez, D., Rivas Jde, L., Cobaleda, C., … Borkhardt, A. (2015). Infection Exposure is a Causal Factor in B-cell Precursor Acute Lymphoblastic Leukemia as a Result of Pax5-Inherited Susceptibility. *Cancer Discov*, *5*(12), 1328–1343. https://doi.org/10.1158/2159-8290.CD-15-0892

Martín-Lorenzo, A., Hauer, J., Vicente-Dueñas, C., Auer, F., González-Herrero, I., García-Ramírez, I., Ginzel, S., Thiele, R., Constantinescu, S. N., Bartenhagen, C., Dugas, M., Gombert, M., Schäfer, D., Blanco, O., Mayado, A., Orfao, A., Alonso-López, D., Rivas, J. D. Las, Cobaleda, C., … Borkhardt, A. (2015). Infection Exposure Is a Causal Factor in B-cell Precursor Acute Lymphoblastic Leukemia as a Result of *Pax5* -Inherited Susceptibility. *Cancer Discovery*, *5*(12), 1328–1343. https://doi.org/10.1158/2159-8290.CD-15-0892

Mayran, A., Pelletier, A., & Drouin, J. (2015). Pax factors in transcription and epigenetic remodelling. *Seminars in Cell & Developmental Biology*, *44*, 135–144. https://doi.org/10.1016/j.semcdb.2015.07.007

McCormack, M. P., Young, L. F., Vasudevan, S., de Graaf, C. A., Codrington, R., Rabbitts, T. H., Jane, S. M., & Curtis, D. J. (2010). The *Lmo2* Oncogene Initiates Leukemia in Mice by Inducing Thymocyte Self-Renewal. *Science*, *327*(5967), 879–883. https://doi.org/10.1126/science.1182378

McLean, K. C., & Mandal, M. (2020). It Takes Three Receptors to Raise a B Cell. *Trends in Immunology*, *41*(7), 629–642. https://doi.org/10.1016/j.it.2020.05.003

McVey, M., & Lee, S. E. (2008). MMEJ repair of double-strand breaks (director's cut): deleted sequences and alternative endings. *Trends in Genetics*, *24*(11), 529–538. https://doi.org/10.1016/j.tig.2008.08.007

Medina, K. L., Pongubala, J. M. R., Reddy, K. L., Lancki, D. W., DeKoter, R., Kieslinger, M., Grosschedl, R., & Singh, H. (2004). Assembling a Gene Regulatory Network for Specification of the B Cell Fate. *Developmental Cell*, *7*(4), 607–617. https://doi.org/10.1016/j.devcel.2004.08.006

Medvedovic, J., Ebert, A., Tagoh, H., & Busslinger, M. (2011a). *Pax5* (pp. 179–206). https://doi.org/10.1016/B978-0-12-385991-4.00005-2

Medvedovic, J., Ebert, A., Tagoh, H., & Busslinger, M. (2011b). Pax5: a master regulator of B cell development and leukemogenesis. *Adv Immunol*, *111*, 179–206. https://doi.org/10.1016/B978-0-12-385991-4.00005-2

Meffre, E., Casellas, R., & Nussenzweig, M. C. (2000). Antibody regulation of B cell development. *Nat Immunol*, *1*(5), 379–385. https://doi.org/10.1038/80816

Melchers, F. (n.d.). B Cell Development and Its Deregulation to Transformed States at the Pre-B Cell Receptor-Expressing Pre-BII Cell Stage. In *Chronic Lymphocytic Leukemia* (pp. 1–17). Springer-Verlag. https://doi.org/10.1007/3-540-29933-5_1

Melchers, F. (2005). The pre-B-cell receptor: selector of fitting immunoglobulin heavy chains for the B-cell repertoire. *Nat Rev Immunol*, *5*(7), 578–584. https://doi.org/10.1038/nri1649

Melchers, F., Haasner, D., Grawunder, U., Kalberer, C., Karasuyama, H., Winkler, T., & Rolink, A. G. (1994). Roles of IGH and L Chains and of Surrogate H and L Chains in the Development of Cells of the B Lymphocyte Lineage. *Annual Review of Immunology*, *12*(1), 209–225. https://doi.org/10.1146/annurev.iy.12.040194.001233

Melchers, F., Strasser, A., Bauer, S. R., Kudo, A., Thalmann, P., & Rolink, A. (1991). *B Cell Development in Fetal Liver* (pp. 201–205). https://doi.org/10.1007/978-1-4684-5943-2_22

Melchers, F., ten Boekel, E., Seidl, T., Kong, X. C., Yamagami, T., Onishi, K., Shimizu, T., Rolink, A. G., & Andersson, J. (2000). Repertoire selection by pre-B-cell receptors and B-cell receptors, and genetic control of B-cell development from immature to mature B cells. *Immunological Reviews*, *175*, 33–46.

Méndez-Ferrer, S., Bonnet, D., Steensma, D. P., Hasserjian, R. P., Ghobrial, I. M., Gribben, J. G., Andreeff, M., & Krause, D. S. (2020). Bone marrow niches in haematological malignancies. *Nature Reviews Cancer*, *20*(5), 285–298. https://doi.org/10.1038/s41568-020-0245-2

Miller, C. L., Dykstra, B., & Eaves, C. J. (2008). Characterization of mouse hematopoietic stem and progenitor cells. *Current Protocols in Immunology*, *Chapter 22*, 22B.2.1-22B.2.31. https://doi.org/10.1002/0471142735.im22b02s80

Mohtashami, M., Shah, D. K., Nakase, H., Kianizad, K., Petrie, H. T., & Zuniga-Pflucker, J. C. (2010). Direct comparison of Dll1- and Dll4-mediated Notch activation levels shows differential lymphomyeloid lineage commitment outcomes. *J Immunol*, *185*(2), 867–876. https://doi.org/10.4049/jimmunol.1000782

Mojica, F. J. M., D□ez-Villase□or, C., Garc□a-Mart□nez, J., & Soria, E. (2005). Intervening Sequences of Regularly Spaced Prokaryotic Repeats Derive from Foreign Genetic Elements. *Journal of Molecular Evolution*, *60*(2), 174–182. https://doi.org/10.1007/s00239-004-0046-3

Monaco, G., Chen, H., Poidinger, M., Chen, J., de Magalhaes, J. P., & Larbi, A. (2016). flowAI: automatic and interactive anomaly discerning tools for flow cytometry data. *Bioinformatics*, *32*(16), 2473–2480. https://doi.org/10.1093/bioinformatics/btw191

Moore, J. K., & Haber, J. E. (1996). Cell Cycle and Genetic Requirements of Two Pathways of Nonhomologous End-Joining Repair of Double-Strand Breaks in *Saccharomyces cerevisiae*. *Molecular and Cellular Biology*, *16*(5), 2164–2173. https://doi.org/10.1128/MCB.16.5.2164

Moorman, A. V, Ensor, H. M., Richards, S. M., Chilton, L., Schwab, C., Kinsey, S. E., Vora, A., Mitchell, C. D., & Harrison, C. J. (2010). Prognostic effect of chromosomal abnormalities in childhood B-cell precursor acute lymphoblastic leukaemia: results from the UK Medical Research Council ALL97/99 randomised trial. *The Lancet Oncology*, *11*(5), 429–438. https://doi.org/10.1016/S1470-2045(10)70066-8

Mori, H., Colman, S. M., Xiao, Z., Ford, A. M., Healy, L. E., Donaldson, C., Hows, J. M., Navarrete, C., & Greaves, M. (2002). Chromosome translocations and covert leukemic clones are generated during normal fetal development. *Proceedings of the National Academy of Sciences*, *99*(12), 8242–8247. https://doi.org/10.1073/pnas.112218799

Morrison, S. J., & Weissman, I. L. (1994). The long-term repopulating subset of hematopoietic stem cells is deterministic and isolatable by phenotype. *Immunity*, *1*(8), 661–673. https://doi.org/10.1016/1074-7613(94)90037-X

Mourcin, F., Breton, C., Tellier, J., Narang, P., Chasson, L., Jorquera, A., Coles, M., Schiff, C., & Mancini, S. J. C. (2011). Galectin-1–expressing stromal cells constitute a specific niche for pre-BII cell development in mouse bone marrow. *Blood*, *117*(24), 6552–6561. https://doi.org/10.1182/blood-2010-12-323113

Mullighan, C. G. (2012). Molecular genetics of B-precursor acute lymphoblastic leukemia. *Journal of Clinical Investigation*, *122*(10), 3407–3415. https://doi.org/10.1172/JCI61203

Mullighan, C. G. (2019). PAX5-driven subtypes of B-progenitor acute lymphoblastic leukemia. *Nature Genetics*, *176*(3), 139–148. https://doi.org/10.1016/j.physbeh.2017.03.040

Mullighan, C. G., Goorha, S., Radtke, I., Miller, C. B., Coustan-Smith, E., Dalton, J. D., Girtman, K., Mathew, S., Ma, J., Pounds, S. B., Su, X., Pui, C. H., Relling, M. V, Evans, W. E., Shurtleff, S. A., & Downing, J. R. (2007a). Genome-wide analysis of genetic alterations in acute lymphoblastic leukaemia. *Nature*, *446*(7137), 758–764. https://doi.org/10.1038/nature05690

Mullighan, C. G., Goorha, S., Radtke, I., Miller, C. B., Coustan-Smith, E., Dalton, J. D., Girtman, K., Mathew, S., Ma, J., Pounds, S. B., Su, X., Pui, C.-H., Relling, M. V., Evans, W. E., Shurtleff, S. A., & Downing, J. R. (2007b). Genome-wide analysis of genetic alterations in acute lymphoblastic leukaemia. *Nature*, *446*(7137), 758–764. https://doi.org/10.1038/nature05690

Mullighan, C. G., Goorha, S., Radtke, I., Miller, C. B., Coustan-Smith, E., Dalton, J. D., Girtman, K., Mathew, S., Ma, J., Pounds, S. B., Su, X., Pui, C.-H., Relling, M. V., Evans, W. E., Shurtleff, S. A., & Downing, J. R. (2007c). Genome-wide analysis of genetic alterations in acute lymphoblastic leukaemia. *Nature*, *446*(7137), 758–764. https://doi.org/10.1038/nature05690

Mullighan, C. G., Goorha, S., Radtke, I., Miller, C. B., Coustan-Smith, E., Dalton, J. D., Girtman, K., Mathew, S., Ma, J., Pounds, S. B., Su, X., Pui, C.-H., Relling, M. V., Evans, W. E., Shurtleff, S. A., & Downing, J. R. (2007d). Genome-wide analysis of genetic alterations in acute lymphoblastic leukaemia. *Nature*, *446*(7137), 758–764. https://doi.org/10.1038/nature05690

Mullighan, C. G., Phillips, L. A., Su, X., Ma, J., Miller, C. B., Shurtleff, S. A., & Downing, J. R. (2008). Genomic Analysis of the Clonal Origins of Relapsed Acute Lymphoblastic Leukemia. *Science*, *322*(5906), 1377–1380. https://doi.org/10.1126/science.1164266

Mullighan, C. G., Zhang, J., Harvey, R. C., Collins-Underwood, J. R., Schulman, B. A., Phillips, L. A., Tasian, S. K., Loh, M. L., Su, X., Liu, W., Devidas, M., Atlas, S. R., Chen, I.-M., Clifford, R. J., Gerhard, D. S., Carroll, W. L., Reaman, G. H., Smith, M., Downing, J. R., … Willman, C. L. (2009). JAK mutations in high-risk childhood acute lymphoblastic leukemia. *Proceedings of the National Academy of Sciences of the United States of America*, *106*(23), 9414–9418. https://doi.org/10.1073/pnas.0811761106

Murakami, H., & Keeney, S. (2008). Regulating the formation of DNA double-strand breaks in meiosis. *Genes & Development*, *22*(3), 286–292. https://doi.org/10.1101/gad.1642308

Murre, C. (2018). 'Big bang' of B-cell development revealed. *Genes & Development*, *32*(2), 93–95. https://doi.org/10.1101/gad.311357.118

Nagasawa, T., Hirota, S., Tachibana, K., Takakura, N., Nishikawa, S., Kitamura, Y., Yoshida, N., Kikutani, H., & Kishimoto, T. (1996). Defects of B-cell lymphopoiesis and bone-marrow myelopoiesis in mice lacking the CXC chemokine PBSF/SDF-1. *Nature*, *382*(6592), 635–638. https://doi.org/10.1038/382635a0

Nagasawa, T., Kikutani, H., & Kishimoto, T. (1994). Molecular cloning and structure of a pre-B-cell growth-stimulating factor. *Proceedings of the National Academy of Sciences*, *91*(6), 2305–2309. https://doi.org/10.1073/pnas.91.6.2305

Namen, A. E., Lupton, S., Hjerrild, K., Wignall, J., Mochizuki, D. Y., Schmierer, A., Mosley, B., March, C. J., Urdal, D., Gillis, S., Cosman, D., & Goodwin, R. G. (1988). Stimulation of B-cell progenitors by cloned murine interleukin-7. *Nature*, *333*(6173), 571–573. https://doi.org/10.1038/333571a0

Nebral, K., Denk, D., Attarbaschi, A., König, M., Mann, G., Haas, O. A., & Strehl, S. (2009). Incidence and diversity of PAX5 fusion genes in childhood acute lymphoblastic leukemia. *Leukemia*, *23*(1), 134–143. https://doi.org/10.1038/leu.2008.306

Nebral, K., Denk, D., Attarbaschi, A., Konig, M., Mann, G., Haas, O. A., & Strehl, S. (2009). Incidence and diversity of PAX5 fusion genes in childhood acute lymphoblastic leukemia. *Leukemia*, *23*(1), 134–143. https://doi.org/10.1038/leu.2008.306

Nera, K. P., Kohonen, P., Narvi, E., Peippo, A., Mustonen, L., Terho, P., Koskela, K., Buerstedde, J. M., & Lassila, O. (2006). Loss of Pax5 promotes plasma cell differentiation. *Immunity*, *24*(3), 283–293. https://doi.org/10.1016/j.immuni.2006.02.003

Nichogiannopoulou, A., Trevisan, M., Neben, S., Friedrich, C., & Georgopoulos, K. (1999). Defects in Hemopoietic Stem Cell Activity in Ikaros Mutant Mice. *Journal of Experimental Medicine*, *190*(9), 1201–1214. https://doi.org/10.1084/jem.190.9.1201

Nishana, M., & Raghavan, S. C. (2012). Role of recombination activating genes in the generation of antigen receptor diversity and beyond. *Immunology*, *137*(4), 271–281. https://doi.org/10.1111/imm.12009

Nobori, T., Miura, K., Wu, D. J., Lois, A., Takabayashi, K., & Carson, D. A. (1994). Deletions of the cyclin-dependent kinase-4 inhibitor gene in multiple human cancers. *Nature*, *368*(6473), 753–756. https://doi.org/10.1038/368753a0

Noll, M. (1993). Evolution and role of Pax genes. *Current Opinion in Genetics & Development*, *3*(4), 595–605. https://doi.org/10.1016/0959-437X(93)90095-7

Nombela-Arrieta, C., Pivarnik, G., Winkel, B., Canty, K. J., Harley, B., Mahoney, J. E., Park, S.-Y., Lu, J., Protopopov, A., & Silberstein, L. E. (2013). Quantitative imaging of haematopoietic stem and progenitor cell localization and hypoxic status in the bone marrow microenvironment. *Nature Cell Biology*, *15*(5), 533–543. https://doi.org/10.1038/ncb2730

Nutt, S. L., Heavey, B., Rolink, A. G., & Busslinger, M. (1999a). Commitment to the B-lymphoid lineage depends on the transcription factor Pax5. *Nature*, *401*(6753), 556–562. https://doi.org/10.1038/44076

Nutt, S. L., Heavey, B., Rolink, A. G., & Busslinger, M. (1999b). Commitment to the B-lymphoid lineage depends on the transcription factor Pax5. *Nature*, *401*(6753), 556–562. https://doi.org/10.1038/44076

Nutt, S. L., Thévenin, C., & Busslinger, M. (1997). Essential Functions of Pax-5 (BSAP) in pro-B Cell Development. *Immunobiology*, *198*(1–3), 227–235. https://doi.org/10.1016/S0171-2985(97)80043-5

Nutt, S. L., Urbanek, P., Rolink, A., & Busslinger, M. (1997). Essential functions of Pax5 (BSAP) in pro-B cell development: difference between fetal and adult B lymphopoiesis and reduced V-to-DJ recombination at the IgH locus. *Genes Dev*, *11*(4), 476–491. https://www.ncbi.nlm.nih.gov/pubmed/9042861

Oefelein, M., Grapey, D., Schaeffer, T., Chin-Chance, C., & Bushman, W. (1996). PAX-2: A Developmental Gene Constitutively Expressed in the Mouse Epididymis and Ductus Deferens. *Journal of Urology*, *156*(3), 1204–1207. https://doi.org/10.1016/S0022-5347(01)65751-3

Ogawa, M., Boekel, E. ten, & Melchers, F. (2000). Identification of CD19–B220+c-Kit+Flt3/Flk-2+cells as early B lymphoid precursors before pre-B-I cells in juvenile mouse bone marrow. *International Immunology*, *12*(3), 313–324. https://doi.org/10.1093/intimm/12.3.313

Olin, A., Henckel, E., Chen, Y., Lakshmikanth, T., Pou, C., Mikes, J., Gustafsson, A., Bernhardsson, A. K., Zhang, C., Bohlin, K., & Brodin, P. (2018). Stereotypic Immune System Development in Newborn Children. *Cell*, *174*(5), 1277-1292.e14. https://doi.org/10.1016/j.cell.2018.06.045

Oppezzo, P., Dumas, G., Lalanne, A. I., Payelle-Brogard, B., Magnac, C., Pritsch, O., Dighiero, G., & Vuillier, F. (2005). Different isoforms of BSAP regulate expression of AID in normal and chronic lymphocytic leukemia B cells. *Blood*, *105*(6), 2495–2503. https://doi.org/10.1182/blood-2004-09-3644

Orlando, E. J., Han, X., Tribouley, C., Wood, P. A., Leary, R. J., Riester, M., Levine, J. E., Qayed, M., Grupp, S. A., Boyer, M., De Moerloose, B., Nemecek, E. R., Bittencourt, H., Hiramatsu, H., Buechner, J., Davies, S. M., Verneris, M. R., Nguyen, K., Brogdon, J. L., … Winckler, W. (2018). Genetic mechanisms of target antigen loss in CAR19 therapy of acute lymphoblastic leukemia. *Nature Medicine*, *24*(10), 1504–1506. https://doi.org/10.1038/s41591-018-0146-z

Osawa, M., Hanada, K., Hamada, H., & Nakauchi, H. (1996). Long-Term Lymphohematopoietic Reconstitution by a Single CD34-Low/Negative Hematopoietic Stem Cell. *Science*, *273*(5272), 242–245. https://doi.org/10.1126/science.273.5272.242

Oshima, K., Khiabanian, H., da Silva-Almeida, A. C., Tzoneva, G., Abate, F., Ambesi-Impiombato, A., Sanchez-Martin, M., Carpenter, Z., Penson, A., Perez-Garcia, A., Eckert, C., Nicolas, C., Balbin, M., Sulis, M. L., Kato, M., Koh, K., Paganin, M., Basso, G., Gastier-Foster, J. M., … Ferrando, A. A. (2016). Mutational landscape, clonal evolution patterns, and role of RAS mutations in relapsed acute lymphoblastic leukemia. *Proceedings of the National Academy of Sciences*, *113*(40), 11306–11311. https://doi.org/10.1073/pnas.1608420113

Paixão-Côrtes, V. R., Salzano, F. M., & Bortolini, M. C. (2015). Origins and evolvability of the PAX family. *Seminars in Cell & Developmental Biology*, *44*, 64–74. https://doi.org/10.1016/j.semcdb.2015.08.014

Pasca di Magliano, M., Di Lauro, R., & Zannini, M. (2000). Pax8 has a key role in thyroid cell differentiation. *Proceedings of the National Academy of Sciences*, *97*(24), 13144–13149. https://doi.org/10.1073/pnas.240336397

Passet, M., Boissel, N., Sigaux, F., Saillard, C., Bargetzi, M., Ba, I., Thomas, X., Graux, C., Chalandon, Y., Leguay, T., Lengliné, E., Konopacki, J., Quentin, S., Delabesse, E., Lafage-Pochitaloff, M., Pastoret, C., Grardel, N., Asnafi, V., Lhéritier, V., … Clappier, E. (2019). PAX5 P80R mutation identifies a novel subtype of B-cell precursor acute lymphoblastic leukemia with favorable outcome. *Blood*, *133*(3), 280–284. https://doi.org/10.1182/blood-2018-10-882142

Passet, M., Boissel, N., Sigaux, F., Saillard, C., Bargetzi, M., Ba, I., Thomas, X., Graux, C., Chalandon, Y., Leguay, T., Lengline, E., Konopacki, J., Quentin, S., Delabesse, E., Lafage-Pochitaloff, M., Pastoret, C., Grardel, N., Asnafi, V., Lheritier, V., … Group for Research on Adult, A. L. L. (2019). PAX5 P80R mutation identifies a novel subtype of B-cell precursor acute lymphoblastic leukemia with favorable outcome. *Blood*, *133*(3), 280–284. https://doi.org/10.1182/blood-2018-10-882142

Peppas, I., Ford, A. M., Furness, C. L., & Greaves, M. F. (2023). Gut microbiome immaturity and childhood acute lymphoblastic leukaemia. *Nature Reviews Cancer*, *23*(8), 565–576. https://doi.org/10.1038/s41568-023-00584-4

Peters, H., Neubüser, A., Kratochwil, K., & Balling, R. (1998). *Pax9* -deficient mice lack pharyngeal pouch derivatives and teeth and exhibit craniofacial and limb abnormalities. *Genes & Development*, *12*(17), 2735–2747. https://doi.org/10.1101/gad.12.17.2735

Pfeffer, P. L., Bouchard, M., & Busslinger, M. (2000). Pax2 and homeodomain proteins cooperatively regulate a 435 bp enhancer of the mouse *Pax5* gene at the midbrain-hindbrain boundary. *Development*, *127*(5), 1017–1028. https://doi.org/10.1242/dev.127.5.1017

Pietras, E. M., Reynaud, D., Kang, Y.-A., Carlin, D., Calero-Nieto, F. J., Leavitt, A. D., Stuart, J. M., Göttgens, B., & Passegué, E. (2015). Functionally Distinct Subsets of Lineage-Biased Multipotent Progenitors Control Blood Production in Normal and Regenerative Conditions. *Cell Stem Cell*, *17*(1), 35–46. https://doi.org/10.1016/j.stem.2015.05.003

Pongubala, J. M. R., Northrup, D. L., Lancki, D. W., Medina, K. L., Treiber, T., Bertolino, E., Thomas, M., Grosschedl, R., Allman, D., & Singh, H. (2008). Transcription factor EBF restricts alternative lineage options and promotes B cell fate commitment independently of Pax5. *Nature Immunology*, *9*(2), 203–215. https://doi.org/10.1038/ni1555

Pourcel, C., Salvignol, G., & Vergnaud, G. (2005). CRISPR elements in Yersinia pestis acquire new repeats by preferential uptake of bacteriophage DNA, and provide additional tools for evolutionary studies. *Microbiology*, *151*(3), 653–663. https://doi.org/10.1099/mic.0.27437-0

Prasad, M. A. J., Ungerbäck, J., Åhsberg, J., Somasundaram, R., Strid, T., Larsson, M., Månsson, R., De Paepe, A., Lilljebjörn, H., Fioretos, T., Hagman, J., & Sigvardsson, M. (2015). Ebf1 heterozygosity results in increased DNA damage in pro-B cells and their synergistic transformation by Pax5 haploinsufficiency. *Blood*, *125*(26), 4052–4059. https://doi.org/10.1182/blood-2014-12-617282

Prasad, M. A., Ungerback, J., Ahsberg, J., Somasundaram, R., Strid, T., Larsson, M., Mansson, R., De Paepe, A., Lilljebjorn, H., Fioretos, T., Hagman, J., & Sigvardsson, M. (2015). Ebf1 heterozygosity results in increased DNA damage in pro-B cells and their synergistic transformation by Pax5 haploinsufficiency. *Blood*, *125*(26), 4052–4059. https://doi.org/10.1182/blood-2014-12-617282

Rabilloud, T., Potier, D., Pankaew, S., Nozais, M., Loosveld, M., & Payet-Bornet, D. (2021). Single-cell profiling identifies pre-existing CD19-negative subclones in a B-ALL patient with CD19-negative relapse after CAR-T therapy. *Nature Communications*, *12*(1), 865. https://doi.org/10.1038/s41467-021-21168-6

Ramadani, F., Bolland, D. J., Garcon, F., Emery, J. L., Vanhaesebroeck, B., Corcoran, A. E., & Okkenhaug, K. (2010). The PI3K Isoforms p110α and p110δ Are Essential for Pre–B Cell Receptor Signaling and B Cell Development. *Science Signaling*, *3*(134). https://doi.org/10.1126/scisignal.2001104

Ramamoorthy, S., Kometani, K., Herman, J. S., Bayer, M., Boller, S., Edwards-Hicks, J., Ramachandran, H., Li, R., Klein-Geltink, R., Pearce, E. L., Grün, D., & Grosschedl, R. (2020). EBF1 and Pax5 safeguard leukemic transformation by limiting IL-7 signaling, Myc expression, and folate metabolism. *Genes & Development*, *34*(21–22), 1503–1519. https://doi.org/10.1101/gad.340216.120

Ramamoorthy, S., Kometani, K., Herman, J. S., Bayer, M., Boller, S., Edwards-Hicks, J., Ramachandran, H., Li, R., Klein-Geltink, R., Pearce, E. L., Grun, D., & Grosschedl, R. (2020). EBF1 and Pax5 safeguard leukemic transformation by limiting IL-7 signaling, Myc

expression, and folate metabolism. *Genes Dev*, *34*(21–22), 1503–1519. https://doi.org/10.1101/gad.340216.120

Rastogi, R. P., Richa, Kumar, A., Tyagi, M. B., & Sinha, R. P. (2010). Molecular Mechanisms of Ultraviolet Radiation-Induced DNA Damage and Repair. *Journal of Nucleic Acids*, *2010*, 1–32. https://doi.org/10.4061/2010/592980

Rath, M. F., Bailey, M. J., Kim, J.-S., Ho, A. K., Gaildrat, P., Coon, S. L., Møller, M., & Klein, D. C. (2009). Developmental and Diurnal Dynamics of Pax4 Expression in the Mammalian Pineal Gland: Nocturnal Down-Regulation Is Mediated by Adrenergic-Cyclic Adenosine 3',5'-Monophosphate Signaling. *Endocrinology*, *150*(2), 803–811. https://doi.org/10.1210/en.2008-0882

Rehe, K., Wilson, K., Bomken, S., Williamson, D., Irving, J., den Boer, M. L., Stanulla, M., Schrappe, M., Hall, A. G., Heidenreich, O., & Vormoor, J. (2013). Acute B lymphoblastic leukaemia-propagating cells are present at high frequency in diverse lymphoblast populations. *EMBO Molecular Medicine*, *5*(1), 38–51. https://doi.org/10.1002/emmm.201201703

Reyman, M., van Houten, M. A., van Baarle, D., Bosch, A. A. T. M., Man, W. H., Chu, M. L. J. N., Arp, K., Watson, R. L., Sanders, E. A. M., Fuentes, S., & Bogaert, D. (2019). Impact of delivery mode-associated gut microbiota dynamics on health in the first year of life. *Nature Communications*, *10*(1), 4997. https://doi.org/10.1038/s41467-019-13014-7

Richardson, C. D., Ray, G. J., DeWitt, M. A., Curie, G. L., & Corn, J. E. (2016). Enhancing homology-directed genome editing by catalytically active and inactive CRISPR-Cas9 using asymmetric donor DNA. *Nature Biotechnology*, *34*(3), 339–344. https://doi.org/10.1038/nbt.3481

Ritz-Laser, B., Estreicher, A., Gauthier, B., & Philippe, J. (2000). The Paired Homeodomain Transcription Factor Pax-2 Is Expressed in the Endocrine Pancreas and Transactivates the Glucagon Gene Promoter. *Journal of Biological Chemistry*, *275*(42), 32708–32715. https://doi.org/10.1074/jbc.M005704200

Roberts, K. G. (2018). Genetics and prognosis of ALL in children vs adults. *Hematology*, *2018*(1), 137–145. https://doi.org/10.1182/asheducation-2018.1.137

Roberts, K. G., & Mullighan, C. G. (2020). The Biology of B-Progenitor Acute Lymphoblastic Leukemia. *Cold Spring Harbor Perspectives in Medicine*, *10*(7), a034835. https://doi.org/10.1101/cshperspect.a034835

Robichaud, G. A., Nardini, M., Laflamme, M., Cuperlovic-Culf, M., & Ouellette, R. J. (2004). Human Pax-5 C-terminal Isoforms Possess Distinct Transactivation Properties and Are Differentially Modulated in Normal and Malignant B Cells. *Journal of Biological Chemistry*, *279*(48), 49956–49963. https://doi.org/10.1074/jbc.M407171200

Rodriguez-Hernandez, G., Opitz, F. V, Delgado, P., Walter, C., Alvarez-Prado, A. F., Gonzalez-Herrero, I., Auer, F., Fischer, U., Janssen, S., Bartenhagen, C., Raboso-Gallego, J., Casado-Garcia, A., Orfao, A., Blanco, O., Alonso-Lopez, D., Rivas, J. L., Tena-Davila, S. G., Muschen, M., Dugas, M., … Borkhardt, A. (2019). Infectious stimuli promote malignant B-cell acute lymphoblastic leukemia in the absence of AID. *Nat Commun*, *10*(1), 5563. https://doi.org/10.1038/s41467-019-13570-y

Rodríguez-Hernández, G., Opitz, F. V., Delgado, P., Walter, C., Álvarez-Prado, Á. F., González-Herrero, I., Auer, F., Fischer, U., Janssen, S., Bartenhagen, C., Raboso-Gallego, J., Casado-García, A., Orfao, A., Blanco, O., Alonso-López, D., Rivas, J. D. Las, Tena-Dávila, S. G. de, Müschen, M., Dugas, M., … Borkhardt, A. (2019). Infectious stimuli promote malignant

B-cell acute lymphoblastic leukemia in the absence of AID. *Nature Communications*, *10*(1), 5563. https://doi.org/10.1038/s41467-019-13570-y

Roessler, S., Györy, I., Imhof, S., Spivakov, M., Williams, R. R., Busslinger, M., Fisher, A. G., & Grosschedl, R. (2007). Distinct Promoters Mediate the Regulation of *Ebf1* Gene Expression by Interleukin-7 and Pax5. *Molecular and Cellular Biology*, *27*(2), 579–594. https://doi.org/10.1128/MCB.01192-06

Rolink, A. G., Nutt, S. L., Melchers, F., & Busslinger, M. (1999a). Long-term in vivo reconstitution of T-cell development by Pax5-deficient B-cell progenitors. *Nature*, *401*(6753), 603–606. https://doi.org/10.1038/44164

Rolink, A. G., Nutt, S. L., Melchers, F., & Busslinger, M. (1999b). Long-term in vivo reconstitution of T-cell development by Pax5-deficient B-cell progenitors. *Nature*, *401*(6753), 603–606. https://doi.org/10.1038/44164

Rolink, A., Kudo, A., Karasuyama, H., Kikuchi, Y., & Melchers, F. (1991). Long-term proliferating early pre B cell lines and clones with the potential to develop to surface Ig-positive, mitogen reactive B cells in vitro and in vivo. *The EMBO Journal*, *10*(2), 327–336. https://doi.org/10.1002/j.1460-2075.1991.tb07953.x

Rolink, A., & Melchers, F. (1996). B-cell development in the mouse. *Immunol Lett*, *54*(2–3), 157–161. https://doi.org/10.1016/s0165-2478(96)02666-1

Rossi, B., Espeli, M., Schiff, C., & Gauthier, L. (2006). Clustering of Pre-B Cell Integrins Induces Galectin-1-Dependent Pre-B Cell Receptor Relocalization and Activation. *The Journal of Immunology*, *177*(2), 796–803. https://doi.org/10.4049/jimmunol.177.2.796

Rouault-Pierre, K., Lopez-Onieva, L., Foster, K., Anjos-Afonso, F., Lamrissi-Garcia, I., Serrano-Sanchez, M., Mitter, R., Ivanovic, Z., de Verneuil, H., Gribben, J., Taussig, D., Rezvani, H. R., Mazurier, F., & Bonnet, D. (2013). HIF-2alpha protects human hematopoietic stem/progenitors and acute myeloid leukemic cells from apoptosis induced by endoplasmic reticulum stress. *Cell Stem Cell*, *13*(5), 549–563. https://doi.org/10.1016/j.stem.2013.08.011

Rumfelt, L. L., Zhou, Y., Rowley, B. M., Shinton, S. A., & Hardy, R. R. (2006). Lineage specification and plasticity in CD19− early B cell precursors. *Journal of Experimental Medicine*, *203*(3), 675–687. https://doi.org/10.1084/jem.20052444

Sarry, J.-E., Murphy, K., Perry, R., Sanchez, P. V., Secreto, A., Keefer, C., Swider, C. R., Strzelecki, A.-C., Cavelier, C., Récher, C., Mansat-De Mas, V., Delabesse, E., Danet-Desnoyers, G., & Carroll, M. (2011). Human acute myelogenous leukemia stem cells are rare and heterogeneous when assayed in NOD/SCID/IL2Rγc-deficient mice. *Journal of Clinical Investigation*, *121*(1), 384–395. https://doi.org/10.1172/JCI41495

Schäfer, D., Olsen, M., Lähnemann, D., Stanulla, M., Slany, R., Schmiegelow, K., Borkhardt, A., & Fischer, U. (2018). Five percent of healthy newborns have an ETV6-RUNX1 fusion as revealed by DNA-based GIPFEL screening. *Blood*, *131*(7), 821–826. https://doi.org/10.1182/blood-2017-09-808402

Schaniel, C., Bruno, L., Melchers, F., & Rolink, A. G. (2002a). Multiple hematopoietic cell lineages develop in vivo from transplanted Pax5-deficient pre-B I–cell clones. *Blood*, *99*(2), 472–478. https://doi.org/10.1182/blood.V99.2.472

Schaniel, C., Bruno, L., Melchers, F., & Rolink, A. G. (2002b). Multiple hematopoietic cell lineages develop in vivo from transplanted Pax5-deficient pre-B I-cell clones. *Blood*, *99*(2), 472–478. https://www.ncbi.nlm.nih.gov/pubmed/11781227

Schebesta, A., McManus, S., Salvagiotto, G., Delogu, A., Busslinger, G. A., & Busslinger, M. (2007). Transcription Factor Pax5 Activates the Chromatin of Key Genes Involved in B

Cell Signaling, Adhesion, Migration, and Immune Function. *Immunity*, *27*(1), 49–63. https://doi.org/10.1016/j.immuni.2007.05.019

Schebesta, M., Pfeffer, P. L., & Busslinger, M. (2002). Control of Pre-BCR Signaling by Pax5-Dependent Activation of the BLNK Gene. *Immunity*, *17*(4), 473–485. https://doi.org/10.1016/S1074-7613(02)00418-1

Schultz, K. R., Carroll, A., Heerema, N. A., Bowman, W. P., Aledo, A., Slayton, W. B., Sather, H., Devidas, M., Zheng, H. W., Davies, S. M., Gaynon, P. S., Trigg, M., Rutledge, R., Jorstad, D., Winick, N., Borowitz, M. J., Hunger, S. P., Carroll, W. L., & Camitta, B. (2014). Long-term follow-up of imatinib in pediatric Philadelphia chromosome-positive acute lymphoblastic leukemia: Children's Oncology Group Study AALL0031. *Leukemia*, *28*(7), 1467–1471. https://doi.org/10.1038/leu.2014.30

Scott, E. W., Fisher, R. C., Olson, M. C., Kehrli, E. W., Simon, M. C., & Singh, H. (1997). PU.1 Functions in a Cell-Autonomous Manner to Control the Differentiation of Multipotential Lymphoid–Myeloid Progenitors. *Immunity*, *6*(4), 437–447. https://doi.org/10.1016/S1074-7613(00)80287-3

Seale, P., Asakura, A., & Rudnicki, M. A. (2001). The Potential of Muscle Stem Cells. *Developmental Cell*, *1*(3), 333–342. https://doi.org/10.1016/S1534-5807(01)00049-1

Sędek, Ł., Theunissen, P., Sobral da Costa, E., van der Sluijs-Gelling, A., Mejstrikova, E., Gaipa, G., Sonsala, A., Twardoch, M., Oliveira, E., Novakova, M., Buracchi, C., van Dongen, J. J. M., Orfao, A., van der Velden, V. H. J., & Szczepański, T. (2019). Differential expression of CD73, CD86 and CD304 in normal vs. leukemic B-cell precursors and their utility as stable minimal residual disease markers in childhood B-cell precursor acute lymphoblastic leukemia. *Journal of Immunological Methods*, *475*, 112429. https://doi.org/10.1016/j.jim.2018.03.005

Seet, C. S., Brumbaugh, R. L., & Kee, B. L. (2004). Early B Cell Factor Promotes B Lymphopoiesis with Reduced Interleukin 7 Responsiveness in the Absence of E2A. *Journal of Experimental Medicine*, *199*(12), 1689–1700. https://doi.org/10.1084/jem.20032202

Sellars, M. (2011a). Ikaros in B cell development and function. *World Journal of Biological Chemistry*, *2*(6), 132. https://doi.org/10.4331/wjbc.v2.i6.132

Sellars, M. (2011b). Ikaros in B cell development and function. *World Journal of Biological Chemistry*, *2*(6), 132. https://doi.org/10.4331/wjbc.v2.i6.132

Shah, S., Schrader, K. A., Waanders, E., Timms, A. E., Vijai, J., Miething, C., Wechsler, J., Yang, J., Hayes, J., Klein, R. J., Zhang, J., Wei, L., Wu, G., Rusch, M., Nagahawatte, P., Ma, J., Chen, S. C., Song, G., Cheng, J., … Offit, K. (2013). A recurrent germline PAX5 mutation confers susceptibility to pre-B cell acute lymphoblastic leukemia. *Nat Genet*, *45*(10), 1226–1231. https://doi.org/10.1038/ng.2754

Shao, Y., Forster, S. C., Tsaliki, E., Vervier, K., Strang, A., Simpson, N., Kumar, N., Stares, M. D., Rodger, A., Brocklehurst, P., Field, N., & Lawley, T. D. (2019). Stunted microbiota and opportunistic pathogen colonization in caesarean-section birth. *Nature*, *574*(7776), 117–121. https://doi.org/10.1038/s41586-019-1560-1

Shin, D. H., Lee, K.-S., Lee, E., Chang, Y. P., Kim, J.-W., Choi, Y. S., Kwon, B.-S., Lee, H. W., & Cho, S. S. (2003). Pax-7 Immunoreactivity in the Post-natal Chicken Central Nervous System. *Anatomia, Histologia, Embryologia: Journal of Veterinary Medicine Series C*, *32*(6), 378–383. https://doi.org/10.1111/j.1439-0264.2003.00496.x

Sivakamasundari, V., Kraus, P., & Lufkin, T. (2018). Regulatory Functions of Pax1 and Pax9 in Mammalian Cells. In *Gene Expression and Regulation in Mammalian Cells - Transcription*

Toward the Establishment of Novel Therapeutics. InTech. https://doi.org/10.5772/intechopen.71920

Smeenk, L., Fischer, M., Jurado, S., Jaritz, M., Azaryan, A., Werner, B., Roth, M., Zuber, J., Stanulla, M., den Boer, M. L., Mullighan, C. G., Strehl, S., & Busslinger, M. (2017a). Molecular role of the <scp>PAX</scp> 5- <scp>ETV</scp> 6 oncoprotein in promoting B-cell acute lymphoblastic leukemia. *The EMBO Journal*, *36*(6), 718–735. https://doi.org/10.15252/embj.201695495

Smeenk, L., Fischer, M., Jurado, S., Jaritz, M., Azaryan, A., Werner, B., Roth, M., Zuber, J., Stanulla, M., den Boer, M. L., Mullighan, C. G., Strehl, S., & Busslinger, M. (2017b). Molecular role of the PAX5-ETV6 oncoprotein in promoting B-cell acute lymphoblastic leukemia. *EMBO J*, *36*(6), 718–735. https://doi.org/10.15252/embj.201695495

Somasundaram, R., Prasad, M. A. J., Ungerbäck, J., & Sigvardsson, M. (2015). Transcription factor networks in B-cell differentiation link development to acute lymphoid leukemia. *Blood*, *126*(2), 144–152. https://doi.org/10.1182/blood-2014-12-575688

Souabni, A., Cobaleda, C., Schebesta, M., & Busslinger, M. (2002a). Pax5 Promotes B Lymphopoiesis and Blocks T Cell Development by Repressing Notch1. *Immunity*, *17*(6), 781–793. https://doi.org/10.1016/S1074-7613(02)00472-7

Souabni, A., Cobaleda, C., Schebesta, M., & Busslinger, M. (2002b). Pax5 promotes B lymphopoiesis and blocks T cell development by repressing Notch1. *Immunity*, *17*(6), 781–793. https://www.ncbi.nlm.nih.gov/pubmed/12479824

Spangrude, G. J., Heimfeld, S., & Weissman, I. L. (1988). Purification and Characterization of Mouse Hematopoietic Stem Cells. *Science*, *241*(4861), 58–62. https://doi.org/10.1126/science.2898810

Stapleton, P., Weith, A., Urbánek, P., Kozmik, Z., & Busslinger, M. (1993). Chromosomal localization of seven PAX genes and cloning of a novel family member, PAX-9. *Nature Genetics*, *3*(4), 292–298. https://doi.org/10.1038/ng0493-292

Sternberg, S. H., Redding, S., Jinek, M., Greene, E. C., & Doudna, J. A. (2014). DNA interrogation by the CRISPR RNA-guided endonuclease Cas9. *Nature*, *507*(7490), 62–67. https://doi.org/10.1038/nature13011

Stewart, C. J., Ajami, N. J., O'Brien, J. L., Hutchinson, D. S., Smith, D. P., Wong, M. C., Ross, M. C., Lloyd, R. E., Doddapaneni, H., Metcalf, G. A., Muzny, D., Gibbs, R. A., Vatanen, T., Huttenhower, C., Xavier, R. J., Rewers, M., Hagopian, W., Toppari, J., Ziegler, A.-G., … Petrosino, J. F. (2018). Temporal development of the gut microbiome in early childhood from the TEDDY study. *Nature*, *562*(7728), 583–588. https://doi.org/10.1038/s41586-018-0617-x

St-Onge, L., Sosa-Pineda, B., Chowdhury, K., Mansouri, A., & Gruss, P. (1997). Pax6 is required for differentiation of glucagon-producing α-cells in mouse pancreas. *Nature*, *387*(6631), 406–409. https://doi.org/10.1038/387406a0

Stoykova, A., & Gruss, P. (1994). Roles of Pax-genes in developing and adult brain as suggested by expression patterns. *The Journal of Neuroscience*, *14*(3), 1395–1412. https://doi.org/10.1523/JNEUROSCI.14-03-01395.1994

Sugimura, R., He, X. C., Venkatraman, A., Arai, F., Box, A., Semerad, C., Haug, J. S., Peng, L., Zhong, X., Suda, T., & Li, L. (2012). Noncanonical Wnt Signaling Maintains Hematopoietic Stem Cells in the Niche. *Cell*, *150*(2), 351–365. https://doi.org/10.1016/j.cell.2012.05.041

Sugiyama, T., Kohara, H., Noda, M., & Nagasawa, T. (2006). Maintenance of the Hematopoietic Stem Cell Pool by CXCL12-CXCR4 Chemokine Signaling in Bone Marrow

Stromal Cell Niches. *Immunity*, *25*(6), 977–988. https://doi.org/10.1016/j.immuni.2006.10.016

Taub, J. W., Konrad, M. A., Ge, Y., Naber, J. M., Scott, J. S., Matherly, L. H., & Ravindranath, Y. (2002). High frequency of leukemic clones in newborn screening blood samples of children with B-precursor acute lymphoblastic leukemia. *Blood*, *99*(8), 2992–2996. https://doi.org/10.1182/blood.V99.8.2992

Theunissen, P. M. J., de Bie, M., van Zessen, D., de Haas, V., Stubbs, A. P., & van der Velden, V. H. J. (2019). Next-generation antigen receptor sequencing of paired diagnosis and relapse samples of B-cell acute lymphoblastic leukemia: Clonal evolution and implications for minimal residual disease target selection. *Leukemia Research*, *76*, 98–104. https://doi.org/10.1016/j.leukres.2018.10.009

Thompson, J. A., Lovicu, F. J., & Ziman, M. (2007). Pax7 and superior collicular polarity: insights from Pax6 (Sey) mutant mice. *Experimental Brain Research*, *178*(3), 316–325. https://doi.org/10.1007/s00221-006-0735-9

Thompson, J. A., Zembrzycki, A., Mansouri, A., & Ziman, M. (2008). Pax7 is requisite for maintenance of a subpopulation of superior collicular neurons and shows a diverging expression pattern to Pax3 during superior collicular development. *BMC Developmental Biology*, *8*(1), 62. https://doi.org/10.1186/1471-213X-8-62

Thompson, J., Lovicu, F., & Ziman, M. (2004). The role of Pax7 in determining the cytoarchitecture of the superior colliculus. *Development, Growth and Differentiation*, *46*(3), 213–218. https://doi.org/10.1111/j.1440-169x.2004.00744.x

TILL, J. E., & McCULLOCH, E. A. (1961). A direct measurement of the radiation sensitivity of normal mouse bone marrow cells. *Radiation Research*, *14*, 213–222.

Tokoyoda, K., Egawa, T., Sugiyama, T., Choi, B.-I., & Nagasawa, T. (2004). Cellular Niches Controlling B Lymphocyte Behavior within Bone Marrow during Development. *Immunity*, *20*(6), 707–718. https://doi.org/10.1016/j.immuni.2004.05.001

Ton, C. C. T., Hirvonen, H., Miwa, H., Weil, M. M., Monaghan, P., Jordan, T., van Heyningen, V., Hastie, N. D., Meijers-Heijboer, H., Drechsler, M., Royer-Pokora, B., Collins, F., Swaroop, A., Strong, L. C., & Saunders, G. F. (1991). Positional cloning and characterization of a paired box- and homeobox-containing gene from the aniridia region. *Cell*, *67*(6), 1059–1074. https://doi.org/10.1016/0092-8674(91)90284-6

Treiber, T., Mandel, E. M., Pott, S., Györy, I., Firner, S., Liu, E. T., & Grosschedl, R. (2010). Early B Cell Factor 1 Regulates B Cell Gene Networks by Activation, Repression, and Transcription- Independent Poising of Chromatin. *Immunity*, *32*(5), 714–725. https://doi.org/10.1016/j.immuni.2010.04.013

Treisman, J., Harris, E., & Desplan, C. (1991). The paired box encodes a second DNA-binding domain in the paired homeo domain protein. *Genes & Development*, *5*(4), 594–604. https://doi.org/10.1101/gad.5.4.594

Tremblay, C. S., Saw, J., Chiu, S. K., Wong, N. C., Tsyganov, K., Ghotb, S., Graham, A. N., Yan, F., Guirguis, A. A., Sonderegger, S. E., Lee, N., Kalitsis, P., Reynolds, J., Ting, S. B., Powell, D. R., Jane, S. M., & Curtis, D. J. (2018). Restricted cell cycle is essential for clonal evolution and therapeutic resistance of pre-leukemic stem cells. *Nature Communications*, *9*(1), 3535. https://doi.org/10.1038/s41467-018-06021-7

Tsitsikov, E., Harris, M. H., Silverman, L. B., Sallan, S. E., & Weinberg, O. K. (2018). Role of CD81 and CD58 in minimal residual disease detection in pediatric B lymphoblastic leukemia. *International Journal of Laboratory Hematology*, *40*(3), 343–351. https://doi.org/10.1111/ijlh.12795

Tsukamoto, K., Nakamura, Y., & Niikawa, N. (1994). Isolation of two isoforms of the PAX3 gene transcripts and their tissue-specific alternative expression in human adult tissues. *Human Genetics*, *93*(3), 270–274. https://doi.org/10.1007/BF00212021

Tzelepis, K., Koike-Yusa, H., De Braekeleer, E., Li, Y., Metzakopian, E., Dovey, O. M., Mupo, A., Grinkevich, V., Li, M., Mazan, M., Gozdecka, M., Ohnishi, S., Cooper, J., Patel, M., McKerrell, T., Chen, B., Domingues, A. F., Gallipoli, P., Teichmann, S., … Yusa, K. (2016). A CRISPR Dropout Screen Identifies Genetic Vulnerabilities and Therapeutic Targets in Acute Myeloid Leukemia. *Cell Rep*, *17*(4), 1193–1205. https://doi.org/10.1016/j.celrep.2016.09.079

Ungerbäck, J., Åhsberg, J., Strid, T., Somasundaram, R., & Sigvardsson, M. (2015). Combined heterozygous loss of *Ebf1* and *Pax5* allows for T-lineage conversion of B cell progenitors. *Journal of Experimental Medicine*, *212*(7), 1109–1123. https://doi.org/10.1084/jem.20132100

Urbánek, P., Wang, Z. Q., Fetka, I., Wagner, E. F., & Busslinger, M. (1994). Complete block of early B cell differentiation and altered patterning of the posterior midbrain in mice lacking Pax5/BSAP. *Cell*, *79*(5), 901–912. https://doi.org/10.1016/0092-8674(94)90079-5

Urbanek, P., Wang, Z. Q., Fetka, I., Wagner, E. F., & Busslinger, M. (1994). Complete block of early B cell differentiation and altered patterning of the posterior midbrain in mice lacking Pax5/BSAP. *Cell*, *79*(5), 901–912. https://www.ncbi.nlm.nih.gov/pubmed/8001127

Urnov, F. D., Rebar, E. J., Holmes, M. C., Zhang, H. S., & Gregory, P. D. (2010). Genome editing with engineered zinc finger nucleases. *Nature Reviews. Genetics*, *11*(9), 636–646. https://doi.org/10.1038/nrg2842

Vallespinós, M., Fernández, D., Rodríguez, L., Alvaro-Blanco, J., Baena, E., Ortiz, M., Dukovska, D., Martínez, D., Rojas, A., Campanero, M. R., & Moreno de Alborán, I. (2011). B Lymphocyte Commitment Program Is Driven by the Proto-Oncogene *c-myc*. *The Journal of Immunology*, *186*(12), 6726–6736. https://doi.org/10.4049/jimmunol.1002753

van der Weyden, L., Giotopoulos, G., Wong, K., Rust, A. G., Robles-Espinoza, C. D., Osaki, H., Huntly, B. J., & Adams, D. J. (2015a). Somatic drivers of B-ALL in a model of ETV6-RUNX1; Pax5(+/-) leukemia. *BMC Cancer*, *15*, 585. https://doi.org/10.1186/s12885-015-1586-1

van der Weyden, L., Giotopoulos, G., Wong, K., Rust, A. G., Robles-Espinoza, C. D., Osaki, H., Huntly, B. J., & Adams, D. J. (2015b). Somatic drivers of B-ALL in a model of ETV6-RUNX1; Pax5 +/− leukemia. *BMC Cancer*, *15*(1), 585. https://doi.org/10.1186/s12885-015-1586-1

Vettermann, C., Herrmann, K., & Jäck, H.-M. (2006). Powered by pairing: The surrogate light chain amplifies immunoglobulin heavy chain signaling and pre-selects the antibody repertoire. *Seminars in Immunology*, *18*(1), 44–55. https://doi.org/10.1016/j.smim.2006.01.001

Vicente-Dueñas, C., Janssen, S., Oldenburg, M., Auer, F., González-Herrero, I., Casado-García, A., Isidro-Hernández, M., Raboso-Gallego, J., Westhoff, P., Pandyra, A. A., Hein, D., Gössling, K. L., Alonso-López, D., De Las Rivas, J., Bhatia, S., García-Criado, F. J., García-Cenador, M. B., Weber, A. P. M., Köhrer, K., … Borkhardt, A. (2020). An intact gut microbiome protects genetically predisposed mice against leukemia. *Blood*, *136*(18), 2003–2017. https://doi.org/10.1182/blood.2019004381

Vicente-Duenas, C., Janssen, S., Oldenburg, M., Auer, F., Gonzalez-Herrero, I., Casado-Garcia, A., Isidro-Hernandez, M., Raboso-Gallego, J., Westhoff, P., Pandyra, A. A., Hein, D., Gossling, K. L., Alonso-Lopez, D., De Las Rivas, J., Bhatia, S., Garcia-Criado, F. J., Garcia-

Cenador, M. B., Weber, A. P. M., Kohrer, K., … Borkhardt, A. (2020). An intact gut microbiome protects genetically predisposed mice against leukemia. *Blood*, *136*(18), 2003–2017. https://doi.org/10.1182/blood.2019004381

von Freeden-Jeffry, U., Vieira, P., Lucian, L. A., McNeil, T., Burdach, S. E., & Murray, R. (1995). Lymphopenia in interleukin (IL)-7 gene-deleted mice identifies IL-7 as a nonredundant cytokine. *Journal of Experimental Medicine*, *181*(4), 1519–1526. https://doi.org/10.1084/jem.181.4.1519

Vyas, P. (2014). Targeting HIF function: the debate continues. *Blood*, *124*(24), 3510–3511. https://doi.org/10.1182/blood-2014-10-605055

Waanders, E., Gu, Z., Dobson, S. M., Antić, Ž., Crawford, J. C., Ma, X., Edmonson, M. N., Payne-Turner, D., van de Vorst, M., Jongmans, M. C. J., McGuire, I., Zhou, X., Wang, J., Shi, L., Pounds, S., Pei, D., Cheng, C., Song, G., Fan, Y., … Mullighan, C. G. (2020). Mutational Landscape and Patterns of Clonal Evolution in Relapsed Pediatric Acute Lymphoblastic Leukemia. *Blood Cancer Discovery*, *1*(1), 96–111. https://doi.org/10.1158/0008-5472.BCD-19-0041

Wallin, J., Mizutani, Y., Imai, K., Miyashita, N., Moriwaki, K., Taniguchi, M., Koseki, H., & Balling, R. (1993). A new Pax gene, Pax-9, maps to mouse Chromosome 12. *Mammalian Genome*, *4*(7), 354–358. https://doi.org/10.1007/BF00360584

Walther, C., Guenet, J.-L., Simon, D., Deutsch, U., Jostes, B., Goulding, M. D., Plachov, D., Balling, R., & Gruss, P. (1991). Pax: A murine multigene family of paired box-containing genes. *Genomics*, *11*(2), 424–434. https://doi.org/10.1016/0888-7543(91)90151-4

Wang, H., La Russa, M., & Qi, L. S. (2016). CRISPR/Cas9 in Genome Editing and Beyond. *Annual Review of Biochemistry*, *85*(1), 227–264. https://doi.org/10.1146/annurev-biochem-060815-014607

Wiemels, J., Cazzaniga, G., Daniotti, M., Eden, O., Addison, G., Masera, G., Saha, V., Biondi, A., & Greaves, M. (1999). Prenatal origin of acute lymphoblastic leukaemia in children. *The Lancet*, *354*(9189), 1499–1503. https://doi.org/10.1016/S0140-6736(99)09403-9

Wilcox, E. R., Rivolta, M. N., Ploplis, B., Potterf, S. B., & Fex, J. (1992). The PAX3 gene is mapped to human chromosome 2 together with a highly informative CA dinucleotide repeat. *Human Molecular Genetics*, *1*(3), 215–215. https://doi.org/10.1093/hmg/1.3.215-a

Wilson, N. K., Foster, S. D., Wang, X., Knezevic, K., Schütte, J., Kaimakis, P., Chilarska, P. M., Kinston, S., Ouwehand, W. H., Dzierzak, E., Pimanda, J. E., de Bruijn, M. F. T. R., & Göttgens, B. (2010). Combinatorial Transcriptional Control In Blood Stem/Progenitor Cells: Genome-wide Analysis of Ten Major Transcriptional Regulators. *Cell Stem Cell*, *7*(4), 532–544. https://doi.org/10.1016/j.stem.2010.07.016

Wojiski, S., Guibal, F. C., Kindler, T., Lee, B. H., Jesneck, J. L., Fabian, A., Tenen, D. G., & Gilliland, D. G. (2009). PML–RARα initiates leukemia by conferring properties of self-renewal to committed promyelocytic progenitors. *Leukemia*, *23*(8), 1462–1471. https://doi.org/10.1038/leu.2009.63

Wossning, T., Herzog, S., Köhler, F., Meixlsperger, S., Kulathu, Y., Mittler, G., Abe, A., Fuchs, U., Borkhardt, A., & Jumaa, H. (2006). Deregulated Syk inhibits differentiation and induces growth factor–independent proliferation of pre–B cells. *Journal of Experimental Medicine*, *203*(13), 2829–2840. https://doi.org/10.1084/jem.20060967

Xu, H. E., Rould, M. A., Xu, W., Epstein, J. A., Maas, R. L., & Pabo, C. O. (1999). Crystal structure of the human Pax6 paired domain-DNA complex reveals specific roles for the

linker region and carboxy-terminal subdomain in DNA binding. *Genes & Development*, *13*(10), 1263–1275. https://doi.org/10.1101/gad.13.10.1263

Xu, W., Rould, M. A., Jun, S., Desplan, C., & Pabo, C. O. (1995). Crystal structure of a paired domain-DNA complex at 2.5 å resolution reveals structural basis for pax developmental mutations. *Cell*, *80*(4), 639–650. https://doi.org/10.1016/0092-8674(95)90518-9

Yang, J. J., Bhojwani, D., Yang, W., Cai, X., Stocco, G., Crews, K., Wang, J., Morrison, D., Devidas, M., Hunger, S. P., Willman, C. L., Raetz, E. A., Pui, C., Evans, W. E., Relling, M. V., & Carroll, W. L. (2008). Genome-wide copy number profiling reveals molecular evolution from diagnosis to relapse in childhood acute lymphoblastic leukemia. *Blood*, *112*(10), 4178–4183. https://doi.org/10.1182/blood-2008-06-165027

Yasuda, T., Sanjo, H., Pagès, G., Kawano, Y., Karasuyama, H., Pouysségur, J., Ogata, M., & Kurosaki, T. (2008). Erk Kinases Link Pre-B Cell Receptor Signaling to Transcriptional Events Required for Early B Cell Expansion. *Immunity*, *28*(4), 499–508. https://doi.org/10.1016/j.immuni.2008.02.015

Yoshida, T., Yao-Ming Ng, S., Zuniga-Pflucker, J. C., & Georgopoulos, K. (2006). Early hematopoietic lineage restrictions directed by Ikaros. *Nature Immunology*, *7*(4), 382–391. https://doi.org/10.1038/ni1314

Zenatti, P. P., Ribeiro, D., Li, W., Zuurbier, L., Silva, M. C., Paganin, M., Tritapoe, J., Hixon, J. A., Silveira, A. B., Cardoso, B. A., Sarmento, L. M., Correia, N., Toribio, M. L., Kobarg, J., Horstmann, M., Pieters, R., Brandalise, S. R., Ferrando, A. A., Meijerink, J. P., … Barata, J. T. (2011). Oncogenic IL7R gain-of-function mutations in childhood T-cell acute lymphoblastic leukemia. *Nature Genetics*, *43*(10), 932–939. https://doi.org/10.1038/ng.924

Zhou, B., Chu, X., Tian, H., Liu, T., Liu, H., Gao, W., Chen, S., Hu, S., Wu, D., & Xu, Y. (2021). The clinical outcomes and genomic landscapes of acute lymphoblastic leukemia patients with <scp>E2A-PBX1</scp> : A 10-year retrospective study. *American Journal of Hematology*, *96*(11), 1461–1471. https://doi.org/10.1002/ajh.26324

Zou, Y.-R., Kottmann, A. H., Kuroda, M., Taniuchi, I., & Littman, D. R. (1998). Function of the chemokine receptor CXCR4 in haematopoiesis and in cerebellar development. *Nature*, *393*(6685), 595–599. https://doi.org/10.1038/31269

Partie III : Conclusions et Discussions

1. *Perte de fonction partielle de Pax5 induit par la mutation PAX5^{P80R}*

Pour mon travail de thèse, j'ai tiré profit de la disponibilité au laboratoire de cellules lymphoïdes provenant de foie fœtal d'embryon *Pax5*$^{-/-}$. Tout d'abord, mon travail a consisté à établir précisément à quel stade de la différenciation les cellules lymphoïdes de foie fœtal *Pax5*$^{-/-}$ étaient bloquées. Grâce à l'utilisation d'un marquage multiparamétrique par FACS permettant de discriminer tous les stades de différenciation B et d'une méthode de clustering non supervisé par UMAP, j'ai pu préciser que ces cellules étaient bloquées aux stades CLP/pré-pro-B juste avant l'engagement définitif dans la différenciation B (**Figure 1**). Ceci faisant de ce modèle un outil relevant pour étudier l'impact de la mutation PAX5^{P80R} sur l'engagement et la différenciation des cellules dans le lignage B. Mes travaux ont démontré que la mutation PAX5^{P80R} permet une progression phénotypique du stade CLP au stade pré-pro-B, mais les cellules restent bloquées juste avant l'engagement définitif, suggérant que la mutation PAX5^{P80R} n'est pas capable de restaurer de façon efficace la différenciation B contrairement à PAX5 WT, qui permet aux cellules de progresser jusqu'au stade pré-BII (**Figure 2C**). Ce blocage de différenciation B a pu être confirmé au niveau moléculaire. En effet, nous avons pu montrer par RT-PCRq que la mutation PAX5^{P80R} ne permettait pas efficacement d'induire l'expression de gènes cibles directs de Pax5 tels que *Cd19* et *Cd79a* impliqués dans la différenciation B (**Figure 4B**).

Du fait de ses observations, j'ai cherché à savoir si la perte de fonction induite par la mutation PAX5^{P80R} était partielle ou totale. Pour cela, j'ai réalisé un test de différenciation T *in vitro* dans le but de déterminer si le mutant était encore capable d'induire la différenciation des cellules vers un autre lignage hématopoïétique que le lignage B. En effet, Pax5 est décrit dans la littérature comme étant un gardien de l'identité B en activant l'expression de gènes impliqués dans la différenciation B d'une part, et en réprimant l'expression de gènes impliqués dans les autres lignages hématopoïétiques d'autre part (Cobaleda, Schebesta, et al., 2007; Delogu et al., 2006). Il a également été démontré que les progéniteurs B *Pax5*$^{-/-}$ ont la capacité de générer l'ensemble des différents lignages hématopoïétiques *in vitro* sous l'action de cytokines appropriées (Nutt et al., 1999a) ou *in vivo* après transplantation (A. G. Rolink et al., 1999a; Schaniel et al., 2002a). Nous avons donc utilisé des cellules stromales MS5 exprimant DL4 à leur surface, qui correspond au ligand de NOTCH le plus physiologique et le plus exprimé dans le thymus. L'interaction entre ces deux protéines est absolument indispensable pour permettre aux cellules de se différencier en cellules lymphoïdes T. Grâce à la visualisation de l'expression

par FACS du CD90/Thy1, j'ai pu montrer que le mutant PAX5 P80R gardait la capacité de réprimer le lignage lymphoïde T tout comme PAX5 WT (**Figure 2E-F**). Cette observation doit être confirmée au niveau moléculaire par RT-qPCR où nous quantifierons l'expression de gènes cibles de Pax5 tels que *Notch* et *Lck*. Ainsi, nous montrerons que la mutation PAX5 P80R permettait d'inhiber de façon efficace l'expression de gènes cibles de Pax5 impliqués dans la différenciation T.

Dans l'ensemble, ces résultats suggèrent que la mutation PAX5^{P80R} induit une perte de fonction partielle en ne restaurant pas la différenciation B mais en gardant la capacité de réprimer le lignage lymphoïde T. Cette perte de fonction partielle pourrait s'expliquer par le fait que la substitution en position 80 de la Proline en Arginine ajoute une charge positive et induit un changement de conformation de la protéine, et est prédite pour altérer soit la fixation sur l'ADN ou soit l'activité transcriptionnelle de PAX5 (Passet, Boissel, Sigaux, Saillard, Bargetzi, Ba, Thomas, Graux, Chalandon, Leguay, Lengliné, et al., 2019). De plus, les équipes de Mullighan en 2007 (Mullighan et al., 2007) et de Martin-Lorenzo (Martín-Lorenzo et al., 2018) en 2018 ont démontré par un test luciférase que la mutation PAX5^{P80R} avait pour conséquence une perte d'activité pour activer l'expression du CD19. Ces résultats, ainsi que la diminution d'expression du Cd19 et du Cd79a observée par RT-qPCR, démontrent que la mutation PAX5^{P80R} altère la fonction de fixation et/ou d'activation de la transcription de PAX5.

De façon intéressante et totalement inattendue, une petite proportion de cellules CD19+ est générée après transduction avec le virus permettant l'expression du mutant PAX5^{P80R}, mais qui finit par disparaitre totalement. Ce phénomène pourrait` s'expliquer par le fait que le mutant commence dans un premier temps par induire le même programme transcriptionnel que PAX5 Wt, poussant ainsi les cellules lymphoïdes non engagées dans la différenciation B précoce (stade pro-B avec l'acquisition du CD19). Cependant, le changement de conformation induit par la substitution de la proline en arginine en position 80 dans le domaine de liaison à l'ADN pourrait impacter la stabilité de la fixation de PAX5^{P80R} sur ses gènes cibles, altérant ainsi le programme transcriptionnel nécessaire pour progresser dans la différenciation B plus tardive. Cette observation corrèle avec ce que nous observons au niveau moléculaire où la mutation PAX5^{P80R} n'est pas capable d'activer de façon efficace l'expression du CD19 et du CD79a.

Cependant, le faible niveau d'expression que nous observons correspond très probablement à la petite proportion de cellules CD19+. Afin de confirmer cette hypothèse, il faudrait trier les différentes populations qui sont générées par le mutant PAX5^{P80R} et démontrer

que seules les cellules qui expriment à leur surface le marqueur CD19 expriment les gènes cibles de Pax5 impliqués dans la différenciation B. En parallèle, dans le but d'expliquer la disparition en culture *in vitro* des cellules CD19+ générées par le mutant $PAX5^{P80R}$, il serait judicieux de mettre en culture ces cellules afin de confirmer qu'elles ne sont pas capables de survivre et finissent par mourir.

En 2007, la comparaison des gènes différentiellement exprimés entre des progéniteurs B $Pax5^{-/-}$ et des cellules B sauvages a permis d'identifier 170 gènes activés et plus de 100 gènes réprimés (A. Schebesta et al., 2007). Afin de comprendre au niveau transcriptionnel le blocage de différenciation induit par la mutation $PAX5^{P80R}$ que l'on observe, nous planifions d'effectuer un RNA-seq afin de comparer les profils d'expression génique des cellules MIG-GFP, PAX5 WT et PAX5 P80R. Ceci permettra de déterminer si l'ensemble des gènes activés par PAX5 le sont également par le mutant, et à l'inverse si l'ensemble des gènes réprimés par PAX5 le sont également par le mutant. De plus, la comparaison entre le mutant et le contrôle nous permettra d'identifier des signatures d'expression génique communes et différentes. Dans l'ensemble, le RNA-seq permettra de confirmer la perte de fonction induite par le mutant d'une part, mais également d'identifier des signatures géniques spécifiques de PAX5 P80R et d'identifier de nouveaux gènes impliqués dans le développement de la LAL-B. Afin de réaliser ce RNA-seq, j'ai pendant ma thèse réalisée les extractions des ARN des cellules MIG-GFP, PAX5 WT et PAX5 P80R mais la qualité n'était pas suffisamment bonne. Une nouvelle expérience est en cours.

Afin de déterminer si la fonction de fixation à l'ADN est impactée par la mutation $PAX5^{P80R}$, nous pourrions également réaliser une expérience de ChiP-seq qui permettrait de savoir si le mutant induit une fermeture de la chromatine au niveau des gènes cibles de PAX5 impliqués dans la différenciation B, ce qui l'empêcherait de se fixer à l'ADN et d'activer leur transcription. Étant donné que le mutant garde la capacité de réprimer l'entrée dans la différenciation lymphoïde T, nous pourrions également valider ce résultat au niveau moléculaire en démontrant par cette approche que la chromatine reste ouverte au niveau des gènes cibles de PAX5 impliqués dans la différenciation T, permettant ainsi au mutant d'inhiber l'expression de ces gènes cibles.

Pax5 est connu pour interagir avec différents partenaires pour former des complexes protéiques qui vont soit permettre d'activer la transcription de ces gènes cibles en formant par

exemple un complexe avec CBP qui va induire l'acétylation des histones et rendre la chromatine active, soit à l'inverse réprimer la transcription de ces gènes cibles en formant un complexe avec NCoR1 qui va induire la désacétylation des histones et rendre la chromatine inactive (Medvedovic et al., 2011a). Afin de déterminer si la diminution d'expression des gènes cibles de Pax5 impliqués dans la différenciation B pourrait être due à une altération dans le recrutement des partenaires de Pax5, nous pourrions réaliser une expérience de co-immunoprécipitation afin de confirmer si les différents partenaires sont toujours recrutés. Afin d'identifier si le mutant induit le recrutement d'autres partenaires que ceux qui sont connus, nous pourrions également utiliser une approche plus large et plus complète en spectrométrie de masse, puis valider les nouveaux partenaires identifiés par co-immunoprécipitations.

Sur le plan fonctionnel, afin de confirmer que le mutant est encore capable de réprimer les différents lignages hématopoïétiques autres que le lignage lymphoïde T, nous pourrions réaliser *in vitro* d'autres tests de différenciation, et notamment des tests de différenciation vers le lignage myéloïde. Nous pourrions également explorer les compartiments T, B, NK, Myéloïde et Erythroïde dans des temps cours après transplantation des cellules MIG-GFP, PAX5 WT et PAX5 P80R. En réalisant cela, nous déterminerons si le mutant PAX5 P80R tout comme PAX5 WT est encore capable de réprimer l'ensemble des lignages hématopoïétiques. Dans l'ensemble, ces différentes approches permettront de démontrer que la perte de fonction induite par la mutation $PAX5^{P80R}$ est partielle, et n'impacte que le versant B.

2. *Développement de la LAL-B induit par la mutation $PAX5^{P80R}$*

Pour déterminer si le blocage de différenciation B observé par la mutation $PAX5^{P80R}$ est associé à une transformation leucémique, nous avons transplanté les cellules dans des souris receveuses préalablement conditionnées au Busulfan (**Figure 3A**). Grâce au marqueur CD45.2 et à la GFP, il nous est possible de discriminer les cellules transplantées qui ont greffées des cellules qui proviennent de la souris receveuse, qui expriment le marqueur CD45.1. Ainsi, nous avons démontré que les cellules non modifiées $Pax5^{-/-}$ sont capables de greffer à long terme, confirmant les données de la littérature (A. G. Rolink et al., 1999a). Contrairement à PAX5 WT qui abroge cette capacité de prise de greffe, le mutant PAX5 P80R induit un potentiel aberrant de prise de greffe aux cellules transplantées. Le phénotype des cellules greffées reste identique à celui des cellules avant transplantation, c'est-à-dire bloquées au stade CLP/pré-pro-B (**Figure 3B**). Lors du sacrifice des souris, nous avons réalisé un immunophénotypage des cellules issues du thymus et de la rate, et nous avons montré que les cellules qui expriment le mutant sont

capables d'envahir d'autres organes lymphoïdes. Cette capacité d'envahissement est révélatrice du développement d'une leucémie, qui se caractérise par la présence de blastes dans la moelle osseuse, le thymus et la rate (induisant une splénomégalie) (**Figure 3C**).

Au niveau moléculaire, nous avons confirmé la clonalité des leucémies en étudiant les réarrangement V(D)J des chaines lourdes des immunoglobulines (**Figure 4C**). En effet, les réarrangements DJ s'effectuent pendant les stades pré-pro-B et pro-B tandis que les réarrangement V(D)J se réalisent au cours du stade pré-BI. Nous avons montré que les cellules présentaient un profil polyclonal pendant la co-culture, que ce soit avec PAX5 WT ou PAX5 P80R. C'est uniquement une fois que les souris sont malades que les réarrangements deviennent clonaux, indiquant que la transformation clonale a eu lieu *in vivo*. A l'aide d'un NGS ciblé sur des mutations que l'on retrouve fréquemment chez les patients, nous avons montré que la transformation leucémique induite par la mutation $PAX5^{P80R}$ dans la souris est associée à l'acquisition de mutations coopératrices affectant la voie JAK/STAT et RAS/MAPK, deux voies de signalisation impliquées dans la prolifération cellulaire (**Figure 4D**). De façon intéressante, ces mutations sont également fréquemment retrouvées dans les LAL-B humaines (Brady et al., 2022; Mullighan, 2019; Passet, Boissel, Sigaux, Saillard, Bargetzi, Ba, Thomas, Graux, Chalandon, Leguay, Lengliné, et al., 2019).

Ces résultats indiquent que notre approche mime le processus multi-étapes de la leucémogenèse humaine. En effet, les leucémies aiguës se caractérisent par l'acquisition d'un premier évènement oncogénique ayant pour conséquence un blocage de différenciation, puis par l'acquisition d'évènements additionnels ayant pour conséquence la prolifération anarchique des cellules. Notre modèle mime ce processus avec comme premier évènement oncogénique la mutation $PAX5^{P80R}$ qui induit un blocage au stade CLP/pré-pro-B, et l'acquisition d'évènements oncogéniques secondaires affectant les voies de signalisation JAK/STAT et RAS/MAPK qui promeut la prolifération incontrôlée des blastes leucémiques dans la souris.

La capacité de prise de greffe et d'auto-renouvellement des cellules exprimant PAX5 P80R comparée aux cellules exprimant PAX5 Wt pourrait s'expliquer par leur localisation aberrante dans la moelle osseuse. En effet, c'est dans la niche périsinusoïdale que l'on trouve les cellules B en devenir à partir du stade CLP puisqu'elles sont dépendantes de l'IL-7. Les cellules CLP et pré-pro-B (qui n'expriment pas encore PAX5) sont retrouvées en contact étroit avec les cellules stromales périsinusoïdales exprimant l'IL-7, tandis que les cellules exprimant

PAX5 se différencient et finissent par ne plus avoir de contact avec les cellules stromales périsinusoïdales exprimant l'IL-7, car l'absence d'IL-7 leur permettent de progresser dans la différenciation B. Grâce à la GFP exprimée par les cellules à la suite de la transduction rétrovirale, des coupes d'os pourraient être réalisées dans le but de déterminer où se localisent les cellules exprimant PAX5 P80R. Ainsi, il serait possible de démontrer que les cellules exprimant la forme mutante de PAX5 ne sont pas capables d'interrompre les interactions avec les cellules stromales périsinusoïdales exprimant l'IL-7, ce qui leur permettrait d'acquérir une capacité de prise de greffe et d'auto-renouvellement.

Nous avons trouvé que les mutations dans les voies de signalisation JAK/STAT et RAS/MAPK coopèrent de façon récurrente avec la mutation $PAX5^{P80R}$ pour induire le développement de la LAL-B. Cependant, aucune mutation dans ces voies de signalisation n'a été trouvée dans certaines souris. Afin d'identifier les mutations additionnelles qui ont permis le développement de la LAL-B dans les souris en question, il faudrait réaliser un exome (*Whole Exome Sequencing* WES) afin d'avoir une vision plus globale. Ainsi, on pourrait très bien imaginer identifier des mutations affectant le récepteur à l'IL-7, étant donné que ce sont des mutations que l'on retrouve fréquemment associées à la mutation $PAX5^{P80R}$ (Passet, Boissel, Sigaux, Saillard, Bargetzi, Ba, Thomas, Graux, Chalandon, Leguay, Lengliné, et al., 2019). Ces mutations induisent généralement une activation constitutive de la voie de l'IL-7R, induisant l'activation constitutive de la voie JAK/STAT (Zenatti et al., 2011). Ainsi, des mutations de l'IL-7R pourraient expliquer une localisation aberrante dans la moelle osseuse des cellules exprimant PAX5 P80R.

Afin de comprendre quels sont les mécanismes biologiques qui sont dérégulés dans les LAL-B PAX5 P80R, un RNA-seq sur les échantillons de LAL-B nous permettrait d'obtenir une liste de gènes dérégulés. Cette liste de gènes pourrait également être comparée avec d'autres listes de gènes venant d'autres altérations de PAX5 (comme avec le modèle murin *PAX5-ELN*^{tg}), ce qui nous permettrait de comprendre par quels mécanismes biologiques les altérations de PAX5 induisent le développement de la LAL-B. À plus large échelle, nous pourrions comparer cette liste de gènes avec celles d'autre sous-types oncogéniques, ce qui nous permettrait d'avoir une liste de gènes spécifiques à la mutation $PAX5^{P80R}$.

À la suite de la découverte de mutations récurrentes dans la voie de signalisation JAK/STAT dans notre modèle, nous nous sommes intéressés à la capacité des cellules à

phosphoryler STAT5 après stimulation avec l'IL-7. Ainsi, nous avons pu montrer que les cellules leucémiques PAX5 P80R sont toutes aussi capables d'induire la phosphorylation de STAT5 que des cellules CTL (**Figure 4E)**. De plus, les cellules leucémiques sont aussi sensibles au Tofacitinib (inhibiteur de JAK) que les cellules CTL (**Figure 4F**). Dans l'ensemble, ces résultats démontrent que la voie est aussi bien activable dans des cellules leucémiques que dans des cellules normales, suggérant que cibler la voie JAK/STAT n'est pas pertinent pour inhiber de façon spécifique la viabilité des cellules leucémiques et impacte également celles des cellules normales. Cette constatation rend encore plus légitime le fait de réaliser un RNA-seq pour comprendre le mécanisme de la leucémogenèse induite par la mutation PAX5^{P80R}, dans le but de cibler de façon spécifique les cellules leucémiques.

Bien que notre modèle mime le processus multi-étapes de la LAL-B, il n'est pas parfait, présente des inconvénients et pourrait être amélioré. En effet, notre approche de transduction rétrovirale ne nous permet pas de contrôler la dose de PAX5 P80R exprimée dans les cellules, mais nous avons pu cependant montrer par FACS que son expression est proche de celle que l'on retrouve dans des cellules B normales. La modélisation optimale serait de placer le mutant dans le locus de Pax5, qui permettrait d'avoir une expression identique à celle de PAX5 Wt. L'équipe de Mullighan a d'ailleurs généré un modèle murin dans lequel *PAX5*^{P80R} est localisé dans le locus de *Pax5* (Gu et al., 2019a). Ces souris développent efficacement une LAL-B avec la présence de cellules leucémiques ayant un phénotype ressemblant à celui de cellules pré-pro-B (B220+CD19-). Ce résultat est similaire à celui que l'on observe dans nos cellules leucémiques PAX5 P80R, permettant ainsi de valider notre approche de complémentation rétrovirale.

3. *Hif2a : un gène candidat impliqué dans la leucémogenèse*

Afin d'identifier des gènes candidats impliqués dans le développement de la LAL-B induit par les mutants de PAX5, nous avons comparé la liste de gènes qui sont activés dans les modèles murins PAX5 P80R (Gu et al., 2019a), PAX5-ELN (Jamrog, Chemin, Fregona, Coster, Pasquet, Oudinet, Rouquié, et al., 2018) et PAX5-ETV6 (Smeenk et al., 2017a). Cette approche nous a permis d'identifier seulement 10 gènes activés dans ces trois modèles (**Figure 5A, panel gauche**). Parmi eux, Hif2α se trouve être le seul facteur de transcription. De plus, en utilisant les données Immgen, nous avons pu montrer que Hif2α n'est pas exprimé dans les cellules B normales de souris (**Figure 5A, panel droit**), suggérant ainsi que l'expression que l'on retrouve dans les modèles *PE*^{tg} et *PAX5*^{P80R} est ectopique. De façon intéressante, nous avons également

montré que Hif2α est absent dans les cellules B normales humaines (**Figure S5C**), et qu'il est surexprimé dans les LAL-B humaines présentant des altérations de PAX5 (**Figure S5C**). Cette expression ectopique fait de Hif2α un gène candidat intéressant.

Afin d'étudier son rôle dans la leucémogenèse, j'ai utilisé le système CRISPR-Cas9 pour inhiber son expression dans les pré-CSL PAX5-ELN et les CSPHs normales (cellules LSK Wt). Ainsi j'ai pu montrer que l'inhibition de Hif2α dans les cellules LSK n'avait pas d'impact sur leur capacité de multipotence (**Figure 6G**), ni sur leur capacité de prise de greffe une fois transplantées dans des souris receveuses (**Figure 6H**), confirmant ainsi les données de la littérature chez la souris (Guitart et al., 2013b). En revanche, l'inhibition de Hif2α dans les pré-CSL diminue statistiquement leur prolifération (**Figure 5E**). Ces résultats convergent vers l'idée que Hif2α est dispensable pour les CSPH, mais qu'il semble critique pour l'activité des pré-CSL PAX5-ELN.

Dans l'objectif de confirmer son rôle dans un modèle de LAL-B induit par un autre mutant de PAX5, il serait intéressant par exemple d'inhiber son expression par un shRNA dans les cellules leucémiques PAX5 P80R. En effet, cela permettrait de confirmer l'importance de Hif2α dans un autre modèle de LAL-B induit par un mutant de PAX5, sur la viabilité des cellules par un test d'Annexine V, sur leur croissance par un test de prolifération et sur leur capacité de prise de greffe.

Nous pourrions tirer profit de l'absence d'expression de Hif2α, comme nous avons pu le démontrer par RT-qPCR, dans les cellules pré-leucémiques PAX5 P80R en co-culture *in vitro* pour étudier l'impact d'une surexpression dans le développement de leucémique. Il serait ainsi possible de prouver si la surexpression de Hif2α accélère la transformation des cellules pour induire l'apparition de la LAL-B.

4. *Identification de l'Acriflavine comme un candidat potentiel grâce à un criblage de composés*

Afin de cibler pharmacologiquement Hif2α, nous avons mis en place un système robuste et miniaturisé en plaque 96 puits de criblages de molécules, et nous l'avons appliqué à un criblage de 19 composés décrits comme étant potentiellement des inhibiteurs de Hifα sur des cellules leucémiques PAX5 P80R et PAX5-ELN (**Figure 7B**). Cette stratégie nous a permis

d'identifier 7 composés candidats qui ont inhibé d'au moins 30% la viabilité des cellules (**Figure 7C**). Parmis eux, nous avons identifié l'Acriflavine, qui se trouvait être le meilleur composé ayant la capacité d'inhiber l'expression de Hif2α (**Figure S7A**). Nous avons ainsi pu valider que l'inhibition de l'expression de Hif2α par l'Acriflavine s'effectue de manière dose-dépendante (**Figure 7E**).

Dans la littérature, Hif2α est présenté comme étant un acteur moléculaire se trouvant en amont de STAT5, et que l'Acriflavine est capable d'inhiber à la fois d'expression de Hif2α et la phosphorylation de STAT5, suggérant que ces deux acteurs moléculaires font partis d'une seule voie de signalisation (Hallal et al., 2020). Dans notre cas, nous avons pu montrer que l'Acriflavine n'était pas capable d'inhiber la phosphorylation de STAT5 (**Figure S7F**), contrairement au Tofacitinib (inhibiteur de JAK) qui sert de contrôle positif. A l'inverse, alors que l'Acriflavine est capable d'inhiber l'expression de Hif2α, le Tofacitinib, quant à lui, en est incapable (**Figure S7C**). Dans l'ensemble, ces résultats semblent montrer que dans notre contexte de leucémogenèse B, Hif2α et STAT5 sont des acteurs moléculaires impliqués dans des voies de signalisation indépendantes.

Pour démontrer la spécificité d'action de l'Acriflavine, il serait intéressant de traiter des cellules lymphoïdes normales, par exemple nos cellules lymphoïdes *Pax5*$^{-/-}$ non modifiées et celles transduites avec le vecteur permettant l'expression de la forme Wt de PAX5, pour démontrer qu'elles ne sont pas impactées ou moins sensibles, du fait de l'absence d'expression de Hif2α. Cette approche nous permettrait de confirmer nos résultats montrant que l'Acriflavine n'est pas capable d'inhiber la voie de signalisation JAK/STAT (qui est tout autant activable dans les cellules normales que dans les cellules leucémiques), et que Hif2α et STAT5 correspondent à des acteurs moléculaires impliqués dans des voies de signalisation indépendantes.

Pour étudier le lien entre Hif2α et le développement de la LAL-B, il serait intéressant de démontrer que le traitement des souris avec l'Acriflavine (i) induit un retard de développement de la LAL-B une fois que les cellules aient greffées en réalisant une ponction de moelle osseuse pour visualiser par FACS les cellules GFP+, et/ou (ii) prolonge la survie des souris une fois que la leucémie s'est développée.

Pour confirmer les résultats obtenus sur les LAL-B PAX5 P80R murines, nous avons mis en place une collaboration avec le Pr. Emmanuelle Clappier et le Dr Marie Passet de l'Hôpital Saint-Louis à Paris afin de récupérer des échantillons de patients présentant une LAL-B PAX5 P80R. Nous venons de transplanter ces quatre échantillons dans des souris NSG afin d'amplifier les cellules pour avoir du matériel en quantité suffisante. Nous prévoyons de confirmer sur les cellules leucémiques humaines que (i) Hif2α est exprimé dans les différents échantillons, (ii) l'Acriflavine est capable d'inhiber l'expression de Hif2a, (iii) l'Acriflavine potentialise l'effet du Tofacitinib de manière synergique, et (iv) augmente la survie des souris transplantées avec les cellules leucémies humaines PAX5 P80R.

Partie IV : Perspectives

Dans l'ensemble, l'objectif principal de ma thèse a été de générer un modèle de leucémogenèse induite par la mutation PAX5^{P80R}. Par les différents résultats que je vous ai présenté au cours de ce manuscrit, mes travaux de thèse offrent ainsi à l'équipe un nouveau système de modélisation du processus multi-étapes de la LAL-B qui mime la leucémogenèse chez les patients.

En parallèle, je me suis également intéressé à un modèle murin impliquant une autre altération de PAX5. En effet, ce modèle murin contient la protéine de fusion PAX5-ELN qui est exprimée spécifiquement dans le lignage B (Jamrog, Chemin, Fregona, Coster, Pasquet, Oudinet, Rouquié, et al., 2018). Les souris développent efficacement une LAL-B avec une médiane de survie de 170 jours. Ce développement leucémique est associé à l'acquisition de mutations secondaires affectant les voies de signalisation JAK/STAT et RAS/MAPK. Le temps de latence de 90 jours avant le développement des premières leucémies nous offre la possibilité d'explorer la phase pré-leucémique qui précède la transformation clonale induite par l'acquisition des mutations secondaires. Ce modèle récapitule donc également le processus multi-étapes des LAL-B et ouvre de nouvelles voies d'investigation pour déchiffrer et cibler les mécanismes biologiques par lesquels une protéine de fusion impliquant PAX5 convertit un progéniteur B normal en pré-CSL.

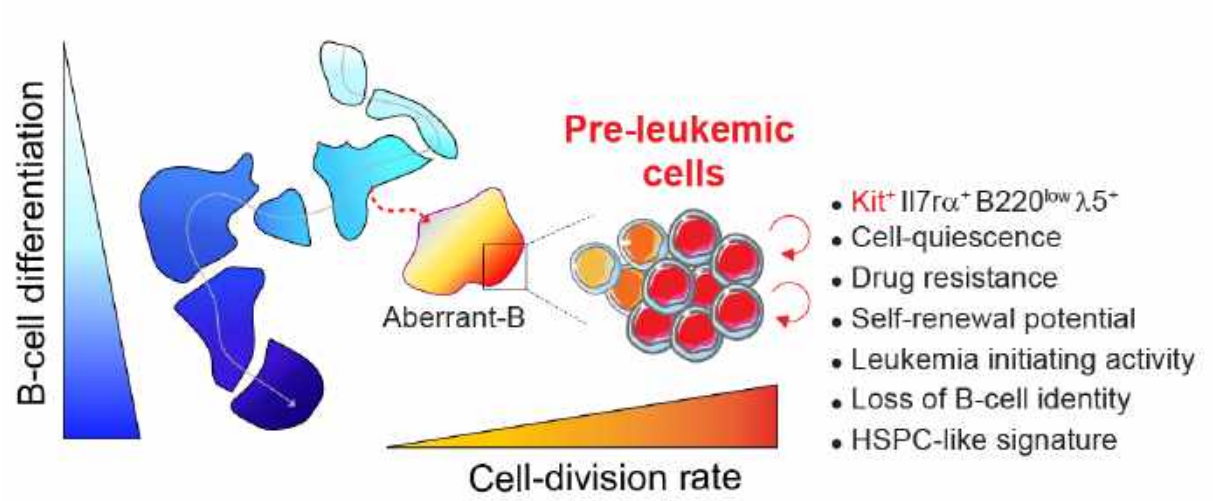

***Figure 34 :** Modèle d'initiation leucémique induite par PAX5-ELN (D'après Fregona et agure).l, in press).*

Dans ce contexte, nous nous sommes intéressés à caractériser la phase pré-leucémique, et nous avons pu montrer que PAX5-ELN induit, en plus des sous-populations B normales, l'apparition d'une population aberrante de progéniteurs B enrichie en cellules quiescentes (**Figure 34**). Phénotypiquement, le caractère aberrant de cette population s'explique notamment par l'expression concomitante et inappropriée de marqueurs de surface. De plus, la population aberrante est résistante aux agents de chimiothérapie conventionnelle. Ce travail fait actuellement l'objet d'une publication

récente dans Journal of Experimental Medicine (JEM), que je signe en deuxième auteure (Annexe I).

Le modèle murin PAX5-ELN, contrairement au modèle de transduction rétrovirale PAX5^{P80R} que je viens de mettre en place, nous offre un accès plus facile et reproductible aux cellules pré-leucémiques. Ainsi, j'ai tiré profit du système miniaturisé que j'ai mis en place pour le criblage des inhibiteurs de Hifα pour l'appliquer à un criblage chimique de plus grande échelle, de 1040 composés provenant de la Chimiothèque Nationale Essentielle, sur les cellules pré-leucémiques PAX5-ELN. J'ai donc mis en place un protocole robuste par FACS pour le criblage de ces composés sur les cellules pré-leucémiques PAX5-ELN. Notre marquage multiparamétrique unique, la population B aberrante contenant les cellules pré-leucémiques et l'ensemble des sous-populations du lignage B normal (**Figure A**).

Mon travail a donc été tout d'abord de miniaturiser en plaque 96 puits la co-culture de cellules B pré-leucémiques PAX5-ELN sur cellules stromales MS5 pendant 48h (N=48). La comparaison du nombre absolu des cellules B aberrantes avec celui des différentes sous-populations B normales s'est montré statistiquement reproductible (valeur de reproductibilité Z' > 0.5) (**Figure B**). Ceci m'offre ainsi la possibilité d'évaluer simultanément l'effet d'un composé chimique sur le nombre de cellules B aberrantes pré-leucémiques et celui des différentes sous-populations B normales.

J'ai donc appliqué cette stratégie au criblage d'une banque de 1040 composés synthétiques et naturels (chimiothèque essentielle) reflétant la diversité chimique de la collection complète de la chimiothèque nationale française (https://chembiofrance.cn.cnrs.fr/fr/composante/chimiotheque) (Mahuteau-Betzer, 2015) (**Figure C+D**). Afin de sélectionner les hits les plus pertinents, j'ai dans un premier temps calculé la valeur statistique SSMD pour tous les composés criblés. Cette valeur permet de quantifier la différence de l'effet d'un composé chimique sur l'ensemble des différentes sous-populations B normales et aberrante PAX5-ELN et la condition CTL non traitée (**Figure E**). Dans un second temps, j'ai déterminé le pourcentage d'inhibition des populations B aberrante et normales de l'ensemble des composés (**Figure F**). Le criblage de la chimiothèque montre que la majorité des composés n'affecte pas la viabilité des cellules, ce qui indique la bonne sélectivité de notre approche et une absence de toxicité générale de la librairie.

Ainsi, ces conditions expérimentales m'ont permis d'identifier 38 molécules candidates (« *hits* ») qui affectent la viabilité des cellules B aberrantes (**Figure G**), certaines affectant également l'ensemble des sous-populations B normales (Groupe A, **Figure G**). De façon intéressante, mon approche m'a permis d'identifier parmi ces hits des molécules épargnant, voire amplifiant, certaines (Groupes B et D, **Figure G**) ou toutes (Groupe C, **Figure G**) les sous-populations B normales. Dans l'ensemble, mon travail montre la faisabilité d'un criblage de petites molécules sur une population de cellules pré-leucémiques prenant en compte la complexité intrinsèque des cellules primaires du lignage B tout en considérant leur microenvironnement.

Afin d'affiner le nombre de composés candidats, j'ai réalisé différents contre-criblage (**Figure H**). Dans un premier temps, j'ai testé la capacité des 38 hits sélectionnés par le crible à inhiber la phosphorylation de STAT5 à la suite de la stimulation par l'IL7. Cette expérience a permis d'éliminer deux sur l'ensemble des composés, qui sont capables d'inhiber partiellement la phosphorylation de STAT5, comparé au Tofacitinib (inhibiteur de JAK) (**Figure I**). Dans un second temps, une dose réponse des 38 composés a été réalisée dans le but d'éliminer tous ceux qui possèdent une IC50 supérieure à 500nM (**Figures J, K**). Cette expérience a permis d'écarter 22 molécules. En parallèle, tous les « frequent hitters », c'est-à-dire les composés qui sont identifiés de façon récurrente comme des hits dans d'autres criblages de la Chimiothèque Nationale Essentielle, qui sont au nombre de 13 ont été identifiés et éliminés (**Figure J**).

Ainsi, l'ensemble de ces contre-cribles ont permis de mettre en exergue cinq composés (**Figure M**) qui : (i) ne sont pas capable d'inhiber la phosphorylation de STAT5 après stimulation à l'IL7, (ii) ont une IC50 inférieure à 500 nM et (iii) ne correspondent pas à des « frequent hitters ».

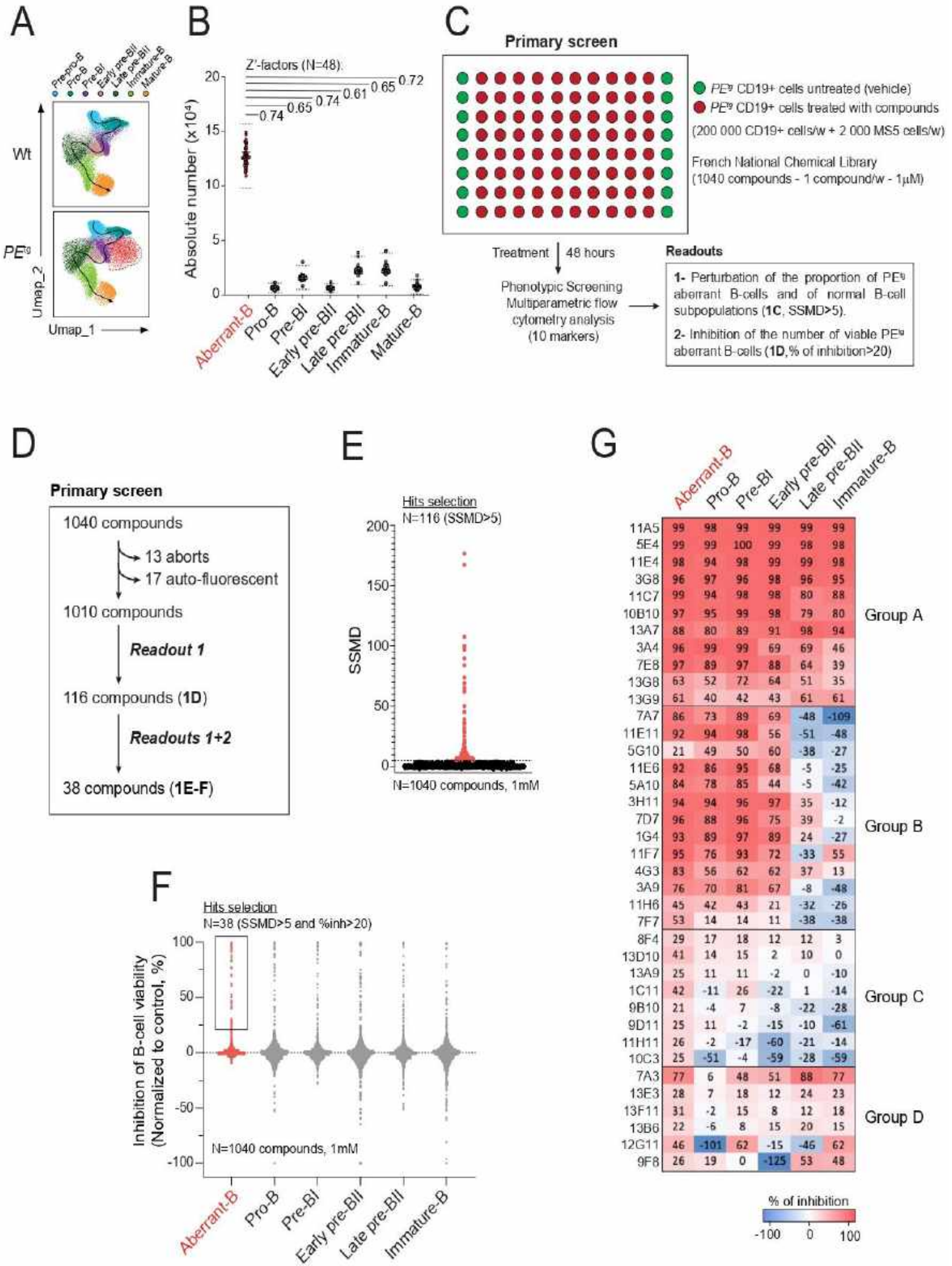
A
Pre-pro-B
Pro-B
Pre-BI
Early pre-BII
Late pre-BII
Immature-B
Mature-B
Wt
PE^tg
Umap_2
Umap_1
B
Z'-factors (N=48):
0.74
0.65
0.74
0.61
0.65
0.72
Absolute number (x10^4)
20
15
10
5
0
Aberrant-B
Pro-B
Pre-BI
Early pre-BII
Late pre-BII
Immature-B
Mature-B
C
Primary screen
PE^tg CD19+ cells untreated (vehicle)
PE^tg CD19+ cells treated with compounds
(200 000 CD19+ cells/w + 2 000 MS5 cells/w)
French National Chemical Library
(1040 compounds - 1 compound/w - 1µM)
Treatment
48 hours
Phenotypic Screening
Multiparametric flow cytometry analysis
(10 markers)
Readouts
1- Perturbation of the proportion of PE^tg aberrant B-cells and of normal B-cell subpopulations (1C, SSMD>5).
2- Inhibition of the number of viable PE^tg aberrant B-cells (1D, % of inhibition>20)
D
Primary screen
1040 compounds
13 aborts
17 auto-fluorescent
1010 compounds
Readout 1
116 compounds (1D)
Readouts 1+2
38 compounds (1E-F)
E
Hits selection
N=116 (SSMD>5)
SSMD
200
150
100
50
0
N=1040 compounds, 1mM
F
Hits selection
N=38 (SSMD>5 and %inh>20)
Inhibition of B-cell viability
(Normalized to control, %)
100
50
0
-50
-100
N=1040 compounds, 1mM
Aberrant-B
Pro-B
Pre-BI
Early pre-BII
Late pre-BII
Immature-B
G
Aberrant-B
Pro-B
Pre-BI
Early pre-BII
Late pre-BII
Immature-B
11A5 99 98 99 99 99 99
5E4 99 99 100 99 98 98
11E4 98 94 98 99 99 98
3G8 96 97 96 98 96 95
11C7 99 94 98 98 80 88
10B10 97 95 99 98 79 80
13A7 88 80 89 91 98 94
3A4 96 99 99 69 69 46
7E8 97 89 97 88 64 39
13G8 63 52 72 64 51 35
13G9 61 40 42 43 61 61
Group A
7A7 86 73 89 69 -48 -109
11E11 92 94 98 56 -51 -48
5G10 21 49 50 60 -38 -27
11E6 92 86 95 68 -5 -25
5A10 84 78 85 44 -5 -42
3H11 94 94 96 97 35 -12
7D7 96 88 96 75 39 -2
1G4 93 89 97 89 24 -27
11F7 95 76 93 72 -33 55
4G3 83 56 62 62 37 13
3A9 76 70 81 67 -8 -48
11H6 45 42 43 21 -32 -26
7F7 53 14 14 11 -38 -38
Group B
8F4 29 17 18 12 12 3
13D10 41 14 15 2 10 0
13A9 25 11 11 -2 0 -10
1C11 42 -11 26 -22 1 -14
9B10 21 -4 7 -8 -22 -28
9D11 25 11 -2 -15 -10 -61
11H11 26 -2 -17 -60 -21 -14
10C3 25 -51 -4 -59 -28 -59
Group C
7A3 77 6 48 51 88 77
13E3 28 7 18 12 24 23
13F11 31 -2 15 8 12 18
13B6 22 -6 8 15 20 15
12G11 46 -101 62 -15 -46 62
9F8 26 19 0 -125 53 48
Group D
% of inhibition
-100
0
100

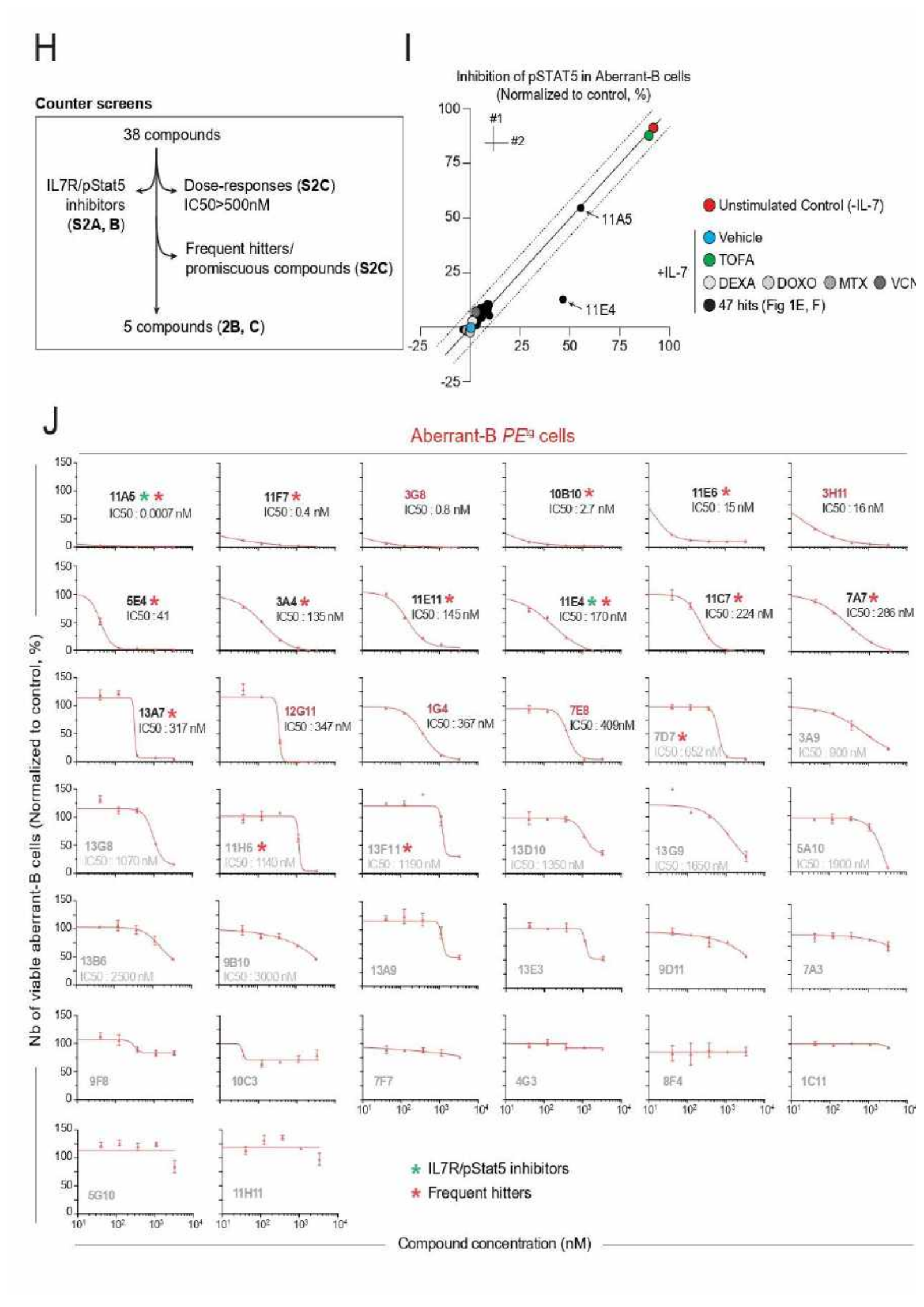
H
Counter screens
38 compounds
IL7R/pStat5 inhibitors (S2A, B)
Dose-responses (S2C) IC50>500nM
Frequent hitters/ promiscuous compounds (S2C)
5 compounds (2B, C)
I
Inhibition of pSTAT5 in Aberrant-B cells (Normalized to control, %)
#1
#2
11A5
11E4
Unstimulated Control (-IL-7)
+IL-7
Vehicle
TOFA
DEXA DOXO MTX VCN
47 hits (Fig 1E, F)
J
Aberrant-B PE^lg cells
11A5 * * IC50 : 0.0007 nM
11F7 * IC50 : 0.4 nM
3G8 IC50 : 0.8 nM
10B10 * IC50 : 2.7 nM
11E6 * IC50 : 15 nM
3H11 IC50 : 16 nM
5E4 * IC50 : 41
3A4 * IC50 : 135 nM
11E11 * IC50 : 145 nM
11E4 * * IC50 : 170 nM
11C7 * IC50 : 224 nM
7A7 * IC50 : 286 nM
13A7 * IC50 : 317 nM
12G11 IC50 : 347 nM
1G4 IC50 : 367 nM
7E8 IC50 : 409nM
7D7 * IC50 : 652 nM
3A9 IC50 : 900 nM
13G8 IC50 : 1070 nM
11H6 * IC50 : 1140 nM
13F11 * IC50 : 1190 nM
13D10 IC50 : 1350 nM
13G9 IC50 : 1650 nM
5A10 IC50 : 1900 nM
13B6 IC50 : 2500 nM
9B10 IC50 : 3000 nM
13A9
13E3
9D11
7A3
9F8
10C3
7F7
4G3
8F4
1C11
5G10
11H11
* IL7R/pStat5 inhibitors
* Frequent hitters
Nb of viable aberrant-B cells (Normalized to control, %)
Compound concentration (nM)

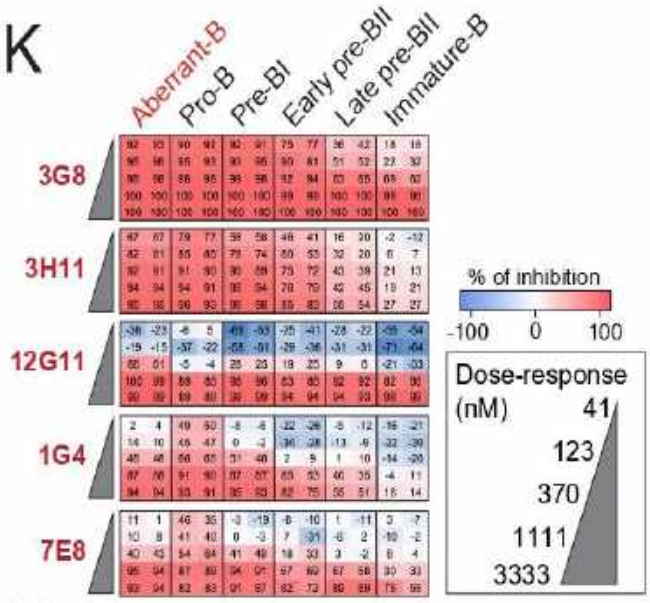

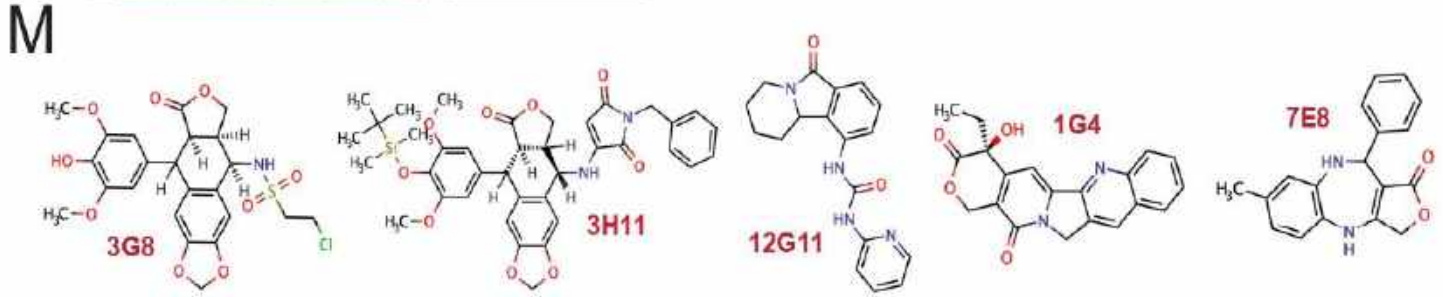

Figure 1.(A) UMAP représentant les différentes sous-populations B présentes dans des souris WT et dans des souris *PE^{tg}* âgées de 35 jours. La population entourée en rouge représente la population aberrante induite par l'expression de l'oncogène PAX5-ELN. **(B)** Les cellules B (CD19+, 2x105 cellules/puits) normales et aberrantes PAX5-ELN ont été cultivées sur la lignée stromale MS5 (2x103 cellules/puits) pendant 48h en plaques 96 puits. Le nombre absolu de cellules B aberrantes et des différentes sous-populations B normales a été évalué par FACS. Les lignes solides représentent la moyenne de chaque groupe et les lignes achurées représentent 3 fois leur déviation standard (N=48). Le facteur Z' est une valeur statistique de reproductibilité prenant en compte ces paramètres (Facteur Z' idéal entre 0.5 et 1). **(C)** Procédure expérimentale pour le criblage chimique des pré-CSLs. **(D)** Stratégie menant à l'identification de 38 composés suite au criblage des 1040 composés de la Chimiothèque Nationale Essentielle. **(E)** Identification de 116 composés ayant une valeur de SSMD>5. Le SSMD est une valeur statistique permettant de quantifier la différence de l'effet d'un composé chimique sur l'ensemble des différentes sous-populations B normales et aberrantes PAX5-ELN et la condition CTL non traité. **(F)** Le pourcentage d'inhibition des différentes populations par les 116 composés identifiées précédemment a été calculé à partir du nombre absolu de cellules vivantes suivant la formule 100 - (composé testé/moyenne des CTL non traité) X 100. La valeur 100% correspond à un composé inhibant totalement la viabilité des cellules. La valeur 0% correspond à un composé ne présentant aucun effet. Et la valeur -100% correspond à un composé expandant les cellules par un facteur 2. 47 composés (top 5% hits) inhibant d'au moins 20% la population aberrante B ont été sélectionnés. **(G)** Heat map de l'impact des 47 composés hits sur la population aberrante et sur les différentes sous-populations B normales. Les nombres indiquent le pourcentage d'inhibition tel que décrit dans le panel D. Les composés ont été classés en 4 groupes en fonction de leur effet soit sur l'ensemble des populations (Groupe A), soit sur les cellules aberrantes et sur les cellules précoces dans la différenciation B (Groupe B), soit sur les cellules aberrantes uniquement (Groupe C) ou soit sur les cellules aberrantes et sur les cellules tardives dans la différenciation B (Groupe D). **(H)** Stratégie des contre-cribles menant à l'identification de 5 composés candidats. **(I)** L'inhibition de la phosphorylation de STAT5 dans les cellules aberrantes B *PE^{tg}* par les 38 composés issus du criblage a été analysée par FACS après stimulation des cellules avec l'IL7, afin d'éliminer les composés qui sont capables d'inhiber la phosphorylation de STAT5. La valeur 100 correspond à un composé inhibant totalement la phosphorylation de STAT5. A l'inverse, la valeur 0 correspond à un composé qui n'a aucun effet. La ligne solide correspond à la moyenne et les lignes hachurées correspondent à 3 fois la déviation standard. **(J)** Dose-réponse des 38 composés sur les cellules aberrantes B *PE^{tg}* afin d'éliminer ceux qui ont une IC50 supérieure à 500 nM. Le symbole * correspond aux composés qui ont la capacité d'inhiber la phosphorylation de STAT5 représenté dans le panel B. Le symbole * correspond aux composés qui sont identifiés de façon récurrente comme des hits dans d'autres criblages de la Chimiothèque Nationale Essentielle. **(K)** Heat maps de l'impact des 5 composés candidats en dose-réponse sur la population aberrante et sur les différentes sous-populations B normales. Les nombres indiquent le pourcentage d'inhibition calculé à partir de la même formule que pour la Figure 1F. **(M)** Structure chimique des 5 composés candidats.

Pour déterminer si ces 5 candidats impactent également la viabilité cellulaire dans d'autres modèles de leucémogenèse, ceux-ci seront testés sur les cellules PAX5 P80R, permettant ainsi de démontrer que l'efficacité des composés peut être généralisable aux LAL-B induite par différents mutants de PAX5. Ils seront également testés sur des lignées cellulaires de LAL-B tel que les RAMOS (IGH-MYC), 697 (TCF3-PBX1) et REH (ETV6-RUNX1) afin de déterminer si l'efficacité des 5 composés peut être généralisable ou non à d'autres sous-types oncogéniques de LAL-B (autres que ceux impliquant des altérations de PAX5).

Afin de savoir quel est l'impact des composés sélectionnés sur le cycle cellulaire, nous avons générés 3 lignées cellulaires de LAL-B humaines qui expriment de façon constitutive le système FUCCI (« Fluorescence Upiquitin Cell Cycle Indicator »). Ce système nous permet de suivre le cycle cellulaire dans les cellules vivantes, et représente un outil d'intérêt majeur pour explorer et cibler les cellules cancéreuses quiescentes et chimio-résistantes. À l'aide de ces 3 lignées, nous pourrons détecter la présence de cellules quiescentes/résistantes aux agents de chimiothérapie couramment utilisés tels que la Dexamethasone, Doxorubicine, Methotrexate et Vincristine. Dans un second temps, nous testerons la capacité de ces composés à inverser la chimiorésistance de ces cellules, en combinaison avec les agents de chimiothérapie.

Pour évaluer l'effet des composés sélectionnés sur l'activité d'auto-renouvellement, nous pourrons réaliser des tests fonctionnels. En effet pour déterminer si les composés diminuent la fréquence des cellules pré-leucémiques PE^{tg} s'auto-renouvelant, les cellules seront traitées *in vitro* puis transplantées en réalisant un test de dilution limite. En parallèle, nous pourrons étudier *in vivo* si les composés sélectionnés ont la capacité d'inverser le blocage de différenciation induit par PAX5-ELN. Pour ce faire, nous transplanterons les cellules et traiterons les souris greffées avec les composés. Ces différents tests fonctionnels pourront également être réalisés sur les cellules PAX5 P80R afin de déterminer si les composés sont capables (i) de lever le blocage de différenciation au stade CLP/pré-pro-B et (ii) d'abroger leur capacité aberrante de prise de greffe.

Partie V : Annexes

Annexe I

JEM Journal of Experimental Medicine

ARTICLE

Stem cell–like reprogramming is required for leukemia-initiating activity in B-ALL

Vincent Fregona[1,2,3], Manon Bayet[1,2,3], Mathieu Bouttier[1,2,3], Laetitia Largeaud[1,2,3,4,5], Camille Hamelle[1,2,3], Laura A. Jamrog[1,2,3], Naïs Prade[1,2,3,4,5], Stéphanie Lagarde[1,2,3,4,5], Sylvie Hebrard[1,2,3], Isabelle Luquet[1,2,3,4,5], Véronique Mansat-De Mas[1,4,5], Marie Nolla[1,2,3,5], Marlène Pasquet[3,2,3,5], Christine Didier[1,2,3], Ahmed Amine Khamlichi[6], Cyril Broccardo[1,2,3], Éric Delabesse[1,2,3,4,5*], Stéphane J.C. Mancini[7*], and Bastien Gerby[1,2,3]

B cell acute lymphoblastic leukemia (B-ALL) is a multistep disease characterized by the hierarchical acquisition of genetic alterations. However, the question of how a primary oncogene reprograms stem cell–like properties in committed B cells and leads to a preneoplastic population remains unclear. Here, we used the *PAX5::ELN* oncogenic model to demonstrate a causal link between the differentiation blockade, the self-renewal, and the emergence of preleukemic stem cells (pre-LSCs). We show that PAX5::ELN disrupts the differentiation of preleukemic cells by enforcing the IL7r/JAK-STAT pathway. This disruption is associated with the induction of rare and quiescent pre-LSCs that sustain the leukemia-initiating activity, as assessed using the *H2B-GFP* model. Integration of transcriptomic and chromatin accessibility data reveals that those quiescent pre-LSCs lose B cell identity and reactivate an immature molecular program, reminiscent of human B-ALL chemo-resistant cells. Finally, our transcriptional regulatory network reveals the transcription factor EGR1 as a strong candidate to control quiescence/resistance of PAX5::ELN pre-LSCs as well as of blasts from human B-ALL.

Introduction

Cell quiescence and self-renewal activity are distinctive characteristics of normal stem cells that are lost throughout the differentiation process. Nevertheless, it is established that molecular reprogramming occurring in cancer cells frequently leads to tumor dedifferentiation and the acquisition of stemness features (Bradner et al., 2017). This notion has been exploited to predict the clinical outcome of patients with solid cancers and hematological malignancies (Malta et al., 2018; Ng et al., 2016; Yan et al., 2020) and supports the idea that cellular plasticity, reprogramming, and cancer resistance are tightly intertwined. Among hematological malignancies, B cell acute lymphoblastic leukemia (B-ALL) is defined as the most frequent pediatric cancer. Although current chemotherapy is efficient at reducing the tumor load by targeting proliferating and metabolically active leukemic cells, the disease relapse points to the presence of resistant cells that escape treatment (Inaba and Mullighan, 2020). Thus, the biological properties of the cell-of-origin of leukemia, including sustained self-renewal activity, cell quiescence, and drug resistance, can significantly affect leukemia treatment and should be considered in the search for new targeted therapies (Fregona et al., 2021).

The evolution and the dynamic of subclones in B-ALL cells have been fully explored in several works through the comparison of the genetic landscape of paired diagnostic and relapse samples (Dobson et al., 2020; Mullighan et al., 2008; van Delft et al., 2011; Waanders et al., 2020). These studies predicted the existence of an ancestral clone of preleukemic stem cells (pre-LSCs) harboring a restricted number of genetic alterations, such as a founding chromosomal translocation, which is not yet transformed but at the apex of the clonal hierarchy. The notion of a multistep process of B-ALL development has also been gained from studies exploring leukemia initiation and progression in monochorionic twins (Greaves, 2018; Hong et al., 2008). These approaches demonstrated that a primary chromosomal translocation by itself does not have the capacity to induce the disease but establishes a preleukemic subclonal compartment in blood cells many years before the leukemia onset. Recurrent chromosomal translocations have been described in B-ALL and

[1]Université de Toulouse, Inserm, Centre Nationale de la Recherche Scientifique, Université Toulouse III-Paul Sabatier, Centre de Recherches en Cancérologie de Toulouse, Toulouse, France; [2]Equipe Labellisée Ligue Contre le Cancer 2023, Toulouse, France; [3]Équipe Labellisée Institut Carnot Opale, Toulouse, France; [4]Institut Universitaire du Cancer de Toulouse-Oncopole, Toulouse, France; [5]Centre Hospitalier Universitaire de Toulouse, Toulouse, France; [6]Institut de Pharmacologie et de Biologie Structurale, Université de Toulouse, Centre Nationale de la Recherche Scientifique, Université Toulouse III—Paul Sabatier (UT3), Toulouse, France; [7]Université de Rennes, Etablissement Français du Sang, Inserm, MOBIDIC—UMR_S 1236, Rennes, France.

*É. Delabesse and S.J.C. Mancini contributed equally to this paper. Correspondence to Bastien Gerby: bastien.gerby@inserm.fr.

lead to the expression of chimeric fusion proteins. These oncoproteins often harbor domains of transcription factors (TFs) (e.g., ETV6::RUNX1, TCF3::PBX1, PAX5::ETV6, and PAX5::ELN) (Coyaud et al., 2010; Familiades et al., 2009; Mullighan et al., 2007). For instance, the TF PAX5, known to play an important role in the transcriptional regulatory networks (TNRs) of early B cells, the definitive B cell commitment, and the plasticity of committed B cells (Cobaleda et al., 2007a, 2007b), was also shown to promote leukemogenesis once translocated in mouse models (Jamrog et al., 2018; Jurado et al., 2022; Smeenk et al., 2017). Thus, it is widely thought that recurrent chromosomal translocations can act as a first oncogenic event in the early steps of B-ALL initiation, though the precise mechanisms at play are yet ill-known.

The development of transgenic mouse models with activated primary oncogenes not only helped to identify the oncogenic collaborators required for leukemia development but also allowed to identify pre-LSCs in the early steps of the disease. Various studies using in vivo models demonstrated that, in both lymphoid and myeloid malignancies, a primary genetic alteration can confer stem cell–like properties to normally committed progenitors and convert them into self-renewing pre-LSCs (Cozzio et al., 2003; Gerby et al., 2014; Huntly et al., 2004; Krivtsov et al., 2006; McCormack et al., 2010; Wojiski et al., 2009). Other studies using T-acute lymphoblastic leukemia (T-ALL) mouse models showed that pre-LSCs are resistant to chemotherapeutic agents because of their distinctive slow-division rate (Gerby et al., 2016; Tremblay et al., 2018). These findings support the view that self-renewal and cell quiescence are early and obligatory events in leukemia initiation, two specific features of the cell-of-origin, and differ from the propagating activity of fully transformed leukemic blasts. However, how a primary oncogene reprograms committed B cell progenitors into pre-LSCs with altered self-renewal and survival properties remains to be fully explored (Fregona et al., 2021).

To this end, we took advantage of a genetically engineered mouse model expressing the human PAX5::ELN fusion oncoprotein (Jamrog et al., 2018), recurrently identified in B-ALL patients (Bousquet et al., 2007). PAX5::ELN-expressing mice efficiently develop B-ALL, reproduce accurately the key features of leukemia development including secondary mutations acquired during the multistep process of human B-ALL, and provide an unrestrictive and reproducible access to a pre-LSC population (Jamrog et al., 2018). Here, by combining genetic and functional assays, together with gene expression and chromatin accessibility profiling, we deciphered the biological mechanisms by which PAX5::ELN reprograms normal B cell progenitors and leads to the emergence of quiescent pre-LSCs. Our data demonstrate that B-lineage identity is perturbed in quiescent pre-LSCs, associated with the reactivation of an immature molecular program. Moreover, our TNR predicted a list of TFs to control pre-LSC reprogramming. Among them, *Early growth response 1* (Egr1) represents a prime candidate TF to regulate pre-LSC quiescence. Finally, our analyses suggest that the pre-LSC signature mimics the resistance/quiescence of human B-ALL cells. In particular, we show that *EGR1* expression is associated with poor clinical outcomes and is activated in quiescent/resistant leukemic blasts from patients.

Results

PAX5::ELN oncoprotein induces aberrant phenotype and function in preleukemic B cells

Adult B cell development is initiated in the bone marrow (BM) by the entry of hematopoietic progenitors into the B cell lineage transcription program and the sequential rearrangement of immunoglobulin heavy (IgH) and light (IgL) chain loci through V(D)J recombination (Hardy et al., 2000). Phenotypic characterization of the different B cell subsets in mice using a combination of cell surface markers was established (Fig. S1 A) (Aurrand-Lions and Mancini, 2018). We previously developed a transgenic mouse model in which the human cDNA encoding the PAX5::ELN oncoprotein was inserted within the *IgH* locus to ensure an early and B cell–restricted expression (Jamrog et al., 2018). To determine whether PAX5::ELN oncoprotein perturbs the normal B cell development at the preleukemic stage, we performed a multiparametric staining by FACS covering exhaustively the steps of B cell differentiation (Fig. S1 A and Table S1). Unsupervised clustering allowed the visualization of the natural phenotypic progression of B cells throughout differentiation and showed that all the normal B cell subpopulations are present in preleukemic PAX5::ELN (PE^{tg}) mice as compared with wild type (wt) littermates (Fig. 1, A and B; and Fig. S1, B and C). Indeed, we distinguished in both lines the presence of pre-pro-B ($B220^+CD19^-CD2^-$), pro-B ($B220^+CD19^+Kit^+$), pre-BI ($B220^+CD19^+BP1^+$), early pre-BII ($B220^+CD19^+CD2^+IL7r^+$), late pre-BII ($B220^+CD19^+CD2^+IL7r^-$), immature B ($B220^+CD19^+Ig\kappa\lambda^+IgM^+$), and circulating/mature-B ($B220^+CD19^+Ig\kappa\lambda^+IgM^-CD23^+$) cell populations, corresponding to the different stages of differentiation (Fig. 1, A–C; and Fig. S1, B and C). However, our clustering approach revealed an aberrant population of B cell progenitors (aberrant B) in the PE^{tg} BMs (Fig. 1, A and B), featuring low expression of B220 ($B220^{low}$) and inappropriate expression of Kit (CD117), IL7r (CD127), IgM, and λ5 (CD179b) (Fig. 1 C), which is directly associated with the transgene expression (Fig. S1 D). Indeed, ELN expression is restricted to aberrant B cells ($CD19^+B220^{low}$) and is negative in all the normal B cell subpopulations ($CD19^+B220^+$) as well as in hematopoietic progenitors ($CD19^-B220^-Kit^{+/low}$) from PE^{tg} mice (Fig. S1 D). Interestingly, we noticed through the exploration of BP1, CD2, CD25 (IL2rα), and Igκλ markers, a phenotypic progression within the aberrant B population that is reminiscent of normal B cell differentiation (Fig. 1 A and Fig. S1 E). Moreover, in addition to the strong expression of Kit, we also observed a concomitant expression of the stem cell surface marker Sca-1 (Morcos et al., 2017) in about 30% of the aberrant B cells from the preleukemic PE^{tg} BM (Fig. S1 F). Together, these results indicate that PAX5::ELN oncoprotein induces a partial blockade of differentiation associated with the emergence of an aberrant B cell population in a steady-state condition.

To explore the functional impact of PAX5::ELN oncoprotein on preleukemic B cells, we performed serial transplantations of wt and PE^{tg} preleukemic total B cells (Fig. 1 D). Short-term

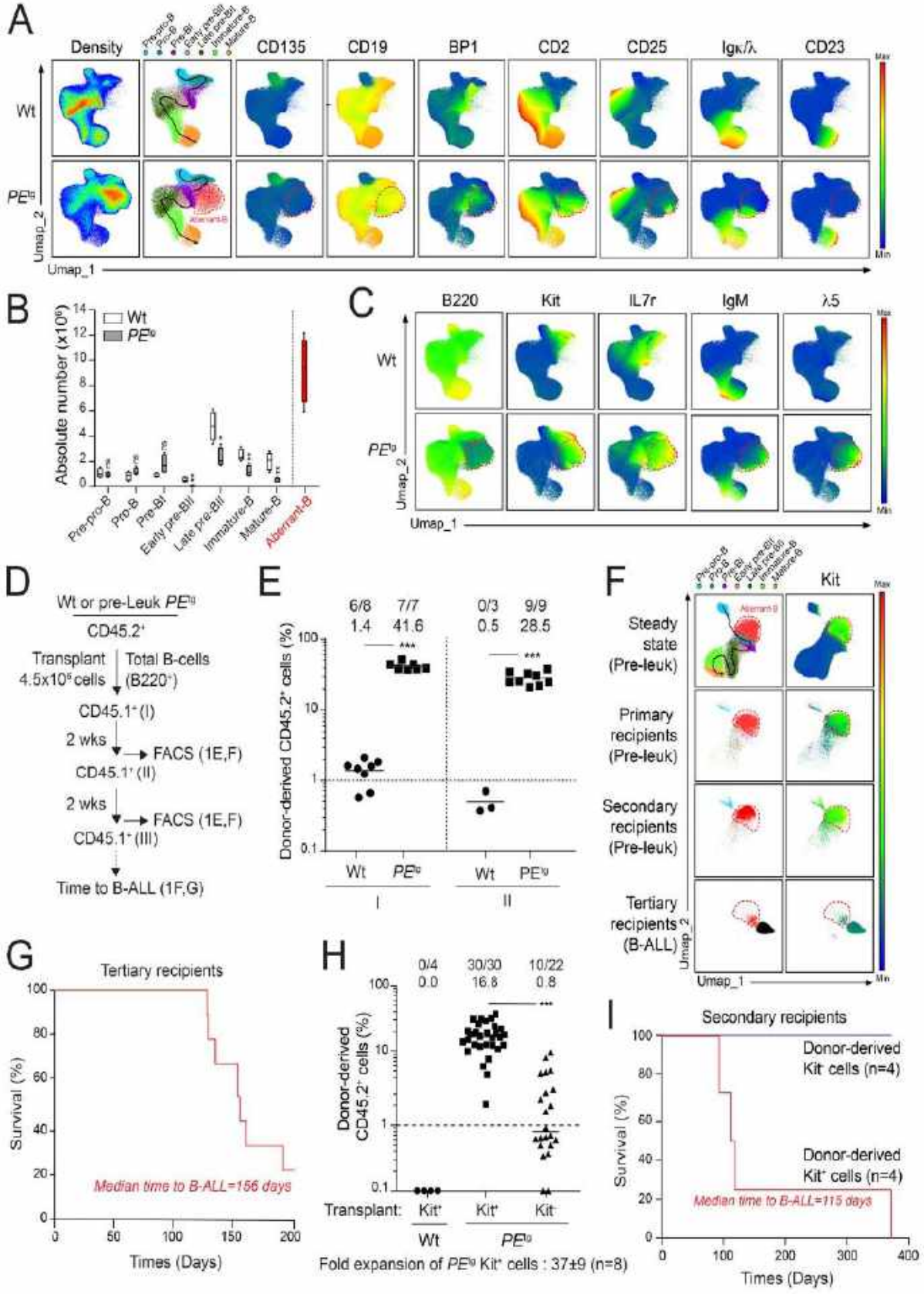

Figure 1. **PAX5::ELN induces aberrant B cells at the preleukemic stage. (A–C)** Phenotypic characterization of the B cell lineage from the BM of wt and PAX5::ELN (*PE*^{tg}) preleukemic mice (30 days old, $n = 4$). UMAP of the cell density (A, left panels), of the clustering analysis of the B cell subpopulations (A, central panels) based on the gating strategy shown in Fig. S1, B and C. Each subset is represented by one color. Black arrow indicates the physiological phenotypic progression of B cells in the differentiation. Red dotted line delimits the aberrant preleukemic B cell population induced by PAX5-ELN (A, central panels). UMAP of the expression level of CD135, CD19, BP1, CD2, CD25, Igκ/λ, and CD23 (A, right panels). Absolute numbers of B cell subpopulations were calculated. The horizontal lines of the box plots indicate the median, while the boxes represent the first and the third quartiles of the data and the whiskers denote the minimum and the maximum values (B, *$P < 0.05$, **$P < 0.01$). UMAP of the expression level of B220, Kit, IL7r, IgM and λ5 (C). Data were compiled

from four mice per condition and are representative at least of two independent experiments (*P < 0.05, **P < 0.01). **(D)** Experimental procedure to study the functional impact of PAX5::ELN on B cells. **(E)** Engraftment efficiency (CD45.2$^+$) in the recipient BM of primary (I) and secondary (II) mice was analyzed each 2 wk after transplantation. The number of positive mice and the median of engraftment are indicated (n = 3–9, ***P < 0.001). **(F)** UMAP of the CD45.2$^+$ *PE*^{tg} B cell subpopulations (left panel) before (steady state) and after transplantation in primary, secondary, and tertiary recipients, associated with the expression level of Kit (right panels). **(G)** Kaplan–Meier survival curve of tertiary recipients transplanted with donor-derived *PE*^{tg} B cells (n = 9). **(H)** Engraftment efficiency in the recipient BM of primary mice was analyzed 3 wk after transplantation. The number of positive mice, the median of engraftment and the in vivo fold expansion of *PE*^{tg} Kit$^+$ cells are indicated. Data were compiled from three independent experiments (n = 4–30, ***P < 0.001). **(I)** Kaplan–Meier survival curve of secondary recipient mice respectively transplanted with donor-derived Kit$^+$ cells (n = 4, red) or Kit$^-$ cells (n = 4, blue).

reconstitution potential was assessed by analyzing the BM engraftment 2 wk after transplantations in primary and secondary recipient mice. In contrast to normal B cells that are devoid of self-renewal potential, preleukemic B cells efficiently engrafted over primary and secondary recipients (Fig. 1 E). The phenotypic characterization of engrafted cells confirmed that this short-term self-renewal activity is associated with the selection and expansion of the aberrant B cell population (Fig. 1 F). Indeed, this phenotype was strongly stable over primary and secondary recipients (Fig. S2 A), as exemplified by the high level of Kit expression (Fig. 1 F). Moreover, tertiary transplantations of preleukemic B cells eventually led to long-term B-ALL development in about 5 mo (Fig. 1 G), which is the delay required to acquire the full pattern of transforming secondary mutations (Jamrog et al., 2018). Strikingly, fully transformed leukemic blasts from tertiary recipients exhibited a distinct phenotype (Fig. 1 F and Fig. S2 A) and were able to efficiently propagate B-ALL a few days only after quaternary transplantations, even with low doses of injected cells (Fig. S2 B). Finally, Kit$^+$ and Kit$^-$ B cells from *PE*^{tg} BMs were purified to compare their short-term engraftment capacity after transplantation in primary mice (Fig. S2 C). We controlled that purified Kit$^+$ cells from wt mice were devoid of engraftment potential, and that the aberrant self-renewal potential of *PE*^{tg} B cells was well enriched in the Kit$^+$ compartment (Fig. 1 H). Moreover, we confirmed that only Kit$^+$ preleukemic B cells sustained long-term B-ALL development after secondary transplantation (Fig. S2 C and Fig. 1 I). Together, our results suggest that PAX5::ELN oncoprotein converts Kit$^+$ B cell progenitors into pre-LSCs that have acquired de novo self-renewing activity in the first steps of the disease.

Preleukemic cells restricted in the cell cycle are chemoresistant and support leukemia-initiating activity

Cell-cycle restriction is a critical feature of normal hematopoietic stem cells (HSCs) to preserve their self-renewal function (Wilson et al., 2008). We therefore hypothesized that cell quiescence could be a biological mark of pre-LSCs in the *PE*^{tg} model. To test this hypothesis, we analyzed Ki67 expression in the different B cell subsets of wt and *PE*^{tg} preleukemic mice in steady-state condition (Fig. 2 A and Table S1). As expected, Ki67 expression followed the physiological proliferation rate of normal B cell differentiation (Tomura et al., 2013) in wt and *PE*^{tg} mice (Fig. 2, A and B; and Fig. S2 D). Furthermore, non-cycling Ki67$^-$ cells were detected within the aberrant *PE*^{tg} B cell population (Fig. 2, A and B; and Fig. S2 D). Since cell-cycle restriction is also an important characteristic of treatment-resistant cells in B-ALL (Ebinger et al., 2016; Turati et al., 2021), we assessed in vitro dose responses of doxorubicin (DOXO), methotrexate (MTX), and vincristine (VCR) on the aberrant *PE*^{tg} B cell population and compared the sensitivity of negative and positive Ki67 cells (Fig. 2 C and Fig. S2 E). We observed that Ki67$^-$ cells were still detected after 48 h of coculture and were strongly selected upon the treatment (Fig. S2 E). Moreover, the analysis of the absolute numbers of each fraction after the treatment showed that Ki67$^-$ cells were less sensitive to the three chemotherapeutic agents than Ki67$^+$ cells (Fig. 2 C).

To further address the question of whether PAX5::ELN perturbs the cell division kinetic of preleukemic B cells, wt and *PE*^{tg} Kit$^+$ B cells were labeled with the cell trace violet (CTV) and cultured for 3 days (Fig. 2 D). This in vitro cell division assay indicated that PAX5::ELN reduced the global proliferation rate of preleukemic cells and revealed the persistence of an undivided (D0) population (Fig. 2, E and F) that maintained the expression of Kit (Fig. S2 F). Next, we purified the slow-cycling (D0–2) *PE*^{tg} B cells population, which represents <1% of total generated cells and are undetectable in CTV-labeled wt counterparts cultured in the same experimental conditions (Fig. 2, E and F). High-cycling (D8–9) cells from both wt and *PE*^{tg} conditions were also purified as controls (Fig. 2 E). RNA sequencing (RNA-seq) demonstrated the presence of *PAX5::ELN* fusion transcript in both D0–2 and D8–9 preleukemic cells (Fig. S2 G) and their polyclonality of $V_H(D_H)J_H$ and V_LJ_L rearrangements (Fig. 2 G), confirming their preleukemic state. These cells were then treated in vitro separately by DOXO, MTX, or VCR (Fig. 2, D and H) with a sublethal concentration that we previously determined by dose-response experiments on total wt and *PE*^{tg} Kit$^+$ B cells (Fig. S2 H). This assay revealed a significant resistance of slow-cycling *PE*^{tg} D0–2 cells in contrast to wt and *PE*^{tg} D8–9 cells (Fig. 2 H). To address at the functional level the role of cell-cycle restriction in pre-LSC activity, equal numbers of D0–2 and D8–9 preleukemic cells were transplanted (Fig. 2 D). Both D0–2 and D8–9 preleukemic *PE*^{tg} B cells were able to engraft the BM of recipient mice 3 wk after transplantation (Fig. 2 I). However, only donor-derived D0–2 *PE*^{tg} cells maintained high-level expression of Kit in vivo (Fig. S2 I), sustained the reconstitution 16 wk after transplantation (Fig. 2 I), and the long-term B-ALL development (Fig. 2 J). Together, our results indicate that cell-cycle restriction of preleukemic cells is associated with chemoresistance and leukemia initiation.

PAX5::ELN oncoprotein disrupts the differentiation of preleukemic cells by enforcing the IL7r/JAK-STAT signaling pathway

PAX5::ELN perturbs B cell differentiation (Fig. 1) and the cell cycle of preleukemic cells (Fig. 2). Thus, we asked whether the main B cell differentiation molecular programs are affected by

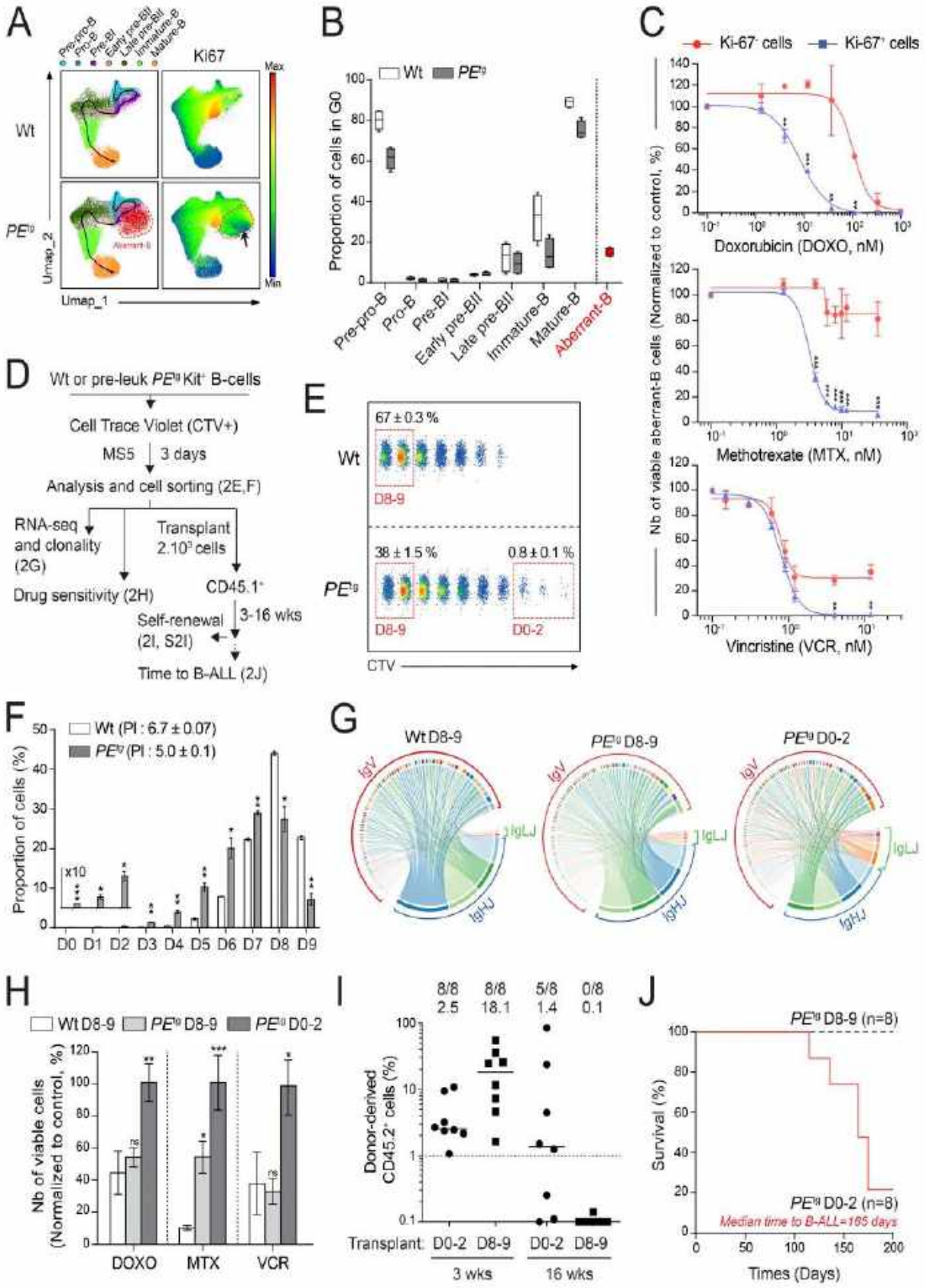

Figure 2. **Cell quiescence is a feature of PAX5::ELN pre-LSCs. (A and B)** UMAP representation of the wt and *PE*^{tg} B cell subpopulations (A, left panel), associated with the Ki67 expression level (A, right panel). The arrow indicates the population in G0 phase (Ki67$^-$ cells in blue) within the aberrant B cell population. Quantification of the proportion of cells in G0 phase (Ki67$^-$ cells) within each wt and *PE*^{tg} B cell subpopulation (B). Data were compiled from four mice per condition and are representative at least of two independent experiments. The horizontal lines of the box plots indicate the median, while the boxes represent the first and the third quartiles of the data and the whiskers denote the minimum and the maximum values. **(C)** Preleukemic *PE*^{tg} cells were treated in vitro on MS5 stromal cells with a dose-response of DOXO, MTX, or VCR for 48 h. Absolute numbers of Ki67$^+$ and Ki67$^-$ cells within the aberrant B cell

population were then analyzed by FACS and normalized to the number of untreated cells ($n = 3$, one experiment, $^{**}P < 0.01$, $^{***}P < 0.001$). **(D)** Experimental procedure to study cell division of Kit$^+$ B-progenitors from wt and preleukemic *PE*^{tg} mice. **(E and F)** The number of cell divisions (D0 to D9) after the coculture was then analyzed (E), the proportion of cells in each division was quantified and the PI (PI ± SD) was calculated for each condition (F, $n = 2$, mean ± SD, representative of two independent experiments, $^{*}P < 0.05$, $^{**}P < 0.01$, $^{***}P < 0.001$). Red dotted gates were used to purify the D0–2 and D8–9 populations (E). **(G)** Cell clonality analysis of *PE*^{tg} D0–2, *PE*^{tg} D8–9 and wt D8–9 populations after RNA-seq. The proportions of $V_H(D_H)J_H$ and V_LJ_L rearranged transcripts were represented by Circos diagrams. **(H)** Drug sensitivity of *PE*^{tg} D0–2 and D8–9 cells and of wt D8–9 cells upon the treatment with an IC50 of DOXO, MTX, and VCR during 48 h. Cell numbers of treated cells were analyzed by FACS and normalized to the number of untreated cells ($n = 3$, one experiment, mean ± SD, $^{*}P < 0.05$, $^{**}P < 0.01$, $^{***}P < 0.001$). **(I and J)** Engraftment efficiency 3 and 16 wk after transplantation (I) and Kaplan–Meier survival curve of recipient mice transplanted with D0–2 and D8–9 *PE*^{tg} cells (J). The number of positive mice and the median of engraftment are indicated (I, $n = 8$). The median of time required to develop the B-ALL is indicated (J).

PAX5::ELN in slow- and high-cycling preleukemic cells. Early B cell development is controlled by the IL7 receptor and the pre-B cell receptor (pre-BCR), two interacting signaling systems that tightly coordinate alternative phases of cell survival and differentiation through the JAK-STAT and pre-BCR/BLNK pathways, respectively (Clark et al., 2014; Reth and Nielsen, 2014). Each pathway has antagonistic and balanced functions to coordinate the proliferation and differentiation switch at the pre-B stage (Fig. 3 A). Interestingly, IL7r is strongly expressed in the aberrant *PE*^{tg} B cell population, together with the accumulation of the surrogate light chain λ5 at their surface (Fig. 1 C). Thus, we analyzed IL7r and pre-BCR/BLNK pathways by using a phosphoflow cytometry approach after ligand and chemical ex vivo stimulations, respectively (Fig. S3 A and Fig. 3 B). Ligand stimulation of IL7r efficiently induced the phosphorylation of its two downstream effectors, STAT5 and FOXO1, in the aberrant B (B220^{low}) *PE*^{tg} population, in a similar way to normal (B220^{high}) pro-B cells (Fig. S3 A and Fig. 3 B, left panels). Accordingly, the presence of IL-7 protected aberrant *PE*^{tg} B cells from apoptosis (Fig. 3 C) and efficiently promoted their proliferation (Fig. 3 D) in vitro. In addition, this process was abrogated in the presence of tofacitinib, a well-known JAK-STAT inhibitor (Fig. 3, C and D), showing that IL-7r signaling is critical to maintaining the survival of preleukemic cells. We also assessed the (pre-)BCR signaling response by mimicking its downstream activation ex vivo with hydrogen peroxide (H_2O_2) (Fig. S3 A and Fig. 3 B, right panels), a well-known inducer of BLNK/PLCγ2 phosphorylation cascade (Patterson et al., 2015; Reth, 2002). As expected, H_2O_2 induced the phosphorylation of BLNK and PLCγ2 along the normal B cell differentiation pathway. In contrast, the aberrant *PE*^{tg} B cell population was unresponsive to BLNK/PLCγ2 stimulation (Fig. S3 A and Fig. 3 B, right panels).

Interestingly, ligand stimulation of IL7r efficiently induced the phosphorylation of STAT5 in both Ki67$^+$ and Ki67$^-$ cells within the aberrant *PE*^{tg} B cell population, which is abrogated in the presence of tofacitinib (Fig. 3 E, right panels). In contrast, IL7r activation is concentrated in cycling Ki67$^+$ cells from normal B cells (Fig. 3 E, left panels), corresponding to cycling pro-B cells (Fig. 2 B and Fig. S2 D). Moreover, gene set enrichment analysis (GSEA) from the RNA-seq of purified *PE*^{tg} D0–2, *PE*^{tg} D8–9, and wt D8–9 cells (Fig. 2 D and Table S2) confirmed that the IL7r/JAK-STAT axis was significantly upregulated by PAX5::ELN oncoprotein in slow- and high-cycling preleukemic cells (Fig. S3 B). This observation was reinforced by the comparison of our PAX5::ELN-modified genes with the Stat5-binding genes arising from the ChIP sequencing of murine *Stat5b*-induced B-ALL cells (Katerndahl et al., 2017), showing a substantial enrichment of Stat5 targets in PAX5::ELN upregulated genes in slow- (D0–2) and high- (D8–9) cycling preleukemic cells (Fig. 3 F and Table S2). Accordingly, the downstream targets of IL7r/JAK-STAT axis, including the prosurvival genes *Cdkn2a*, *Il2rα*, *Tnfrsf13b*, and *Socs3*, were significantly activated in both D0–2 and D8–9 cells (Fig. 3 G, left panels). In contrast, several components of the pre-BCR/BLNK signaling including *CD79b*, *CD79a*, *Lyn*, *Syk*, *Blnk*, *Ikzf3*, and *Irf8* were downregulated in both D0–2 and D8–9 cells (Fig. 3 G, right panels). Among them, the pre-B cell differentiation genes *Blnk*, *Ikzf3*, and *Syk* also belong to Stat5 targets (Fig. 3 F), reinforcing the notion that IL7r/JAK-STAT axis negatively regulates the B cell differentiation (Fig. 3 A).

Collectively, combined with our phosphoflow cytometry results, our RNA-seq data suggest that the activation of IL7r/JAK-STAT pathway favors the maintenance and survival of preleukemic cells, in slow- and high-cycling fractions.

B cell molecular identity is impaired in quiescent pre-LSCs

While the above results demonstrate that the leukemia-initiating potential is enriched in slow-cycling population, the imbalance between IL7r/JAK-STAT and pre-BCR/BLNK molecular circuits is a shared feature of all *PAX5::ELN* preleukemic cells. Thus, to further identify and characterize quiescent pre-LSCs, we generated *PE*^{tg}*::H2B-GFP*^{tg} mice, derived from doxycycline-inducible *H2B-GFP*^{tg} mice, an in vivo model allowing the study of cell quiescence in normal HSCs (Foudi et al., 2009; Wilson et al., 2008). After a doxycycline pulse, we compared the cell division kinetics in vivo between wt and preleukemic *PE*^{tg} B cells based on the loss of GFP expression during a time course of doxycycline chase (Fig. 4 A). At the end of the doxycycline pulse, almost all B cells in both wt and preleukemic BM expressed the H2B-GFP marker (Fig. 4 B). However, the decrease of GFP after the withdrawal (chase period) of doxycycline revealed a substantial delay of the global GFP loss in preleukemic *PE*^{tg} B cells, with the persistence of GFP^{high} *PE*^{tg} cells after 1-wk chase of doxycycline (Fig. 4 B). Based on the loss of GFP after 2- and 3-wk chase of doxycycline, we defined GFP^{high} cells as quiescent rather than dormant cells, such as reported for normal stem cells (Foudi et al., 2009; Wilson et al., 2008). Therefore, we adapted the multiparametric staining to identify the quiescent GFP^{high} B cell subset. Quiescent cells were exclusively found in the aberrant B cell population of *PE*^{tg} BM (Fig. S3 C and Fig. 4 C). Additionally, we observed that GFP loss was proportional to the acquisition of the Ki67 marker, almost all GFP^{high} cells did not express Ki67 (Fig. 4 D), and only this non-

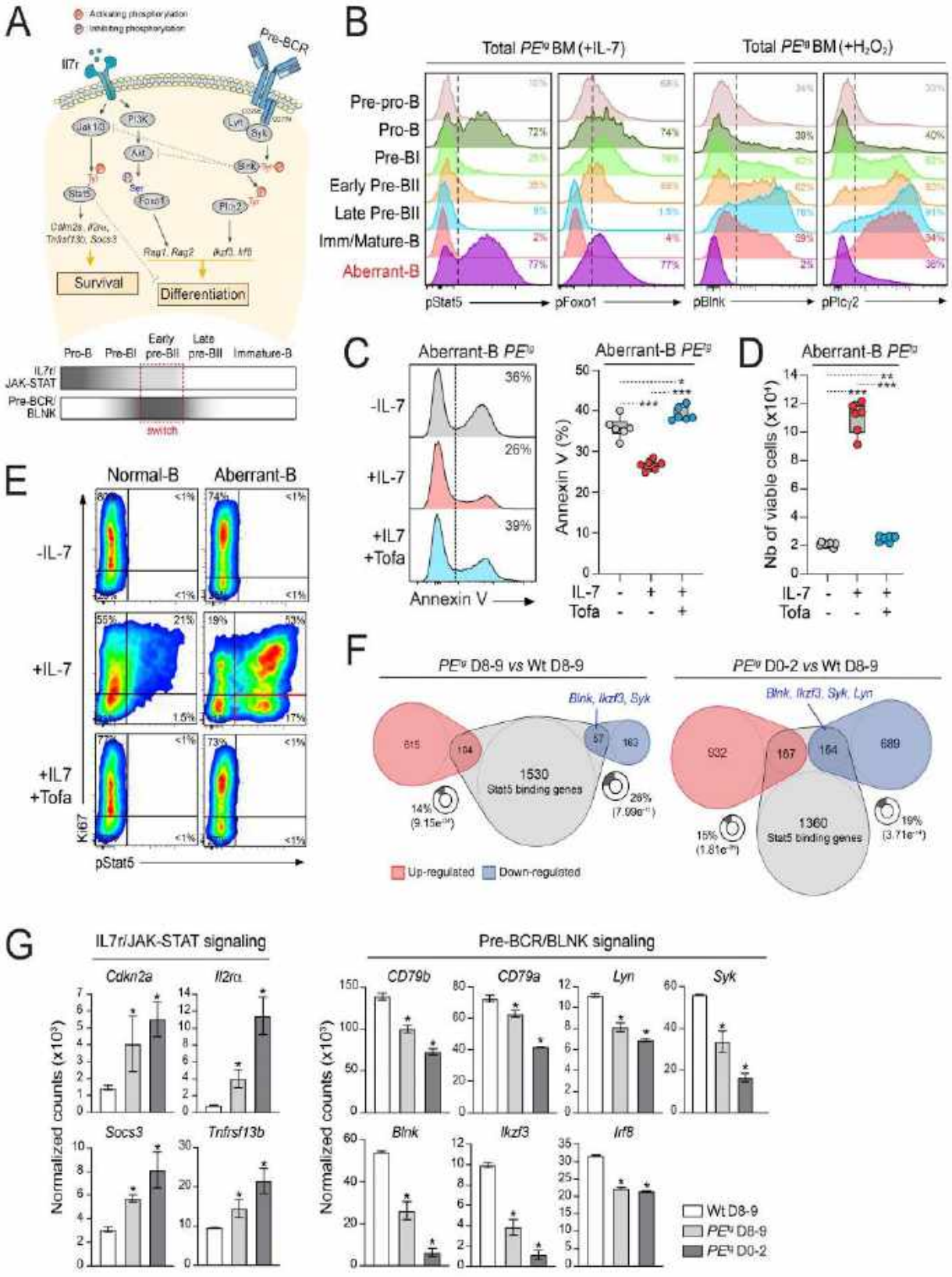

Figure 3. **Imbalance of IL7r/JAK-STAT and pre-BCR/BLNK pathways in PAX5::ELN preleukemic cells. (A)** Simplified schematic representation of the IL7r and pre-BCR signaling pathways adapted from Clark et al. (2014). **(B)** FACS analysis of pStat5 and pFoxo1 on the aberrant B cell population and on each normal B cell subsets from preleukemic PE^{tg} mice after ex vivo IL-7 stimulation (+IL-7) (left panels). FACS analysis of pBlnk and pPlcγ2 after ex vivo H_2O_2 stimulation ($+H_2O_2$) is shown in right panels. **(C and D)** Preleukemic PE^{tg} cells were treated in vitro on MS5 stromal cells with IL-7 (+IL-7) or not (−IL-7) for 48 h. The proportion of Annexin V⁺ cells within the aberrant B PE^{tg} population was measured (left panel) and quantified (right panel) by FACS and the absolute numbers of viable aberrant B PE^{tg} cells were calculated (D). Cells treated with 1 µM tofacitinib (Tofa) were used as controls ($n = 6$, representative of two independent experiments, $^*P < 0.05$, $^{**}P < 0.01$, $^{***}P < 0.001$). The horizontal lines of the box plots indicate the median, while the boxes represent the first and the third quartiles of the data and the whiskers denote the minimum and the maximum values. **(E)** Representative FACS analysis of pStat5 after IL-7 stimulation (+IL-7)

in presence or not (vehicle) of 1 µM tofacitinib associated with Ki67 expression in normal B cells and in aberrant B PE^{tg} cells. Unstimulated (−IL-7) cells were used as controls. **(F)** Venn diagram of PAX5::ELN-modified genes overlapped with a list of Stat5-binding genes arising from the ChIP sequencing of murine *Stat5b*-induced B-ALL cells (Katerndahl et al., 2017). Numbers in the plot indicate quantification of genes in each group. Indicated P value was calculated by hypergeometric test. **(G)** Expression level of selected genes involved in IL7r/JAK-STAT (left panel, *Cdkn2a*, *Il2rα*, *Tnfrsf13b*, and *Socs3*) and in pre-BCR/BLNK (right panel, CD79b, CD79a, *Lyn*, *Syk*, *Blnk*, *Ikzf3*, and *Irf8*) signaling pathways extracted from the RNA-seq of PE^{tg} D0–2, PE^{tg} D8–9 and wt D8–9 cells ($n = 2$, mean ± SD, $^*P < 0.05$).

cycling population sustained engraftment capacity after transplantation (Fig. 4 E) and the long-term B-ALL development (Fig. S3 D).

To refine the molecular characterization of quiescent pre-LSCs in vivo, GFP^{high} and GFP^{low} cells were purified from aberrant B cells of PE^{tg}*H2B-GFP*^{tg} mice after 1-wk chase of doxycycline, and an integrative molecular approach was performed comparing both gene expression profiles by RNA-seq and chromatin accessibility by assay for transposase-accessible chromatin sequencing (ATAC-seq) (Fig. 4 F) (Buenrostro et al., 2013). Transcriptome analysis identified 836 upregulated and 789 downregulated genes with an expression difference of >1.5-fold and an adjusted P value of <0.05 in quiescent GFP^{high} pre-LSCs (Fig. 4 F and Table S3). Combined with an expected downregulation of cell cycle–related pathways, the analysis revealed that cytokine signaling pathways were upregulated in quiescent GFP^{high} pre-LSCs (Fig. S3 E). Indeed, these modifications, involving the downregulation of E2f/Myc targets and the upregulation of TNFα signaling (Fig. S3 E), are crucial for HSC and cancer stem cell survival (Cabezas-Wallscheid et al., 2017; Vazquez-Santillan et al., 2015; Yamashita and Passegué, 2019; Zhang et al., 2022). Differentially accessible chromatin regions were revealed by ATAC-seq analysis in preleukemic GFP^{high} (7,439 peaks) and GFP^{low} (5,360 peaks) cells (Fig. 4 F and Table S4). Their associated genes were enriched for molecular pathways similar to those identified at the mRNA level (Fig. S3, E and F). These observations highlight the direct relationship between the expression of genes and their surrounding accessibilities, allowing the identification of specific regulators.

To this end, we combined footprinting analysis using hint-ATAC and "diffTF" computational tools (Berest et al., 2019) to identify and classify TF motif accessibilities that were differentially regulated in quiescent GFP^{high} pre-LSCs (Fig. 4 G). We observed that the motif accessibility of critical TFs involved in the B cell identity, such as Ebf and Pax, or in the cell cycle, such as E2f, was significantly downregulated in quiescent GFP^{high} pre-LSCs (Fig. 4 G and Fig. S4 A). While the accessibility footprint (Tn5 insertion site) of Ebf and Pax was decreased in quiescent GFP^{high} pre-LSCs (Fig. S4 A), we observed that the expression of *Ebf1* and total *Pax5* was tightly increased at the transcriptional level (significantly for *Ebf1* but not for total *Pax5*, Fig. S4 B). Of note, the expressions of *Pax5* WT and *PAX5-ELN* were quietly similar between H2B-GFP^{high} and H2B-GFP^{low} cells (Fig. S4 B). This observation indicates that the binding activity of these two TF is affected in H2B-GFP^{high} pre-LSCs, but not their expression. Interestingly, we observed that Pax5-repressed genes, but not Pax5-activated genes (Revilla-I-Domingo et al., 2012), were drastically enriched in GFP^{high} pre-LSCs (Fig. 4 H and Fig. S4 C). Together, these results strongly suggest that Pax5 has lost its repressive activity in quiescent pre-LSCs, allowing the upregulation of a non-B cell molecular program. Indeed, we observed the upregulation of the chromatin accessibility to Spi and Runx motifs in quiescent GFP^{high} pre-LSCs (Fig. 4 G and Fig. S4 A). This was associated with increased expression of Spi1 (PU.1) and Runx1 (Fig. S4 B), two critical TFs regulating the quiescence and the myeloid differentiation process of normal HSCs (Chavez et al., 2021; Imperato et al., 2015; Staber et al., 2014). This observation was also associated with a downstream activation of a myeloid program in quiescent GFP^{high} pre-LSCs at the transcriptional level. Indeed, the analysis mainly revealed the upregulation of genes involved in TNFα signaling and in myeloid differentiation in GFP^{high} pre-LSCs (Fig. 4 I). Finally, we observed a strong enrichment of both murine (Fig. 4 J and Table S3) (Venezia et al., 2004) and human (Fig. S4 D and Table S3) (Garcia-Prat et al., 2021) dormant/quiescent HSC signature in the GFP^{high} pre-LSCs, suggesting redundant molecular mechanisms between pre-LSCs and HSCs. Collectively, our data indicate that quiescent pre-LSCs partially lose B-lineage molecular identity and concomitantly reactivate an inappropriate and immature transcriptional program.

Multi-lymphoid progenitor (MLP)/hematopoietic stem and progenitor cell (HSPC) molecular signatures are partially reprogrammed in quiescent pre-LSCs

The above findings raise the question as to what extent stem cell–like molecular features are reprogrammed in quiescent pre-LSCs. Thus, we integrated our results within ATAC-seq and RNA-seq data from the Immunological Genome Project (ImmGen) consortium (https://www.immgen.org/). First, we extracted both chromatin accessibility and gene expression profiles from normal HSPCs (LT-HSCs, MPP1, ST-HSCs, MPP4), MLPs, common lymphoid progenitor (CLP), Fr.A (i.e., Pre-pro-B), and B cells (Fr.B/Pro-B to Fr.E/immature-B) (Fig. 5 A). Then, differentially accessible peaks and expressed genes from preleukemic GFP^{high} and GFP^{low} cells were clustered by a k-means approach according to their signal in the different steps of normal differentiation (Fig. 5, A–C and Table S5). Strikingly, ATAC-seq data revealed that open chromatin regions from HSPCs, including LT-HSCs and other multipotent immature progenitors (clusters C1 to C4), were enriched in quiescent GFP^{high} pre-LSCs, contrasting in this regard with GFP^{low} cycling cells that were rather enriched in accessible regions from committed B cells (clusters C7, C8) (Fig. 5 B). Furthermore, RNA-seq data identified four clusters of genes in preleukemic GFP^{high} and three clusters of genes in GFP^{low} cells. This analysis notably revealed a unique "$HSPC^{like}$ cluster" in quiescent GFP^{high} cells, composed of genes mostly upregulated in LT-HSCs, MPP1, ST-HSCs, and MPP4 fractions (Fig. 5 C). An "MLP^{like} cluster" was

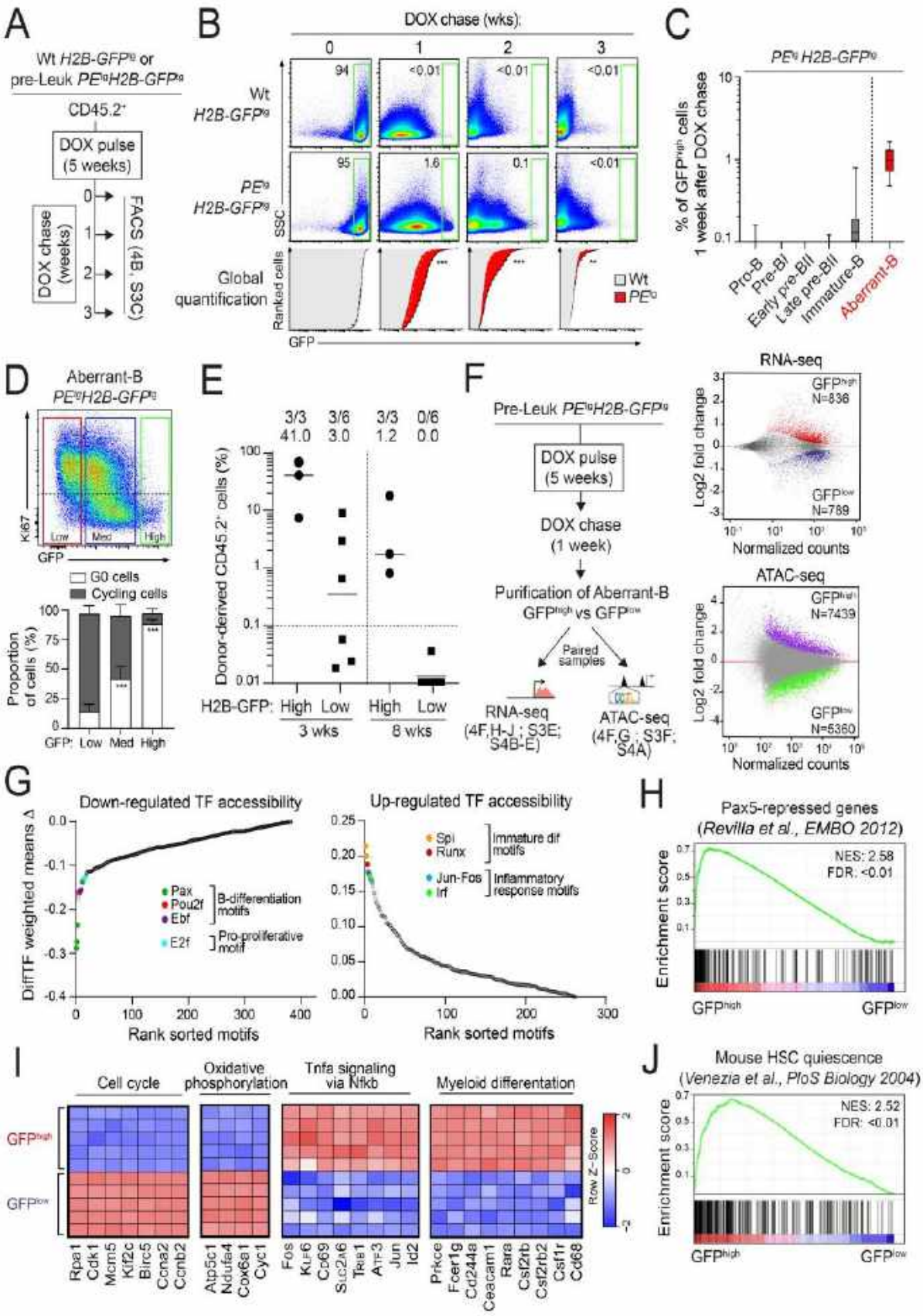

Figure 4. **Loss of B cell molecular identity in quiescent pre-LSCs. (A)** Experimental procedure to study the cell division kinetics in vivo of wt and pre-leukemic B cells. TFBS, TF binding site. **(B)** Representative FACS analysis of GFP expression in B cells ($CD19^+CD23^-$) from the BM of wt *H2B-GFP*^{tg} ($n = 14$, upper panels) and preleukemic *PE*^{tg}*H2B-GFP*^{tg} ($n = 12$, central panels) mice after 0, 1, 2, and 3 wk of DOX chase. AUC quantification of the GFP was compared between the two conditions (lower panels, $^{**}P < 0.01$, $^{***}P < 0.001$). **(C)** Quantification of the proportion of GFP^{high} within preleukemic *PE*^{tg}*H2B-GFP*^{tg} ($n = 12$) B cell subpopulations after 1 wk of DOX chase. The horizontal lines of the box plots indicate the median, while the boxes represent the first and the third quartiles of the data and the whiskers denote the minimum and the maximum values. **(D)** Representative FACS analysis (upper panel) and quantification (lower panel, $n =$

8, mean ± SD, ***P < 0.001) of the proportion of G0 (Ki67-) and cycling (Ki67+) cells in GFP^{low}, GFP^{med} and GFP^{high} populations. Data from B–D were representative at least of two independent experiments. **(E)** Engraftment efficiency of purified GFP^{high} (n = 3) and GFP^{low} (n = 6) cells from *PE^{tg}H2B-GFP^{tg}* mice was analyzed by FACS 3 and 8 wk after transplantation. The number of positive mice and the median of engraftment are indicated. **(F)** Experimental procedure for the molecular characterization of quiescent pre-LSCs in vivo (left panel). Scatter plots showing differentially expressed genes (RNA-seq, n = 5) and differentially chromatin accessibility (ATAC-seq signal, n = 3) between purified GFP^{high} and GFP^{low} cells from *PE^{tg}H2B-GFP^{tg}* mice (right panels). **(G)** TF motifs with differential chromatin accessibility between GFP^{high} and GFP^{low} cells identified and sorted using the DiffTF computational tool (Berest et al., 2019). Down- (left panel) and up- (right panel) regulated TF accessible regions in quiescent GFP^{high} cells were represented. **(H)** GSEA of the well-established list of in vivo PAX5-repressed genes (Revilla-I-Domingo et al., 2012) between GFP^{high} and GFP^{low} cells. **(I)** Heatmap of genes involved in indicated pathways between GFP^{high} (n = 5) and GFP^{low} (n = 5) cells. **(J)** GSEA of the established list of in vivo mouse HSC quiescence genes (Venezia et al., 2004) between GFP^{high} and GFP^{low} cells. The normalized enrichment score (NES) and the false discovery rate (FDR) are indicated in H and J.

also defined in quiescent GFP^{high} cells, composed of genes upregulated in CLP and pre-pro-B precursors, two populations that retain multilymphoid potential (Fig. 5 C). This MLP signature, which is strongly activated in quiescent GFP^{high} cells, was also observed in human B-ALL chemoresistant cells (Turati et al., 2021).

These observations revealed at the transcriptional level the plasticity and reprogramming of quiescent pre-LSCs that can partially reactivate a non-B cell molecular program.

TRN reveals Egr1 to control pre-LSC quiescence

According to the global upregulation of the cell-cycle program in GFP^{low} cells (Fig. 4 I and Fig. S3 E), we identified a cluster of genes named "cell-cycle^{like} cluster," whose expression pattern followed the normal proliferation rate of each subset in the differentiation (Fig. 5 C). Conversely, a "quiescence^{like} cluster" corresponding to the mirror image of the "cell-cycle^{like} cluster" was detected within GFP^{high} cells (Fig. 5 C).

To predict the "core" TFs defining pre-LSC identity, and in particular pre-LSC quiescence, we built a TRN from ATAC-seq (Fig. 5 B) and RNA-seq (Fig. 5 C) data using LASSO-StARS algorithm (Miraldi et al., 2019; Pokrovskii et al., 2019). This algorithm integrates (i) motif analyses, (ii) differential accessibility motifs, and (iii) gene expression to construct a set of TF–gene interactions. This analysis predicted TFs that positively (activating) or negatively (repressive) regulate their target genes. Thus, we contrasted five specific TRNs (#1 to #5) to one shared TRN involved in the pre-LSC signature (Fig. 5 D). In particular, a quiescence module (TRN #1) was identified in GFP^{high} pre-LSCs composed of four TFs (Egr1, Mnt, Klf6, and Atf3) (Fig. 5 D). Among them, *Early growth response 1* (Egr1) regulates the higher number of target genes (121 activated and 242 repressed genes). Moreover, Egr1 was the top predicted TF to regulate positively the quiescence and negatively the cell cycle (TRN#1, Fig. 5 D). Accordingly, we observed a strong downregulation of the quiescence^{like} cluster and upregulation of the cell-cycle^{like} cluster in human HSPCs in which EGR1 has been silenced by RNA interference (Stoddart et al., 2022) (Fig. S4 E). Consistent with the critical role of Egr1 in controlling normal HSC dormancy and functions (Cabezas-Wallscheid et al., 2017; Min et al., 2008; Scheicher et al., 2015), our result suggests that it may be also relevant in pre-LSCs.

To address this question, we used a loss-of-function approach by CRISPR/Cas9 strategy (Fig. S4 F). We generated *PE^{tg}Cas9^{tg}* mice that constitutively express the Cas9 endonuclease (Tzelepis et al., 2016) and designed two single-guide RNAs (sgRNAs) (sgEgr1 T5 and sgEgr1 T7) that target the genomic region encoding the exon 1 of *Egr1* gene (Table S1). Aberrant B cells from preleukemic *PE^{tg}Cas9^{tg}* mice were purified and transduced with lentiviral vectors encoding sgEgr1 T5 or sgEgr1 T7 or a non-targeted control sgRNA (sgCTL). Transduced *PE^{tg}Cas9^{tg}* GFP^{+} cells were then purified (Fig. S4 G) and genome editing efficiency was determined by analyzing the rate of insertions/deletions (InDels) induced in the targeted region. Although sgEgr1 T5 did not induce InDels in the *Egr1* locus, sgEgr1 T7 allowed for almost a complete (93%) genome editing of the *Egr1* locus (Fig. S4 H). Subsequent in vitro cell division assay indicated that Egr1 genomic editing by sgEgr1 T7 slightly but significantly increases the global proliferation rate of aberrant B cells (Fig. S4, I and J). Interestingly, this observation was associated with a reduction of the proportion of slow-cycling (D0–2) cells (Fig. 5 E), with a decrease of Kit expression and an increase of IgM expression at the surface of aberrant B cells (Fig. 5 F). Thus, our results show that Egr1 genomic editing reverses, at least partially, the quiescence and the aberrant expression of Kit of preleukemic cells.

Finally, we built the molecular network of genes involved in TRN#1 from Fig. 5 D (Fig. S4 K). Strikingly, several members of the network such as the TFs Atf3 (Liu et al., 2020) and Klf6 (Adelman et al., 2019), the GTPase Gimap5 (Chen et al., 2011), and the transcriptional coactivator Taz (Althoff et al., 2020) have been also documented to control HSC functions.

Collectively, the data arising from our integrative molecular approach predict a list of TFs and their target genes to control molecular reprogramming in pre-LSCs and highlights Egr1 as a strong candidate to regulate pre-LSC quiescence.

EGR1 is activated in quiescent and therapy-resistant leukemic blasts from human B-ALL

Finally, we addressed the relevance of the expression modifications of murine pre-LSCs in human-resistant and quiescent leukemic cells. Interestingly, the downregulation of E2f/Myc targets (Fig. S3 E) and cell cycle/oxidative phosphorylation program (Fig. 4 I), combined with the upregulation of TNFα signaling (Fig. S3 E and Fig. 4 I) and HSPC/MLP signatures (Fig. 5 C) that we identified in GFP^{high} pre-LSCs from the *PAX5::ELN* model, have been also observed in treatment-resistant (minimal residual disease [MRD]) cells and in CFSE label-retaining cells (LRC) from B-ALL patient-derived xenografts (PDXs) in two independent studies (Ebinger et al., 2016; Turati et al., 2021). These molecular similarities (Fig. 6, A and B; and Fig. S5 A) suggest that PAX5::ELN pre-LSC signature mimics in some aspect the resistance/quiescence of human B-ALL cells.

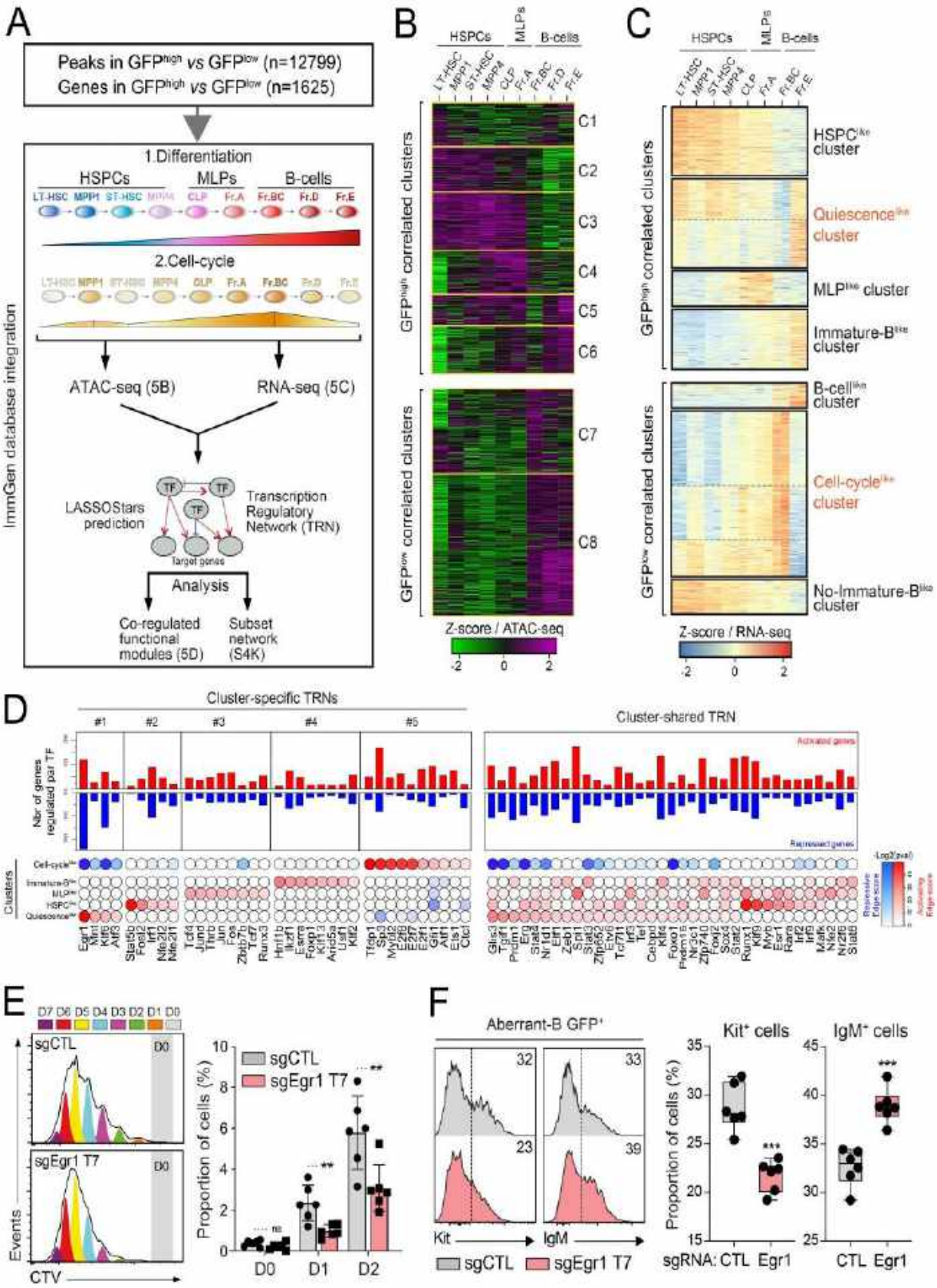

Figure 5. **Transcriptional molecular network reprogrammed in quiescent pre-LSCs. (A)** Study design for the generation of the pre-LSC transcription regulatory network. **(B and C)** Heatmap of k-means clustering for the differentially accessible region (B) or differentially expressed genes (C) integrating the different subsets of the normal B-lymphopoiesis. Clusters are separated depending on the correlation with GFP^{high} or GFP^{low}. **(D)** Core TRNs are defined according to enriched positive regulation of upregulated gene (red) or negative regulation of downregulated genes (blue) in a given cluster identified in Fig. 5 C (lower panels). The significance of enrichment is displayed on the right. The upper panels displayed the number of positive (red) and negative (blue) regulatory interactions per TF. The analysis defined five cluster-specific TRNs and one cluster-shared TRN of the pre-LSC signature. **(E and F)** Cell division assay (E) and

cell differentiation assay (F) of $PE^{tg}Cas9^{tg}$ aberrant B cells expressing sgCTL or sgEgr1 T7 (GFP$^+$) according to the experimental procedure detailed in Fig. S4 F. The number of cell divisions (D0 to D7) after 6 days of coculture was then analyzed (E, left panel) and the proportion of cells in the divisions D0, D1, and D2 was quantified (E, right panel, $n = 6$, one experiment, mean ± SD, $^{**}P < 0.01$). The proportion of Kit$^+$ and IgM$^+$ cells was evaluated by FACS (F, left panel) and quantified (F, right panel, $n = 6$, one experiment, $^{***}P < 0.001$). The horizontal lines of the box plots indicate the median, while the boxes represent the first and the third quartiles of the data and the whiskers denote the minimum and the maximum values.

Thus, we explored *EGR1* expression in resistant and/or quiescent human B-ALL cells. We transplanted leukemic blasts from two "de novo" *ETV6-RUNX1* B-ALL patients (HB#010 and HB#007) into immunodeficient NOD.*Cg-Prkdc*^{scid}*Il2rg*^{tm1Wjl} (referred to as NSG) mice and monitored for engraftment before treatment with a chemotherapeutic cocktail (dexamethasone [DEXA] + VCR) or vehicle control (Fig. 6, C and D; and Fig. S5, B and C). Strikingly, B-ALL progression was prevented in chemotherapy-treated mice characterized by a significant reduction of the leukemic burden in the BM and the spleen (Fig. 6, E and F; and Fig. S5, D and E). This drastic reduction of human B-ALL cells in vivo was associated with an enrichment of quiescent Ki67$^-$ leukemic blasts (Fig. 6 G and Fig. S5 F). This resistance was also associated with a significant upregulation of *EGR1* transcript in purified residual leukemic blasts (Fig. 6 H and Fig. S5 G). Interestingly, we observed that residual leukemic blasts developed leukemia in secondary recipients with a significant delay as compared with untreated cells (Fig. S5 H). This result reinforces the notion that quiescent/resistant cells from PDX models exhibit a long-term leukemia-initiating activity and mimics, in some aspects, relapse-initiating cells from B-ALL patients.

Based on our previous observations, we hypothesized that *EGR1* expression was already upregulated in quiescent cells within the tumor burden of B-ALL. Thus, leukemic blasts from two other *ETV6::RUNX1* B-ALL patients (HB#002 and HB#008) were labeled with CTV and cocultured on MS5 stromal cells (Fig. 6 I and Fig. S5 I). Strikingly, our data showed the feasibility of identifying undividing/slow-dividing cells from "de novo" B-ALL samples using this in vitro cell division approach (Fig. 6 J and Fig. S5 J). Of note, we observed that these cells were enriched in the CD45$^{neg/low}$ phenotype (Fig. 6 J and Fig. S5 J), which has been associated with drug-tolerant leukemic clones leading to B-ALL relapse in patients (Dobson et al., 2020). Therefore, we confirmed that *EGR1* expression was higher in purified undivided (CTV^{high}) B-ALL cells from the two patients as compared with cycling (CTV^{low}) leukemic cells (Fig. 6 K and Fig. S5 K). Together, our observations suggest that EGR1 overexpression is a "de novo" molecular characteristic of quiescent/resistant cells within the tumor bulk.

Finally, we took advantage of the RNA-seq and clinical data of a large cohort of B-ALL patients (Gu et al., 2019) to explore *EGR1* expression and its clinical outcome. The analysis of the event-free survival (EFS) curves showed that the clinical outcome was drastically affected for all B-ALL patients with high levels of *EGR1* (Fig. S5 L). This is partially explained by the observation that *EGR1* expression was higher in high-risk genetic subgroups (i.e., Ph-like and *KMT2A*-rearranged subgroups) than in B-ALL subgroups associated with a better prognosis (i.e., *ETV6::RUNX1*, *TCF3::PBX1*, hyperdiploid, and *PAX5*alt) (Inaba and Pui, 2021) (Fig. S5 M). Furthermore, the poor clinical outcome was also strikingly associated with EGR1 expression within the different B-ALL oncogenic subgroups (Fig. 6 L). Collectively, our observations strongly suggest that cell quiescence and *EGR1* activation are common and oncogene-independent features of treatment-resistant B-ALL cells.

Discussion

In the present study, we found that a single primary oncogenic event of B-ALL is sufficient to confer stem cell–like features to a subset of committed B cell progenitors, converting them to pre-LSCs. Combined with an unsupervised clustering representation of FACS data, our multiparametric immunophenotypic approach allowed for a precise visualization of the normal progression of B cells throughout differentiation. In addition, this strategy revealed concomitantly the presence of an aberrant B cell population in preleukemic PE^{tg} mice, characterized by the abnormal co-occurrence of phenotypic markers. To date, this exhaustive coverage of the B cell differentiation has not yet been described in leukemic mouse models, mainly limited by the number of simultaneously assayed markers. However, the identification of aberrant antigen coexpression is commonly used in clinics to define the MRD in B-ALL (Cherian and Soma, 2021; Hassanein et al., 2009) based on the principle that leukemic cells express phenotypic features that can be used to distinguish them from normal hematopoietic cells. Moreover, the development of single-cell mass cytometry (CyTOF) approach, quantifying simultaneously a large number of surface markers and intracellular phosphorylated proteins, allowed for the identification of several features involved in normal and pathological B cell development in humans with unprecedented resolution (Bendall et al., 2014; Good et al., 2018). Thus, our approach reinforces the notion that exploring abnormal coexpression using a large number of phenotypic markers is a valuable approach to predict the aberrant differentiation state occurring in cells.

Combined with RNA-seq, the integration of intracellular phosphorylated proteins established that the ectopic activation of IL7r/JAK-STAT pathway, which is normally shut down by the pre-BCR/BLNK axis, favors the differentiation blockade of preleukemic cells. Thus, the imbalance between the IL7r/JAK-STAT pathway and pre-BCR/BLNK axis appears as a critical feature of B-ALL initiation. Interestingly, this molecular imbalance, including unresponsive pre-BCR signaling, has been shown to predict patient relapse in B-ALL (Good et al., 2018). Moreover, secondary alterations in human B-ALL frequently mimic cytokine-receptor signaling through the constitutive phosphorylation of STAT5 (*IL7R*, *CRLF2*, and *JAK* mutations) or mimic the pre-BCR downstream pathway through the constitutive activation of the RAS/MAPK signaling (*NRAS*, *KRAS*, and *PTPN11*

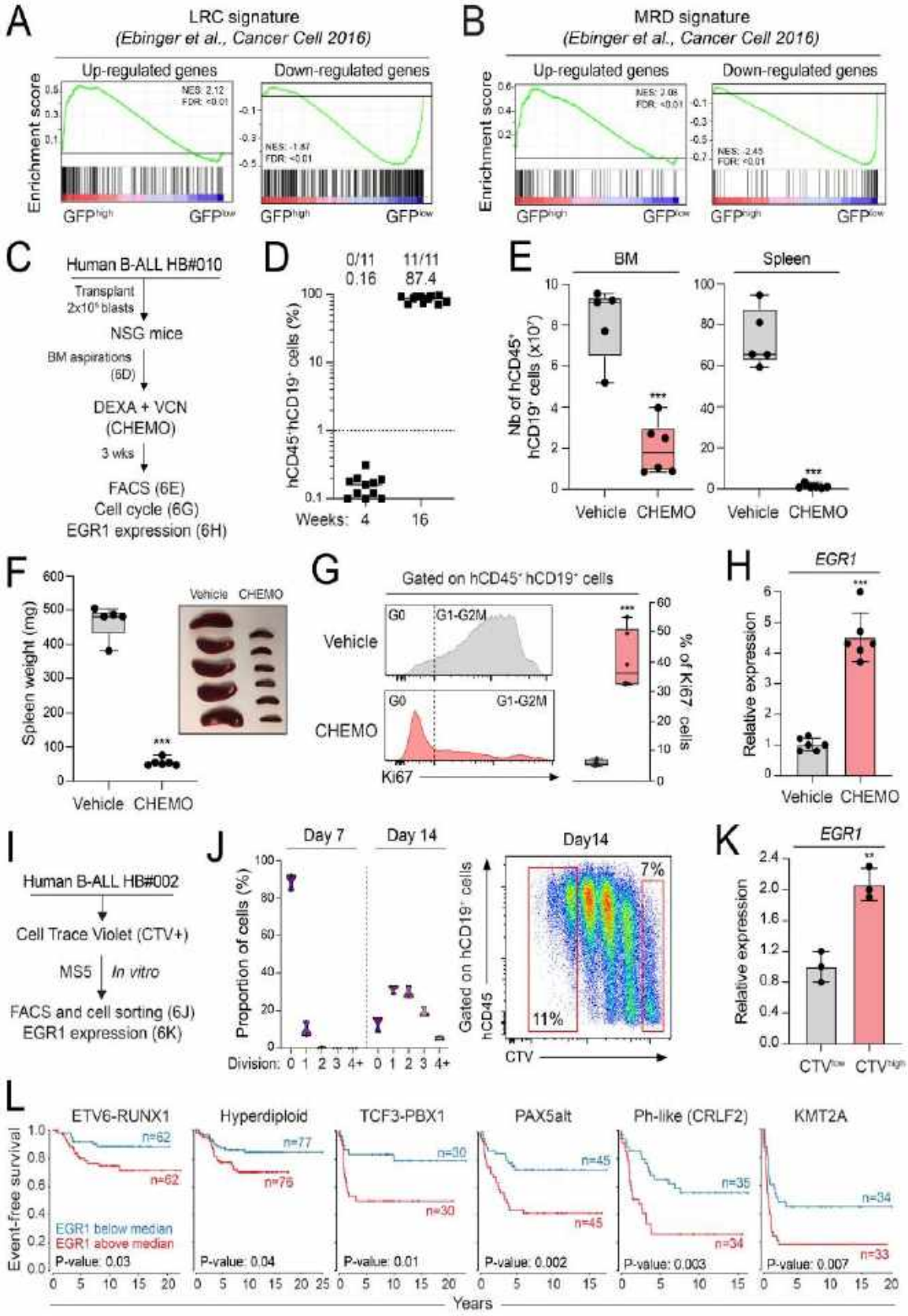

Figure 6. **EGR1 activation in quiescent and therapy-resistant human B-ALL. (A and B)** GSEA of the up- (left panels) and down- (right panels) regulated genes from CFSE label-retaining human B-ALL cells (LRC signature, A) or from residual human B-ALL cells after chemotherapies (MRD signature, B) (Ebinger et al., 2016) between GFP^{high} and GFP^{low} cells. NES and FDR values are indicated. **(C–H)** Experimental procedure to explore EGR1 expression in resistant human B-ALL cells (C). Leukemic blasts from the "de novo" B-ALL patient HB#010 were transplanted into NSG mice ($n = 11$). The proportion of hCD45$^+$hCD19$^+$ B-ALL blasts in BM aspirations was assessed 4 and 16 wk after transplantation (D). Engrafted mice were randomly selected for treatment (CHEMO) or not (vehicle) with a chemotherapeutic cocktail (DEXA+VCR) during 3 wk. Human B-ALL reconstitution (number of hCD45$^+$hCD19$^+$ B-ALL blasts) was monitored by FACS in the BM and the spleen after the treatment (E). Spleen weight was measured, and a picture of the spleen is shown (F). Ki67 expression was determined by FACS

in blasts from the BM of treated and untreated mice (G). Data obtained with B-ALL patient HB#010 were compiled from five (vehicle) and six (CHEMO) mice per condition (***P < 0.001). The horizontal lines of the box plots indicate the median, while the boxes represent the first and the third quartiles of the data and the whiskers denote the minimum and the maximum values. Engrafted blasts were purified and mRNA levels of the human *EGR1* were determined by quantitative RT-PCR and normalized to *ABL1* gene. Error bars indicate mean ± SD (n = 6, ***P < 0.001) from two independent experiments (H). **(I–K)** Experimental procedure to explore EGR1 expression in quiescent human B-ALL cells (I). Leukemic blasts from the "de novo" B-ALL patient HB#002 were stained with CTV and the number of cell divisions (D0 to D4–5) after the coculture was then analyzed (J). The proportion of cells in each division was quantified (J, left panel). Red dotted gates were used to purify the D0 (CTV^{high}) and D4–5 (CTV^{low}) populations (J, right panel) and the expression of human *EGR1* were determined by quantitative RT-PCR (K, mean ± SD, n = 3, one experiment, **P < 0.01). **(L)** *EGR1* expression and its associated clinical outcome in B-ALL patient extracted from Gu et al. (2019). EFS curves of B-ALL patients with *EGR1* expression below (blue) and above (red) to the median. Patients are classified within the different B-ALL oncogenic subgroups.

mutations) (Jamrog et al., 2018; Mullighan et al., 2007). It has been recently demonstrated that mutations in these two pathways are mutually exclusive in human B-ALL (Chan et al., 2020). In addition, the concurrent reactivation of one pathway affects the activity of the other, reciprocally, leading to the subversion of B-ALL transformation (Chan et al., 2020). B-ALL development in the PAX5::ELN model is also associated with the acquisition of secondary mutations in genes of either JAK/STAT (*Jak3* mutations) or RAS/MAPK (*Kras* and *Ptpn11* mutations) signaling pathways (Jamrog et al., 2018). These observations, therefore, suggest that secondary mutations either reinforce the aberrant activation of the JAK/STAT pathway already primed in preleukemic cells or allow for a bypass of pre-BCR signaling deficiency to trigger B-ALL transformation.

Various studies suggest that the restricted cell cycle is an important mechanism of therapeutic resistance in both human and murine leukemia models (Ebinger et al., 2016; Gerby et al., 2016; Prost et al., 2015; Tremblay et al., 2018; Trumpp et al., 2010; Turati et al., 2021). In parallel with an in vitro cell division assay, we used the doxycycline-inducible *H2B-GFP*^{tg} mouse model to demonstrate in vivo the existence of a slow-cycling and drug-resistant population of pre-LSCs in the PAX5::ELN-induced B-ALL model. In particular, our work corroborates that self-renewal and clonal evolution could be restricted to a rare and slow-cycling population of preleukemic cells, as previously observed in the *Lmo2*-induced T-ALL model (Tremblay et al., 2018). This not only reinforces the importance of cell-cycle restriction in pre-LSC activities in two distinct lineages but also makes the *H2B-GFP* system a powerful in vivo tool to develop strategies targeting the quiescence and the resistance of relapse-inducing clones in different models.

Additionally, the present study brings new insights regarding the molecular mechanisms of the cell-of-origin of B-ALL demonstrating that quiescent pre-LSCs are characterized by a partial loss of B cell lineage identity and activate an HSPC-like molecular program. This finding is in agreement with pioneer works in acute myeloid leukemia and T-ALL demonstrating that a primary oncogene can activate an aberrant stem cell–like program in committed myeloid progenitors (Krivtsov et al., 2006) or thymocytes (McCormack et al., 2010). While the presence of PAX5::ELN induces the emergence of quiescent cells in committed B cells, its expression level in quiescent and cycling cells is quite similar. Notwithstanding the fact that functional and molecular stem cell–like features were focused in quiescent cells, this observation raises at least two questions: (i) whether cell-cycle restriction is a common aberrant characteristic of pre-LSCs or is a critical property to prime leukemia initiation, and (ii) whether stem cell properties of pre-LSCs such as self-renewal, drug resistance, and leukemia-initiating activity are reversible processes, as demonstrated on human B-ALL blasts (Ebinger et al., 2016).

The question of whether a primary genetic alteration induces sufficient molecular and functional plasticity to cause lineage subversion remains poorly explored. A previous investigation on the cell-of-origin in mixed phenotype acute leukemia supports the notion that a founding alteration, rather than the secondary events, induces lineage plasticity in preleukemic clones (Alexander et al., 2018). Another study using lineage-specific oncogene activation also shows that *ETV6::RUNX1* fusion protein can induce both B-ALL and T-ALL, and that leukemia transformation is dependent on the nature of the secondary mutations (Rodríguez-Hernández et al., 2021). While *ETV6::RUNX1* is associated with B-ALL in humans, this work suggests that preleukemic clones can exhibit a T cell potential when expressed in the appropriate lineage. Our results revealed that the TF activity of PAX5 and EBF1, considered master factors to maintain B cell identity by suppressing alternative lineage choices (Busslinger, 2004; Nutt et al., 1999; Ramamoorthy et al., 2020), is downregulated in quiescent pre-LSCs. The downregulation of PAX5 and EBF1 activity is associated with the upregulation of PU-1 and RUNX1 activity, and with the activation of a non-B cell molecular program. Integrating chromatin accessibility and gene expression data recently brought major insights and facilitated the identification of putative regulatory regions and their candidate binding TFs, thus allowing a more precise definition of the regulatory networks in immune cells (Miraldi et al., 2019; Pokrovskii et al., 2019). Here, we applied this computational method to build cluster-specific TRNs that define the molecular identity and plasticity of quiescent pre-LSCs in our model. In particular, this approach allowed us to identify Egr1 as a strong TF candidate regulating positively pre-LSC quiescence. In addition, our loss-of-function approach demonstrated that Egr1 inhibition reverses, at least partially, the cell quiescence of preleukemic PAX5-ELN cells. This observation is consistent with its critical role in controlling normal HSC dormancy, localization, and functions that have been described using both *Egr1*$^{-/-}$ mouse model (Min et al., 2008) and RNA interference in human $CD34^+$ cord blood–derived HSPCs (Stoddart et al., 2022). Finally, molecular similarities with resistant clones in B-ALL patients after chemotherapy (Ebinger et al., 2016; Turati et al., 2021), including the upregulation of *EGR1*, strongly make our PAX5::ELN quiescent pre-LSCs a

relevant drug-resistant cellular platform to develop new targeted therapies.

Materials and methods

Mice

PAX5::ELN (*PE*^{tg}) transgenic mouse model was developed by our team as previously described (Jamrog et al., 2018). Briefly, cDNA encoding the human PAX5::ELN fusion protein was inserted at the *IgH* locus under the control of a VH promoter (PVH) and the endogenous Eμ enhancer to trigger PAX5::ELN expression in the early phase of B cell development. The previously developed inducible *TetOP-H2B-GFP* (*H2B-GFP*^{tg}) mouse model (Foudi et al., 2009) was purchased from Jackson Laboratory. *Rosa26-Cas9* (*Cas9*^{tg}) mice (Tzelepis et al., 2016) were generously provided by the Wellcome Sanger Institute of Cambridge (UK). Homozygous *PE*^{tg}, *H2B-GFP*^{tg}, and *Cas9*^{tg} mice were maintained by crossbreeding, their genotypes were verified by PCR, and all the experiments were performed in heterozygous mice. C57BL6 (Ly6.2, CD45.2) mice were purchased from Charles River Laboratories and Pep3b (Ly6.1, CD45.1) B6.SJL congenic mice were initially obtained from The Jackson Laboratory. All animals were housed in pathogen-free conditions (Anexplo US006 CREFRE) in accordance with the European Directive 2010/63/EU and the French Institutional Guidelines for animal handling. Mice were handled according to protocols approved by the Regional Ethical Committee (agreement #A31555010). Mice were backcrossed into the C57BL6 background for >10 generations.

FACS analysis and cell sorting

Single-cell suspensions were prepared from BM of wt and *PE*^{tg} mice of the indicated ages in Iscove's modified Dulbecco's medium (IMDM; Gibco) supplemented with 2% fetal bovine serum (FBS) (Stemcell Technologies). Immunostainings were performed using antibodies for flow cytometry obtained from Pharmingen (BD Biosciences), Invitrogen, and Miltenyi are listed in Table S1. FACS analysis was performed on a Fortessa cytometer (BD Biosciences) using FlowJo (BD Biosciences) software. For surface staining, cells were incubated with the antibodies for 20 min in IMDM 2% FBS at 4°C and washed twice with PBS1X before analysis. For cell-cycle analysis, cells were fixed and permeabilized (CytofixCytoperm Plus; BD Bioscience) for 30 min before staining with the anti-Ki67 antibody, in accordance with the manufacturer's instructions. For cell sorting, BM cells from wt or preleukemic *PE*^{tg} mice were flushed, and B cell fraction were enriched by B220 magnetics microbead sorting (Miltenyi Biotech). B cell fraction was subsequently incubated with anti-CD19, -CD23, and -Kit antibodies listed in Table S1. Cell sorting of Kit$^+$ and Kit$^-$ (CD19$^+$CD23$^-$) B cells was performed on a MoFlo Astrios sorter (Beckman Coulter).

Uniform manifold approximation and projection (UMAP) analysis

UMAP analysis was performed using FlowJo software. At least four samples per condition were pregated on single cells of the population of interest. Then, informatic cleaning and normalization were performed using FlowAI package (V2.1) (Monaco et al., 2016) and CytoNorm package (V1.0) (Van Gassen et al., 2020) for each sample and the same number of cells were then concatenated. Arc sin transformation was performed manually for each marker to discriminate the different B cell populations. The dimension reduction algorithm UMAP (umap-learn Python package v2.4.0) (Becht et al., 2018) was run using Euclidian distance with 15 nearest neighbors and 0.5 distance parameters. Thus, the UMAP analysis was performed using a multiparametric staining by FACS integrating the 12 markers shown in Fig. S1 A covering all the steps of the B cell differentiation. UMAP representations of the cell density and the clustering analysis of the different B cell subpopulations are based on the gating strategy shown in Fig. S1, B and C. In the UMAP analyses, each subset is represented by one color. Black arrow indicates the physiological phenotypic progression of B cells in the differentiation, and red dotted line delimits the aberrant preleukemic B cell population induced by PAX5::ELN.

In vitro coculture assays

B cell populations were cocultured on MS5 stromal cells in a B cell medium composed of IMDM 10% FBS, 0.05 mM β-mercaptoethanol (Sigma-Aldrich), 2 mM *L*-glutamine (Invitrogen), penicillin (100 U/ml), and streptomycin (100 U/ml), and supplemented with 5 ng/ml of murine Il7, 10 ng/ml of murine Flt3L, and 10 ng/ml of murine stem cell factor (SCF) (Peprotech).

In vivo transplantation assays

Donor and recipient mice were on C57BL6 (Ly6.2, CD45.2) and Pep3b (Ly6.1, CD45.1) backgrounds, respectively, allowing for the discrimination of host- and donor-derived cells on the basis of CD45 alleles. For the serial transplantation assay, total B cells (B220$^+$) from the BM of wt or preleukemic *PE*^{tg} mice (30 days old; CD45.2$^+$) were purified and transplanted intravenously in equal numbers (4.5×10^6 cells per mouse) into primary (I) recipient mice (6–8 wk-old; CD45.1$^+$). Then, one fifth of the total BM cells from primary mice were transplanted in equal numbers (~20×10^6 cells per mouse) into secondary (II) recipients. To measure the short-term reconstitution potential of preleukemic B cells, the chimerism was analyzed by flow cytometry (FACS) 2 wk after each transplantation and was illustrated by the percentage of donor-derived cells (% CD45.2$^+$) found in the BM of recipient mice. Finally, one fifth of the total BM cells from secondary mice were transplanted in equal numbers (~20×10^6 cells per mouse) into tertiary (III) recipients to assess the long-term B-ALL development, represented by Kaplan–Meier survival curves. All the recipient mice (CD45.1$^+$) were pretreated, 24 h before transplantation, with 30 mg/kg of Busulfan (Busilvex; Pierre Fabre) (related to Fig. 1, D–G).

Kit$^+$ and Kit$^-$ (CD19$^+$CD23$^-$) B cells from the BM of preleukemic *PE*^{tg} mice (CD45.2) were purified and intravenously transplanted in equal numbers (5×10^4 per mouse) in primary (I) recipient CD45.1 mice. Kit$^+$ (CD19$^+$CD23$^-$) B cells from the BM of wt mice were purified and transplanted (5×10^4 per mouse) as control. BM cells from the primary transplantation with preleukemic *PE*^{tg} Kit$^+$ et Kit$^-$ cells were transplanted in secondary (II) recipients (related to Fig. S2 C and Fig. 1, H and I).

Purified D0–2 and D8–9 cells (CD45.2$^+$) from CTV-labeled preleukemic *PE*^{tg} cells were transplanted in equal numbers (2 × 10^3 per mouse) in recipient CD45.1 mice (related to Fig. 2, D, I, and J).

Purified GFP^{high} and GFP^{low} cells from preleukemic *PE*^{tg}*H2B-GFP*^{tg} mice (CD45.2$^+$) were transplanted in equal numbers (1.5 × 10^4 per mouse) in recipient CD45.1 mice. Engraftment was monitored by FACS and was illustrated by the percentage of donor-derived cells (% CD45.2$^+$) found in recipient mice after BM punctions. For all transplantation experiments, the number of positive mice and the median of engraftment are indicated. Statistical significance was calculated using an unpaired *t* test. For Kaplan–Meyer survival curves, the median of time required to develop the B-ALL is indicated on the curve (related to Fig. 4 E and Fig. S3 D).

In vitro cell division assay

Cell division of Kit$^+$ (CD19$^+$CD23$^-$) wt and *PE*^{tg} B cells were analyzed by using CTV dilution. Briefly, total B cells (10^6 cells/ml) from wt and preleukemic *PE*^{tg} mice (30 days old) were labeled with 5 µM CTV (C34557; Thermo Fisher Scientific) in PBS1X during 20 min at 37°C. CTV-labeled B cells were then washed twice in PBS1X 1% FBS according to the manufacturer's recommendations and plated on MS5 stromal cells for 24 h to stabilize the staining. Then, Kit$^+$ (CD19$^+$CD23$^-$) CTV-labeled B cells were purified by cell sorting and cocultured for 3 days on an MS5 cell line in a supplemented B cell medium. Since dividing cells equally distribute the dye to daughter cells, the number of cell divisions can be followed by a decrease in the fluorescence intensity. Cell division was analyzed using Winlist (Verity Software House), and proliferation index (PI) was calculated as described (Roederer, 2011). Slow- (D0–2) and high- (D8–9) cycling *PE*^{tg} cells were purified by cell sorting. High- (D8–9) cycling wt cells were also purified as a control to perform the subsequent functional and molecular experiments as indicated in the experimental procedure detailed in Fig. 2 D.

In vivo cell division assay

Wt or homozygous *PE*^{tg} mice were bred with homozygous *H2B-GFP*^{tg} mice to obtain heterozygous *H2B-GFP*^{tg} and *PE*^{tg}*H2B-GFP*^{tg} mice, respectively. To induce *H2B-GFP* transgene expression, 20-day-old mice were intraperitoneally treated with 40 mg/kg of doxycyxline (DOX, D9891; Sigma-Aldrich) and 2 mg/ml of DOX, supplemented with sucrose (S9378; Sigma-Aldrich) at 10 mg/ml, was added to drinking water for 5 wk (DOX pulse). GFP expression in all B cell subpopulations was then examined following withdrawal of doxycycline (DOX chase) for 0, 1, 2 and 3 wk. Quantification of GFP was determined for each time point by ranking 10^4 wt or *PE*^{tg} cells from the lowest to the highest value of their GFP fluorescence intensity and the area under the curve (AUC) was then calculated. White and black dotted lines indicate the standard error of the mean (SEM) of wt and *PE*^{tg} AUC, respectively. The proportion of persisting GFP-retained (GFP^{high}) cells is indicated for each time point (related to Fig. 4, A–C). Purification of GFP^{high}, GFP^{med}, and GFP^{low} B cells was performed after 1 wk of DOX chase using a MoFlo Astrios cell sorter (Beckman Coulter).

Phosphoflow cytometry

Phosphoflow cytometry experiments are related to Fig. 3, B and E; and Fig. S3 A to explore IL7r and pre-BCR signaling pathways in preleukemic B cells. As shown in Fig. 3 A, the IL7r signal induces Stat5 phosphorylation that activates the transcription of *Cdkn2a*, *IL2rα*, *Tnfrsf13b*, and *Socs3* to promote cell survival and proliferation. In parallel, IL7r activates the PI3K signaling pathway that phosphorylates and represses Foxo1, the inducer of *Rag1* and *Rag2* gene transcription, therefore inhibiting *Igκ* gene recombination. In contrast, pre-BCR signal induces Syk/Blnk/Plcγ2 phosphorylation cascade that converges to the transcription of *Ikzf3* and *Irf8* that inhibit pre-B cell proliferation and initiate *Igκ* gene recombination, respectively. Together, each receptor has antagonistic and balanced functions to coordinate the proliferation and differentiation switch in pre-B cells.

1.5 × 10^6 cells from each wt and preleukemic *PE*^{tg} BM were mixed, and surface markers were stained in RPMI (Gibco) supplemented with 2% FBS for 10 min at 37°C and washed with RPMI (centrifugation, 5 min; 1,200 rpm).

IL7r-ligand stimulation was assessed by phosphoflow cytometry after the ex vivo activation of preleukemic *PE*^{tg} BM cells with IL-7 (+IL-7). Unstimulated (−IL-7) cells were used as control. Normal B cells and aberrant B *PE*^{tg} cells were distinguished according to the level of B220 expression, and pStat5 and pFoxo1 expression were detected by FACS. IL7r-ligand stimulation was performed by incubating the cells with RPMI 2% FBS supplemented or not with 30 ng/ml IL-7 (Peprotech) for 15 min at 37°C for the detection of pStat5 and for 16 h at 37°C for the detection of pFoxo1. For the staining of pStat5, cells were then fixed with prewarmed Lyse/Fix buffer 1× for 12 min at 37°C, washed twice (centrifugation, 7 min; 500 rpm) in RPMI 2% FBS, and permeabilized with cold Perm Buffer III for 30 min at 4°C, according to the manufacturer's instructions (BD Phosphoflow). Cells were washed twice in PermWash buffer and the intracellular immunostainings with the anti-pStat5 antibody combined with the anti-Ki67 antibody were performed for 30 min at room temperature, followed by two washes before FACS analysis. For the staining of pFoxo1, cells were fixed and permeabilized with cold CytofixCytoperm Plus buffer (BD Bioscience) for 24 h at 4°C and washed twice (centrifugation, 7 min; 500 rpm) in PermWash buffer (BD Bioscience). The intracellular immunostainings with the anti-pFoxo1 antibody combined with the anti-Ki67 antibody were performed in PermWash buffer for 1 h at room temperature, followed by two washes (centrifugation, 7 min; 500 rpm) before FACS analysis.

(Pre-)BCR stimulation was assessed by phosphoflow cytometry after the ex vivo activation of preleukemic *PE*^{tg} BM cells with H_2O_2 ($H_2O_2^+$). Unstimulated ($H_2O_2^-$) cells were used as control. Normal B cells and aberrant B *PE*^{tg} cells were distinguished according to the level of B220 expression, and pBlnk and pPlcγ2 expression was detected by FACS. (Pre-)BCR stimulation was performed by incubating the cells with RPMI 2% FBS supplemented or not with 1 mM H_2O_2 for 5 min at 37°C. Cells were then fixed and permeabilized with cold CytofixCytoperm Plus buffer (BD Bioscience) for 45 min at 4°C and washed twice (centrifugation, 7 min; 500 rpm) in PermWash buffer (BD Bioscience). The intracellular immunostainings with the anti-pBlnk

or the anti-pPlcγ2 antibodies combined with the anti-Ki67 antibody were performed in PermWash buffer for 30 min at room temperature, followed by two washes (centrifugation, 7 min; 500 rpm) before FACS analysis. Immunostaining combinations used for the phospflow cytometry are listed in Table S1.

Lentiviral production and transduction for gene editing by CRISPR/Cas9

sgRNAs targeting the exon 1 of *Egr1* (Table S1) were designed using CCTop-CRISPR/Cas9 target online predictor software (Center for Organismal Studies Heidelberg) and subcloned in pLKO5-sgRNA-EFS-GFP, in which the sgRNA and GFP coding sequences are controlled by the U6 and the EF1α promoters, respectively (Heckl et al., 2014). Concentrated VSV/G pseudotyped lentiviral vectors pLKO5-sgRNA-EFS-GFP encoding sgRNA *Egr1* (sgEgr1 T5 and T7) or sgCTL were produced by the vectorology facility Vect'UB (TBMCore—CNRS UAR3427, INSERM US005, Universtiy of Bordeaux, Bordeaux, France). Titrations of produced lentiviral vectors were performed on the HEK293T cell line. Homozygous PE^{tg} mice were bred with homozygous $Cas9^{tg}$ mice to obtain heterozygous $PE^{tg}Cas9^{tg}$ mice. Aberrant B cells from the BM of preleukemic $PE^{tg}Cas9^{tg}$ mice were purified by cell sorting, plated in suspension culture in B cell medium and transduced with lentiviral vectors expressing sgCTL or sgEgr1 T5 and sgEgr1 T7 at a multiplicity of infection of 30 in the presence of 4 µg/ml of polybrene (Sigma-Aldrich) for 24 h. Transduced cells were then washed in PBS1X and cocultured on MS5 stromal cells in a fresh supplemented B cell medium for 3 days. Transduced GFP^+ cells were then purified by cell sorting to perform in vitro cell division assay and cell differentiation assay in coculture on MS5 stromal cells in a B cell medium supplemented with a low concentration of Il-7 (0.5 ng/ml) and with Flt3L (10 ng/ml) and SCF (10 ng/ml) (related to Fig. 5, E and F; and Fig. S4, F–J).

Next-generation sequencing (NGS) of targeted gene regions

The targeted region (exon 1) of *Egr1* was performed by NGS, and the genomic editing efficiency was analyzed by the proportion (%) of insertions and deletions (InDel) induced by the sgRNA Egr1 T5 and T7. Genomic DNA was extracted and purified using QIAamp DNA mini kit (Qiagen). Sequencing was performed using a MiSeq sequencer (Illumina) using a Miseq Reagent kit V2 (paired-end sequencing 2 × 150 cycles). Genome editing efficiency of the targeted *Egr1* region (exon 1) was analyzed using the online CRISPResso software (https://crispresso.pinellolab.partners.org/submission; Canver et al., 2018). Targets and primers are listed in Table S1.

Human B-ALL samples

Human B-ALL samples were obtained from the Toulouse University Hospital (Toulouse, France) after signed written informed consent for research use in accordance with the Declaration of Helsinki and stored at the Hémopathies malignes de l'Inserm en Midi-Pyrénées (HIMIP) collection (BB-0033-00060). According to the French law, HIMIP biobank collection has been declared to the Ministry of Higher Education and Research (DC 2008-307, collection 1) and obtained a transfer agreement for research applications (AC 2008-129) after approbation by our institutional review board and ethics committee (Comité de Protection des Personnes Sud-Oust et Outremer II). Biological annotations of the samples have been declared to the Comité National Informatique et Libertés (i.e., Data Processing and Liberties National Committee). For in vitro cell division assay using CTV dilution, human B-ALL blasts (HB#002 and HB#008) were stained as previously described, and CTV-labeled cells were grown in cocultured on MS5 cell line in supplemented B cell medium and analyzed at the indicated time points in the Fig. 6 J and Fig. S5 J.

PDX model and in vivo treatment with chemotherapy

NSG mice were produced at the Génotoul-Anexplo platform in Toulouse, France, using breeders obtained from Charles River Laboratories. Mice were housed in sterile conditions using high-efficiency particulate arrestance-filtered microisolators and fed with irradiated food and sterile water. Mice (6–9 wk old) were sublethally treated with busulfan 30 mg/kg 24 h before injection of leukemic cells. Leukemic blasts from B-ALL patients were thawed at room temperature, washed twice in PBS, and transplanted by intravenous injection (2×10^5 cells per mouse). At the indicated time points in Fig. 6 D and Fig. S5 C, leukemia engraftment was monitored by FACS with hCD45 (557748; BD Bioscience) and hCD19 (562294; BD Bioscience) staining after BM punctions. For combination therapy, a chemotherapeutic cocktail composed of DEXA (10 mg/kg) and VCR (0.5 mg/kg) was administered weekly for 3 wk (HB#010; Fig. 6 C) and for 1 wk (HB#007; Fig. S5 B) via intraperitoneal injection. A daily administration of 10 mg/kg DEXA was supplemented during the period of treatment. Mice were euthanized and analyzed after the treatment.

Quantitative RT-PCR

RNA was isolated using the Trizol method, and cDNA was synthesized using SuperScript VILO cDNA Synthesis Kit (Invitrogen) according to the manufacturer's instructions. Quantitative SYBR Green PCR was performed on a LightCycler480 II System (Roche) to quantify human *EGR1* cDNAs expression in Fig. 6, H and K; and Fig. S5, G and K using LightCycler480 SYBR Green I Master (Roche Diagnostics GmbH) according to the manufacturer's instructions. All PCR were carried out as follows in a 20 µl volume: 5 min at 95°C, followed by 45 cycles of 10 s at 95°C, 10 s at annealing temperature of 60°C and 10 s at 72°C. Quantification was performed using the ΔCt method with normalization to the human *ABL1* gene expression levels. Data were analyzed using the LC480 software (Roche Diagnostics). The forward (Fw) and reverse (Rev) primers used were as follows: for EGR1 (Fw: 5′-CAGCCCTACGAGCACCTGAC-3′ and Rev: 5′-GTGGTTTGGCTGGGGTAACT-3′); for ABL1 (Fw: 5′-TGGAGATAACACTCTAAGCATAACTAAAGGT-3′ and Rev: 5′-GATGTAGTTGCTTGGGACCCA-3′).

Statistical analysis

The number of biological replicates is indicated in the relevant figure legends. Error bars for pooled replicates represent standard deviation (SD). Statistical differences were determined

using a two-tailed unpaired Student's *t* test for comparison of quantitative variables, assuming normality and equal distribution of variance between the different groups analyzed. All statistical analyses were performed using GraphPad Prism software, version 7 (GraphPad). A P value of <0.05 was considered statistically significant (*P < 0.05, **P < 0.01, ***P < 0.001). Survival in mouse experiments was represented with Kaplan–Meier curves (GraphPad Prism).

RNA-seq

RNA from purified PE^{tg} D0–2 ($n = 2$) and D8–9 ($n = 2$) cells and from wt D8–9 ($n = 2$) cells was isolated with the RNeasy Plus Mini Kit (Qiagen). RNA-seq libraries were prepared using TruSeq Stranded mRNA Low Sample kit (Illumina) according to the manufacturer's protocol, starting with 300 ng mRNA. Cluster generation and sequencing were carried out by using the Illumina NEXTSEQ 550 system and NEXTSEQ 500/550 HIGH OUTPUT KIT v2.5 (150 cycles) with a read length of 2 × 75 nucleotides according to the manufacturer's guidelines. The expression of mRNA transcripts rearranged for the *IgH* and *IgL* loci was analyzed using Mixcr software and represented by Circos diagrams using VDJ tool software (related to Fig. 2 G).

ULI RNA-seq

GFP^{high} and GFP^{low} cells from the aberrant B population of preleukemic *PE^{tg}H2B-GFP^{tg}* mice after 1 wk of DOX chase were purified by cell sorting (Melody, BD) directly in RLT buffer, and the RNA was isolated with the RNeasy plus micro kit (Qiagen). Smart-seqv4 libraries were prepared as previously described (Picelli et al., 2014) using the Takara SMART-Seq v4 full-length transcriptome analysis kit according to the manufacture's guidelines. Paired-end sequencing was performed on an Illumina NextSeq 500 using 2 × 75 bp reads. Low-quality reads were trimmed, and adaptor sequence was removed using fastp (v). Short reads were then mapped to mm10 genome using RNA-STAR (v2.7.8a) with doublepass parameter. Low-quality mapping and duplicated reads were removed and the remaining reads was count using featurecount (v) with default paired-end parameter.

A specific region in the exon 7 of Pax5 (Chr4: 44,609,844–44,609,786), which is enriched in SNPs, was for the quantification of reads from murine *Pax5* (Pax5 WT) and from human *PAX5* (PAX5-ELN) (related to Fig. S4 B).

GSEA of top 500 differentially expressed genes (bulk RNA-seq EGAD00001006133) of residual human B-ALL cells after chemotherapies published in Turati et al. (2021) (corresponding to acutely treated versus untreated PDX from patient 2) was performed in preleukemic *PE^{tg}H2B-GFP^{tg}* (Fig. S5 A).

For the integration of the ImmGen database, the same preprocessing pipeline was used for all the ImmGen fastq (GSE109125) except that the reads of the *PE^{tg}H2B-GFP^{tg}* samples were trimmed to 25 bp to match the ImmGen reads length and avoid mappability bias. The ComBat function in the sva R package was used to correct the batch effect between our and ImmGen samples. Regularized log-transformed (rlog) values were calculated by DESeq2, used to calculate k-means, and perform our integrative approach.

ATAC-seq libraries generation and processing

Sorted *PE^{tg}H2B-GFP^{tg}* populations were prepared according to Buenrostro et al. (2013) using ATAC-Seq kit (#53150; Active-motif). The size distribution and concentration of the libraries were assessed on Tapestation with a DNA High Sensitivity kit (Agilent Technologies). Paired-end 37.5 bp sequences were generated from samples on an NextSeq 500 (Illumina), generating an average of 125 millions of reads per sample.

First, FastQC was used to assess the sequence quality. Foreign sequences removal and trimming are realized with Sickle (qual threshold 20 and length threshold 20). Sequences were mapped to the murine genome with Bowtie2 (2.4.2) (Langmead and Salzberg, 2012) with -X 2,000 (maximal fragment length), very sensitive, and against mm10. Next, we performed various cleaning steps according to Berest et al. (2019): in brief, removing mitochondrial reads, filtering reads with mapping quality <20, removing duplicate reads, and adjusting read start sites as described previously (Buenrostro et al., 2013) (+4 −5). Lastly, a GC bias diagnosis and correction using deepTools was run for each sample. The output of this preprocessing pipeline was used to peak calling using MACS2 with -SE -200 -100 -lambdafix parameter and removal of blacklisted regions.

diffTF and HINT-atac analysis

The complete diffTF pipeline (Berest et al., 2019) was run using TF binding sites generated by PWMscan analysis (cutoff P val: 0.00001; background base composition: 0.29;0.21;0.21;0.29) of each JASPAR2020 PWM motif to obtain the position of 644 nonredundant and specific motifs. The analytical approach was preferred due to the small size of the sample, and paired design was used for DeSeq2 parameter. For the plotting of individual activity for each TF, we used Hint-atac pipeline (Li et al., 2019) with a standard parameter on the combination of the bam for each condition to scan the JASPAR2020 database.

Fastq ATAC-seq data of interest from the ImmGen database was extracted from GSE100738 preprocessed as described previously, and the totality of the reads from all samples was normalized together using local loess normalization as described in Reske et al. (2020) with csaw package. Finally, to represent pile-up traces of the integrated data, Becorrect (Gontarz et al., 2020) was used on each bedgraph file with their corresponding normalized counts.

TNR inference

Peaks were associated with putative TF binding events and target genes to generate a prior network: $P\varepsilon R^{|genes|\ \times\ |TFs|}$ of TF–gene interactions. We used vertebrate motifs from JASPAR2020 to scan the differential *PE^{tg}H2B-GFP^{tg}* peaks, running construct_atac_prior.R script (P val cutoff = 10^{-5}; window_-feature = 25 kb; background set as A = 0.29, C = 0.21, G = 0.21, T = 0.29). We built gene expression models according to Miraldi et al. (2019) and included in our study a target gene expression matrix containing the 1,625 core *PE^{tg}H2B-GFP^{tg}* genes for a total of 26 samples: LT-HSC ($n = 2$), MPP1 ($n = 2$), ST-HSC ($n = 2$), MPP4 ($n = 2$), CLP ($n = 2$), FrA ($n = 2$), FrBC ($n = 2$), FrE ($n = 2$), $H2B^{high}$ ($n = 5$), and $H2B^{low}$ ($n = 5$). We considered 275 potential TF regulators corresponding to most variable TFs across the samples. The parameters used were moderate prior reinforcement (λbias = 0.05), 50 subsamples of size 0.90 × |samples|, and an instability cutoff of

0.05 to solve the TF-gene interactions. The *PE*^{tg}*H2B-GFP*^{tg} TRN size was set to an average of 15 TFs per gene and resulted in a total of 24,275 TF-gene interactions.

Online supplemental material

Fig. S1 describes the gating strategy of the different B cell subpopulations from the BM of wt and *PE*^{tg} preleukemic mice, and the expression of intracytoplasmic ELN and of Sca-1 surface marker are explored. Fig. S2 displays the immunophenotype of *PE*^{tg} B cells after serial transplantations; the survival curve of quaternary recipient mice after transplantation of *PE*^{tg} B-ALL cells; the cell-cycle status (Ki67) of wt and *PE*^{tg} preleukemic B cells in steady state and in response to chemotherapy; the expression of Kit in CTV-labeled wt and preleukemic *PE*^{tg} cells; the expression of PAX5-ELN in *PE*^{tg} D0–2, *PE*^{tg} D8–9, and wt D8–9 cells; the dose-response of chemotherapy on wt and preleukemic *PE*^{tg} Kit^{+} cells; and the immunophenotype of engrafted cells in recipient mice transplanted with D0–2 and D8–9 preleukemic *PE*^{tg} cells. Fig. S3 shows FACS analysis of pStat5/pFoxo1 and of pBlnk/pPlcγ2 on *PE*^{tg} B cells after IL-7 and H_2O_2 stimulation respectively; signaling pathways that are up- and down-regulated in *PE*^{tg} D0–2 and *PE*^{tg} D8–9 cells; the kinetic of GFP expression in the different B cell subsets from wt *H2B-GFP*^{tg}; and preleukemic *PE*^{tg}*H2B-GFP*^{tg} mice after DOX chase, the survival curve of recipient mice transplanted with purified GFP^{high} and GFP^{low} cells from *PE*^{tg}*H2B-GFP*^{tg} mice and the heatmaps of signaling pathways up- and downregulated in GFP^{high} from RNA-seq and ATAC-seq data. Fig. S4 shows the accessibility footprints (ATAC-seq) and the expression levels (RNA-seq) of *Ebf1*, *Spi1*, *Runx1*, and *Pax5* in GFP^{high} and GFP^{low} cells from *PE*^{tg}*H2B-GFP*^{tg} mice; GSEA highlighting the quiescent state of GFP^{high} cells; the transduction efficiency of preleukemic *PE*^{tg}*Cas9*^{tg} B cells with sgCTL, sgEgr1 T5, and sgEgr1 T7 lentiviral vectors combined to the genomic editing efficiency of the Egr1 locus; the impact of Egr1 editing on the cell division and proliferation of preleukemic cells; and the molecular network of genes involving Egr1 from TRN#1. Fig. S5 displays the molecular similarities between GFP^{high} cells and residual human B-ALL cells after chemotherapies and shows EGR1 activation in quiescent and therapy-resistant human B-ALL. Table S1 contains the list of FACS antibodies and the sequence of oligonucleotide primers used in the study. Table S2 contains the RNA-seq data of *PE*^{tg} D0–2, *PE*^{tg} D8–9, and Wt D8–9 cells. Tables S3 and S4 contain the RNA-seq data and the ATAC-seq data of GFP^{high} and GFP^{low} cells, respectively. Table S5 presents the clustering data of modified genes and peaks from GFP^{high} and GFP^{low} cells according to their signal in the different steps of the normal differentiation.

Data availability

The RNA-seq and ATAC-seq data reported in this study (Tables S2, S3, and S4) are available at the at the Gene Expression Omnibus repository under the accession number GSE210926.

Acknowledgments

We acknowledge Pr. Tariq Enver and Pr. Javier Herrero for having shared their molecular data published in Turati et al. (2021). We acknowledge Manon Farcé from the cytometry and cell sorting facility of the Cancer Research Center of Toulouse (Institut National de la Santé et de la Recherche Médicale [INSERM] U1037) and the Anexplo/Genotoul platforms (UMS006) for technical assistance. We thank the vectorology facility Vect'UB for providing lentiviral particles and for technical support, TBMCore (Centre National de la Recherche Scientifique [CNRS] UAR3427, INSERM US005, University of Bordeaux, Bordeaux, France).

This study was supported by institutional grants from INSERM, from CNRS, the Institut National du Cancer (INCa-2020-096), the Agence Nationale de la Recherche (ANR-18-CE13-0002-01), and the Fondation ARC pour la Recherche sur le Cancer (PJA-20181207977). The team is supported by the Ligue Contre le Cancer and the associations "Laurette Fugain," "111 des arts," "Cassandra," and "Constance la petite guerrière astronaute."

Author contributions: V. Fregona designed the study, performed and analyzed the experiments, and wrote the manuscript. M. Bayet, M. Bouttier, L. Largeaud, C. Hamelle, L.A. Jamrog, N. Prade, S. Lagarde, S. Hebrard, I. Luquet, V. Mansat-De Mas, and M. Nolla performed experiments. M. Pasquet, C. Didier, A.A. Khamlichi, C. Broccardo, É. Delabesse, and S.J.C. Mancini reviewed the data and the manuscript. B. Gerby performed and analyzed experiments, conceived and supervised the project, and wrote the manuscript. All authors contributed to the final draft.

Disclosures: The authors declare no competing interests exist.

Submitted: 14 February 2023
Revised: 31 August 2023
Accepted: 3 October 2023

References

Adelman, E.R., H.T. Huang, A. Roisman, A. Olsson, A. Colaprico, T. Qin, R.C. Lindsley, R. Bejar, N. Salomonis, H.L. Grimes, and M.E. Figueroa. 2019. Aging human hematopoietic stem cells manifest profound epigenetic reprogramming of enhancers that may predispose to leukemia. *Cancer Discov.* 9:1080–1101. https://doi.org/10.1158/2159-8290.CD-18-1474

Alexander, T.B., Z. Gu, I. Iacobucci, K. Dickerson, J.K. Choi, B. Xu, D. Payne-Turner, H. Yoshihara, M.L. Loh, J. Horan, et al. 2018. The genetic basis and cell of origin of mixed phenotype acute leukaemia. *Nature.* 562:373–379. https://doi.org/10.1038/s41586-018-0436-0

Althoff, M.J., R.C. Nayak, S. Hegde, A.M. Wellendorf, B. Bohan, M.D. Filippi, M. Xin, Q.R. Lu, H. Geiger, Y. Zheng, et al. 2020. Yap1-scribble polarization is required for hematopoietic stem cell division and fate. *Blood.* 136:1824–1836. https://doi.org/10.1182/blood.2019004113

Aurrand-Lions, M., and S.J.C. Mancini. 2018. Murine bone marrow niches from hematopoietic stem cells to B cells. *Int. J. Mol. Sci.* 19:2353. https://doi.org/10.3390/ijms19082353

Becht, E., L. McInnes, J. Healy, C.A. Dutertre, I.W.H. Kwok, L.G. Ng, F. Ginhoux, and E.W. Newell. 2018. Dimensionality reduction for visualizing single-cell data using UMAP. *Nat. Biotechnol.* https://doi.org/10.1038/nbt.4314

Bendall, S.C., K.L. Davis, E.A.D. Amir, M.D. Tadmor, E.F. Simonds, T.J. Chen, D.K. Shenfeld, G.P. Nolan, and D. Pe'er. 2014. Single-cell trajectory detection uncovers progression and regulatory coordination in human B cell development. *Cell.* 157:714–725. https://doi.org/10.1016/j.cell.2014.04.005

Berest, I., C. Arnold, A. Reyes-Palomares, G. Palla, K.D. Rasmussen, H. Giles, P.M. Bruch, W. Huber, S. Dietrich, K. Helin, and J.B. Zaugg. 2019. Quantification of differential transcription factor activity and multiomics-based classification into activators and repressors: diffTF. *Cell Rep.* 29:3147–3159.e12. https://doi.org/10.1016/j.celrep.2019.10.106

Bousquet, M., C. Broccardo, C. Quelen, F. Meggetto, E. Kuhlein, G. Delsol, N. Dastugue, and P. Brousset. 2007. A novel PAX5-ELN fusion protein identified in B-cell acute lymphoblastic leukemia acts as a dominant negative on wild-type PAX5. *Blood.* 109:3417–3423. https://doi.org/10.1182/blood-2006-05-025221

Bradner, J.E., D. Hnisz, and R.A. Young. 2017. Transcriptional addiction in cancer. *Cell.* 168:629–643. https://doi.org/10.1016/j.cell.2016.12.013

Buenrostro, J.D., P.G. Giresi, L.C. Zaba, H.Y. Chang, and W.J. Greenleaf. 2013. Transposition of native chromatin for fast and sensitive epigenomic profiling of open chromatin, DNA-binding proteins and nucleosome position. *Nat. Methods.* 10:1213–1218. https://doi.org/10.1038/nmeth.2688

Busslinger, M. 2004. Transcriptional control of early B cell development. *Annu. Rev. Immunol.* 22:55–79. https://doi.org/10.1146/annurev.immunol.22.012703.104807

Cabezas-Wallscheid, N., F. Buettner, P. Sommerkamp, D. Klimmeck, L. Ladel, F.B. Thalheimer, D. Pastor-Flores, L.P. Roma, S. Renders, P. Zeisberger, et al. 2017. Vitamin A-retinoic acid signaling regulates hematopoietic stem cell dormancy. *Cell.* 169:807–823.e19. https://doi.org/10.1016/j.cell.2017.04.018

Canver, M.C., M. Haeussler, D.E. Bauer, S.H. Orkin, N.E. Sanjana, O. Shalem, G.C. Yuan, F. Zhang, J.P. Concordet, and L. Pinello. 2018. Integrated design, execution, and analysis of arrayed and pooled CRISPR genome-editing experiments. *Nat. Protoc.* 13:946–986. https://doi.org/10.1038/nprot.2018.005

Chan, L.N., M.A. Murakami, M.E. Robinson, R. Caeser, T. Sadras, J. Lee, K.N. Cosgun, K. Kume, V. Khairnar, G. Xiao, et al. 2020. Signalling input from divergent pathways subverts B cell transformation. *Nature.* 583:845–851. https://doi.org/10.1038/s41586-020-2513-4

Chavez, J.S., J.L. Rabe, D. Loeffler, K.C. Higa, G. Hernandez, T.S. Mills, N. Ahmed, R.L. Gessner, Z. Ke, B.M. Idler, et al. 2021. PU.1 enforces quiescence and limits hematopoietic stem cell expansion during inflammatory stress. *J. Exp. Med.* 218:e20201169. https://doi.org/10.1084/jem.20201169

Chen, Y., M. Yu, X. Dai, M. Zogg, R. Wen, H. Weiler, and D. Wang. 2011. Critical role for Gimap5 in the survival of mouse hematopoietic stem and progenitor cells. *J. Exp. Med.* 208:923–935. https://doi.org/10.1084/jem.20101192

Cherian, S., and L.A. Soma. 2021. How I diagnose minimal/measurable residual disease in B lymphoblastic leukemia/lymphoma by flow cytometry. *Am. J. Clin. Pathol.* 155:38–54. https://doi.org/10.1093/ajcp/aqaa242

Clark, M.R., M. Mandal, K. Ochiai, and H. Singh. 2014. Orchestrating B cell lymphopoiesis through interplay of IL-7 receptor and pre-B cell receptor signalling. *Nat. Rev. Immunol.* 14:69–80. https://doi.org/10.1038/nri3570

Cobaleda, C., W. Jochum, and M. Busslinger. 2007a. Conversion of mature B cells into T cells by dedifferentiation to uncommitted progenitors. *Nature.* 449:473–477. https://doi.org/10.1038/nature06159

Cobaleda, C., A. Schebesta, A. Delogu, and M. Busslinger. 2007b. Pax5: The guardian of B cell identity and function. *Nat. Immunol.* 8:463–470. https://doi.org/10.1038/ni1454

Coyaud, E., S. Struski, N. Prade, J. Familiades, R. Eichner, C. Quelen, M. Bousquet, F. Mugneret, P. Talmant, M.P. Pages, et al. 2010. Wide diversity of PAX5 alterations in B-ALL: A Groupe Francophone de Cytogenetique Hematologique study. *Blood.* 115:3089–3097. https://doi.org/10.1182/blood-2009-07-234229

Cozzio, A., E. Passegué, P.M. Ayton, H. Karsunky, M.L. Cleary, and I.L. Weissman. 2003. Similar MLL-associated leukemias arising from self-renewing stem cells and short-lived myeloid progenitors. *Genes Dev.* 17:3029–3035. https://doi.org/10.1101/gad.1143403

Dobson, S.M., L. García-Prat, R.J. Vanner, J. Wintersinger, E. Waanders, Z. Gu, J. McLeod, O.I. Gan, I. Grandal, D. Payne-Turner, et al. 2020. Relapse-fated latent diagnosis subclones in acute B lineage leukemia are drug tolerant and possess distinct metabolic programs. *Cancer Discov.* 10:568–587. https://doi.org/10.1158/2159-8290.CD-19-1059

Ebinger, S., E.Z. Ozdemir, C. Ziegenhain, S. Tiedt, C. Castro Alves, M. Grunert, M. Dworzak, C. Lutz, V.A. Turati, T. Enver, et al. 2016. Characterization of rare, dormant, and therapy-resistant cells in acute lymphoblastic leukemia. *Cancer Cell.* 30:849–862. https://doi.org/10.1016/j.ccell.2016.11.002

Familiades, J., M. Bousquet, M. Lafage-Pochitaloff, M.C. Béné, K. Beldjord, J. De Vos, N. Dastugue, E. Coyaud, S. Struski, C. Quelen, et al. 2009. PAX5 mutations occur frequently in adult B-cell progenitor acute lymphoblastic leukemia and PAX5 haploinsufficiency is associated with BCR-ABL1 and TCF3-PBX1 fusion genes: A GRAALL study. *Leukemia.* 23:1989–1998. https://doi.org/10.1038/leu.2009.135

Foudi, A., K. Hochedlinger, D. Van Buren, J.W. Schindler, R. Jaenisch, V. Carey, and H. Hock. 2009. Analysis of histone 2B-GFP retention reveals slowly cycling hematopoietic stem cells. *Nat. Biotechnol.* 27:84–90. https://doi.org/10.1038/nbt.1517

Fregona, V., M. Bayet, and B. Gerby. 2021. Oncogene-induced reprogramming in acute lymphoblastic leukemia: Towards targeted therapy of leukemia-initiating cells. *Cancers.* 13:5511. https://doi.org/10.3390/cancers13215511

García-Prat, L., K.B. Kaufmann, F. Schneiter, V. Voisin, A. Murison, J. Chen, M. Chan-Seng-Yue, O.I. Gan, J.L. McLeod, S.A. Smith, et al. 2021. TFEB-mediated endolysosomal activity controls human hematopoietic stem cell fate. *Cell Stem Cell.* 28:1838–1850.e10. https://doi.org/10.1016/j.stem.2021.07.003

Gerby, B., C.S. Tremblay, M. Tremblay, S. Rojas-Sutterlin, S. Herblot, J. Hébert, G. Sauvageau, S. Lemieux, E. Lécuyer, D.F.T. Veiga, and T. Hoang. 2014. SCL, LMO1 and Notch1 reprogram thymocytes into self-renewing cells. *PLoS Genet.* 10:e1004768. https://doi.org/10.1371/journal.pgen.1004768

Gerby, B., D.F.T. Veiga, J. Krosl, S. Nourreddine, J. Ouellette, A. Haman, G. Lavoie, I. Fares, M. Tremblay, V. Litalien, et al. 2016. High-throughput screening in niche-based assay identifies compounds to target pre-leukemic stem cells. *J. Clin. Invest.* 126:4569–4584. https://doi.org/10.1172/JCI86489

Gontarz, P., S. Fu, X. Xing, S. Liu, B. Miao, V. Bazylianska, A. Sharma, P. Madden, K. Cates, A. Yoo, et al. 2020. Comparison of differential accessibility analysis strategies for ATAC-seq data. *Sci. Rep.* 10:10150. https://doi.org/10.1038/s41598-020-66998-4

Good, Z., J. Sarno, A. Jager, N. Samusik, N. Aghaeepour, E.F. Simonds, L. White, N.J. Lacayo, W.J. Fantl, G. Fazio, et al. 2018. Single-cell developmental classification of B cell precursor acute lymphoblastic leukemia at diagnosis reveals predictors of relapse. *Nat. Med.* 24:474–483. https://doi.org/10.1038/nm.4505

Greaves, M. 2018. A causal mechanism for childhood acute lymphoblastic leukaemia. *Nat. Rev. Cancer.* 18:471–484. https://doi.org/10.1038/s41568-018-0015-6

Gu, Z., M.L. Churchman, K.G. Roberts, I. Moore, X. Zhou, J. Nakitandwe, K. Hagiwara, S. Pelletier, S. Gingras, H. Berns, et al. 2019. PAX5-driven subtypes of B-progenitor acute lymphoblastic leukemia. *Nat. Genet.* 51:296–307. https://doi.org/10.1038/s41588-018-0315-5

Hardy, R.R., and K. Hayakawa. 2001. B cell development pathways. *Annu. Rev. Immunol.* 19:595–621. https://doi.org/10.1146/annurev.immunol.19.1.595

Hardy, R.R., Y.S. Li, D. Allman, M. Asano, M. Gui, and K. Hayakawa. 2000. B-cell commitment, development and selection. *Immunol. Rev.* 175:23–32. https://doi.org/10.1111/j.1600-065X.2000.imr017517.x

Hassanein, N.M., F. Alcancia, K.R. Perkinson, P.J. Buckley, and A.S. Lagoo. 2009. Distinct expression patterns of CD123 and CD34 on normal bone marrow B-cell precursors ("hematogones") and B lymphoblastic leukemia blasts. *Am. J. Clin. Pathol.* 132:573–580. https://doi.org/10.1309/AJCPO4DS0GTLSOEI

Heckl, D., M.S. Kowalczyk, D. Yudovich, R. Belizaire, R.V. Puram, M.E. McConkey, A. Thielke, J.C. Aster, A. Regev, and B.L. Ebert. 2014. Generation of mouse models of myeloid malignancy with combinatorial genetic lesions using CRISPR-Cas9 genome editing. *Nat. Biotechnol.* 32:941–946. https://doi.org/10.1038/nbt.2951

Hong, D., R. Gupta, P. Ancliff, A. Atzberger, J. Brown, S. Soneji, J. Green, S. Colman, W. Piacibello, V. Buckle, et al. 2008. Initiating and cancer-propagating cells in TEL-AML1-associated childhood leukemia. *Science.* 319:336–339. https://doi.org/10.1126/science.1150648

Huntly, B.J.P., H. Shigematsu, K. Deguchi, B.H. Lee, S. Mizuno, N. Duclos, R. Rowan, S. Amaral, D. Curley, I.R. Williams, et al. 2004. MOZ-TIF2, but not BCR-ABL, confers properties of leukemic stem cells to committed murine hematopoietic progenitors. *Cancer Cell.* 6:587–596. https://doi.org/10.1016/j.ccr.2004.10.015

Imperato, M.R., P. Cauchy, N. Obier, and C. Bonifer. 2015. The RUNX1-PU.1 axis in the control of hematopoiesis. *Int. J. Hematol.* 101:319–329. https://doi.org/10.1007/s12185-015-1762-8

Inaba, H., and C.G. Mullighan. 2020. Pediatric acute lymphoblastic leukemia. *Haematologica.* 105:2524–2539. https://doi.org/10.3324/haematol.2020.247031

Inaba, H., and C.H. Pui. 2021. Advances in the diagnosis and treatment of pediatric acute lymphoblastic leukemia. *J. Clin. Med.* 10:1926. https://doi.org/10.3390/jcm10091926

Jamrog, L., G. Chemin, V. Fregona, L. Coster, M. Pasquet, C. Oudinet, N. Rouquie, N. Prade, S. Lagarde, C. Cresson, et al. 2018. PAX5-ELN oncoprotein promotes multistep B-cell acute lymphoblastic leukemia in

mice. *Proc. Natl. Acad. Sci. USA.* 115:10357–10362. https://doi.org/10.1073/pnas.1721678115

Jurado, S., A.S. Fedl, M. Jaritz, D. Kostanova-Poliakova, S.G. Malin, C.G. Mullighan, S. Strehl, M. Fischer, and M. Busslinger. 2022. The PAX5-JAK2 translocation acts as dual-hit mutation that promotes aggressive B-cell leukemia via nuclear STAT5 activation. *EMBO J.* 41:e108397. https://doi.org/10.15252/embj.2021108397

Katerndahl, C.D.S., L.M. Heltemes-Harris, M.J.L. Willette, C.M. Henzler, S. Frietze, R. Yang, H. Schjerven, K.A.T. Silverstein, L.B. Ramsey, G. Hubbard, et al. 2017. Antagonism of B cell enhancer networks by STAT5 drives leukemia and poor patient survival. *Nat. Immunol.* 18:694–704. https://doi.org/10.1038/ni.3716

Krivtsov, A.V., D. Twomey, Z. Feng, M.C. Stubbs, Y. Wang, J. Faber, J.E. Levine, J. Wang, W.C. Hahn, D.G. Gilliland, et al. 2006. Transformation from committed progenitor to leukaemia stem cell initiated by MLL-AF9. *Nature.* 442:818–822. https://doi.org/10.1038/nature04980

Langmead, B., and S.L. Salzberg. 2012. Fast gapped-read alignment with Bowtie 2. *Nat. Methods.* 9:357–359. https://doi.org/10.1038/nmeth.1923

Li, Z., M.H. Schulz, T. Look, M. Begemann, M. Zenke, and I.G. Costa. 2019. Identification of transcription factor binding sites using ATAC-seq. *Genome Biol.* 20:45. https://doi.org/10.1186/s13059-019-1642-2

Liu, Y., Y. Chen, X. Deng, and J. Zhou. 2020. ATF3 prevents stress-induced hematopoietic stem cell exhaustion. *Front. Cell Dev. Biol.* 8:585771. https://doi.org/10.3389/fcell.2020.585771

Malta, T.M., A. Sokolov, A.J. Gentles, T. Burzykowski, L. Poisson, J.N. Weinstein, B. Kamińska, J. Huelsken, L. Omberg, O. Gevaert, et al. 2018. Machine learning identifies stemness features associated with oncogenic dedifferentiation. *Cell.* 173:338–354.e15. https://doi.org/10.1016/j.cell.2018.03.034

McCormack, M.P., L.F. Young, S. Vasudevan, C.A. de Graaf, R. Codrington, T.H. Rabbitts, S.M. Jane, and D.J. Curtis. 2010. The Lmo2 oncogene initiates leukemia in mice by inducing thymocyte self-renewal. *Science.* 327:879–883. https://doi.org/10.1126/science.1182378

Min, I.M., G. Pietramaggiori, F.S. Kim, E. Passegué, K.E. Stevenson, and A.J. Wagers. 2008. The transcription factor EGR1 controls both the proliferation and localization of hematopoietic stem cells. *Cell Stem Cell.* 2:380–391. https://doi.org/10.1016/j.stem.2008.01.015

Miraldi, E.R., M. Pokrovskii, A. Watters, D.M. Castro, N. De Veaux, J.A. Hall, J.Y. Lee, M. Ciofani, A. Madar, N. Carriero, et al. 2019. Leveraging chromatin accessibility for transcriptional regulatory network inference in T Helper 17 Cells. *Genome Res.* 29:449–463. https://doi.org/10.1101/gr.238253.118

Monaco, G., H. Chen, M. Poidinger, J. Chen, J.P. de Magalhães, and A. Larbi. 2016. flowAI: Automatic and interactive anomaly discerning tools for flow cytometry data. *Bioinformatics.* 32:2473–2480. https://doi.org/10.1093/bioinformatics/btw191

Morcos, M.N.F., K.B. Schoedel, A. Hoppe, R. Behrendt, O. Basak, H.C. Clevers, A. Roers, and A. Gerbaulet. 2017. SCA-1 expression level identifies quiescent hematopoietic stem and progenitor cells. *Stem Cell Rep.* 8:1472–1478. https://doi.org/10.1016/j.stemcr.2017.04.012

Mullighan, C.G., S. Goorha, I. Radtke, C.B. Miller, E. Coustan-Smith, J.D. Dalton, K. Girtman, S. Mathew, J. Ma, S.B. Pounds, et al. 2007. Genome-wide analysis of genetic alterations in acute lymphoblastic leukaemia. *Nature.* 446:758–764. https://doi.org/10.1038/nature05690

Mullighan, C.G., L.A. Phillips, X. Su, J. Ma, C.B. Miller, S.A. Shurtleff, and J.R. Downing. 2008. Genomic analysis of the clonal origins of relapsed acute lymphoblastic leukemia. *Science.* 322:1377–1380. https://doi.org/10.1126/science.1164266

Ng, S.W.K., A. Mitchell, J.A. Kennedy, W.C. Chen, J. McLeod, N. Ibrahimova, A. Arruda, A. Popescu, V. Gupta, A.D. Schimmer, et al. 2016. A 17-gene stemness score for rapid determination of risk in acute leukaemia. *Nature.* 540:433–437. https://doi.org/10.1038/nature20598

Nutt, S.L., B. Heavey, A.G. Rolink, and M. Busslinger. 1999. Commitment to the B-lymphoid lineage depends on the transcription factor Pax5. *Nature.* 401:556–562. https://doi.org/10.1038/44076

Patterson, H.C., C. Gerbeth, P. Thiru, N.F. Vögtle, M. Knoll, A. Shahsafaei, K.E. Samocha, C.X. Huang, M.M. Harden, R. Song, et al. 2015. A respiratory chain controll signal transduction cascade in the mitochondrial intermembrane space mediates hydrogen peroxide signaling. *Proc. Natl. Acad. Sci. USA.* 112:E5679–E5688. https://doi.org/10.1073/pnas.1517932112

Picelli, S., O.R. Faridani, A.K. Björklund, G. Winberg, S. Sagasser, and R. Sandberg. 2014. Full-length RNA-seq from single cells using Smart-seq2. *Nat. Protoc.* 9:171–181. https://doi.org/10.1038/nprot.2014.006

Pokrovskii, M., J.A. Hall, D.E. Ochayon, R. Yi, N.S. Chaimowitz, H. Seelamneni, N. Carriero, A. Watters, S.N. Waggoner, D.R. Littman, et al. 2019. Characterization of transcriptional regulatory networks that promote and restrict identities and functions of intestinal innate lymphoid cells. *Immunity.* 51:185–197.e6. https://doi.org/10.1016/j.immuni.2019.06.001

Prost, S., F. Relouzat, M. Spentchian, Y. Ouzegdouh, J. Saliba, G. Massonnet, J.P. Beressi, E. Verhoeyen, V. Raggueneau, B. Maneglier, et al. 2015. Erosion of the chronic myeloid leukaemia stem cell pool by PPARγ agonists. *Nature.* 525:380–383. https://doi.org/10.1038/nature15248

Ramamoorthy, S., K. Kometani, J.S. Herman, M. Bayer, S. Boller, J. Edwards-Hicks, H. Ramachandran, R. Li, R. Klein-Geltink, E.L. Pearce, et al. 2020. EBF1 and Pax5 safeguard leukemic transformation by limiting IL-7 signaling, Myc expression, and folate metabolism. *Genes Dev.* 34:1503–1519. https://doi.org/10.1101/gad.340216.120

Reske, J.J., M.R. Wilson, and R.L. Chandler. 2020. ATAC-seq normalization method can significantly affect differential accessibility analysis and interpretation. *Epigenetics Chromatin.* 13:22. https://doi.org/10.1186/s13072-020-00342-y

Reth, M. 2002. Hydrogen peroxide as second messenger in lymphocyte activation. *Nat. Immunol.* 3:1129–1134. https://doi.org/10.1038/ni1202-1129

Reth, M., and P. Nielsen. 2014. Signaling circuits in early B-cell development. *Adv. Immunol.* 122:129–175. https://doi.org/10.1016/B978-0-12-800267-4.00004-3

Revilla-I-Domingo, R., I. Bilic, B. Vilagos, H. Tagoh, A. Ebert, I.M. Tamir, L. Smeenk, J. Trupke, A. Sommer, M. Jaritz, and M. Busslinger. 2012. The B-cell identity factor Pax5 regulates distinct transcriptional programmes in early and late B lymphopoiesis. *EMBO J.* 31:3130–3146. https://doi.org/10.1038/emboj.2012.155

Rodríguez-Hernández, G., A. Casado-García, M. Isidro-Hernández, D. Picard, J. Raboso-Gallego, S. Alemán-Arteaga, A. Orfao, O. Blanco, S. Riesco, P. Prieto-Matos, et al. 2021. The second oncogenic hit determines the cell fate of ETV6-RUNX1 positive leukemia. *Front. Cell Dev. Biol.* 9:704591. https://doi.org/10.3389/fcell.2021.704591

Roederer, M. 2011. Interpretation of cellular proliferation data: Avoid the panglossian. *Cytometry A.* 79:95–101. https://doi.org/10.1002/cyto.a.21010

Rolink, A., and F. Melchers. 1996. B-cell development in the mouse. *Immunol. Lett.* 54:157–161. https://doi.org/10.1016/S0165-2478(96)02666-1

Scheicher, R., A. Hoelbl-Kovacic, F. Bellutti, A.S. Tigan, M. Prchal-Murphy, G. Heller, C. Schneckenleithner, M. Salazar-Roa, S. Zöchbauer-Müller, J. Zuber, et al. 2015. CDK6 as a key regulator of hematopoietic and leukemic stem cell activation. *Blood.* 125:90–101. https://doi.org/10.1182/blood-2014-06-584417

Smeenk, L., M. Fischer, S. Jurado, M. Jaritz, A. Azaryan, B. Werner, M. Roth, J. Zuber, M. Stanulla, M.L. den Boer, et al. 2017. Molecular role of the PAX5-ETV6 oncoprotein in promoting B-cell acute lymphoblastic leukemia. *EMBO J.* 36:718–735. https://doi.org/10.15252/embj.201695495

Staber, P.B., P. Zhang, M. Ye, R.S. Welner, E. Levantini, A. Di Ruscio, A.K. Ebralidze, C. Bach, H. Zhang, J. Zhang, et al. 2014. The Runx-PU.1 pathway preserves normal and AML/ETO9a leukemic stem cells. *Blood.* 124:2391–2399. https://doi.org/10.1182/blood-2014-01-550855

Stoddart, A., A.A. Fernald, E.M. Davis, M.E. McNerney, and M.M. Le Beau. 2022. EGR1 haploinsufficiency confers a Fitness advantage to hematopoietic stem cells following chemotherapy. *Exp. Hematol.* 115:54–67. https://doi.org/10.1016/j.exphem.2022.08.003

Tomura, M., A. Sakaue-Sawano, Y. Mori, M. Takase-Utsugi, A. Hata, K. Ohtawa, O. Kanagawa, and A. Miyawaki. 2013. Contrasting quiescent G0 phase with mitotic cell cycling in the mouse immune system. *PLoS One.* 8:e73801. https://doi.org/10.1371/journal.pone.0073801

Tremblay, C.S., J. Saw, S.K. Chiu, N.C. Wong, K. Tsyganov, S. Ghotb, A.N. Graham, F. Yan, A.A. Guirguis, S.E. Sonderegger, et al. 2018. Restricted cell cycle is essential for clonal evolution and therapeutic resistance of pre-leukemic stem cells. *Nat. Commun.* 9:3535. https://doi.org/10.1038/s41467-018-06021-7

Trumpp, A., M. Essers, and A. Wilson. 2010. Awakening dormant haematopoietic stem cells. *Nat. Rev. Immunol.* 10:201–209. https://doi.org/10.1038/nri2726

Turati, V.A., J.A. Guerra-Assunção, N.E. Potter, R. Gupta, S. Ecker, A. Daneviciute, M. Tarabichi, A.P. Webster, C. Ding, G. May, et al. 2021. Chemotherapy induces canalization of cell state in childhood B-cell precursor acute lymphoblastic leukemia. *Nat. Cancer.* 2:835–852. https://doi.org/10.1038/s43018-021-00219-3

Tzelepis, K., H. Koike-Yusa, E. De Braekeleer, Y. Li, E. Metzakopian, O.M. Dovey, A. Mupo, V. Grinkevich, M. Li, M. Mazan, et al. 2016. A CRISPR dropout screen identifies genetic vulnerabilities and therapeutic targets in acute myeloid leukemia. *Cell Rep.* 17:1193–1205. https://doi.org/10.1016/j.celrep.2016.09.079

van Delft, F.W., S. Horsley, S. Colman, K. Anderson, C. Bateman, H. Kempski, J. Zuna, C. Eckert, V. Saha, L. Kearney, et al. 2011. Clonal origins of relapse in ETV6-RUNX1 acute lymphoblastic leukemia. *Blood*. 117: 6247–6254. https://doi.org/10.1182/blood-2010-10-314674

Van Gassen, S., B. Gaudilliere, M.S. Angst, Y. Saeys, and N. Aghaeepour. 2020. CytoNorm: A normalization algorithm for cytometry data. *Cytometry A*. 97:268–278. https://doi.org/10.1002/cyto.a.23904

Vazquez-Santillan, K., J. Melendez-Zajgla, L. Jimenez-Hernandez, G. Martínez-Ruiz, and V. Maldonado. 2015. NF-κB signaling in cancer stem cells: A promising therapeutic target? *Cell Oncol*. 38:327–339. https://doi.org/10.1007/s13402-015-0236-6

Venezia, T.A., A.A. Merchant, C.A. Ramos, N.L. Whitehouse, A.S. Young, C.A. Shaw, and M.A. Goodell. 2004. Molecular signatures of proliferation and quiescence in hematopoietic stem cells. *PLoS Biol*. 2:e301. https://doi.org/10.1371/journal.pbio.0020301

Waanders, E., Z. Gu, S.M. Dobson, Ž. Antić, J.C. Crawford, X. Ma, M.N. Edmonson, D. Payne-Turner, M. van de Vorst, M.C.J. Jongmans, et al. 2020. Mutational landscape and patterns of clonal evolution in relapsed pediatric acute lymphoblastic leukemia. *Blood Cancer Discov*. 1:96–111. https://doi.org/10.1158/0008-5472.BCD-19-0041

Wilson, A., E. Laurenti, G. Oser, R.C. van der Wath, W. Blanco-Bose, M. Jaworski, S. Offner, C.F. Dunant, L. Eshkind, E. Bockamp, et al. 2008. Hematopoietic stem cells reversibly switch from dormancy to self-renewal during homeostasis and repair. *Cell*. 135:1118–1129. https://doi.org/10.1016/j.cell.2008.10.048

Wojiski, S., F.C. Guibal, T. Kindler, B.H. Lee, J.L. Jesneck, A. Fabian, D.G. Tenen, and D.G. Gilliland. 2009. PML-RARalpha initiates leukemia by conferring properties of self-renewal to committed promyelocytic progenitors. *Leukemia*. 23:1462–1471. https://doi.org/10.1038/leu.2009.63

Yamashita, M., and E. Passegué. 2019. TNF-A coordinates hematopoietic stem cell survival and myeloid regeneration. *Cell Stem Cell*. 25:357–372.e7. https://doi.org/10.1016/j.stem.2019.05.019

Yan, F., N.C. Wong, D.R. Powell, and D.J. Curtis. 2020. A 9-gene score for risk stratification in B-cell acute lymphoblastic leukemia. *Leukemia*. 34: 3070–3074. https://doi.org/10.1038/s41375-020-0888-8

Zhang, Y.W., J. Mess, N. Aizarani, P. Mishra, C. Johnson, M.C. Romero-Mulero, J. Rettkowski, K. Schönberger, N. Obier, K. Jäcklein, et al. 2022. Hyaluronic acid-GPRC5C signalling promotes dormancy in haematopoietic stem cells. *Nat. Cell Biol*. 24:1038–1048. https://doi.org/10.1038/s41556-022-00931-x

Supplemental material

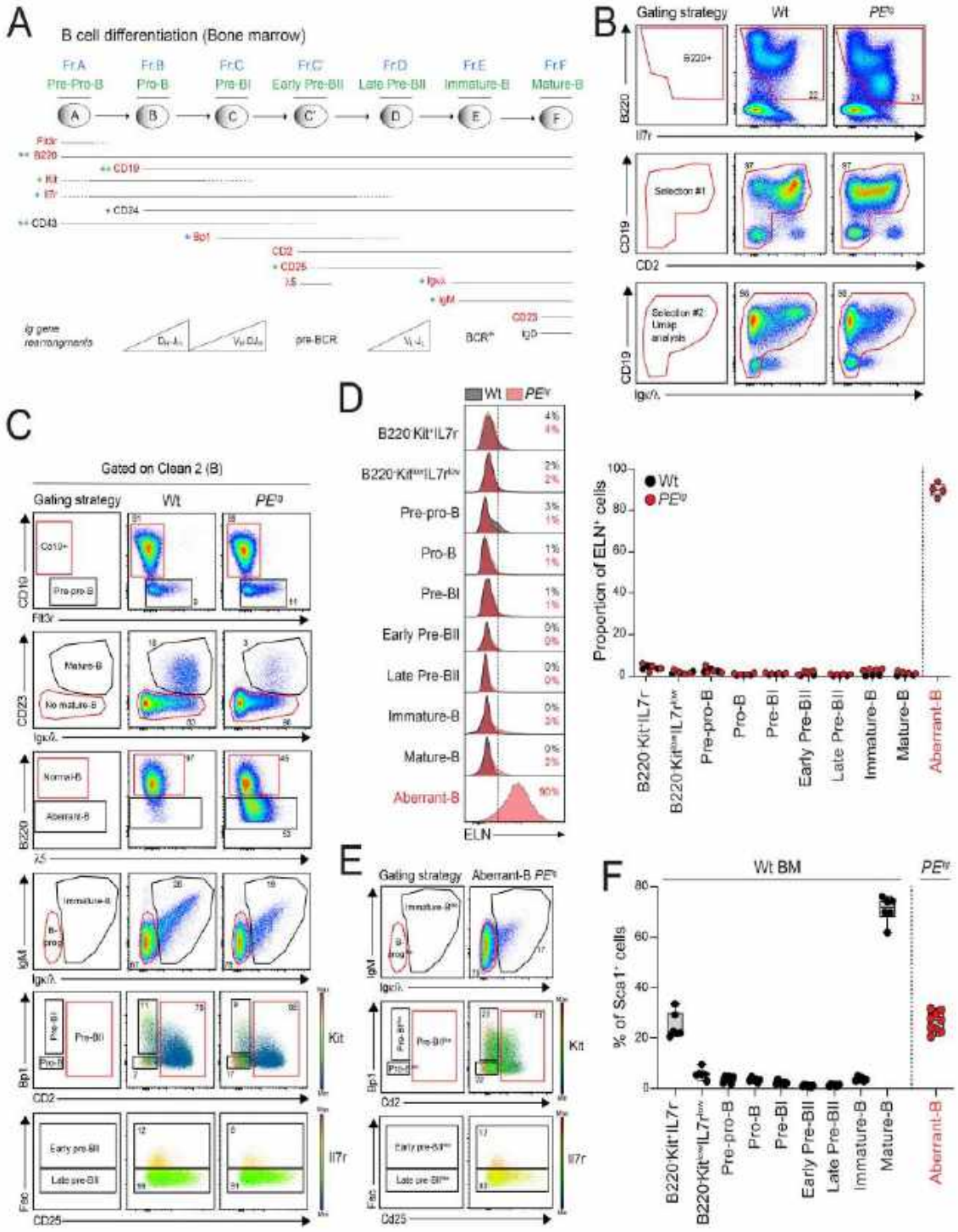

Figure S1. **Phenotypic characterization of preleukemic mice. (A)** Schematic representation of the murine BM B cell differentiation. Representation of the different B cell differentiation stages (pre-pro-B, pro-B, pre-BI, early pre-BII, late pre-BII, immature-B, and mature-B) and pattern of expression of the main markers used to characterize each subset. Both Philadelphia (Hardy and Hayakawa, 2001) and Basel (Rolink and Melchers, 1996) nomenclatures are indicated in blue and green, respectively. Blue and green stars indicate the markers used in the respective nomenclatures. The thickness of the line is representative of the expression level. The dotted lines indicate subsets where expression is progressively acquired or lost. The markers used to perform the multiparametric staining by FACS, and the UMAP representation are indicated in red. $V_HD_HJ_H$ and V_LJ_L rearrangements are indicated. **(B and C)** Gating strategy of the B cell compartment (B) and of the different B cell subpopulations (C) from the BM of wt and *PE*^{ts} preleukemic mice to perform the clustering analysis by UMAP shown in Fig. 1 A. Each red gate represents the parent population of the following below set of FACS plots. Kit expression level in pro-B, pre-BI, and pre-BII subsets and IL7r expression level in early and late pre-BII subsets are shown. **(D)** Expression of intracytoplasmic ELN in aberrant B cells (CD19$^+$B220^{low}), in all the steps of B cell differentiation (CD19$^+$B220$^+$), in HSPC-enriched (CD19$^-$B220$^-$Kit$^+$IL7r$^-$) and CLP-enriched (CD19$^-$B220$^-$Kit^{low}IL7r^{low}) populations from preleukemic PE^{ts} mice (n = 4). Wt mice (n = 4) were used as controls. **(E)** Representative immunophenotype of the aberrant B population from PE^{ts} preleukemic BM identified in Fig. S1 C. The aberrant B PE^{ts} population was subdivided into the different phenotypic-like subsets pro-B^{like}, pre-BI^{like}, early pre-BII^{like}, late pre-BII^{like}, immature-B^{like}. Kit expression levels in pro-B^{like}, pre-BI^{like}, and pre-BII^{like} subsets and Il7r expression levels in early and late pre-BII^{like} subsets are shown. **(F)** Expression of Sca-1 in aberrant B cells (CD19$^+$B220^{low}), in all the steps of B cell differentiation (CD19$^+$B220$^+$), in HSPC-enriched (CD19$^-$B220$^-$Kit$^+$IL7r$^-$) and CLP-enriched (CD19$^-$B220$^-$Kit^{low}IL7r^{low}) populations from PE^{ts} mice (n = 9). Wt mice (n = 6) were used as controls.

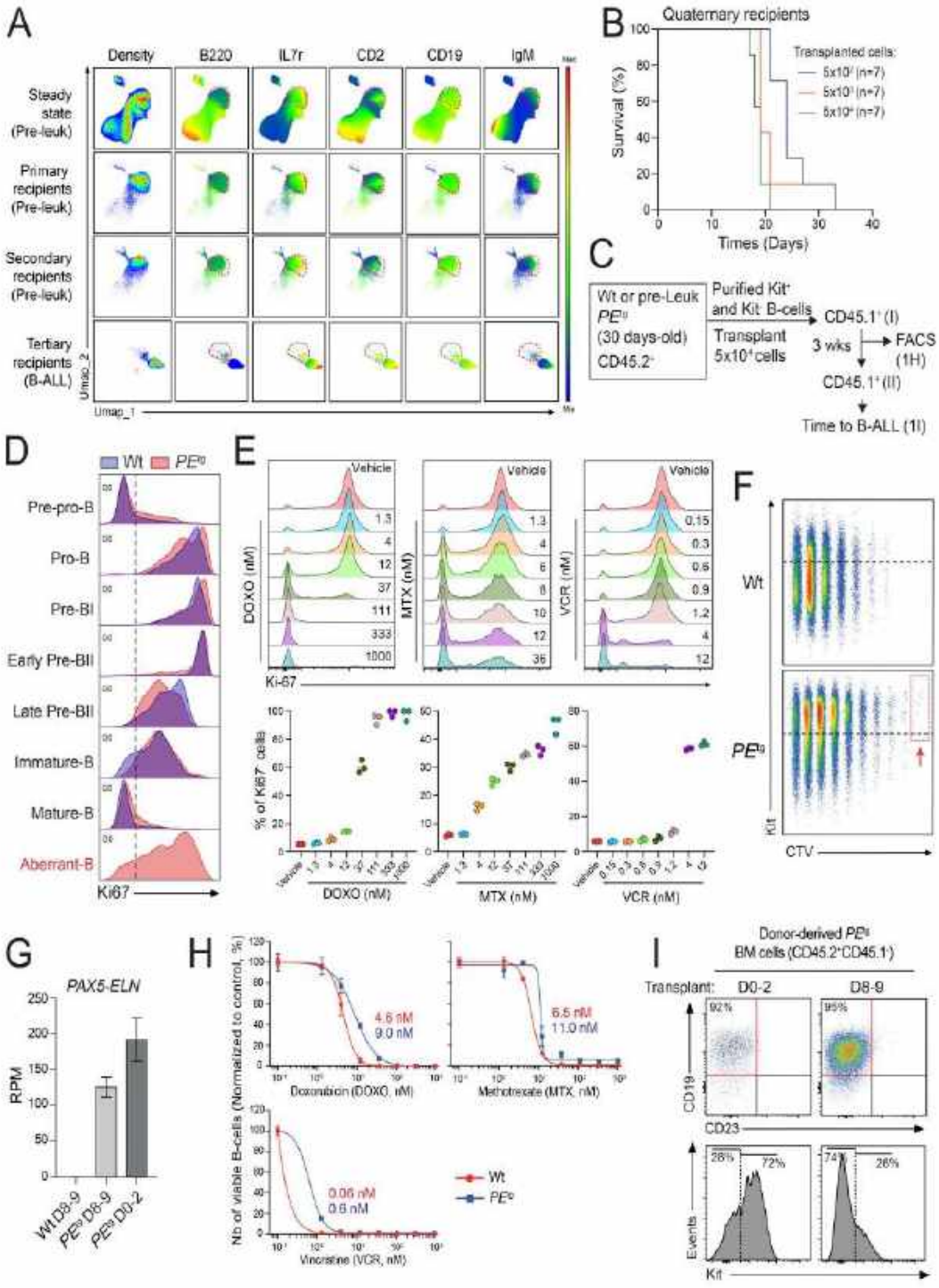

Figure S2. **Cell-cycle status of preleukemic B cells. (A)** UMAP of the cell density (left panel) before (steady state) and after transplantation in primary, secondary, and tertiary recipients, associated with the expression level of B220, IL7r, CD2, CD19, and IgM (right panels). **(B)** Kaplan–Meier survival curve of quaternary recipient mice transplanted with 5×10^2 ($n = 7$), 5×10^3 ($n = 7$), and 5×10^4 ($n = 7$) donor-derived blasts from tertiary B-ALL *PE*^{tg} mice. **(C)** Experimental procedure to study the engraftment potential of kit$^+$ aberrant B cells. **(D)** Ki67 staining was performed on B cells from the BM of wt and preleukemic *PE*^{tg} mice according to Fig. 2 A ($n = 4$). Representative FACS analysis of the proportion of cells in G0 phase (Ki67$^-$ cells) within each wt and *PE*^{tg} B cell subpopulation. **(E)** Preleukemic *PE*^{tg} cells were plated on MS5 stromal cells and treated with increasing doses ($n = 3$ for each dose, one experiment) of DOXO, MTX, or VCR for 48 h. Ki67 staining was then performed, and the proportion of Ki67$^+$ and Ki67$^-$ within the aberrant B cell population was shown (upper panels) and quantified (lower panels) for each dose. **(F)** FACS analysis (Winlist software) of the cell divisions (CTV) in function of Kit expression level after the coculture of CTV-labeled wt and preleukemic *PE*^{tg} cells. Red arrow indicates the undivided (D0) population. **(G)** Expression level of the *PAX5::ELN* fusion transcript in *PE*^{tg} D0–2 ($n = 2$), *PE*^{tg} D8–9 ($n = 2$), and wt D8–9 ($n = 2$) cells (mean ± SD). RNA-seq data were aligned independently on the sequence of *PAX5::ELN* human transgene. Expression levels are represented in "reads" per million (RPM). **(H)** Purified wt and preleukemic *PE*^{tg} Kit$^+$ cells were plated on MS5 stromal cells and treated with increasing doses ($n = 3$ for each dose, one experiment) of DOXO, MTX, or VCR for 48 h. Cell numbers of treated cells were then analyzed by FACS and normalized to the number of untreated cells. IC50 of each compound on wt and preleukemic *PE*^{tg} cells were determined according to the respective dose-response curves. **(I)** Representative immunophenotype of donor-derived (CD45.2$^+$CD45.1$^-$) cells in engrafted recipient BM 3 wk after the transplantation of slow- (D0–2) and high- (D8–9) cycling preleukemic *PE*^{tg} cells.

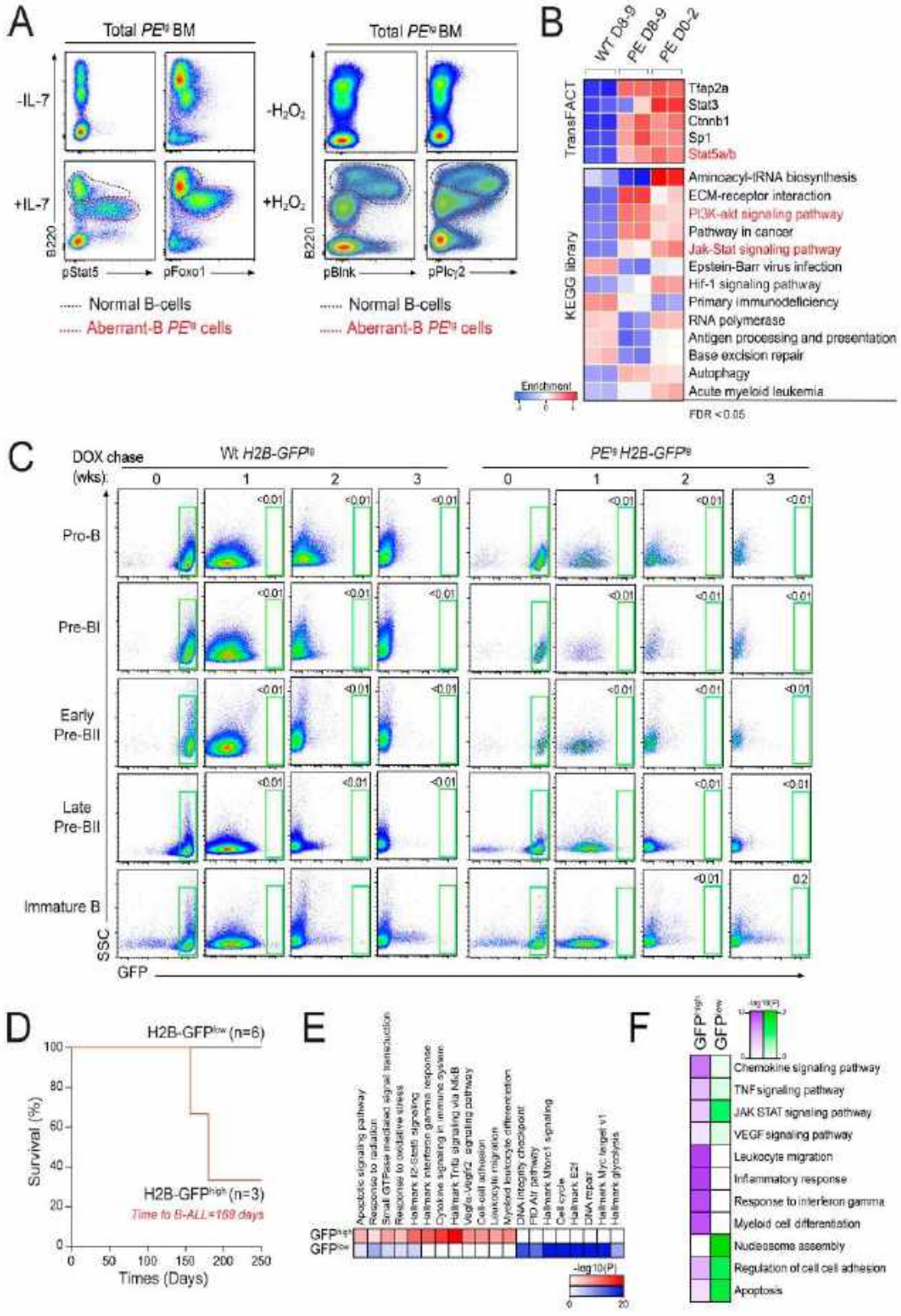

Figure S3. **Molecular characterization of quiescent preleukemic B cells. (A)** Representative FACS analysis of pStat5 and pFoxo1 on total BM from preleukemic PE^tg mice after ex vivo IL-7 stimulation (+IL-7). Unstimulated (−IL-7) cells were used as control (left panels). FACS analysis of pBlnk and pPlcγ2 on total BM from preleukemic PE^tg mice after ex vivo H_2O_2 stimulation (+H_2O_2). Unstimulated (−H_2O_2) cells were used as control (right panels). **(B)** Gene set variation analysis of PE^tg D0–2 ($n = 2$), PE^tg D8–9 ($n = 2$), and wt D8–9 ($n = 2$) cells was performed using TransFACT and KEGG libraries and top gene sets were represented in heatmap. **(C)** Representative FACS analysis of GFP expression in the different B cell subsets from wt *H2B-GFP*^tg (left panels) and preleukemic PE^tgH2B-GFP^tg (right panels) mice after 0, 1, 2, and 3 wk of DOX chase. The proportion of GFP^high cells is indicated for each time point. **(D)** Kaplan–Meier survival curve of recipient mice transplanted with purified GFP^high ($n = 3$) and GFP^low ($n = 6$) cells from *PE^tgH2B-GFP^tg* mice. **(E)** Heatmap of Metascape results of the top selected pathways between all the differentially expressed genes between GFP^high ($n = 5$) and GFP^low ($n = 5$) cells. **(F)** Heatmap of enrichment analysis of differentially accessible regions obtained with Cistrome-GO.

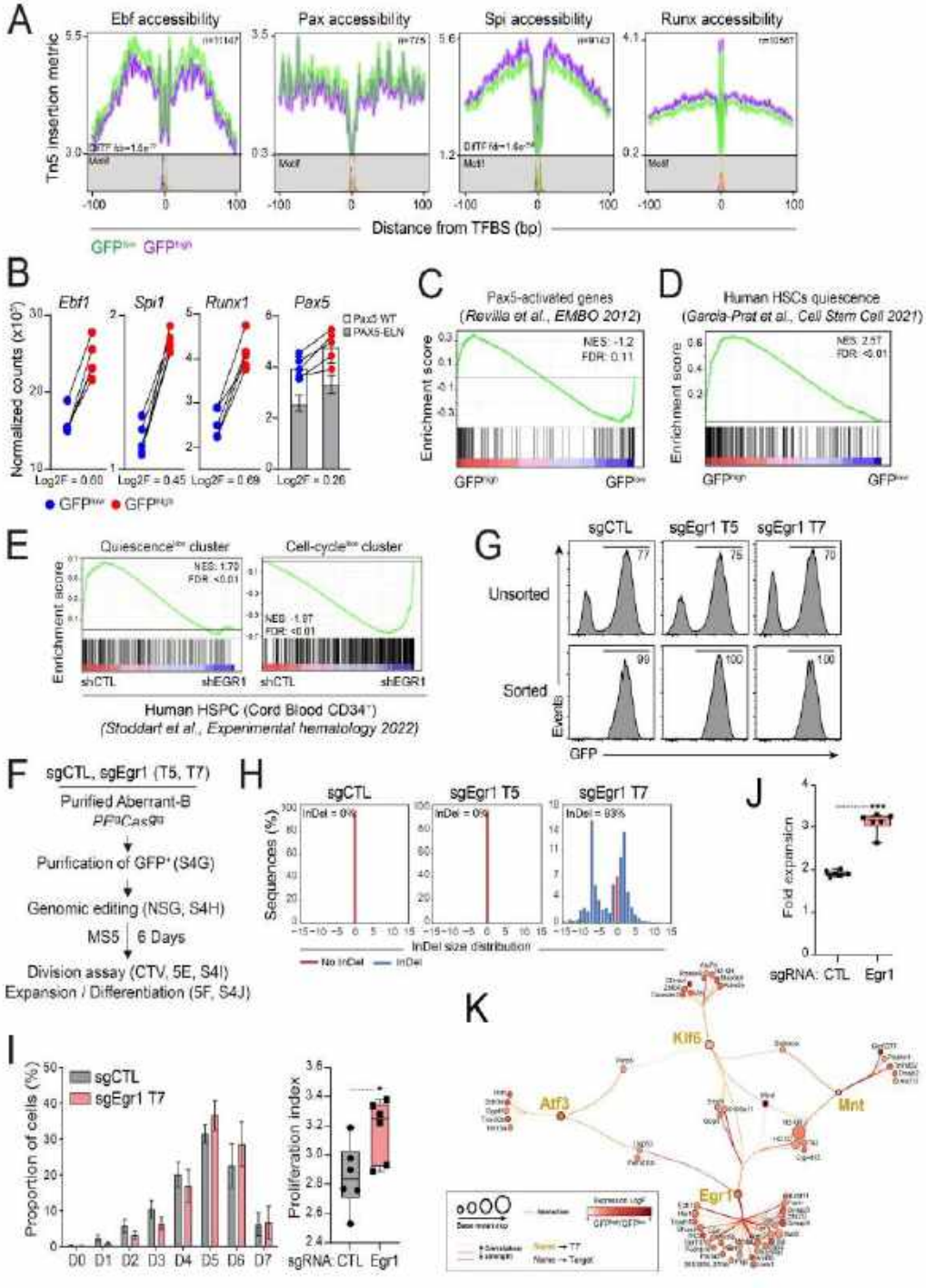

Figure S4. **Impact of Egr1 editing on cell proliferation of preleukemic B cells. (A)** Comparison of the accessibility footprint of Ebf, Pax, Spi, and Runx motifs (ATAC-seq data) between GFP^{high} (purple) and GFP^{low} (green) cells. **(B)** Comparison of *Ebf1*, *Spi1*, *Runx1*, and of total *Pax5* expression (RNA-seq data, n = 5, mean ± SD) between GFP^{high} (red) and GFP^{low} (blue) cells. The proportions of murine *Pax5* (*Pax5* WT) and of human *PAX5* (*PAX5-ELN*) are shown. **(C)** GSEA of the well-established list of in vivo PAX5-activated genes (Revilla-I-Domingo et al., 2012) between GFP^{high} and GFP^{low} cells. **(D)** GSEA of the established list of in vivo human HSC quiescence genes (Garcia-Prat et al., 2021) between GFP^{high} (red) and GFP^{low} (blue) cells. **(E)** GSEA of the list of genes in the quiescence^{like} cluster (left panel) and in the cell-cycle^{like} cluster (right panel) and identified in Fig. 5 C between human CD34^{+} HSPCs modified or not (shCTL) with *EGR1* shRNA (shEGR1) (Stoddart et al., 2022). **(F)** Experimental procedure to study the role of Egr1 in PE^{tg} pre-LSC activity. **(G)** Transduction efficiency of preleukemic PE^{tg}*Cas9*^{tg} aberrant B cells expressing sgCTL, sgEgr1 T5, and sgEgr1 T7 was assessed by FACS by monitoring the percentage of GFP for each condition (upper panels). Transduced PE^{tg}*Cas9*^{tg} GFP^{+} cells were purified by cell sorting and cell purity was then verified (lower panels). **(H)** Analysis of the targeted region (exon 1) of *Egr1* by NGS and quantification of the genomic editing efficiency. **(I)** The number of cell divisions (D0 to D7) of aberrant B GFP^{+} cells expressing sgCTL or sgEgr1 T7 after 6 days of coculture was analyzed (left panel) and the PI was calculated for each condition (right panel, n = 6, one experiment, $^{*}P < 0.05$). **(J)** In vitro cell growth of GFP^{+} sgCTL and sgEgr1 T7 cells. Results represent the fold expansion of aberrant B GFP^{+} cells after 6 days of coculture on MS5 stromal cells (n = 6, one experiment, $^{***}P < 0.001$). The horizontal lines of the box plots indicate the median, while the boxes represent the first and the third quartiles of the data and the whiskers denote the minimum and the maximum values. **(K)** Molecular network of genes from TRN#1 of Fig. 5 D. Node color represents the log-fold difference between GFP^{high} and GFP^{low} subset and node size represents the base-mean expression. Target genes positively regulated by the four TFs, Egr1, Mnt, Klf6, and Atf3, were annotated.

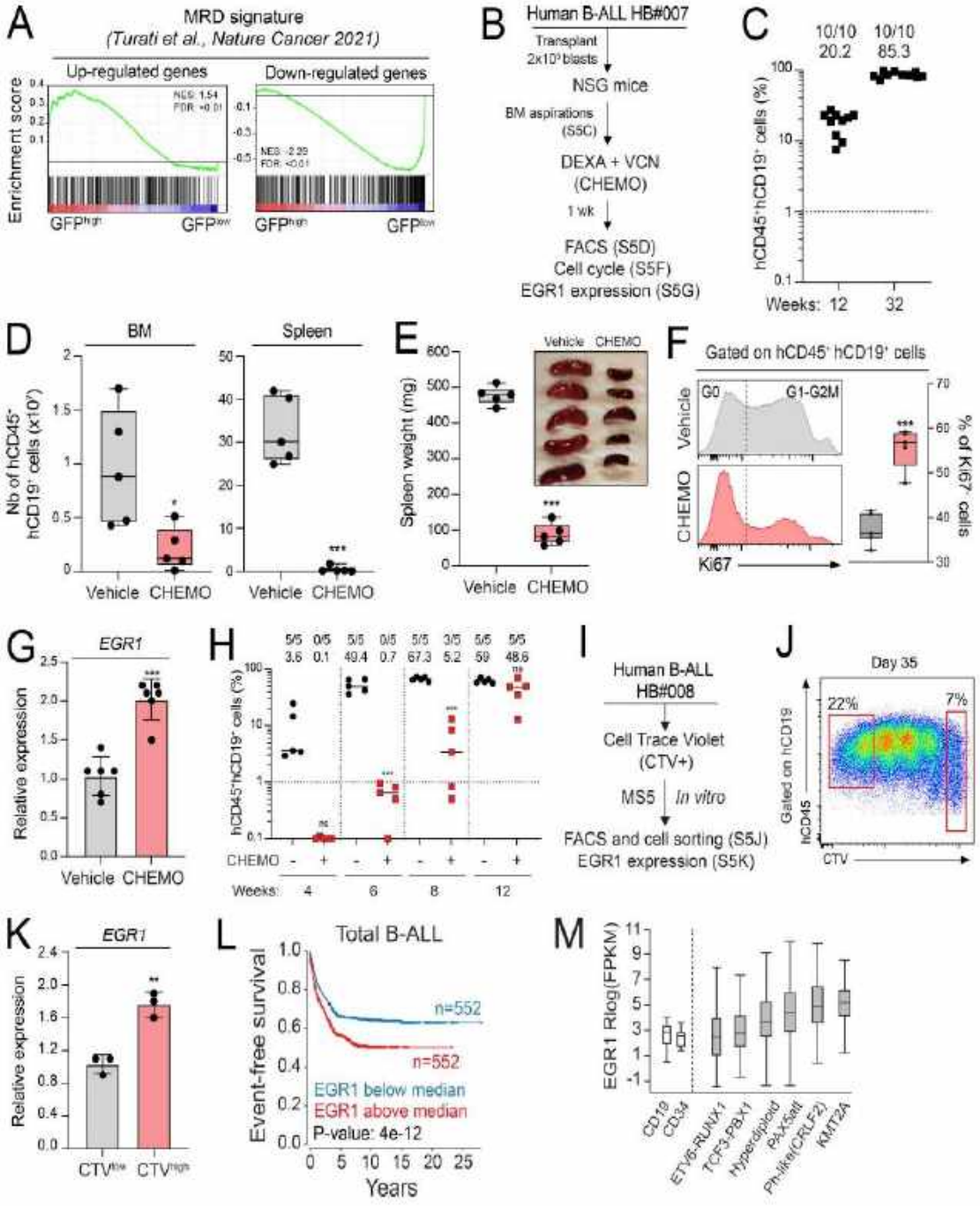

Figure S5. **Upregulation of *EGR1* expression in residual leukemic blasts. (A)** GSEA of the up- (left panel) and down- (right panel) regulated genes from residual human B-ALL cells after chemotherapies (Turati et al., 2021) between GFP^{high} and GFP^{low} cells. **(B–G)** Experimental procedure to explore EGR1 expression in resistant human B-ALL cells (B). Leukemic blasts from the "de novo" B-ALL patient HB#007 were transplanted into NSG mice (n = 11). The proportion of hCD45$^+$hCD19$^+$ B-ALL blasts in BM aspirations was assessed 12 and 32 wk after transplantation (C). Engrafted mice were randomly selected for treatment (CHEMO) or not (vehicle) with a chemotherapeutic cocktail (DEXA+VCR) for 1 wk. Human B-ALL reconstitution (number of hCD45$^+$hCD19$^+$ B-ALL blasts) was monitored by FACS in the BM and the spleen after the treatment (D). Spleen weight was measured, and a picture of the spleen is shown (E). Ki67 expression was determined by FACS in blasts from the BM of treated and untreated mice (F). Data obtained with B-ALL patient HB#007 were compiled from five (vehicle) and five (CHEMO) mice per condition (*P < 0.05, ***P < 0.001). The horizontal lines of the box plots indicate the median, while the boxes represent the first and the third quartiles of the data and the whiskers denote the minimum and the maximum values. Engrafted blasts were purified and mRNA levels of the human *EGR1* were determined by quantitative RT-PCR and normalized to *ABL1* gene. Error bars indicate mean ± SD (n = 6, ***P < 0.001) from two independent experiments (G). **(H)** Engrafted blasts (B-ALL patient HB#010) from the BM of treated (CHEMO) and untreated (Vehicle) mice (Fig. 6 E) were purified and transplanted in equal number (2 × 10^5 cells/mouse) in secondary recipients. The proportion of hCD45$^+$hCD19$^+$ B-ALL blasts in BM aspirations was assessed 4, 6, 8, and 12 wk after transplantation was monitored by FACS (n = 5, one experiment, ***P < 0.001). **(I–K)** Experimental procedure to explore EGR1 expression in quiescent human B-ALL cells (I). Leukemic blasts from the "de novo" B-ALL patient HB#008 were stained with CTV and the number of cell divisions (D0 to D4–5) after the coculture was then analyzed. Red dotted gates were used to purify the D0 (CTV^{high}) and D4–5 (CTV^{low}) populations (J) and the expression of human *EGR1* were determined by quantitative RT-PCR (K, mean ± SD, n = 3, one experiment, **P < 0.01). **(L)** *EGR1* expression and its associated clinical outcome in B-ALL patient extracted from Gu et al. (2019). EFS curves of total B-ALL patients with *EGR1* expression below (blue) and above (red) to the median. **(M)** *EGR1* expression in the different B-ALL oncogenic subgroups was shown.

Provided online are Table S1, Table S2, Table S3, Table S4, and Table S5. Table S1 is a list of FACS antibodies used for the phenotypic characterization of the B cell lineage. Table S2 shows results of differentially expressed genes of PE^{tg} D0–2, PE^{tg} D8–9, and Wt D8–9 cells analyzed with DESeq2 ($Log_2F > 0.65$; P adj <0.05). Table S3 shows results of differentially expressed genes (RNA-seq) of H2B-GFP^{high} and H2B-GFP^{low} cells analyzed with DESeq2 ($Log_2F > 0.6$; P adj <0.05). Table S4 shows results of differentially accessible regions (ATAC-seq) of GFP^{high} and GFP^{low} cells and their associated TF activity analyzed with diffTF pipeline. Table S5 shows clustering data (k-means) of significantly modified genes (related to Fig. 5 C and Table S3) and peaks (related to Fig. 5 B and Table S4) from preleukemic GFP^{high} and GFP^{low} cells according to their signal in the different steps of the normal differentiation (extracted from RNA-seq and ATAC-seq ImmGen datasets).

Annexe II

cancers

MDPI

Review

Oncogene-Induced Reprogramming in Acute Lymphoblastic Leukemia: Towards Targeted Therapy of Leukemia-Initiating Cells

Vincent Fregona †, Manon Bayet † and Bastien Gerby *

Centre de Recherches en Cancérologie de Toulouse (CRCT), Université de Toulouse, Institut National de la Santé et de la Recherche Médicale (INSERM), UMR-1037, Université Toulouse III Paul Sabatier (UPS), 31100 Toulouse, France; vincent.fregona@inserm.fr (V.F.); manon.bayet@inserm.fr (M.B.)

* Correspondence: bastien.gerby@inserm.fr

† These authors contributed equally to this work.

Simple Summary: Acute lymphoblastic leukemia is a heterogeneous disease characterized by a diversity of genetic alterations, following a sophisticated and controversial organization. In this review, we present and discuss the concepts exploring the cellular, molecular and functional heterogeneity of leukemic cells. We also review the emerging evidence indicating that cell plasticity and oncogene-induced reprogramming should be considered at the biological and clinical levels as critical mechanisms for identifying and targeting leukemia-initiating cells.

Abstract: Our understanding of the hierarchical structure of acute leukemia has yet to be fully translated into therapeutic approaches. Indeed, chemotherapy still has to take into account the possibility that leukemia-initiating cells may have a distinct chemosensitivity profile compared to the bulk of the tumor, and therefore are spared by the current treatment, causing the relapse of the disease. Therefore, the identification of the cell-of-origin of leukemia remains a longstanding question and an exciting challenge in cancer research of the last few decades. With a particular focus on acute lymphoblastic leukemia, we present in this review the previous and current concepts exploring the phenotypic, genetic and functional heterogeneity in patients. We also discuss the benefits of using engineered mouse models to explore the early steps of leukemia development and to identify the biological mechanisms driving the emergence of leukemia-initiating cells. Finally, we describe the major prospects for the discovery of new therapeutic strategies that specifically target their aberrant stem cell-like functions.

Keywords: oncogene-induced reprogramming; (pre-)leukemic stem cells; cell plasticity; self-renewal; oncogenic transcription factors; acute lymphoblastic leukemia

Citation: Fregona, V.; Bayet, M.; Gerby, B. Oncogene-Induced Reprogramming in Acute Lymphoblastic Leukemia: Towards Targeted Therapy of Leukemia-Initiating Cells. *Cancers* **2021**, *13*, 5511. https://doi.org/10.3390/cancers13215511

Academic Editor: David Wong

Received: 7 October 2021
Accepted: 28 October 2021
Published: 2 November 2021

1. Introduction

Cell plasticity is a property required for cell reprogramming. The specification of cellular fate during development and differentiation is a dynamic and evolving process that initiates in stem/progenitor cells. A network of transcription factors controls the balance between the maintenance of stem cell identity and the process of lineage specification. However, somatic cell identity is not fixed and can be modified since cellular reprogramming has been achieved. Especially, the concept of the stability of stem cell function has been challenged by the finding that only the Oct4, Sox2, c-Myc and Klf4 transcription factors are required for the reprogramming of somatic cells into induced pluripotent stem cells (iPS) [1]. Interestingly, these four factors have been shown to be oncogenic in different contexts [2], suggesting a link between cell reprogramming and tumorigenesis. This observation is along the lines of the notion that cancer progression is characterized by the gradual loss of a differentiated state associated with the reprogramming of stem cell-like features.

Indeed, transcriptional and epigenetic modifications occurring in malignant cells frequently lead to tumor dedifferentiation and the acquisition of stemness features [3] and can be exploited using machine learning approaches to predict the clinical outcome and to identify potential drugs targeting the stemness signature [4]. Thus, cell plasticity, oncogene-induced reprogramming, self-renewal, perturbation of lineage identity and cancer initiation appear to be tightly intertwined and should be considered as critical mechanisms for identifying and targeting the cell-of-origin of cancer.

Self-renewal is defined by the functional property of stem cell populations that undergo symmetric or asymmetric divisions to preserve tissue integrity and homeostasis in normal development. In adult hematopoiesis, sustained self-renewal is a distinctive function of normal hematopoietic stem cells (HSCs) which is tightly controlled by a network of transcription factors [5], whereas committed hematopoietic progenitors are devoid of this stem cell property. Thus, it was originally thought in myeloid malignancies that the biological features of leukemic stem cells (LSCs) come from reminiscent states of normal HSCs in which self-renewal is a central property in the process of leukemia initiation. In particular, pioneering studies in chronic myeloid leukemia (CML) considered that the primary oncogenic event takes place in rare and self-renewing multipotent stem cells [6,7], and established the concept that these cells are prone to transformation because of their unique self-renewal capacity. In acute myeloid leukemia (AML), the notion that leukemia originates from an HSC or a committed progenitor is debated in the field. The phenotypic characterization of LSCs in the original studies led to the idea that AML is organized in a hierarchical pattern, in a way similar to that of normal hematopoiesis and derive from the malignant transformation of a primitive hematopoietic cell [8,9]. Supporting this notion, some murine leukemia models have led to show that AML-initiating mutations occur at the level of HSCs and alter their self-renewal properties [10,11]. However, there is evidence that leukemia-initiating activity can be observed not only in an immature cell population but also in populations corresponding to a range of normal committed progenitors. Indeed, a number of studies brought evidence that more mature progenitors, that normally lack any potential for self-renewal, may be the cells-of-origin in AML [12–16]. Thus, oncogenic transcription factors can destabilize the normal molecular program of target cells, leading to changes in gene expression and to a total or partial loss of the original cell identity.

Defined as the most frequent pediatric cancer, acute lymphoblastic leukemia (ALL) is a multistep disease characterized by the acquisition of diverse genetic alterations that can be classified into more than 20 B-lineage subtypes (B-ALL) and more than 10 T-lineage subtypes (T-ALL). These different oncogenic subgroups are established according to the identity of the first oncogenic event carrying in the leukemic cells [17]. Chemotherapy is efficient at inducing long-term remission in child but is associated with severe side effects and undesirable consequences, including second malignant neoplasms. Indeed, while the 5-year survival rates now exceed 90%, the most common cause of treatment failure in pediatric ALL remains relapse that occurs in approximately 15–20% of patients [17]. In addition, the treatment is also limited by indiscriminate toxicity towards normal HSCs. Over the last decade, genome-wide analyses, mainly through next generation sequencing approaches, have been extensively used to draw the genomic landscape and the gene expression profile of ALL patients. As recently reviewed and updated both in T-ALL [18] and B-ALL [19,20], this offered major insights regarding the diversity of oncogenic subtypes associated with altered signaling pathways and led to patient stratification and to the discovery of new therapeutic opportunities. However, although current chemotherapy is efficient at reducing the tumor load by targeting proliferating and metabolically active leukemic cells, the disease relapse points to the presence of resistant cells that escape treatment [21]. Thus, pioneering works and emerging studies converge around the notion that the biological properties of pre-leukemic and/or leukemic stem cells, including oncogene-induced reprogramming, cell plasticity, sustained self-renewal activity, cell-quiescence and drug-resistance, can significantly affect leukemia treatment and should be considered in the search for new and more targeted therapies.

With a focus on B-ALL and T-ALL, we present in this review previous and current studies exploring the cellular, molecular and functional heterogeneity in leukemic cells from patients. With a particular emphasis on the lymphoid lineage, we also review the engineered mouse models that led to the recognition that a single primary oncogene could be sufficient to confer stem cell-like properties to committed progenitors, converting them to a population of pre-LSCs. Finally, we describe the perspectives for the identification of new therapeutic agents that specifically target their aberrant stem cell-like functions.

2. Cellular and Molecular Heterogeneity in Acute Leukemia: In Search of Leukemic Stem Cells

2.1. The Origin of the Leukemic Stem Cell Concept

According to several pioneering works [22–27], normal hematopoiesis is a well-known tightly regulated process based on a hierarchical organization in which a small number of multipotent stem cells maintain all of the hematopoietic lineages. Similar to the normal hematopoietic system, the concept of leukemic stem cells (LSCs) supports the idea that leukemic cells are functionally heterogeneous, following a hierarchical model in which only a minor population of LSCs residing are able to initiate and indefinitely maintain the neoplastic tissue. Historically and experimentally built on xenograft transplantations, this concept has come from pioneering studies on AML from Dick's laboratory, which have defined a distinct subpopulation of tumor cells characterized by their capacity to initiate and propagate the disease when transplanted into immunodeficient mice [8,9]. Since this finding, xenotransplantation of human leukemic cells has become the gold standard assay to study LSC activity [28]. Based on an immunophenotypic identification, AML was thus the first hematological malignancy with a reported LSC population within the tumor bulk that sustains the long-term leukemia development. This has been confirmed by a number of subsequent studies describing a rare and specialized population of LSCs enriched in the CD34+CD38-Lineage- fraction from AML patients [29–32]. However, transplantable LSCs from AML samples could also be found in the CD34+CD38+ and CD34- subpopulations, albeit with lower frequency [28,33–35], and therefore could be phenotypically more diverse than originally thought. Despite this controversy, it is still inferred that in contrast to leukemic blasts that have limited self-renewal potentials, LSC-enriched populations reside at the apex of the leukemia hierarchy, are able to sustain long-term tumor growth and constitute an important driver of relapse through their slow division rate that make them resistant to conventional therapies [28,36].

2.2. Phenotypic and Functional Plasticity in ALL

The notion of cellular and functional heterogeneity in leukemic cells is of fundamental interest to understand the leukemia initiation and development in patients. Therefore, the hierarchical model of the LSC concept was applied to acute lymphoblastic leukemia, in both B-ALL and T-ALL. In B-ALL, scientists extensively used CD34, CD38 and CD19 markers to explore cellular and functional heterogeneity in leukemic blasts from adult and infant patients, which lead to many controversies [37]. It has originally been proposed that leukemic cells with the HSC-like immunophenotype CD34+CD19- exclusively contained LSCs in both high and standard risk B-ALL [38,39]. However, the following investigations demonstrated that self-renewal activity can be enriched in leukemic subpopulations expressing the CD19 marker [40–43], corresponding phenotypically to a range of normal B-cell precursors. Nevertheless, the prospective enrichment of LSCs in B-ALL using the CD34 and CD38 surface markers, associated or not with CD19, led to highly variable results [37,42–44]. These controversial conclusions could be explained by the possibility that the majority of blasts among the tumor can sustain leukemia-initiating activity, thus following a stochastic model of B-ALL. Indeed, Vormoor and colleagues challenged the hierarchical stem cell concept by demonstrating using limiting dilution assays (LDAs) that B-ALL cells able to engraft immunodeficient mice are highly frequent and are not restricted to a population with a specific immunophenotype [43,45]. Using

an in vivo tracking approach by cellular barcoding of B-ALL samples combined with deep sequencing, the same group reported that leukemia-initiating clones are abundant and functionally equipotent, exhibiting a similar ability to reconstitute the disease over serial transplantations [46]. Other investigations by Rieger and colleagues demonstrated at the single-cell level that the expression of CD34 and CD38 markers is a highly plastic and dynamic process at the surface of B-ALL blasts [47], which also could explain the previous discrepancies in using these two markers for the enrichment of LSC activity. In the same line of thought, the loss of CD19 antigen expression at the surface of leukemic cells enabling the tumor to evade chimeric antigen receptor (CAR) immunotherapy [48,49] is a well-known representative example of antigen plasticity and evolved adaptation of leukemic cells upon the treatment. Therefore, the identification of several stable surface markers aberrantly expressed in leukemic cells is critical to follow the disease evolution and to monitor resistant cells [50,51]. Together, phenotypic and functional plasticity should be considered in experimental approaches to identify LSC-enriched populations, but also at the clinical level to explain therapy escape mechanisms and B-ALL relapse.

In contrast to B-ALL, there are few published studies of cell populations enriched in LSCs from human T-ALL samples. Nevertheless, original works demonstrated that leukemia-initiating activity can be explored by using in vivo xenografts and in vitro assays [52,53]. The functional heterogeneity in human T-ALL combined with the phenotypic characterization of the LSC compartment has been explored using CD34, CD7 and CD4 surface markers. In particular, the work from Pflumio's group reported that CD34+CD7-CD4- fraction from the blood of T-ALL patients does not produce leukemic blasts but undergoes normal hematopoiesis in vitro and after transplantation into immune-deficient mice [54], which is quite similar to what has been observed for the CD34+CD19-CD38- population from B-ALL patients [41,42], and that correspond to the residual and circulating normal hematopoietic stem and progenitor cells (HSPCs). In fact, LSC activity seems to be exclusively present in the CD7+ fraction [54,55], suggesting that T-ALL initiation is triggered in a committed T-cell. Finally, T-ALL development is significantly pronounced after the xenograft of CD7+CD34+ leukemic cell population, as demonstrated in three independent studies [54,56,57]. Interestingly, despite the fact that the CD34 marker seems to be useful to enrich LSC activity from T-ALL samples, immunophenotyping of donor-derived blasts in xenograft samples revealed that CD34+ blasts may lose the CD34 maker after transplantation, and vice versa [57]. This observation suggests that CD34 could be a plastic marker at the surface of T-ALL blasts, as it has been shown at the clonal level in B-ALL [47], and asks about the functional relevance and the correspondence of LSC surface markers between blasts from patients and blasts from patient-derived xenografts (PDX).

Collectively, these studies challenge the hierarchical organization of the stem cell concept in ALL by raising the question of whether surface marker plasticity is connected to functional plasticity within the tumor. Indeed, T-ALL characteristics such as cell-surface immunophenotype, but also dormancy and chemoresistance, are under the influence of the bone marrow (BM) niches, indicating an important cellular and functional plasticity of leukemic cells in response to their in vivo microenvironment [58]. Using ALL xenograft models combined with in vivo cell-division assay, Jeremias and colleagues also addressed this notion by demonstrating that stem cell properties, such as dormancy, treatment-resistance and leukemia-initiating activity, are reversible [59]. In addition, the authors showed that the functional plasticity of dormant clones is dependent of their in vivo environment and suggest that this reversible mechanism could be involved in treatment failure and ALL relapse. The molecular characterization of those dormant and chemo-resistant clones recently led to the extraction of a core subset of genes that would help for the risk stratification of ALL patients [60], as previously achieved in AML [61]. Together, these findings raise the importance of considering cellular and functional plasticity in the clinical outcome of ALL patients. This points to the need to focus on the functional mechanisms of leukemic cells, such as self-renewal, cell-quiescence and -resistance, to identify new specific LSC markers.

2.3. When Molecular Diversity and Clonal Evolution Meet the LSC Theory

Accurately addressing the cell-of-origin in leukemic patients using surface markers seems to be obviously limited, not only by the plastic properties of leukemic blasts as previously described, but also by their genetic heterogeneity, which represents a major hallmark of cancers, including ALL [62,63]. Indeed, the development of acute leukemia is a multistep process characterized by the acquisition of accumulated mutations. Consistent with the observation that acute leukemias exhibit a limited number of genetic alterations [64], each mutation can perturb critical cellular functions and their combinatorial interaction would be sufficient to cause leukemia.

Through a cytogenetic approach by multiplex fluorescence in situ hybridization (M-FISH), Greaves and colleagues explored in a ground-breaking study the intraclonal genetic architecture of leukemic cells from B-ALL patients. Since the M-FISH approach allows for the detection of up to eight genetic alterations at the single-cell level, the authors provided the first direct evidence for genetic diversity of leukemic cells by establishing phylogenetic trees of clonal evolution within individual patients [65]. Major insights in the composition and the dynamic of subclones in leukemic cells have been also gained through the comparison of the genetic landscape of paired diagnostic and relapse ALL samples, as performed in numerous works [66–75]. Thus, genome-wide studies, including single nucleotide polymorphism (SNP), next generation sequencing (NGS), comparative genomic hybridization (CGH) and multiplex ligation-dependent probe amplification (MLPA) analyses of matched diagnosis-relapse ALL samples, led to an exhaustive characterization of the genetic profile of patients during the evolution of their disease. These integrative approaches helped to establish the complex architecture of individual leukemia and revealed that a relapse may be generated from major, minor or ancestral clones from the initial diagnosis. Remarkably, Mullighan and colleagues demonstrated that more than half of the relapse ALL samples lacked some of the genomic copy number abnormalities (CNAs) present at the diagnosis and acquired new and distinct genetic lesions [66,75,76]. This observation indicated that in the majority of ALL cases, relapse leukemic cells have evolved not from the bulk of the diagnosis cells but from a clone that harbored a restricted number of genetic alterations, such as a founding chromosomal translocation. Indeed, while a relapse may be produced from a predominant clone at the diagnosis, the majority of them arise from pre-existing minor subclones highly diluted within the diagnosis sample or from the clonal evolution of an ancestral clone [66,75,77,78].

By the same way of evidence, whole- and targeted-exome sequencing of peripheral blood cells from a large cohort of healthy individuals identified that 10 to 20% of people aged over 70 harbor pre-leukemic mutations resulting in the dominance of a small number of HSC-derived clones, a process called age-related clonal hematopoiesis (ARCH) [79,80]. While these pre-leukemic HSCs still have the capacity to differentiate and produce healthy blood cells, additional mutations can lead to disease progression towards myeloid malignancies such as AML [81]. In addition, ultra-sensitive deep sequencing of targeted genomic regions from AML patients revealed the existence of long-lasting clones carrying pre-neoplastic mutations, referred to as pre-leukemic HSCs hidden within the bulk of the tumor and that serve as a reservoir for disease progression [82–84]. These cells can thus acquire stem cell-like drug resistance mechanisms and by way of consequences, are spared by current treatment and are involved in the disease evolution and relapse. Despite of their low abundance in patients, it has been recently shown using clonal tracking from single-cell transcriptomics that these pre-LSCs exhibit a specific gene expression profile, distinct from that of leukemic cells and of normal HSCs [85].

Since xenotransplantation remains the gold standard assay to evaluate leukemia-initiating activity, the notion that genetic subclones are frequently selected in xenograft models adds a level of complexity to the LSC definition. Nevertheless, tracking leukemic clones in immunodeficient mice not only provides insights into the genetic and clonal architecture of human ALL, but also can be used to isolate resistant and adaptative subclones that participate to disease progression. Indeed, it has been shown that xenograft models

of T-ALL can recapitulate at the genetic and functional levels to the gain of malignancy observed at relapse of the disease, including aggressiveness and therapy resistance [86]. Consistent with a branched rather than linear evolution, oncogenic trees showed that xenograft and relapse samples had frequently derived from an ancestral pre-leukemic clone, and not from diagnosis cells. Interestingly, in the case of *ETV6-RUNX1*-induced B-ALL, the putative ancestral pre-leukemic clone harboring the *ETV6-RUNX1* fusion only observed at the time of diagnosis does not regenerate neither over serial transplantations nor at the relapse [65]. This finding suggests that although xenografting leukemic cells allow us to explore the genetic progression and the aggressiveness of the disease, it does not represent a relevant approach to expand and isolate ancestral pre-leukemic clones. The branching and multi-clonal evolution model of leukemogenesis has been similarly explored using xenotransplantation approaches in *BCR-ABL1* [87] and in *MLL*-rearranged [88] ALL. Therefore, although debated in the literature [89,90], genetic and clonal variegations should definitely be considered to define LSCs by using transplantation in immunodeficient mice. Through an unprecedented large-scale LDA xenografting approach combined with targeted sequencing, this point was recently clarified by the isolation and the characterization of subclones from diagnosis B-ALL samples responsible for a relapse [91]. These clones, referred to as diagnosis Relapse-Initiating (dRI) clones, can be revealed only in a minor proportion of xenografted mice and display low sensitivity to chemotherapeutic agents. At the molecular level, dRI clones activate the mitochondria metabolism and unfolded protein response (UPR) [91], two stress molecular pathways that have been described to be critical in the maintenance of stem cell homeostasis and function [92,93].

A better understanding about the dynamic and the selection of leukemic cells during disease progression has also been gained through single-cell developmental classification methods. In particular, Nolan and colleagues developed a single-cell mass cytometry (CyTOF) approach [94] allowing for the simultaneous quantification of up to 35 proteins, including surface markers and intracellular phosphorylated proteins involved in normal and pathological B-cell development [95,96]. Using this strategy, they were able to align human B-cell subpopulations into a unified trajectory and to precise their regulatory signaling pathways during early differentiation checkpoints [96]. Built on this expertise and combined to machine learning approaches, they recently established a single-cell classification of human B-ALL at the diagnosis and identified specific features, such as activated mTOR signaling and unresponsive pre-BCR signaling, which were sufficient to predict patient relapse [95]. In addition, Müschen and colleagues recently used single-cell amplicon sequencing combined with a single-cell phosphoprotein analysis to study the interaction of oncogenic lesions in STAT5 and ERK signaling pathways during normal B-cell development and malignant transformation [97]. Using these approaches, the authors showed that the driver mutations in these two pathways are mutually exclusive in human B-ALL, consistent with the segregation of STAT5 and ERK phosphorylation. Moreover, the following functional experiments showed that concurrent oncogenic STAT5 and ERK activation can subvert leukemia development, demonstrating the proof of concept that the reactivation of divergent and conflicting signaling pathways represents a powerful barrier to transformation [97]. Recently, single-cell amplicon sequencing has also been applied in human T-ALL to study their clonal heterogeneity and evolution [98]. Strikingly, this approach allowed for the detection of clinically relevant subclones at diagnosis that evolved to major clones at later disease stages.

Collectively, these studies uncovered a considerable and interconnected subclonal diversity in leukemic cells from ALL patients, resulting from a complex, nonlinear and branching evolutionary pathway. They have also demonstrated that the majority of ALL relapses after chemotherapy arise from persisting and resistant minor clones already existing at the time of diagnosis, which can be revealed using xenograft models. These studies predicted the existence of an ancestral pre-diagnostic clone harboring a minimal set of genetic alterations which is not yet transformed but at the top of the tumoral hierarchy and heterogeneity. In addition to genomic approaches, this set of publications also highlights

the relevance in using single-cell phosphoprotein analyses to define a precise trajectory of normal and pathological B-cell development and to anticipate the relapse of the disease.

3. Oncogene-Induced Reprogramming in ALL: Tracking (Pre-)Leukemic Stem Cells

3.1. Self-Renewal Property and Lineage Plasticity: Early Events of Leukemogenesis?

Major insights about the multistep process and the prenatal origin of ALL development have been gained from 25 years of outstanding studies by Greaves and his group, exploring leukemia initiation and progression in monochorionic twins [99]. These studies revealed that chromosomal translocations, in particular *ETV6-RUNX1*, could be detected in blood cells many years before the leukemia onset, establishing a pre-leukemic sub-clonal compartment. Thus, these pre-leukemic cells contain the founding genetic alteration but do not have the capacity to induce the disease by themselves. Later in life, the acquisition of full complement mutations transforms them into malignant leukemic cells, subject to clonal evolution and selection processes, and leads to the genetic heterogeneity of the tumor bulk at the time of diagnosis [99]. Therefore, it seems to be clear that *ETV6-RUNX1* originates prenatally during fetal hematopoiesis and acts as a first oncogenic event in a committed B-cell to induce the emergence of a pre-leukemic clone with altered self-renewal and survival properties [100]. Interestingly, the self-renewing pre-leukemic clone exhibits the combination of surface markers CD34+CD38-CD19+CD10- that corresponds neither to a normal B-cell subpopulation nor to fully transformed leukemic blasts. Together, these findings support the view that self-renewal is an early and obligatory event in leukemia initiation, a specific feature of the cell-of-origin, and differs from the propagating activity of fully transformed leukemic blasts. Obviously, the major limit is that pre-leukemic clones are very infrequent in ALL patients [65,75]. Therefore, except in rare cases of paired leukemic and pre-leukemic monochorionic twins [99], exploring their biological properties remains highly challenging.

To tackle this issue, the development of engineered mouse models in which there are activated particular oncogenes in specific lineages is of critical interest. Indeed, transgenic mice represent a valuable tool to understand the biological mechanisms by which a primary oncogene induces the disease and their use opens new challenges and has several perspectives: (i) it allows us to decipher biological mechanisms by which an oncogenic pathway perturbs normal hematopoietic development and reprograms a committed progenitor into a pre-LSC during the disease initiation; (ii) it helps to understand the multistep process of the disease from the pre-leukemic to the leukemic stages by identifying the oncogenic collaborative events driving malignant transformation; (iii) it allows us to explore at the molecular and functional levels the crosstalk between pre-leukemic and leukemic cells with their microenvironment; and (iv) finally, it aims to develop therapies that specifically target markers and/or biological mechanisms involved in leukemia development and resistance (Figure 1).

The use of AML mouse models corroborated that the genetic alterations of transcription factors are early events in leukemia development and can interfere with essential cellular functions of somatic cells. As examples, oncogenes such as *MOZ-TIF2* [12], *MLL-AF9* [13], *MLL-ENL* [14] or *PML-RAR* [15,16] were shown to be able to induce AML development when introduced into committed target cells. Precisely, the molecular and cellular characterization of the cell-of-origin from the AML mouse models led to the recognition that these cells can self-renew and exhibit a self-renewal gene signature induced by such oncogenic transcription factors. For example, *AML1-ETO* and *MLL-AF9* disrupt the normal hematopoietic functions by inducing self-renewal activity of myeloid progenitors prior the progression towards overt leukemia [13,101,102]. In the case of *MLL-AF9*, gene expression arrays have revealed that the oncogene can activate an HSC-like program in committed granulocyte–macrophage progenitors [13,102]. However, other oncogenes such as *BCR-ABLp190* are unable to confer self-renewal properties to hematopoietic progenitor cells [12]. In these cases, the self-renewal function must be conferred by the targeted cell or by additional genetic alterations. On the other hand, the abrogation of transcription factor

activity could also result in impaired differentiation and the development of hematopoietic malignancies, such as myelodysplastic syndrome (MDS) and AML. For example, the loss of function mutations of the two important transcription factors RUNX1 and CEBPα have been identified in rare familial hematopoietic disorders involving a predisposition to MDS and AML. Furthermore, murine models with diminished expression of key transcription factors such as JunB, Gata1 and Gata2 have shown to perturb HSC regulation and function, establishing a pre-leukemic state, primed to undergo subsequent AML transformation [103–105]. These observations support the view that the loss of function of key transcription factors can also lead to the emergence of an aberrant pre-leukemic stem cell population prior to clonal transformation.

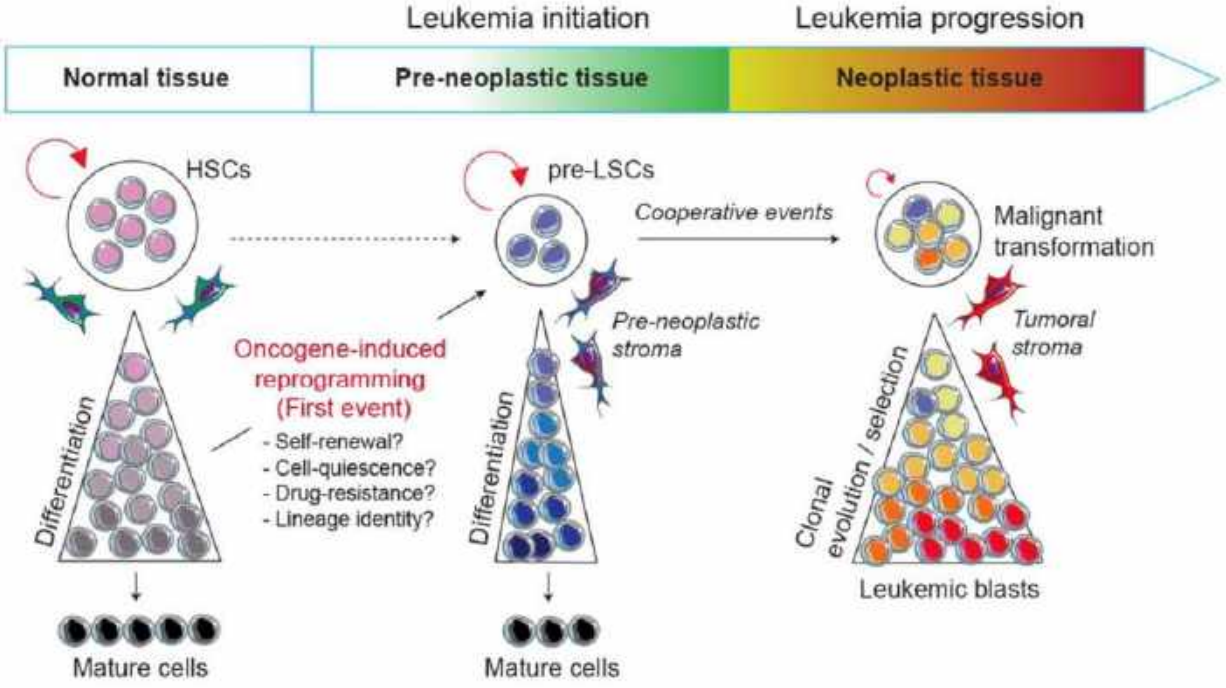

Figure 1. Model of leukemic evolution. A first oncogenic event can either convert a normal HSC or reprogram a normal committed progenitor into a self-renewing pre-LSC. Thus, pre-LSCs are the first cells carrying the initial pre-leukemic lesion but are still able to differentiate and give rise to mature cells. Next, following secondary and cooperative events transform pre-LSCs into malignant leukemic cells that are subjected to clonal evolution and selection processes.

Considering the importance of self-renewal in leukemia initiation, an outstanding question remains how one oncogenic transcription factor can modify or reprogram stem cell-like properties in normal cells and can lead to the emergence of a pre-neoplastic population (Figure 1). The occurrence of biphenotypic leukemias and the concept of lineage infidelity in acute leukemias have long been thought of as a degree of plasticity in leukemic cells which either is conferred by the cell-of-origin, such as a pluripotent stem/progenitor, or results from the oncogene subversion of the process of lineage determination in a committed progenitor [106]. This long-lasting idea revives the question of to what extent oncogenic transcription factors in acute leukemias lead to the reactivation of self-renewal genes with or without pluripotency. It also asks to what extent oncogenic alterations that arise in committed progenitors lead to a whole or partial reprogramming of a normal cellular fate and open a new pathologic developmental program. Moreover, the exploration of the cell-of-origin in mixed phenotype acute leukemia (MPAL) led to the idea that a founding alteration, rather than the secondary events, primes pre-leukemic clones for lineage plasticity [107].

3.2. Pre-Leukemic Thymocyte Self-Renewal: Lesson from bHLH Transcription Factors

In ALL, the demonstration that an oncogenic transcription factor can reprogram a committed progenitor into an aberrant self-renewing pre-LSC has been made for the first time in thymocytes. Since bone marrow-derived progenitors settle in the thymus and gradually lose stemness properties and acquire T-cell characteristics, normal thymocytes have a very limited self-renewal capability [108]. Indeed, thymic output requires continuous seeding from HSCs-derived progenitors, and thymic progenitors progress into the thymus through several stages of differentiation (DN1-4, ISP8, DP) before giving rise to $CD4^+$ or $CD8^+$ immunocompetent cells [109,110]. Therefore, the thymus represents a relevant cellular platform to study oncogene-induced reprogramming. As assessed by serial transplantation of pre-leukemic thymocytes, McCormack and colleagues reported that the overexpression of the *Lmo2* oncogene in the thymus induces the emergence of a population of pre-LSCs [111]. Precisely, using Cd2-Lmo2 transgenic mouse model that recapitulate the human T-ALL, the study showed that enforced expression of Lmo2 converts normal DN3 thymocytes into a self-renewing, pre-leukemic population by reprogramming a stem cell-like gene program.

LMO proteins, members of the LIM-domain only family, lack the DNA-binding ability and require a protein interaction with basic helix-loop-helix (bHLH) transcription factors such as SCL/TAL1 (SCL) or LYL1 to form a multiprotein complex on DNA and activate the transcription that controls HSPC functions [112]. Based on this molecular evidence, protein–protein interaction should occur between bHLH and LMO1/2 oncoproteins to activate the aberrant stem cell gene program in pre-LSCs. Indeed, Hoang and colleagues showed that the ectopic expression, the interaction and the collaboration of SCL and LMO1 oncoproteins are critical to alter thymocyte differentiation [113] and to induce a self-renewal molecular network for the emergence of pre-LSCs in the thymus [114,115]. Therefore, the capacity of SCL-LMO1 to reprogram DN3 thymocytes into self-renewing pre-LSCs mirrors in some aspect the physiological function of SCL, which controls the repopulation ability and the maintenance of HSPCs [116–118]. Furthermore, associated with LMO1, LYL1 ectopic expression mimics the effect of SCL to activate the self-renewal function in pre-LSCs [114], corroborating their functional redundancy described in normal HSCs [119]. In contrast, the loss of function approaches showed that Lyl1, but not Scl, is required for *Lmo2*-induced thymocyte self-renewal [120]. This observation suggests that Lmo2 oncoprotein interacts preferentially with endogenous Lyl1 than with Scl for thymocyte reprogramming. According to the importance of *Scl* gene dosage in normal HSPCs [117,118], the alternative explanation would be that the physiological levels of Scl in thymocyte progenitors are not sufficient for its efficient interaction with Lmo2 oncoprotein.

Cell purification indicates that only DN3 thymocytes in both *Lmo2* or *SCL-LMO1* mouse models are able to colonize the thymus of recipient mice in transplantation assays [111,114]. The intriguing question then is what predisposes DN3 subsets to reprogramming by these primary oncogenes? The DN3 stage represents a critical restriction point in the thymus when thymocytes are committed to the T-lineage and lose non-T potential under the influence of NOTCH and pre-TCR signaling pathways. Reprogramming self-renewal activity likely occurs just prior to pre-TCR signaling since self-renewal can be induced in $Cd3\varepsilon^{-/-}$ DN3a cells [114]. Thus, while pre-TCR signaling represents a collaborating event in T-ALL progression and transformation [121], it is dispensable for the initial transition from DN3 thymocytes to pre-LSCs. Therefore, NOTCH signaling, which is activated at highest levels in DN3 cells [122], represents a strong candidate to collaborate with *Lmo2* or *SCL-LMO1* oncogenes in thymocyte reprogramming. NOTCH signaling is essential for T-cell commitment and specification [123] but its role in stem cell self-renewal is controversial. Indeed, some studies indicate that NOTCH does not exert an essential function in adult HSCs [124–126], while others suggest that NOTCH activation enhances their self-renewal capacity [127,128]. The frequent occurrence of activating mutations of the *NOTCH1* gene in T-ALL patients [129] and in mouse models of the disease [110,130], as well as the sensitivity of both human [52,56] and murine leukemic blasts [131] to NOTCH1

inhibitors, strongly indicates that a gain of function of NOTCH1 represents a critical step in cell transformation. Nonetheless, enforced expression of NOTCH signaling by itself does not convert thymocyte progenitors into pre-LSCs [111,114], comforting the notion that *NOTCH1* mutations observed in patients are collaborating and not initiating events in the leukemogenesis process. However, pre-LSC self-renewal induced by *SCL-LMO1* collaborates with the physiological levels of the NOTCH-MYC signaling axis [114], which is provided by the cellular interactions with thymic stromal cells. Thus, in contrast to leukemia propagating cells which have acquired different sets of secondary mutations, pre-LSCs are believed to be genetically and phenotypically stable, are still capable of differentiating into mature and functional T-cells and remain highly dependent on their thymic microenvironment [111,114,121].

The major advantage of the transgenic models is to provide unrestricted and reproducible access to pre-LSCs that allow us to study and target their cellular and molecular mechanisms and particularly those involved in therapy resistance. Recent works showed that pre-LSCs are resistant to chemotherapeutic agents because of their distinctive slow-division rate [132,133]. Indeed, it is well known that cell quiescence may be an important limitation for therapeutic efficiency, as exemplified at the clinical level in CML [134,135]. Using doxycycline-inducible *H2B-GFP*^{tg} mice, a gold standard in vivo model to study cell quiescence of normal HSCs [136,137], Curtis and colleagues demonstrated that self-renewal, drug resistance and clonal evolution are restricted to a rare and slow-cycling population of pre-LSCs in the *Lmo2*-induced T-ALL model [133]. This work not only defines for the first time the importance of the cell cycle restriction in pre-LSC activities, but also makes the *H2B-GFP* system as a powerful in vivo tool to purify slow-cycling pre-LSCs in other models and to develop strategies targeting the quiescence and the resistance of relapse-inducing clones.

Collectively, this set of publications provided new insights into the long-lasting questions concerning the cell-of-origin of T-ALL and the molecular mechanisms by which oncogenic transcription factors can reprogram the self-renewal property to thymocytes, thus establishing a pre-leukemic state before malignant transformation. These studies demonstrate that the main effect of the transcription factor SCL, associated with its partner LMO1/2, is to induce DN3 thymocyte self-renewal. While thymocyte reprogramming induced by other T-ALL transcription factors such as TLX1, TLX3 or HOXA remains unexplored, emerging studies indicate that chromosomal rearrangements generating NUP98 fusion proteins can induce thymocyte self-renewal prior the DN3 stage [138,139]. These observations suggest that only particular cells possess the necessary molecular background to allow for oncogene reprogramming, and conversely, only some oncogenes, in the right cellular context, can induce stem cell-like properties. Despite this, the question of whether a primary oncogene in ALL induces sufficient molecular and functional plasticity to cause lineage subversion remains poorly explored. Interestingly, SCL and LMO2 belong to the five transcription factors that convert adult fibroblasts to multipotent hematopoietic progenitors [140], suggesting their critical functions in cellular and molecular reprogramming of committed cells. Using the generation of targeted mouse lines conditionally expressing *Lmo2*, two recent studies demonstrate that *Lmo2* acts as a "hit-and-run" oncogene in T-ALL development [141,142]. Precisely, while pre-LSC self-renewal activity required continuous Lmo2 expression, overt leukemia frequently evolves in a Lmo2-independent manner [142]. This observation strongly suggests that oncogenic evolution occurring in fully transformed blasts overcomes the requirement of the initiating event. In addition, B-cell-restricted expression of Lmo2 reprograms committed B-cells into malignant T-ALL [141], demonstrating the proof of concept that a primary oncogene can induce sufficient reprogramming to switch from a B-cell fate to a T-cell neoplastic process. The cell-of-origin and the role of the primary oncogene *ETV6-RUNX1* in lineage organization have also been addressed recently [143]. Using a lineage-specific oncogenic activation approach, Vicente-Duenas and colleagues demonstrated that *ETV6-RUNX1* can give rise to both B-ALL and T-ALL and that leukemia transformation is dependent from the nature of the acquired secondary

mutations [143]. Although *ETV6-RUNX1* is always associated with B-ALL in humans, this strategy predicts that pre-leukemic clones exhibit a T-cell potential. Together, these findings have important implications to develop targeted therapies of pre-LSCs.

3.3. Cell Reprogramming by PAX5 Mutants: To B-Cells or Not to B-Cells?

Adult B-cell development is initiated in the BM by the entry of hematopoietic progenitors into the B-cell lineage transcription program and the concomitant sequential rearrangements of the immunoglobulin genes through V(D)J recombination, leading to the generation of immune-competent plasma cells. B-cell development can be dissected into pre-pro-B, pro-B, pre-B, immature B and mature-B cell populations corresponding to different stages of differentiation [144]. B-lineage commitment is characterized by the rearrangement of the immunoglobulin heavy-chain (*IgH*) locus that occurs during the differentiation of pre-pro-B cells to pro-B cells. Productive V_H-D_H-J_H recombination leads to the expression of the Igμ protein as part of the pre-B cell receptor (pre-BCR), which promotes the transition from the pro-B to the pre-B cell stage [145]. Then, successful immunoglobulin light-chain (*IgL*) gene rearrangement in pre-B cells results in the emergence of immature IgM^+ B cells that emigrate from the BM to peripheral lymphoid organs [146]. B-cell lineage is generated from HSCs by a complex and tightly regulated differentiation processes. Among them, the *PAX5* gene encodes the crucial transcription factor PAX5, which has been described as the guardian of B-cell identity [147,148]. Indeed, while the developmental progression from early B progenitors to plasma cells is regulated by several extracellular signals and transcription factors [149], PAX5 is considered as a master piece to control the irreversible commitment of lymphoid progenitors to the B-cell lineage by activating the transcription of B-cell-specific programs and by suppressing alternative lineage choices [147,150,151]. The initial work demonstrated that B-cell differentiation is completely blocked at the transition between pre-pro-B and pro-B stages in $Pax5^{-/-}$ mice, revealing the critical role of Pax5 in the B-cell commitment [152]. Then, functional experiments, including transplantation assays, revealed that $Pax5^{-/-}$ B-cells had the ability to home in on the BM, where they exhibited aberrant engraftment activity [153]. In addition, uncommitted $Pax5^{-/-}$ B-cells are able to differentiate into several hematopoietic cell types, either in vitro in the presence of appropriate cytokines or in vivo after transplantation [147,153–155]. Finally, Pax5 inactivation in mature B-cells leads to the downregulation of B-cell-specific genes and the reactivation of lineage-inappropriate genes [156–158]. This process allowed for their conversion into functional T cells exhibiting *IgH* and *IgL* gene rearrangements by dedifferentiation back to early uncommitted progenitors [159]. Interestingly, the loss of lineage identity by the elimination of Pax5 in mature B-cells is also associated with an increased risk of lymphoma development [159]. Together, these findings highlight the critical role of Pax5 in B-lineage commitment and in maintaining the B-cell identity. Given the importance of normal Pax5 in the B-cell development and the degree of plasticity of committed B-cells, the question of whether and to what extent genetic alterations involving *PAX5* could reprogram B-cell progenitors and perturb their identity and function remain to be fully explored.

PAX5 is a well-known haploinsufficient tumor suppressor gene in human B-ALL. Indeed, heterozygous deletions of *PAX5* are found in about one-third of patients [160–162]. These alterations, which are considered as secondary events in B-ALL development, result in the reduction of PAX5 expression or impairment of DNA-binding activity and/or transcriptional activity of PAX5. However, *Pax5* heterozygous mice exhibit normal B-cell development and is not sufficient to induce leukemia in the absence of other oncogenic lesions [163]. The tumor suppressor role of Pax5 has been revealed in these mice using chemical-induced mutagenesis approaches [164]. In addition, the Pax5 tumor-suppressor activity has been demonstrated through the modulation of other critical transcription factors, such as Ebf1 [165,166], Ikzf1 [167] and Stat5 [168]. Since genetic lesions of *PAX5*, *EBF1* and *IKZF1* are commonly found in human B-ALL, it suggests that the dosage of these three genes is critical to prevent the disease [169,170]. Interestingly, combined

heterozygous deletion of *Pax5* and *Ebf1* partially blocks the differentiation of pro-B cells and increases their lineage plasticity before the leukemia onset [165,166,171]. Indeed, $Pax5^{+/-}Ebf1^{+/-}$ pro-B cells downregulated critical genes for the preservation and the stability of the B-cell identity, revealing their response to NOTCH signaling and their T-cell potential in vitro and in vivo. Although the authors did not detect any sign of dedifferentiation into classical hematopoietic progenitors, they demonstrated in this study that simultaneous reduction of Pax5 and Ebf1 induces at the molecular and functional levels a process of lineage conversion in pre-leukemic pro-B cells [171]. Interestingly, molecular reprogramming has been also observed in *Ikzf1* [172] deficient mouse models before the leukemia onset. Thus, these studies reinforce the notion that reprogramming, a partial loss of B-cell identity and leukemia initiation are critical mechanisms involved in pre-leukemic cells prior to malignant transformation. Interestingly, recent works from Sanchez-Garcia and colleagues demonstrated that leukemia initiation and progression can be triggered upon natural infection exposure [173,174] or by altering the gut microbiome [175] in *Pax5* heterozygous mice as well as in the *Sca1-ETV6-RUNX1* model. Indeed, the production of inflammatory cytokines triggered by infection can promote leukemia growth in $Pax5^{+/-}$ mice [176]. These studies strongly support the epidemiological evidence suggesting that patterns of infection and inflammation after birth have a causal role in triggering the acquisition of full complement mutations in pre-neoplastic cells to transform them into malignant leukemia [99]. Indeed, emerging evidence demonstrates that a major driver for the conversion from a pre-leukemic clone to fully transformed B-ALL is the exposure to immune stressors, which currently represent a major therapeutic opportunity in the field [177].

PAX5 is also rearranged in 2.6% of pediatric B-ALL cases, being fused to a wide diversity of fusion partners involving other transcription factors such as ETV6 and FOXP1, chromatin regulators such as NCoR1 and BRD1, a protein kinase such as JAK2 and an estrogen-related receptor such as ESRRB [160,178–181]. All PAX5 fusion proteins conserve the N-terminal DNA-binding paired domain of PAX5 and lack the C-terminal domain, including the transactivation domain [160,180]. Chromosomal translocations involving *PAX5* have been associated with a blockage of B-cell differentiation, the first reported and frequent example being *PAX5-ETV6*, which fuses the PAX5 paired domain to almost the entire ETV6 transcription factor [182]. In contrast to *PAX5* deletions, *PAX5* translocations act as primary oncogenic events, altering normal B-cell development in the early steps of the disease. Therefore, PAX5 fusion proteins represent strong candidates to reprogram stem cell features in B-cell progenitors. However, studying their role in leukemia development is highly limited by the lack of animal models. Exhaustively, transgenic mice expressing PAX5-ETV6 and PAX5-FOXP1 fusion proteins from the *Pax5* locus have been generated. While they failed to induce B-ALL on their own, both fusion proteins blocked the B-cell development at the pro-B/pre-B cell transition [183]. Recently, our group developed a new genetically engineered mouse model of B-ALL induced by PAX5-ELN [184], a fusion protein previously identified in patients [179]. Driven by the *IgH* locus, PAX5-ELN efficiently induced the B-ALL in mice associated with the acquisition of secondary mutations in genes involved in the JAK/STAT and RAS/MAPK pathways, which are recurrently found in B-ALL patients [162] and in other oncogene-induced B-ALL models such as *ETV6-RUNX1* [185] and *TCF3-PBX1* [186] transgenic mice. Thus, these transgenic mice accurately reproduce the key features of leukemia development and provide a valuable in vivo model mimicking the multistep process of human B-ALL. Importantly, the leukemia development is preceded by three months of a pre-leukemic phase which is also associated with a partial blockade of differentiation at the transition of pro-B/pre-B stages. Thus, our in vivo model opens the way for deciphering the biological mechanisms by which a PAX5 fusion protein reprograms normal B-cell progenitors, perturbs B-cell identity and leads to the emergence of pre-LSCs. In addition, it should help us to explore the molecular and the functional crosstalk between pre-LSCs and their BM niches.

Point mutations of *PAX5* are found in about 7% of both adult and childhood B-ALL [161,162]. Somatic mutations of *PAX5* are a hallmark of B-ALL [161,162] and inherited *PAX5* mutations have also been reported [187,188]. In contrast to PAX5 translocations that lead to the loss of trans-activating/inhibitory domains and conserves the integrity of the DNA-binding domain, *PAX5* point mutations are predicted to result in lost or altered DNA-binding or transcriptional regulatory functions [162,189]. The somatic mutation *P80R* of *PAX5* (*PAX5-P80R*) was recurrently identified within the exon 3 encoding the paired DNA-binding domain and represents the most frequent *PAX5* point mutation [161,162]. Recently, it has been shown that the *PAX5-P80R* mutation induces a unique transcriptional program in patients, defining an independent B-ALL subtype and supporting the notion that *PAX5-P80R* is an initiating lesion in the process of leukemogenesis [190–193]. However, the question of whether *PAX5* mutations and PAX5 fusion proteins exhibit different molecular mechanisms in driving B-ALL remains unanswered. Therefore, comparing the effect of PAX5 fusion proteins and *PAX5* mutations on B-cell reprograming and B-cell identity should bring novel insight on the general biological mechanisms required for normal and pathological B-cell development.

4. Murine Models as Tools to Explore the Multistep Process of ALL

As documented in the previous sections, murine models represent valuable tools to explore oncogene-induced reprogramming that occurs in the early step of leukemia development. Furthermore, their use has greatly contributed to understanding the natural history of the human disease from the pre-leukemic state to the following fully transformed stages. Here, we review and update the mouse models that have been developed for mimicking the multistep process of leukemia development both in T-ALL and B-ALL. Thus, we summarize the mouse strains that have been used to study the impact of the inappropriate expression of an oncogenic transcription factor on pre-leukemic T- or B-cell lineages, and to identify their associated collaborative events driving malignant transformation (Table 1).

Table 1. T-ALL and B-ALL mouse models exploring the biological mechanisms by which an oncogenic transcription factor perturbs normal hematopoietic development during the pre-leukemic phase and leads to malignant transformation.

Transgene	Additional Modifications	Pre-Leukemic State/ Reprogramming	Disease Evolution/ Collab. Events	Ref.
T-ALL mouse models				
bHLH transcription factors and partners				
Scl (*pSil*, *Cd2 or Sca1* promoters)	-	Perturb T-cell differentiation	No leukemia	[194–196]
Scl (*Lck* promoter)	-	Perturb T-cell differentiation	T-ALL (low penetrance)	[131,197–199]
Lmo2 (*Lck* promoter)	-	Perturb T-cell differentiation	T-ALL (low penetrance)	
Scl-Lmo2 (*Lck* promoters)	-	Expansion of DN3/DN4 populations	T-ALL (~3 months) *Notch1* mutations	
Lmo2 (*Cd2* promoter)	-	Pre-leukemic DN3 thymocyte self-renewal (pre-LSCs) ETP-ALL-like molecular signature	T-ALL (~10 months) *NOTCH1* and *Dnm2* mutations	[111,133,200]
	$Scl^{\Delta/-}$ or $Lyl1^{-/-}$	Lyl1, but not Scl, required for pre-LSC self-renewal	Lyl1 is required for T-ALL development	[120]
	$Hhex^{\Delta/-}$ or $Kit^{Wv/Wv}$	Hhex regulates Kit to promote radioresistance and pre-LSC self-renewal	Hhex and Kit are not required for T-ALL development	[201]
	$Dnm2^{V235G}$	Restore cycling and survival of pre-LSCs	Accelerate T-ALL progression	[200]
	H2B-GFP (Tet-on system)	Identification of chemo-resistant and cell cycle-restricted pre-LSCs	Cell cycle restriction is critical for clonal evolution	[133]
	H2B-GFP $Cdkn1a^{-/-}$	Loss of asymmetric cell division and cell cycle restriction	Reduce T-ALL progression	
Lmo2 (*Tet-off* system)	-	Lmo2 expression required for pre-LSC self-renewal	Lmo2-independent T-ALL development (~12 months) *Ikzf1* deletions	[142]
Lmo2 (*Cre*-driving *Rosa26* promoter)	-	Lmo2 reprograms committed B-cells into malignant T-ALL	Lmo2: "hit-and-run" oncogene in T-ALL	[141]

Table 1. *Cont.*

Transgene	Additional Modifications	Pre-Leukemic State/ Reprogramming	Disease Evolution/ Collab. Events	Ref.
SCL-LMO1 (*pSil and Lck* promoters, respectively)	-	Impaired T-cell differentiation Pre-leukemic DN3a thymocyte self-renewal (pre-LSCs) Activation of a stem cell gene signature Pre-LSCs low proliferation rate and chemosensitivity	T-ALL (~4 months) *NOTCH1* mutations	[113,114,121,132]
	NOTCH1 (*Lck* promoter)	Enhance pre-LSC self-renewal Expand the pool of pre-LSC to DN1-4 and ISP8 populations	Accelerate T-ALL progression (~1 month)	[114,121]
	$Cd3\varepsilon^{-/-}$ and NOTCH1 $Cd3\varepsilon^{-/-}$	Pre-TCR dispensable for pre-LSC self-renewal	Pre-TCR required for T-ALL development	
LYL1-LMO1 (*Lck* promoters)	-	Pre-leukemic DN3 thymocyte self-renewal	ND	[114]
Fusion proteins				
NUP98-HOXD13 (*Vav* promoter)	-	Pre-leukemic DN2 thymocyte self-renewal (pre-LSCs) Overexpression of HOXA cluster genes	MDS/AML (mostly)/T-ALL (~15%)	[138,202]
	$Lyl1^{-/-}$	Lyl1 required for pre-LSC self-renewal	T-ALL (100%)	
B-ALL mouse models				
Pax5 dosage				
$Pax5^{-/-}$	-	Blockade at pre-pro-B stage ($B220^{+}CD19^{-}Kit^{+}$) Self-renewal activity, multilineage potential	No leukemia	[147,153]
$Pax5^{\Delta/-}$ (*Cre*-mediated deletion)	-	Lineage plasticity and dedifferentiation of mature B-cells Conversion of B-cells into BCR-rearranged functional T-cells	B-cell lymphoma	[159]

Table 1. *Cont.*

Transgene	Additional Modifications	Pre-Leukemic State/ Reprogramming	Disease Evolution/ Collab. Events	Ref.
$Pax5^{+/-}$	-	No differentiation blockade	No leukemia	[163,203]
	Chemical (ENU) or retroviral (MMLV) mutagenesis	-	B-ALL (~6 to 8 months) *Pax5* and *Ikzf1* deletions, *Jak1* and Jak3 mutations	[164]
	Infection exposure or microbiome disturbance	-	B-ALL (~6 to 16 months) *JAK3*, *Stat5b* and *Pax5* mutations	[173–175]
	$Ebf1^{+/-}$	Partial blockage at pro-B stage Reveal oncogenic potential of Il7-Myc axis Lineage plasticity of pro-B cells (T-lineage conversion)	B-ALL (~7 months) *Jak1*, *Stat5b*, *Cblb* and *Myb* mutations	[165,166,171]
	$Ebf1^{+/-}$ $Ikzf1^{+/-}$	-	B-ALL (40%) T-ALL (35%)	[204]
	CA-Stat5b	-	B-ALL (~2 months)	[168]
Pax5 mutations				
Pax5 P80R	- $Pax5^{P80R/+}$	-	B-ALL (~5 months)	[190]
	-$Pax5^{P80R/P80R}$	-	B-ALL (~3 months) *Jak1* and *Jak3* mutations	
PAX5 Y351*	-$Pax5^{Y351*/+}$	-	B-ALL (~25 months)	[205]
	-$Pax5^{Y351*/Y351*}$	-	B-ALL (~8 months) *Jak3* and *Ptpn11* mutations	
Pax5 rearrangements				
PAX5-ETV6 (*Pax5* promoter)	-	Blockade between pro-B/pre-B cells	B-ALL (<10%)	[183]
	$Cdkn2ab^{+/-}$	-	B-ALL (~6 months)	
PAX5-ELN (*IgH* enhancer)	-	Partial blockage at pro-B stage Aberrant expansion potential of pre-leukemic pro-B	B-ALL (~6 months) *Ptpn11*, *Kras*, *Jak3* and *Pax5* mutations	[184]

Table 1. *Cont.*

Transgene	Additional Modifications	Pre-Leukemic State/ Reprogramming	Disease Evolution/ Collab. Events	Ref.
Other rearrangements				
ETV6-RUNX1 (*Etv6* promoter)	-		No leukemia	[185]
	Sleeping beauty (SB) transposon system	-	B-ALL (~6 months) Jak1 and Jak3 mutations	
ETV6-RUNX1 (*Sca1* promoter)	-	-	No leukemia	[175,206]
	Infection exposure or microbiome disturbance	Perturb B-cell development	B-ALL (~11%)	
ETV6-RUNX1 (*Cre*-driving *Etv6* promoter)	-	Pre-leukemic *ETV6-RUNX1* HSPC (*Sca1*-Cre/Infectious stimuli) Propensity to trigger T and B malignancies	B-ALL (*Pax5* mutations) T-ALL (*NOTCH1* and *Bcl11b* mutations)	[143]
TCF3-PBX1 (*TCR Vβ* and *Lck* promoters /*Igμ* enhancer)	-	-	B-ALL (13%) and T-ALL (33%)	[207]
	$CD3\varepsilon^{-/-}$	-	B-ALL (40%)	
TCF3-PBX1 (Cre-driving *TCF3* promoter)	-	Partial blockage at pro-B/pre-B stage	B-ALL (Cd19-Cre, 7%) B-ALL (Mb1-Cre, 53%) B-ALL (Mx1-Cre, 59%) *Ptpn11*, *Kras*, *Nras*, *Jak1*, *Jak3* and *Il7r* mutations *Cdkn2a* deletions	[186]
	$Pax5^{+/-}$	-	B-ALL (increased penetrance)	
BCR-ABL1 (*Sca1* promoter)	-	Pre-leukemic *BCR-ABL1* HSPCs	B-ALL (low penetrance)	[208]
	$Pax5^{+/-}$	Pro-B/pre-B cells permissive for B-ALL development	B-ALL (high penetrance, ~10 months)	

5. Targeting Cell- and Non-Cell-Autonomous Properties of (Pre-)LSCs

The search for more targeted therapies remains an important challenge based on an understanding of both cell-autonomous and non-cell-autonomous mechanisms involved in leukemia initiation and propagation. Targeting genes encoding for key players in controlling proliferation and differentiation in leukemia remains a dream and, unfortunately, represents very few examples of success in the clinic so far. In addition, most transcription factors, which exert intrinsic functions on cancer cells, are considered "undruggable" by small molecules or blocking antibodies due to their structural configurations, their protein–protein or protein–DNA interactions and their cellular localizations [209,210]. Despite this, the treatment of acute promyelocytic leukemia (APL) represents a prime example of a drug combination that targets both differentiation blockade and the self-renewal activity of LSCs through the proteasome-dependent degradation of the PML-RARα fusion protein, as described in the pioneer work from de The and colleagues [211,212]. This strategy underscores the importance of targeting the oncoprotein functions as this allowed for a more than 90% cure rate and very rare relapses, representing a major success in the field of hematologic malignancies [213]. In addition, this demonstrates the proof of concept that targeted degradation of a driver oncogenic transcription factor, along with its associated self-renewal and stem cell-like functions, is the strategy of choice for the long-term cure of leukemia. In ALL, while deciphering the diversity of the different oncogenic subtypes associated with their altered signaling pathways led to the discovery of new therapeutic opportunities [18,19], a significant proportion of patients still have unsatisfactory outcomes. Thus, the importance of challenging therapeutic approaches and of finding new druggable targets that enhance anti-leukemic efficiency remains a topical issue. In that purpose and as a representative example of targeted therapy, it has been demonstrated that the demethylase activity of UTX is essential for the maintenance of SCL/TAL1-positive T-ALL and not for other oncogenic subtypes [214]. Consistently, pharmacological inhibition of UTX with the H3K27 demethylase inhibitor GSK-J4 selectively targets SCL/TAL1-positive leukemic cells. Based on this targeted epigenetic vulnerability, the authors proposed for the first time a subtype-specific therapy in T-ALL [214].

The current cancer therapies target proliferating and metabolically active cancer cells and efficiently reduce the tumor load. However, frequent relapses indicate the persistence of residual resistant cells that escape treatment likely due to a protective microenvironment that blunt their chemosensitivity [215–219]. Indeed, specific locations within the niche may modify the chemosensitivity of primary leukemic blasts [58,220]. In addition, growing evidence supports the notion that leukemic cells can remodel their niche into an abnormal environment that contributes to neoplastic progression at the expense of normal hematopoiesis [221]. Thus, the interactions between leukemic cells with the molecular cues provided by their microenvironment are critical to promote leukemia progression and to design new targeted therapies, as is well documented elsewhere both in T-ALL [222,223] and in B-ALL [224]. Interestingly, non-cell-autonomous mechanisms can control the vulnerability of leukemic cells upon treatment, as exemplified by mitochondria transfer from activated stromal cells to rescue ALL cells from drug-induced oxidative stress [225]. Non-cell-autonomous pathways can also be exploited to develop therapeutic opportunities, as recently documented by Van Vlierberghe and colleagues showing that endogenous IL7, a cytokine abundantly secreted by the microenvironment, collaborates with glucocorticoids to reveal the sensitivity of residual leukemic cells upon the PIM inhibitor [226,227]. Together, the impact of extrinsic signals in leukemic cells, especially the molecular crosstalk between (pre-)LSCs and their microenvironment should be considered to develop new therapeutic approaches. Modifying the BM niche represents an innovative therapeutic approach to prevent leukemia re-initiation from residual (pre-)LSCs after complete remission. Thus, there is a need to characterize the adhesion molecules and soluble factors involved in the crosstalk between (pre-)LSCs and BM stromal cells. While the in vivo method stays the gold standard approach to study the molecular interactions between (pre-)LSCs and the BM microenvironment, a 3D organotypic "leukemia on-a-chip" microphysiological

system has been recently developed. This ex vivo bioengineered strategy recapitulates the heterogeneity of the leukemic BM microenvironment and opens the opportunity to perform a niche-based drug screening assay [228].

As described previously using transgenic T-ALL models, a primary oncogene can introduce cell quiescence, drug resistance and self-renewal to pre-LSCs [132,133], three critical properties that can be controlled by their niches. Thus, the development of new drugs targeting specific non-cell-autonomous mechanisms in (pre-)LSCs could open new therapeutic opportunities for more selective treatments. This notion has recently been exploited through the demonstration that a potent inhibitor of dynamin GTPase activity overcome the chemoresistance of pre-LSCs by inhibiting the transduction of key signaling pathways provided by the microenvironment [229]. Therefore, the reliance of leukemic cells on their niches and on non-cell-autonomous pathways together with the failure of chemotherapy in a significant proportion of patients point to the need for novel drug screening strategies incorporating elements of the microenvironment. This has been challenged by the design of the niche-based screening in multiple myeloma (MM) to identify Food and Drug Administration (FDA)-approved compounds that overcome stroma-induced drug resistance [230]. Precisely, this strategy led to the discovery of a chemical inhibitor specifically targeting microtubule-bound kinesin-5 in MM cells and allowing a greater selectivity over normal hematopoietic cells [230]. Obviously, the major limit is to target these (pre-)LSCs in primary patient samples, which are not easily amenable to high-throughput screening (HTS) for drug discovery due to their extreme rarity. Despite this, the critical dependency of primary (pre-)LSCs for their microenvironment has been challenged by the design of miniaturized, niche-based assays for chemical screening strategies using both *MLL-AF9*-induced AML [231] and *SCL-LMO1*-induced T-ALL [132] models. The latter led to the identification of the 2-methoxyestradiol, an FDA-approved drug inhibiting both the cell-intrinsic SCL oncoprotein and the stroma-dependent NOTCH1-Myc pathway, together with an absence of toxicity towards normal HSC functions. As previously reported, *MYC* is indeed essential for NOTCH1 activity in T-ALL [232,233], and inhibiting *Myc* expression via a BRD4 inhibitor effectively killed leukemia-initiating cells [234,235].

Collectively, recapitulating tissue-like properties of primary (pre-)LSCs represents a promising avenue for developing new cancer therapies. In addition, drug repositioning seems to be a powerful alternative strategy to discover novel biological applications of existing drugs that have a well-established dose regimen with favorable pharmacokinetics and pharmacodynamics properties as well as tolerable side effects [236]. In addition, drug repositioning should significantly reduce the time and the cost of the pre-clinical trial. Therefore, the chemical screen of FDA-approved compounds represents an attractive approach to the discovery of novel biological applications of a known drug and its rapid translation to the clinic.

6. Conclusions

The leukemic stem cell concept has important clinical implications and is already applied for patient stratification and for the development of more effective therapies against hematopoietic malignancies. In this review, we presented multiple lines of evidence for the complexity of leukemic cells from ALL patients that include cellular, molecular, genetic and functional heterogeneity. We described the different technological approaches that led to the recognition that leukemic cells evolve towards a nonlinear evolution process during the progression of the disease. Then, we focused on the development of improved methods, particularly the use of transgenic mice, to detect, purify and characterize pre-malignant stem cells before they have acquired additional genetic alterations and propagating properties. We described how a primary oncogenic transcription factor can reprogram stem cell-like functions to normal progenitors, such as self-renewal and cell dormancy, and that led to the emergence of pre-LSCs. Finally, we discussed the biological as well as the clinical importance of studying and targeting the intrinsic and extrinsic properties of pre-LSCs.

Over the last decade, genome-wide studies greatly improved the classification of ALL patients, enabling the identification of diverse and heterogeneous oncogenic subtypes that led to a better patient stratification, clinical prognosis and treatment orientation. Despite considerable improvements in overall survival, a significant proportion of ALL patients still have unsatisfactory outcomes. Moreover, the finding of therapeutic strategies targeting both the self-renewal and differentiation blockade of leukemic cells in ALL has not yet been achieved. Based on a better understanding of the intratumoral heterogeneity and on the deciphering of both the cell-autonomous and non-cell-autonomous mechanisms driving the emergence of leukemia-initiating cells, we expect in the near future the identification of new druggable targets and therapeutic opportunities that might render ALL a curable disease.

Funding: This research received no external funding.

Conflicts of Interest: The authors declare no conflict of interest.

References

1. Takahashi, K.; Yamanaka, S. Induction of pluripotent stem cells from mouse embryonic and adult fibroblast cultures by defined factors. *Cell* **2006**, *126*, 663–676. [CrossRef] [PubMed]
2. Wuputra, K.; Ku, C.C.; Wu, D.C.; Lin, Y.C.; Saito, S.; Yokoyama, K.K. Prevention of tumor risk associated with the reprogramming of human pluripotent stem cells. *J. Exp. Clin. Cancer. Res.* **2020**, *39*, 100. [CrossRef] [PubMed]
3. Bradner, J.E.; Hnisz, D.; Young, R.A. Transcriptional addiction in cancer. *Cell* **2017**, *168*, 629–643. [CrossRef] [PubMed]
4. Malta, T.M.; Sokolov, A.; Gentles, A.J.; Burzykowski, T.; Poisson, L.; Weinstein, J.N.; Kaminska, B.; Huelsken, J.; Omberg, L.; Gevaert, O.; et al. Machine learning identifies stemness features associated with oncogenic dedifferentiation. *Cell* **2018**, *173*, 338–354. [CrossRef]
5. Swiers, G.; Patient, R.; Loose, M. Genetic regulatory networks programming hematopoietic stem cells and erythroid lineage specification. *Dev. Biol.* **2006**, *294*, 525–540. [CrossRef]
6. Sloma, I.; Jiang, X.; Eaves, A.C.; Eaves, C.J. Insights into the stem cells of chronic myeloid leukemia. *Leukemia* **2010**, *24*, 1823–1833. [CrossRef]
7. Fialkow, P.J.; Gartler, S.M.; Yoshida, A. Clonal origin of chronic myelocytic leukemia in man. *Proc. Natl. Acad. Sci. USA* **1967**, *58*, 1468–1471. [CrossRef]
8. Lapidot, T.; Sirard, C.; Vormoor, J.; Murdoch, B.; Hoang, T.; Caceres-Cortes, J.; Minden, M.; Paterson, B.; Caligiuri, M.A.; Dick, J.E. A cell initiating human acute myeloid leukaemia after transplantation into scid mice. *Nature* **1994**, *367*, 645–648. [CrossRef]
9. Bonnet, D.; Dick, J.E. Human acute myeloid leukemia is organized as a hierarchy that originates from a primitive hematopoietic cell. *Nat. Med.* **1997**, *3*, 730–737. [CrossRef]
10. Bereshchenko, O.; Mancini, E.; Moore, S.; Bilbao, D.; Mansson, R.; Luc, S.; Grover, A.; Jacobsen, S.E.; Bryder, D.; Nerlov, C. Hematopoietic stem cell expansion precedes the generation of committed myeloid leukemia-initiating cells in c/ebpalpha mutant aml. *Cancer Cell* **2009**, *16*, 390–400. [CrossRef]
11. Miyamoto, T.; Weissman, I.L.; Akashi, K. Aml1/eto-expressing nonleukemic stem cells in acute myelogenous leukemia with 8;21 chromosomal translocation. *Proc. Natl. Acad. Sci. USA* **2000**, *97*, 7521–7526. [CrossRef]
12. Huntly, B.J.; Shigematsu, H.; Deguchi, K.; Lee, B.H.; Mizuno, S.; Duclos, N.; Rowan, R.; Amaral, S.; Curley, D.; Williams, I.R.; et al. Moz-tif2, but not bcr-abl, confers properties of leukemic stem cells to committed murine hematopoietic progenitors. *Cancer Cell* **2004**, *6*, 587–596. [CrossRef]
13. Krivtsov, A.V.; Twomey, D.; Feng, Z.; Stubbs, M.C.; Wang, Y.; Faber, J.; Levine, J.E.; Wang, J.; Hahn, W.C.; Gilliland, D.G.; et al. Transformation from committed progenitor to leukaemia stem cell initiated by mll-af9. *Nature* **2006**, *442*, 818–822. [CrossRef]
14. Cozzio, A.; Passegue, E.; Ayton, P.M.; Karsunky, H.; Cleary, M.L.; Weissman, I.L. Similar mll-associated leukemias arising from self-renewing stem cells and short-lived myeloid progenitors. *Genes Dev.* **2003**, *17*, 3029–3035. [CrossRef]
15. Guibal, F.C.; Alberich-Jorda, M.; Hirai, H.; Ebralidze, A.; Levantini, E.; Di Ruscio, A.; Zhang, P.; Santana-Lemos, B.A.; Neuberg, D.; Wagers, A.J.; et al. Identification of a myeloid committed progenitor as the cancer-initiating cell in acute promyelocytic leukemia. *Blood* **2009**, *114*, 5415–5425. [CrossRef]
16. Wojiski, S.; Guibal, F.C.; Kindler, T.; Lee, B.H.; Jesneck, J.L.; Fabian, A.; Tenen, D.G.; Gilliland, D.G. Pml-raralpha initiates leukemia by conferring properties of self-renewal to committed promyelocytic progenitors. *Leukemia* **2009**, *23*, 1462–1471. [CrossRef]
17. Inaba, H.; Pui, C.H. Advances in the diagnosis and treatment of pediatric acute lymphoblastic leukemia. *J. Clin. Med.* **2021**, *10*, 1926. [CrossRef]
18. Lato, M.W.; Przysucha, A.; Grosman, S.; Zawitkowska, J.; Lejman, M. The new therapeutic strategies in pediatric t-cell acute lymphoblastic leukemia. *Int. J. Mol. Sci.* **2021**, *22*, 4502. [CrossRef]
19. Ratti, S.; Lonetti, A.; Follo, M.Y.; Paganelli, F.; Martelli, A.M.; Chiarini, F.; Evangelisti, C. B-all complexity: Is targeted therapy still a valuable approach for pediatric patients? *Cancers* **2020**, *12*, 3498. [CrossRef]
20. Tardif, M.; Souza, A.; Krajinovic, M.; Bittencourt, H.; Tran, T.H. Molecular-based and antibody-based targeted pharmacological approaches in childhood acute lymphoblastic leukemia. *Expert Opin. Pharmacother.* **2021**, *22*, 1871–1887. [CrossRef]

21. Valent, P.; Bonnet, D.; De Maria, R.; Lapidot, T.; Copland, M.; Melo, J.V.; Chomienne, C.; Ishikawa, F.; Schuringa, J.J.; Stassi, G.; et al. Cancer stem cell definitions and terminology: The devil is in the details. *Nat. Rev. Cancer* **2012**, *12*, 767–775. [CrossRef]
22. Till, J.E.; Mc, C.E. A direct measurement of the radiation sensitivity of normal mouse bone marrow cells. *Radiat. Res.* **1961**, *14*, 213–222. [CrossRef]
23. Spangrude, G.J.; Heimfeld, S.; Weissman, I.L. Purification and characterization of mouse hematopoietic stem cells. *Science* **1988**, *241*, 58–62. [CrossRef]
24. Morrison, S.J.; Weissman, I.L. The long-term repopulating subset of hematopoietic stem cells is deterministic and isolatable by phenotype. *Immunity* **1994**, *1*, 661–673. [CrossRef]
25. Osawa, M.; Hanada, K.; Hamada, H.; Nakauchi, H. Long-term lymphohematopoietic reconstitution by a single cd34-low /negative hematopoietic stem cell. *Science* **1996**, *273*, 242–245. [CrossRef]
26. Berenson, R.J.; Andrews, R.G.; Bensinger, W.I.; Kalamasz, D.; Knitter, G.; Buckner, C.D.; Bernstein, I.D. Antigen cd34+ marrow cells engraft lethally irradiated baboons. *J. Clin. Investig.* **1988**, *81*, 951–955. [CrossRef]
27. Bhatia, M.; Wang, J.C.; Kapp, U.; Bonnet, D.; Dick, J.E. Purification of primitive human hematopoietic cells capable of repopulating immune-deficient mice. *Proc. Natl. Acad. Sci. USA* **1997**, *94*, 5320–5325. [CrossRef]
28. Kreso, A.; Dick, J.E. Evolution of the cancer stem cell model. *Cell Stem Cell* **2014**, *14*, 275–291. [CrossRef]
29. Hope, K.J.; Jin, L.; Dick, J.E. Acute myeloid leukemia originates from a hierarchy of leukemic stem cell classes that differ in self-renewal capacity. *Nat. Immunol.* **2004**, *5*, 738–743. [CrossRef]
30. Ishikawa, F.; Yoshida, S.; Saito, Y.; Hijikata, A.; Kitamura, H.; Tanaka, S.; Nakamura, R.; Tanaka, T.; Tomiyama, H.; Saito, N.; et al. Chemotherapy-resistant human aml stem cells home to and engraft within the bone-marrow endosteal region. *Nat. Biotechnol.* **2007**, *25*, 1315–1321. [CrossRef]
31. Eppert, K.; Takenaka, K.; Lechman, E.R.; Waldron, L.; Nilsson, B.; van Galen, P.; Metzeler, K.H.; Poeppl, A.; Ling, V.; Beyene, J.; et al. Stem cell gene expression programs influence clinical outcome in human leukemia. *Nat. Med.* **2011**, *17*, 1086–1093. [CrossRef] [PubMed]
32. Goardon, N.; Marchi, E.; Atzberger, A.; Quek, L.; Schuh, A.; Soneji, S.; Woll, P.; Mead, A.; Alford, K.A.; Rout, R.; et al. Coexistence of lmpp-like and gmp-like leukemia stem cells in acute myeloid leukemia. *Cancer Cell* **2011**, *19*, 138–152. [CrossRef] [PubMed]
33. Sarry, J.E.; Murphy, K.; Perry, R.; Sanchez, P.V.; Secreto, A.; Keefer, C.; Swider, C.R.; Strzelecki, A.C.; Cavelier, C.; Recher, C.; et al. Human acute myelogenous leukemia stem cells are rare and heterogeneous when assayed in nod/scid/il2rgammac-deficient mice. *J. Clin. Investig.* **2011**, *121*, 384–395. [CrossRef] [PubMed]
34. Thomas, D.; Majeti, R. Biology and relevance of human acute myeloid leukemia stem cells. *Blood* **2017**, *129*, 1577–1585. [CrossRef]
35. Taussig, D.C.; Miraki-Moud, F.; Anjos-Afonso, F.; Pearce, D.J.; Allen, K.; Ridler, C.; Lillington, D.; Oakervee, H.; Cavenagh, J.; Agrawal, S.G.; et al. Anti-cd38 antibody-mediated clearance of human repopulating cells masks the heterogeneity of leukemia-initiating cells. *Blood* **2008**, *112*, 568–575. [CrossRef]
36. Greaves, M. Leukaemia 'firsts' in cancer research and treatment. *Nat. Rev. Cancer* **2016**, *16*, 163–172. [CrossRef]
37. Lang, F.; Wojcik, B.; Rieger, M.A. Stem cell hierarchy and clonal evolution in acute lymphoblastic leukemia. *Stem Cells Int.* **2015**, *2015*, 137164. [CrossRef]
38. Cobaleda, C.; Gutierrez-Cianca, N.; Perez-Losada, J.; Flores, T.; Garcia-Sanz, R.; Gonzalez, M.; Sanchez-Garcia, I. A primitive hematopoietic cell is the target for the leukemic transformation in human philadelphia-positive acute lymphoblastic leukemia. *Blood* **2000**, *95*, 1007–1013. [CrossRef]
39. Cox, C.V.; Evely, R.S.; Oakhill, A.; Pamphilon, D.H.; Goulden, N.J.; Blair, A. Characterization of acute lymphoblastic leukemia progenitor cells. *Blood* **2004**, *104*, 2919–2925. [CrossRef]
40. Hotfilder, M.; Rottgers, S.; Rosemann, A.; Jurgens, H.; Harbott, J.; Vormoor, J. Immature cd34+cd19- progenitor/stem cells in tel/aml1-positive acute lymphoblastic leukemia are genetically and functionally normal. *Blood* **2002**, *100*, 640–646. [CrossRef]
41. Castor, A.; Nilsson, L.; Astrand-Grundstrom, I.; Buitenhuis, M.; Ramirez, C.; Anderson, K.; Strombeck, B.; Garwicz, S.; Bekassy, A.N.; Schmiegelow, K.; et al. Distinct patterns of hematopoietic stem cell involvement in acute lymphoblastic leukemia. *Nat. Med.* **2005**, *11*, 630–637. [CrossRef]
42. Kong, Y.; Yoshida, S.; Saito, Y.; Doi, T.; Nagatoshi, Y.; Fukata, M.; Saito, N.; Yang, S.M.; Iwamoto, C.; Okamura, J.; et al. Cd34+cd38+cd19+ as well as cd34+cd38-cd19+ cells are leukemia-initiating cells with self-renewal capacity in human b-precursor all. *Leukemia* **2008**, *22*, 1207–1213. [CrossRef]
43. Le Viseur, C.; Hotfilder, M.; Bomken, S.; Wilson, K.; Rottgers, S.; Schrauder, A.; Rosemann, A.; Irving, J.; Stam, R.W.; Shultz, L.D.; et al. In childhood acute lymphoblastic leukemia, blasts at different stages of immunophenotypic maturation have stem cell properties. *Cancer Cell* **2008**, *14*, 47–58. [CrossRef]
44. Aoki, Y.; Watanabe, T.; Saito, Y.; Kuroki, Y.; Hijikata, A.; Takagi, M.; Tomizawa, D.; Eguchi, M.; Eguchi-Ishimae, M.; Kaneko, A.; et al. Identification of cd34+ and cd34- leukemia-initiating cells in mll-rearranged human acute lymphoblastic leukemia. *Blood* **2015**, *125*, 967–980. [CrossRef]
45. Rehe, K.; Wilson, K.; Bomken, S.; Williamson, D.; Irving, J.; den Boer, M.L.; Stanulla, M.; Schrappe, M.; Hall, A.G.; Heidenreich, O.; et al. Acute b lymphoblastic leukaemia-propagating cells are present at high frequency in diverse lymphoblast populations. *EMBO Mol. Med.* **2013**, *5*, 38–51. [CrossRef]
46. Elder, A.; Bomken, S.; Wilson, I.; Blair, H.J.; Cockell, S.; Ponthan, F.; Dormon, K.; Pal, D.; Heidenreich, O.; Vormoor, J. Abundant and equipotent founder cells establish and maintain acute lymphoblastic leukaemia. *Leukemia* **2017**, *31*, 2577–2586. [CrossRef]

47. Lang, F.; Wojcik, B.; Bothur, S.; Knecht, C.; Falkenburg, J.H.; Schroeder, T.; Serve, H.; Ottmann, O.G.; Rieger, M.A. Plastic cd34 and cd38 expression in adult b-cell precursor acute lymphoblastic leukemia explains ambiguity of leukemia-initiating stem cell populations. *Leukemia* **2017**, *31*, 731–734. [CrossRef]
48. Orlando, E.J.; Han, X.; Tribouley, C.; Wood, P.A.; Leary, R.J.; Riester, M.; Levine, J.E.; Qayed, M.; Grupp, S.A.; Boyer, M.; et al. Genetic mechanisms of target antigen loss in car19 therapy of acute lymphoblastic leukemia. *Nat. Med.* **2018**, *24*, 1504–1506. [CrossRef]
49. Rabilloud, T.; Potier, D.; Pankaew, S.; Nozais, M.; Loosveld, M.; Payet-Bornet, D. Single-cell profiling identifies pre-existing cd19-negative subclones in a b-all patient with cd19-negative relapse after car-t therapy. *Nat. Commun.* **2021**, *12*, 865. [CrossRef]
50. Sedek, L.; Theunissen, P.; Sobral da Costa, E.; van der Sluijs-Gelling, A.; Mejstrikova, E.; Gaipa, G.; Sonsala, A.; Twardoch, M.; Oliveira, E.; Novakova, M.; et al. Differential expression of cd73, cd86 and cd304 in normal vs. Leukemic b-cell precursors and their utility as stable minimal residual disease markers in childhood b-cell precursor acute lymphoblastic leukemia. *J. Immunol. Methods* **2019**, *475*, 112429. [CrossRef]
51. Tsitsikov, E.; Harris, M.H.; Silverman, L.B.; Sallan, S.E.; Weinberg, O.K. Role of cd81 and cd58 in minimal residual disease detection in pediatric b lymphoblastic leukemia. *Int. J. Lab. Hematol.* **2018**, *40*, 343–351. [CrossRef]
52. Armstrong, F.; de la Grange, P.B.; Gerby, B.; Rouyez, M.C.; Calvo, J.; Fontenay, M.; Boissel, N.; Dombret, H.; Baruchel, A.; Landman-Parker, J.; et al. Notch is a key regulator of human t-cell acute leukemia initiating cell activity. *Blood* **2009**, *113*, 1730–1740. [CrossRef]
53. Cox, C.V.; Martin, H.M.; Kearns, P.R.; Virgo, P.; Evely, R.S.; Blair, A. Characterization of a progenitor cell population in childhood t-cell acute lymphoblastic leukemia. *Blood* **2007**, *109*, 674–682. [CrossRef]
54. Gerby, B.; Clappier, E.; Armstrong, F.; Deswarte, C.; Calvo, J.; Poglio, S.; Soulier, J.; Boissel, N.; Leblanc, T.; Baruchel, A.; et al. Expression of cd34 and cd7 on human t-cell acute lymphoblastic leukemia discriminates functionally heterogeneous cell populations. *Leukemia* **2011**, *25*, 1249–1258. [CrossRef]
55. Chiu, P.P.; Jiang, H.; Dick, J.E. Leukemia-initiating cells in human t-lymphoblastic leukemia exhibit glucocorticoid resistance. *Blood* **2010**, *116*, 5268–5279. [CrossRef]
56. Ma, W.; Gutierrez, A.; Goff, D.J.; Geron, I.; Sadarangani, A.; Jamieson, C.A.; Court, A.C.; Shih, A.Y.; Jiang, Q.; Wu, C.C.; et al. Notch1 signaling promotes human t-cell acute lymphoblastic leukemia initiating cell regeneration in supportive niches. *PLoS ONE* **2012**, *7*, e39725.
57. Poglio, S.; Lewandowski, D.; Calvo, J.; Caye, A.; Gros, A.; Laharanne, E.; Leblanc, T.; Landman-Parker, J.; Baruchel, A.; Soulier, J.; et al. Speed of leukemia development and genetic diversity in xenograft models of t cell acute lymphoblastic leukemia. *Oncotarget* **2016**, *7*, 41599–41611. [CrossRef]
58. Cahu, X.; Calvo, J.; Poglio, S.; Prade, N.; Colsch, B.; Arcangeli, M.-L.; Leblanc, T.; Petit, A.; Baleydier, F.; Baruchel, A.; et al. Bone marrow sites differently imprint dormancy and chemoresistance to T-cell acute lymphoblastic leukemia. *Blood Adv.* **2017**, *1*, 1760–1772. [CrossRef]
59. Ebinger, S.; Ozdemir, E.Z.; Ziegenhain, C.; Tiedt, S.; Castro Alves, C.; Grunert, M.; Dworzak, M.; Lutz, C.; Turati, V.A.; Enver, T.; et al. Characterization of rare, dormant, and therapy-resistant cells in acute lymphoblastic leukemia. *Cancer Cell* **2016**, *30*, 849–862. [CrossRef]
60. Yan, F.; Wong, N.C.; Powell, D.R.; Curtis, D.J. A 9-gene score for risk stratification in b-cell acute lymphoblastic leukemia. *Leukemia* **2020**, *34*, 3070–3074. [CrossRef]
61. Ng, S.W.; Mitchell, A.; Kennedy, J.A.; Chen, W.C.; McLeod, J.; Ibrahimova, N.; Arruda, A.; Popescu, A.; Gupta, V.; Schimmer, A.D.; et al. A 17-gene stemness score for rapid determination of risk in acute leukaemia. *Nature* **2016**, *540*, 433–437. [CrossRef] [PubMed]
62. Inaba, H.; Mullighan, C.G. Pediatric acute lymphoblastic leukemia. *Haematologica* **2020**, *105*, 2524–2539. [CrossRef] [PubMed]
63. Kimura, S.; Mullighan, C.G. Molecular markers in all: Clinical implications. *Best Pract. Res. Clin. Haematol.* **2020**, *33*, 101193. [CrossRef] [PubMed]
64. Alexandrov, L.B.; Nik-Zainal, S.; Wedge, D.C.; Aparicio, S.A.; Behjati, S.; Biankin, A.V.; Bignell, G.R.; Bolli, N.; Borg, A.; Borresen-Dale, A.L.; et al. Signatures of mutational processes in human cancer. *Nature* **2013**, *500*, 415–421. [CrossRef] [PubMed]
65. Anderson, K.; Lutz, C.; van Delft, F.W.; Bateman, C.M.; Guo, Y.; Colman, S.M.; Kempski, H.; Moorman, A.V.; Titley, I.; Swansbury, J.; et al. Genetic variegation of clonal architecture and propagating cells in leukaemia. *Nature* **2011**, *469*, 356–361. [CrossRef] [PubMed]
66. Mullighan, C.G.; Phillips, L.A.; Su, X.; Ma, J.; Miller, C.B.; Shurtleff, S.A.; Downing, J.R. Genomic analysis of the clonal origins of relapsed acute lymphoblastic leukemia. *Science* **2008**, *322*, 1377–1380. [CrossRef]
67. Mullighan, C.G.; Zhang, J.; Kasper, L.H.; Lerach, S.; Payne-Turner, D.; Phillips, L.A.; Heatley, S.L.; Holmfeldt, L.; Collins-Underwood, J.R.; Ma, J.; et al. Crebbp mutations in relapsed acute lymphoblastic leukaemia. *Nature* **2011**, *471*, 235–239. [CrossRef]
68. Yang, J.J.; Bhojwani, D.; Yang, W.; Cai, X.; Stocco, G.; Crews, K.; Wang, J.; Morrison, D.; Devidas, M.; Hunger, S.P.; et al. Genome-wide copy number profiling reveals molecular evolution from diagnosis to relapse in childhood acute lymphoblastic leukemia. *Blood* **2008**, *112*, 4178–4183. [CrossRef]
69. Tosello, V.; Mansour, M.R.; Barnes, K.; Paganin, M.; Sulis, M.L.; Jenkinson, S.; Allen, C.G.; Gale, R.E.; Linch, D.C.; Palomero, T.; et al. Wt1 mutations in t-all. *Blood* **2009**, *114*, 1038–1045. [CrossRef]

70. Kuster, L.; Grausenburger, R.; Fuka, G.; Kaindl, U.; Krapf, G.; Inthal, A.; Mann, G.; Kauer, M.; Rainer, J.; Kofler, R.; et al. Etv6/runx1-positive relapses evolve from an ancestral clone and frequently acquire deletions of genes implicated in glucocorticoid signaling. *Blood* **2011**, *117*, 2658–2667. [CrossRef]
71. Van Delft, F.W.; Horsley, S.; Colman, S.; Anderson, K.; Bateman, C.; Kempski, H.; Zuna, J.; Eckert, C.; Saha, V.; Kearney, L.; et al. Clonal origins of relapse in etv6-runx1 acute lymphoblastic leukemia. *Blood* **2011**, *117*, 6247–6254. [CrossRef]
72. Ribera, J.; Zamora, L.; Morgades, M.; Mallo, M.; Solanes, N.; Batlle, M.; Vives, S.; Granada, I.; Junca, J.; Malinverni, R.; et al. Copy number profiling of adult relapsed b-cell precursor acute lymphoblastic leukemia reveals potential leukemia progression mechanisms. *Genes Chromosomes Cancer* **2017**, *56*, 810–820. [CrossRef]
73. Theunissen, P.M.J.; de Bie, M.; van Zessen, D.; de Haas, V.; Stubbs, A.P.; van der Velden, V.H.J. Next-generation antigen receptor sequencing of paired diagnosis and relapse samples of b-cell acute lymphoblastic leukemia: Clonal evolution and implications for minimal residual disease target selection. *Leuk. Res.* **2019**, *76*, 98–104. [CrossRef]
74. Forero-Castro, M.; Montano, A.; Robledo, C.; Garcia de Coca, A.; Fuster, J.L.; de Las Heras, N.; Queizan, J.A.; Hernandez-Sanchez, M.; Corchete-Sanchez, L.A.; Martin-Izquierdo, M.; et al. Integrated genomic analysis of chromosomal alterations and mutations in b-cell acute lymphoblastic leukemia reveals distinct genetic profiles at relapse. *Diagnostics* **2020**, *10*, 455. [CrossRef]
75. Waanders, E.; Gu, Z.; Dobson, S.M.; Antic, Z.; Crawford, J.C.; Ma, X.; Edmonson, M.N.; Payne-Turner, D.; van der Vorst, M.; Jongmans, M.C.J.; et al. Mutational landscape and patterns of clonal evolution in relapsed pediatric acute lymphoblastic leukemia. *Blood Cancer Discov.* **2020**, *1*, 96–111. [CrossRef]
76. Mullighan, C.G. Molecular genetics of b-precursor acute lymphoblastic leukemia. *J. Clin. Investig.* **2012**, *122*, 3407–3415. [CrossRef]
77. Ma, X.; Edmonson, M.; Yergeau, D.; Muzny, D.M.; Hampton, O.A.; Rusch, M.; Song, G.; Easton, J.; Harvey, R.C.; Wheeler, D.A.; et al. Rise and fall of subclones from diagnosis to relapse in pediatric b-acute lymphoblastic leukaemia. *Nat. Commun.* **2015**, *6*, 6604. [CrossRef]
78. Oshima, K.; Khiabanian, H.; da Silva-Almeida, A.C.; Tzoneva, G.; Abate, F.; Ambesi-Impiombato, A.; Sanchez-Martin, M.; Carpenter, Z.; Penson, A.; Perez-Garcia, A.; et al. Mutational landscape, clonal evolution patterns, and role of ras mutations in relapsed acute lymphoblastic leukemia. *Proc. Natl. Acad. Sci. USA* **2016**, *113*, 11306–11311. [CrossRef]
79. Jaiswal, S.; Fontanillas, P.; Flannick, J.; Manning, A.; Grauman, P.V.; Mar, B.G.; Lindsley, R.C.; Mermel, C.H.; Burtt, N.; Chavez, A.; et al. Age-related clonal hematopoiesis associated with adverse outcomes. *N. Engl. J. Med.* **2014**, *371*, 2488–2498. [CrossRef]
80. Acuna-Hidalgo, R.; Sengul, H.; Steehouwer, M.; van de Vorst, M.; Vermeulen, S.H.; Kiemeney, L.; Veltman, J.A.; Gilissen, C.; Hoischen, A. Ultra-sensitive sequencing identifies high prevalence of clonal hematopoiesis-associated mutations throughout adult life. *Am. J. Hum. Genet.* **2017**, *101*, 50–64. [CrossRef] [PubMed]
81. Bowman, R.L.; Busque, L.; Levine, R.L. Clonal hematopoiesis and evolution to hematopoietic malignancies. *Cell Stem Cell* **2018**, *22*, 157–170. [CrossRef] [PubMed]
82. Shlush, L.I.; Zandi, S.; Mitchell, A.; Chen, W.C.; Brandwein, J.M.; Gupta, V.; Kennedy, J.A.; Schimmer, A.D.; Schuh, A.C.; Yee, K.W.; et al. Identification of pre-leukaemic haematopoietic stem cells in acute leukaemia. *Nature* **2014**, *506*, 328–333. [CrossRef] [PubMed]
83. Corces-Zimmerman, M.R.; Hong, W.J.; Weissman, I.L.; Medeiros, B.C.; Majeti, R. Preleukemic mutations in human acute myeloid leukemia affect epigenetic regulators and persist in remission. *Proc. Natl. Acad. Sci. USA* **2014**, *111*, 2548–2553. [CrossRef]
84. Shlush, L.I.; Mitchell, A.; Heisler, L.; Abelson, S.; Ng, S.W.K.; Trotman-Grant, A.; Medeiros, J.J.F.; Rao-Bhatia, A.; Jaciw-Zurakowsky, I.; Marke, R.; et al. Tracing the origins of relapse in acute myeloid leukaemia to stem cells. *Nature* **2017**, *547*, 104–108. [CrossRef]
85. Velten, L.; Story, B.A.; Hernandez-Malmierca, P.; Raffel, S.; Leonce, D.R.; Milbank, J.; Paulsen, M.; Demir, A.; Szu-Tu, C.; Fromel, R.; et al. Identification of leukemic and pre-leukemic stem cells by clonal tracking from single-cell transcriptomics. *Nat. Commun.* **2021**, *12*, 1366. [CrossRef]
86. Clappier, E.; Gerby, B.; Sigaux, F.; Delord, M.; Touzri, F.; Hernandez, L.; Ballerini, P.; Baruchel, A.; Pflumio, F.; Soulier, J. Clonal selection in xenografted human t cell acute lymphoblastic leukemia recapitulates gain of malignancy at relapse. *J. Exp. Med.* **2011**, *208*, 653–661. [CrossRef]
87. Notta, F.; Mullighan, C.G.; Wang, J.C.; Poeppl, A.; Doulatov, S.; Phillips, L.A.; Ma, J.; Minden, M.D.; Downing, J.R.; Dick, J.E. Evolution of human bcr-abl1 lymphoblastic leukaemia-initiating cells. *Nature* **2011**, *469*, 362–367. [CrossRef]
88. Bardini, M.; Woll, P.S.; Corral, L.; Luc, S.; Wittmann, L.; Ma, Z.; Lo Nigro, L.; Basso, G.; Biondi, A.; Cazzaniga, G.; et al. Clonal variegation and dynamic competition of leukemia-initiating cells in infant acute lymphoblastic leukemia with mll rearrangement. *Leukemia* **2015**, *29*, 38–50. [CrossRef]
89. Richter-Pechanska, P.; Kunz, J.B.; Bornhauser, B.; von Knebel Doeberitz, C.; Rausch, T.; Erarslan-Uysal, B.; Assenov, Y.; Frismantas, V.; Marovca, B.; Waszak, S.M.; et al. Pdx models recapitulate the genetic and epigenetic landscape of pediatric t-cell leukemia. *EMBO Mol. Med.* **2018**, *10*, e9443. [CrossRef]
90. Wang, K.; Sanchez-Martin, M.; Wang, X.; Knapp, K.M.; Koche, R.; Vu, L.; Nahas, M.K.; He, J.; Hadler, M.; Stein, E.M.; et al. Patient-derived xenotransplants can recapitulate the genetic driver landscape of acute leukemias. *Leukemia* **2017**, *31*, 151–158. [CrossRef]
91. Dobson, S.M.; Garcia-Prat, L.; Vanner, R.J.; Wintersinger, J.; Waanders, E.; Gu, Z.; McLeod, J.; Gan, O.I.; Grandal, I.; Payne-Turner, D.; et al. Relapse-fated latent diagnosis subclones in acute b lineage leukemia are drug tolerant and possess distinct metabolic programs. *Cancer Discov.* **2020**, *10*, 568–587. [CrossRef] [PubMed]

92. Van Galen, P.; Kreso, A.; Mbong, N.; Kent, D.G.; Fitzmaurice, T.; Chambers, J.E.; Xie, S.; Laurenti, E.; Hermans, K.; Eppert, K.; et al. The unfolded protein response governs integrity of the haematopoietic stem-cell pool during stress. *Nature* **2014**, *510*, 268–272. [CrossRef] [PubMed]
93. Van Galen, P.; Mbong, N.; Kreso, A.; Schoof, E.M.; Wagenblast, E.; Ng, S.W.K.; Krivdova, G.; Jin, L.; Nakauchi, H.; Dick, J.E. Integrated stress response activity marks stem cells in normal hematopoiesis and leukemia. *Cell Rep.* **2018**, *25*, 1109–1117. [CrossRef] [PubMed]
94. Spitzer, M.H.; Nolan, G.P. Mass cytometry: Single cells, many features. *Cell* **2016**, *165*, 780–791. [CrossRef]
95. Good, Z.; Sarno, J.; Jager, A.; Samusik, N.; Aghaeepour, N.; Simonds, E.F.; White, L.; Lacayo, N.J.; Fantl, W.J.; Fazio, G.; et al. Single-cell developmental classification of b cell precursor acute lymphoblastic leukemia at diagnosis reveals predictors of relapse. *Nat. Med.* **2018**, *24*, 474–483. [CrossRef]
96. Bendall, S.C.; Davis, K.L.; Amir, E.-A.D.; Tadmor, M.D.; Simonds, E.F.; Chen, T.J.; Shenfeld, D.K.; Nolan, G.P.; Pe'er, D. Single-cell trajectory detection uncovers progression and regulatory coordination in human b cell development. *Cell* **2014**, *157*, 714–725. [CrossRef]
97. Chan, L.N.; Murakami, M.A.; Robinson, M.E.; Caeser, R.; Sadras, T.; Lee, J.; Cosgun, K.N.; Kume, K.; Khairnar, V.; Xiao, G.; et al. Signalling input from divergent pathways subverts b cell transformation. *Nature* **2020**, *583*, 845–851. [CrossRef]
98. Alberti-Servera, L.; Demeyer, S.; Govaerts, I.; Swings, T.; de Bie, J.; Gielen, O.; Brociner, M.; Michaux, L.; Maertens, J.; Uyttebroeck, A.; et al. Single-cell DNA amplicon sequencing reveals clonal heterogeneity and evolution in T-cell acute lymphoblastic leukemia. *Blood* **2021**, *137*, 801–811. [CrossRef]
99. Greaves, M. A causal mechanism for childhood acute lymphoblastic leukaemia. *Nat. Rev. Cancer* **2018**, *18*, 471–484. [CrossRef]
100. Hong, D.; Gupta, R.; Ancliff, P.; Atzberger, A.; Brown, J.; Soneji, S.; Green, J.; Colman, S.; Piacibello, W.; Buckle, V.; et al. Initiating and cancer-propagating cells in tel-aml1-associated childhood leukemia. *Science* **2008**, *319*, 336–339. [CrossRef]
101. De Guzman, C.G.; Warren, A.J.; Zhang, Z.; Gartland, L.; Erickson, P.; Drabkin, H.; Hiebert, S.W.; Klug, C.A. Hematopoietic stem cell expansion and distinct myeloid developmental abnormalities in a murine model of the aml1-eto translocation. *Mol. Cell. Biol.* **2002**, *22*, 5506–5517. [CrossRef]
102. Chen, W.; Kumar, A.R.; Hudson, W.A.; Li, Q.; Wu, B.; Staggs, R.A.; Lund, E.A.; Sam, T.N.; Kersey, J.H. Malignant transformation initiated by mll-af9: Gene dosage and critical target cells. *Cancer Cell* **2008**, *13*, 432–440. [CrossRef]
103. Passegue, E.; Wagner, E.F.; Weissman, I.L. Junb deficiency leads to a myeloproliferative disorder arising from hematopoietic stem cells. *Cell* **2004**, *119*, 431–443. [CrossRef]
104. Shimizu, R.; Kuroha, T.; Ohneda, O.; Pan, X.; Ohneda, K.; Takahashi, S.; Philipsen, S.; Yamamoto, M. Leukemogenesis caused by incapacitated gata-1 function. *Mol. Cell. Biol.* **2004**, *24*, 10814–10825. [CrossRef]
105. Rodrigues, N.P.; Tipping, A.J.; Wang, Z.; Enver, T. Gata-2 mediated regulation of normal hematopoietic stem/progenitor cell function, myelodysplasia and myeloid leukemia. *Int. J. Biochem. Cell. Biol.* **2012**, *44*, 457–460. [CrossRef]
106. Smith, L.J.; Curtis, J.E.; Messner, H.A.; Senn, J.S.; Furthmayr, H.; McCulloch, E.A. Lineage infidelity in acute leukemia. *Blood* **1983**, *61*, 1138–1145. [CrossRef]
107. Alexander, T.B.; Gu, Z.; Iacobucci, I.; Dickerson, K.; Choi, J.K.; Xu, B.; Payne-Turner, D.; Yoshihara, H.; Loh, M.L.; Horan, J.; et al. The genetic basis and cell of origin of mixed phenotype acute leukaemia. *Nature* **2018**, *562*, 373–379. [CrossRef]
108. Peaudecerf, L.; Krenn, G.; Goncalves, P.; Vasseur, F.; Rocha, B. Thymocytes self-renewal: A major hope or a major threat? *Immunol. Rev.* **2016**, *271*, 173–184. [CrossRef]
109. Han, J.; Zuniga-Pflucker, J.C. A 2020 view of thymus stromal cells in t cell development. *J. Immunol.* **2021**, *206*, 249–256. [CrossRef]
110. Tremblay, C.S.; Hoang, T.; Hoang, T. Early t cell differentiation lessons from t-cell acute lymphoblastic leukemia. *Prog. Mol. Biol. Transl. Sci.* **2010**, *92*, 121–156.
111. McCormack, M.P.; Young, L.F.; Vasudevan, S.; de Graaf, C.A.; Codrington, R.; Rabbitts, T.H.; Jane, S.M.; Curtis, D.J. The lmo2 oncogene initiates leukemia in mice by inducing thymocyte self-renewal. *Science* **2010**, *327*, 879–883. [CrossRef]
112. Wilson, N.K.; Foster, S.D.; Wang, X.; Knezevic, K.; Schutte, J.; Kaimakis, P.; Chilarska, P.M.; Kinston, S.; Ouwehand, W.H.; Dzierzak, E.; et al. Combinatorial transcriptional control in blood stem/progenitor cells: Genome-wide analysis of ten major transcriptional regulators. *Cell Stem Cell* **2010**, *7*, 532–544. [CrossRef]
113. Herblot, S.; Steff, A.M.; Hugo, P.; Aplan, P.D.; Hoang, T. Scl and lmo1 alter thymocyte differentiation: Inhibition of e2a-heb function and pre-t alpha chain expression. *Nat. Immunol.* **2000**, *1*, 138–144. [CrossRef]
114. Gerby, B.; Tremblay, C.S.; Tremblay, M.; Rojas-Sutterlin, S.; Herblot, S.; Hebert, J.; Sauvageau, G.; Lemieux, S.; Lecuyer, E.; Veiga, D.F.; et al. Scl, lmo1 and notch1 reprogram thymocytes into self-renewing cells. *PLoS Genet.* **2014**, *10*, e1004768. [CrossRef]
115. Goossens, S.; van Vlierberghe, P. Controlling pre-leukemic thymocyte self-renewal. *PLoS Genet.* **2014**, *10*, e1004881. [CrossRef] [PubMed]
116. Curtis, D.J.; Hall, M.A.; van Stekelenburg, L.J.; Robb, L.; Jane, S.M.; Begley, C.G. Scl is required for normal function of short-term repopulating hematopoietic stem cells. *Blood* **2004**, *103*, 3342–3348. [CrossRef]
117. Reynaud, D.; Ravet, E.; Titeux, M.; Mazurier, F.; Renia, L.; Dubart-Kupperschmitt, A.; Romeo, P.H.; Pflumio, F. Scl/tal1 expression level regulates human hematopoietic stem cell self-renewal and engraftment. *Blood* **2005**, *106*, 2318–2328. [CrossRef]
118. Lacombe, J.; Herblot, S.; Rojas-Sutterlin, S.; Haman, A.; Barakat, S.; Iscove, N.N.; Sauvageau, G.; Hoang, T. Scl regulates the quiescence and the long-term competence of hematopoietic stem cells. *Blood* **2010**, *115*, 792–803. [CrossRef] [PubMed]

119. Souroullas, G.P.; Salmon, J.M.; Sablitzky, F.; Curtis, D.J.; Goodell, M.A. Adult hematopoietic stem and progenitor cells require either lyl1 or scl for survival. *Cell Stem Cell* **2009**, *4*, 180–186. [CrossRef] [PubMed]
120. McCormack, M.P.; Shields, B.J.; Jackson, J.T.; Nasa, C.; Shi, W.; Slater, N.J.; Tremblay, C.S.; Rabbitts, T.H.; Curtis, D.J. Requirement for lyl1 in a model of lmo2-driven early t-cell precursor all. *Blood* **2013**, *122*, 2093–2103. [CrossRef] [PubMed]
121. Tremblay, M.; Tremblay, C.S.; Herblot, S.; Aplan, P.D.; Hebert, J.; Perreault, C.; Hoang, T. Modeling t-cell acute lymphoblastic leukemia induced by the scl and lmo1 oncogenes. *Genes Dev.* **2010**, *24*, 1093–1105. [CrossRef]
122. Shi, J.; Fallahi, M.; Luo, J.L.; Petrie, H.T. Nonoverlapping functions for notch1 and notch3 during murine steady-state thymic lymphopoiesis. *Blood* **2011**, *118*, 2511–2519. [CrossRef]
123. Radtke, F.; Wilson, A.; Mancini, S.J.; MacDonald, H.R. Notch regulation of lymphocyte development and function. *Nat. Immunol.* **2004**, *5*, 247–253. [CrossRef]
124. Mancini, S.J.; Mantei, N.; Dumortier, A.; Suter, U.; MacDonald, H.R.; Radtke, F. Jagged1-dependent notch signaling is dispensable for hematopoietic stem cell self-renewal and differentiation. *Blood* **2005**, *105*, 2340–2342. [CrossRef]
125. Maillard, I.; Koch, U.; Dumortier, A.; Shestova, O.; Xu, L.; Sai, H.; Pross, S.E.; Aster, J.C.; Bhandoola, A.; Radtke, F.; et al. Canonical notch signaling is dispensable for the maintenance of adult hematopoietic stem cells. *Cell Stem Cell* **2008**, *2*, 356–366. [CrossRef]
126. Chiang, M.Y.; Shestova, O.; Xu, L.; Aster, J.C.; Pear, W.S. Divergent effects of supraphysiological notch signals on leukemia stem cells and hematopoietic stem cells. *Blood* **2012**, *121*, 905–917. [CrossRef]
127. Karanu, F.N.; Murdoch, B.; Gallacher, L.; Wu, D.M.; Koremoto, M.; Sakano, S.; Bhatia, M. The notch ligand jagged-1 represents a novel growth factor of human hematopoietic stem cells. *J. Exp. Med.* **2000**, *192*, 1365–1372. [CrossRef]
128. Varnum-Finney, B.; Xu, L.; Brashem-Stein, C.; Nourigat, C.; Flowers, D.; Bakkour, S.; Pear, W.S.; Bernstein, I.D. Pluripotent, cytokine-dependent, hematopoietic stem cells are immortalized by constitutive notch1 signaling. *Nat. Med.* **2000**, *6*, 1278–1281. [CrossRef]
129. Weng, A.P.; Ferrando, A.A.; Lee, W.; Morris, J.P.t.; Silverman, L.B.; Sanchez-Irizarry, C.; Blacklow, S.C.; Look, A.T.; Aster, J.C. Activating mutations of notch1 in human t cell acute lymphoblastic leukemia. *Science* **2004**, *306*, 269–271. [CrossRef]
130. O'Neil, J.; Calvo, J.; McKenna, K.; Krishnamoorthy, V.; Aster, J.C.; Bassing, C.H.; Alt, F.W.; Kelliher, M.; Look, A.T. Activating notch1 mutations in mouse models of t-all. *Blood* **2006**, *107*, 781–785. [CrossRef]
131. Tatarek, J.; Cullion, K.; Ashworth, T.; Gerstein, R.; Aster, J.C.; Kelliher, M.A. Notch1 inhibition targets the leukemia-initiating cells in a tal1/lmo2 mouse model of t-all. *Blood* **2011**, *118*, 1579–1590. [CrossRef] [PubMed]
132. Gerby, B.; Veiga, D.F.; Krosl, J.; Nourreddine, S.; Ouellette, J.; Haman, A.; Lavoie, G.; Fares, I.; Tremblay, M.; Litalien, V.; et al. High-throughput screening in niche-based assay identifies compounds to target preleukemic stem cells. *J. Clin. Investig.* **2016**, *126*, 4569–4584. [CrossRef] [PubMed]
133. Tremblay, C.S.; Saw, J.; Chiu, S.K.; Wong, N.C.; Tsyganov, K.; Chotb, S.; Graham, A.N.; Yan, F.; Guirguis, A.A.; Sonderegger, S.E.; et al. Restricted cell cycle is essential for clonal evolution and therapeutic resistance of pre-leukemic stem cells. *Nat. Commun.* **2018**, *9*, 3535. [CrossRef] [PubMed]
134. Barnes, D.J.; Melo, J.V. Primitive, quiescent and difficult to kill: The role of non-proliferating stem cells in chronic myeloid leukemia. *Cell Cycle* **2006**, *5*, 2862–2866. [CrossRef]
135. Prost, S.; Relouzat, F.; Spentchian, M.; Ouzegdouh, Y.; Saliba, J.; Massonnet, G.; Beressi, J.P.; Verhoeyen, E.; Raggueneau, V.; Maneglier, B.; et al. Erosion of the chronic myeloid leukaemia stem cell pool by ppargamma agonists. *Nature* **2015**, *525*, 380–383. [CrossRef]
136. Foudi, A.; Hochedlinger, K.; van Buren, D.; Schindler, J.W.; Jaenisch, R.; Carey, V.; Hock, H. Analysis of histone 2b-gfp retention reveals slowly cycling hematopoietic stem cells. *Nat. Biotechnol.* **2009**, *27*, 84–90. [CrossRef]
137. Wilson, A.; Laurenti, E.; Oser, G.; van der Wath, R.C.; Blanco-Bose, W.; Jaworski, M.; Offner, S.; Dunant, C.F.; Eshkind, L.; Bockamp, E.; et al. Hematopoietic stem cells reversibly switch from dormancy to self-renewal during homeostasis and repair. *Cell* **2008**, *135*, 1118–1129. [CrossRef]
138. Shields, B.J.; Slape, C.I.; Vo, N.; Jackson, J.T.; Pliego-Zamora, A.; Ranasinghe, H.; Shi, W.; Curtis, D.J.; McCormack, M.P. The nup98-hoxd13 fusion oncogene induces thymocyte self-renewal via lmo2/lyl1. *Leukemia* **2019**, *33*, 1868–1880. [CrossRef]
139. Tardif, M.; Gerby, B.; Hoang, T. NUP98-PHF23 and NUP98-HOXD13 oncogenes confer aberrant self-renewal potential to thymocyte progenitors. *Exp. Hematol.* **2014**, *42*, S62. [CrossRef]
140. Batta, K.; Florkowska, M.; Kouskoff, V.; Lacaud, G. Direct reprogramming of murine fibroblasts to hematopoietic progenitor cells. *Cell Rep.* **2014**, *9*, 1871–1884. [CrossRef]
141. Garcia-Ramirez, I.; Bhatia, S.; Rodriguez-Hernandez, G.; Gonzalez-Herrero, I.; Walter, C.; Gonzalez de Tena-Davila, S.; Parvin, S.; Haas, O.; Woessmann, W.; Stanulla, M.; et al. Lmo2 expression defines tumor cell identity during t-cell leukemogenesis. *EMBO J.* **2018**, *37*, e98783. [CrossRef]
142. Abdulla, H.; Vo, A.; Shields, B.J.; Davies, T.J.; Jackson, J.T.; Alserihi, R.; Viney, E.M.; Wong, T.; Yan, F.; Wong, N.C.; et al. T-all can evolve to oncogene independence. *Leukemia* **2021**, *35*, 2205–2219. [CrossRef]
143. Rodriguez-Hernandez, G.; Casado-Garcia, A.; Isidro-Hernandez, M.; Picard, D.; Raboso-Gallego, J.; Aleman-Arteaga, S.; Orfao, A.; Blanco, O.; Riesco, S.; Prieto-Matos, P.; et al. The second oncogenic hit determines the cell fate of etv6-runx1 positive leukemia. *Front. Cell Dev. Biol.* **2021**, *9*, 704591. [CrossRef]
144. Hardy, R.R.; Li, Y.S.; Allman, D.; Asano, M.; Gui, M.; Hayakawa, K. B-cell commitment, development and selection. *Immunol. Rev.* **2000**, *175*, 23–32. [CrossRef]

145. Melchers, F. The pre-b-cell receptor: Selector of fitting immunoglobulin heavy chains for the b-cell repertoire. *Nat. Rev. Immunol.* **2005**, *5*, 578–584. [CrossRef]
146. Meffre, E.; Casellas, R.; Nussenzweig, M.C. Antibody regulation of b cell development. *Nat. Immunol.* **2000**, *1*, 379–385. [CrossRef]
147. Nutt, S.L.; Heavey, B.; Rolink, A.G.; Busslinger, M. Commitment to the b-lymphoid lineage depends on the transcription factor pax5. *Nature* **1999**, *401*, 556–562. [CrossRef]
148. Cresson, C.; Peron, S.; Jamrog, L.; Rouquie, N.; Prade, N.; Dubois, M.; Hebrard, S.; Lagarde, S.; Gerby, B.; Mancini, S.J.C.; et al. Pax5a and pax5b isoforms are both efficient to drive b cell differentiation. *Oncotarget* **2018**, *9*, 32841–32854. [CrossRef]
149. Busslinger, M. Transcriptional control of early b cell development. *Annu. Rev. Immunol.* **2004**, *22*, 55–79. [CrossRef]
150. Souabni, A.; Cobaleda, C.; Schebesta, M.; Busslinger, M. Pax5 promotes b lymphopoiesis and blocks t cell development by repressing notch1. *Immunity* **2002**, *17*, 781–793. [CrossRef]
151. Nera, K.P.; Kohonen, P.; Narvi, E.; Peippo, A.; Mustonen, L.; Terho, P.; Koskela, K.; Buerstedde, J.M.; Lassila, O. Loss of pax5 promotes plasma cell differentiation. *Immunity* **2006**, *24*, 283–293. [CrossRef]
152. Urbanek, P.; Wang, Z.Q.; Fetka, I.; Wagner, E.F.; Busslinger, M. Complete block of early b cell differentiation and altered patterning of the posterior midbrain in mice lacking pax5/bsap. *Cell* **1994**, *79*, 901–912. [CrossRef]
153. Rolink, A.G.; Nutt, S.L.; Melchers, F.; Busslinger, M. Long-term in vivo reconstitution of t-cell development by pax5-deficient b-cell progenitors. *Nature* **1999**, *401*, 603–606. [CrossRef]
154. Schaniel, C.; Bruno, L.; Melchers, F.; Rolink, A.G. Multiple hematopoietic cell lineages develop in vivo from transplanted pax5-deficient pre-b i-cell clones. *Blood* **2002**, *99*, 472–478. [CrossRef]
155. Hoflinger, S.; Kesavan, K.; Fuxa, M.; Hutter, C.; Heavey, B.; Radtke, F.; Busslinger, M. Analysis of notch1 function by in vitro t cell differentiation of pax5 mutant lymphoid progenitors. *J. Immunol.* **2004**, *173*, 3935–3944. [CrossRef]
156. Delogu, A.; Schebesta, A.; Sun, Q.; Aschenbrenner, K.; Perlot, T.; Busslinger, M. Gene repression by pax5 in b cells is essential for blood cell homeostasis and is reversed in plasma cells. *Immunity* **2006**, *24*, 269–281. [CrossRef]
157. Schebesta, A.; McManus, S.; Salvagiotto, G.; Delogu, A.; Busslinger, G.A.; Busslinger, M. Transcription factor pax5 activates the chromatin of key genes involved in b cell signaling, adhesion, migration, and immune function. *Immunity* **2007**, *27*, 49–63. [CrossRef]
158. Revilla, I.D.R.; Bilic, I.; Vilagos, B.; Tagoh, H.; Ebert, A.; Tamir, I.M.; Smeenk, L.; Trupke, J.; Sommer, A.; Jaritz, M.; et al. The b-cell identity factor pax5 regulates distinct transcriptional programmes in early and late b lymphopoiesis. *EMBO J.* **2012**, *31*, 3130–3146. [CrossRef]
159. Cobaleda, C.; Jochum, W.; Busslinger, M. Conversion of mature b cells into t cells by dedifferentiation to uncommitted progenitors. *Nature* **2007**, *449*, 473–477. [CrossRef] [PubMed]
160. Nebral, K.; Denk, D.; Attarbaschi, A.; Konig, M.; Mann, G.; Haas, O.A.; Strehl, S. Incidence and diversity of pax5 fusion genes in childhood acute lymphoblastic leukemia. *Leukemia* **2009**, *23*, 134–143. [CrossRef] [PubMed]
161. Familiades, J.; Bousquet, M.; Lafage-Pochitaloff, M.; Bene, M.C.; Beldjord, K.; De Vos, J.; Dastugue, N.; Coyaud, E.; Struski, S.; Quelen, C.; et al. Pax5 mutations occur frequently in adult b-cell progenitor acute lymphoblastic leukemia and pax5 haploinsufficiency is associated with bcr-abl1 and tcf3-pbx1 fusion genes: A graall study. *Leukemia* **2009**, *23*, 1989–1998. [CrossRef]
162. Mullighan, C.G.; Goorha, S.; Radtke, I.; Miller, C.B.; Coustan-Smith, E.; Dalton, J.D.; Girtman, K.; Mathew, S.; Ma, J.; Pounds, S.B.; et al. Genome-wide analysis of genetic alterations in acute lymphoblastic leukaemia. *Nature* **2007**, *446*, 758–764. [CrossRef] [PubMed]
163. Cobaleda, C.; Schebesta, A.; Delogu, A.; Busslinger, M. Pax5: The guardian of b cell identity and function. *Nat. Immunol.* **2007**, *8*, 463–470. [CrossRef]
164. Dang, J.; Wei, L.; de Ridder, J.; Su, X.; Rust, A.G.; Roberts, K.G.; Payne-Turner, D.; Cheng, J.; Ma, J.; Qu, C.; et al. Pax5 is a tumor suppressor in mouse mutagenesis models of acute lymphoblastic leukemia. *Blood* **2015**, *125*, 3609–3617. [CrossRef]
165. Ramamoorthy, S.; Kometani, K.; Herman, J.S.; Bayer, M.; Boller, S.; Edwards-Hicks, J.; Ramachandran, H.; Li, R.; Klein-Geltink, R.; Pearce, E.L.; et al. Ebf1 and pax5 safeguard leukemic transformation by limiting il-7 signaling, myc expression, and folate metabolism. *Genes Dev.* **2020**, *34*, 1503–1519. [CrossRef]
166. Prasad, M.A.; Ungerback, J.; Ahsberg, J.; Somasundaram, R.; Strid, T.; Larsson, M.; Mansson, R.; De Paepe, A.; Lilljebjorn, H.; Fioretos, T.; et al. Ebf1 heterozygosity results in increased DNA damage in pro-b cells and their synergistic transformation by pax5 haploinsufficiency. *Blood* **2015**, *125*, 4052–4059. [CrossRef]
167. Chan, L.N.; Chen, Z.; Braas, D.; Lee, J.W.; Xiao, G.; Geng, H.; Cosgun, K.N.; Hurtz, C.; Shojaee, S.; Cazzaniga, V.; et al. Metabolic gatekeeper function of b-lymphoid transcription factors. *Nature* **2017**, *542*, 479–483. [CrossRef]
168. Heltemes-Harris, L.M.; Willette, M.J.; Ramsey, L.B.; Qiu, Y.H.; Neeley, E.S.; Zhang, N.; Thomas, D.A.; Koeuth, T.; Baechler, E.C.; Kornblau, S.M.; et al. Ebf1 or pax5 haploinsufficiency synergizes with stat5 activation to initiate acute lymphoblastic leukemia. *J. Exp. Med.* **2011**, *208*, 1135–1149. [CrossRef]
169. Roberts, K.G.; Mullighan, C.G. The biology of b-progenitor acute lymphoblastic leukemia. *Cold Spring Harb. Perspect. Med.* **2020**, *10*, a034835. [CrossRef]
170. Somasundaram, R.; Prasad, M.A.; Ungerback, J.; Sigvardsson, M. Transcription factor networks in b-cell differentiation link development to acute lymphoid leukemia. *Blood* **2015**, *126*, 144–152. [CrossRef]
171. Ungerback, J.; Ahsberg, J.; Strid, T.; Somasundaram, R.; Sigvardsson, M. Combined heterozygous loss of ebf1 and pax5 allows for t-lineage conversion of b cell progenitors. *J. Exp. Med.* **2015**, *212*, 1109–1123. [CrossRef] [PubMed]

172. Hu, Y.; Zhang, Z.; Kashiwagi, M.; Yoshida, T.; Joshi, I.; Jena, N.; Somasundaram, R.; Emmanuel, A.O.; Sigvardsson, M.; Fitamant, J.; et al. Superenhancer reprogramming drives a b-cell-epithelial transition and high-risk leukemia. *Genes Dev.* **2016**, *30*, 1971–1990. [CrossRef]
173. Rodriguez-Hernandez, G.; Opitz, F.V.; Delgado, P.; Walter, C.; Alvarez-Prado, A.F.; Gonzalez-Herrero, I.; Auer, F.; Fischer, U.; Janssen, S.; Bartenhagen, C.; et al. Infectious stimuli promote malignant b-cell acute lymphoblastic leukemia in the absence of aid. *Nat. Commun.* **2019**, *10*, 5563. [CrossRef] [PubMed]
174. Martin-Lorenzo, A.; Hauer, J.; Vicente-Duenas, C.; Auer, F.; Gonzalez-Herrero, I.; Garcia-Ramirez, I.; Ginzel, S.; Thiele, R.; Constantinescu, S.N.; Bartenhagen, C.; et al. Infection exposure is a causal factor in b-cell precursor acute lymphoblastic leukemia as a result of pax5-inherited susceptibility. *Cancer Discov.* **2015**, *5*, 1328–1343. [CrossRef]
175. Vicente-Duenas, C.; Janssen, S.; Oldenburg, M.; Auer, F.; Gonzalez-Herrero, I.; Casado-Garcia, A.; Isidro-Hernandez, M.; Raboso-Gallego, J.; Westhoff, P.; Pandyra, A.A.; et al. An intact gut microbiome protects genetically predisposed mice against leukemia. *Blood* **2020**, *136*, 2003–2017. [CrossRef]
176. Isidro-Hernandez, M.; Mayado, A.; Casado-Garcia, A.; Martinez-Cano, J.; Palmi, C.; Fazio, G.; Orfao, A.; Ribera, J.; Ribera, J.M.; Zamora, L.; et al. Inhibition of inflammatory signaling in pax5 mutant cells mitigates b-cell leukemogenesis. *Sci. Rep.* **2020**, *10*, 19189. [CrossRef]
177. Cobaleda, C.; Vicente-Duenas, C.; Sanchez-Garcia, I. Infectious triggers and novel therapeutic opportunities in childhood b cell leukaemia. *Nat. Rev. Immunol.* **2021**, *21*, 570–581. [CrossRef]
178. Medvedovic, J.; Ebert, A.; Tagoh, H.; Busslinger, M. Pax5: A master regulator of b cell development and leukemogenesis. *Adv. Immunol.* **2011**, *111*, 179–206.
179. Bousquet, M.; Broccardo, C.; Quelen, C.; Meggetto, F.; Kuhlein, E.; Delsol, G.; Dastugue, N.; Brousset, P. A novel pax5-eln fusion protein identified in b-cell acute lymphoblastic leukemia acts as a dominant negative on wild-type pax5. *Blood* **2007**, *109*, 3417–3423. [CrossRef]
180. Coyaud, E.; Struski, S.; Prade, N.; Familiades, J.; Eichner, R.; Quelen, C.; Bousquet, M.; Mugneret, F.; Talmant, P.; Pages, M.P.; et al. Wide diversity of pax5 alterations in b-all: A groupe francophone de cytogenetique hematologique study. *Blood* **2010**, *115*, 3089–3097. [CrossRef]
181. Marincevic-Zuniga, Y.; Zachariadis, V.; Cavelier, L.; Castor, A.; Barbany, G.; Forestier, E.; Fogelstrand, L.; Heyman, M.; Abrahamsson, J.; Lönnerholm, G.; et al. PAX5-ESRRB is a recurrent fusion gene in B-cell precursor pediatric acute lymphoblastic leukemia. *Haematologica* **2015**, *101*, e20–e23. [CrossRef] [PubMed]
182. Cazzaniga, G.; Daniotti, M.; Tosi, S.; Giudici, G.; Aloisi, A.; Pogliani, E.; Kearney, L.; Biondi, A. The paired box domain gene pax5 is fused to etv6/tel in an acute lymphoblastic leukemia case. *Cancer Res.* **2001**, *61*, 4666–4670. [PubMed]
183. Smeenk, L.; Fischer, M.; Jurado, S.; Jaritz, M.; Azaryan, A.; Werner, B.; Roth, M.; Zuber, J.; Stanulla, M.; den Boer, M.L.; et al. Molecular role of the pax5-etv6 oncoprotein in promoting b-cell acute lymphoblastic leukemia. *EMBO J.* **2017**, *36*, 718–735. [CrossRef] [PubMed]
184. Jamrog, L.; Chemin, G.; Fregona, V.; Coster, L.; Pasquet, M.; Oudinet, C.; Rouquie, N.; Prade, N.; Lagarde, S.; Cresson, C.; et al. Pax5-eln oncoprotein promotes multistep b-cell acute lymphoblastic leukemia in mice. *Proc. Natl. Acad. Sci. USA* **2018**, *115*, 10357–10362. [CrossRef]
185. Van der Weyden, L.; Giotopoulos, G.; Wong, K.; Rust, A.G.; Robles-Espinoza, C.D.; Osaki, H.; Huntly, B.J.; Adams, D.J. Somatic drivers of b-all in a model of etv6-runx1; pax5(+/-) leukemia. *BMC Cancer* **2015**, *15*, 585. [CrossRef]
186. Duque-Afonso, J.; Feng, J.; Scherer, F.; Lin, C.H.; Wong, S.H.; Wang, Z.; Iwasaki, M.; Cleary, M.L. Comparative genomics reveals multistep pathogenesis of e2a-pbx1 acute lymphoblastic leukemia. *J. Clin. Investig.* **2015**, *125*, 3667–3680. [CrossRef]
187. Shah, S.; Schrader, K.A.; Waanders, E.; Timms, A.E.; Vijai, J.; Miething, C.; Wechsler, J.; Yang, J.; Hayes, J.; Klein, R.J.; et al. A recurrent germline pax5 mutation confers susceptibility to pre-b cell acute lymphoblastic leukemia. *Nat. Genet.* **2013**, *45*, 1226–1231. [CrossRef]
188. Duployez, N.; Jamrog, L.A.; Fregona, V.; Hamelle, C.; Fenwarth, L.; Lejeune, S.; Helevaut, N.; Geffroy, S.; Caillault, A.; Marceau-Renaut, A.; et al. Germline pax5 mutation predisposes to familial b-cell precursor acute lymphoblastic leukemia. *Blood* **2021**, *137*, 1424–1428. [CrossRef]
189. An, Q.; Wright, S.L.; Konn, Z.J.; Matheson, E.; Minto, L.; Moorman, A.V.; Parker, H.; Griffiths, M.; Ross, F.M.; Davies, T.; et al. Variable breakpoints target pax5 in patients with dicentric chromosomes: A model for the basis of unbalanced translocations in cancer. *Proc. Natl. Acad. Sci. USA* **2008**, *105*, 17050–17054. [CrossRef]
190. Gu, Z.; Churchman, M.L.; Roberts, K.G.; Moore, I.; Zhou, X.; Nakitandwe, J.; Hagiwara, K.; Pelletier, S.; Gingras, S.; Berns, H.; et al. Pax5-driven subtypes of b-progenitor acute lymphoblastic leukemia. *Nat. Genet.* **2019**, *51*, 296–307. [CrossRef]
191. Passet, M.; Boissel, N.; Sigaux, F.; Saillard, C.; Bargetzi, M.; Ba, I.; Thomas, X.; Graux, C.; Chalandon, Y.; Leguay, T.; et al. Pax5 p80r mutation identifies a novel subtype of b-cell precursor acute lymphoblastic leukemia with favorable outcome. *Blood* **2019**, *133*, 280–284. [CrossRef]
192. Li, J.F.; Dai, Y.T.; Lilljebjorn, H.; Shen, S.H.; Cui, B.W.; Bai, L.; Liu, Y.F.; Qian, M.X.; Kubota, Y.; Kiyoi, H.; et al. Transcriptional landscape of b cell precursor acute lymphoblastic leukemia based on an international study of 1,223 cases. *Proc. Natl. Acad. Sci. USA* **2018**, *115*, E11711–E11720. [CrossRef]

193. Bastian, L.; Schroeder, M.P.; Eckert, C.; Schlee, C.; Tanchez, J.O.; Kampf, S.; Wagner, D.L.; Schulze, V.; Isaakidis, K.; Lazaro-Navarro, J.; et al. Pax5 biallelic genomic alterations define a novel subgroup of b-cell precursor acute lymphoblastic leukemia. *Leukemia* **2019**, *33*, 1895–1909. [CrossRef]
194. Aplan, P.D.; Jones, C.A.; Chervinsky, D.S.; Zhao, X.; Ellsworth, M.; Wu, C.; McGuire, E.A.; Gross, K.W. An scl gene product lacking the transactivation domain induces bony abnormalities and cooperates with lmo1 to generate t-cell malignancies in transgenic mice. *EMBO J.* **1997**, *16*, 2408–2419. [CrossRef]
195. Curtis, D.J.; Robb, L.; Strasser, A.; Begley, C.G. The cd2-scl transgene alters the phenotype and frequency of t-lymphomas in n-ras transgenic or p53 deficient mice. *Oncogene* **1997**, *15*, 2975–2983. [CrossRef]
196. Goardon, N.; Schuh, A.; Hajar, I.; Ma, X.; Jouault, H.; Dzierzak, E.; Romeo, P.H.; Maouche-Chretien, L. Ectopic expression of tal-1 protein in ly-6e.1-htal-1 transgenic mice induces defects in b- and t-lymphoid differentiation. *Blood* **2002**, *100*, 491–500. [CrossRef]
197. Condorelli, G.L.; Facchiano, F.; Valtieri, M.; Proietti, E.; Vitelli, L.; Lulli, V.; Huebner, K.; Peschle, C.; Croce, C.M. T-cell-directed tal-1 expression induces t-cell malignancies in transgenic mice. *Cancer Res.* **1996**, *56*, 5113–5119.
198. Kelliher, M.A.; Seldin, D.C.; Leder, P. Tal-1 induces t cell acute lymphoblastic leukemia accelerated by casein kinase iialpha. *EMBO J.* **1996**, *15*, 5160–5166. [CrossRef]
199. Draheim, K.M.; Hermance, N.; Yang, Y.; Arous, E.; Calvo, J.; Kelliher, M.A. A DNA-binding mutant of tal1 cooperates with lmo2 to cause t cell leukemia in mice. *Oncogene* **2011**, *30*, 1252–1260. [CrossRef]
200. Tremblay, C.S.; Brown, F.C.; Collett, M.; Saw, J.; Chiu, S.K.; Sonderegger, S.E.; Lucas, S.E.; Alserihi, R.; Chau, N.; Toribio, M.L.; et al. Loss-of-function mutations of dynamin 2 promote t-all by enhancing il-7 signalling. *Leukemia* **2016**, *30*, 1993–2001. [CrossRef]
201. Shields, B.J.; Alserihi, R.; Nasa, C.; Bogue, C.; Alexander, W.S.; McCormack, M.P. Hhex regulates kit to promote radioresistance of self-renewing thymocytes in lmo2-transgenic mice. *Leukemia* **2015**, *29*, 927–938. [CrossRef]
202. Choi, C.W.; Chung, Y.J.; Slape, C.; Aplan, P.D. A nup98-hoxd13 fusion gene impairs differentiation of b and t lymphocytes and leads to expansion of thymocytes with partial tcrb gene rearrangement. *J. Immunol.* **2009**, *183*, 6227–6235. [CrossRef]
203. Nutt, S.L.; Vambrie, S.; Steinlein, P.; Kozmik, Z.; Rolink, A.; Weith, A.; Busslinger, M. Independent regulation of the two pax5 alleles during b-cell development. *Nat. Genet.* **1999**, *21*, 390–395. [CrossRef]
204. Heltemes-Harris, L.M.; Hubbard, G.K.; La Rue, R.S.; Munro, S.A.; Knudson, T.P.; Yang, R.; Henzler, C.M.; Starr, T.K.; Sarver, A.L.; Kornblau, M.S.; et al. Identification of mutations that cooperate with defects in B cell transcription factors to initiate leukemia. *bioRxiv* **2020**. [CrossRef]
205. Boast, B.; Helian, K.; Andrews, T.D.; Vicky Cho, X.L.; Closa, A.; Sutton, H.J.; Reed, J.H.; Bergmann, H.; Roots, C.M.; Yabas, M.; et al. Dysregulation of PAX5 causes uncommitted B cell development and tumorigenesis in mice. *bioRxiv* **2021**. [CrossRef]
206. Rodriguez-Hernandez, G.; Hauer, J.; Martin-Lorenzo, A.; Schafer, D.; Bartenhagen, C.; Garcia-Ramirez, I.; Auer, F.; Gonzalez-Herrero, I.; Ruiz-Roca, L.; Gombert, M.; et al. Infection exposure promotes etv6-runx1 precursor b-cell leukemia via impaired h3k4 demethylases. *Cancer Res.* **2017**, *77*, 4365–4377. [CrossRef]
207. Bijl, J.; Sauvageau, M.; Thompson, A.; Sauvageau, G. High incidence of proviral integrations in the Hoxa locus in a new model of E2a-PBX1-induced B-cell leukemia. *Genes Dev.* **2005**, *19*, 224–233. [CrossRef]
208. Martin-Lorenzo, A.; Auer, F.; Chan, L.N.; Garcia-Ramirez, I.; Gonzalez-Herrero, I.; Rodriguez-Hernandez, G.; Bartenhagen, C.; Dugas, M.; Gombert, M.; Ginzel, S.; et al. Loss of pax5 exploits sca1-bcr-abl(p190) susceptibility to confer the metabolic shift essential for pb-all. *Cancer Res.* **2018**, *78*, 2669–2679. [CrossRef]
209. Hopkins, A.L.; Groom, C.R. The druggable genome. *Nat. Rev. Drug Discov.* **2002**, *1*, 727–730. [CrossRef]
210. Verdine, G.L.; Walensky, L.D. The challenge of drugging undruggable targets in cancer: Lessons learned from targeting bcl-2 family members. *Clin. Cancer Res.* **2007**, *13*, 7264–7270. [CrossRef]
211. Nasr, R.; Guillemin, M.C.; Ferhi, O.; Soilihi, H.; Peres, L.; Berthier, C.; Rousselot, P.; Robledo-Sarmiento, M.; Lallemand-Breitenbach, V.; Gourmel, B.; et al. Eradication of acute promyelocytic leukemia-initiating cells through pml-rara degradation. *Nat. Med.* **2008**, *14*, 1333–1342. [CrossRef] [PubMed]
212. De The, H.; Pandolfi, P.P.; Chen, Z. Acute promyelocytic leukemia: A paradigm for oncoprotein-targeted cure. *Cancer Cell* **2017**, *32*, 552–560. [CrossRef] [PubMed]
213. Conneely, S.E.; Stevens, A.M. Advances in pediatric acute promyelocytic leukemia. *Children* **2020**, *7*, 11. [CrossRef] [PubMed]
214. Benyoucef, A.; Palii, C.G.; Wang, C.; Porter, C.J.; Chu, A.; Dai, F.; Tremblay, V.; Rakopoulos, P.; Singh, K.; Huang, S.; et al. Utx inhibition as selective epigenetic therapy against tal1-driven t-cell acute lymphoblastic leukemia. *Genes Dev.* **2016**, *30*, 508–521. [CrossRef]
215. McMillin, D.W.; Delmore, J.; Weisberg, E.; Negri, J.M.; Geer, D.C.; Klippel, S.; Mitsiades, N.; Schlossman, R.L.; Munshi, N.C.; Kung, A.L.; et al. Tumor cell-specific bioluminescence platform to identify stroma-induced changes to anticancer drug activity. *Nat. Med.* **2010**, *16*, 483–489. [CrossRef]
216. Tabe, Y.; Konopleva, M. Role of microenvironment in resistance to therapy in aml. *Curr. Hematol. Malig. Rep.* **2015**, *10*, 96–103. [CrossRef]
217. Lane, S.W.; Scadden, D.T.; Gilliland, D.G. The leukemic stem cell niche: Current concepts and therapeutic opportunities. *Blood* **2009**, *114*, 1150–1157. [CrossRef]
218. Batsivari, A.; Haltalli, M.L.R.; Passaro, D.; Pospori, C.; Celso, C.L.; Bonnet, D. Dynamic responses of the haematopoietic stem cell niche to diverse stresses. *Nat. Cell Biol.* **2020**, *22*, 7–17. [CrossRef]

219. Medyouf, H. The microenvironment in human myeloid malignancies: Emerging concepts and therapeutic implications. *Blood* **2017**, *129*, 1617–1626. [CrossRef]
220. Xia, B.; Tian, C.; Guo, S.; Zhang, L.; Zhao, D.; Qu, F.; Zhao, W.; Wang, Y.; Wu, X.; Da, W.; et al. C-myc plays part in drug resistance mediated by bone marrow stromal cells in acute myeloid leukemia. *Leuk. Res.* **2015**, *39*, 92–99. [CrossRef]
221. Sanchez-Aguilera, A.; Mendez-Ferrer, S. The hematopoietic stem-cell niche in health and leukemia. *Cell. Mol. Life Sci.* **2017**, *74*, 579–590. [CrossRef]
222. Passaro, D.; Quang, C.T.; Ghysdael, J. Microenvironmental cues for t-cell acute lymphoblastic leukemia development. *Immunol. Rev.* **2016**, *271*, 156–172. [CrossRef]
223. Calvo, J.; Fahy, L.; Uzan, B.; Pflumio, F. Desperately seeking a home marrow niche for t-cell acute lymphoblastic leukaemia. *Adv. Biol. Regul.* **2019**, *74*, 100640. [CrossRef]
224. Delahaye, M.C.; Salem, K.I.; Pelletier, J.; Aurrand-Lions, M.; Mancini, S.J.C. Toward therapeutic targeting of bone marrow leukemic niche protective signals in b-cell acute lymphoblastic leukemia. *Front. Oncol.* **2020**, *10*, 606540. [CrossRef]
225. Burt, R.; Dey, A.; Aref, S.; Aguiar, M.; Akarca, A.; Bailey, K.; Day, W.; Hooper, S.; Kirkwood, A.; Kirschner, K.; et al. Activated stromal cells transfer mitochondria to rescue acute lymphoblastic leukemia cells from oxidative stress. *Blood* **2019**, *134*, 1415–1429. [CrossRef]
226. De Smedt, R.; Morscio, J.; Reunes, L.; Roels, J.; Bardelli, V.; Lintermans, B.; van Loocke, W.; Almeida, A.; Cheung, L.C.; Kotecha, R.S.; et al. Targeting cytokine- and therapy-induced pim1 activation in preclinical models of t-cell acute lymphoblastic leukemia and lymphoma. *Blood* **2020**, *135*, 1685–1695. [CrossRef]
227. Gerby, B.; Hoang, T. A targetable cue in t-cell malignancy. *Blood* **2020**, *135*, 1616–1617. [CrossRef]
228. Ma, C.; Witkowski, M.T.; Harris, J.; Dolgalev, I.; Sreeram, S.; Qian, W.; Tong, J.; Chen, X.; Aifantis, I.; Chen, W. Leukemia-on-a-chip: Dissecting the chemoresistance mechanisms in b cell acute lymphoblastic leukemia bone marrow niche. *Sci. Adv.* **2020**, *6*, eaba5536. [CrossRef]
229. Tremblay, C.S.; Chiu, S.K.; Saw, J.; McCalmont, H.; Litalien, V.; Boyle, J.; Sonderegger, S.E.; Chau, N.; Evans, K.; Cerruti, L.; et al. Small molecule inhibition of dynamin-dependent endocytosis targets multiple niche signals and impairs leukemia stem cells. *Nat. Commun.* **2020**, *11*, 6211. [CrossRef]
230. Chattopadhyay, S.; Stewart, A.L.; Mukherjee, S.; Huang, C.; Hartwell, K.A.; Miller, P.G.; Subramanian, R.; Carmody, L.C.; Yusuf, R.Z.; Sykes, D.B.; et al. Niche-based screening in multiple myeloma identifies a kinesin-5 inhibitor with improved selectivity over hematopoietic progenitors. *Cell Rep.* **2015**, *10*, 755–770. [CrossRef]
231. Hartwell, K.A.; Miller, P.G.; Mukherjee, S.; Kahn, A.R.; Stewart, A.L.; Logan, D.J.; Negri, J.M.; Duvet, M.; Jaras, M.; Puram, R.; et al. Niche-based screening identifies small-molecule inhibitors of leukemia stem cells. *Nat. Chem. Biol.* **2013**, *9*, 840–848. [CrossRef] [PubMed]
232. Weng, A.P.; Millholland, J.M.; Yashiro-Ohtani, Y.; Arcangeli, M.L.; Lau, A.; Wai, C.; Del Bianco, C.; Rodriguez, C.G.; Sai, H.; Tobias, J.; et al. C-myc is an important direct target of notch1 in t-cell acute lymphoblastic leukemia/lymphoma. *Genes Dev.* **2006**, *20*, 2096–2109. [CrossRef] [PubMed]
233. Palomero, T.; Lim, W.K.; Odom, D.T.; Sulis, M.L.; Real, P.J.; Margolin, A.; Barnes, K.C.; O'Neil, J.; Neuberg, D.; Weng, A.P.; et al. Notch1 directly regulates c-myc and activates a feed-forward-loop transcriptional network promoting leukemic cell growth. *Proc. Natl. Acad. Sci. USA* **2006**, *103*, 18261–18266. [CrossRef] [PubMed]
234. Roderick, J.E.; Tesell, J.; Shultz, L.D.; Brehm, M.A.; Greiner, D.L.; Harris, M.H.; Silverman, L.B.; Sallan, S.E.; Gutierrez, A.; Look, A.T.; et al. C-myc inhibition prevents leukemia initiation in mice and impairs the growth of relapsed and induction failure pediatric t-all cells. *Blood* **2014**, *123*, 1040–1050. [CrossRef]
235. Yashiro-Ohtani, Y.; Wang, H.; Zang, C.; Arnett, K.L.; Bailis, W.; Ho, Y.; Knoechel, B.; Lanauze, C.; Louis, L.; Forsyth, K.S.; et al. Long-range enhancer activity determines myc sensitivity to notch inhibitors in t cell leukemia. *Proc. Natl. Acad. Sci. USA* **2014**, *111*, E4946–E4953. [CrossRef]
236. Jin, G.; Wong, S.T. Toward better drug repositioning: Prioritizing and integrating existing methods into efficient pipelines. *Drug Discov. Today* **2014**, *19*, 637–644. [CrossRef]

Partie VI : Bibliographie

Adams, B., Dörfler, P., Aguzzi, A., Kozmik, Z., Urbánek, P., Maurer-Fogy, I., & Busslinger, M. (1992). Pax-5 encodes the transcription factor BSAP and is expressed in B lymphocytes, the developing CNS, and adult testis. *Genes & Development*, *6*(9), 1589–1607. https://doi.org/10.1101/gad.6.9.1589

Adams, G. B., Chabner, K. T., Alley, I. R., Olson, D. P., Szczepiorkowski, Z. M., Poznansky, M. C., Kos, C. H., Pollak, M. R., Brown, E. M., & Scadden, D. T. (2006). Stem cell engraftment at the endosteal niche is specified by the calcium-sensing receptor. *Nature*, *439*(7076), 599–603. https://doi.org/10.1038/nature04247

Adolfsson, J., Månsson, R., Buza-Vidas, N., Hultquist, A., Liuba, K., Jensen, C. T., Bryder, D., Yang, L., Borge, O.-J., Thoren, L. A. M., Anderson, K., Sitnicka, E., Sasaki, Y., Sigvardsson, M., & Jacobsen, S. E. W. (2005). Identification of Flt3+ Lympho-Myeloid Stem Cells Lacking Erythro-Megakaryocytic Potential. *Cell*, *121*(2), 295–306. https://doi.org/10.1016/j.cell.2005.02.013

Aird, E. J., Lovendahl, K. N., St. Martin, A., Harris, R. S., & Gordon, W. R. (2018). Increasing Cas9-mediated homology-directed repair efficiency through covalent tethering of DNA repair template. *Communications Biology*, *1*(1), 54. https://doi.org/10.1038/s42003-018-0054-2

Aiuti, A., Webb, I. J., Bleul, C., Springer, T., & Gutierrez-Ramos, J. C. (1997). The Chemokine SDF-1 Is a Chemoattractant for Human CD34+ Hematopoietic Progenitor Cells and Provides a New Mechanism to Explain the Mobilization of CD34+ Progenitors to Peripheral Blood. *The Journal of Experimental Medicine*, *185*(1), 111–120. https://doi.org/10.1084/jem.185.1.111

Alberti-Servera, L., von Muenchow, L., Tsapogas, P., Capoferri, G., Eschbach, K., Beisel, C., Ceredig, R., Ivanek, R., & Rolink, A. (2017). Single-cell RNA sequencing reveals developmental heterogeneity among early lymphoid progenitors. *The EMBO Journal*, *36*(24), 3619–3633. https://doi.org/10.15252/embj.201797105

Alexandrov, L. B., Nik-Zainal, S., Wedge, D. C., Aparicio, S. A. J. R., Behjati, S., Biankin, A. V., Bignell, G. R., Bolli, N., Borg, A., Børresen-Dale, A.-L., Boyault, S., Burkhardt, B., Butler, A. P., Caldas, C., Davies, H. R., Desmedt, C., Eils, R., Eyfjörd, J. E., Foekens, J. A., … Stratton, M. R. (2013). Signatures of mutational processes in human cancer. *Nature*, *500*(7463), 415–421. https://doi.org/10.1038/nature12477

Amir, A., Erez-Granat, O., Braun, T., Sosnovski, K., Hadar, R., BenShoshan, M., Heiman, S., Abbas-Egbariya, H., Glick Saar, E., Efroni, G., & Haberman, Y. (2022). Gut microbiome development in early childhood is affected by day care attendance. *Npj Biofilms and Microbiomes*, *8*(1), 2. https://doi.org/10.1038/s41522-021-00265-w

An, Q., Wright, S. L., Konn, Z. J., Matheson, E., Minto, L., Moorman, A. V, Parker, H., Griffiths, M., Ross, F. M., Davies, T., Hall, A. G., Harrison, C. J., Irving, J. A., & Strefford, J. C. (2008). Variable breakpoints target PAX5 in patients with dicentric chromosomes: a model for the basis of unbalanced translocations in cancer. *Proc Natl Acad Sci U S A*, *105*(44), 17050–17054. https://doi.org/10.1073/pnas.0803494105

Anderson, K., Lutz, C., van Delft, F. W., Bateman, C. M., Guo, Y., Colman, S. M., Kempski, H., Moorman, A. V., Titley, I., Swansbury, J., Kearney, L., Enver, T., & Greaves, M. (2011). Genetic variegation of clonal architecture and propagating cells in leukaemia. *Nature*, *469*(7330), 356–361. https://doi.org/10.1038/nature09650

Aoki, Y., Watanabe, T., Saito, Y., Kuroki, Y., Hijikata, A., Takagi, M., Tomizawa, D., Eguchi, M., Eguchi-Ishimae, M., Kaneko, A., Ono, R., Sato, K., Suzuki, N., Fujiki, S., Koh, K., Ishii, E., Shultz, L. D., Ohara, O., Mizutani, S., & Ishikawa, F. (2015). Identification of CD34+ and

CD34− leukemia-initiating cells in MLL-rearranged human acute lymphoblastic leukemia. *Blood*, *125*(6), 967–980. https://doi.org/10.1182/blood-2014-03-563304

Asada, N., Kunisaki, Y., Pierce, H., Wang, Z., Fernandez, N. F., Birbrair, A., Ma'ayan, A., & Frenette, P. S. (2017). Differential cytokine contributions of perivascular haematopoietic stem cell niches. *Nature Cell Biology*, *19*(3), 214–223. https://doi.org/10.1038/ncb3475

Aurrand-Lions, M., & Mancini, S. (2018). Murine Bone Marrow Niches from Hematopoietic Stem Cells to B Cells. *International Journal of Molecular Sciences*, *19*(8), 2353. https://doi.org/10.3390/ijms19082353

Bain, G., Maandag, E. C., Izon, D. J., Amsen, D., Kruisbeek, A. M., Weintraub, B. C., Krop, I., Schlissel, M. S., Feeney, A. J., & van Roon, M. (1994). E2A proteins are required for proper B cell development and initiation of immunoglobulin gene rearrangements. *Cell*, *79*(5), 885–892. https://doi.org/10.1016/0092-8674(94)90077-9

Balczarek, K. A., Lai, Z. C., & Kumar, S. (1997). Evolution of functional diversification of the paired box (Pax) DNA- binding domains. *Molecular Biology and Evolution*, *14*(8), 829–842. https://doi.org/10.1093/oxfordjournals.molbev.a025824

Bao, E. L., Cheng, A. N., & Sankaran, V. G. (2019). The genetics of human hematopoiesis and its disruption in disease. *EMBO Molecular Medicine*, *11*(8). https://doi.org/10.15252/emmm.201910316

Barlev, N. A., Emelyanov, A. V., Castagnino, P., Zegerman, P., Bannister, A. J., Sepulveda, M. A., Robert, F., Tora, L., Kouzarides, T., Birshtein, B. K., & Berger, S. L. (2003). A Novel Human Ada2 Homologue Functions with Gcn5 or Brg1 To Coactivate Transcription. *Molecular and Cellular Biology*, *23*(19), 6944–6957. https://doi.org/10.1128/MCB.23.19.6944-6957.2003

Barrangou, R., Fremaux, C., Deveau, H., Richards, M., Boyaval, P., Moineau, S., Romero, D. A., & Horvath, P. (2007). CRISPR Provides Acquired Resistance Against Viruses in Prokaryotes. *Science*, *315*(5819), 1709–1712. https://doi.org/10.1126/science.1138140

Bastian, L., Schroeder, M. P., Eckert, C., Schlee, C., Tanchez, J. O., Kampf, S., Wagner, D. L., Schulze, V., Isaakidis, K., Lazaro-Navarro, J., Hanzelmann, S., James, A. R., Ekici, A., Burmeister, T., Schwartz, S., Schrappe, M., Horstmann, M., Vosberg, S., Krebs, S., … Baldus, C. D. (2019). PAX5 biallelic genomic alterations define a novel subgroup of B-cell precursor acute lymphoblastic leukemia. *Leukemia*, *33*(8), 1895–1909. https://doi.org/10.1038/s41375-019-0430-z

Becht, E., McInnes, L., Healy, J., Dutertre, C. A., Kwok, I. W. H., Ng, L. G., Ginhoux, F., & Newell, E. W. (2018). Dimensionality reduction for visualizing single-cell data using UMAP. *Nat Biotechnol*. https://doi.org/10.1038/nbt.4314

Berenson, R. J., Andrews, R. G., Bensinger, W. I., Kalamasz, D., Knitter, G., Buckner, C. D., & Bernstein, I. D. (1988). Antigen CD34+ marrow cells engraft lethally irradiated baboons. *Journal of Clinical Investigation*, *81*(3), 951–955. https://doi.org/10.1172/JCI113409

Berry, R., Chen, Z., McCluskey, J., & Rossjohn, J. (2011). Insight into the basis of autonomous immunoreceptor activation. *Trends in Immunology*, *32*(4), 165–170. https://doi.org/10.1016/j.it.2011.01.007

Bhatia, M., Wang, J. C. Y., Kapp, U., Bonnet, D., & Dick, J. E. (1997). Purification of primitive human hematopoietic cells capable of repopulating immune-deficient mice. *Proceedings of the National Academy of Sciences*, *94*(10), 5320–5325. https://doi.org/10.1073/pnas.94.10.5320

Bhatia, S., Pooja, & Yadav, S. K. (2023). CRISPR-Cas for genome editing: Classification, mechanism, designing and applications. *International Journal of Biological Macromolecules*, *238*, 124054. https://doi.org/10.1016/j.ijbiomac.2023.124054

Bolotin, A., Quinquis, B., Sorokin, A., & Ehrlich, S. D. (2005). Clustered regularly interspaced short palindrome repeats (CRISPRs) have spacers of extrachromosomal origin. *Microbiology*, *151*(8), 2551–2561. https://doi.org/10.1099/mic.0.28048-0

Bonnet, D., & Dick, J. E. (1997). Human acute myeloid leukemia is organized as a hierarchy that originates from a primitive hematopoietic cell. *Nature Medicine*, *3*(7), 730–737. https://doi.org/10.1038/nm0797-730

Bousquet, M., Broccardo, C., Quelen, C., Meggetto, F., Kuhlein, E., Delsol, G., Dastugue, N., & Brousset, P. (2007). A novel PAX5-ELN fusion protein identified in B-cell acute lymphoblastic leukemia acts as a dominant negative on wild-type PAX5. *Blood*, *109*(8), 3417–3423. https://doi.org/10.1182/blood-2006-05-025221

Brady, S. W., Roberts, K. G., Gu, Z., Shi, L., Pounds, S., Pei, D., Cheng, C., Dai, Y., Devidas, M., Qu, C., Hill, A. N., Payne-Turner, D., Ma, X., Iacobucci, I., Baviskar, P., Wei, L., Arunachalam, S., Hagiwara, K., Liu, Y., … Mullighan, C. G. (2022). The genomic landscape of pediatric acute lymphoblastic leukemia. *Nature Genetics*, *54*(9), 1376–1389. https://doi.org/10.1038/s41588-022-01159-z

Broudy, V. C. (1997). Stem cell factor and hematopoiesis. *Blood*, *90*(4), 1345–1364.

Broxmeyer, H. E., Orschell, C. M., Clapp, D. W., Hangoc, G., Cooper, S., Plett, P. A., Liles, W. C., Li, X., Graham-Evans, B., Campbell, T. B., Calandra, G., Bridger, G., Dale, D. C., & Srour, E. F. (2005). Rapid mobilization of murine and human hematopoietic stem and progenitor cells with AMD3100, a CXCR4 antagonist. *The Journal of Experimental Medicine*, *201*(8), 1307–1318. https://doi.org/10.1084/jem.20041385

Brun, T., Franklin, I., St-Onge, L., Biason-Lauber, A., Schoenle, E. J., Wollheim, C. B., & Gauthier, B. R. (2004). The diabetes-linked transcription factor PAX4 promotes β-cell proliferation and survival in rat and human islets. *Journal of Cell Biology*, *167*(6), 1123–1135. https://doi.org/10.1083/jcb.200405148

Busslinger, M. (2004). Transcriptional control of early B cell development. *Annu Rev Immunol*, *22*, 55–79. https://doi.org/10.1146/annurev.immunol.22.012703.104807

Busslinger, M., Klix, N., Pfeffer, P., Graninger, P. G., & Kozmik, Z. (1996). Deregulation of PAX-5 by translocation of the Emu enhancer of the IgH locus adjacent to two alternative PAX-5 promoters in a diffuse large-cell lymphoma. *Proceedings of the National Academy of Sciences*, *93*(12), 6129–6134. https://doi.org/10.1073/pnas.93.12.6129

Cai, Q., Dmitrieva, N. I., Ferraris, J. D., Brooks, H. L., van Balkom, B. W. M., & Burg, M. (2005). Pax2 expression occurs in renal medullary epithelial cells *in vivo* and in cell culture, is osmoregulated, and promotes osmotic tolerance. *Proceedings of the National Academy of Sciences*, *102*(2), 503–508. https://doi.org/10.1073/pnas.0408840102

Canver, M. C., Haeussler, M., Bauer, D. E., Orkin, S. H., Sanjana, N. E., Shalem, O., Yuan, G. C., Zhang, F., Concordet, J. P., & Pinello, L. (2018). Integrated design, execution, and analysis of arrayed and pooled CRISPR genome-editing experiments. *Nat Protoc*, *13*(5), 946–986. https://doi.org/10.1038/nprot.2018.005

Castor, A., Nilsson, L., Åstrand-Grundström, I., Buitenhuis, M., Ramirez, C., Anderson, K., Strömbeck, B., Garwicz, S., Békássy, A. N., Schmiegelow, K., Lausen, B., Hokland, P., Lehmann, S., Juliusson, G., Johansson, B., & Jacobsen, S. E. W. (2005). Distinct patterns of hematopoietic stem cell involvement in acute lymphoblastic leukemia. *Nature Medicine*, *11*(6), 630–637. https://doi.org/10.1038/nm1253

Cazzaniga, G., Daniotti, M., Tosi, S., Giudici, G., Aloisi, A., Pogliani, E., Kearney, L., & Biondi, A. (2001). The paired box domain gene PAX5 is fused to ETV6/TEL in an acute lymphoblastic leukemia case. *Cancer Res*, *61*(12), 4666–4670. https://www.ncbi.nlm.nih.gov/pubmed/11406533

Chan, L. N., Chen, Z., Braas, D., Lee, J. W., Xiao, G., Geng, H., Cosgun, K. N., Hurtz, C., Shojaee, S., Cazzaniga, V., Schjerven, H., Ernst, T., Hochhaus, A., Kornblau, S. M., Konopleva, M., Pufall, M. A., Cazzaniga, G., Liu, G. J., Milne, T. A., … Muschen, M. (2017). Metabolic gatekeeper function of B-lymphoid transcription factors. *Nature*, *542*(7642), 479–483. https://doi.org/10.1038/nature21076

Chapman, J. R., Taylor, M. R. G., & Boulton, S. J. (2012). Playing the End Game: DNA Double-Strand Break Repair Pathway Choice. *Molecular Cell*, *47*(4), 497–510. https://doi.org/10.1016/j.molcel.2012.07.029

Chi, N., & Epstein, J. A. (2002). Getting your Pax straight: Pax proteins in development and disease. *Trends in Genetics*, *18*(1), 41–47. https://doi.org/10.1016/S0168-9525(01)02594-X

Clark, M. R., Mandal, M., Ochiai, K., & Singh, H. (2014). Orchestrating B cell lymphopoiesis through interplay of IL-7 receptor and pre-B cell receptor signalling. *Nat Rev Immunol*, *14*(2), 69–80. https://doi.org/10.1038/nri3570

Cobaleda, C., Gutiérrez-Cianca, N., Pérez-Losada, J., Flores, T., García-Sanz, R., González, M., & Sánchez-García, I. (2000). A primitive hematopoietic cell is the target for the leukemic transformation in human philadelphia-positive acute lymphoblastic leukemia. *Blood*, *95*(3), 1007–1013.

Cobaleda, C., Schebesta, A., Delogu, A., & Busslinger, M. (2007). Pax5: the guardian of B cell identity and function. *Nat Immunol*, *8*(5), 463–470. https://doi.org/10.1038/ni1454

Cong, L., Ran, F. A., Cox, D., Lin, S., Barretto, R., Habib, N., Hsu, P. D., Wu, X., Jiang, W., Marraffini, L. A., & Zhang, F. (2013). Multiplex Genome Engineering Using CRISPR/Cas Systems. *Science*, *339*(6121), 819–823. https://doi.org/10.1126/science.1231143

Corcoran, A. E., Riddell, A., Krooshoop, D., & Venkitaraman, A. R. (1998). Impaired immunoglobulin gene rearrangement in mice lacking the IL-7 receptor. *Nature*, *391*(6670), 904–907. https://doi.org/10.1038/36122

Cordeiro Gomes, A., Hara, T., Lim, V. Y., Herndler-Brandstetter, D., Nevius, E., Sugiyama, T., Tani-ichi, S., Schlenner, S., Richie, E., Rodewald, H.-R., Flavell, R. A., Nagasawa, T., Ikuta, K., & Pereira, J. P. (2016). Hematopoietic Stem Cell Niches Produce Lineage-Instructive Signals to Control Multipotent Progenitor Differentiation. *Immunity*, *45*(6), 1219–1231. https://doi.org/10.1016/j.immuni.2016.11.004

Cox, C. V., Evely, R. S., Oakhill, A., Pamphilon, D. H., Goulden, N. J., & Blair, A. (2004). Characterization of acute lymphoblastic leukemia progenitor cells. *Blood*, *104*(9), 2919–2925. https://doi.org/10.1182/blood-2004-03-0901

Coyaud, E., Struski, S., Prade, N., Familiades, J., Eichner, R., Quelen, C., Bousquet, M., Mugneret, F., Talmant, P., Pages, M. P., Lefebvre, C., Penther, D., Lippert, E., Nadal, N., Taviaux, S., Poppe, B., Luquet, I., Baranger, L., Eclache, V., … Broccardo, C. (2010). Wide diversity of PAX5 alterations in B-ALL: a Groupe Francophone de Cytogenetique Hematologique study. *Blood*, *115*(15), 3089–3097. https://doi.org/10.1182/blood-2009-07-234229

Cozzio, A., Passegué, E., Ayton, P. M., Karsunky, H., Cleary, M. L., & Weissman, I. L. (2003). Similar MLL-associated leukemias arising from self-renewing stem cells and short-lived

myeloid progenitors. *Genes & Development*, *17*(24), 3029–3035. https://doi.org/10.1101/gad.1143403

Cresson, C., Péron, S., Jamrog, L., Rouquié, N., Prade, N., Dubois, M., Hébrard, S., Lagarde, S., Gerby, B., Mancini, S. J. C., Cogné, M., Delabesse, E., Delpy, L., & Broccardo, C. (2018). *PAX5A* and *PAX5B* isoforms are both efficient to drive B cell differentiation. *Oncotarget*, *9*(67), 32841–32854. https://doi.org/10.18632/oncotarget.26003

Cvekl, A., Kashanchi, F., Brady, J. N., & Piatigorsky, J. (1999). Pax-6 interactions with TATA-box-binding protein and retinoblastoma protein. *Investigative Ophthalmology & Visual Science*, *40*(7), 1343–1350.

Czerny, T., & Busslinger, M. (1995). DNA-Binding and Transactivation Properties of Pax-6: Three Amino Acids in the Paired Domain Are Responsible for the Different Sequence Recognition of Pax-6 and BSAP (Pax-5). *Molecular and Cellular Biology*, *15*(5), 2858–2871. https://doi.org/10.1128/MCB.15.5.2858

Czerny, T., Schaffner, G., & Busslinger, M. (1993). DNA sequence recognition by Pax proteins: bipartite structure of the paired domain and its binding site. *Genes & Development*, *7*(10), 2048–2061. https://doi.org/10.1101/gad.7.10.2048

Dang, J., Wei, L., de Ridder, J., Su, X., Rust, A. G., Roberts, K. G., Payne-Turner, D., Cheng, J., Ma, J., Qu, C., Wu, G., Song, G., Huether, R. G., Schulman, B., Janke, L., Zhang, J., Downing, J. R., van der Weyden, L., Adams, D. J., & Mullighan, C. G. (2015). PAX5 is a tumor suppressor in mouse mutagenesis models of acute lymphoblastic leukemia.

Danial, N. N., & Korsmeyer, S. J. (2004). Cell Death. *Cell*, *116*(2), 205–219. https://doi.org/10.1016/S0092-8674(04)00046-7

Davis, A. J., & Chen, D. J. (2013). DNA double strand break repair via non-homologous end-joining. *Translational Cancer Research*, *2*(3), 130–143. https://doi.org/10.3978/j.issn.2218-676X.2013.04.02

Decker, T., Pasca di Magliano, M., McManus, S., Sun, Q., Bonifer, C., Tagoh, H., & Busslinger, M. (2009). Stepwise Activation of Enhancer and Promoter Regions of the B Cell Commitment Gene Pax5 in Early Lymphopoiesis. *Immunity*, *30*(4), 508–520. https://doi.org/10.1016/j.immuni.2009.01.012

DeKoter, R. P., & Singh, H. (2000). Regulation of B Lymphocyte and Macrophage Development by Graded Expression of PU.1. *Science*, *288*(5470), 1439–1441. https://doi.org/10.1126/science.288.5470.1439

Delahaye, M. C., Salem, K.-I., Pelletier, J., Aurrand-Lions, M., & Mancini, S. J. C. (2021). Toward Therapeutic Targeting of Bone Marrow Leukemic Niche Protective Signals in B-Cell Acute Lymphoblastic Leukemia. *Frontiers in Oncology*, *10*. https://doi.org/10.3389/fonc.2020.606540

Delogu, A., Schebesta, A., Sun, Q., Aschenbrenner, K., Perlot, T., & Busslinger, M. (2006). Gene Repression by Pax5 in B Cells Is Essential for Blood Cell Homeostasis and Is Reversed in Plasma Cells. *Immunity*, *24*(3), 269–281. https://doi.org/10.1016/j.immuni.2006.01.012

Deltcheva, E., Chylinski, K., Sharma, C. M., Gonzales, K., Chao, Y., Pirzada, Z. A., Eckert, M. R., Vogel, J., & Charpentier, E. (2011). CRISPR RNA maturation by trans-encoded small RNA and host factor RNase III. *Nature*, *471*(7340), 602–607. https://doi.org/10.1038/nature09886

Dick, J. E. (2003). Self-renewal writ in blood. *Nature*, *423*(6937), 231–232. https://doi.org/10.1038/423231a

Ding, L., & Morrison, S. J. (2013). Haematopoietic stem cells and early lymphoid progenitors occupy distinct bone marrow niches. *Nature*, *495*(7440), 231–235. https://doi.org/10.1038/nature11885

Ding, L., Saunders, T. L., Enikolopov, G., & Morrison, S. J. (2012). Endothelial and perivascular cells maintain haematopoietic stem cells. *Nature*, *481*(7382), 457–462. https://doi.org/10.1038/nature10783

Dörfler, P., & Busslinger, M. (1996). C-terminal activating and inhibitory domains determine the transactivation potential of BSAP (Pax-5), Pax-2 and Pax-8. *The EMBO Journal*, *15*(8), 1971–1982.

Downes, C. E. J., McClure, B. J., Bruning, J. B., Page, E., Breen, J., Rehn, J., Yeung, D. T., & White, D. L. (2021). Acquired JAK2 mutations confer resistance to JAK inhibitors in cell models of acute lymphoblastic leukemia. *NPJ Precision Oncology*, *5*(1), 75. https://doi.org/10.1038/s41698-021-00215-x

Driessen, E. M. C., van Roon, E. H. J., Spijkers-Hagelstein, J. A. P., Schneider, P., de Lorenzo, P., Valsecchi, M. G., Pieters, R., & Stam, R. W. (2013). Frequencies and prognostic impact of RAS mutations in MLL-rearranged acute lymphoblastic leukemia in infants. *Haematologica*, *98*(6), 937–944. https://doi.org/10.3324/haematol.2012.067983

Duployez, N., Jamrog, L. A., Fregona, V., Hamelle, C., Fenwarth, L., Lejeune, S., Helevaut, N., Geffroy, S., Caillault, A., Marceau-Renaut, A., Poulain, S., Roche-Lestienne, C., Largeaud, L., Prade, N., Dufrechou, S., Hebrard, S., Berthon, C., Nelken, B., Fernandes, J., … Broccardo, C. (2021). Germline PAX5 mutation predisposes to familial B-cell precursor acute lymphoblastic leukemia. *Blood*, *137*(10), 1424–1428. https://doi.org/10.1182/blood.2020005756

Duque-Afonso, J., Feng, J., Scherer, F., Lin, C. H., Wong, S. H., Wang, Z., Iwasaki, M., & Cleary, M. L. (2015). Comparative genomics reveals multistep pathogenesis of E2A-PBX1 acute lymphoblastic leukemia. *J Clin Invest*, *125*(9), 3667–3680. https://doi.org/10.1172/JCI81158

Eberhard, D., & Busslinger, M. (1999). The partial homeodomain of the transcription factor Pax-5 (BSAP) is an interaction motif for the retinoblastoma and TATA-binding proteins. *Cancer Research*, *59*(7 Suppl), 1716s–1724s; discussion 1724s-1725s.

Eberhard, D., Jiménez, G., Heavey, B., & Busslinger, M. (2000). Transcriptional repression by Pax5 (BSAP) through interaction with corepressors of the Groucho family. *The EMBO Journal*, *19*(10), 2292–2303. https://doi.org/10.1093/emboj/19.10.2292

Ebinger, S., Özdemir, E. Z., Ziegenhain, C., Tiedt, S., Castro Alves, C., Grunert, M., Dworzak, M., Lutz, C., Turati, V. A., Enver, T., Horny, H.-P., Sotlar, K., Parekh, S., Spiekermann, K., Hiddemann, W., Schepers, A., Polzer, B., Kirsch, S., Hoffmann, M., … Jeremias, I. (2016). Characterization of Rare, Dormant, and Therapy-Resistant Cells in Acute Lymphoblastic Leukemia. *Cancer Cell*, *30*(6), 849–862. https://doi.org/10.1016/j.ccell.2016.11.002

Elantak, L., Espeli, M., Boned, A., Bornet, O., Bonzi, J., Gauthier, L., Feracci, M., Roche, P., Guerlesquin, F., & Schiff, C. (2012). Structural Basis for Galectin-1-dependent Pre-B Cell Receptor (Pre-BCR) Activation. *Journal of Biological Chemistry*, *287*(53), 44703–44713. https://doi.org/10.1074/jbc.M112.395152

Emelyanov, A. V., Kovac, C. R., Sepulveda, M. A., & Birshtein, B. K. (2002). The Interaction of Pax5 (BSAP) with Daxx Can Result in Transcriptional Activation in B Cells. *Journal of Biological Chemistry*, *277*(13), 11156–11164. https://doi.org/10.1074/jbc.M111763200

Eppert, K., Takenaka, K., Lechman, E. R., Waldron, L., Nilsson, B., van Galen, P., Metzeler, K. H., Poeppl, A., Ling, V., Beyene, J., Canty, A. J., Danska, J. S., Bohlander, S. K., Buske, C.,

Minden, M. D., Golub, T. R., Jurisica, I., Ebert, B. L., & Dick, J. E. (2011). Stem cell gene expression programs influence clinical outcome in human leukemia. *Nature Medicine*, *17*(9), 1086–1093. https://doi.org/10.1038/nm.2415

Espeli, M., Mancini, S. J. C., Breton, C., Poirier, F., & Schiff, C. (2009). Impaired B-cell development at the pre-BII-cell stage in galectin-1–deficient mice due to inefficient pre-BII/stromal cell interactions. *Blood*, *113*(23), 5878–5886. https://doi.org/10.1182/blood-2009-01-198465

Familiades, J., Bousquet, M., Lafage-Pochitaloff, M., Bene, M. C., Beldjord, K., De Vos, J., Dastugue, N., Coyaud, E., Struski, S., Quelen, C., Prade-Houdellier, N., Dobbelstein, S., Cayuela, J. M., Soulier, J., Grardel, N., Preudhomme, C., Cave, H., Blanchet, O., Lheritier, V., … Delabesse, E. (2009). PAX5 mutations occur frequently in adult B-cell progenitor acute lymphoblastic leukemia and PAX5 haploinsufficiency is associated with BCR-ABL1 and TCF3-PBX1 fusion genes: a GRAALL study. *Leukemia*, *23*(11), 1989–1998. https://doi.org/10.1038/leu.2009.135

Fisher, A. L., & Caudy, M. (1998). Groucho proteins: transcriptional corepressors for specific subsets of DNA-binding transcription factors in vertebrates and invertebrates. *Genes & Development*, *12*(13), 1931–1940. https://doi.org/10.1101/gad.12.13.1931

Fitzsimmons, D., Hodsdon, W., Wheat, W., Maira, S. M., Wasylyk, B., & Hagman, J. (1996). Pax-5 (BSAP) recruits Ets proto-oncogene family proteins to form functional ternary complexes on a B-cell-specific promoter. *Genes & Development*, *10*(17), 2198–2211. https://doi.org/10.1101/gad.10.17.2198

Flemming, A., Brummer, T., Reth, M., & Jumaa, H. (2003). The adaptor protein SLP-65 acts as a tumor suppressor that limits pre-B cell expansion. *Nature Immunology*, *4*(1), 38–43. https://doi.org/10.1038/ni862

Forestier, E., Heyman, M., Andersen, M. K., Autio, K., Blennow, E., Borgström, G., Golovleva, I., Heim, S., Heinonen, K., Hovland, R., Johannsson, J. H., Kerndrup, G., Nordgren, A., Rosenquist, R., Swolin, B., & Johansson, B. (2008). Outcome of ETV6/RUNX1-positive childhood acute lymphoblastic leukaemia in the NOPHO-ALL-1992 protocol: frequent late relapses but good overall survival. *British Journal of Haematology*, *140*(6), 665–672. https://doi.org/10.1111/j.1365-2141.2008.06980.x

Fregona, V., Bayet, M., & Gerby, B. (2021). Oncogene-Induced Reprogramming in Acute Lymphoblastic Leukemia: Towards Targeted Therapy of Leukemia-Initiating Cells. *Cancers (Basel)*, *13*(21). https://doi.org/10.3390/cancers13215511

Fuxa, M., Skok, J., Souabni, A., Salvagiotto, G., Roldan, E., & Busslinger, M. (2004). Pax5 induces *V* -to- *DJ* rearrangements and locus contraction of the *immunoglobulin heavy-chain* gene. *Genes & Development*, *18*(4), 411–422. https://doi.org/10.1101/gad.291504

Garneau, J. E., Dupuis, M.-È., Villion, M., Romero, D. A., Barrangou, R., Boyaval, P., Fremaux, C., Horvath, P., Magadán, A. H., & Moineau, S. (2010). The CRISPR/Cas bacterial immune system cleaves bacteriophage and plasmid DNA. *Nature*, *468*(7320), 67–71. https://doi.org/10.1038/nature09523

Gauthier, L., Rossi, B., Roux, F., Termine, E., & Schiff, C. (2002). Galectin-1 is a stromal cell ligand of the pre-B cell receptor (BCR) implicated in synapse formation between pre-B and stromal cells and in pre-BCR triggering. *Proceedings of the National Academy of Sciences*, *99*(20), 13014–13019. https://doi.org/10.1073/pnas.202323999

Georgopoulos, K., Bigby, M., Wang, J.-H., Molnar, A., Wu, P., Winandy, S., & Sharpe, A. (1994). The ikaros gene is required for the development of all lymphoid lineages. *Cell*, *79*(1), 143–156. https://doi.org/10.1016/0092-8674(94)90407-3

Gerby, B., Tremblay, C. S., Tremblay, M., Rojas-Sutterlin, S., Herblot, S., Hébert, J., Sauvageau, G., Lemieux, S., Lécuyer, E., Veiga, D. F. T., & Hoang, T. (2014). SCL, LMO1 and Notch1 Reprogram Thymocytes into Self-Renewing Cells. *PLoS Genetics*, *10*(12), e1004768. https://doi.org/10.1371/journal.pgen.1004768

Gerby, B., Veiga, D. F., Krosl, J., Nourreddine, S., Ouellette, J., Haman, A., Lavoie, G., Fares, I., Tremblay, M., Litalien, V., Ottoni, E., Kosic, M., Geoffrion, D., Ryan, J., Maddox, P. S., Chagraoui, J., Marinier, A., Hebert, J., Sauvageau, G., … Hoang, T. (2016). High-throughput screening in niche-based assay identifies compounds to target preleukemic stem cells. *J Clin Invest*. https://doi.org/10.1172/JCI86489

Glodek, A. M., Honczarenko, M., Le, Y., Campbell, J. J., & Silberstein, L. E. (2003). Sustained Activation of Cell Adhesion Is a Differentially Regulated Process in B Lymphopoiesis. *The Journal of Experimental Medicine*, *197*(4), 461–473. https://doi.org/10.1084/jem.20021477

Goardon, N., Marchi, E., Atzberger, A., Quek, L., Schuh, A., Soneji, S., Woll, P., Mead, A., Alford, K. A., Rout, R., Chaudhury, S., Gilkes, A., Knapper, S., Beldjord, K., Begum, S., Rose, S., Geddes, N., Griffiths, M., Standen, G., … Vyas, P. (2011). Coexistence of LMPP-like and GMP-like Leukemia Stem Cells in Acute Myeloid Leukemia. *Cancer Cell*, *19*(1), 138–152. https://doi.org/10.1016/j.ccr.2010.12.012

Goetz, C. A., Harmon, I. R., O'Neil, J. J., Burchill, M. A., & Farrar, M. A. (2004). STAT5 Activation Underlies IL7 Receptor-Dependent B Cell Development. *The Journal of Immunology*, *172*(8), 4770–4778. https://doi.org/10.4049/jimmunol.172.8.4770

Goode, D. K., & Elgar, G. (2009). The *PAX258* gene subfamily: A comparative perspective. *Developmental Dynamics*, *238*(12), 2951–2974. https://doi.org/10.1002/dvdy.22146

Goossens, S., & Van Vlierberghe, P. (2014). Controlling Pre-leukemic Thymocyte Self-Renewal. *PLoS Genetics*, *10*(12), e1004881. https://doi.org/10.1371/journal.pgen.1004881

Grawunder, U., Leu, T. M. J., Schatz, D. G., Werner, A., Rolink, A. G., Melchers, F., & Winkler, T. H. (1995). Down-regulation of RAG1 and RAG2 gene expression in PreB cells after functional immunoglobulin heavy chain rearrangement. *Immunity*, *3*(5), 601–608. https://doi.org/10.1016/1074-7613(95)90131-0

Greaves, M. (2016). Leukaemia "firsts" in cancer research and treatment. *Nature Reviews Cancer*, *16*(3), 163–172. https://doi.org/10.1038/nrc.2016.3

Greaves, M. (2018). A causal mechanism for childhood acute lymphoblastic leukaemia. *Nature Reviews Cancer*, *18*(8), 471–484. https://doi.org/10.1038/s41568-018-0015-6

Gruenbacher, S., Jaritz, M., Hill, L., Schäfer, M., & Busslinger, M. (2023). Essential role of the Pax5 C-terminal domain in controlling B cell commitment and development. *Journal of Experimental Medicine*, *220*(12). https://doi.org/10.1084/jem.20230260

Gu, Z., Churchman, M. L., Roberts, K. G., Moore, I., Zhou, X., Nakitandwe, J., Hagiwara, K., Pelletier, S., Gingras, S., Berns, H., Payne-Turner, D., Hill, A., Iacobucci, I., Shi, L., Pounds, S., Cheng, C., Pei, D., Qu, C., Newman, S., … Mullighan, C. G. (2019). PAX5-driven subtypes of B-progenitor acute lymphoblastic leukemia. *Nature Genetics*, *51*(2), 296–307. https://doi.org/10.1038/s41588-018-0315-5

Guibal, F. C., Alberich-Jorda, M., Hirai, H., Ebralidze, A., Levantini, E., Di Ruscio, A., Zhang, P., Santana-Lemos, B. A., Neuberg, D., Wagers, A. J., Rego, E. M., & Tenen, D. G. (2009). Identification of a myeloid committed progenitor as the cancer-initiating cell in acute promyelocytic leukemia. *Blood*, *114*(27), 5415–5425. https://doi.org/10.1182/blood-2008-10-182071

Guitart, A. V, Subramani, C., Armesilla-Diaz, A., Smith, G., Sepulveda, C., Gezer, D., Vukovic, M., Dunn, K., Pollard, P., Holyoake, T. L., Enver, T., Ratcliffe, P. J., & Kranc, K. R. (2013). Hif-2alpha is not essential for cell-autonomous hematopoietic stem cell maintenance. *Blood*, *122*(10), 1741–1745. https://doi.org/10.1182/blood-2013-02-484923

Hallal, R., Nehme, R., Brachet-Botineau, M., Nehme, A., Dakik, H., Deynoux, M., Dello Sbarba, P., Levern, Y., Zibara, K., Gouilleux, F., & Mazurier, F. (2020). Acriflavine targets oncogenic STAT5 signaling in myeloid leukemia cells. *Journal of Cellular and Molecular Medicine*, *24*(17), 10052–10062. https://doi.org/10.1111/jcmm.15612

Hamasaki, A., Yamada, Y., Kurose, T., Ban, N., Nagashima, K., Takahashi, A., Fujimoto, S., Shimono, D., Fujiwara, M., Toyokuni, S., Seino, Y., & Inagaki, N. (2007). Adult pancreatic islets require differential pax6 gene dosage. *Biochemical and Biophysical Research Communications*, *353*(1), 40–46. https://doi.org/10.1016/j.bbrc.2006.11.105

Hardy, R. R., Carmack, C. E., Shinton, S. A., Kemp, J. D., & Hayakawa, K. (2012). Resolution and characterization of pro-B and pre-pro-B cell stages in normal mouse bone marrow. 1991. *Journal of Immunology (Baltimore, Md. : 1950)*, *189*(7), 3271–3283.

Hardy, R. R., & Hayakawa, K. (2001). B Cell Development Pathways. *Annual Review of Immunology*, *19*(1), 595–621. https://doi.org/10.1146/annurev.immunol.19.1.595

Hardy, R. R., Kincade, P. W., & Dorshkind, K. (2007). The Protean Nature of Cells in the B Lymphocyte Lineage. *Immunity*, *26*(6), 703–714. https://doi.org/10.1016/j.immuni.2007.05.013

Hardy, R. R., Li, Y. S., Allman, D., Asano, M., Gui, M., & Hayakawa, K. (2000). B-cell commitment, development and selection. *Immunol Rev*, *175*, 23–32. https://www.ncbi.nlm.nih.gov/pubmed/10933588

Hauser, J., Grundström, C., Kumar, R., & Grundström, T. (2016). Regulated localization of an AID complex with E2A, PAX5 and IRF4 at the Igh locus. *Molecular Immunology*, *80*, 78–90. https://doi.org/10.1016/j.molimm.2016.10.014

He, T., Hong, S. Y., Huang, L., Xue, W., Yu, Z., Kwon, H., Kirk, M., Ding, S., Su, K., & Zhang, Z. (2011). Histone Acetyltransferase p300 Acetylates Pax5 and Strongly Enhances Pax5-mediated Transcriptional Activity. *Journal of Biological Chemistry*, *286*(16), 14137–14145. https://doi.org/10.1074/jbc.M110.176289

Heckl, D., Kowalczyk, M. S., Yudovich, D., Belizaire, R., Puram, R. V, McConkey, M. E., Thielke, A., Aster, J. C., Regev, A., & Ebert, B. L. (2014). Generation of mouse models of myeloid malignancy with combinatorial genetic lesions using CRISPR-Cas9 genome editing. *Nat Biotechnol*, *32*(9), 941–946. https://doi.org/10.1038/nbt.2951

Heidenreich, E. (2003). Non-homologous end joining as an important mutagenic process in cell cycle-arrested cells. *The EMBO Journal*, *22*(9), 2274–2283. https://doi.org/10.1093/emboj/cdg203

Heltemes-Harris, L. M., Willette, M. J. L., Ramsey, L. B., Qiu, Y. H., Neeley, E. S., Zhang, N., Thomas, D. A., Koeuth, T., Baechler, E. C., Kornblau, S. M., & Farrar, M. A. (2011). *Ebf1* or *Pax5* haploinsufficiency synergizes with STAT5 activation to initiate acute lymphoblastic leukemia. *Journal of Experimental Medicine*, *208*(6), 1135–1149. https://doi.org/10.1084/jem.20101947

Herblot, S., Steff, A.-M., Hugo, P., Aplan, P. D., & Hoang, T. (2000). SCL and LMO1 alter thymocyte differentiation: inhibition of E2A-HEB function and pre-Tα chain expression. *Nature Immunology*, *1*(2), 138–144. https://doi.org/10.1038/77819

Hiebert, S. W., Sun, W., Nathan Davis, J., Golub, T., Shurtleff, S., Buijs, A., Downing, J. R., Grosveld, G., Roussel, M. F., Gary Gilliland, D., Lenny, N., & Meyers, S. (1996). The

t(12;21) Translocation Converts AML-1B from an Activator to a Repressor of Transcription. *Molecular and Cellular Biology*, *16*(4), 1349–1355. https://doi.org/10.1128/MCB.16.4.1349

Hoflinger, S., Kesavan, K., Fuxa, M., Hutter, C., Heavey, B., Radtke, F., & Busslinger, M. (2004). Analysis of Notch1 function by in vitro T cell differentiation of Pax5 mutant lymphoid progenitors. *J Immunol*, *173*(6), 3935–3944. https://doi.org/10.4049/jimmunol.173.6.3935

Holmes, M. L., Carotta, S., Corcoran, L. M., & Nutt, S. L. (2006). Repression of *Flt3* by Pax5 is crucial for B-cell lineage commitment. *Genes & Development*, *20*(8), 933–938. https://doi.org/10.1101/gad.1396206

Hong, D., Gupta, R., Ancliff, P., Atzberger, A., Brown, J., Soneji, S., Green, J., Colman, S., Piacibello, W., Buckle, V., Tsuzuki, S., Greaves, M., & Enver, T. (2008). Initiating and Cancer-Propagating Cells in *TEL-AML1* -Associated Childhood Leukemia. *Science*, *319*(5861), 336–339. https://doi.org/10.1126/science.1150648

Hope, K. J., Jin, L., & Dick, J. E. (2004). Acute myeloid leukemia originates from a hierarchy of leukemic stem cell classes that differ in self-renewal capacity. *Nature Immunology*, *5*(7), 738–743. https://doi.org/10.1038/ni1080

Horcher, M., Souabni, A., & Busslinger, M. (2001). Pax5/BSAP Maintains the Identity of B Cells in Late B Lymphopoiesis. *Immunity*, *14*(6), 779–790. https://doi.org/10.1016/S1074-7613(01)00153-4

Hotfilder, M., Röttgers, S., Rosemann, A., Jürgens, H., Harbott, J., & Vormoor, J. (2002). Immature CD34+CD19− progenitor/stem cells in TEL/AML1-positive acute lymphoblastic leukemia are genetically and functionally normal. *Blood*, *100*(2), 640–646. https://doi.org/10.1182/blood.V100.2.640

Hsu, P. D., Lander, E. S., & Zhang, F. (2014). Development and Applications of CRISPR-Cas9 for Genome Engineering. *Cell*, *157*(6), 1262–1278. https://doi.org/10.1016/j.cell.2014.05.010

Hsu, P. D., Scott, D. A., Weinstein, J. A., Ran, F. A., Konermann, S., Agarwala, V., Li, Y., Fine, E. J., Wu, X., Shalem, O., Cradick, T. J., Marraffini, L. A., Bao, G., & Zhang, F. (2013). DNA targeting specificity of RNA-guided Cas9 nucleases. *Nature Biotechnology*, *31*(9), 827–832. https://doi.org/10.1038/nbt.2647

Huang, X., Trinh, T., Aljoufi, A., & Broxmeyer, H. E. (2018). Hypoxia Signaling Pathway in Stem Cell Regulation: Good and Evil. *Current Stem Cell Reports*, *4*(2), 149–157. https://doi.org/10.1007/s40778-018-0127-7

Ikawa, T., Kawamoto, H., Wright, L. Y. T., & Murre, C. (2004). Long-Term Cultured E2A-Deficient Hematopoietic Progenitor Cells Are Pluripotent. *Immunity*, *20*(3), 349–360. https://doi.org/10.1016/S1074-7613(04)00049-4

Inaba, H., & Mullighan, C. G. (2020). Pediatric acute lymphoblastic leukemia. *Haematologica*, *105*(11), 2524–2539. https://doi.org/10.3324/haematol.2020.247031

Inlay, M. A., Bhattacharya, D., Sahoo, D., Serwold, T., Seita, J., Karsunky, H., Plevritis, S. K., Dill, D. L., & Weissman, I. L. (2009). Ly6d marks the earliest stage of B-cell specification and identifies the branchpoint between B-cell and T-cell development. *Genes & Development*, *23*(20), 2376–2381. https://doi.org/10.1101/gad.1836009

Ishikawa, F., Yoshida, S., Saito, Y., Hijikata, A., Kitamura, H., Tanaka, S., Nakamura, R., Tanaka, T., Tomiyama, H., Saito, N., Fukata, M., Miyamoto, T., Lyons, B., Ohshima, K., Uchida, N., Taniguchi, S., Ohara, O., Akashi, K., Harada, M., & Shultz, L. D. (2007). Chemotherapy-resistant human AML stem cells home to and engraft within the bone-marrow

endosteal region. *Nature Biotechnology*, *25*(11), 1315–1321. https://doi.org/10.1038/nbt1350

Ishino, Y., Krupovic, M., & Forterre, P. (2018). History of CRISPR-Cas from Encounter with a Mysterious Repeated Sequence to Genome Editing Technology. *Journal of Bacteriology*, *200*(7). https://doi.org/10.1128/JB.00580-17

Ishino, Y., Shinagawa, H., Makino, K., Amemura, M., & Nakata, A. (1987). Nucleotide sequence of the iap gene, responsible for alkaline phosphatase isozyme conversion in Escherichia coli, and identification of the gene product. *Journal of Bacteriology*, *169*(12), 5429–5433. https://doi.org/10.1128/jb.169.12.5429-5433.1987

Isidro-Hernández, M., Casado-García, A., Oak, N., Alemán-Arteaga, S., Ruiz-Corzo, B., Martínez-Cano, J., Mayado, A., Sánchez, E. G., Blanco, O., Gaspar, M. L., Orfao, A., Alonso-López, D., De Las Rivas, J., Riesco, S., Prieto-Matos, P., González-Murillo, Á., Criado, F. J. G., Cenador, M. B. G., Ramírez-Orellana, M., … Sánchez-García, I. (2023). Immune stress suppresses innate immune signaling in preleukemic precursor B-cells to provoke leukemia in predisposed mice. *Nature Communications*, *14*(1), 5159. https://doi.org/10.1038/s41467-023-40961-z

Isidro-Hernández, M., Mayado, A., Casado-García, A., Martínez-Cano, J., Palmi, C., Fazio, G., Orfao, A., Ribera, J., Ribera, J. M., Zamora, L., Raboso-Gallego, J., Blanco, O., Alonso-López, D., De Las Rivas, J., Jiménez, R., García Criado, F. J., García Cenador, M. B., Ramírez-Orellana, M., Cazzaniga, G., … Sánchez-García, I. (2020). Inhibition of inflammatory signaling in Pax5 mutant cells mitigates B-cell leukemogenesis. *Scientific Reports*, *10*(1), 19189. https://doi.org/10.1038/s41598-020-76206-y

Itkin, T., Gur-Cohen, S., Spencer, J. A., Schajnovitz, A., Ramasamy, S. K., Kusumbe, A. P., Ledergor, G., Jung, Y., Milo, I., Poulos, M. G., Kalinkovich, A., Ludin, A., Golan, K., Khatib, E., Kumari, A., Kollet, O., Shakhar, G., Butler, J. M., Rafii, S., … Lapidot, T. (2016). Distinct bone marrow blood vessels differentially regulate haematopoiesis. *Nature*, *532*(7599), 323–328. https://doi.org/10.1038/nature17624

Jamrog, L., Chemin, G., Fregona, V., Coster, L., Pasquet, M., Oudinet, C., Rouquié, N., Prade, N., Lagarde, S., Cresson, C., Hébrard, S., Nguyen Huu, N. S., Bousquet, M., Quelen, C., Brousset, P., Mancini, S. J. C., Delabesse, E., Khamlichi, A. A., Gerby, B., & Broccardo, C. (2018). PAX5-ELN oncoprotein promotes multistep B-cell acute lymphoblastic leukemia in mice. *Proceedings of the National Academy of Sciences*, *115*(41), 10357–10362. https://doi.org/10.1073/pnas.1721678115

Jansen, Ruud., Embden, Jan. D. A. van, Gaastra, Wim., & Schouls, Leo. M. (2002). Identification of genes that are associated with DNA repeats in prokaryotes. *Molecular Microbiology*, *43*(6), 1565–1575. https://doi.org/10.1046/j.1365-2958.2002.02839.x

Jiang, F., & Doudna, J. A. (2017). CRISPR–Cas9 Structures and Mechanisms. *Annual Review of Biophysics*, *46*(1), 505–529. https://doi.org/10.1146/annurev-biophys-062215-010822

Jiang, Q., Li, W. Q., Hofmeister, R. R., Young, H. A., Hodge, D. R., Keller, J. R., Khaled, A. R., & Durum, S. K. (2004). Distinct Regions of the Interleukin-7 Receptor Regulate Different Bcl2 Family Members. *Molecular and Cellular Biology*, *24*(14), 6501–6513. https://doi.org/10.1128/MCB.24.14.6501-6513.2004

Jinek, M., Chylinski, K., Fonfara, I., Hauer, M., Doudna, J. A., & Charpentier, E. (2012). A Programmable Dual-RNA–Guided DNA Endonuclease in Adaptive Bacterial Immunity. *Science*, *337*(6096), 816–821. https://doi.org/10.1126/science.1225829

Johnson, R. D., & Jasin, M. (2001). Double-strand-break-induced homologous recombination in mammalian cells. *Biochemical Society Transactions*, *29*(2), 196. https://doi.org/10.1042/0300-5127:0290196

Jurado, S., Fedl, A. S., Jaritz, M., Kostanova-Poliakova, D., Malin, S. G., Mullighan, C. G., Strehl, S., Fischer, M., & Busslinger, M. (2022). The PAX5-JAK2 translocation acts as dual-hit mutation that promotes aggressive B-cell leukemia via nuclear STAT5 activation. *EMBO J*, *41*(7), e108397. https://doi.org/10.15252/embj.2021108397

Kaeser, G., & Chun, J. (2020). Brain cell somatic gene recombination and its phylogenetic foundations. *Journal of Biological Chemistry*, *295*(36), 12786–12795. https://doi.org/10.1074/jbc.REV120.009192

Kamb, A., Gruis, N. A., Weaver-Feldhaus, J., Liu, Q., Harshman, K., Tavtigian, S. V., Stockert, E., Day, R. S., Johnson, B. E., & Skolnick, M. H. (1994). A Cell Cycle Regulator Potentially Involved in Genesis of Many Tumor Types. *Science*, *264*(5157), 436–440. https://doi.org/10.1126/science.8153634

Kamb, A., Shattuck-Eidens, D., Eeles, R., Liu, Q., Gruis, N. A., Ding, W., Hussey, C., Tran, T., Miki, Y., Weaver-Feldhaus, J., McClure, M., Aitken, J. F., Anderson, D. E., Bergman, W., Frants, R., Goldgar, D. E., Green, A., MacLennan, R., Martin, N. G., … Cannon-Albright, L. A. (1994). Analysis of the p16 gene (CDKN2) as a candidate for the chromosome 9p melanoma susceptibility locus. *Nature Genetics*, *8*(1), 22–26. https://doi.org/10.1038/ng0994-22

Kiel, M. J., Yilmaz, Ö. H., Iwashita, T., Yilmaz, O. H., Terhorst, C., & Morrison, S. J. (2005). SLAM Family Receptors Distinguish Hematopoietic Stem and Progenitor Cells and Reveal Endothelial Niches for Stem Cells. *Cell*, *121*(7), 1109–1121. https://doi.org/10.1016/j.cell.2005.05.026

Kirstetter, P., Thomas, M., Dierich, A., Kastner, P., & Chan, S. (2002). Ikaros is critical for B cell differentiation and function. *European Journal of Immunology*, *32*(3), 720. https://doi.org/10.1002/1521-4141(200203)32:3<720::AID-IMMU720>3.0.CO;2-P

Koch, U., Fiorini, E., Benedito, R., Besseyrias, V., Schuster-Gossler, K., Pierres, M., Manley, N. R., Duarte, A., Macdonald, H. R., & Radtke, F. (2008). Delta-like 4 is the essential, nonredundant ligand for Notch1 during thymic T cell lineage commitment. *J Exp Med*, *205*(11), 2515–2523. https://doi.org/10.1084/jem.20080829

Komor, A. C., Badran, A. H., & Liu, D. R. (2017). CRISPR-Based Technologies for the Manipulation of Eukaryotic Genomes. *Cell*, *169*(3), 559. https://doi.org/10.1016/j.cell.2017.04.005

Kong, Y., Yoshida, S., Saito, Y., Doi, T., Nagatoshi, Y., Fukata, M., Saito, N., Yang, S. M., Iwamoto, C., Okamura, J., Liu, K. Y., Huang, X. J., Lu, D. P., Shultz, L. D., Harada, M., & Ishikawa, F. (2008). CD34+CD38+CD19+ as well as CD34+CD38−CD19+ cells are leukemia-initiating cells with self-renewal capacity in human B-precursor ALL. *Leukemia*, *22*(6), 1207–1213. https://doi.org/10.1038/leu.2008.83

Koop, K. E., MacDonald, L. M., & Lobe, C. G. (1996). Transcripts of Grg4, a murine groucho-related gene, are detected in adjacent tissues to other murine neurogenic gene homologues during embryonic development. *Mechanisms of Development*, *59*(1), 73–87. https://doi.org/10.1016/0925-4773(96)00582-5

Kovac, C. R., Emelyanov, A., Singh, M., Ashouian, N., & Birshtein, B. K. (2000). BSAP (Pax5)-Importin α1 (Rch1) Interaction Identifies a Nuclear Localization Sequence. *Journal of Biological Chemistry*, *275*(22), 16752–16757. https://doi.org/10.1074/jbc.M001551200

Kozmik, Z., Wang, S., Dörfler, P., Adams, B., & Busslinger, M. (1992). The Promoter of the CD19 Gene Is a Target for the B-Cell-Specific Transcription Factor BSAP. *Molecular and Cellular Biology*, *12*(6), 2662–2672. https://doi.org/10.1128/mcb.12.6.2662-2672.1992

Kreso, A., & Dick, J. E. (2014). Evolution of the Cancer Stem Cell Model. *Cell Stem Cell*, *14*(3), 275–291. https://doi.org/10.1016/j.stem.2014.02.006

Krivtsov, A. V., Twomey, D., Feng, Z., Stubbs, M. C., Wang, Y., Faber, J., Levine, J. E., Wang, J., Hahn, W. C., Gilliland, D. G., Golub, T. R., & Armstrong, S. A. (2006). Transformation from committed progenitor to leukaemia stem cell initiated by MLL–AF9. *Nature*, *442*(7104), 818–822. https://doi.org/10.1038/nature04980

Kunisaki, Y., Bruns, I., Scheiermann, C., Ahmed, J., Pinho, S., Zhang, D., Mizoguchi, T., Wei, Q., Lucas, D., Ito, K., Mar, J. C., Bergman, A., & Frenette, P. S. (2013). Arteriolar niches maintain haematopoietic stem cell quiescence. *Nature*, *502*(7473), 637–643. https://doi.org/10.1038/nature12612

Kuster, L., Grausenburger, R., Fuka, G., Kaindl, U., Krapf, G., Inthal, A., Mann, G., Kauer, M., Rainer, J., Kofler, R., Hall, A., Metzler, M., Meyer, L. H., Meyer, C., Harbott, J., Marschalek, R., Strehl, S., Haas, O. A., & Panzer-Grümayer, R. (2011). ETV6/RUNX1-positive relapses evolve from an ancestral clone and frequently acquire deletions of genes implicated in glucocorticoid signaling. *Blood*, *117*(9), 2658–2667. https://doi.org/10.1182/blood-2010-03-275347

Lang, D., Powell, S. K., Plummer, R. S., Young, K. P., & Ruggeri, B. A. (2007). PAX genes: Roles in development, pathophysiology, and cancer. *Biochemical Pharmacology*, *73*(1), 1–14. https://doi.org/10.1016/j.bcp.2006.06.024

Lang, F., Wojcik, B., Bothur, S., Knecht, C., Falkenburg, J. H. F., Schroeder, T., Serve, H., Ottmann, O. G., & Rieger, M. A. (2017). Plastic CD34 and CD38 expression in adult B–cell precursor acute lymphoblastic leukemia explains ambiguity of leukemia-initiating stem cell populations. *Leukemia*, *31*(3), 731–734. https://doi.org/10.1038/leu.2016.315

Lang, F., Wojcik, B., & Rieger, M. A. (2015). Stem Cell Hierarchy and Clonal Evolution in Acute Lymphoblastic Leukemia. *Stem Cells International*, *2015*, 1–13. https://doi.org/10.1155/2015/137164

Lapidot, T., Sirard, C., Vormoor, J., Murdoch, B., Hoang, T., Caceres-Cortes, J., Minden, M., Paterson, B., Caligiuri, M. A., & Dick, J. E. (1994). A cell initiating human acute myeloid leukaemia after transplantation into SCID mice. *Nature*, *367*(6464), 645–648. https://doi.org/10.1038/367645a0

le Viseur, C., Hotfilder, M., Bomken, S., Wilson, K., Röttgers, S., Schrauder, A., Rosemann, A., Irving, J., Stam, R. W., Shultz, L. D., Harbott, J., Jürgens, H., Schrappe, M., Pieters, R., & Vormoor, J. (2008). In Childhood Acute Lymphoblastic Leukemia, Blasts at Different Stages of Immunophenotypic Maturation Have Stem Cell Properties. *Cancer Cell*, *14*(1), 47–58. https://doi.org/10.1016/j.ccr.2008.05.015

Lieber, M. R., Yu, K., & Raghavan, S. C. (2006). Roles of nonhomologous DNA end joining, V(D)J recombination, and class switch recombination in chromosomal translocations. *DNA Repair*, *5*(9–10), 1234–1245. https://doi.org/10.1016/j.dnarep.2006.05.013

Lin, H., & Grosschedl, R. (1995). Failure of B-cell differentiation in mice lacking the transcription factor EBF. *Nature*, *376*(6537), 263–267. https://doi.org/10.1038/376263a0

Lin, Y. C., Jhunjhunwala, S., Benner, C., Heinz, S., Welinder, E., Mansson, R., Sigvardsson, M., Hagman, J., Espinoza, C. A., Dutkowski, J., Ideker, T., Glass, C. K., & Murre, C. (2010). A

global network of transcription factors, involving E2A, EBF1 and Foxo1, that orchestrates B cell fate. *Nature Immunology*, *11*(7), 635–643. https://doi.org/10.1038/ni.1891

Liu, M.-L., Rahman, M., Hirabayashi, Y., & Sasaki, T. (2002). Sequence analysis of 5'-flanking region of human pax-5 gene exon 1B. *Zhongguo Shi Yan Xue Ye Xue Za Zhi*, *10*(2), 100–103.

Lowen, M., Scott, G., & Zwollo, P. (2001). Functional Analyses of Two Alternative Isoforms of the Transcription Factor Pax-5. *Journal of Biological Chemistry*, *276*(45), 42565–42574. https://doi.org/10.1074/jbc.M106536200

Ma, Q., Jones, D., Borghesani, P. R., Segal, R. A., Nagasawa, T., Kishimoto, T., Bronson, R. T., & Springer, T. A. (1998). Impaired B-lymphopoiesis, myelopoiesis, and derailed cerebellar neuron migration in CXCR4- and SDF-1-deficient mice. *Proceedings of the National Academy of Sciences*, *95*(16), 9448–9453. https://doi.org/10.1073/pnas.95.16.9448

Ma, Q., Jones, D., & Springer, T. A. (1999). The Chemokine Receptor CXCR4 Is Required for the Retention of B Lineage and Granulocytic Precursors within the Bone Marrow Microenvironment. *Immunity*, *10*(4), 463–471. https://doi.org/10.1016/S1074-7613(00)80046-1

Ma, X., Edmonson, M., Yergeau, D., Muzny, D. M., Hampton, O. A., Rusch, M., Song, G., Easton, J., Harvey, R. C., Wheeler, D. A., Ma, J., Doddapaneni, H., Vadodaria, B., Wu, G., Nagahawatte, P., Carroll, W. L., Chen, I.-M., Gastier-Foster, J. M., Relling, M. V., … Zhang, J. (2015). Rise and fall of subclones from diagnosis to relapse in pediatric B-acute lymphoblastic leukaemia. *Nature Communications*, *6*(1), 6604. https://doi.org/10.1038/ncomms7604

Mahuteau-Betzer, F. (2015). Chimiothèque Nationale. *Médecine/Sciences*, *31*(4), 417–422. https://doi.org/10.1051/medsci/20153104016

Maia, A. T., van der Velden, V. H. J., Harrison, C. J., Szczepanski, T., Williams, M. D., Griffiths, M. J., van Dongen, J. J. M., & Greaves, M. F. (2003). Prenatal origin of hyperdiploid acute lymphoblastic leukemia in identical twins. *Leukemia*, *17*(11), 2202–2206. https://doi.org/10.1038/sj.leu.2403101

Makarova, K. S., Grishin, N. V, Shabalina, S. A., Wolf, Y. I., & Koonin, E. V. (2006). A putative RNA-interference-based immune system in prokaryotes: computational analysis of the predicted enzymatic machinery, functional analogies with eukaryotic RNAi, and hypothetical mechanisms of action. *Biology Direct*, *1*(1), 7. https://doi.org/10.1186/1745-6150-1-7

Mali, P., Yang, L., Esvelt, K. M., Aach, J., Guell, M., DiCarlo, J. E., Norville, J. E., & Church, G. M. (2013). RNA-Guided Human Genome Engineering via Cas9. *Science*, *339*(6121), 823–826. https://doi.org/10.1126/science.1232033

Malin, S., McManus, S., Cobaleda, C., Novatchkova, M., Delogu, A., Bouillet, P., Strasser, A., & Busslinger, M. (2010). Role of STAT5 in controlling cell survival and immunoglobulin gene recombination during pro-B cell development. *Nature Immunology*, *11*(2), 171–179. https://doi.org/10.1038/ni.1827

Malu, S., Malshetty, V., Francis, D., & Cortes, P. (2012). Role of non-homologous end joining in V(D)J recombination. *Immunologic Research*, *54*(1–3), 233–246. https://doi.org/10.1007/s12026-012-8329-z

Månsson, R., Hultquist, A., Luc, S., Yang, L., Anderson, K., Kharazi, S., Al-Hashmi, S., Liuba, K., Thorén, L., Adolfsson, J., Buza-Vidas, N., Qian, H., Soneji, S., Enver, T., Sigvardsson, M., & Jacobsen, S. E. W. (2007). Molecular Evidence for Hierarchical Transcriptional Lineage

Priming in Fetal and Adult Stem Cells and Multipotent Progenitors. *Immunity*, *26*(4), 407–419. https://doi.org/10.1016/j.immuni.2007.02.013

Mansson, R., Zandi, S., Welinder, E., Tsapogas, P., Sakaguchi, N., Bryder, D., & Sigvardsson, M. (2010). Single-cell analysis of the common lymphoid progenitor compartment reveals functional and molecular heterogeneity. *Blood*, *115*(13), 2601–2609. https://doi.org/10.1182/blood-2009-08-236398

Marnett, L. J. (2000). Oxyradicals and DNA damage. *Carcinogenesis*, *21*(3), 361–370. https://doi.org/10.1093/carcin/21.3.361

Marshall, A. J., Fleming, H. E., Wu, G. E., & Paige, C. J. (1998). Modulation of the IL-7 dose-response threshold during pro-B cell differentiation is dependent on pre-B cell receptor expression. *Journal of Immunology (Baltimore, Md. : 1950)*, *161*(11), 6038–6045.

Martín-Lorenzo, A., Auer, F., Chan, L. N., García-Ramírez, I., González-Herrero, I., Rodríguez-Hernández, G., Bartenhagen, C., Dugas, M., Gombert, M., Ginzel, S., Blanco, O., Orfao, A., Alonso-López, D., Rivas, J. D. Las, García-Cenador, M. B., García-Criado, F. J., Müschen, M., Sánchez-García, I., Borkhardt, A., … Hauer, J. (2018). Loss of Pax5 Exploits Sca1-BCR-ABLp190 Susceptibility to Confer the Metabolic Shift Essential for pB-ALL. *Cancer Research*, *78*(10), 2669–2679. https://doi.org/10.1158/0008-5472.CAN-17-3262

Martin-Lorenzo, A., Hauer, J., Vicente-Duenas, C., Auer, F., Gonzalez-Herrero, I., Garcia-Ramirez, I., Ginzel, S., Thiele, R., Constantinescu, S. N., Bartenhagen, C., Dugas, M., Gombert, M., Schafer, D., Blanco, O., Mayado, A., Orfao, A., Alonso-Lopez, D., Rivas Jde, L., Cobaleda, C., … Borkhardt, A. (2015). Infection Exposure is a Causal Factor in B-cell Precursor Acute Lymphoblastic Leukemia as a Result of Pax5-Inherited Susceptibility. *Cancer Discov*, *5*(12), 1328–1343. https://doi.org/10.1158/2159-8290.CD-15-0892

Mayran, A., Pelletier, A., & Drouin, J. (2015). Pax factors in transcription and epigenetic remodelling. *Seminars in Cell & Developmental Biology*, *44*, 135–144. https://doi.org/10.1016/j.semcdb.2015.07.007

McCormack, M. P., Young, L. F., Vasudevan, S., de Graaf, C. A., Codrington, R., Rabbitts, T. H., Jane, S. M., & Curtis, D. J. (2010). The *Lmo2* Oncogene Initiates Leukemia in Mice by Inducing Thymocyte Self-Renewal. *Science*, *327*(5967), 879–883. https://doi.org/10.1126/science.1182378

McLean, K. C., & Mandal, M. (2020). It Takes Three Receptors to Raise a B Cell. *Trends in Immunology*, *41*(7), 629–642. https://doi.org/10.1016/j.it.2020.05.003

McVey, M., & Lee, S. E. (2008). MMEJ repair of double-strand breaks (director's cut): deleted sequences and alternative endings. *Trends in Genetics*, *24*(11), 529–538. https://doi.org/10.1016/j.tig.2008.08.007

Medina, K. L., Pongubala, J. M. R., Reddy, K. L., Lancki, D. W., DeKoter, R., Kieslinger, M., Grosschedl, R., & Singh, H. (2004). Assembling a Gene Regulatory Network for Specification of the B Cell Fate. *Developmental Cell*, *7*(4), 607–617. https://doi.org/10.1016/j.devcel.2004.08.006

Medvedovic, J., Ebert, A., Tagoh, H., & Busslinger, M. (2011). *Pax5* (pp. 179–206). https://doi.org/10.1016/B978-0-12-385991-4.00005-2

Meffre, E., Casellas, R., & Nussenzweig, M. C. (2000). Antibody regulation of B cell development. *Nat Immunol*, *1*(5), 379–385. https://doi.org/10.1038/80816

Melchers, F. (n.d.). B Cell Development and Its Deregulation to Transformed States at the Pre-B Cell Receptor-Expressing Pre-BII Cell Stage. In *Chronic Lymphocytic Leukemia* (pp. 1–17). Springer-Verlag. https://doi.org/10.1007/3-540-29933-5_1

Melchers, F. (2005). The pre-B-cell receptor: selector of fitting immunoglobulin heavy chains for the B-cell repertoire. *Nat Rev Immunol*, *5*(7), 578–584. https://doi.org/10.1038/nri1649

Melchers, F., Haasner, D., Grawunder, U., Kalberer, C., Karasuyama, H., Winkler, T., & Rolink, A. G. (1994). Roles of IGH and L Chains and of Surrogate H and L Chains in the Development of Cells of the B Lymphocyte Lineage. *Annual Review of Immunology*, *12*(1), 209–225. https://doi.org/10.1146/annurev.iy.12.040194.001233

Melchers, F., Strasser, A., Bauer, S. R., Kudo, A., Thalmann, P., & Rolink, A. (1991). *B Cell Development in Fetal Liver* (pp. 201–205). https://doi.org/10.1007/978-1-4684-5943-2_22

Melchers, F., ten Boekel, E., Seidl, T., Kong, X. C., Yamagami, T., Onishi, K., Shimizu, T., Rolink, A. G., & Andersson, J. (2000). Repertoire selection by pre-B-cell receptors and B-cell receptors, and genetic control of B-cell development from immature to mature B cells. *Immunological Reviews*, *175*, 33–46.

Méndez-Ferrer, S., Bonnet, D., Steensma, D. P., Hasserjian, R. P., Ghobrial, I. M., Gribben, J. G., Andreeff, M., & Krause, D. S. (2020). Bone marrow niches in haematological malignancies. *Nature Reviews Cancer*, *20*(5), 285–298. https://doi.org/10.1038/s41568-020-0245-2

Miller, C. L., Dykstra, B., & Eaves, C. J. (2008). Characterization of mouse hematopoietic stem and progenitor cells. *Current Protocols in Immunology*, *Chapter 22*, 22B.2.1-22B.2.31. https://doi.org/10.1002/0471142735.im22b02s80

Mohtashami, M., Shah, D. K., Nakase, H., Kianizad, K., Petrie, H. T., & Zuniga-Pflucker, J. C. (2010). Direct comparison of Dll1- and Dll4-mediated Notch activation levels shows differential lymphomyeloid lineage commitment outcomes. *J Immunol*, *185*(2), 867–876. https://doi.org/10.4049/jimmunol.1000782

Mojica, F. J. M., D□ez-Villase□or, C., Garc□a-Mart□nez, J., & Soria, E. (2005). Intervening Sequences of Regularly Spaced Prokaryotic Repeats Derive from Foreign Genetic Elements. *Journal of Molecular Evolution*, *60*(2), 174–182. https://doi.org/10.1007/s00239-004-0046-3

Monaco, G., Chen, H., Poidinger, M., Chen, J., de Magalhaes, J. P., & Larbi, A. (2016). flowAI: automatic and interactive anomaly discerning tools for flow cytometry data. *Bioinformatics*, *32*(16), 2473–2480. https://doi.org/10.1093/bioinformatics/btw191

Moore, J. K., & Haber, J. E. (1996). Cell Cycle and Genetic Requirements of Two Pathways of Nonhomologous End-Joining Repair of Double-Strand Breaks in *Saccharomyces cerevisiae*. *Molecular and Cellular Biology*, *16*(5), 2164–2173. https://doi.org/10.1128/MCB.16.5.2164

Moorman, A. V, Ensor, H. M., Richards, S. M., Chilton, L., Schwab, C., Kinsey, S. E., Vora, A., Mitchell, C. D., & Harrison, C. J. (2010). Prognostic effect of chromosomal abnormalities in childhood B-cell precursor acute lymphoblastic leukaemia: results from the UK Medical Research Council ALL97/99 randomised trial. *The Lancet Oncology*, *11*(5), 429–438. https://doi.org/10.1016/S1470-2045(10)70066-8

Mori, H., Colman, S. M., Xiao, Z., Ford, A. M., Healy, L. E., Donaldson, C., Hows, J. M., Navarrete, C., & Greaves, M. (2002). Chromosome translocations and covert leukemic clones are generated during normal fetal development. *Proceedings of the National Academy of Sciences*, *99*(12), 8242–8247. https://doi.org/10.1073/pnas.112218799

Morrison, S. J., & Weissman, I. L. (1994). The long-term repopulating subset of hematopoietic stem cells is deterministic and isolatable by phenotype. *Immunity*, *1*(8), 661–673. https://doi.org/10.1016/1074-7613(94)90037-X

Mourcin, F., Breton, C., Tellier, J., Narang, P., Chasson, L., Jorquera, A., Coles, M., Schiff, C., & Mancini, S. J. C. (2011). Galectin-1–expressing stromal cells constitute a specific niche for pre-BII cell development in mouse bone marrow. *Blood*, *117*(24), 6552–6561. https://doi.org/10.1182/blood-2010-12-323113

Mullighan, C. G. (2012). Molecular genetics of B-precursor acute lymphoblastic leukemia. *Journal of Clinical Investigation*, *122*(10), 3407–3415. https://doi.org/10.1172/JCI61203

Mullighan, C. G. (2019). PAX5-driven subtypes of B-progenitor acute lymphoblastic leukemia. *Nature Genetics*, *176*(3), 139–148. https://doi.org/10.1016/j.physbeh.2017.03.040

Mullighan, C. G., Goorha, S., Radtke, I., Miller, C. B., Coustan-Smith, E., Dalton, J. D., Girtman, K., Mathew, S., Ma, J., Pounds, S. B., Su, X., Pui, C. H., Relling, M. V, Evans, W. E., Shurtleff, S. A., & Downing, J. R. (2007). Genome-wide analysis of genetic alterations in acute lymphoblastic leukaemia. *Nature*, *446*(7137), 758–764. https://doi.org/10.1038/nature05690

Mullighan, C. G., Phillips, L. A., Su, X., Ma, J., Miller, C. B., Shurtleff, S. A., & Downing, J. R. (2008). Genomic Analysis of the Clonal Origins of Relapsed Acute Lymphoblastic Leukemia. *Science*, *322*(5906), 1377–1380. https://doi.org/10.1126/science.1164266

Mullighan, C. G., Zhang, J., Harvey, R. C., Collins-Underwood, J. R., Schulman, B. A., Phillips, L. A., Tasian, S. K., Loh, M. L., Su, X., Liu, W., Devidas, M., Atlas, S. R., Chen, I.-M., Clifford, R. J., Gerhard, D. S., Carroll, W. L., Reaman, G. H., Smith, M., Downing, J. R., … Willman, C. L. (2009). JAK mutations in high-risk childhood acute lymphoblastic leukemia. *Proceedings of the National Academy of Sciences of the United States of America*, *106*(23), 9414–9418. https://doi.org/10.1073/pnas.0811761106

Murakami, H., & Keeney, S. (2008). Regulating the formation of DNA double-strand breaks in meiosis. *Genes & Development*, *22*(3), 286–292. https://doi.org/10.1101/gad.1642308

Murre, C. (2018). 'Big bang' of B-cell development revealed. *Genes & Development*, *32*(2), 93–95. https://doi.org/10.1101/gad.311357.118

Nagasawa, T., Hirota, S., Tachibana, K., Takakura, N., Nishikawa, S., Kitamura, Y., Yoshida, N., Kikutani, H., & Kishimoto, T. (1996). Defects of B-cell lymphopoiesis and bone-marrow myelopoiesis in mice lacking the CXC chemokine PBSF/SDF-1. *Nature*, *382*(6592), 635–638. https://doi.org/10.1038/382635a0

Nagasawa, T., Kikutani, H., & Kishimoto, T. (1994). Molecular cloning and structure of a pre-B-cell growth-stimulating factor. *Proceedings of the National Academy of Sciences*, *91*(6), 2305–2309. https://doi.org/10.1073/pnas.91.6.2305

Namen, A. E., Lupton, S., Hjerrild, K., Wignall, J., Mochizuki, D. Y., Schmierer, A., Mosley, B., March, C. J., Urdal, D., Gillis, S., Cosman, D., & Goodwin, R. G. (1988). Stimulation of B-cell progenitors by cloned murine interleukin-7. *Nature*, *333*(6173), 571–573. https://doi.org/10.1038/333571a0

Nebral, K., Denk, D., Attarbaschi, A., König, M., Mann, G., Haas, O. A., & Strehl, S. (2009). Incidence and diversity of PAX5 fusion genes in childhood acute lymphoblastic leukemia. *Leukemia*, *23*(1), 134–143. https://doi.org/10.1038/leu.2008.306

Nera, K. P., Kohonen, P., Narvi, E., Peippo, A., Mustonen, L., Terho, P., Koskela, K., Buerstedde, J. M., & Lassila, O. (2006). Loss of Pax5 promotes plasma cell differentiation. *Immunity*, *24*(3), 283–293. https://doi.org/10.1016/j.immuni.2006.02.003

Nichogiannopoulou, A., Trevisan, M., Neben, S., Friedrich, C., & Georgopoulos, K. (1999). Defects in Hemopoietic Stem Cell Activity in Ikaros Mutant Mice. *Journal of Experimental Medicine*, *190*(9), 1201–1214. https://doi.org/10.1084/jem.190.9.1201

Nishana, M., & Raghavan, S. C. (2012). Role of recombination activating genes in the generation of antigen receptor diversity and beyond. *Immunology*, *137*(4), 271–281. https://doi.org/10.1111/imm.12009

Nobori, T., Miura, K., Wu, D. J., Lois, A., Takabayashi, K., & Carson, D. A. (1994). Deletions of the cyclin-dependent kinase-4 inhibitor gene in multiple human cancers. *Nature*, *368*(6473), 753–756. https://doi.org/10.1038/368753a0

Noll, M. (1993). Evolution and role of Pax genes. *Current Opinion in Genetics & Development*, *3*(4), 595–605. https://doi.org/10.1016/0959-437X(93)90095-7

Nombela-Arrieta, C., Pivarnik, G., Winkel, B., Canty, K. J., Harley, B., Mahoney, J. E., Park, S.-Y., Lu, J., Protopopov, A., & Silberstein, L. E. (2013). Quantitative imaging of haematopoietic stem and progenitor cell localization and hypoxic status in the bone marrow microenvironment. *Nature Cell Biology*, *15*(5), 533–543. https://doi.org/10.1038/ncb2730

Nutt, S. L., Heavey, B., Rolink, A. G., & Busslinger, M. (1999). Commitment to the B-lymphoid lineage depends on the transcription factor Pax5. *Nature*, *401*(6753), 556–562. https://doi.org/10.1038/44076

Nutt, S. L., Thévenin, C., & Busslinger, M. (1997). Essential Functions of Pax-5 (BSAP) in pro-B Cell Development. *Immunobiology*, *198*(1–3), 227–235. https://doi.org/10.1016/S0171-2985(97)80043-5

Nutt, S. L., Urbanek, P., Rolink, A., & Busslinger, M. (1997). Essential functions of Pax5 (BSAP) in pro-B cell development: difference between fetal and adult B lymphopoiesis and reduced V-to-DJ recombination at the IgH locus. *Genes Dev*, *11*(4), 476–491. https://www.ncbi.nlm.nih.gov/pubmed/9042861

Oefelein, M., Grapey, D., Schaeffer, T., Chin-Chance, C., & Bushman, W. (1996). PAX-2: A Developmental Gene Constitutively Expressed in the Mouse Epididymis and Ductus Deferens. *Journal of Urology*, *156*(3), 1204–1207. https://doi.org/10.1016/S0022-5347(01)65751-3

Ogawa, M., Boekel, E. ten, & Melchers, F. (2000). Identification of CD19–B220+c-Kit+Flt3/Flk-2+cells as early B lymphoid precursors before pre-B-I cells in juvenile mouse bone marrow. *International Immunology*, *12*(3), 313–324. https://doi.org/10.1093/intimm/12.3.313

Olin, A., Henckel, E., Chen, Y., Lakshmikanth, T., Pou, C., Mikes, J., Gustafsson, A., Bernhardsson, A. K., Zhang, C., Bohlin, K., & Brodin, P. (2018). Stereotypic Immune System Development in Newborn Children. *Cell*, *174*(5), 1277-1292.e14. https://doi.org/10.1016/j.cell.2018.06.045

Oppezzo, P., Dumas, G., Lalanne, A. I., Payelle-Brogard, B., Magnac, C., Pritsch, O., Dighiero, G., & Vuillier, F. (2005). Different isoforms of BSAP regulate expression of AID in normal and chronic lymphocytic leukemia B cells. *Blood*, *105*(6), 2495–2503. https://doi.org/10.1182/blood-2004-09-3644

Orlando, E. J., Han, X., Tribouley, C., Wood, P. A., Leary, R. J., Riester, M., Levine, J. E., Qayed, M., Grupp, S. A., Boyer, M., De Moerloose, B., Nemecek, E. R., Bittencourt, H., Hiramatsu, H., Buechner, J., Davies, S. M., Verneris, M. R., Nguyen, K., Brogdon, J. L., … Winckler, W. (2018). Genetic mechanisms of target antigen loss in CAR19 therapy of

acute lymphoblastic leukemia. *Nature Medicine*, *24*(10), 1504–1506. https://doi.org/10.1038/s41591-018-0146-z

Osawa, M., Hanada, K., Hamada, H., & Nakauchi, H. (1996). Long-Term Lymphohematopoietic Reconstitution by a Single CD34-Low/Negative Hematopoietic Stem Cell. *Science*, *273*(5272), 242–245. https://doi.org/10.1126/science.273.5272.242

Oshima, K., Khiabanian, H., da Silva-Almeida, A. C., Tzoneva, G., Abate, F., Ambesi-Impiombato, A., Sanchez-Martin, M., Carpenter, Z., Penson, A., Perez-Garcia, A., Eckert, C., Nicolas, C., Balbin, M., Sulis, M. L., Kato, M., Koh, K., Paganin, M., Basso, G., Gastier-Foster, J. M., … Ferrando, A. A. (2016). Mutational landscape, clonal evolution patterns, and role of RAS mutations in relapsed acute lymphoblastic leukemia. *Proceedings of the National Academy of Sciences*, *113*(40), 11306–11311. https://doi.org/10.1073/pnas.1608420113

Paixão-Côrtes, V. R., Salzano, F. M., & Bortolini, M. C. (2015). Origins and evolvability of the PAX family. *Seminars in Cell & Developmental Biology*, *44*, 64–74. https://doi.org/10.1016/j.semcdb.2015.08.014

Pasca di Magliano, M., Di Lauro, R., & Zannini, M. (2000). Pax8 has a key role in thyroid cell differentiation. *Proceedings of the National Academy of Sciences*, *97*(24), 13144–13149. https://doi.org/10.1073/pnas.240336397

Passet, M., Boissel, N., Sigaux, F., Saillard, C., Bargetzi, M., Ba, I., Thomas, X., Graux, C., Chalandon, Y., Leguay, T., Lengliné, E., Konopacki, J., Quentin, S., Delabesse, E., Lafage-Pochitaloff, M., Pastoret, C., Grardel, N., Asnafi, V., Lhéritier, V., … Clappier, E. (2019). PAX5 P80R mutation identifies a novel subtype of B-cell precursor acute lymphoblastic leukemia with favorable outcome. *Blood*, *133*(3), 280–284. https://doi.org/10.1182/blood-2018-10-882142

Peppas, I., Ford, A. M., Furness, C. L., & Greaves, M. F. (2023). Gut microbiome immaturity and childhood acute lymphoblastic leukaemia. *Nature Reviews Cancer*, *23*(8), 565–576. https://doi.org/10.1038/s41568-023-00584-4

Peters, H., Neubüser, A., Kratochwil, K., & Balling, R. (1998). *Pax9* -deficient mice lack pharyngeal pouch derivatives and teeth and exhibit craniofacial and limb abnormalities. *Genes & Development*, *12*(17), 2735–2747. https://doi.org/10.1101/gad.12.17.2735

Pfeffer, P. L., Bouchard, M., & Busslinger, M. (2000). Pax2 and homeodomain proteins cooperatively regulate a 435 bp enhancer of the mouse *Pax5* gene at the midbrain-hindbrain boundary. *Development*, *127*(5), 1017–1028. https://doi.org/10.1242/dev.127.5.1017

Pietras, E. M., Reynaud, D., Kang, Y.-A., Carlin, D., Calero-Nieto, F. J., Leavitt, A. D., Stuart, J. M., Göttgens, B., & Passegué, E. (2015). Functionally Distinct Subsets of Lineage-Biased Multipotent Progenitors Control Blood Production in Normal and Regenerative Conditions. *Cell Stem Cell*, *17*(1), 35–46. https://doi.org/10.1016/j.stem.2015.05.003

Pongubala, J. M. R., Northrup, D. L., Lancki, D. W., Medina, K. L., Treiber, T., Bertolino, E., Thomas, M., Grosschedl, R., Allman, D., & Singh, H. (2008). Transcription factor EBF restricts alternative lineage options and promotes B cell fate commitment independently of Pax5. *Nature Immunology*, *9*(2), 203–215. https://doi.org/10.1038/ni1555

Pourcel, C., Salvignol, G., & Vergnaud, G. (2005). CRISPR elements in Yersinia pestis acquire new repeats by preferential uptake of bacteriophage DNA, and provide additional tools for evolutionary studies. *Microbiology*, *151*(3), 653–663. https://doi.org/10.1099/mic.0.27437-0

Prasad, M. A. J., Ungerbäck, J., Åhsberg, J., Somasundaram, R., Strid, T., Larsson, M., Månsson, R., De Paepe, A., Lilljebjörn, H., Fioretos, T., Hagman, J., & Sigvardsson, M. (2015). Ebf1 heterozygosity results in increased DNA damage in pro-B cells and their synergistic transformation by Pax5 haploinsufficiency. *Blood*, *125*(26), 4052–4059. https://doi.org/10.1182/blood-2014-12-617282

Rabilloud, T., Potier, D., Pankaew, S., Nozais, M., Loosveld, M., & Payet-Bornet, D. (2021). Single-cell profiling identifies pre-existing CD19-negative subclones in a B-ALL patient with CD19-negative relapse after CAR-T therapy. *Nature Communications*, *12*(1), 865. https://doi.org/10.1038/s41467-021-21168-6

Ramadani, F., Bolland, D. J., Garcon, F., Emery, J. L., Vanhaesebroeck, B., Corcoran, A. E., & Okkenhaug, K. (2010). The PI3K Isoforms p110α and p110δ Are Essential for Pre–B Cell Receptor Signaling and B Cell Development. *Science Signaling*, *3*(134). https://doi.org/10.1126/scisignal.2001104

Ramamoorthy, S., Kometani, K., Herman, J. S., Bayer, M., Boller, S., Edwards-Hicks, J., Ramachandran, H., Li, R., Klein-Geltink, R., Pearce, E. L., Grün, D., & Grosschedl, R. (2020). EBF1 and Pax5 safeguard leukemic transformation by limiting IL-7 signaling, Myc expression, and folate metabolism. *Genes & Development*, *34*(21–22), 1503–1519. https://doi.org/10.1101/gad.340216.120

Rastogi, R. P., Richa, Kumar, A., Tyagi, M. B., & Sinha, R. P. (2010). Molecular Mechanisms of Ultraviolet Radiation-Induced DNA Damage and Repair. *Journal of Nucleic Acids*, *2010*, 1–32. https://doi.org/10.4061/2010/592980

Rath, M. F., Bailey, M. J., Kim, J.-S., Ho, A. K., Gaildrat, P., Coon, S. L., Møller, M., & Klein, D. C. (2009). Developmental and Diurnal Dynamics of Pax4 Expression in the Mammalian Pineal Gland: Nocturnal Down-Regulation Is Mediated by Adrenergic-Cyclic Adenosine 3’,5’-Monophosphate Signaling. *Endocrinology*, *150*(2), 803–811. https://doi.org/10.1210/en.2008-0882

Rehe, K., Wilson, K., Bomken, S., Williamson, D., Irving, J., den Boer, M. L., Stanulla, M., Schrappe, M., Hall, A. G., Heidenreich, O., & Vormoor, J. (2013). Acute B lymphoblastic leukaemia-propagating cells are present at high frequency in diverse lymphoblast populations. *EMBO Molecular Medicine*, *5*(1), 38–51. https://doi.org/10.1002/emmm.201201703

Reyman, M., van Houten, M. A., van Baarle, D., Bosch, A. A. T. M., Man, W. H., Chu, M. L. J. N., Arp, K., Watson, R. L., Sanders, E. A. M., Fuentes, S., & Bogaert, D. (2019). Impact of delivery mode-associated gut microbiota dynamics on health in the first year of life. *Nature Communications*, *10*(1), 4997. https://doi.org/10.1038/s41467-019-13014-7

Richardson, C. D., Ray, G. J., DeWitt, M. A., Curie, G. L., & Corn, J. E. (2016). Enhancing homology-directed genome editing by catalytically active and inactive CRISPR-Cas9 using asymmetric donor DNA. *Nature Biotechnology*, *34*(3), 339–344. https://doi.org/10.1038/nbt.3481

Ritz-Laser, B., Estreicher, A., Gauthier, B., & Philippe, J. (2000). The Paired Homeodomain Transcription Factor Pax-2 Is Expressed in the Endocrine Pancreas and Transactivates the Glucagon Gene Promoter. *Journal of Biological Chemistry*, *275*(42), 32708–32715. https://doi.org/10.1074/jbc.M005704200

Roberts, K. G. (2018). Genetics and prognosis of ALL in children vs adults. *Hematology*, *2018*(1), 137–145. https://doi.org/10.1182/asheducation-2018.1.137

Roberts, K. G., & Mullighan, C. G. (2020). The Biology of B-Progenitor Acute Lymphoblastic Leukemia. *Cold Spring Harbor Perspectives in Medicine*, *10*(7), a034835. https://doi.org/10.1101/cshperspect.a034835

Robichaud, G. A., Nardini, M., Laflamme, M., Cuperlovic-Culf, M., & Ouellette, R. J. (2004). Human Pax-5 C-terminal Isoforms Possess Distinct Transactivation Properties and Are Differentially Modulated in Normal and Malignant B Cells. *Journal of Biological Chemistry*, *279*(48), 49956–49963. https://doi.org/10.1074/jbc.M407171200

Rodriguez-Hernandez, G., Opitz, F. V, Delgado, P., Walter, C., Alvarez-Prado, A. F., Gonzalez-Herrero, I., Auer, F., Fischer, U., Janssen, S., Bartenhagen, C., Raboso-Gallego, J., Casado-Garcia, A., Orfao, A., Blanco, O., Alonso-Lopez, D., Rivas, J. L., Tena-Davila, S. G., Muschen, M., Dugas, M., … Borkhardt, A. (2019). Infectious stimuli promote malignant B-cell acute lymphoblastic leukemia in the absence of AID. *Nat Commun*, *10*(1), 5563. https://doi.org/10.1038/s41467-019-13570-y

Roessler, S., Györy, I., Imhof, S., Spivakov, M., Williams, R. R., Busslinger, M., Fisher, A. G., & Grosschedl, R. (2007). Distinct Promoters Mediate the Regulation of *Ebf1* Gene Expression by Interleukin-7 and Pax5. *Molecular and Cellular Biology*, *27*(2), 579–594. https://doi.org/10.1128/MCB.01192-06

Rolink, A. G., Nutt, S. L., Melchers, F., & Busslinger, M. (1999). Long-term in vivo reconstitution of T-cell development by Pax5-deficient B-cell progenitors. *Nature*, *401*(6753), 603–606. https://doi.org/10.1038/44164

Rolink, A., Kudo, A., Karasuyama, H., Kikuchi, Y., & Melchers, F. (1991). Long-term proliferating early pre B cell lines and clones with the potential to develop to surface Ig-positive, mitogen reactive B cells in vitro and in vivo. *The EMBO Journal*, *10*(2), 327–336. https://doi.org/10.1002/j.1460-2075.1991.tb07953.x

Rolink, A., & Melchers, F. (1996). B-cell development in the mouse. *Immunol Lett*, *54*(2–3), 157–161. https://doi.org/10.1016/s0165-2478(96)02666-1

Rossi, B., Espeli, M., Schiff, C., & Gauthier, L. (2006). Clustering of Pre-B Cell Integrins Induces Galectin-1-Dependent Pre-B Cell Receptor Relocalization and Activation. *The Journal of Immunology*, *177*(2), 796–803. https://doi.org/10.4049/jimmunol.177.2.796

Rouault-Pierre, K., Lopez-Onieva, L., Foster, K., Anjos-Afonso, F., Lamrissi-Garcia, I., Serrano-Sanchez, M., Mitter, R., Ivanovic, Z., de Verneuil, H., Gribben, J., Taussig, D., Rezvani, H. R., Mazurier, F., & Bonnet, D. (2013). HIF-2alpha protects human hematopoietic stem/progenitors and acute myeloid leukemic cells from apoptosis induced by endoplasmic reticulum stress. *Cell Stem Cell*, *13*(5), 549–563. https://doi.org/10.1016/j.stem.2013.08.011

Rumfelt, L. L., Zhou, Y., Rowley, B. M., Shinton, S. A., & Hardy, R. R. (2006). Lineage specification and plasticity in CD19− early B cell precursors. *Journal of Experimental Medicine*, *203*(3), 675–687. https://doi.org/10.1084/jem.20052444

Sarry, J.-E., Murphy, K., Perry, R., Sanchez, P. V., Secreto, A., Keefer, C., Swider, C. R., Strzelecki, A.-C., Cavelier, C., Récher, C., Mansat-De Mas, V., Delabesse, E., Danet-Desnoyers, G., & Carroll, M. (2011). Human acute myelogenous leukemia stem cells are rare and heterogeneous when assayed in NOD/SCID/IL2Rγc-deficient mice. *Journal of Clinical Investigation*, *121*(1), 384–395. https://doi.org/10.1172/JCI41495

Schäfer, D., Olsen, M., Lähnemann, D., Stanulla, M., Slany, R., Schmiegelow, K., Borkhardt, A., & Fischer, U. (2018). Five percent of healthy newborns have an ETV6-RUNX1 fusion as revealed by DNA-based GIPFEL screening. *Blood*, *131*(7), 821–826. https://doi.org/10.1182/blood-2017-09-808402

Schaniel, C., Bruno, L., Melchers, F., & Rolink, A. G. (2002). Multiple hematopoietic cell lineages develop in vivo from transplanted Pax5-deficient pre-B I–cell clones. *Blood*, *99*(2), 472–478. https://doi.org/10.1182/blood.V99.2.472

Schebesta, A., McManus, S., Salvagiotto, G., Delogu, A., Busslinger, G. A., & Busslinger, M. (2007). Transcription Factor Pax5 Activates the Chromatin of Key Genes Involved in B Cell Signaling, Adhesion, Migration, and Immune Function. *Immunity*, *27*(1), 49–63. https://doi.org/10.1016/j.immuni.2007.05.019

Schebesta, M., Pfeffer, P. L., & Busslinger, M. (2002). Control of Pre-BCR Signaling by Pax5-Dependent Activation of the BLNK Gene. *Immunity*, *17*(4), 473–485. https://doi.org/10.1016/S1074-7613(02)00418-1

Schultz, K. R., Carroll, A., Heerema, N. A., Bowman, W. P., Aledo, A., Slayton, W. B., Sather, H., Devidas, M., Zheng, H. W., Davies, S. M., Gaynon, P. S., Trigg, M., Rutledge, R., Jorstad, D., Winick, N., Borowitz, M. J., Hunger, S. P., Carroll, W. L., & Camitta, B. (2014). Long-term follow-up of imatinib in pediatric Philadelphia chromosome-positive acute lymphoblastic leukemia: Children's Oncology Group Study AALL0031. *Leukemia*, *28*(7), 1467–1471. https://doi.org/10.1038/leu.2014.30

Scott, E. W., Fisher, R. C., Olson, M. C., Kehrli, E. W., Simon, M. C., & Singh, H. (1997). PU.1 Functions in a Cell-Autonomous Manner to Control the Differentiation of Multipotential Lymphoid–Myeloid Progenitors. *Immunity*, *6*(4), 437–447. https://doi.org/10.1016/S1074-7613(00)80287-3

Seale, P., Asakura, A., & Rudnicki, M. A. (2001). The Potential of Muscle Stem Cells. *Developmental Cell*, *1*(3), 333–342. https://doi.org/10.1016/S1534-5807(01)00049-1

Sędek, Ł., Theunissen, P., Sobral da Costa, E., van der Sluijs-Gelling, A., Mejstrikova, E., Gaipa, G., Sonsala, A., Twardoch, M., Oliveira, E., Novakova, M., Buracchi, C., van Dongen, J. J. M., Orfao, A., van der Velden, V. H. J., & Szczepański, T. (2019). Differential expression of CD73, CD86 and CD304 in normal vs. leukemic B-cell precursors and their utility as stable minimal residual disease markers in childhood B-cell precursor acute lymphoblastic leukemia. *Journal of Immunological Methods*, *475*, 112429. https://doi.org/10.1016/j.jim.2018.03.005

Seet, C. S., Brumbaugh, R. L., & Kee, B. L. (2004). Early B Cell Factor Promotes B Lymphopoiesis with Reduced Interleukin 7 Responsiveness in the Absence of E2A. *Journal of Experimental Medicine*, *199*(12), 1689–1700. https://doi.org/10.1084/jem.20032202

Sellars, M. (2011). Ikaros in B cell development and function. *World Journal of Biological Chemistry*, *2*(6), 132. https://doi.org/10.4331/wjbc.v2.i6.132

Shah, S., Schrader, K. A., Waanders, E., Timms, A. E., Vijai, J., Miething, C., Wechsler, J., Yang, J., Hayes, J., Klein, R. J., Zhang, J., Wei, L., Wu, G., Rusch, M., Nagahawatte, P., Ma, J., Chen, S. C., Song, G., Cheng, J., … Offit, K. (2013). A recurrent germline PAX5 mutation confers susceptibility to pre-B cell acute lymphoblastic leukemia. *Nat Genet*, *45*(10), 1226–1231. https://doi.org/10.1038/ng.2754

Shao, Y., Forster, S. C., Tsaliki, E., Vervier, K., Strang, A., Simpson, N., Kumar, N., Stares, M. D., Rodger, A., Brocklehurst, P., Field, N., & Lawley, T. D. (2019). Stunted microbiota and opportunistic pathogen colonization in caesarean-section birth. *Nature*, *574*(7776), 117–121. https://doi.org/10.1038/s41586-019-1560-1

Shin, D. H., Lee, K.-S., Lee, E., Chang, Y. P., Kim, J.-W., Choi, Y. S., Kwon, B.-S., Lee, H. W., & Cho, S. S. (2003). Pax-7 Immunoreactivity in the Post-natal Chicken Central Nervous System.

Anatomia, Histologia, Embryologia: Journal of Veterinary Medicine Series C, *32*(6), 378–383. https://doi.org/10.1111/j.1439-0264.2003.00496.x

Sivakamasundari, V., Kraus, P., & Lufkin, T. (2018). Regulatory Functions of Pax1 and Pax9 in Mammalian Cells. In *Gene Expression and Regulation in Mammalian Cells - Transcription Toward the Establishment of Novel Therapeutics*. InTech. https://doi.org/10.5772/intechopen.71920

Smeenk, L., Fischer, M., Jurado, S., Jaritz, M., Azaryan, A., Werner, B., Roth, M., Zuber, J., Stanulla, M., den Boer, M. L., Mullighan, C. G., Strehl, S., & Busslinger, M. (2017). Molecular role of the PAX5-ETV6 oncoprotein in promoting B-cell acute lymphoblastic leukemia. *EMBO J*, *36*(6), 718–735. https://doi.org/10.15252/embj.201695495

Somasundaram, R., Prasad, M. A. J., Ungerbäck, J., & Sigvardsson, M. (2015). Transcription factor networks in B-cell differentiation link development to acute lymphoid leukemia. *Blood*, *126*(2), 144–152. https://doi.org/10.1182/blood-2014-12-575688

Souabni, A., Cobaleda, C., Schebesta, M., & Busslinger, M. (2002). Pax5 Promotes B Lymphopoiesis and Blocks T Cell Development by Repressing Notch1. *Immunity*, *17*(6), 781–793. https://doi.org/10.1016/S1074-7613(02)00472-7

Spangrude, G. J., Heimfeld, S., & Weissman, I. L. (1988). Purification and Characterization of Mouse Hematopoietic Stem Cells. *Science*, *241*(4861), 58–62. https://doi.org/10.1126/science.2898810

Stapleton, P., Weith, A., Urbánek, P., Kozmik, Z., & Busslinger, M. (1993). Chromosomal localization of seven PAX genes and cloning of a novel family member, PAX-9. *Nature Genetics*, *3*(4), 292–298. https://doi.org/10.1038/ng0493-292

Sternberg, S. H., Redding, S., Jinek, M., Greene, E. C., & Doudna, J. A. (2014). DNA interrogation by the CRISPR RNA-guided endonuclease Cas9. *Nature*, *507*(7490), 62–67. https://doi.org/10.1038/nature13011

Stewart, C. J., Ajami, N. J., O'Brien, J. L., Hutchinson, D. S., Smith, D. P., Wong, M. C., Ross, M. C., Lloyd, R. E., Doddapaneni, H., Metcalf, G. A., Muzny, D., Gibbs, R. A., Vatanen, T., Huttenhower, C., Xavier, R. J., Rewers, M., Hagopian, W., Toppari, J., Ziegler, A.-G., … Petrosino, J. F. (2018). Temporal development of the gut microbiome in early childhood from the TEDDY study. *Nature*, *562*(7728), 583–588. https://doi.org/10.1038/s41586-018-0617-x

St-Onge, L., Sosa-Pineda, B., Chowdhury, K., Mansouri, A., & Gruss, P. (1997). Pax6 is required for differentiation of glucagon-producing α-cells in mouse pancreas. *Nature*, *387*(6631), 406–409. https://doi.org/10.1038/387406a0

Stoykova, A., & Gruss, P. (1994). Roles of Pax-genes in developing and adult brain as suggested by expression patterns. *The Journal of Neuroscience*, *14*(3), 1395–1412. https://doi.org/10.1523/JNEUROSCI.14-03-01395.1994

Sugimura, R., He, X. C., Venkatraman, A., Arai, F., Box, A., Semerad, C., Haug, J. S., Peng, L., Zhong, X., Suda, T., & Li, L. (2012). Noncanonical Wnt Signaling Maintains Hematopoietic Stem Cells in the Niche. *Cell*, *150*(2), 351–365. https://doi.org/10.1016/j.cell.2012.05.041

Sugiyama, T., Kohara, H., Noda, M., & Nagasawa, T. (2006). Maintenance of the Hematopoietic Stem Cell Pool by CXCL12-CXCR4 Chemokine Signaling in Bone Marrow Stromal Cell Niches. *Immunity*, *25*(6), 977–988. https://doi.org/10.1016/j.immuni.2006.10.016

Taub, J. W., Konrad, M. A., Ge, Y., Naber, J. M., Scott, J. S., Matherly, L. H., & Ravindranath, Y. (2002). High frequency of leukemic clones in newborn screening blood samples of

children with B-precursor acute lymphoblastic leukemia. *Blood*, *99*(8), 2992–2996. https://doi.org/10.1182/blood.V99.8.2992

Theunissen, P. M. J., de Bie, M., van Zessen, D., de Haas, V., Stubbs, A. P., & van der Velden, V. H. J. (2019). Next-generation antigen receptor sequencing of paired diagnosis and relapse samples of B-cell acute lymphoblastic leukemia: Clonal evolution and implications for minimal residual disease target selection. *Leukemia Research*, *76*, 98–104. https://doi.org/10.1016/j.leukres.2018.10.009

Thompson, J. A., Lovicu, F. J., & Ziman, M. (2007). Pax7 and superior collicular polarity: insights from Pax6 (Sey) mutant mice. *Experimental Brain Research*, *178*(3), 316–325. https://doi.org/10.1007/s00221-006-0735-9

Thompson, J. A., Zembrzycki, A., Mansouri, A., & Ziman, M. (2008). Pax7 is requisite for maintenance of a subpopulation of superior collicular neurons and shows a diverging expression pattern to Pax3 during superior collicular development. *BMC Developmental Biology*, *8*(1), 62. https://doi.org/10.1186/1471-213X-8-62

Thompson, J., Lovicu, F., & Ziman, M. (2004). The role of Pax7 in determining the cytoarchitecture of the superior colliculus. *Development, Growth and Differentiation*, *46*(3), 213–218. https://doi.org/10.1111/j.1440-169x.2004.00744.x

TILL, J. E., & McCULLOCH, E. A. (1961). A direct measurement of the radiation sensitivity of normal mouse bone marrow cells. *Radiation Research*, *14*, 213–222.

Tokoyoda, K., Egawa, T., Sugiyama, T., Choi, B.-I., & Nagasawa, T. (2004). Cellular Niches Controlling B Lymphocyte Behavior within Bone Marrow during Development. *Immunity*, *20*(6), 707–718. https://doi.org/10.1016/j.immuni.2004.05.001

Ton, C. C. T., Hirvonen, H., Miwa, H., Weil, M. M., Monaghan, P., Jordan, T., van Heyningen, V., Hastie, N. D., Meijers-Heijboer, H., Drechsler, M., Royer-Pokora, B., Collins, F., Swaroop, A., Strong, L. C., & Saunders, G. F. (1991). Positional cloning and characterization of a paired box- and homeobox-containing gene from the aniridia region. *Cell*, *67*(6), 1059–1074. https://doi.org/10.1016/0092-8674(91)90284-6

Treiber, T., Mandel, E. M., Pott, S., Györy, I., Firner, S., Liu, E. T., & Grosschedl, R. (2010). Early B Cell Factor 1 Regulates B Cell Gene Networks by Activation, Repression, and Transcription- Independent Poising of Chromatin. *Immunity*, *32*(5), 714–725. https://doi.org/10.1016/j.immuni.2010.04.013

Treisman, J., Harris, E., & Desplan, C. (1991). The paired box encodes a second DNA-binding domain in the paired homeo domain protein. *Genes & Development*, *5*(4), 594–604. https://doi.org/10.1101/gad.5.4.594

Tremblay, C. S., Saw, J., Chiu, S. K., Wong, N. C., Tsyganov, K., Ghotb, S., Graham, A. N., Yan, F., Guirguis, A. A., Sonderegger, S. E., Lee, N., Kalitsis, P., Reynolds, J., Ting, S. B., Powell, D. R., Jane, S. M., & Curtis, D. J. (2018). Restricted cell cycle is essential for clonal evolution and therapeutic resistance of pre-leukemic stem cells. *Nature Communications*, *9*(1), 3535. https://doi.org/10.1038/s41467-018-06021-7

Tsitsikov, E., Harris, M. H., Silverman, L. B., Sallan, S. E., & Weinberg, O. K. (2018). Role of CD81 and CD58 in minimal residual disease detection in pediatric B lymphoblastic leukemia. *International Journal of Laboratory Hematology*, *40*(3), 343–351. https://doi.org/10.1111/ijlh.12795

Tsukamoto, K., Nakamura, Y., & Niikawa, N. (1994). Isolation of two isoforms of the PAX3 gene transcripts and their tissue-specific alternative expression in human adult tissues. *Human Genetics*, *93*(3), 270–274. https://doi.org/10.1007/BF00212021

Tzelepis, K., Koike-Yusa, H., De Braekeleer, E., Li, Y., Metzakopian, E., Dovey, O. M., Mupo, A., Grinkevich, V., Li, M., Mazan, M., Gozdecka, M., Ohnishi, S., Cooper, J., Patel, M., McKerrell, T., Chen, B., Domingues, A. F., Gallipoli, P., Teichmann, S., … Yusa, K. (2016). A CRISPR Dropout Screen Identifies Genetic Vulnerabilities and Therapeutic Targets in Acute Myeloid Leukemia. *Cell Rep*, *17*(4), 1193–1205. https://doi.org/10.1016/j.celrep.2016.09.079

Ungerbäck, J., Åhsberg, J., Strid, T., Somasundaram, R., & Sigvardsson, M. (2015). Combined heterozygous loss of *Ebf1* and *Pax5* allows for T-lineage conversion of B cell progenitors. *Journal of Experimental Medicine*, *212*(7), 1109–1123. https://doi.org/10.1084/jem.20132100

Urbánek, P., Wang, Z. Q., Fetka, I., Wagner, E. F., & Busslinger, M. (1994). Complete block of early B cell differentiation and altered patterning of the posterior midbrain in mice lacking Pax5/BSAP. *Cell*, *79*(5), 901–912. https://doi.org/10.1016/0092-8674(94)90079-5

Urnov, F. D., Rebar, E. J., Holmes, M. C., Zhang, H. S., & Gregory, P. D. (2010). Genome editing with engineered zinc finger nucleases. *Nature Reviews. Genetics*, *11*(9), 636–646. https://doi.org/10.1038/nrg2842

Vallespinós, M., Fernández, D., Rodríguez, L., Alvaro-Blanco, J., Baena, E., Ortiz, M., Dukovska, D., Martínez, D., Rojas, A., Campanero, M. R., & Moreno de Alborán, I. (2011). B Lymphocyte Commitment Program Is Driven by the Proto-Oncogene *c-myc*. *The Journal of Immunology*, *186*(12), 6726–6736. https://doi.org/10.4049/jimmunol.1002753

van der Weyden, L., Giotopoulos, G., Wong, K., Rust, A. G., Robles-Espinoza, C. D., Osaki, H., Huntly, B. J., & Adams, D. J. (2015). Somatic drivers of B-ALL in a model of ETV6-RUNX1; Pax5(+/-) leukemia. *BMC Cancer*, *15*, 585. https://doi.org/10.1186/s12885-015-1586-1

Vettermann, C., Herrmann, K., & Jäck, H.-M. (2006). Powered by pairing: The surrogate light chain amplifies immunoglobulin heavy chain signaling and pre-selects the antibody repertoire. *Seminars in Immunology*, *18*(1), 44–55. https://doi.org/10.1016/j.smim.2006.01.001

Vicente-Dueñas, C., Janssen, S., Oldenburg, M., Auer, F., González-Herrero, I., Casado-García, A., Isidro-Hernández, M., Raboso-Gallego, J., Westhoff, P., Pandyra, A. A., Hein, D., Gössling, K. L., Alonso-López, D., De Las Rivas, J., Bhatia, S., García-Criado, F. J., García-Cenador, M. B., Weber, A. P. M., Köhrer, K., … Borkhardt, A. (2020). An intact gut microbiome protects genetically predisposed mice against leukemia. *Blood*, *136*(18), 2003–2017. https://doi.org/10.1182/blood.2019004381

von Freeden-Jeffry, U., Vieira, P., Lucian, L. A., McNeil, T., Burdach, S. E., & Murray, R. (1995). Lymphopenia in interleukin (IL)-7 gene-deleted mice identifies IL-7 as a nonredundant cytokine. *Journal of Experimental Medicine*, *181*(4), 1519–1526. https://doi.org/10.1084/jem.181.4.1519

Vyas, P. (2014). Targeting HIF function: the debate continues. *Blood*, *124*(24), 3510–3511. https://doi.org/10.1182/blood-2014-10-605055

Waanders, E., Gu, Z., Dobson, S. M., Antić, Ž., Crawford, J. C., Ma, X., Edmonson, M. N., Payne-Turner, D., van de Vorst, M., Jongmans, M. C. J., McGuire, I., Zhou, X., Wang, J., Shi, L., Pounds, S., Pei, D., Cheng, C., Song, G., Fan, Y., … Mullighan, C. G. (2020). Mutational Landscape and Patterns of Clonal Evolution in Relapsed Pediatric Acute Lymphoblastic Leukemia. *Blood Cancer Discovery*, *1*(1), 96–111. https://doi.org/10.1158/0008-5472.BCD-19-0041

Wallin, J., Mizutani, Y., Imai, K., Miyashita, N., Moriwaki, K., Taniguchi, M., Koseki, H., & Balling, R. (1993). A new Pax gene, Pax-9, maps to mouse Chromosome 12. *Mammalian Genome*, *4*(7), 354–358. https://doi.org/10.1007/BF00360584

Walther, C., Guenet, J.-L., Simon, D., Deutsch, U., Jostes, B., Goulding, M. D., Plachov, D., Balling, R., & Gruss, P. (1991). Pax: A murine multigene family of paired box-containing genes. *Genomics*, *11*(2), 424–434. https://doi.org/10.1016/0888-7543(91)90151-4

Wang, H., La Russa, M., & Qi, L. S. (2016). CRISPR/Cas9 in Genome Editing and Beyond. *Annual Review of Biochemistry*, *85*(1), 227–264. https://doi.org/10.1146/annurev-biochem-060815-014607

Wiemels, J., Cazzaniga, G., Daniotti, M., Eden, O., Addison, G., Masera, G., Saha, V., Biondi, A., & Greaves, M. (1999). Prenatal origin of acute lymphoblastic leukaemia in children. *The Lancet*, *354*(9189), 1499–1503. https://doi.org/10.1016/S0140-6736(99)09403-9

Wilcox, E. R., Rivolta, M. N., Ploplis, B., Potterf, S. B., & Fex, J. (1992). The PAX3 gene is mapped to human chromosome 2 together with a highly informative CA dinucleotide repeat. *Human Molecular Genetics*, *1*(3), 215–215. https://doi.org/10.1093/hmg/1.3.215-a

Wilson, N. K., Foster, S. D., Wang, X., Knezevic, K., Schütte, J., Kaimakis, P., Chilarska, P. M., Kinston, S., Ouwehand, W. H., Dzierzak, E., Pimanda, J. E., de Bruijn, M. F. T. R., & Göttgens, B. (2010). Combinatorial Transcriptional Control In Blood Stem/Progenitor Cells: Genome-wide Analysis of Ten Major Transcriptional Regulators. *Cell Stem Cell*, *7*(4), 532–544. https://doi.org/10.1016/j.stem.2010.07.016

Wojiski, S., Guibal, F. C., Kindler, T., Lee, B. H., Jesneck, J. L., Fabian, A., Tenen, D. G., & Gilliland, D. G. (2009). PML–RARα initiates leukemia by conferring properties of self-renewal to committed promyelocytic progenitors. *Leukemia*, *23*(8), 1462–1471. https://doi.org/10.1038/leu.2009.63

Wossning, T., Herzog, S., Köhler, F., Meixlsperger, S., Kulathu, Y., Mittler, G., Abe, A., Fuchs, U., Borkhardt, A., & Jumaa, H. (2006). Deregulated Syk inhibits differentiation and induces growth factor–independent proliferation of pre–B cells. *Journal of Experimental Medicine*, *203*(13), 2829–2840. https://doi.org/10.1084/jem.20060967

Xu, H. E., Rould, M. A., Xu, W., Epstein, J. A., Maas, R. L., & Pabo, C. O. (1999). Crystal structure of the human Pax6 paired domain-DNA complex reveals specific roles for the linker region and carboxy-terminal subdomain in DNA binding. *Genes & Development*, *13*(10), 1263–1275. https://doi.org/10.1101/gad.13.10.1263

Xu, W., Rould, M. A., Jun, S., Desplan, C., & Pabo, C. O. (1995). Crystal structure of a paired domain-DNA complex at 2.5 å resolution reveals structural basis for pax developmental mutations. *Cell*, *80*(4), 639–650. https://doi.org/10.1016/0092-8674(95)90518-9

Yang, J. J., Bhojwani, D., Yang, W., Cai, X., Stocco, G., Crews, K., Wang, J., Morrison, D., Devidas, M., Hunger, S. P., Willman, C. L., Raetz, E. A., Pui, C., Evans, W. E., Relling, M. V., & Carroll, W. L. (2008). Genome-wide copy number profiling reveals molecular evolution from diagnosis to relapse in childhood acute lymphoblastic leukemia. *Blood*, *112*(10), 4178–4183. https://doi.org/10.1182/blood-2008-06-165027

Yasuda, T., Sanjo, H., Pagès, G., Kawano, Y., Karasuyama, H., Pouysségur, J., Ogata, M., & Kurosaki, T. (2008). Erk Kinases Link Pre-B Cell Receptor Signaling to Transcriptional Events Required for Early B Cell Expansion. *Immunity*, *28*(4), 499–508. https://doi.org/10.1016/j.immuni.2008.02.015

Yoshida, T., Yao-Ming Ng, S., Zuniga-Pflucker, J. C., & Georgopoulos, K. (2006). Early hematopoietic lineage restrictions directed by Ikaros. *Nature Immunology*, *7*(4), 382–391. https://doi.org/10.1038/ni1314

Zenatti, P. P., Ribeiro, D., Li, W., Zuurbier, L., Silva, M. C., Paganin, M., Tritapoe, J., Hixon, J. A., Silveira, A. B., Cardoso, B. A., Sarmento, L. M., Correia, N., Toribio, M. L., Kobarg, J., Horstmann, M., Pieters, R., Brandalise, S. R., Ferrando, A. A., Meijerink, J. P., … Barata, J. T. (2011). Oncogenic IL7R gain-of-function mutations in childhood T-cell acute lymphoblastic leukemia. *Nature Genetics*, *43*(10), 932–939. https://doi.org/10.1038/ng.924

Zhou, B., Chu, X., Tian, H., Liu, T., Liu, H., Gao, W., Chen, S., Hu, S., Wu, D., & Xu, Y. (2021). The clinical outcomes and genomic landscapes of acute lymphoblastic leukemia patients with <scp>E2A-PBX1</scp> : A 10-year retrospective study. *American Journal of Hematology*, *96*(11), 1461–1471. https://doi.org/10.1002/ajh.26324

Zou, Y.-R., Kottmann, A. H., Kuroda, M., Taniuchi, I., & Littman, D. R. (1998). Function of the chemokine receptor CXCR4 in haematopoiesis and in cerebellar development. *Nature*, *393*(6685), 595–599. https://doi.org/10.1038/31269